PB97-152292

CAPABILITIES OF ATOMIC WEAPONS
SANITIZED VERSION

ARMED FORCES SPECIAL WEAPONS PROJECT
WASHINGTON, DC

NOVEMBER 1957

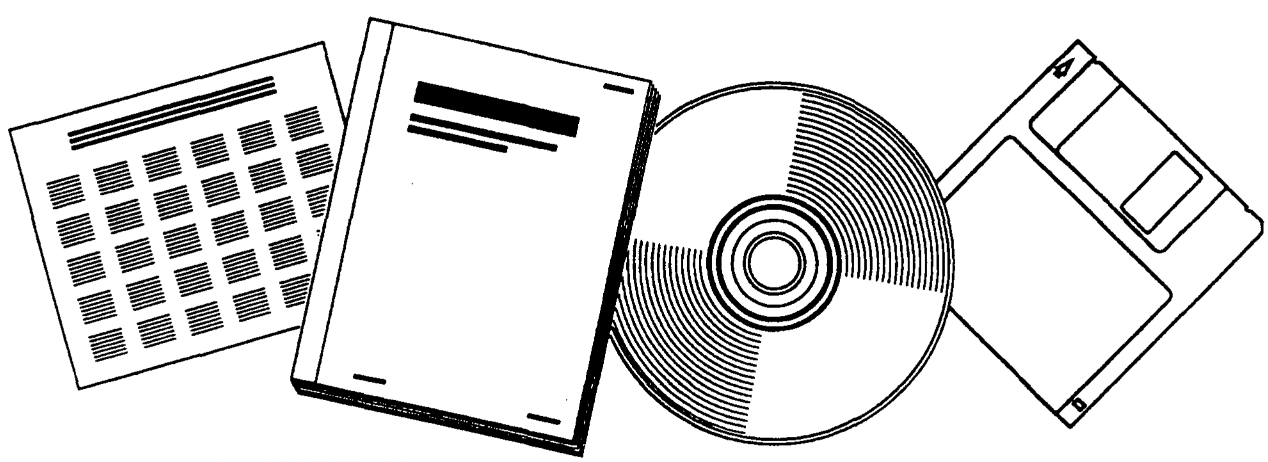

U.S. DEPARTMENT OF COMMERCE
National Technical Information Service

~~CONFIDENTIAL~~

DEPARTMENT OF THE ARMY TECHNICAL MANUAL — TM 23-200

DEPARTMENT OF THE NAVY — OPNAV INSTRUCTION 03400.1B

DEPARTMENT OF THE AIR FORCE — AFL 136-1

MARINE CORPS PUBLICATIONS — NAVMC 1104 REV

CAPABILI[redacted]

OF

ATOMIC WEAPONS ([redacted])

sanitized version

Prepared by
Armed Forces Special Weapons Project

REGRADING DATA CANNOT BE PREDETERMINED

DEPARTMENTS OF THE ARMY, THE NAVY AND THE AIR FORCE

REVISED EDITION NOVEMBER 1957

~~CONFIDENTIAL~~

1884

CONFIDENTIAL

TM 23-200/OPNAV INSTRUCTION 03400.1B/AFL 136-1/NAVMC 1104 REV

THIS PUBLICATION SUPERSEDES TM 23-200, OPNAV INSTRUCTION 003400.1A, AFL 136-4/NAVMC 1104, 1 JUNE 1955, INCLUDING C 1, 1 APRIL 1956, C 2, 17 OCTOBER 1956, AND C 3, 19 SEPTEMBER 1957

CAPABILITIES OF ATOMIC WEAPONS (U)

United States Government Printing Office
Washington : 1957

CONFIDENTIAL

ATTENTION!

This Document, PB97-152292

is considered old but it has been determined that

there is an audience for it.

Do NOT follow established procedures which call for

data base only.

THIS DOCUMENT IS TO BE ANNOUNCED.

Please code it for full announcement in all

applicable announcement material.

ATTENTION!

DISK 1/cdataold.doc/pph

Defense Special Weapons Agency
6801 Telegraph Road
Alexandria, Virginia 22310-3398

TRC

25 March 1997

National Technical Information Service
ATTN: Receiving
5285 Port Royal Road
Springfield, Virginia 22161

Dear Sir:

The Defense Special Weapons Agency (formerly Defense Nuclear Agency) Public Affairs Office submits the following sanitized report under distribution statement **"A"** to be released to the public:

PB97-152292

TM-23-200-SAN
OPNAV-INSTRUCTION-03400.1B-SAN
AFL-136-1-SAN
NAVMC-1104-REV-SAN
Capabilities of Atomic Weapons, Sanitized Version
Departments of the Army, The Navy and the Air Force
Revised Edition November 1957.

Please send us the assigned accession number for this report, so that it can be referenced to our users.

Sincerely,

ARDITH JARRETT
Chief, Technical Resource Center

2 Enclosures:
A/S

BLANK

DEPARTMENT OF THE ARMY TECHNICAL MANUAL
DEPARTMENT OF THE NAVY
DEPARTMENT OF THE AIR FORCE MANUAL
MARINE CORPS PUBLICATIONS

C 2, TM 23-200
OPNAVINST 03400.1B, CH-2
AFM 136-1B
NAVMC 1104 REV, CH-2

CAPABILITIES OF ATOMIC WEAPONS

CHANGES No. 2

DEPARTMENTS OF THE ARMY, THE NAVY AND THE AIR FORCE
WASHINGTON 25, D.C., *3 October 1960*

TM 23-200/OPNAV Instruction 03400.1B/AFM 136-1/NAVMC 1104, REV, 29 November 1957, is changed as follows:

1. Make the following pen and ink changes in Changes No. 1:

a. Page (I). Change item 11 to read: Remove pages I-29 and I-30 and substitute pages I-29 through I-32 Changes No. One.

b. Page (IV). Change Navy distribution to read:

F9 (Station CNO)
H23 (AV Med Ctr)

c. Page v. Change column 1, line 15 to read: 4-22a through 4-22d .... Change 1
4-23 and 4-24 .... Change 1
Change column 1, line 16 to read: 4-25 through 4-88 .... Original
Change column 2, line 9 to read: I-9 through I-28 .... Original

d. Index. Change page numbers 9 and 10 to read 11 and 12, respectively. Add C 1, 24 June 1960, in the upper inside corners of pages 1, 2, 5 through 8, and renumbered pages 11 and 12.

2. Destroy, according to proper security procedures, the page of the Index issued in Changes No. 1 as page 12. The reverse of page 12 is blank.

3. After necessary action, file the transmittal sheet in the front of the manual for reference.

[AG 461 (9 Aug 60)]

BY ORDER OF THE SECRETARIES OF THE ARMY, THE NAVY, AND THE AIR FORCE:

G. H. DECKER,
General, United States Army,
Chief of Staff.

OFFICIAL:
R. V. LEE,
Major General, United States Army,
The Adjutant General.

G. R. DONAHO,
Rear Admiral, United States Navy,
Assistant Vice Chief of Naval Operations,
Director of Naval Administration.

THOMAS D. WHITE,
Chief of Staff, United States Air Force.

OFFICIAL:
J. L. TARR,
Colonel, United States Air Force,
Director of Administrative Services.

F. L. WIESEMAN,
Major General, U.S. Marine Corps,
Deputy Chief of Staff (Plans).

DISTRIBUTION:

Active Army:

CofSA (2)
VCofSA (2)
DCSPER (5)
ACSI (5)
DCSOPS (12)
DCSLOG (5)
ACSRC (2)
SGS (5)
CA (2)
CUSARROTC (2)
CINFO (1)
CNGB (2)
CRD (2)
CLL (1)
TIG (1)
TAG (2)
TJAG (1)
CMH (2)
CofCH (2)
USASA (2)
Tech Stf, DA (5) except CofT (1)
Tech Stf Bd (2)
USCONARC (20)
USA Arty Bd (2)
USA Armor Bd (2)
USA Inf Bd (2)
USA AD Bd (2)
USA Avn Bd (2)
US ARADCOM (5)
US ARADCOM Rgn (5)
OS Maj Comd (5)
OS Base Comd (5)
Log Comd (5)
MDW (2)
Armies (10) except First US Army (12)
Corps (10)
Div (10) except Armored Div (25), (Each CC 5)
Bde (5)
Rgt/Gp/bg (5)
Bn (2)
USATC (2)
USMA (2)
USAWC (5)
USACGSC (1500)
Joint Sch (2)
Br Svc Sch (2) except
  US ARADSCH (220)
  USAAMS (250)
  USAARMS (500)
  USACMLCSCH (200)
  USAES (300)
  USAIS (445)
  AMSS (175)
  USA Ord Sch (85)
  PMGS (60)
  USA QM Sch (35)
  USATSCH (100)
Specialist Sch (2) except
  USAAVNS (38)
  USAOGMS (50)
  USASWS (75)
USAINTC (5)
AH (1)
Ports of Emb (OS) (5)
Dist Engr (5)
Div Engr (5)
GENDEP (1)
PG (2)
Arsenals (1) except Picatinny Arsenal (2)
MAAG (2)
Mil Msn (2)

NG: State AG (3).

USAR: Div (2).

For explanation of abbreviations used, see AR 320-50.

Navy:

SNDL
Part I (Operating Forces)—(less Annex A)
Part II
A3 (CNO)
A5 (Bureaus)
A6 (Hdqtrs, U.S. MarCorps)
E4 (Laboratory ONR)
E5 (Research Office ONR)
F2 (NavDist & River Comd Comdts)
F3 (Base)
F9 (Station CNO)
F17 (Comm Sta)
F18 (Comm Unit)
F21 (Admin Cmd & Unit CNO)
F22 (Dipt Duty Intell)
F23 (Dipl Duty Missions)
F28 (Intell Off Naval Dist)
F40 (Comm Facility)
F41 (Security Sta)
F42 (Radio Sta)
F43 (Radio Fac)
F46 (Mar Bks CNO)
F48 (Sec Grp Hdqtrs Act)
F56 (Flt Weather Cent)
F57 (Flt Weather Fac)
H5 (Lab BUMED)
H23 (Av Med Ctr)
H24 (Scol AV Med)
J1 (Admin Command & Unit BUPERS)
J3 (Air Def Trng Ctr)
J4 (Amphib Base)
J12 (Flt Trng Ctr)
J28 (Res Trng Ctr)
J29 (Res Trng Fac)
J30 (Tra Pubs Ctr)
J33 (Ser Scol Comd)
J34 (Station BUPERS)
J35 (Sub Trng Fac)
J36 (Trng Ctr)
J48 (Constr Trng Unit)
J56 (Schools Command)
J60 (School Academy)
J65 (Schol CEC Off's)
J66 (Scol Constr)
J71 (Scol Expl Ord Disp)
J73 (Scol Flt Sonor)
J76 (Scol Flt Gunnary)
J79 (Scol Intell)
J81 (Scol Mine Warfare)
J84 (Scol Postgraduate)
J87 (Service Scols)
J88 (Scol Submarine)
J93 (Scol Adv Undersea Wpns)
J94 (Scol ROTC)
J95 (Scol War College)
J98 (Scol Guided Missiles)
J104 (Nuc Pwr Trng Unit)
J105 (Res Trng Comd)
L1 (Shipyard)
L7 (Lab BUSHIPS)
L24 (Nav Acts)
L26 (Nav Fac)
L30 (Sub Base)
L32 (Nav Supp Acts)
L35 (Station, BUSHIPS)
L38 (Base BUSHIPS)
L42 (Flt Acts)
L45 (Oceanographic Unit)
M17 (Ord Supp Dep)
M18 (Overseas Air Cargo Term)
M26 (Supply Annex)
M27 (Supply Ctr)
M28 (Supply Dep)
M44 (Nuclear Wpns Supp Annex)
M45 (Nuclear Wpns Supp Dep)
M46 (Ord Sup Off)
N2 (Public Works Off)
N8 (Lab BUDOCKS)
N9 (Pub Wks Ctr)
R1 (Hdq Dept of Pac)
R20 (Mar Cor Scol Quantico)
R36 (Hdqtrs Batt)
R64 (Mar Corps Base)
W1A (Air Station)
W1B (Air Sta Auxiliary)
W1C (Air Fac BUAER)
W1E (Mar Cor Air Stations)
W1F (Mar Cor Aux Air Sta)
W1G (Mar Cor Air Fac)
W1H (Station BUAER)
W1J (Flt Air Serv Ron Spec)
W2 (Air Bases Comd)
W2B (Mar Cor Air Base Cmdrs)
W3A (Air Trng Comd)
W3B (Air Adv Trng Comd)
W3C (Air Basic Trng Comd)
W3E (Air Reserve Trng Comd)
W3F (Air Tech Trng Comd)
W3G (Mar Air Res Trng Comd)
W4A (Air Tech Trng Ctr)
W4B (Air Tech Tra Unit)
W4C (Air Res Trng Unit)
W4E (Mar Air Res Trng Det)
W4F (Nav Tech Tra Unit)
W4G (Hel Trng Grp)
W4H (School Pre Flt)
W4J (CIC School)
W5A (Naval Activities)
W5E (Flt Act BUWEPS)
W5K (Flt Intell Ctr)
W5L (Flt Air Intell Aug Unit)
W5M (Mob Intel Prod Unit)
W6A (BUWEPS Gen Rep)
W6B (BUWEPS Rep Off)
W7A (Air Dev & Mat Ctr)
W7B (Air Mat Ctr)
W7C (Air Test Ctr)
W7E (Air Dev Ctr)
W7F (EODT Ctr)
W7J (Ord Miss Test Fac)
W7K (Air Spec Wpns Fac)
W7N (Air Min Def Dev Unit)
W7P (Weapons Laboratory)
W7Q (Lab BUWEPS)
W7T (Air Rocket Test Sta)
W7V (Underwater Ord Sta)
W7X (G M Unit)
W8B (Miss Ctr)
W9A (Weapons Plant)
W9C (Propellent Plant)
W9F (Mine Eng Fac)
W9G (Ord Fac)
W11A (Ammo Depot)
W11F (Tor Sta)
W11H (Mag)
W11J (Net Dep & Fac)
W12B (G M Serv Unit)
Copy to:
A1 (Sec & Exec Assts)
A2 (Exec Off of the Sec)
GSD NORVA (Stock 100 copies)
GSD OAKLAND (Stock 150 copies)
NWP WASH (Stock 50 copies)

Air Force: X

Headquarters USAF	230
Tactical Air Command	150
Air Training Command	2
Military Air Transport Service	25
Air University	200
Pacific Air Forces	50
Air Materiel Command	35
U.S. Air Forces in Europe	60
Air Defense Command	35
Continental Air Command	25
Air Research & Development Command, ATTN: RDAPD	250
Alaskan Air Command	28
Strategic Air Command	375
Caribbean Air Command	10
Headquarters Command, USAF	3
USAF Security Service	4
AF Special Weapons Center	30

U.S. GOVERNMENT PRINTING OFFICE: 1960

Department of the Army Technical Manual
Department of the Navy
Department of the Air Force Manual
Marine Corps Publications

C 1, TM 23-200
OPNAV Instruction 03400.1B, CH-1
AFM 136-1A
NAVMC 1104 REV, CH-1

Capabilities of Atomic Weapons (U)

CHANGES No. 1

DEPARTMENTS OF THE ARMY, THE NAVY, AND THE AIR FORCE
WASHINGTON 25, D.C., *24 June 1960*

TM 23-200/OPNAV Instruction 03400.1B/AFM 136-1/NAVMC 1104 REV, 29 November 1957, is changed as follows:

1. Change the Air Force number to read: **AFM 136-1.**
2. Remove pages v and vi and substitute pages v and vi of Changes Number One.
3. Remove pages xv through xxii and substitute pages xv through xxii of Changes Number One.
4. Remove pages 2-15 through 2-18 and substitute pages 2-15 through 2-18 of Changes Number One.
5. Remove pages 4-1 through 4-8 and substitute pages 4-1 through 4-8 of Changes Number One.
6. Following page 4-16, add pages 4-16a through 4-16d of Changes Number One.
7. Remove pages 4-21 through 4-24 and substitute pages 4-21, 4-22, 4-22a through 4-22d, 4-23, and 4-24 of Changes Number One.
8. Remove pages 9-3 and 9-4 and substitute pages 9-3 and 9-4 of Changes Number One.
9. Remove pages 9-9 through 9-12 and substitute pages 9-9 through 9-12 of Changes Number One.
10. Remove pages I-7 and I-8 and substitute pages I-7 and I-8 of Changes Number One.
11. Remove pages I-29 through I-32 and substitute pages I-29 through I-32 of Changes Number One.
12. Remove pages II-3 and II-4 and substitute pages II-3 and II-4 of Changes Number One.
13. Remove pages 1, 2, 5 through 8, and 11 and substitute pages 1, 2, 5 through 8, 11 and 12 of Changes Number One.

BY ORDER OF THE SECRETARIES OF THE ARMY, THE NAVY, AND THE AIR FORCE:

L. L. LEMNITZER,
General, United States Army,
Chief of Staff.

OFFICIAL:
R. V. LEE,
Major General, United States Army,
The Adjutant General.

ARLEIGH BURKE,
Chief of Naval Operations.

OFFICIAL:
G. R. DONAHO,
Rear Admiral, United States Navy,
Assistant Vice Chief of Naval Operations,
Director of Naval Administration.

THOMAS D. WHITE,
Chief of Staff, United States Air Force.

OFFICIAL:
J. L. TARR,
Colonel, United States Air Force,
Director of Administrative Services.

DAVID M. SHOUP,
General, U.S. Marine Corps,
Commandant of the Marine Corps.

OFFICIAL:
F. L. WIESEMAN,
Major General, U.S. Marine Corps,
Deputy Chief of Staff (Plans).

Distribution:

Active Army:

CofSA (2)
VCofSA (2)
DCSPER (5)
ACSI (5)
DCSOPS (12)
DCSLOG (5)
ACSRC (2)
SGS (5)
CA (2)
CUSARROTC (2)
CINFO (1)
CNGB (2)
CRD (2)
CLL (1)
TIG (1)
TAG (2)
TJAG (1)
CMH (2)
CofCh (2)
USASA (2)
Tech Stf, DA (5) except CofT (1)
Tech Stf Bd (2)
USCONARC (20)
USA Arty Bd (2)
USA Armor Bd (2)
USA Inf Bd (2)
USA AD Bd (2)
USA Avn Bd (2)
US ARADCOM (5)
US ARADCOM, Rgn (5)
OS Maj Comd (5)
OS Base Comd (5)
Log Comd (5)
MDW (2)
Armies (10) except First USA (12)
Corps (10)
Div (10) (ea CC) (5)
Bde (5)
Regt/Gp/Bg (5)
Bn (2)
USATC (2)
USMA (2)
USAWC (5)
USACGSC (1500)
Joint Sch (2)
Br Svc Sch (2) except
  US ARADSCH (220)
  USAAMS (250)
  USAARMS (500)
  USACMLSCH (200)
  USAES (300)
  USAIS (445)
  USAMSS (175)
  USA Ord Sch (85)
  PMGS (60)
  USA QM Sch (35)
  USATSCH (100)
Specialist Sch (2) except
  USAAVNS (38)
  USAOGMS (50)
  USASWS (75)
USAINTC (5)
AH (1)
Ports of Emb (OS) (5)
Dist Engr (5)
Div Engr (5)
GENDEP (1)
PG (2)
Arsenals (1) except Picatinny Arsenal (2)
SHARPE (Attn: USMMR) (10)
USA Corps (Res) (5)
MAAG (2)
Mil Msn (2)

NG: State AG (3).

USAR: Div (2).

For explanation of abbreviations used, see AR 320–50.

Navy:

SNDL
Part I (Operating Forces)—(less Annex A)
Part II
A3 (CNO)
A5 (Bureaus)
A6 (Hdqtrs, U.S. MarCorps)
E4 (Laboratory ONR)
E5 (Research Office ONR)
F2 (NavDist & River Comd Comdts)
F3 (Base)
F9 (Section CNO)
F17 (Comm Sta)
F18 (Comm Unit)
F21 (Admin Cmd & Unit CNO)
F22 (Dipt Duty Intell)
F23 (Dipl Duty Missions)
F28 (Intell Off Naval Dist)
F40 (Comm Facility)
F41 (Security Sta)
F42 (Radio Sta)
F43 (Radio Fac)
F46 (Mar Bks CNO)
F48 (Sec Grp Hdqtrs Act)
F56 (Flt Weather Cent)
F57 (Flt Weather Fac)
H5 (Lab BUMED)
H25 (Av Med Ctr)
H24 (Scol AV Med)
J1 (Admin Command & Unit BUPERS)
J3 (Air Def Trng Ctr)
J4 (Amphib Base)
J12 (Flt Trng Ctr)
J28 (Res Trng Ctr)
J29 (Res Trng Fac)
J30 (Tra Pubs Ctr)
J33 (Ser Scol Comd)
J34 (Station BUPERS)
J35 (Sub Trng Fac)
J36 (Trng Ctr)
J48 (Constr Trng Unit)
J56 (Schools Command)
J60 (School Academy)
J65 (Schol CEC Off's)
J66 (Scol Constr)
J71 (Scol Expl Ord Disp)
J73 (Scol Flt Sonor)
J76 (Scol Flt Gunnary)
J79 (Scol Intell)
J81 (Scol Mine Warfare)
J84 (Scol Postgraduate)
J87 (Service Scols)
J88 (Scol Submarine)
J93 (Scol Adv Undersea Wpns)
J94 (Scol ROTC)
J95 (Scol War College)
J98 (Scol Guided Missiles)
J104 (Nuc Pwr Trng Unit)
J105 (Res Trng Comd)
L1 (Shipyard)
L7 (Lab BUSHIPS)
L24 (Nav Acts)
L26 (Nav Fac)
L30 (Sub Base)
L32 (Nav Supp Acts)
L35 (Station, BUSHIPS)
L38 (Base BUSHIPS)
L42 (Flt Acts)
L45 (Oceanographic Unit)
M17 (Ord Supp Dep)
M18 (Overseas Air Cargo Term)
M26 (Supply Annex)
M27 (Supply Ctr)
M28 (Supply Dep)
M44 (Nuclear Wpns Supp Annex)
M45 (Nuclear Wpns Supp Dep)
M46 (Ord Sup Off)
N2 (Public Works Off)
N8 (Lab BUDOCKS)
N9 (Pub Wks Ctr)
R1 (Hdq Dept of Pac)
R20 (Mar Cor Scol Quantico)
R36 (Hdqtrs Batt)
R64 (Mar Corps Base)
W1A (Air Station)
W1B (Air Sta Auxiliary)
W1C (Air Fac BUAER)
W1E (Mar Cor Air Stations)
W1F (Mar Cor Aux Air Sta)
W1G (Mar Cor Air Fac)
W1H (Station BUAER)
W1J (Flt Air Serv Ron Spec)
W2 (Air Bases Comd)
W2B (Mar Cor Air Base Cmdrs)
W3A (Air Trng Comd)
W3B (Air Adv Trng Comd)
W3C (Air Basic Trng Comd)
W3E (Air Reserve Trng Comd)
W3F (Air Tech Trng Comd)
W3G (Mar Air Res Trng Comd)
W4A (Air Tech Trng Ctr)
W4B (Air Tech Tra Unit)
W4C (Air Res Trng Unit)
W4E (Mar Air Res Trng Det)
W4F (Nav Tech Tra Unit)
W4G (Hel Trng Grp)
W4H (School Pre Flt)
W4J (CIC School)
W5A (Naval Activities)
W5E (Flt Act BUWEPS)
W5K (Flt Intell Ctr)
W5L (Flt Air Intell Aug Unit)
W5M (Mob Intel Prod Unit)
W6A (BUWEPS Gen Rep)
W6B (BUWEPS Rep Off)
W7A (Air Dev & Mat Ctr)
W7B (Air Mat Ctr)
W7C (Air Test Ctr)
W7E (Air Dev Ctr)
W7F (EODT Ctr)
W7J (Ord Miss Test Fac)
W7K (Air Spec Wpns Fac)
W7N (Air Min Def Dev Unit)
W7P (Weapons Laboratory)
W7Q (Lab BUWEPS)
W7T (Air Rocket Test Sta)
W7V (Underwater Ord Sta)
W7X (G M Unit)
W8B (Miss Ctr)
W9A (Weapons Plant)
W9C (Propellent Plant)
W9F (Mine Eng Fac)
W9G (Ord Fac)
W11A (Ammo Depot)
W11F (Tor Sta)
W11H (Mag)
W11J (Net Dep & Fac)
W12B (G M Serv Unit)

Copy to:
A1 (Sec & Exec Assts)
A2 (Exec Off of the Sec)
GSD NORVA (Stock 100 copies)
GSD OAKLAND (Stock 150 copies)
NWP WASH (Stock 50 copies)

Air Force: X

Headquarters USAF	230
Tactical Air Command	150
Air Training Command	2
Military Air Transport Service	25
Air University	200
Pacific Air Forces	50
Air Materiel Command	35
U.S. Air Forces in Europe	60
Air Defense Command	35
Continental Air Command	25
Air Research & Development Command, ATTN: RDAPD	250
Alaskan Air Command	28
Strategic Air Command	375
Caribbean Air Command	10
Headquarters Command, USAF	3
USAF Security Service	4
AF Special Weapons Center	30

Contents

TM 23–200
OPNAV INSTRUCTION 03400.1B
AFL 136–1
NAVMC 1104 Rev

DEPARTMENTS OF THE ARMY,
THE NAVY, AND
THE AIR FORCE
WASHINGTON 25, D. C., *29 November 1957*

TM 23–200/OPNAV INSTRUCTION 03400.1B/AFL 136–1/NAVMC 1104 Rev, Capabilities of Atomic Weapons (U), is published for the use of all concerned.

[AG 461 (7 Oct 57)]

BY ORDER OF THE SECRETARIES OF THE ARMY, THE NAVY, AND THE AIR FORCE:

MAXWELL D. TAYLOR,
General, United States Army,
Chief of Staff.

OFFICIAL:
HERBERT M. JONES,
Major General, United States Army,
The Adjutant General.

ARLEIGH BURKE,
Chief of Naval Operations.

OFFICIAL
R. N. SMOOT,
Rear Admiral, United States Navy,
Deputy Chief of Naval Operations
(Administration).

THOMAS D. WHITE,
Chief of Staff,
United States Air Force.

OFFICIAL:
J. L. TARR,
Colonel, United States Air Force,
Air Adjutant General.

R. McC. PATE,
General, U. S. Marine Corps,
Commandant of the Marine Corps.

OFFICIAL:
ROBT. E. HOGABOOM,
Major General, U. S. Marine Corps,
Deputy Chief of Staff (Plans).

Distribution:

Active Army:

DCSPER	Technical Stf, DA	Brig	USA Ord Sch
ACSI	Technical Stf Bd	Regt/Gp/bg	AMSS
DCSOPS	USCONARC	Bn	Br Svc Sch
DCSLOG	USA Arty Bd	Ft & Camps	Army Intel Cen
ACSRC	USA Armor Bd	USMA	Army Log Maint Cen
SGS	USA Inf Bd	USAWC	RTC
CAMG	USA Air Def Bd	USACGSC	Arsenals
CoA	USA Abn & Elct Bd	USAARMS	Mil Dist
CUSARROTC	USA Avn Bd	USAAMS	MAAG
CofT	USA Armor Bd Test Sec	USARADSCH	Mil Mis
CINFO	USA Air Def Bd Test Sec	USAIS	ARMA
CNGB	CDEC	TAGSUSA	USMMR-SHAPE
CLL	USARADCOM	USACMLCSCH	AH
TIG	OS Maj Comd	USAES	Ports of Emb (OS)
TJAG	MDW	PMGS	Engr Dist
CMH	Armies	USATSCH	Div Engr
OCSpWar	Corps	USASCS	PG
ASA	Div		

NG: State AG; units—same as Active Army.
USAR: Same as Active Army.
For explanation of abbreviations used, see AR 320-50.

Air Force:

Zone of Interior and Overseas:

Headquarters USAF	230
Air Proving Ground Command	22
Tactical Air Command	150
Air Training Command	2
Crew Training Air Force	10
Flying Training Air Force	10
Technical Training Air Force	40
Military Air Transport Service	25
Air University	200
Far East Air Forces	50
Air Materiel Command	35
U. S. Air Forces in Europe	60
Air Defense Command	35
Continental Air Command	25
Air Research & Development Command, ATTN: RDAPD	250
Alaskan Air Command	28
Strategic Air Command	375
Carribean Air Command	10
Headquarters Command, USAF	3
USAF Security Service	4
AF Special Weapons Center	30

LIST OF EFFECTIVE PAGES

BLANK

CONTENTS

PART ONE. PHYSICAL PHENOMENA

PART ONE. PHYSICAL PHENOMENA—Continued

SECTION II. BLAST AND SHOCK PHENOMENA

PART ONE. PHYSICAL PHENOMENA—Continued

SECTION II. BLAST AND SHOCK PHENOMENA—Continued

SECTION III. THERMAL RADIATION PHENOMENA

PART ONE. PHYSICAL PHENOMENA—Continued

SECTION IV. NUCLEAR RADIATION PHENOMENA

PART TWO. DAMAGE CRITERIA

SECTION V. INTRODUCTION

PART TWO. DAMAGE CRITERIA—Continued

PART TWO. DAMAGE CRITERIA—Continued

PART TWO. DAMAGE CRITERIA—Continued

SECTION VIII. DAMAGE TO NAVAL EQUIPMENT

SECTION IX. DAMAGE TO AIRCRAFT

SECTION X. DAMAGE TO MILITARY FIELD EQUIPMENT

SECTION X. DAMAGE TO MILITARY FIELD EQUIPMENT—Continued

SECTION XI. FOREST STANDS

SECTION XII. MISCELLANEOUS RADIATION DAMAGE CRITERIA

APPENDIX I. SUPPLEMENTARY BLAST DATA

PART TWO. DAMAGE CRITERIA—Continued

Page

FIGURES—Continued

FIGURES—Continued

Page

FIGURES—Continued

TABLES:

BLANK

PAGE LOCATOR FOR PHYSICAL PHENOMENA FIGURES AND TABLES*

	Free air	Air	Transition	Land surface	Water surface	Underground	Underwater
BLAST AND SHOCK:							
Altitude Effects	2-9; I-29, 30.	I-29, 30	I-29, 30	I-29, 30	I-29, 30		
Base Surge						2-86	2-94
Crater:							
Depth			2-65, 72	2-65, 72	2-78	2-65, 72	2-78
Lip			2-50	2-50	2-80	2-50	2-80
Profile			2-50	2-50		2-50	
Radius (Diameter)			2-63, 68	2-63, 68	2-76	2-63, 68	2-76
Dynamic Pressure:							
Impulse	I-19						
Peak *vs.* Distance	2-21	2-40, 41	2-40, 41	2-40, 41	2-40		
Versus Time	2-1; I-16, 21.	2-1	2-1	2-1	2-1		
Wave Forms	I-5	I-5	I-5	I-5	I-5		
Ground Shock		2-83	2-83	2-53, 83			
Mach Stem		2-4, 23	2-4, 23				
Overpressure:							
Effect of Rain or Fog	2-43	2-43	2-43	2-43	2-43		
Impulse	I-13	I-24	I-24	I-24	I-24		
Peak *vs.* Distance	2-17	2-30, 32	2-30, 32	2-30, 32; I-32	2-30, I-32	2-47	2-47
Versus Time	2-1; I-15, 16.	2-1	2-1	2-1	2-1		
Wave Forms	I-3	I-3, 27	I-3, 27	I-3, 27	I-3		
Positive Phase:							
Duration	2-19	2-36	2-36	2-36	2-36		
Effect of Cut-Off							2-56, 57
Precursor		2-45	2-12, 45	2-45			
Relations of Various Parameters	*2-3*; I-11	I-11	I-11				
Time of Arrival	2-15	2-26	2-26	2-26	2-26		
Velocity:							
Peak Particle	*2-3*; I-10						
Shock	I-9						
Water Shock							2-59, 89
Water Waves					2-91		2-91
THERMAL:							
Atmospheric Transmissivity	3-14	3-14	3-14	3-14	3-14		
Fireball	3-5	3-5					
Generalized Pulse and Percent Emitted	3-7; 6-15	3-7; 6-15	3-7; 6-15	3-7; 6-15	3-7; 6-15		
Radiant Exposure	3-12, 18	3-18	3-18	3-18	3-18		
Times	3-10	3-10	3-10	3-10	3-10		
Yield *vs.* Altitude	3-12						
NUCLEAR:							
Cloud:							
Diameter	4-84	4-84	4-84	4-84	4-84	4-84	4-84
Height	4-81, 83	4-81, 83	4-81, 83	4-81, 83	4-81, 83	4-81, 83	4-81, 83
Penetration Dose	4-87	4-87	4-87	4-87	4-87	4-87	4-87
Initial Gamma:							
Dose *vs.* Distance	4-14, 15, 16, 16a, 16b, 16c, 16d.	4-14, 15, 16, 16a, 16b, 16c, 16d.	4-10, 11, 12, 13.	4-10, 11, 12, 13.	4-10, 11, 12, 13.	4-19	4-19
Percent *vs.* Time	4-20	4-20	4-20	4-20	4-20		
Shielding (Transmission) Factors	*6-11*; 6-19.	*6-11*; 6-19.	*6-11*; 6-19.	*6-11*; 6-19.	*6-11*; 6-19.	*6-11*; 6-19.	*6-11*; 6-19.

*Page numbers in italics are for tables.

PAGE LOCATOR FOR PHYSICAL PHENOMENA FIGURES AND TABLES*—Continued

	Free air	Air	Transition	Land surface	Water surface	Underground	Underwater
NUCLEAR—Continued							
Neutron:							
Dose, Fission Weapons	4-22a, 22b, 22c, 22d, 23.	4-22a, 22b, 22c, 22d, 23.	4-22a, 22b, 22c, 22d, 23.	4-22a, 22b, 22c, 22d, 23.	4-22a, 22b, 22c, 22d, 23.		
Dose, Thermonuclear Weapons	4-25	4-25	4-25	4-25	4-25		
Flux	12-9	12-9	12-9	12-9	12-9		
Induced Activity	----------	----------	*4-66*; 4-70, 73, 75, 76, 77, 78.				
Transmission Factors	*6-11*	*6-11*	*6-11*	*6-11*	*6-11*		
Fall-Out:							
Contours	----------	----------	4-38, 40, 42, 44, 46, 48.	4-29, 38, 40, 42, 44, 46.	4-38, 40, 42, 44, 46.	4-53, 54, 55, 56, 57.	4-59
Gamma Decay	----------	----------	4-35	4-35	4-35	4-35	4-35
Shielding (Transmission) Factors	----------	----------	*6-11*; 6-20.	*6-11*; 6-20.	*6-11*; 6-20.	*6-11*; 6-20.	*6-11*; 6-20.
Total Dose	----------	----------	4-61, 63	4-61, 63	4-61, 63	4-61, 63	4-61, 63
GENERAL:							
Atmospheric Conditions	*11-3, 4*; II-9, 10.	*11-3, 4*; II-9, 10.	*11-3, 4*; II-9, 10.	*11-3, 4*; II-9, 10.	*11-3, 4*; II-9, 10.		
Comparison of Phenomena	----------	5-13, 18	5-13, 18	5-13, 18	5-13, 18		
Relative Air Density	*4-2*; II-9	*4-2*; II-9	*4-2*; II-9	*4-2*; II-9	*4-2*; II-9		
Water Vapor Density	II-10	II-10	II-10	II-10	II-10		

PAGE LOCATOR FOR DAMAGE FIGURES AND TABLES*

	Blast	Thermal	Nuclear
Aircraft	9-5, 7, 9, 11	9-11	
Clothing	----------	*12-3*	
Earth-Covered Structures	*7-4, 8*; 7-40, 42, 46		
Electronics Equipment	10-15		
Engineer Equipment	10-21, 23		
Field Fortifications	*7-9*; 7-53, 54, 55		
Forests	*11-2*; 11-7, 8, 9, 10, 11, 12	*11-3, 4*; 11-15	
Land Mines	*10-4*		
Materials	----------	*12-3*; 12-5, 10	
Ordnance Equipment	*10-2*		
Personnel	*6-3*; 6-13, 17	*6-4, 5*; 6-14, 15, 17	*6-7, 11*; 6-17, 19, 20
Railroad Equipment	10-17, 19		
Submarines	*8-2*; 8-10, 11		
Supply Dumps	10-13		
Surface Ships	*8-2*; 8-6, 7, 8		
Surface Structures:			
Bridges	*7-4*; 7-34, 36, 38, 46		
Buildings	*7-3, 4*; 7-14, 16, 18, 20, 22, 26, 28, 30, 32, 45, 46		
Oil Tanks	*7-3*; 7-24, 45		
Tanks and Artillery	10-11		
Tunnels	7-51		
Underwater Mines	8-13, 14, 15		
Urban Areas	----------	*12-1*; 12-5, 6, 7	
Vehicles	10-9		
Subsurface burst damage distance reduction for surface targets	7-49		

*Page numbers in italics are for tables.

FOREWORD

The purpose of this manual is to provide the military Services with a compendium of the phenomena manifested by the detonation of nuclear weapons and the effects thereof in terms of damage to targets of military interest.

This edition of *Capabilities of Atomic Weapons* represents the continuing effort by the Armed Forces Special Weapons Project to make available the progressively improved data resulting from field testing, scaled tests, laboratory and theoretical analyses.

The manual is intended to serve as a basis for the preparation of operational manuals, not as an operational or employment manual of itself. Every effort has been made to include the best available data which will assist the using Services in meeting their particular operational requirements. As additional or better data becomes available it will be incorporated herein.

EDWARD N. PARKER
Rear Admiral, USN
Chief, Armed Forces Special Weapons Project

PART ONE—PHENOMENA
1. Introduction

This publication supersedes TM 23-200/OPNAV INSTRUCTION 003400.1A/AFL 136-4/NAVMC 1104, 1 June 1955, including C 1, 1 April 1956; C 2, 17 October 1956; and C 3, 19 September 1957

PART ONE
PHYSICAL PHENOMENA

SECTION I
INTRODUCTION

1.1 Explosion of a Nuclear Weapon

a. General. An explosion is defined as the sudden release of a large amount of energy in a small space. For high explosives, this energy manifests itself primarily as blast energy, regardless of environmental conditions. In a nuclear explosion, on the other hand, the energy manifests itself in the form of blast, thermal radiation, and nuclear radiation. In addition, the energy released from a nuclear detonation is essentially from a point source, whereas a comparable amount of energy released from a high explosive detonation would require an enormous volume of explosive. Further, the energy released in a nuclear detonation results from a fission process, a fusion process or a combination of the two, while the energy released in a high explosive detonation results from a chemical process which does not affect the nuclei of the atoms involved. In the fission process, heavy atoms are split into pairs of lighter radioactive atoms, whereas in the fusion process two light atoms are combined to form a heavier atom. In both processes, there is a net loss of mass which appears as energy, and there is also an emission of neutrons and gamma rays. The high temperatures resulting from either of these processes in turn cause large pressures to develop, hence rapid expansion and the creation of a shock wave.

b. Energy Partition. Energy partition is defined as the distribution of the total energy released by a nuclear detonation among nuclear radiation, thermal radiation, and blast. Energy partition depends primarily upon environmental conditions, i. e., whether the detonation takes place in air, underground, or underwater. Furthermore, energy partition has meaning only when related to a particular time after detonation. For example, the energy partition of a nuclear detonation in free air under ambient conditions varying from a homogeneous sea level atmosphere to the conditions existing at 50,000 feet altitude is in the proportion of about 50 percent blast, 35 percent thermal, and 15 percent nuclear (5 percent initial radiations, 10 percent in fission products), if evaluated within the first minute. The energy partition of an underground burst, on the other hand, is entirely different. There is a reduction of thermal radiation received at a distance due to the amount of heat used in vaporizing the surrounding soil and a reduction of air blast due to the amount of blast energy used to produce cratering and ground shock.

1.2 Weapon Ratings

a. In order to provide a yardstick for rating the total energy release of a nuclear detonation, it has become the practice to express the total yield of a nuclear device in terms of a TNT energy equivalent. For example, if the total energy of the blast, thermal radiation, and nuclear radiation released by a nuclear weapon is the same as the energy released by the detonation of 1,000 tons of TNT, the nuclear weapon is rated as a 1,000-ton, or 1-kiloton, weapon. When 1 kilogram of U-235 or plutonium undergoes fission nearly one gram (1/450 pound) of matter is converted into energy. This energy expressed in terms of TNT energy equivalence would be the same as for the detonation of 20,000 tons of TNT. Similarly, the fusion of 1 kilogram of deuterium results in the transformation of 2.65 grams of matter into energy, with an energy release equivalent to that resulting from the detonation of 57,000 tons of TNT.

b. Another method of rating in common usage, and one which is often confused with the rating of *energy* in terms of TNT *energy* equivalence, is the rating of *effects* in terms of TNT *effects* equivalence, i. e., the *effect* of a particular phenomenon of a nuclear detonation expressed in terms of the amount of TNT which would produce the same *effect*. An example of TNT effect equivalence would be the expression of the crater radius of a nuclear surface burst in terms of the amount of TNT which would be required to produce the same radius.

c. For convenience these TNT equivalences are expressed in 1,000 ton or 1,000,000 ton units, KT (kiloton) or MT (megaton), where 1 ton equals 2,000 pounds and the energy content of TNT is defined as 1100 calories per gram.

d. A "nominal" weapon is one the yield of which is 20 KT. The use of this term arose from the approximately 20 KT yields at Hiroshima, Nagasaki, and the Bikini (Crossroads) tests. In some reports nuclear weapons effects data are based on the nominal weapon.

1.3 Data Presentation

This manual is divided into two parts. Part One, *Physical Phenomena*, treats the basic phenomena of blast and shock, thermal radiation, and nuclear radiation resulting from a nuclear explosion in various media and under various conditions. Part Two, *Damage Criteria*, discusses the mechanism of casualty production and damage to military targets, correlating the basic physical phenomena of a nuclear detonation with various defined degrees of damage.

Relatively simple scaling procedures exist for relating the majority of phenomena associated with weapons of one yield to weapons of other yields. For simplicity and convenience in the use of the manual, most physical phenomena data and much of the damage data are presented for 1 KT bursts, from which the phenomena or damage for other yields may be readily obtained by means of the appropriate scaling procedures which are explained wherever their use is required.

An estimate of the degree of reliability accompanies the presentation of nearly all physical phenomena data. This estimated reliability indicates a range of values above and below the curve such that, for a large number of events, 90 percent of the data will fall within this range. Statements regarding reliability of damage data, on the other hand, describe the source and relative quantity of the data. Reliability estimates do not include operational considerations such as aiming error, target intelligence, and height of burst or yield variations.

1.4 Types of Burst

a. General. The medium in which a weapon is burst determines in great measure the relative magnitudes of the various physical phenomena. In particular, large differences result depending upon whether the detonation occurs in air above the surface, at the surface, or beneath the surface. It is often convenient to discuss weapon phenomena by these types of burst.

b. Brief Description of an Air Burst.

(1) *Definition.* An air burst is defined as the explosion of a nuclear weapon at such a height that the weapon phenomenon of interest is not significantly modified by the earth's surface. For example, from a blast standpoint, this height is such that the reflected wave passing through the fireball does not overtake the incident wave above the fireball (heights greater than about 160 $W^{1/3}$ feet $\pm$ 15%, where W is the weapon yield in kilotons). For thermal radiation an airburst occurs at such heights above the surface that the apparent thermal yield viewed from the ground is not affected by surface phenomena, such as heat transfer to the surface, distortion of the fireball by the reflected shock wave, thermal reflection from the surface, etc. (heights above the surface greater than about 180 $W^{0.4}$ feet $\pm 20\%$ for yields of 10 KT to 100 KT, and $\pm 30\%$ for other yields). From the standpoint of fallout, an airburst occurs at such heights that militarily significant local fallout does not result (for yields less than 100 KT, a minimum height of burst of 100 $W^{1/3}$ feet; for yields greater than 100 KT, in the absence of data,

FIGURE 1-1

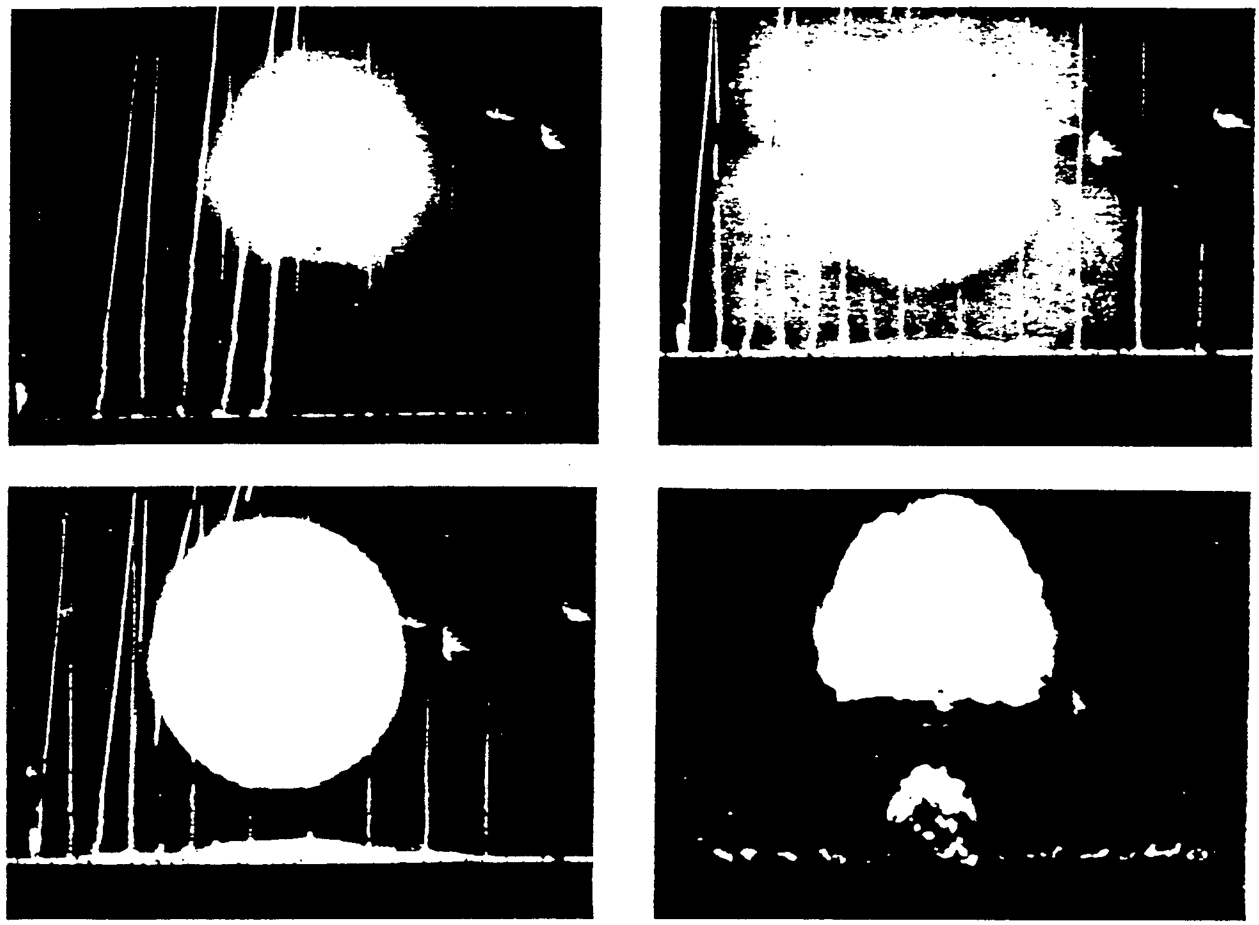

DEVELOPMENT OF AN AIR BURST

the minimum height of burst may be taken conservatively to equal 180 $W^{0.4}$ feet). For certain other phenomena of interest, e. g., neutron induced activity, initial gamma or neutron flux, the height of burst at which the earth's surface fails to produce an effect is difficult or impossible to distinguish.

(2) *Development.* Upon the detonation of a nuclear weapon, there occurs as a direct result of the fission and/or fusion process an emission of neutrons and of electromagnetic radiation in the form of a burst of gamma rays. The nuclear radiations are discussed further in (5) below and section IV.

The tremendous amount of energy created by the nuclear reaction gives rise to extremely high temperatures, which in turn result in the vaporization of the fission products and the components of the weapon, and the emission of additional electromagnetic radiation covering a wide range of wave lengths from infrared through visible to soft X-rays.

Until the temperature falls to about 300,000° K. (540,000° F.), this additional electromagnetic radiation is the most rapid means of energy transfer, and hence is the means by which the surrounding air is heated to incandescence. When the temperature drops below about 300,000° K., a shock wave becomes the primary mechanism for making the surrounding air incandescent. As long as the shock wave is strong enough to cause the shock-heated air to be luminescent, the boundary of the observable luminous sphere (the fireball) is the shock front. Actually this observable sphere consists of two concentric regions. The inner (hotter) region is a sphere of uniform temperature, surrounded by a layer of shock-heated air at a somewhat lower but still very high temperature.

During the early stages of expansion of the incandescent shock front, the emitted radiant power increases as the luminous sphere increases in size, in spite of the fact that expansion causes a temperature decrease, until a maximum (the first maximum) is reached. At this point, the effect of the rapid rate of decrease in temperature overrides the enhancement of radiant power resulting from the increasing area of the luminous sphere.

Subsequently, further expansion causes a reduction in the radiant power. Eventually the shock front temperature is reduced to a point where the shock front is no longer incandescent; therefore, the rate of emission of radiation from the shock front is negligible. In effect, the shock front has become transparent, and the hotter incandescent inner core would be expected to be observable. Initially, however, the radiation emitted from the inner core is absorbed by compounds formed in the shock heated air, and the radiant power reaches a minimum. As these compounds break down, the radiant power emitted from the inner core begins to pass through, and the inner core becomes the visible source of radiation. Thus, the radiant power increases again. This change in boundary of the observable luminous sphere from the shock front to the incandescent inner core gives rise to the term "breakaway."

As the opacity of the shock-heated air decreases, the apparent temperature as measured from a distance approaches that of the hot gases of the inner core, and the emitted radiant power approaches a second maximum. Further expansion and radiative cooling of the hot gases, however, give rise to a slow decrease in the radiant power. This decrease is so slow, relative to the previous rises and decline, that a large percentage of the total radiant energy emitted is delivered during this period. Finally, the rate of delivery of radiant energy drops to a low value.

The subsequent characteristics of the shock, or blast, wave are discussed in (3) below and section II. The effects of the thermal pulse are discussed in section III.

(3) *Blast wave.* A blast wave is characterized by a sharp rise in pressure, temperature and density at its shock front. Thus, upon the arrival of a blast wave at a given location from the burst point, the sequence of events is a sudden increase in pressure, temperature and density, followed by a subsequent decrease in pressure, temperature and density to values below ambient, and a more gradual return to ambient conditions with the temperature going slightly above ambient. The overall characteristics of the blast wave are preserved over long distances from the burst point, but vary in magnitude with distance. With increase in distance, for example, the maximum pressure in the shock wave decreases, and the length of time over which the blast pressure is above ambient, the "positive phase," increases. In addition, under conditions of high relative humidity (50 percent or higher), the drop in air pressure below ambient lowers the temperature sufficiently to cause condensation of atmospheric moisture to form a large cloud called the Wilson Cloud. When the air pressure again becomes normal, in a matter of seconds, the cloud disappears. Although quite spectacular, the Wilson Cloud always occurs too far behind the shock front to modify the blast effects and too late to reduce the thermal effects appreci-

ably; therefore, the cloud has no military significance.

Also characteristic of a blast wave is the motion of the air away from the burst point during the positive phase and toward the burst point during the negative phase. The pattern of the air motion or air velocity is the same as for the other characteristics, with maximum velocity occurring just behind the shock front and decreasing with distance from the burst point. At 300 yards from the burst point of a 1 KT weapon, the peak wind velocity is about 240 miles per hour.

(4) *Thermal radiation.* The relatively large amount of thermal radiation emitted in a nuclear detonation is one of its most striking characteristics. This radiant energy amounts to approximately one-third of the total energy of an air burst weapon. For a 1 KT weapon most of this radiation is emitted in less than a second, and is sufficient to cause serious burns to exposed personnel and to start fires in some combustible materials out to distances of about a thousand yards.

(5) *Nuclear radiation.* A unique feature of a nuclear explosion is the nuclear radiation released. This consists of gamma rays, neutrons, alpha particles and beta particles. About a third of this energy is emitted within the first second after detonation, the remainder being released from radioactive fission products and unfissioned bomb materials over long periods of time after the burst. Nuclear radiation is primarily an anti-personnel effect, with the penetrating radiations (gamma rays and neutrons) being the most dangerous. Lethal doses of initial gamma radiation from a 1 KT burst are received by exposed personnel out to about 700 yards. Residual nuclear radiation, due either to fallout or to neutron-induced gamma activity, can under certain conditions deny entry into a bombed area for some period of time after a detonation. Nuclear radiation effects on materials and equipment are negligible, except for sensitive photographic materials and certain electronic components.

(6) *Cloud.* Because of its relatively low density compared to ambient conditions, the mass of hot gases comprising the fireball rises. The rate of rise may reach several hundred feet per second, after which it decreases rapidly. As the gases rise, they expand, cool and condense, forming a radioactive cloud which consists largely of water vapor and metallic oxides from the weapon. As the fireball cools, the color changes gradually from red to a reddish brown, and ultimately water vapor from the air condenses sufficiently to produce a white color. As the heated mass of air in the fireball rises, cool air is pulled in from the sides and below, which may cause a doughnut shaped ring to form around the column of hot air. This part of the cloud rolls violently as it rises. The cloud from a 1 KT detonation may reach a height of 5,000 to 10,000 feet above the burst point, after which it is gradually dispersed by the winds.

c. *Brief Description of a Surface Burst.*

(1) *Definition.* A surface burst is defined as the explosion of a nuclear weapon at the earth's surface.

(2) *Development and air blast wave.* When a nuclear weapon is burst at the surface of the earth the sequence of events in the development of the fireball and the formation of the blast wave is the same as that for an air burst, except that the fireball boundary and the shock front are roughly hemispherical. Since the earth's surface is an almost perfect reflector for the blast wave, the resulting blast effects are about the same as for a burst of twice the yield in free air.

(3) *Ground shock.* When a burst takes place on the ground surface, a portion of the energy is directly transmitted to the earth in the form of ground shock. In addition, the air blast wave induces a ground shock wave which at shallow depths has essentially the same mag-

FIGURE 1-2

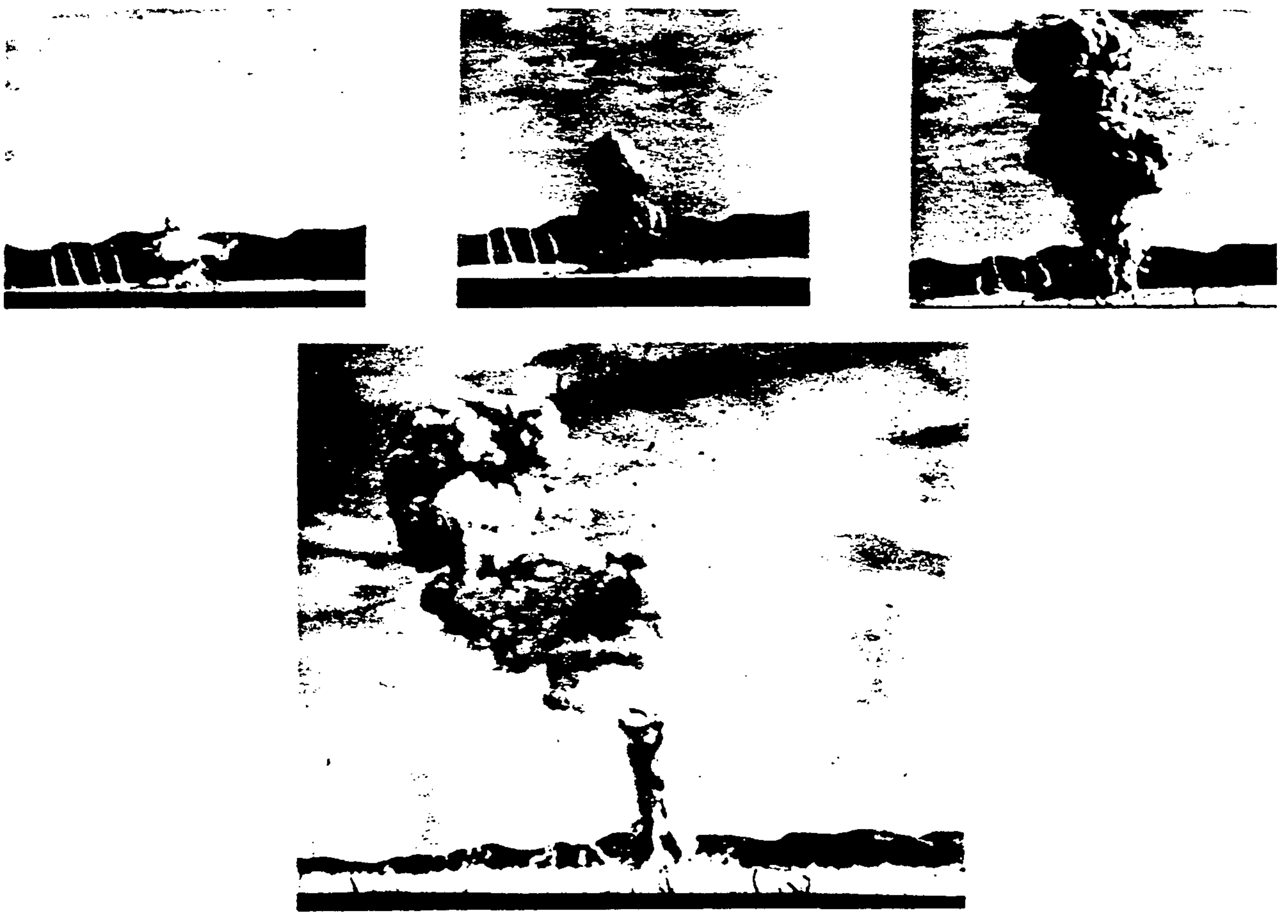

DEVELOPMENT OF A SURFACE BURST

nitude as the air blast wave at the same distance from the burst. The directly transmitted ground shock, although of higher magnitude initially, attenuates faster than the air blast induced shock.

(4) *Crater.* For a burst on land, pressures of hundreds of thousands of pounds per square inch are exerted on the earth's surface, displacing material to form a crater and causing a downward compression of the soil. In addition to the material thrown out and compressed, a considerable quantity of earth is vaporized by the intense heat. A crater approximately 125 feet in diameter and 28 feet in depth is formed by a 1 KT weapon burst on a dry soil surface.

(5) *Thermal radiation.* Because of the heat transfer to the surface, the hemispherical shape of the fireball and the partial obscuration of the fireball by earth or water, the radiant exposure received by surface targets from a nuclear weapon burst on the surface is somewhat less than would be delivered by an air burst nuclear weapon of the same yield.

(6) *Nuclear radiation.*

(*a*) *Initial.* For a small yield weapon, owing largely to absorption by the surface, the initial gamma radiation from a surface burst is somewhat less at the same distance from the burst point than that from a burst of the same yield in free air. For high yield weapons, where hydrodynamic effects become important, a surface burst can be expected to produce as much or more initial gamma radiation as a burst of the same yield in free air, at the same distance from the burst point.

(*b*) *Residual.* The contamination effects of residual nuclear radiation from a surface burst are very much greater than for an air burst, and hazardous radiological effects are produced over areas much greater than those seriously affected by blast or by thermal radiation. Roughly half of the available radioactivity resulting from a nuclear explosion on land, for example, can be expected to fall out in the general vicinity of the burst point. Dose rate contours near the burst point as great as 10,000 r/hr at $H+1$ hour have been observed at tests, regardless of yield.

(7) *Cloud.* For a burst on the surface, a great quantity of material is thrown out from the point of detonation. As the fireball rises, some material is drawn up under the fireball, forming a stem and sometimes forming a second cloud below the one which develops from the fireball. The stem and cloud(s) continue to rise and follow the course described for an air burst.

(8) *Surface bursts on water.* In general, the phenomena as outlined in (2), (5), (6), and (7) above will occur for a surface burst on water. In addition, the expanding sphere of hot gases depresses the water, causing the formation of a surface wave train and the transmission of a directly coupled shock wave into the water. The expanding air blast wave induces a shock wave in the water, which at shallow depths has essentially the same magnitude as the air blast wave at the same distance from the burst. Although the directly coupled water shock is of higher magnitude initially, it attenuates faster than the air blast induced water shock. As the height of burst increases from zero, depression, surface waves, and directly coupled water shock become smaller in magnitude. The formation of a crater on the bottom as the result of a surface burst in shallow water will depend on the depth of the water yield of the weapon and other factors. A 1 KT weapon, for example, detonated on the surface of water 50 feet deep with a soft rock bottom, will form a crater 130 feet in diameter and 4 feet deep.

d. Brief Description of a Burst in the Transition Zone Between an Air Burst and a Surface Burst.

(1) *General.* There is a sizable zone above the earth's surface such that, for weapons detonated in the zone, the presence of the earth's surface significantly modifies one or more of the basic weapon phenomena. As the height of burst is successively lowered in this transition zone, the earth's surface plays an increasingly important role in modifying weapon phenomena; there is a gradual transition from the characteristics of an air burst to those of a surface burst. The upper boundary of the transition zone varies depending upon the phenomenon being considered, since the effect of the earth's surface ceases to be of importance at different scaled heights of burst for different phenomena, as mentioned in *b*(1) above and covered in more detail in the discussion of specific weapon phenomena.

(2) *Development.* The development of a burst in the transition zone generally follows the sequence of events described in *b*(2) above for an air burst.

(3) *Blast wave, thermal and nuclear radiation.* From the standpoint of blast, as the height of burst decreases from that of an air burst, peak air overpressures are more and more affected by the blast wave reflected from the surface, until total coalescence of the incident wave and the reflected wave occurs for a surface burst. From the standpoint of thermal radiation, the apparent thermal yield viewed from the ground decreases with increasing distortion of the fireball by the reflected blast wave, until the thermal yield and the fireball shape approach those characteristic of a surface burst. For nuclear radiation, local fall-out becomes increasingly more significant with decreasing height of burst.

and, especially for large yield weapons burst close to the surface, the hydrodynamic enhancement of the initial gamma radiation (see par. 4.2*a*(1)) becomes of considerable importance.

(4) *Ground shock and crater formation.* As the height of burst is lowered, ground shock increases in magnitude. Crater formation commences at a height of burst in the region of $60W^{1/3}$ feet by the mechanism of compression and scouring of the soil. At a height of burst less than about $10W^{1/3}$ feet, the expanding gases from a nuclear detonation form a crater by vaporization, throwing and compressing the soil in an outward direction from the detonation. Below this height of burst, crater radius and depth approach those of a surface burst.

e. Brief Description of an Underground Burst.

(1) *Definition.* An underground burst is defined as the explosion of a nuclear weapon in which the center of the detonation lies at any point beneath the surface of the ground.

(2) *Development.* When an atomic weapon is detonated at a sufficient depth underground, the ball of fire formed is composed primarily of vaporized materials from the bomb and vaporized earth. At shallow depths light from the fireball generally may be seen from the time it breaks through the surface until it is obscured by dust and vapor clouds, a matter of a few milliseconds. The characteristics of the explosion and their related effects depend upon the depth, yield, and soil type. As the depth below the surface is increased, the characteristics depart gradually from those of a surface burst and finally, at depths of the order of 20 feet for a 1 KT detonation, the explosion exhibits the phenomena commonly associated with underground explosions. It is emphasized that the transition from the observed characteristics of a surface burst to those of an underground burst is not sudden, but that the characteristics change gradually.

(3) *Air blast.* Bursts at depths shallow enough to permit significant venting will produce air blast waves similar to those of air or surface bursts. As the depth of burst increases, the magnitude of the air blast will decrease.

(4) *Column, cloud and base surge.* The first physical manifestation of an underground explosion at shallow depths is an incandescence at the ground surface directly above the point of detonation. This is almost immediately followed by large quantities of material being thrown vertically as a consequence of the direct ground shock reflection along the ground surface. Concurrently large quantities of gas are released. These gases entrain additional quantities of material and carry them high into the air in the form of a cylindrical column. As the column rises it fans out and forms a dense cloud. Some of the particles thrown vertically, together with the entrained particles, behave like an aerosol with a density considerably greater than the surrounding air. This aerosol subsequently falls downward in the immediate vicinity of ground zero, and the finer soil particles spread out radially along the ground to form a low dust cloud called the base surge. For a 1 KT weapon burst at a depth of 20 feet, it is estimated that the column will reach a height of approximately 420 feet and a diameter of 660 feet, and the cloud will be 4,400 feet in diameter and 5,000 feet in height. Dimensions of the base surge are discussed in paragraph 2.2. For shallower depths of burst, the column tends to assume the shape of an inverted cone rather than a cylindrical column and has a more pronounced radial throwout. Shallower depths of burst also become less favorable for the formation

1.4e (5)

FIGURE 1-3

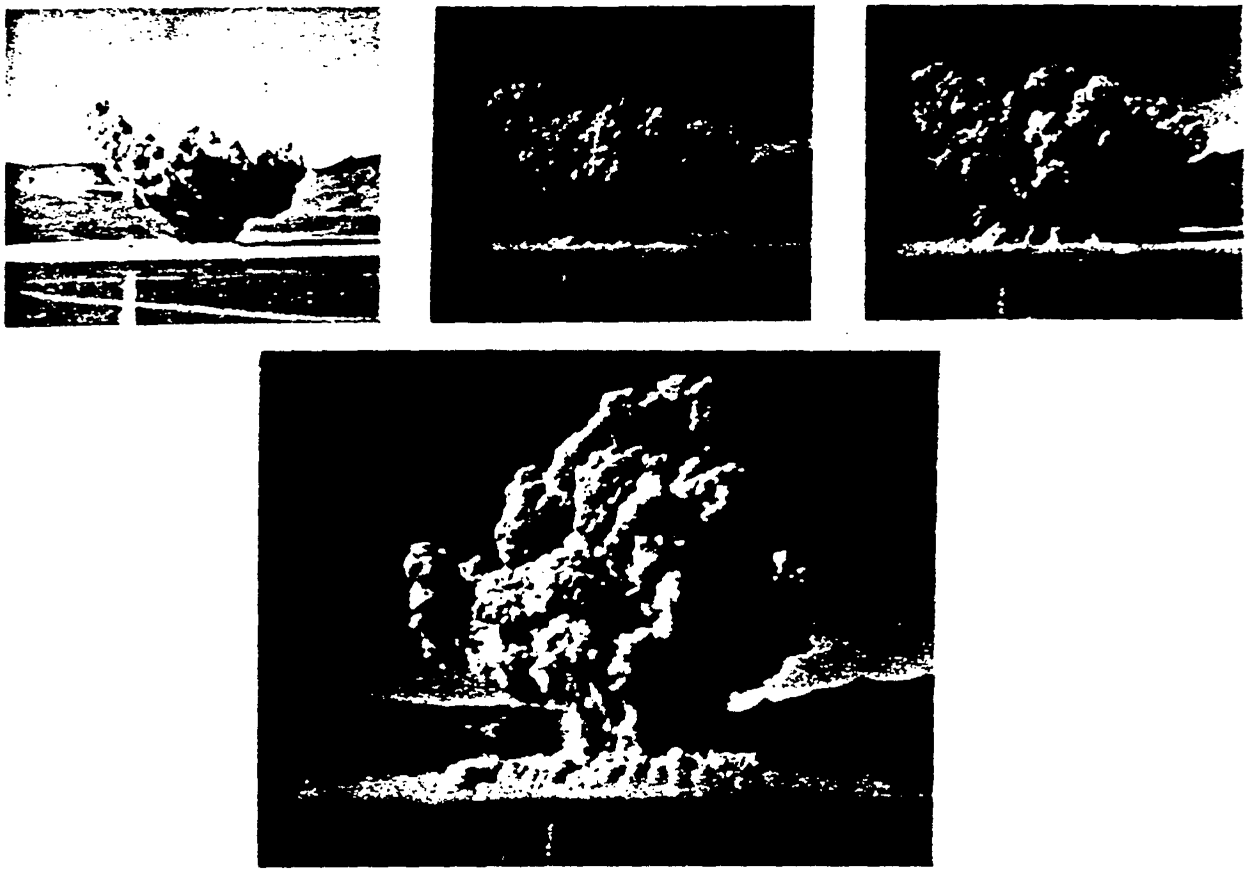

DEVELOPMENT OF A SHALLOW UNDERGROUND BURST

of a base surge, approaching the conditions of a surface burst where no base surge is expected.

(5) *Ground shock.* As a burst is moved deeper and deeper into the ground, the directly transmitted ground shock increases in importance and the air induced ground shock becomes less important.

(6) *Crater.* Formation of the crater from an underground burst is essentially the same as for the surface burst, except that more material is thrown vertically. At sufficiently deep depths the explosion will not vent to the surface and a cavity (camouflet) will be formed. There may or may not be disturbances at the surface, depending on the depth of the detonation and the material comprising the ground.

(7) *Thermal radiation.* If the underground burst is sufficiently deep, the fireball is obscured by the earth column; therefore thermal radiation effects are negligible.

(8) *Nuclear radiation.*

(*a*) *Initial.* The initial gamma radiation becomes less than that described for a surface burst as the depth of burst increases, until it becomes insignificant for depths where a camouflet is formed.

(*b*) *Residual.* For shallow depths of burst, the residual radiation effects are similar to those of a surface burst; a large amount of residual radiation is deposited by the column, the cloud and the base surge. However, as the depth of burst increases, more and more of the contaminant is deposited in the immediate vicinity of the detonation,

FIGURE 1-4

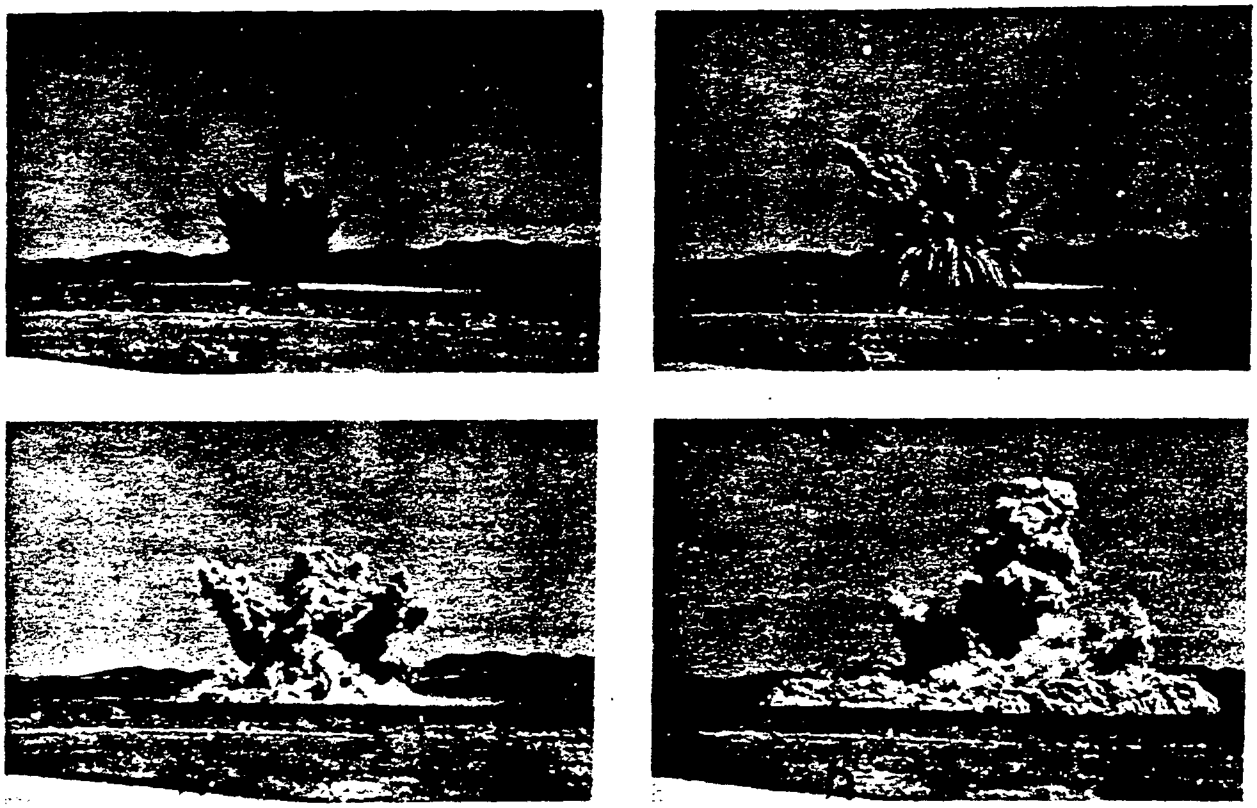

DEVELOPMENT OF A DEEP UNDERGROUND BURST

until for the case of no surface venting, all of the contaminant is contained in the volume of the ruptured earth surrounding the point of detonation.

f. Brief Description of an Underwater Burst.

(1) *Definition.* An underwater burst is defined as the explosion of a nuclear weapon in which the center of the detonation lies at any point beneath the surface of the water.

(2) *Development and gas bubble.* As in other types of bursts, a ball of fire is formed but of lesser magnitude. Although distortion due to waves may prevent a clear view of the fireball for deep underwater bursts, the water in the vicinity of the explosion will be observed to light up momentarily. This luminosity remains but a few milliseconds. The reason that the fireball is of lesser magnitude is that the energy of detonation is rapidly used up in dissociating and vaporizing the water in the immediate vicinity of the weapon. The consequence of this dissociation and vaporization of water is the formation of a gaseous bubble and the initiation of a shock wave. This shock wave moves away from the gaseous bubble during the early stages of the bubble's formation. As it does so, additional quantities of water are vaporized. This additional vaporized water increases the size of the expanding bubble appreciably. Due to the inertia of the water moving in front of the increasing bubble, the bubble expands to a radius considerably beyond the point of pressure equilibrium with the surrounding water. It then contracts and continues a series of successive expansions and contractions, meanwhile rising because of its buoyancy, until it reaches the surface. For shallow underwater bursts the bubble may vent before it reaches maximum first expansion. For deep bursts the bubble may break up before it reaches the surface.

FIGURE 1-5

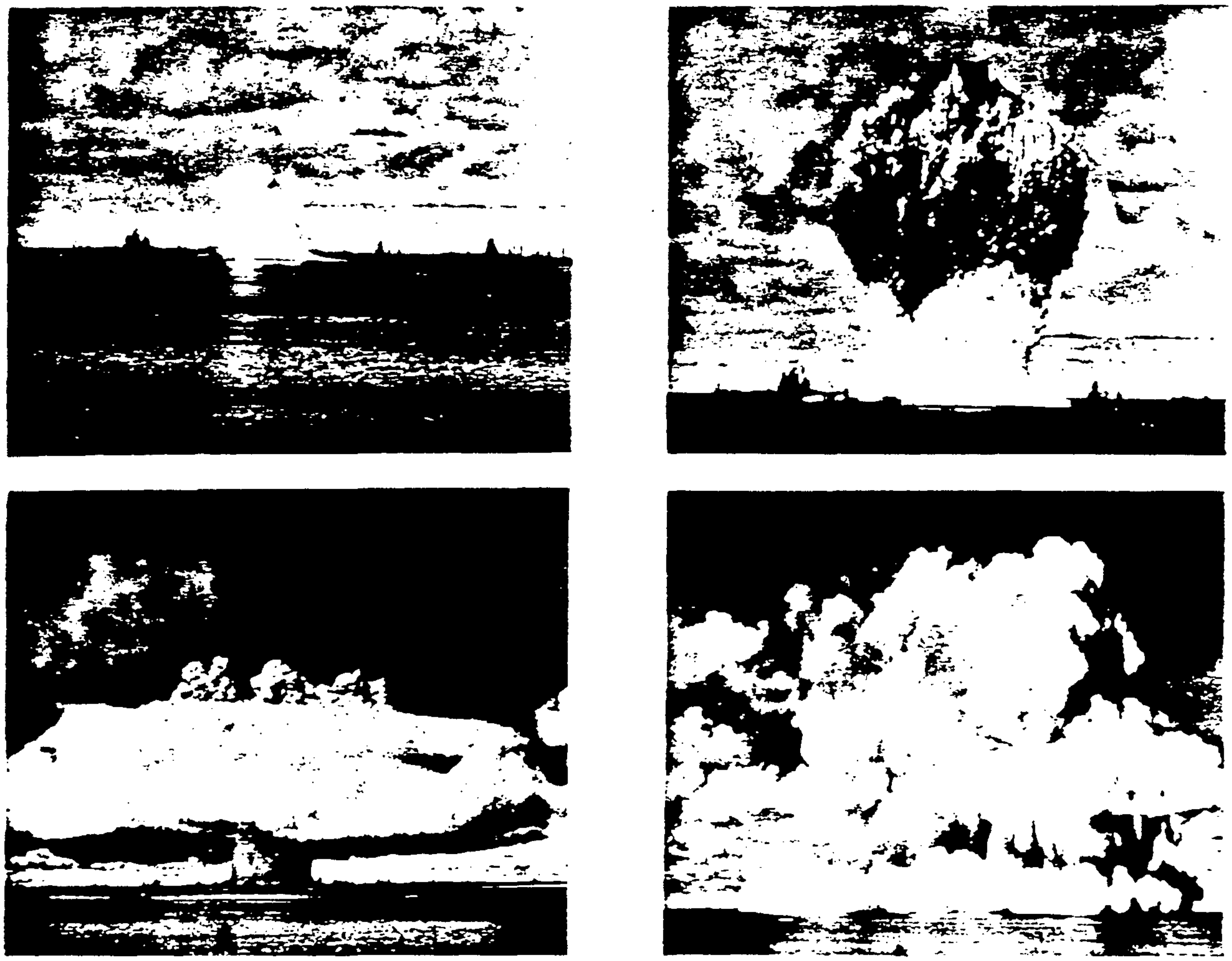

DEVELOPMENT OF A SHALLOW UNDERWATER BURST

The characteristics and related effects of the explosion depend on the depth of water, depth of burst, yield and other factors. For bursts in shallow water, the presence of the bottom significantly alters effects phenomena. For bursts at very shallow depths, the characteristics are essentially those of a water surface burst. These characteristics change gradually as the depth of burst increases.

(3) *Water shock.* The water shock wave exhibits an extremely high initial peak overpressure as it moves at a great rate ahead of the bubble. In free water, the characteristics of the water shock wave are the same as those of the air blast wave, although of differing magnitudes. However, the relatively close presence of boundaries provides for complex shock wave forms due to reflections and rarefactions. In addition to the water shock wave preceding the bubble during its first expansion, subsequent water shock waves are produced by pulsations of the bubble, reflections from the bottom and other effects. The shock waves from pulsations of the bubble, however, are of a lower magnitude and longer in duration. An additional source of shock waves in shallow water is the shock re-transmitted to the water from shock waves traveling through the air above and the ground beneath the water. Again, these shock

waves are of lower magnitude than the directly transmitted initial shock wave from the detonation. Shallow bursts are the least effective in producing water shock, since more energy is manifested as air blast. For depths of burst greater than one maximum bubble radius, the effectiveness of an underwater nuclear burst in producing water shock is about 60 percent compared to TNT.

(4) *Air blast.* As in the underground burst, air blast waves are formed whose propagation depends upon the depth of burst. The first air blast wave from an underwater burst is that formed by the transfer of the shock front across the water-air interface. This front appears as a flat dome. The second air blast wave is transmitted by the venting bubble. This front will propagate essentially hemispherically. For shallow burst depths, the air blast wave resulting from venting is more intense than the shock wave transmitted across the water-air interface. For deep bursts, on the other hand, the shock wave transmitted across the water-air interface yields the higher pressures.

(5) *Surface effects.* An underwater burst produces spectacular effects on the surface. As the water shock wave strikes the surface and is reflected, a rarefaction is formed which cavitates a thin layer near the surface, projecting a white, frothy "spray dome" into the air. For a shallow burst, soon after this phenomenon the gas bubble vents the surface, throwing the water near the bubble's upper surface into the air in the form of a hollow "column". For deep bursts additional spray domes may be formed prior to venting. These additional domes result from the shock waves from the bubble oscillations striking the surface. The venting phenomena accompanying this deep geometry are unpredictable, as they depend upon the state of expansion or contraction of the bubble at the moment it breaks the surface. The venting of the gas bubble and the subsequent collapse of the water cavity formed therefrom initiate a series of "surface waves". The air blast transferred across the water-air interface by the initial water shock and the later air blast resulting from the venting of the gas bubble usually produce a "Wilson Cloud", as described in *b*(3) above. In addition, the "column" upon starting to collapse will form a "base surge" similar in mechanism to that from the underground burst (*e*(4) above).

(6) *Thermal and nuclear radiation.* Thermal and nuclear effects are considered insignificant for underwater bursts, except in shallow water where the effects will approximate those of a ground surface burst.

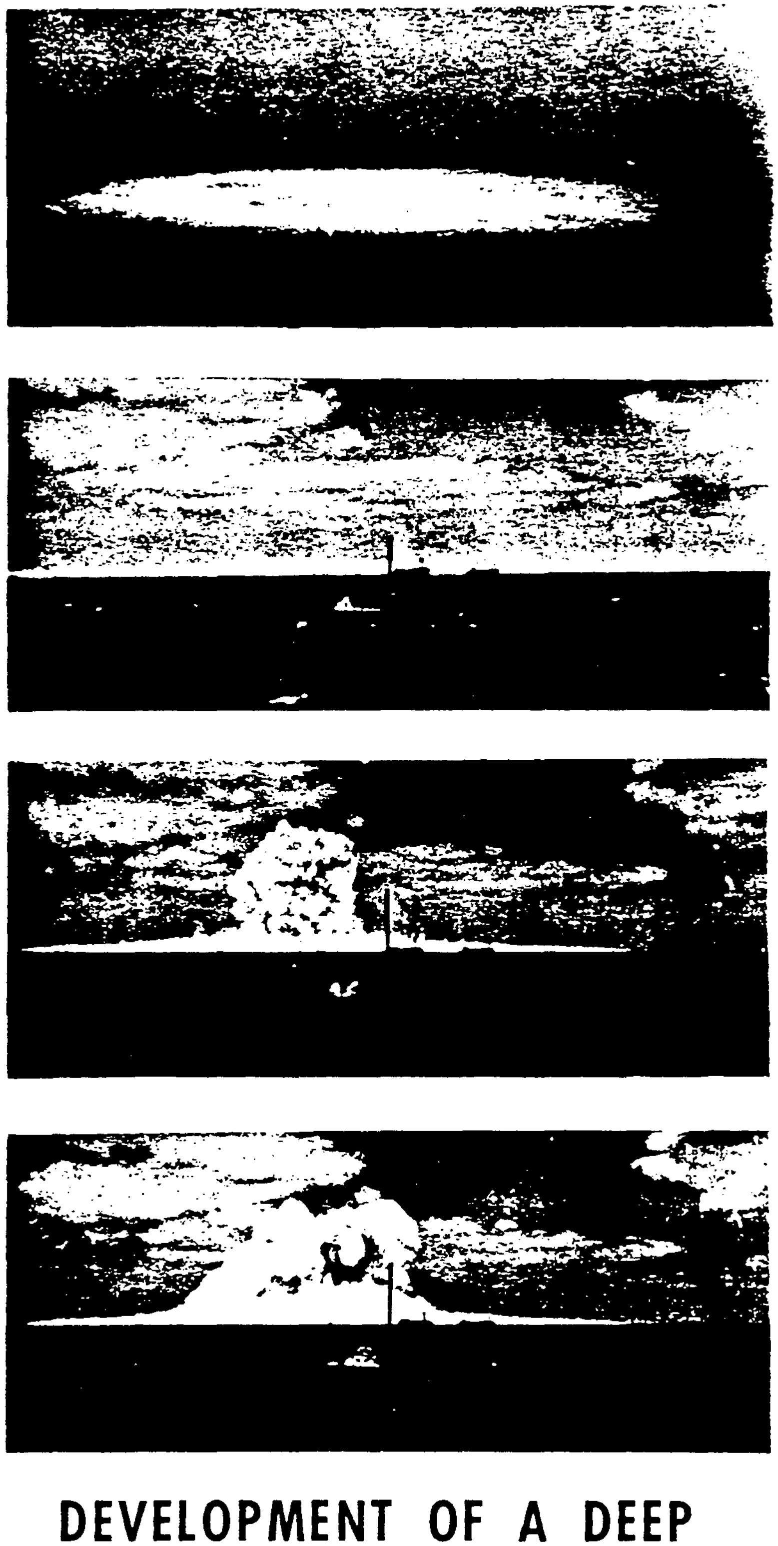

DEVELOPMENT OF A DEEP UNDERWATER BURST

BLANK

2
Blast

Air Blast

SECTION II
BLAST AND SHOCK PHENOMENA

2.1 Air Blast Phenomena

a. General. The shock wave which propagates through air as a consequence of a nuclear explosion is commonly referred to as a blast wave. The head of the blast wave, called the shock front, causes an abrupt rise in both overpressure and dynamic pressure as it passes a given point, as illustrated at point B in figure 2-1. In the case of overpressure, this abrupt rise is followed by a decline to a pressure below ambient and then a gradual return to ambient. The portion of the wave in which the overpressure is above ambient is termed the positive overpressure phase, while the remaining portion, where the pressure is below ambient, is called the negative pressure phase. The decrease in pressure below ambient in the negative phase is usually small in comparison with the increase in pressure in the positive phase.

The dynamic pressure associated with mass motion of air has a positive duration somewhat

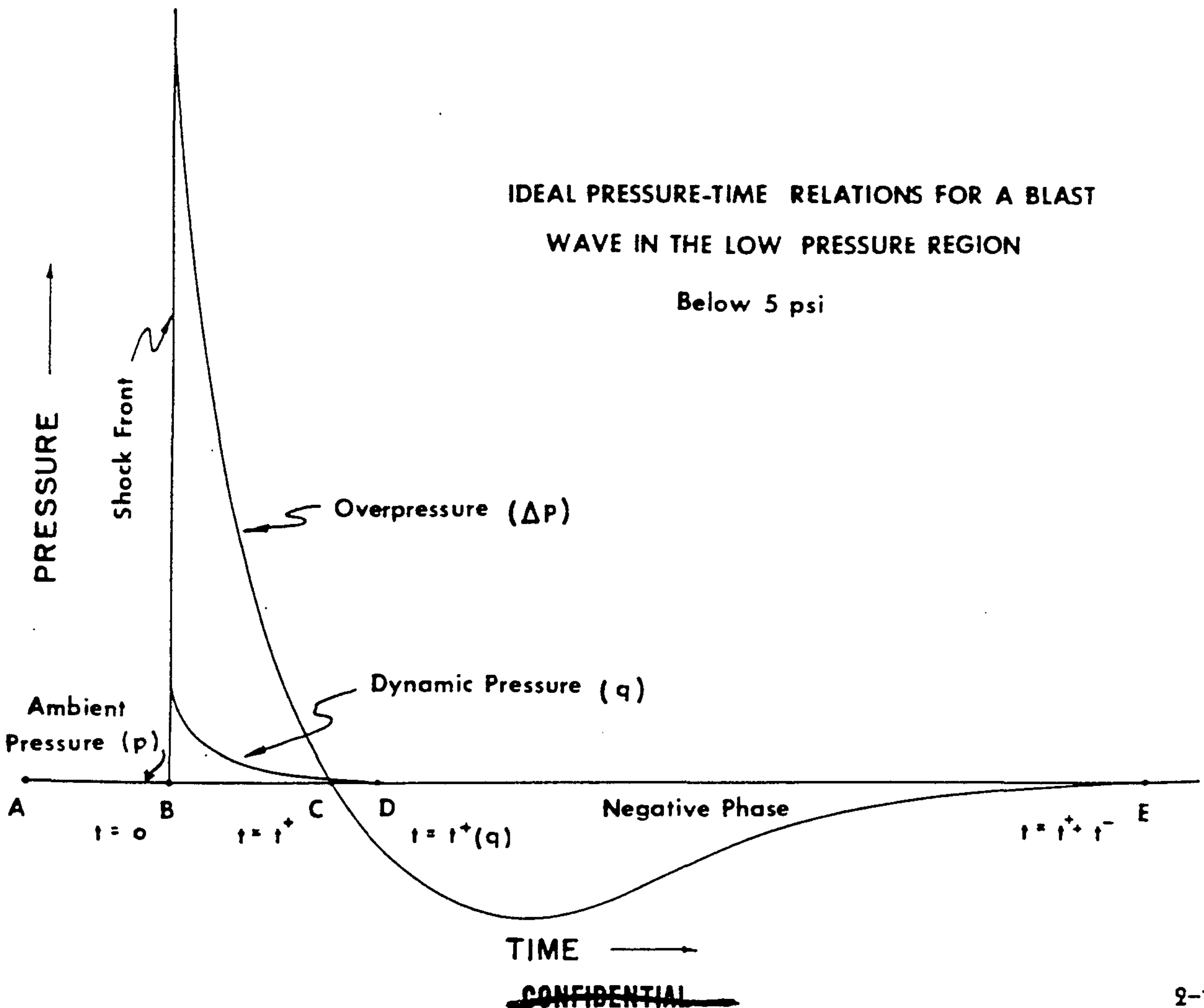

SECTION II
BLAST AND SHOCK PHENOMENA

2.1 Air Blast Phenomena

a. General. The shock wave which propagates through air as a consequence of a nuclear explosion is commonly referred to as a blast wave. The head of the blast wave, called the shock front, causes an abrupt rise in both overpressure and dynamic pressure as it passes a given point, as illustrated at point B in figure 2-1. In the case of overpressure, this abrupt rise is followed by a decline to a pressure below ambient and then a gradual return to ambient. The portion of the wave in which the overpressure is above ambient is termed the positive overpressure phase, while the remaining portion, where the pressure is below ambient, is called the negative pressure phase. The decrease in pressure below ambient in the negative phase is usually small in comparison with the increase in pressure in the positive phase.

The dynamic pressure associated with mass motion of air has a positive duration somewhat

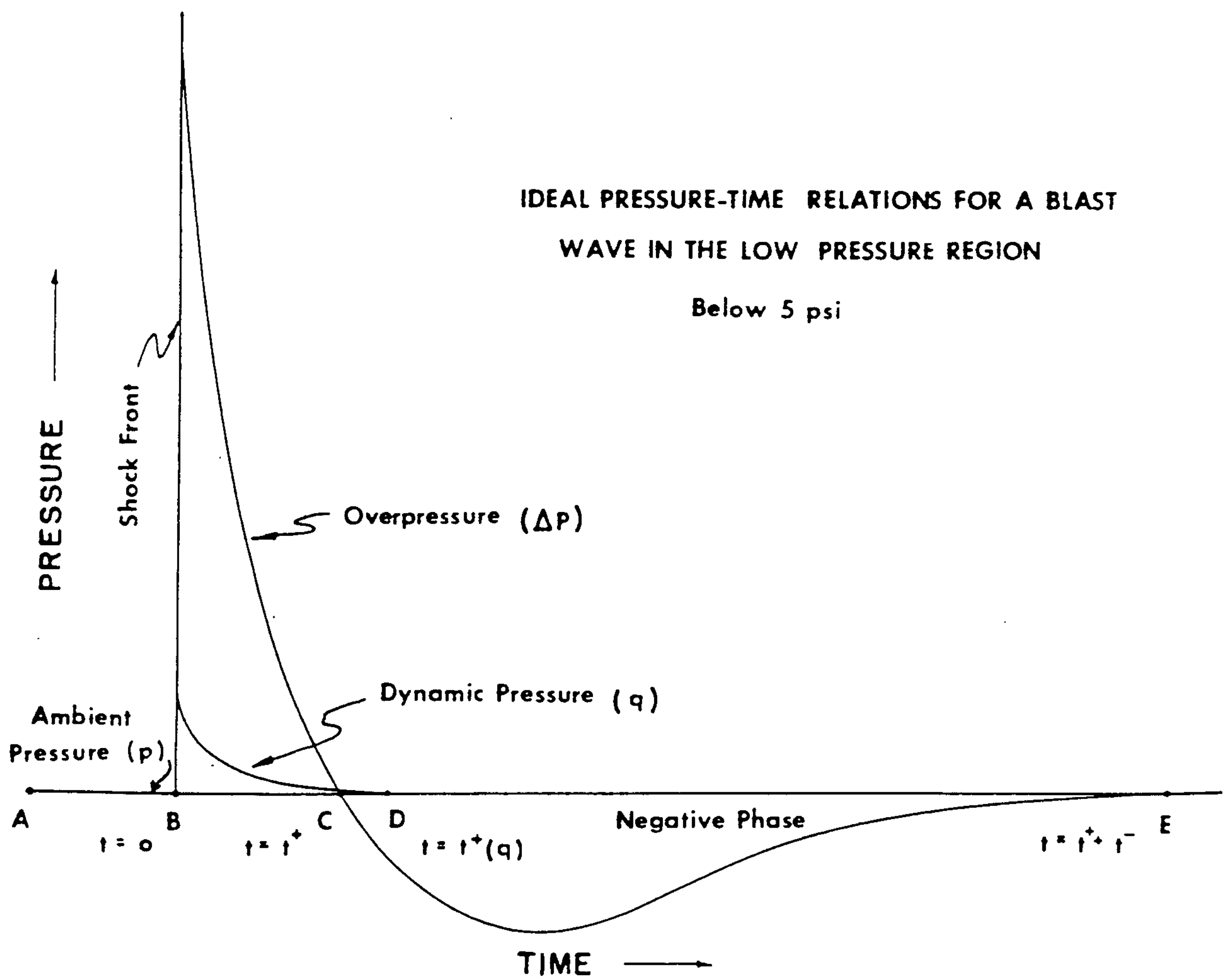

greater than the overpressure positive duration. During this period the transient winds blow in the direction of shock motion. The wind velocity after decreasing to zero reverses direction and flows toward the direction of the nuclear explosion. The dynamic pressure associated with this reverse flow of air is insignificant. The pressure-time histories of the overpressure and dynamic pressure are shown schematically in figure 2–1.

b. Propagation in Free Air.

(1) *General.* As the blast wave moves out from the fireball region, various changes in its physical characteristics occur as a function of time and distance. In free air, i. e., in a homogeneous atmosphere where no boundaries or surfaces are present, these changes take place in a definite manner as a result of spherical divergence and irreversible energy losses to the air through which the blast wave propagates. As previously noted in paragraph 1.4*b*(3), the shock front velocity and peak overpressure decrease with increasing distance, while the duration of the positive phase increases. Other blast wave parameters are affected in a similar way, so that the blast wave is said to be attenuated with distance. The manner in which these changes take place for the different blast wave parameters is described in succeeding paragraphs.

(2) *Time of arrival.* As the shock front travels away from an explosion under sea level conditions, its velocity of propagation at breakaway is approximately seven times the velocity of sound. As the peak overpressure approaches zero, however, the shock front velocity approximates sonic velocity. The time of arrival of the shock front as a function of distance in free air for 1 KT burst in a homogeneous sea level atmosphere is shown in figure 2–2. The time of arrival for other yields can be computed using the scaling procedure accompanying the figure.

(3) *Overpressure.*

(*a*) *Peak overpressure.* The term *overpressure,* expressed in pounds per square inch (psi), is used to describe an increase in pressure over ambient. *Peak overpressure* is the highest overpressure reached during the passage of the blast wave. The basic free air curve for the attenuation of peak overpressure with distance for a 1 KT explosion in a standard sea level atmosphere is given in figure 2–3. Standard sea level atmospheric conditions are given in appendix II. The distance to which a given peak overpressure extends for other yields may be computed by use of the scaling procedure accompanying figure 2–3.

(*b*) *Duration.* The duration of the positive overpressure phase of a blast wave from a nuclear detonation of a given yield increases as the peak overpressure decreases with distance. Also the duration of the positive overpressure phase for a given peak overpressure increases as the yield increases. The variation of positive phase duration with distance is illustrated in figure 2–4. Accompanying this figure is the scaling procedure for other yields.

(*c*) *Impulse and wave forms.* In many cases, the damage resulting from a nuclear detonation is more nearly a function of both the positive phase overpressure and its duration, specifically the *overpressure impulse,* than upon peak overpressure alone. The overpressure impulse (I_p) of the positive phase of the blast wave is the area under the positive portion of the overpressure-time curve as illustrated in figure 2–1. This curve or wave form varies in an exponential fashion, depending on the peak overpressure. Negative phase impulse is similarly defined in terms of the underpressure; however, it is usually less significant than the positive phase impulse. For a more detailed discussion of impulse and wave forms, refer to appendix I.

(4) *Dynamic pressure.*

(*a*) *General.* As mentioned in *a*, above, a wind of high velocity blowing in the direction of shock motion exists immediately behind the shock front. Dynamic pressures are a measure of the drag forces associated with these winds and are a function of the density and particle velocity of the air behind the shock front. Dynamic pressure is usually denoted by "q" and is expressed in pounds per square inch. Examples of the maximum winds or peak particle velocities expected for various free air peak overpressures in a homogeneous sea level atmosphere are shown in table 2–1. The wind velocities shown therein coincide with the onset of the shock front, but thereafter diminish as the blast wave overpressure decreases. It is emphasized that wind velocities following the shock front exist only for short periods of time, and the effects cannot be compared directly with steady winds of the same velocity. However, the duration of the blast wind for a given dynamic pressure increases with increase in yield. The relation between free air peak dynamic pressure and distance for a 1 KT burst in a homogeneous sea level atmosphere is given in figure 2–5. The distance to which a given peak dynamic pressure extends for other yields may be computed by use of the scaling procedure accompanying this figure. During the negative overpressure phase, the transient winds reverse and blow at reduced velocities; the resulting values of dynamic pressure are small and act in the opposite direction.

(*b*) *Duration.* The time during which dynamic pressure acts in the direction of shock motion at a given distance from the detonation is somewhat longer than the positive phase duration of the overpressure at the same distance. The wind velocity does not go to zero at the same time the overpressure becomes zero due to the inertia of the air in motion. This "overshoot" is usually not significant because of the very rapid decay of the dynamic pressure behind the shock front. As shown by figure 2–1, the dynamic pressure is very small at the end of the overpressure positive phase.

(*c*) *Impulse and wave forms.* The dynamic pressure impulse is the area under the dynamic pressure-time curve. This curve or wave form varies in an exponential fashion, depending upon the peak dynamic pressure. For a more detailed discussion of impulse and wave forms, refer to appendix I.

Table 2–1. Related Values Among Various Free Air Blast Parameters (Homogeneous Sea Level Atmosphere)

Peak overpressure (psi)	Peak particle velocity		Dynamic pressure (psi)	Peak density (slugs/ft³)
	(ft/sec)	(mph)		
72	1,730	1,180	75	0.0074
50	1,320	935	41	0.0063
30	982	670	17	0.0051
20	743	580	8.2	0.0043
10	431	295	2.2	0.0034
5	239	160	0.6	0.0029
2	103	70	0.1	0.0026

c. Surface Influences.

(1) *General.* When an incident air blast wave strikes a more dense medium, such as the earth's surface, it is reflected as shown in figure 2–6. The reflected wave near the earth's surface moves faster than the incident wave because the former travels through a region which, as a result of the passage of the incident shock front, is hotter and more dense than the ambient atmosphere. Therefore, under appropriate conditions, that portion of the reflected shock near the surface overtakes and merges with the incident shock to form a single shock front called the Mach stem. Due to the reflection process, higher peak overpressures and higher peak dynamic pressures are realized at or near the surface than would be obtained at the same distance in free air.

FIGURE 2-6

GROWTH OF THE MACH STEM
(IDEALIZED)

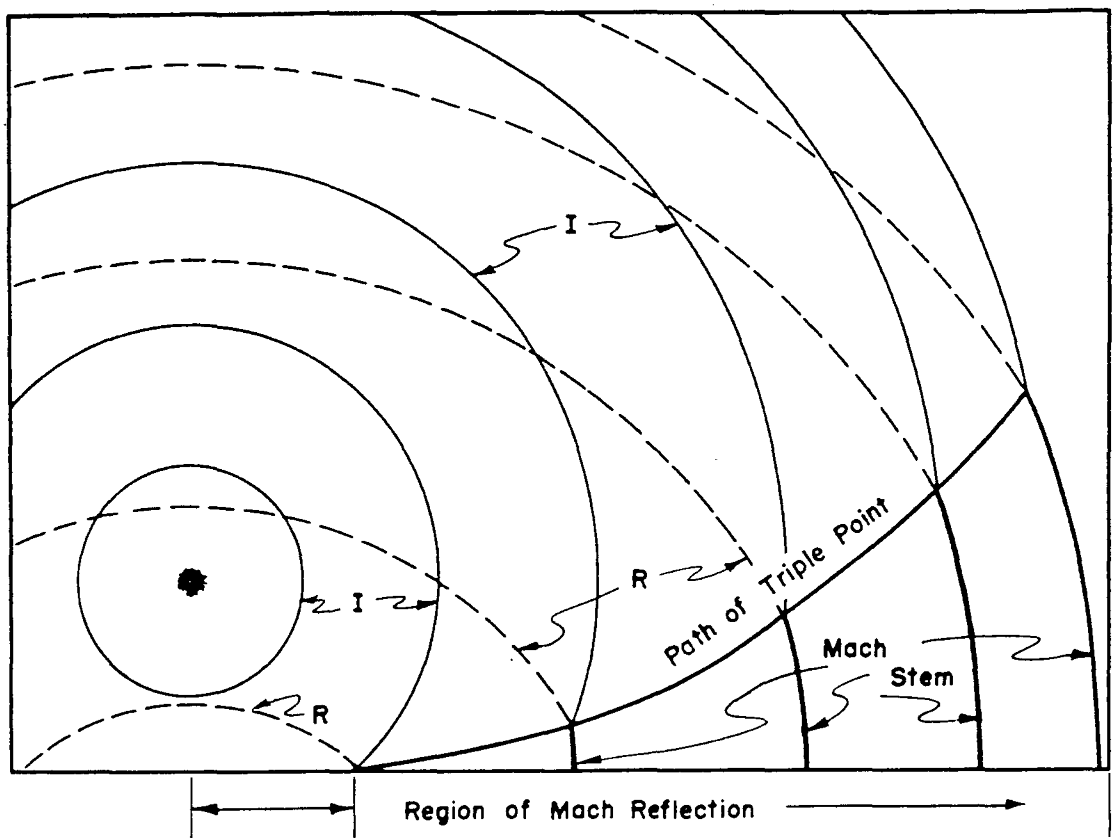

I — Incident Wave

R — Reflected Wave

The characteristics of the blast wave at or near the surface, as well as the formation of the Mach stem, are dependent upon yield, height of burst, and the boundary or reflecting surface conditions. The region where the incident and reflected shocks have not merged to form a Mach stem is often referred to as the region of regular reflection; the region where they have merged is referred to as the region of Mach reflection. As the Mach stem travels along the surface, the triple point (the point of intersection of the incident wave, reflected wave, and the Mach stem) rises. The estimated height of the Mach stem as a function of height of burst and distance from ground zero is given in figure 2–7, for a 1 KT burst. The procedure for scaling to other yields is illustrated in the example accompanying this figure. In addition to the fusing of the reflected and incident blast waves to form a Mach stem as just described, that portion of the reflected wave passing through the fireball of a burst in the transition zone will also fuse with that portion of the incident wave directly above the fireball. This fusion is primarily a result of the increased velocity of the reflected wave as it passes through the fireball, and as a consequence, is relatively narrow in lateral extent. As the height of burst varies from the surface to about 160 $W^{1/3}$, the peak overpressures in the fused wave above the fireball vary from those expected from a particular weapon burst at the earth's surface to those expected from a free air burst of the same weapon. This is primarily the consequence of the spherical divergence of the reflected shock together with the dissipative effect of passing through a heated region.

(a) *Good surface conditions.* The preceding description of the reflection process considers the earth's surface as if it were an ideal reflector. For bursts over real target areas, however, the condition and nature of the surface must be considered, since it has been determined that under certain circumstances severe modifications of the blast wave may occur. These modifications are due to the physical characteristics of the surface, which result in thermal and mechanical effects on the blast wave. These effects will be discussed further in *d*(4) below. In a practical sense, the surfaces which most closely approach the ideal are ice, snow and water. These surfaces are considered as "good," since the influence of such surfaces in altering the blast wave is expected to be a minimum. The air blast characteristics for nuclear detonations over such "good" surfaces are presented in figures 2–8A, 2–9, and 2–11A.

(b) *Average surface conditions.* As noted above, the characteristics of the blast wave can be appreciably influenced by the type and condition of the surface over which it passes. In many target areas, it is expected that a significant thermal layer will form near the surface prior to shock arrival. The interaction of the incident blast wave with this thermal layer may affect the reflection process to a considerable degree, depending on the intensity of the thermal layer. Thus individual blast wave parameters such as shock velocity, peak overpressure, particle velocity, peak dynamic pressure and duration, as well as arrival times, wave forms and impulse values, will be affected. The nature of these perturbations depends on the height of burst and ground range involved, and to a lesser extent on the yield. They are important for surface bursts, bursts in the transition zone, and air bursts over such surfaces as desert sand, coral, wooded and agricultural areas. In general, severe thermal effects on the blast wave may be expected over such surfaces for burst heights up to 650 $W^{1/3}$ feet, while moderate to light thermal effects may be expected for burst heights between 650 $W^{1/3}$ and 800 $W^{1/3}$. However, these thermal effects are not expected in regions where pressures are below 6 psi for bursts over any surface. Mechanical influences on the blast wave may be present for any pressure level, but their relative importance is considerably less than the thermal effects previously mentioned. A detailed discussion of thermal and mechanical effects is given in *d*(4) below. The air blast characteristics for nuclear detonations over the real surfaces described above are presented in figures 2–8B, 2–10, and 2–11B. These figures should be used as representative for all target areas where surface conditions cannot be considered as *good*.

(2) *Time of arrival.* The time of arrival of the shock front on the surface is given in figure 2–8 as a function of height of burst and ground range for a 1 KT burst in a homogeneous sea level atmosphere. For other yields, cube root scaling applies to burst heights, ground range and time. Figure 2–8A applies to good surface conditions while 2–8B applies to average surface conditions.

(3) *Peak overpressure.*

(a) *General.* For given surface conditions, the variation of peak overpressure with distance as a function of the height of burst is presented in "height of burst" curves. Curves for good surface conditions are shown in figure

2–9, while those presented in figure 2–10 are considered appropriate for all other target areas. These figures give distances from ground zero at which various peak overpressures will be attained on the ground surface from a 1 KT explosion at different heights of burst in a homogeneous sea level atmosphere. In order to scale to other yields, the height of burst and the distance at which a given overpressure occurs are multiplied by the cube root of the selected yield. This procedure is illustrated in the example which accompanies these figures. Study of figure 2–10 reveals that if it is desired to obtain the maximum ground range for an overpressure of 10 psi or less, a height of burst should be selected which coincides as nearly as possible with the extreme right projection, sometimes called the "knee," of the desired pressure contour. If the range of an overpressure at the surface greater than 10 psi is of interest, it will be seen that the maximum coverage is obtained from bursts close to the ground (i. e., the extreme right projection of the curve occurs at low heights of burst).

(*b*) *Duration.* The duration of the positive phase of the blast wave at the surface depends upon height of burst, distance from ground zero, yield, and surface conditions. This dependence is illustrated in figure 2–11 for a 1 KT burst at sea level. Figure 2–11A applies to good surface conditions while 2–11B applies to average surface conditions. Accompanying figure 2–11 is the scaling procedure for other yields with an example of its use.

(*c*) *Impulse and wave forms.* The overpressure positive phase impulse is obtained from the area under the positive phase of the overpressure-time curve. The exact value at or near a reflecting surface for a particular range depends on the height of burst and yield, as well as the extent of perturbation of the wave form as noted above. The classical wave form previously discussed for free air overpressures (characterized by an instantaneous rise to a peak value at shock arrival, followed by an exponential decay in some manner dependent upon shock strength) is seldom found along the surface for overpressure levels above 6 psi. Only for such specialized surface conditions as snow, ice and water, where thermal effects on the blast wave are expected to be at a minimum, do the wave forms for higher overpressure levels approach the ideal. Even then, minor mechanical effects may be present; for example, over water the rise time may not be instantaneous and there may be a slight rounding of the peak value of the overpressure wave form. In general, non-ideal overpressure wave forms which reflect precursor action will result for those bursts over such real surfaces as desert sand, coral, wooded and agricultural areas where significant thermal effects on the blast wave may be expected. The variation in the overpressure wave shape depends on height of burst and ground distance. For a detailed discussion of wave form types and overpressure impulse to be expected under various conditions, refer to appendix I. A detailed discussion of the precursor is given in *d*(4) below.

(4) *Dynamic pressure.*

(*a*) *General.* For given surface conditions, the variation of peak dynamic pressure at the surface with range depends on the yield and height of burst. This dependence is shown in the form of height of burst curves, such as those presented in figure 2–12 for 1 KT in a homogeneous sea level atmosphere for good surface conditions. These curves approach the ideal situation where thermal effects on the blast wave are considered to be at a minimum over such surfaces as ice, snow and water. Under these conditions, wave forms are more nearly ideal. It should be noted that the curves in figure 2–12 show only the horizontal component of particle velocity, or the flow of air parallel to the surface. Consequently, all dynamic pressure levels fall to zero at ground zero, where the mass motion of the air has no horizontal component. However, peak overpressures in this close-in region of low horizontal dynamic pressures may be very high (see fig. 2–9). To scale to other yields, the height of burst and the distance to which a given dynamic pressure at the surface extends are multiplied by the cube root of the selected yield. This procedure is illustrated in the example which accompanies figure 2–12.

For average surface conditions, the variation of peak dynamic pressure at the surface with height of burst is presented in figure 2–13 for 1 KT in a homogeneous sea level atmosphere. This curve is based on limited empirical data which reflect both thermal and mechanical effects on the blast wave. As a result, wave forms above 1.5 psi are distorted in varying degree, depending upon the range and height of burst. Under such conditions, the classical shock front disappears, and peak values of the various air blast parameters occur at different times after shock arrival at a given range. The entire behavior of the blast wave in this region may be described as non-ideal. It is believed that the peak values of dynamic pressure reflect both increased particle velocities and dust loading in the precursor region. These effects are discussed further in *d*(4) below.

(*b*) *Duration*. As with the overpressure positive duration, the duration of dynamic pressure is dependent upon height of burst, ground range, yield and surface conditions. The limited data available indicate that dynamic pressure duration may be assumed equal to overpressure positive phase duration without serious error at the same range and height of burst. Therefore, dynamic pressure durations may be determined from figure 2–11A for good surface conditions and figure 2–11B for average surface conditions.

(*c*) *Impulse and wave forms*. Dynamic pressure impulse is the total area under the dynamic pressure-time curve. It is not possible at this time to establish a quantitative relation between height of burst, ground range, yield and surface conditions, due to the extreme variations in the limited full-scale data presently available. However, a few general statements concerning wave form variations with surface conditions are possible. For good surface conditions, that is, where thermal effects on the blast wave are minimized, wave forms for dynamic pressure approach the ideal or classical case. However, minor perturbations may sometimes occur for blast waves traveling over water due to the "pickup" of water near the surface. A further discussion of water loading of the shock wave is found under *d*(4)(*d*) below.

For bursts over such real surfaces as desert sand, coral, wooded and agricultural areas, where significant thermal effects on the blast wave may be expected, considerably disturbed non-ideal wave forms will be observed. Mechanical effects such as dust loading also contribute to wave form modification under such conditions. Measurements in this region often show high frequency fluctuations which indicate the extreme turbulence of the dusty air medium. For a more detailed discussion of dynamic pressure wave forms, see appendix I.

d. Other Influences on Air Blast Propagation.

(1) *General*. The material on air blast presented in previous sections is strictly

applicable only to standard homogeneous sea level conditions (app. II) and flat "open" terrain. Some modification of the data presented may be necessary under the following conditions:

(*a*) Heavy rains or fogs.
(*b*) Temperature inversions.
(*c*) Target or burst height at altitudes above sea level.
(*d*) Terrain with large hill masses, severe inclines or depressions, and obstructions.

The effects of these conditions are discussed in some detail below, together with an expanded discussion of the thermal and mechanical influences which cause the blast parameter curves for "average" surface conditions to differ from those representing the ideal situation, or "good" surface conditions.

(2) *Atmospheric effects.*

(*a*) *Effects of rain and fog.* The effects of atmospheric moisture on blast propagation are not completely known. An estimate of the effect on overpressure for moderate and heavy rains and fogs is given in figures 2–14A and 2–14B. Although the probability of encountering high concentrations of atmospheric liquid water is small, calculations indicate that for a high burst in very heavy rains or fogs a significant reduction may occur in the range to which overpressures less than 10 psi extend. Attenuation of air blast will be less severe in the higher overpressure regions, for lighter rains or fogs and for low heights of burst. Little is known about the effect of atmospheric moisture on other blast parameters such as time of arrival, positive phase duration, and dynamic pressure. No allowance for the effect of weather conditions on blast need be made if only hard targets (requiring greater than 15 psi overpressure) are being considered, since these targets require lower heights of burst and reductions in this overpressure range for low burst heights are small. Reductions for rain or fog effects should not be made unless it is definitely established that the extent of the rain or fog is large enough to cover a volume which includes the target and the burst.

(*b*) *Effects of temperature inversions.* A temperature inversion is a region in the atmosphere in which the temperature increases with increasing altitude, instead of decreasing. Temperature inversions tend to modify the blast wave on the ground because they are mild reflecting surfaces. An enhancement of surface or near surface overpressures at large ground distances may result when a burst is below a temperature inversion. The overpressures on the ground may be lessened somewhat if the explosion takes place above a temperature inversion. Since the corrections at close-in ground distances are small, quantitative adjustments to blast data to correct for the effect of a temperature inversion are usually unnecessary. However, the enhancement of lower overpressures at or near the surface produced by bursts below inversions may increase the possibility of damage to blast sensitive structures and equipment at greater distances.

(*c*) *Effects of altitude.*

1. Blast yield reduction with altitude. For burst altitudes up to 50,000 feet the total blast energy available from a given size weapon is essentially the same as that produced when the weapon is burst in a sea level atmosphere. In the less dense atmospheres at higher altitudes, and at times and ranges of importance to military targets, more of the weapon energy is emitted as thermal energy and less is available in the form of blast. An estimate of this variation of blast yield as a function of altitude is presented in figure 2–15.

RELATIVE BLAST YIELD Vs. ALTITUDE OF BURST

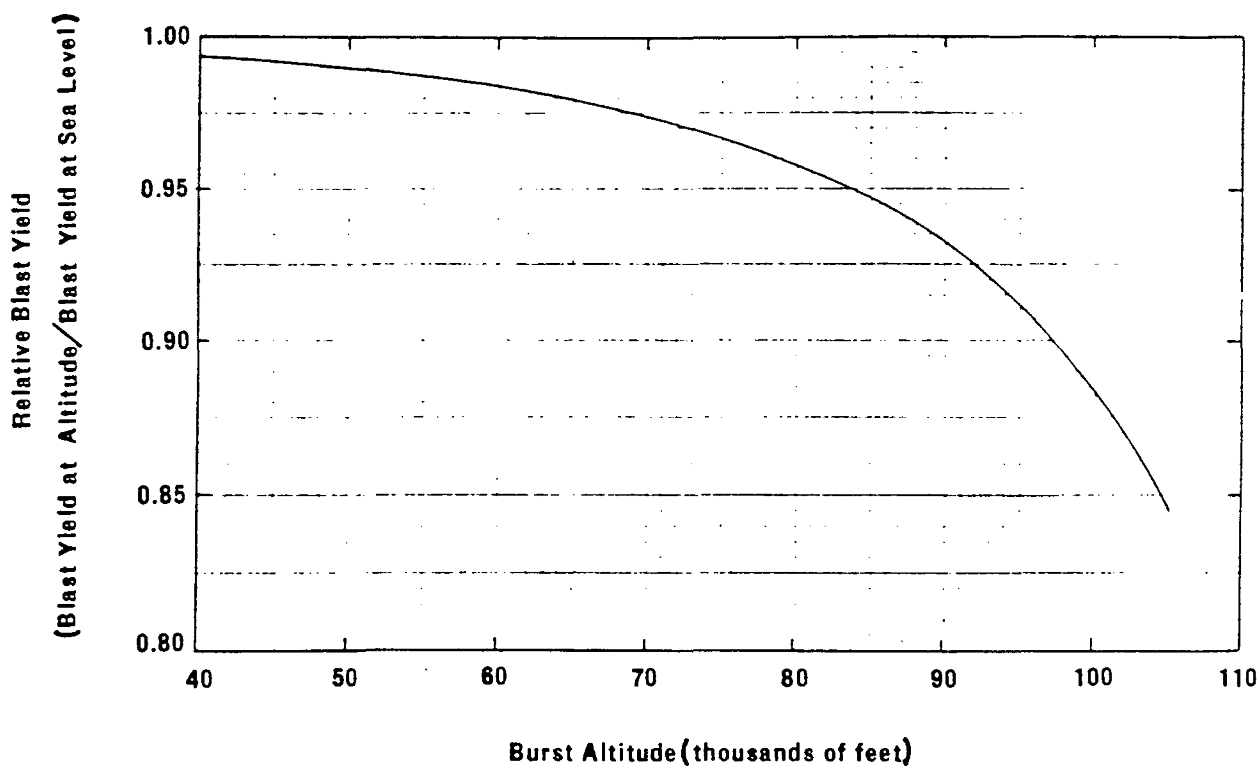

As indicated, the estimated reduction in blast yield is probably of minor significance up to altitudes of 100,000 feet. Until additional information is available, it is recommended that no correction be made for blast yield variation with altitude.

2. *Blast propagation at altitude.* The overpressure, distance and time relationships describing the propagation of a blast wave in air depend on the ambient atmospheric conditions. Blast wave propagation data presented for the standard sea level atmosphere may be converted to the atmospheric conditions of other altitudes by a procedure presented in appendix I. For targets at mean sea level altitudes of 5,000 feet or less, the altitude scaling corrections are small and are usually of no practical importance.

(3) *Effects of topography.*

(*a*) *General.* In addition to the effects on blast wave propagation caused by atmospheric conditions, the characteristics of the blast wave along or near the surface may be modified by various natural and artificial, or man-made, factors. These modifications are generally regarded as topographic effects. They include such non-local effects on the individual parameters of the blast wave as are caused by gross terrain features, cities or forested areas; and such local effects as are caused by small areas which are significantly different from the general surroundings and should therefore be considered separately.

(*b*) *Terrain.* Small-scale high explosive tests and limited full-scale nuclear tests indicate that in the Mach reflection region steep slopes may significantly affect the overpressure wave shape of the blast wave. Depending upon the effective slope, positive or negative slopes may result in respective increases or decreases in peak overpressures by a factor of as much as two. The former is attributable to the reflection of the blast wave from the positive slope, whereas the latter is attributable to the diffraction of the blast wave as it moves over the crest of the hill and down the rear slope. In the Mach region, the qualitative changes in pulse or wave shape which occur for a positive slope are the formation of a spike on the front of the pulse at the base of the slope, and the gradual widening of this spike as the blast wave progresses up the slope. The peak pressure ratio (the ratio of the peak pressures on the slope to those which would exist in the absence of the slope) increases as the positive slope angle increases and the incident pressure decreases. On a negative slope, the qualitative changes in pulse shape which occur are a rounding of the front of the pulse at the beginning of the negative slope with a return to the normal shape as the blast wave moves down the slope. The peak pressure ratio in this instance is reduced as the negative slope angle increases and the incident pressure decreases. These changes in the pressure pulse apply to the gross terrain features only, and not to local accidents of the terrain. There is no known procedure for relating local terrain accidents to gross terrain features.

Contrary to popular opinion, a "line of sight" concept does not apply to blast shielding by terrain features. However, severe local irregularities or terrain accidents may result in significant shielding from drag or dynamic pressure effects. In addition, the effects of an isolated terrain feature on the blast wave are essentially limited to the immediate vicinity of the terrain feature itself. The total energy of the blast wave is such that recovery from perturbations is quite rapid. The precursor effects on the blast wave, when coupled with the effects of terrain features, are unknown, but are believed to be significant.

(*c*) *Cities.* As with terrain features, the effect of a city as a whole on blast wave phenomena is limited essentially to the immediate vicinity of the city itself. This gross effect is usually less significant than localized changes in the characteristics of a passing blast wave. Although some local shielding similar to that afforded by terrain accidents is expected to result from intervening objects and structures, reflection and channeling phenomena may, in certain instances, result in increases in peak overpressures and peak dynamic pressures. These local effects cannot be quantitatively related to the gross effects of cities on blast wave phenomena. The general air blast characteristics in cities and urban areas are essentially the same as those for open terrain of average surface conditions.

(*d*) *Forests.* Forests may be effective in altering blast wave characteristics. However, non-local effects are less significant than localized effects. The extent of the alteration depends on forest area, tree size, state of foliation, distance from ground zero, and other variables. The shielding provided within a forest is not well known. Air blast characteristics in forested areas are essentially the same as those for open terrain, average surface conditions.

(4) *Surface conditions.*

(*a*) *General.* The nature of the surface over which the blast wave moves has been found to exert a considerable influence on the individual characteristics of the blast wave. For example, significant differences between the peak values of a given blast wave parameter may occur when considering the effects of a nuclear weapon burst over an "average" surface as compared to those expected for the same weapon burst at the same height over a "good" surface. (See $c(1)$ above for discussion of "good" and "average" surfaces.) These differences, as reflected in the iso-pressure height of burst curves, are a consequence of the thermal and mechanical influences of the earth's surface on the blast wave propagation.

(*b*) *Thermal influences.* For relatively low scaled heights of burst the earth's surface in the vicinity of ground zero absorbs sufficient thermal energy to reach a temperature of several thousand degrees in a relatively short period of time. If certain surface conditions exist, a hot layer of air or other gases, or a mixture of gases and solid matter, will form with explosive rapidity above the earth's surface. This layer may be no more than 10 feet thick, and is rapidly dissipated once the principal portion of the thermal energy has been emitted. If this thermal layer is sufficiently intense, a separate and distinct pressure wave forms and moves ahead of the incident and reflected blast waves. This detached wave, known as the "precursor," is illustrated in figure 2–16. The surface characteristics necessary for the formation and development of a precursor are not completely understood. However, precursors have been observed over coral and desert type soils, forest areas, and large artificial surfaces such as asphalt. In addition, they are expected to occur over other surfaces such as agricultural and urban areas. No precursor is expected to occur over water, snow or ice, or over ground covered by a white smoke layer. The criteria for precursor formation are shown graphically in figure 2–17.

(*c*) *Precursor characteristics.* As indicated in the discussion on impulse and wave forms in $c(3)(c)$ above, the precursor produces non-ideal wave forms. The rise in pressure above ambient at shock arrival is not nearly as instantaneous as in free air; instead, there is a relatively gradual and somewhat irregular increase to the peak value. There is also an increase in positive phase duration over that which is expected at a given range in the absence of a precursor. These degraded peak pressures, in combination with the increased positive phase durations at a given range, result in slightly larger impulse values. At ranges where the peak overpressure has fallen below about 6 psi, the precursor ceases to exist, and the blast wave form again becomes normal in shape. Although the reductions in peak pressure which may occur are on the order of one-third the ideal overpressure, reductions may be more or less than that value, depending upon the degree of development of the precursor. Overpressures in the precursor region, or where strong thermal effects on the blast wave are expected, may be obtained from figure 2–10.

The effect of the precursor on dynamic pressures is less well known than its effect on overpressures. It is known, however, that in the presence of a precursor, measured dynamic pressures over a dusty desert surface are considerably higher than those which are calculated from the peak overpressures over a "good" surface. Dynamic pressures to be expected where there are strong thermal influences on the blast wave are shown in figure 2–13.

A more detailed discussion of wave form variations reflecting precursor action is contained in appendix I.

(*d*) *Mechanical influences.* Mechanical influences of the earth's surface include air-to-earth or air-to-water coupling, reflectivity, surface roughness, and dust or water loading. Energy losses from air or surface bursts due to cou-

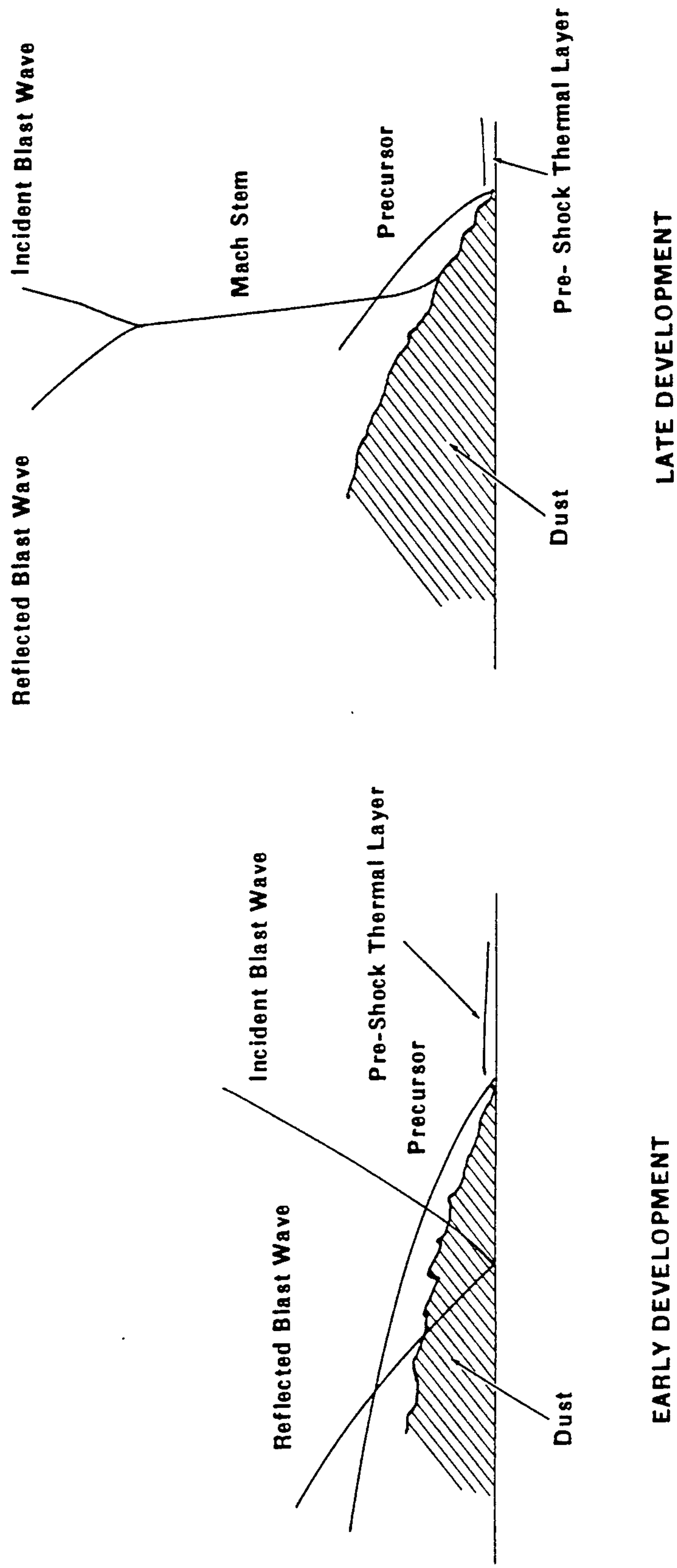

PRECURSOR CHARACTERISTICS

pling across the air-ground or air-water interface may be regarded as negligible. The reflectivity and roughness of the earth's surface exert only a minor influence on attenuation of pressure with distance, but may affect Mach stem formation and growth. Dust loading, however, may increase the peak dynamic pressure for a given peak overpressure over that which occurs in the absence of dust. Conditions for dust loading are maximized for bursts occurring over dry, fine-grained soils. The amount of dust produced will depend on the burst position, the type and moisture content of the soil, and the surface wind conditions. An effect similar to dust loading also occurs when water is picked up by the blast wave. With the possible exception of dust or water loading, mechanical influences on the blast wave are usually less significant than the thermal influences described in (*b*) above. In addition to the effects of dust on loading, dust also may limit visibility and movement in the target area for some time after a detonation.

e. *Air Blast From a Subsurface Explosion.*

(1) *General.* As discussed previously, there is no abrupt change in the air blast phenomena as the height of burst is varied. The changes occur gradually, as the earth's surface exerts a greater and greater influence on the air blast wave. The same is true for a subsurface burst. As the depth of burst increases, the magnitude of the air blast gradually decreases, until a depth of burst is reached at which any air blast effect is essentially nonexistent.

(2) *Underground.* Figure 2–18 gives the air blast peak overpressure at the ground surface for a 1 KT yield weapon detonated under sea level conditions, as a function of depth of burst and distance from surface zero. To scale to other yields, the depth of burst and distance at which a given peak overpressure occurs are multiplied by the cube root of the yield. The scaling procedure and an illustrative example accompany figure 2–18.

Thermal influences, discussed in *d*(4) above, have little or no effect on air blast propagation resulting from a subsurface burst.

(3) *Underwater.* For shallow depths of burst, peak air overpressures from underwater explosions are expected to be approximately equal to those from underground explosions at the same depth of burst. Therefore, figure 2–18 may be used to determine peak pressure at the surface versus distance for a 1 KT detonation at the depths of burst represented. As the depth of burst is lowered below those depths given in figure 2–18, the shock wave transmitted across the water-air interface gradually becomes the predominate cause of the air blast, and the significance of changes in depth of burst becomes smaller. For example, it is predicted that a 1 KT burst at a depth of 180 feet would produce a peak air blast pressure of 1.5 psi at a range of 150 yards from surface zero. If the depth of burst were lowered to 360 feet, the 1.5 psi pressure would still extend as far as 150 yards.

FREE AIR TIME OF ARRIVAL OF SHOCK FRONT

Shock arrival time vs. distance in free air for a 1 KT burst in a homogeneous sea level atmosphere is given in figure 2-2.

Scaling. To calculate the distance and time of shock arrival for a yield other than 1 KT, use the following scaling:

$$\frac{t_1}{t_2}=\frac{W_1^{1/3}}{W_2^{1/3}}=\frac{d_1}{d_2},$$

where t_2=time of arrival of shock front from explosion of yield W_2 KT at range d_2, and t_1=time of arrival of shock front from explosion of W_1 KT at range d_1.

Example.

Given: A 100 KT burst in free air.

Find: The time of arrival of the shock front at 40,000 feet.

Solution: The corresponding distance for 1 KT is,

$$d_1=\frac{d_2\times W_1^{1/3}}{W_2^{1/3}}=\frac{40{,}000\times 1}{(100)^{1/3}}=8{,}600 \text{ ft.}$$

From figure 2-2, the time of arrival t_1 for a 1 KT burst at 8,600 feet is 7 seconds. Thus, the time of arrival of the shock front from a 100 KT detonation at a distance of 40,000 feet is,

$$t_2=\frac{W_2^{1/3}\times t^1}{W_1^{1/3}}=\frac{(100)^{1/3}\times 7}{1}=$$

32.5 (±4.8) seconds. *Answer.*

Reliability. Times of arrival obtained from this curve are considered to be reliable to ±15 percent (0.1 KT to 100 MT).

Related material.

See paragraphs 2.1.*b*(2) and I-3.

See also figures 2-3, 2-4, 2-5, and 2-8.

TIME OF ARRIVAL OF SHOCK FRONT Vs SLANT RANGE IN FREE AIR
HOMOGENEOUS ATMOSPHERE OF STANDARD SEA LEVEL PROPERTIES
1 KILOTON YIELD

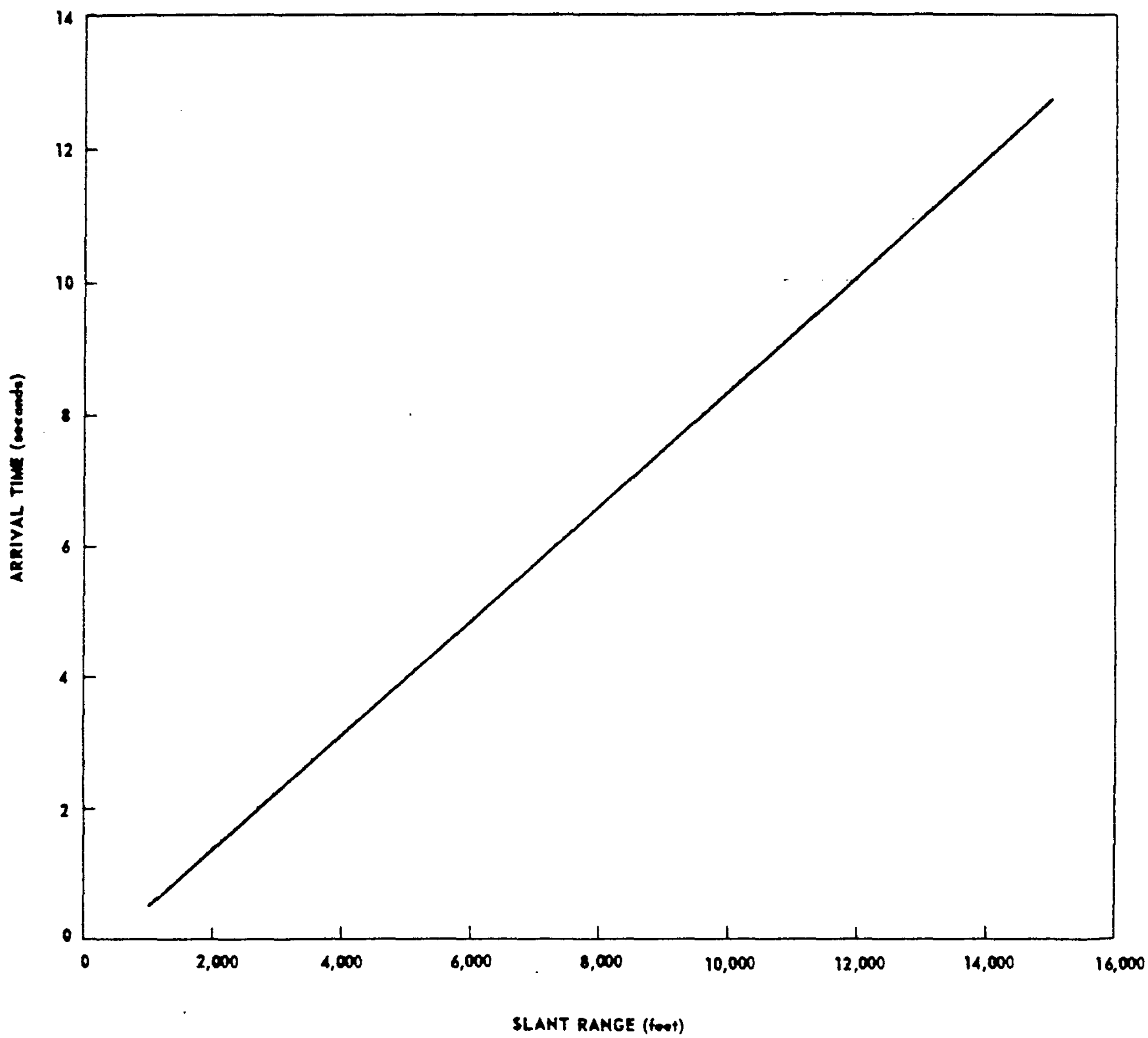

"FREE AIR PEAK OVERPRESSURE VS. SLANT RANGE"

A curve of peak overpressure vs. slant range in free air for a 1 KT burst in a homogeneous sea level atmosphere is presented in figure 2-3. This curve may be used to predict incident pressures near the surface from air bursts at heights up to 40,000 feet. Reflected overpressures at the surface for moderate bursts heights (up to 5200 feet for 1 KT) may be determined from the height of burst curve, figures 2-9 and 2-10. Reflected overpressures at the surface for high burst heights (above 5200 ft. for 1 KT) may be calculated by use of the reflection factors given on page I-31 in appendix I as a function of incident pressure and angle of reflection as explained in paragraph I.4. The above procedures should be used for predicting effects on surface targets. For predicting effects on air-borne targets, figure I-14 in appendix I should be used as explained in paragraph I.3b.

Scaling. In order to calculate the distance to which a given overpressure extends for yields other than 1 KT, use the following scaling:

$$\frac{d_1}{d_2}=\frac{W_1^{1/3}}{W_2^{1/3}}$$

where d_1 = distance at which a given overpressure occurs from an explosion of yield W_1 KT, and d_2 = distance at which the same overpressure occurs for an explosion of yield W_2 KT.

This scaling is often referred to as "cube root" scaling.

Example:

Given: A 100 KT detonation in free air.

Find: The distance to which 7 psi overpressure extends.

Solution: From figure 2-3 a 1 KT burst produces 7 psi at a distance of 1,000 feet.

Scaling to 100 KT:

$$\frac{1{,}000}{d_2}=\frac{1}{(100)^{1/3}} \text{ or } d_2=\frac{1{,}000\times(100)^{1/3}}{1}=$$

$$1{,}000\times4.64=4{,}640 \text{ feet.} \quad \textit{Answer.}$$

Reliability. For ranges less than 1,000 feet (overpressures greater than 7 psi) the values of peak overpressure obtained from the curve are considered reliable to ±5%. This portion of the curve is based largely on analysis of data obtained by high-speed photography. For overpressures less than 7 psi the curve is based on data obtained with pressure gages near the ground. The reliability of this portion of the curve is estimated to be ±30%.

Related material:

See paragraphs 2.1.b(3), I.3, and I.4.

See also figures 2-2, 2-4, 2-5, 2-9, and 2-10.

PEAK OVERPRESSURE VS. SLANT RANGE IN FREE AIR

HOMOGENEOUS ATMOSPHERE OF STANDARD SEA LEVEL PROPERTIES

1 KT. YIELD

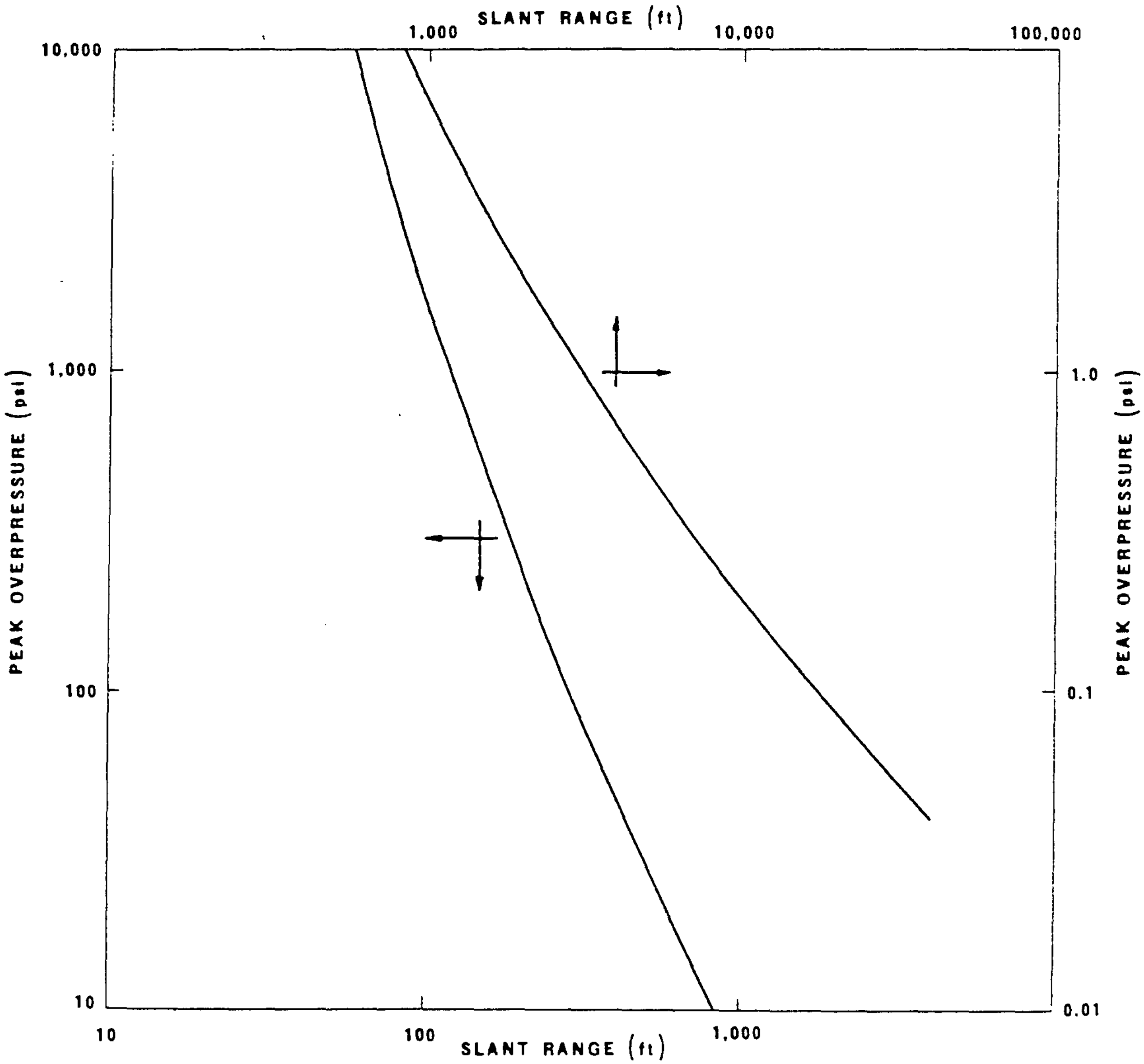

FREE AIR DURATION OF POSITIVE PHASE VS. SLANT RANGE

Figure 2-4 shows the duration of the positive pressure phase as a function of distance in free air for a 1 KT burst in a sea level homogeneous atmosphere.

Scaling. To scale to yields other than 1 KT, use the following scaling:

$$\frac{t_1^+}{t_2^+}=\frac{W_1^{1/3}}{W_2^{1/3}}=\frac{d_1}{d_2}$$

where t_1^+ = duration of the positive phase for yield W_1 KT at distance d_1, and t_2^+ = duration of the positive phase for yield W_2 KT at distance d_2.

Example.

Given: A 160 KT detonation in free air.

Find: The positive phase duration at 27,000 feet.

Solution:

$$d_1=\frac{W_1^{1/3}\times d_2}{W_2^{1/3}}=\frac{1\times 27{,}000}{(160)^{1/3}}=5{,}000 \text{ feet}$$

(corresponding distance for 1 KT).

From figure 2-4, t_1, the duration of the positive phase for 1 KT at 5,000 feet is 0.35 second. For 160 KT the duration is,

$$t_2^+=\frac{t_1^+\times W_2^{1/3}}{W_1^{1/3}}=\frac{0.35\times(160)^{1/3}}{1}=$$

1.90 (±0.57) seconds. *Answer.*

Reliability. Durations obtained from this curve are considered to be reliable to ±30 percent (0.1 KT to 20 MT).

Related material.

See paragraph 2.1.*b*(3)(*b*).

See also figures 2-2, 2-3, 2-5, and 2-11.

FREE AIR DURATION OF POSITIVE PHASE VS SLANT RANGE FOR A 1 KT BURST IN A HOMOGENEOUS SEA LEVEL ATMOSPHERE

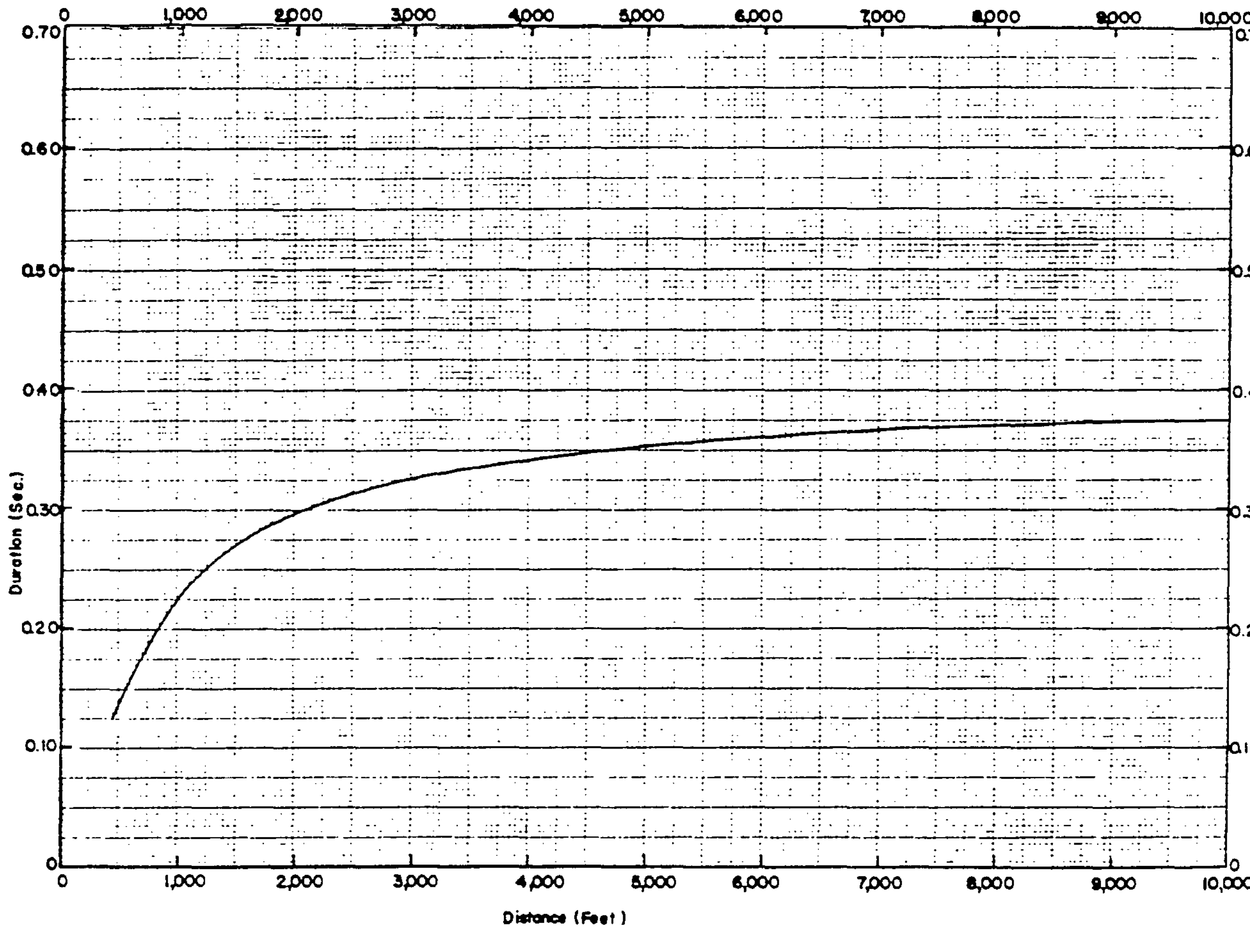

FREE AIR PEAK DYNAMIC PRESSURE VS. SLANT RANGE

A curve of free air peak dynamic pressure for a 1 KT burst in a homogeneous sea level atmosphere is presented in figure 2–5.

Scaling. To calculate the distance at which a given dynamic pressure extends for a yield other than 1 KT, use the following scaling:

$$\frac{d_1}{d_2}=\frac{W_1^{1/3}}{W_2^{1/3}},$$

where d_1=distance to which a given dynamic pressure extends for yield W_1, and d_2=distance to which the same dynamic pressure extends for yield W_2.

Example.

Given: A 100 KT detonation in free air.

Find: The distance to which 10 psi dynamic pressure extends.

Solution: From figure 2–5, one KT produces 10 psi at a distance of 560 feet. Hence,

$$\frac{560}{d_2}=\frac{1}{(100)^{1/3}},$$

and

$$d_2=560\times(100)^{1/3}=560\times(4.64)=$$
$$2{,}590 \text{ feet.} \quad \textit{Answer.}$$

Reliability. Peak dynamic pressures obtained from this curve are considered to be reliable to ±5 percent for pressures greater than 2 psi and to ±10 percent for pressures below 2 psi (0.1 KT to 100 MT).

Related material.

See paragraph 2.1.*b*(4).

See also figures 2–2 through 2–4, 2–12, and 2–13.

FREE AIR PEAK DYNAMIC PRESSURE VS SLANT RANGE FOR A 1 KT BURST IN A HOMOGENEOUS SEA LEVEL ATMOSPHERE.

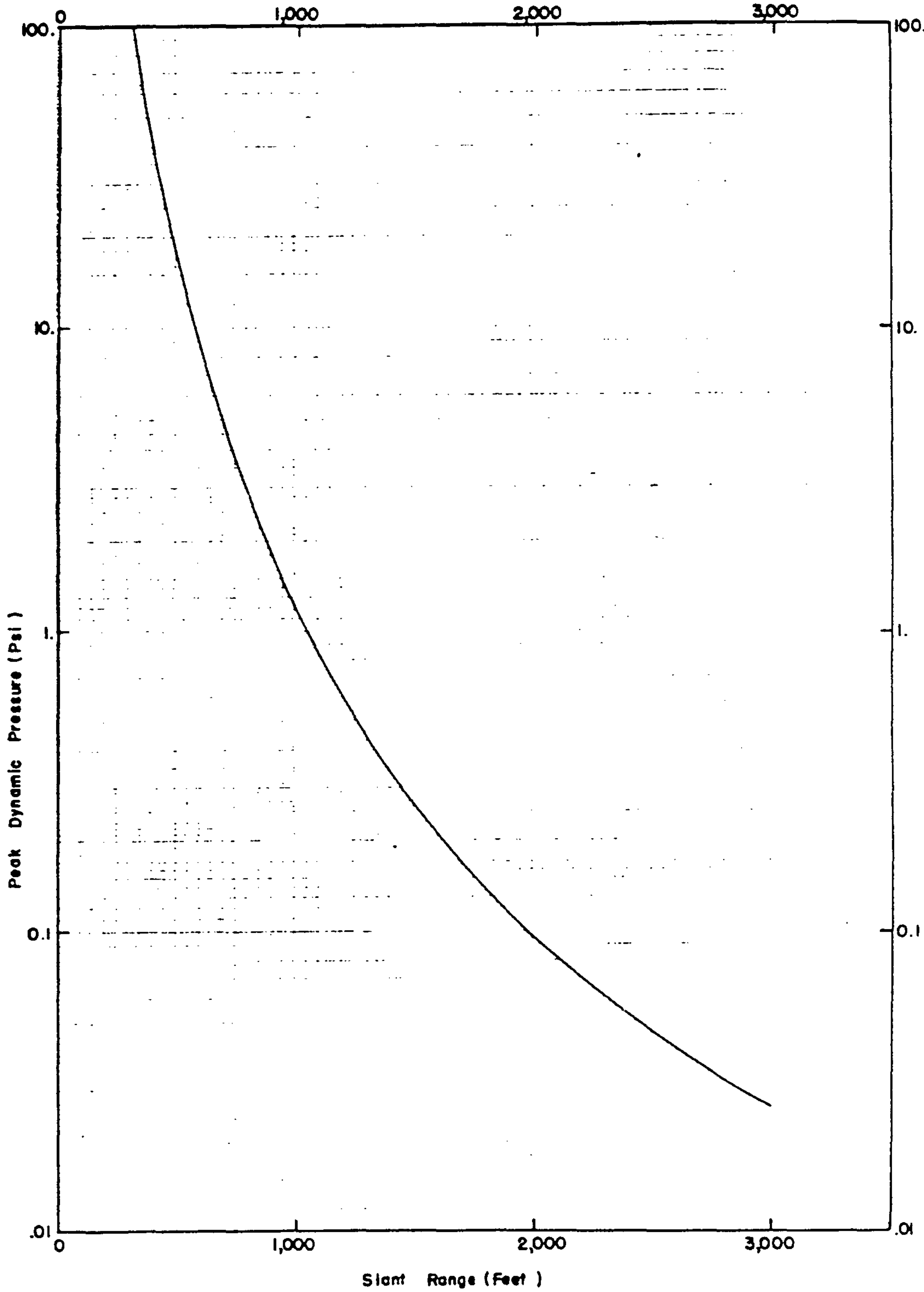

MACH STEM HEIGHT

Figure 2–7 is a plot of ground distance vs. Mach stem height for various heights of burst of a 1 KT detonation in a sea level atmosphere. These curves are for average surface conditions; depending upon the thermal qualities and the roughness of the surface, the triple point rise may be somewhat different from that shown.

Scaling. Distances scale as the cube root of the yield, so that—

$$\frac{H_1}{H_2}=\frac{h_1}{h_2}=\frac{d_1}{d_2}=\frac{W_1^{1/3}}{W_2^{1/3}}$$

where H_1, h_1 and d_1 are Mach stem height, height of burst and ground distance for yield W_1, and H_2, h_2 and d_2 are the corresponding Mach stem height, height of burst and ground distance for yield W_2.

Example.

Given: A 60 KT detonation at 1,000 feet height of burst.

Find:

(*a*) The range at which the Mach stem is 50 feet high.

(*b*) The minimum ground range for which an aircraft at 5,000 feet altitude is in the Mach reflection region.

Solution:

(*a*) The corresponding burst height for 1 KT is—

$$h_1=\frac{1{,}000\times 1}{(60)^{1/3}}=255 \text{ feet.}$$

The corresponding Mach stem height for a 1 KT burst is—

$$H_1=\frac{50\times 1}{(60)^{1/3}}=13 \text{ feet.}$$

From figure 2–7, a Mach stem height of 13 feet is found at 95 yards for a 1 KT burst at 255 feet HOB. For a 60 KT burst, the range is $95\times(60)^{1/3}=$ 370 yards. *Answer.*

(*b*) 5,000 feet altitude for a 60 KT burst corresponds to $\frac{5{,}000}{(60)^{1/3}}=1{,}280$ feet altitude for a 1 KT burst. Interpolating between the 200 feet and 300 feet burst height curves, the ground range for a Mach stem height of 1,280 feet is 810 yards. The corresponding range for a 60 KT burst is $810\times(60)^{1/3}=$ 3,200 yards. *Answer.* This indicates that for the burst condition and altitude specified, an aircraft at ranges greater than 3,200 yards will experience a single shock.

Reliability. The range at which a given Mach stem height occurs as obtained from figure 2–7 is considered to be reliable to ± 10 percent for 1 KT and to ± 25 percent for 20 MT. This decrease in reliability with increasing yield is a result of the lack of knowledge concerning the effect of atmospheric inhomogeneity on the triple point trajectory. It is suggested that no correction be made for altitude effects; however, when the basic data are applied to high yield air bursts, the results should be treated with somewhat less confidence.

Related material.

See paragraph 2.1.*c*(1).

See also figure 2–6.

MACH STEM HEIGHT (1 KT)

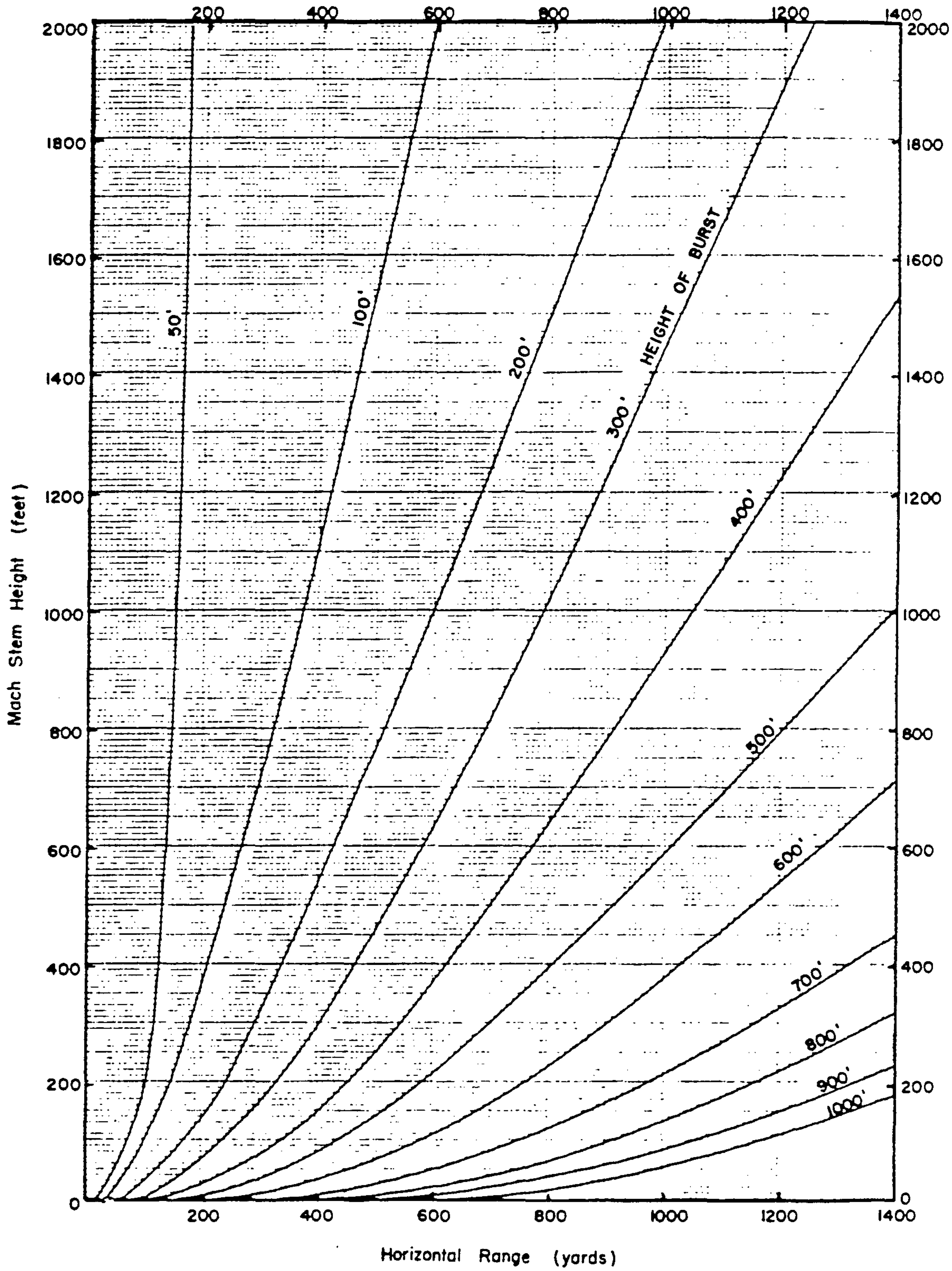

447555 O - 58 - 5

BLANK

BLAST WAVE ARRIVAL TIMES AT THE SURFACE

Figures 2-8A and 2-8B show families of curves representing the arrival time of the blast wave on the ground as a function of burst height and ground distance. The curves are drawn for a 1 KT burst in sea level atmospheric conditions. Figure 2-8A is for good surface conditions; figure 2-8B is for average surface conditions.

Scaling. The height of burst, the range, and the arrival times all scale as the cube root of the yield:

$$\frac{h_1}{h_2}=\frac{d_1}{d_2}=\frac{W_1^{1/3}}{W_2^{1/3}}=\frac{t_1}{t_2},$$

where h_1, d_1 and t_1 are the height of burst, range, and arrival time for W_1 KT; and h_2, d_2, and t_2 are the corresponding height of burst, range, and arrival time for W_2 KT.

Example.

Given: A 160 KT detonation at a height of 3,000 feet.

Find: The arrival time at a ground range of 2,000 yards, for good surface conditions.

Solution: The corresponding burst height for 1 KT is:

$$h_1=\frac{3{,}000\times 1}{(160)^{1/3}}=550 \text{ feet.}$$

The corresponding range for 1 KT is:

$$d_1=\frac{2{,}000\times 1}{(160)^{1/3}}=370 \text{ yards.}$$

From figure 2-8A, at a range of 370 yards and a burst height of 550 feet, the arrival time is approximately 0.65 second (for 1 KT). The corresponding arrival time for 160 KT is $0.65\times(160)^{1/3}=$ 3.5 ($\pm$0.4) seconds. *Answer.*

Reliability. Arrival times obtained from these curves are considered to be reliable to $\pm$10 percent for 0.1 KT to 20 MT. In the region of precursor formation, because of thermal effects on shock velocity, the values given are less certain. The curves may be used outside this range of yields with somewhat less confidence.

Related material.

See paragraphs 2.1c(1) and (2).

See also figures 2-2 and 2-9 through 2-13.

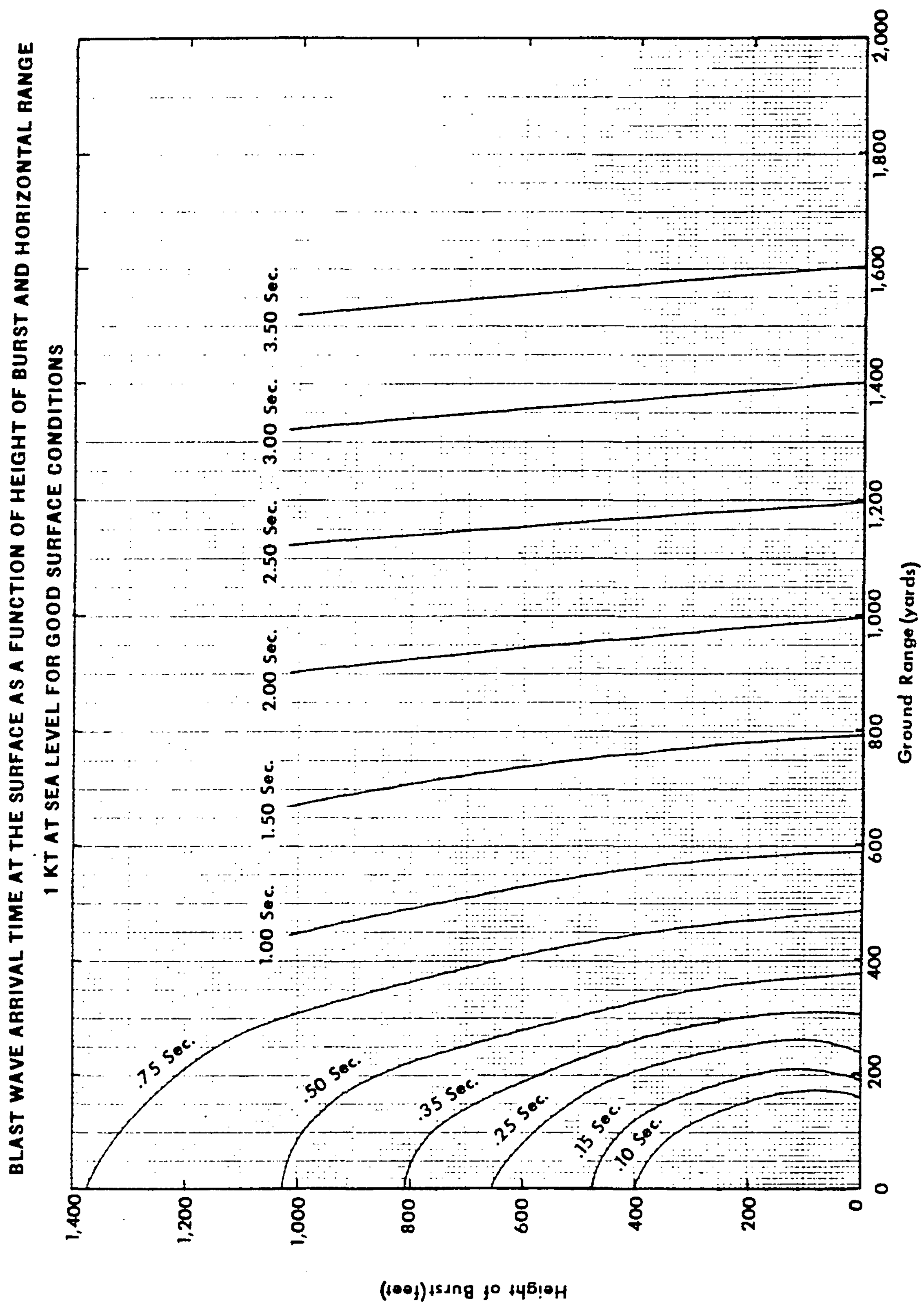
BLAST WAVE ARRIVAL TIME AT THE SURFACE AS A FUNCTION OF HEIGHT OF BURST AND HORIZONTAL RANGE
1 KT AT SEA LEVEL FOR GOOD SURFACE CONDITIONS
3.50 Sec.
3.00 Sec.
2.50 Sec.
2.00 Sec.
1.50 Sec.
1.00 Sec.
.75 Sec.
.50 Sec.
.35 Sec.
.25 Sec.
.15 Sec.
.10 Sec.
Ground Range (yards)
0
200
400
600
800
1,000
1,200
1,400
1,600
1,800
2,000
Height of Burst (feet)
1,400
1,200
1,000
800
600
400
200
0

BLAST WAVE ARRIVAL TIME AT THE SURFACE AS A FUNCTION OF HEIGHT OF BURST AND HORIZONTAL RANGE

1 KT AT SEA LEVEL FOR AVERAGE SURFACE CONDITIONS

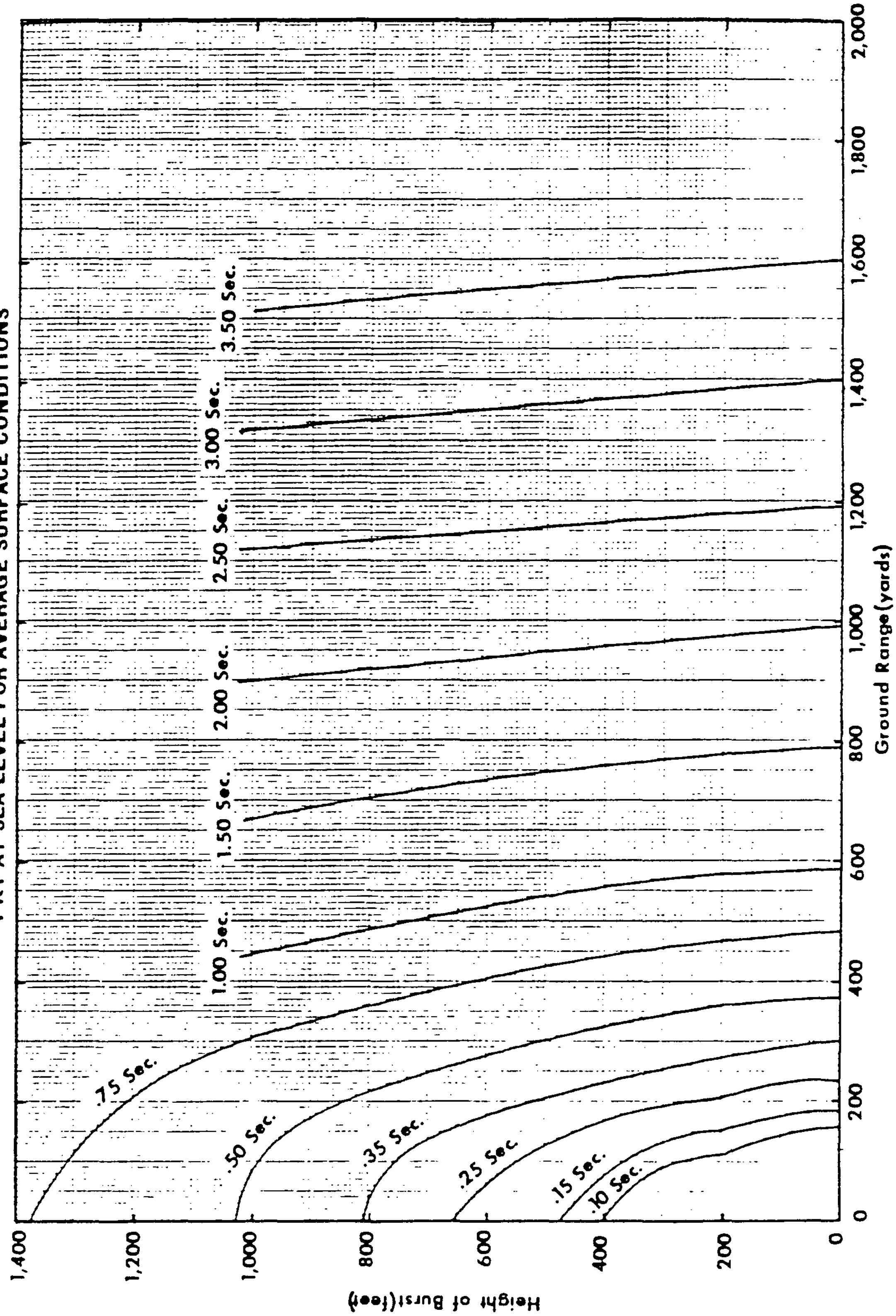

BLANK

PEAK OVERPRESSURES ON THE SURFACE

(Good and Average Surface Conditions)

Figures 2–9 and 2–10 are families of curves representing peak overpressures on the ground as a function of ground range and height of burst for a 1 KT burst under sea level conditions. The solid lines are based upon experimental data established as a result of full-scale nuclear explosions and the dashed portions are based upon theory and high explosive experiments. The curves in figures 2–9A and 2–9B are considered representative for "good" target surfaces approaching the ideal, while the curves in figures 2–10A and 2–10B are considered appropriate for all other target conditions ("average"). Surface influences are discussed in paragraphs 2.1*c* and *d*(4).

Scaling. The height of burst and the range to which a given peak overpressure extends scale as the cube root of the yield, i. e.,

$$\frac{d_1}{d_2}=\frac{h_1}{h_2}=\frac{W_1^{1/3}}{W_2^{1/3}},$$

where for a given peak overpressure, d_1 and h_1 are ground range and height of burst for W_1 KT, and d_2 and h_2 are the corresponding ground range and height of burst for W_2 KT.

Example.

Given: An 80 KT detonation 2,580 feet above an average surface.

Find: The distance to which 3 psi extends.

Solution: The corresponding burst height for 1 KT is—

$$h_1=\frac{W_1^{1/3}\times h_2}{W_2^{1/3}}=\frac{1\times 2{,}580}{(80)^{1/3}}=600 \text{ ft.}$$

From figure 2–10B, 3 psi extends to 920 yards for a 600 foot burst height for a 1 KT weapon. The corresponding distance for 80 KT is:

$$d_2=\frac{W_2^{1/3}\times d_1}{W_1^{1/3}}=\frac{(80)^{1/3}\times 920}{1}=$$

3,960 yards. *Answer.*

Reliability. The pressures obtained from figures 2–9 and 2–10 are considered to be reliable to ±20 percent for yields of 1 KT to 20 MT. Outside this range of yields the figures may be used with somewhat less confidence.

Related Material.

See paragraphs 2.1*c*(3) and *d*(4).

See also figures 2–3, 2–8, 2–11 through 2–13, and 2–18.

PEAK OVERPRESSURE ON THE SURFACE AS A FUNCTION OF HEIGHT OF BURST AND HORIZONTAL RANGE
1 KT AT SEA LEVEL FOR GOOD SURFACE CONDITIONS

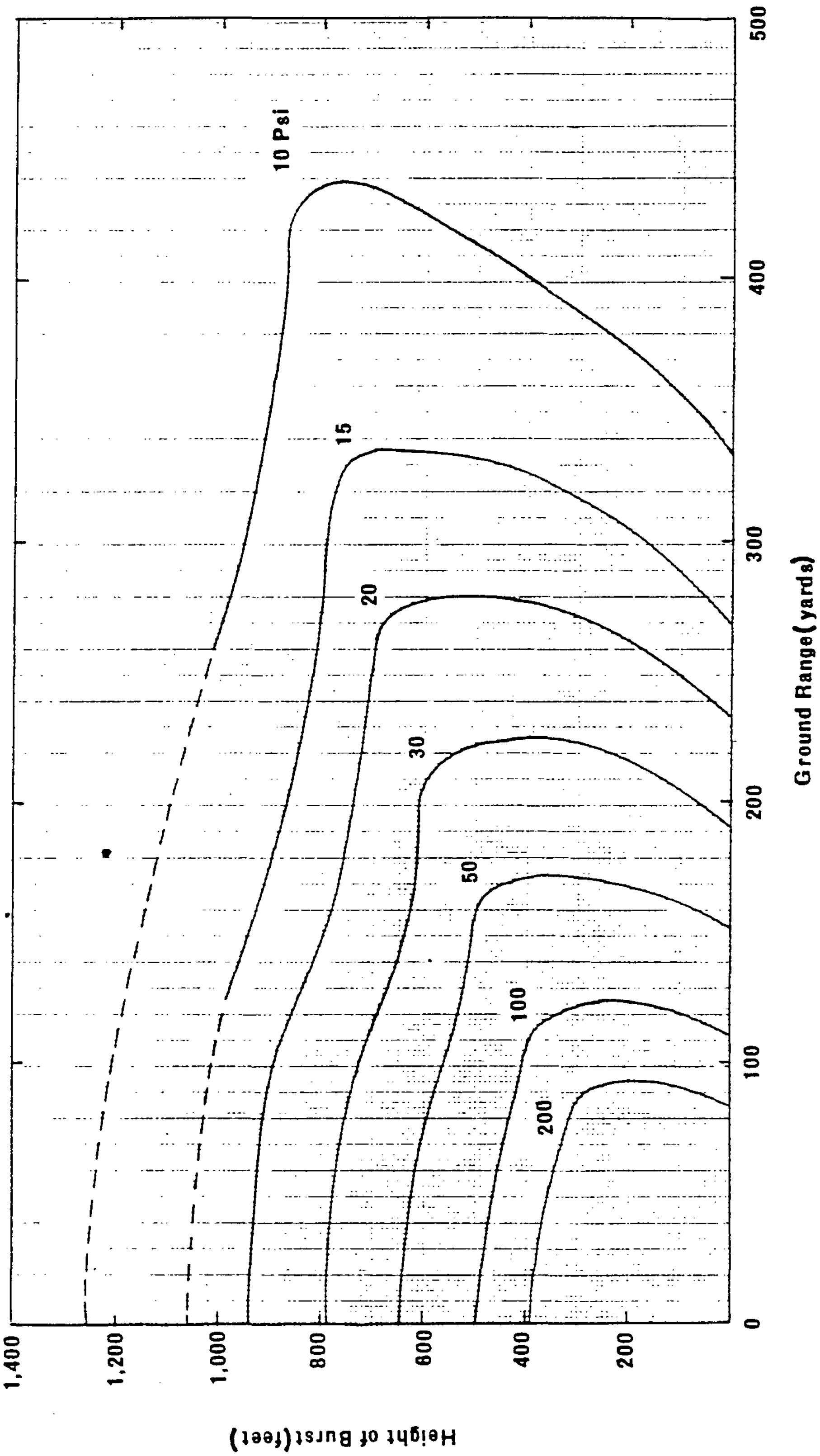

PEAK OVERPRESSURE ON THE SURFACE AS A FUNCTION OF HEIGHT OF BURST AND GROUND RANGE
1 KT AT SEA LEVEL FOR GOOD SURFACE CONDITIONS

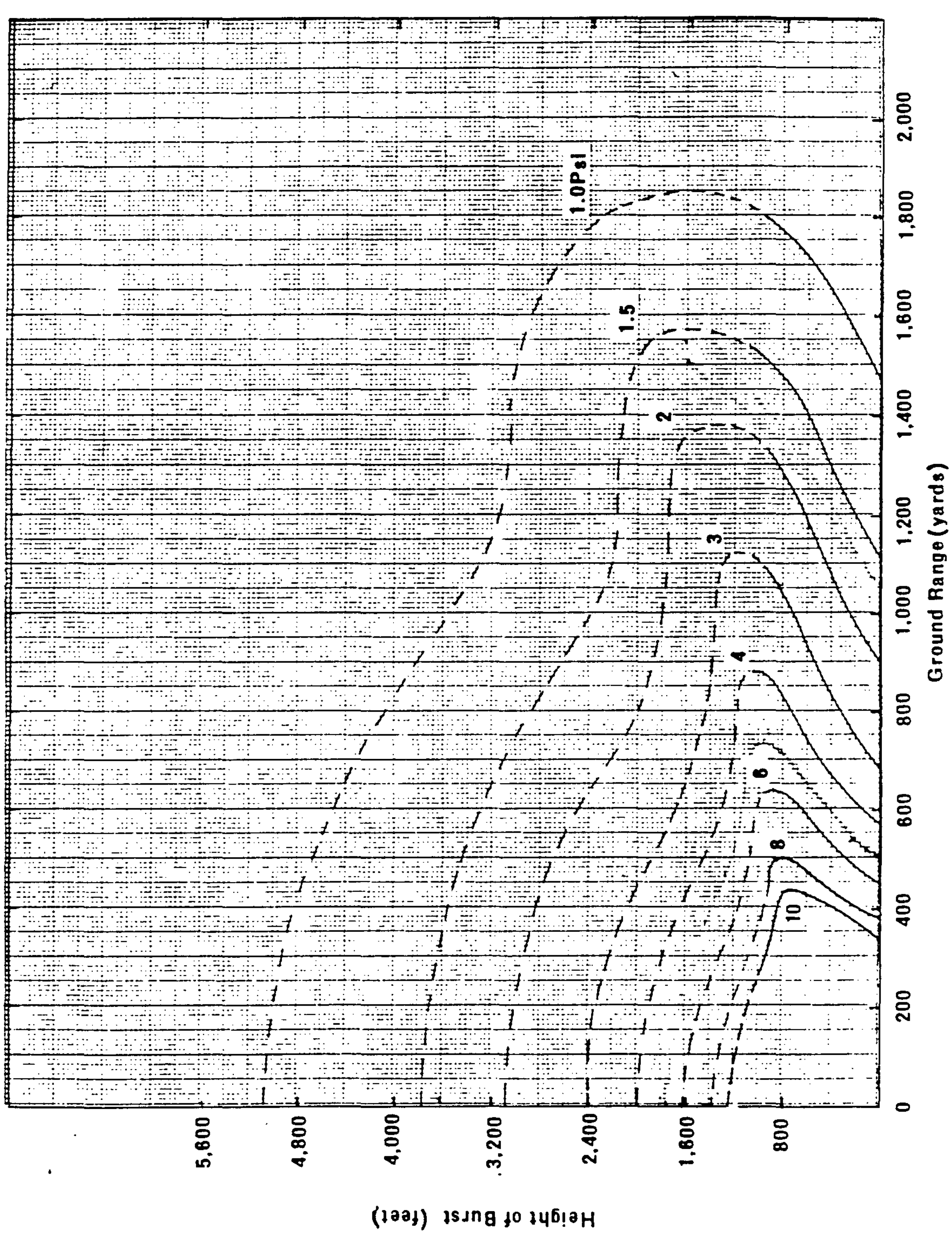

PEAK OVERPRESSURE ON THE SURFACE AS A FUNCTION OF HEIGHT OF BURST AND GROUND RANGE

1 KT AT SEA LEVEL FOR AVERAGE SURFACE CONDITIONS

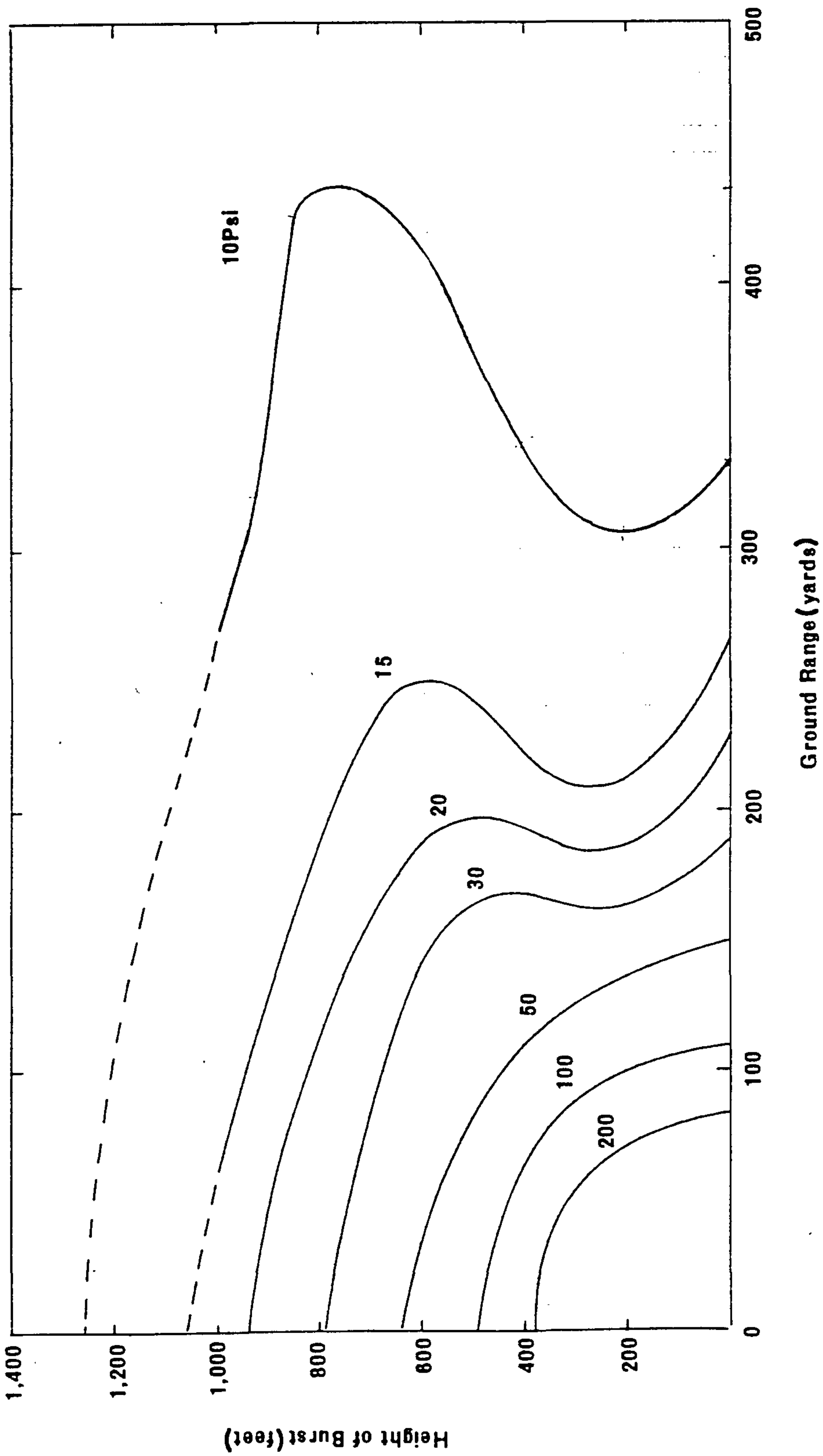

PEAK OVERPRESSURES ON THE SURFACE
AS A FUNCTION OF HEIGHT OF BURST AND HORIZONTAL RANGE
1 KT AT SEA LEVEL FOR AVERAGE SURFACE CONDITIONS

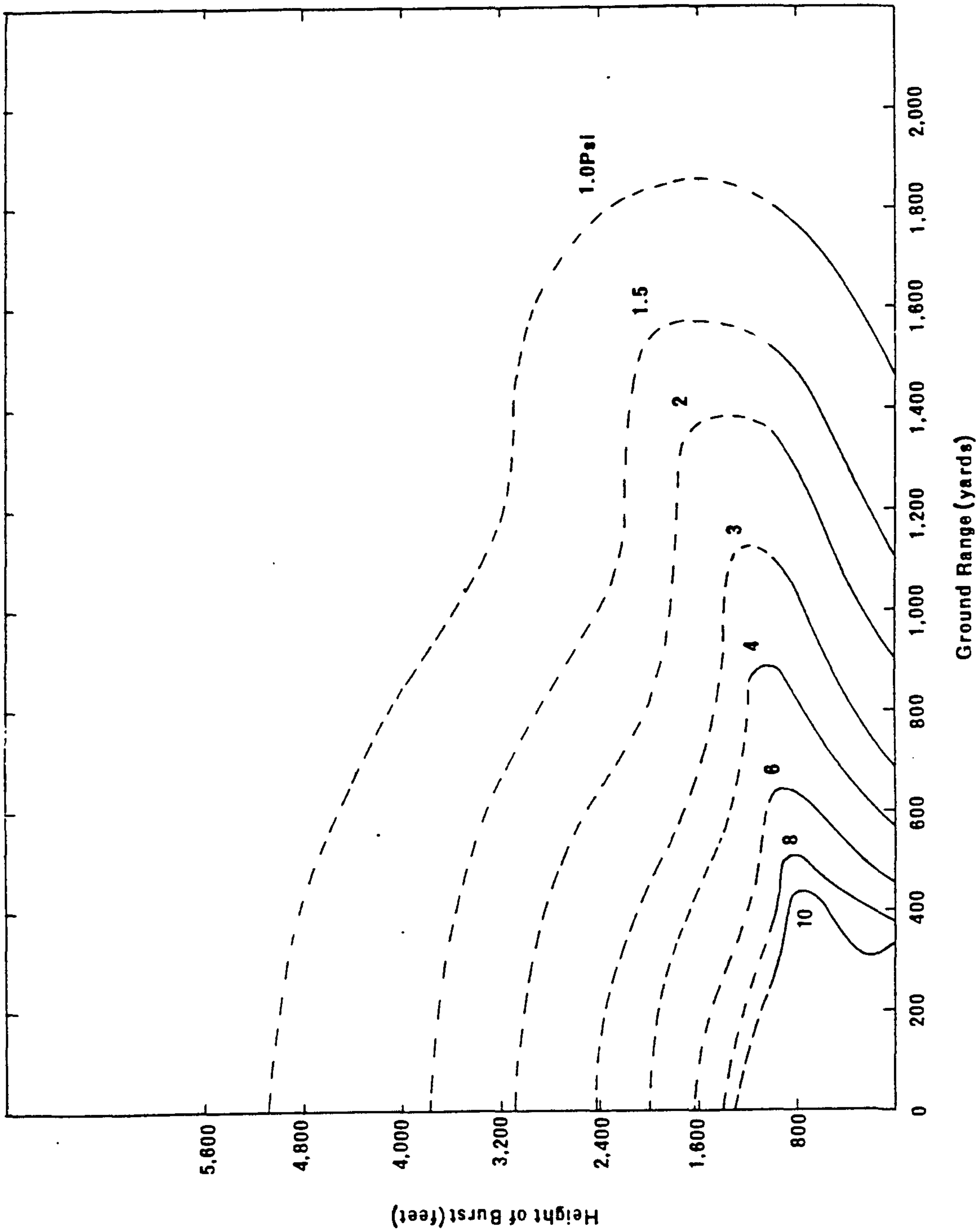

BLANK

POSITIVE PHASE DURATION ON THE SURFACE

Figures 2-11A and 2-11B are families of curves representing positive phase durations on the ground as functions of ground range and burst height for a 1 KT burst under sea level conditions. Figure 2-11A represents positive phase duration under good surface conditions, while 2-11B represents the same values under average surface conditions.

Scaling: Use:

$$\frac{h_1}{h_2}=\frac{d_1}{d_2}=\frac{W_1^{1/3}}{W_2^{1/3}}=\frac{t_1}{t_2},$$

where h_1, d_1, and t_1 are the height of burst, range, and duration for W_1 KT; and h_2, d_2, and t_2 are the corresponding height of burst, range, and duration for W_2 KT.

Example.

Given: A 160 KT explosion at a height of 3,000 feet.

Find: The positive phase duration at 4,000 yards for average surface conditions.

Solution: The corresponding 1 KT height of burst is:

$$h_1=\frac{3{,}000}{(160)^{1/3}}=550 \text{ feet};$$

and the corresponding ground range is:

$$d_1=\frac{4{,}000}{(160)^{1/3}}=740 \text{ yards}.$$

From figure 2-11B, the positive phase duration for 1 KT at 740 yards and a burst height of 550 feet is 0.34 second. The corresponding duration for 160 KT is: $t_2=0.34\times(160)^{1/3}=1.8$ (± 0.9) seconds. *Answer.*

Reliability. Durations obtained from these curves are considered to be reliable to ± 50 percent for 0.1 KT to 20 MT. The curves may be used outside this range of yields with somewhat less confidence.

Related material.

See paragraphs 2.1.*c*(1) and (3).

See also figures 2-4 and 2-8 through 2-13.

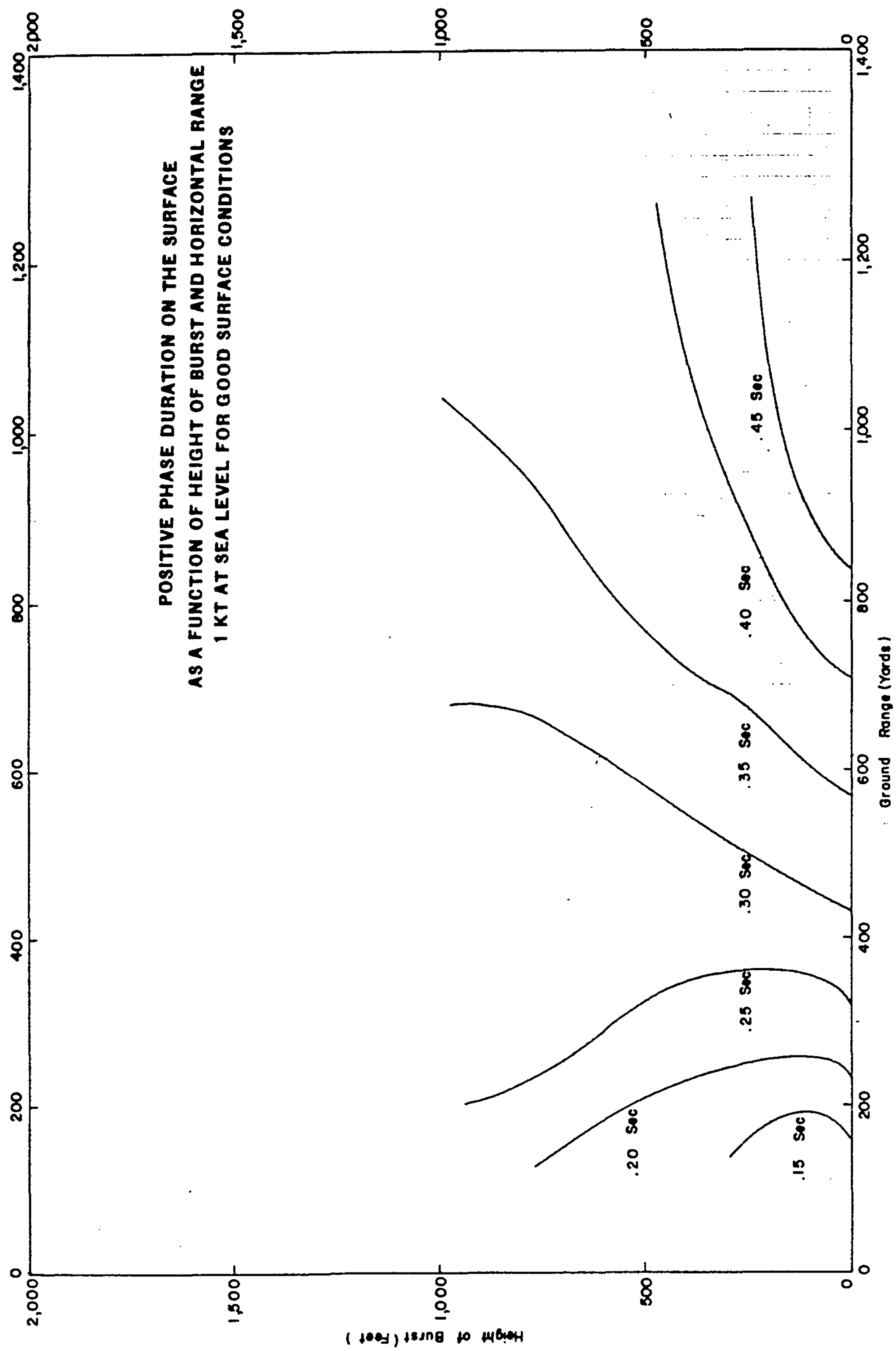
POSITIVE PHASE DURATION ON THE SURFACE
AS A FUNCTION OF HEIGHT OF BURST AND HORIZONTAL RANGE
1 KT AT SEA LEVEL FOR GOOD SURFACE CONDITIONS
.15 Sec
.20 Sec
.25 Sec
.30 Sec
.35 Sec
.40 Sec
.45 Sec
Ground Range (Yards)
Height of Burst (Feet)
0
200
400
600
800
1,000
1,200
1,400
500
1,500
2,000

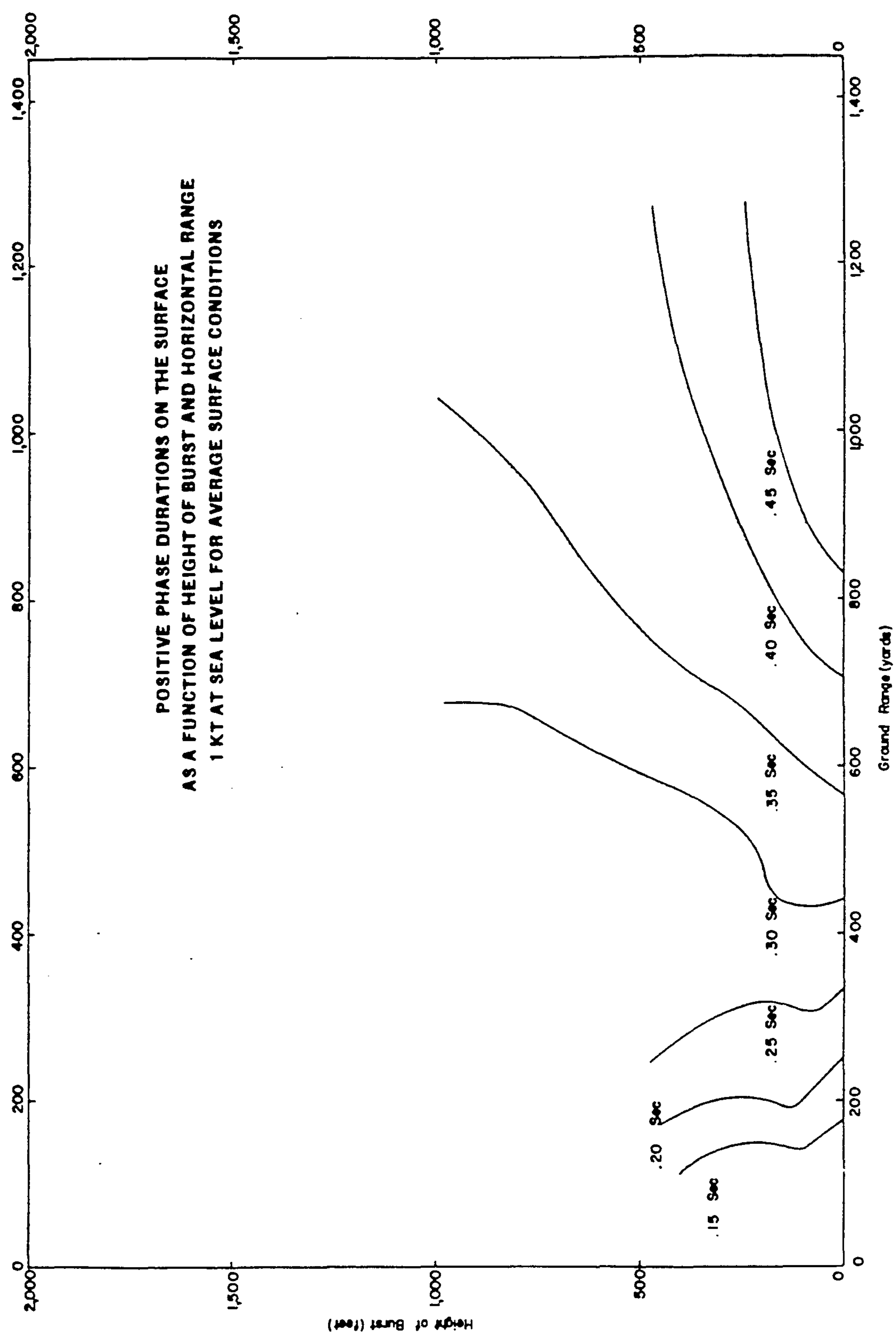
POSITIVE PHASE DURATIONS ON THE SURFACE
AS A FUNCTION OF HEIGHT OF BURST AND HORIZONTAL RANGE
1 KT AT SEA LEVEL FOR AVERAGE SURFACE CONDITIONS
.15 Sec
.20 Sec
.25 Sec
.30 Sec
.35 Sec
.40 Sec
.45 Sec
Ground Range (yards)
Height of Burst (feet)
0
200
400
600
800
1,000
1,200
1,400
500
1,000
1,500
2,000

BLANK

PEAK DYNAMIC PRESSURE ON THE SURFACE

(Good and Average Surface Conditions)

Figures 2–12 and 2–13 are families of curves representing the horizontal component of peak dynamic pressure on the ground as a function of burst height and ground distance. The curves are drawn for a 1 KT burst in sea level atmospheric conditions. The curves in figure 2–12 are considered representative for "good" target surfaces approaching the ideal, while the curves in figure 2–13 are considered appropriate for all other target conditions ("average"). Surface influences are discussed in paragraphs 2.1*c* and *d*(4).

Scaling. The height of burst and range to which a given peak dynamic pressure extends scale as the cube root of the yield:

$$\frac{h_1}{h_2}=\frac{d_1}{d_2}=\frac{W_1^{1/3}}{W_2^{1/3}},$$

where for a given peak dynamic pressure, h_1 and d_1 are the height of burst and range for yield W_1; and h_2 and d_2 are the corresponding height of burst and range for yield W_2.

Example.

Given: A 160 KT burst at a height of 3,000 feet, with *average* surface conditions.

Find: The horizontal component of peak dynamic pressure on the ground at a range of 2,000 yards.

Solution: The corresponding burst height for 1 KT is:

$$h_1=\frac{3,000\times 1}{(160)^{1/3}}=550 \text{ feet.}$$

The corresponding range for 1 KT is:

$$d_1=\frac{2,000\times 1}{(160)^{1/3}}=370 \text{ yards.}$$

From figure 2–13, at a range of 370 yards and a burst height of 550 feet, the dynamic pressure is approximately 3.7 psi. *Answer.*

Reliability. Ranges for peak values of dynamic pressure less than 10 psi are considered to be reliable to ±25 percent. This reliability factor applies from 1 KT to 20 MT. Outside these limits the curves may be used with somewhat less confidence.

Related material.

See paragraphs 2.1*c*(1), (4) and *d*(4).

See also figures 2–5, 2–8 through 2–11, and 2–17.

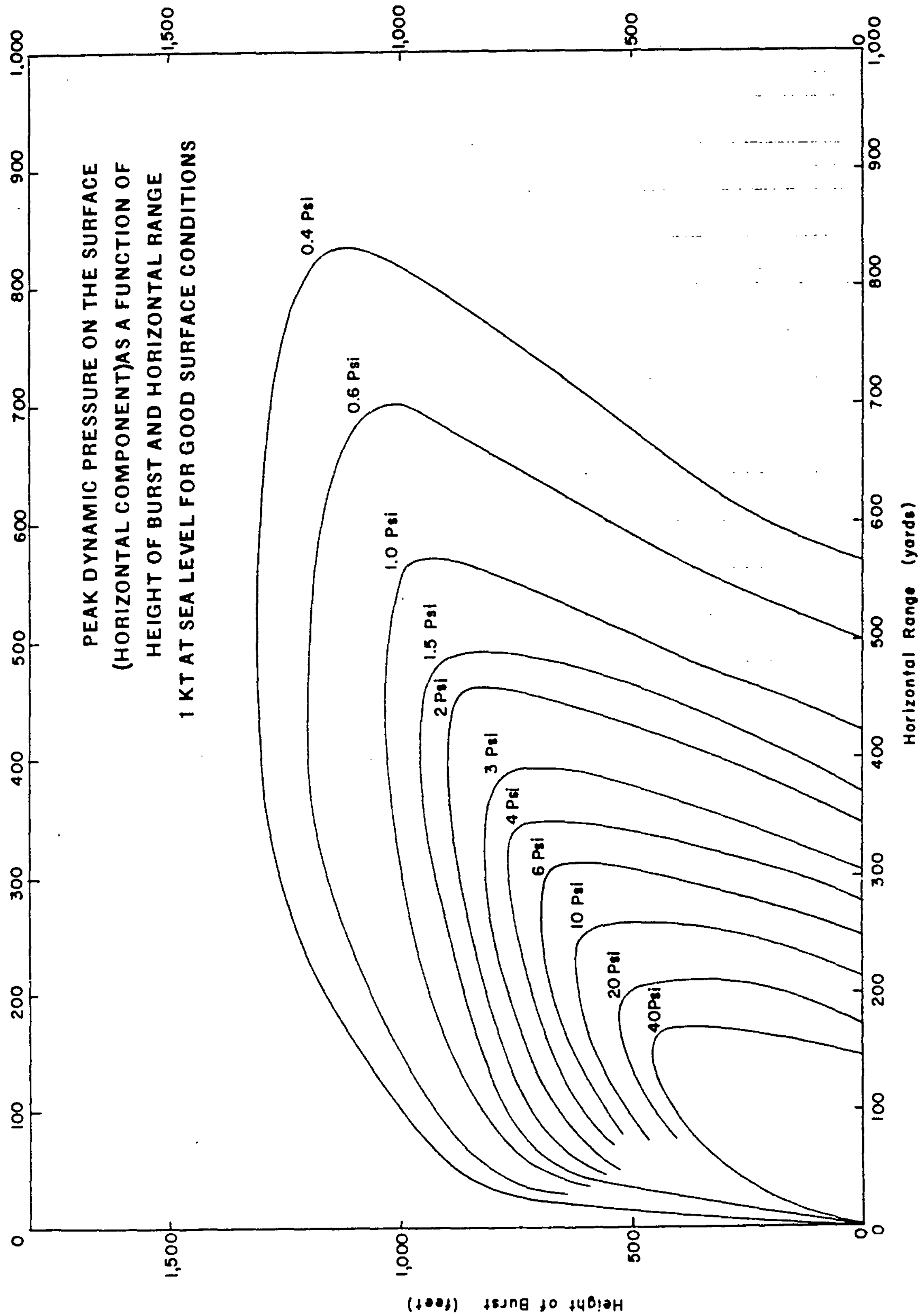
PEAK DYNAMIC PRESSURE ON THE SURFACE
(HORIZONTAL COMPONENT)AS A FUNCTION OF
HEIGHT OF BURST AND HORIZONTAL RANGE
1 KT AT SEA LEVEL FOR GOOD SURFACE CONDITIONS
0.4 Psi
0.6 Psi
1.0 Psi
1.5 Psi
2 Psi
3 Psi
4 Psi
6 Psi
10 Psi
20 Psi
40Psi
Horizontal Range (yards)
Height of Burst (feet)
0
100
200
300
400
500
600
700
800
900
1,000
1,500
1,000
500

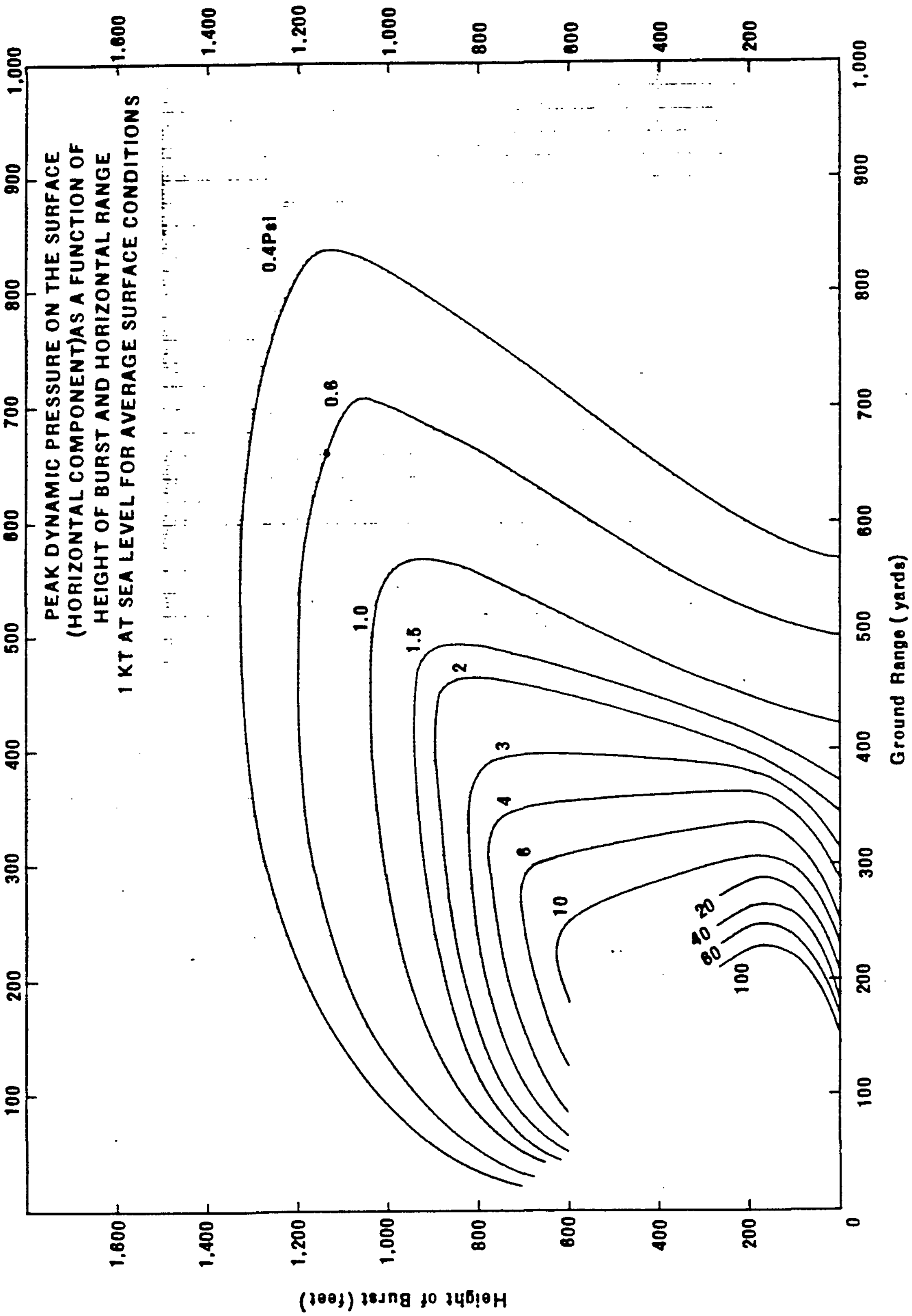
PEAK DYNAMIC PRESSURE ON THE SURFACE
(HORIZONTAL COMPONENT)AS A FUNCTION OF
HEIGHT OF BURST AND HORIZONTAL RANGE
1 KT AT SEA LEVEL FOR AVERAGE SURFACE CONDITIONS
0.4Psi
0.6
1.0
1.5
2
3
4
6
10
20
40
60
100
Ground Range (yards)
Height of Burst (feet)
0
100
200
300
400
500
600
700
800
900
1,000
200
400
600
800
1,000
1,200
1,400
1,600

RAIN OR FOG EFFECTS ON PEAK OVERPRESSURE

Figures 2–14A and 2–14B present range correction factors as a function of height of burst and overpressure for a 1 KT detonation in rain or fog. The range to which a given overpressure would extend under normal conditions is multiplied by the correction factor to account for the presence of the rain or fog.

Scaling. Use the relation:

$$\frac{h_1}{h_2}=\frac{W_1^{1/3}}{W_2^{1/3}},$$

where h_1=height of burst for yield W_1, and h_2= the corresponding height of burst for yield W_2.

Example.

Given: A 30 KT burst at 600 feet in a moderate rain.

Find: The distances to which 8 and 30 psi extend on the ground surface under average surface conditions.

Solution: The corresponding burst height for 1 KT is:

$$h_1=\frac{600\times 1}{(30)^{1/3}}=190 \text{ feet.}$$

From figure 2–10, the ground range for 8 psi overpressure is 380 yards and for 30 psi overpressure is 164 yards for a 1 KT burst. The corresponding ranges for a 30 KT burst are 1,200 yards (for 8 psi) and 530 yards (for 30 psi). From figure 2–14A (moderate rain), the correction factors for a burst at 190 feet are 0.9 (for 8 psi) and >0.99 (for 30 psi).

The range to which 8 psi extends in moderate rain is 1,200×(0.9)=1,100 yards. *Answer.*

The reduction in range for 30 psi is negligible; it therefore extends to 530 yards. *Answer.*

Reliability. At a given range obtained in this manner, overpressures are considered to be reliable within ±40 percent.

Related material. See paragraph 2.1.*d*(2). See also figures 2–9, 2–10, and 2–18.

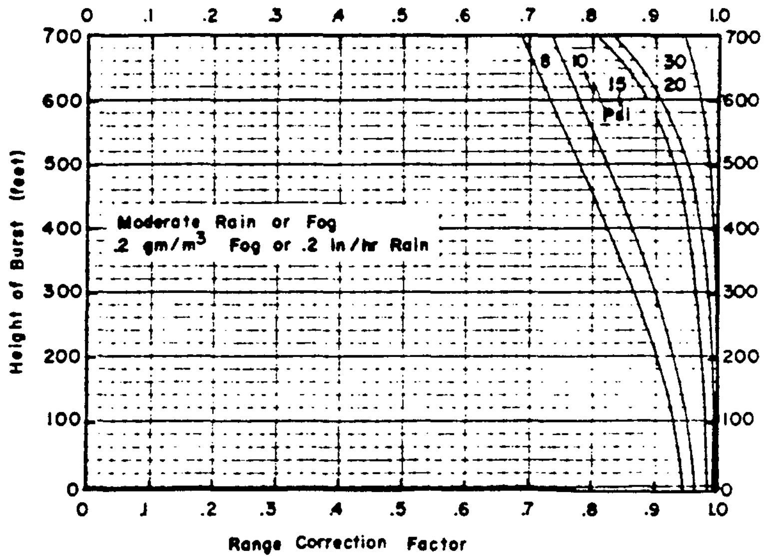

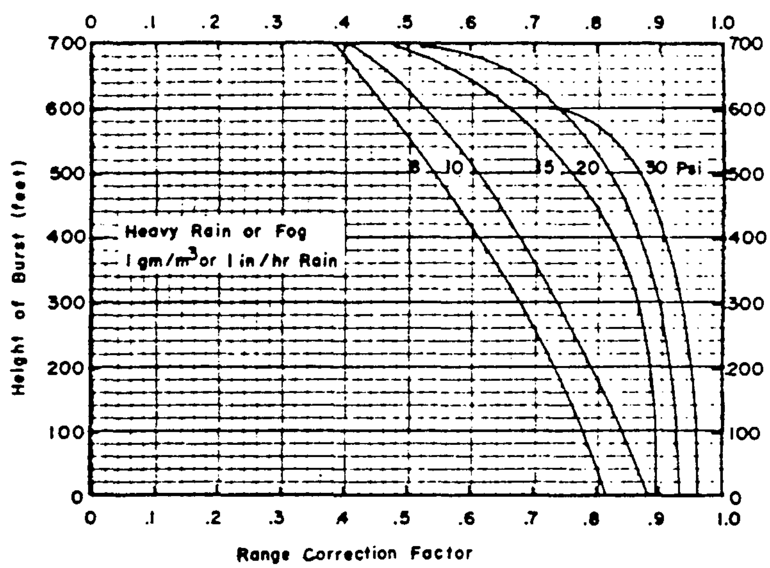

RAIN OR FOG EFFECTS ON PEAK OVERPRESSURE AS A FUNCTION OF HEIGHT OF BURST FOR 1 KT AT SEA LEVEL

CRITERIA FOR PRECURSOR FORMATION

Figure 2-17 gives conditions of burst height and yield for precursor formation over average surfaces, and may be utilized to predict precursor formation if these conditions are known.

Example.

Given: A 100 KT burst at 600 feet over an "average" surface.

Find: Whether or not a precursor may be expected.

Solution: Enter figure 2-17 with a height of burst of 600 feet and a yield of 100 kilotons. The intercept falls within the portion of the figure indicating a precursor will form. *Answer.*

Reliability. Based on data obtained from extensive full scale testing over desert surfaces and limited tests over coral.

Related material.

See paragraphs 2.1*c* and *d*(4), and appendix I.
See also figure 2-16.

CRITERIA FOR PRECURSOR FORMATION(AVERAGE SURFACE CONDITIONS)

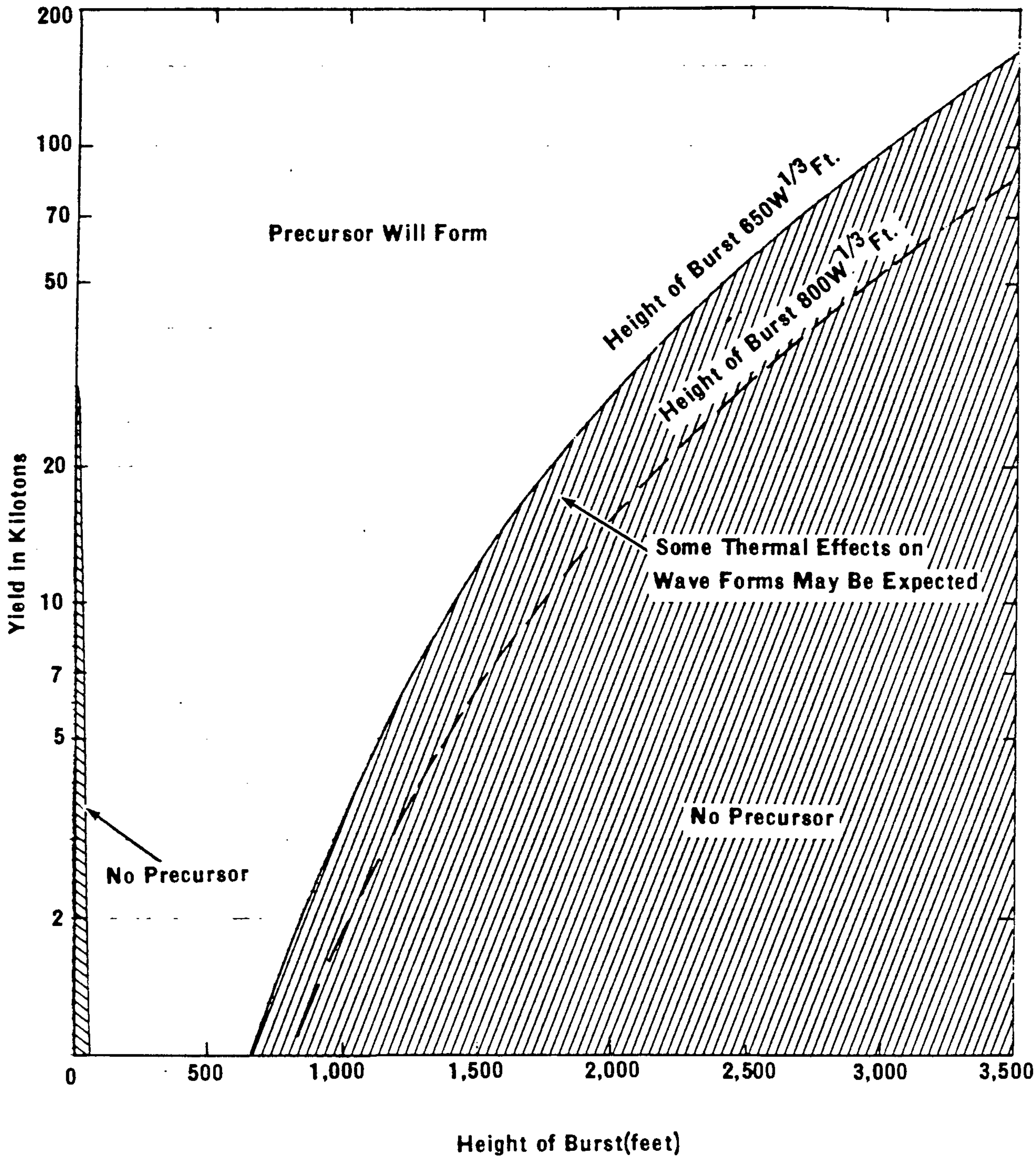

PEAK AIR OVERPRESSURES AT THE SURFACE AS A FUNCTION OF DEPTH OF BURST IN EARTH OR WATER AND HORIZONTAL RANGE

Figure 2-18 is a family of curves representing peak air overpressures on the surface as a function of depth of burst and surface range for a yield of 1 KT.

Scaling. The depth of burst and the range to which a given peak overpressure extends are directly proportional to the cube root of the yield:

$$\frac{d_1}{d_2}=\frac{h_1}{h_2}=\frac{W_1^{1/3}}{W_2^{1/3}}$$

where h_1=depth of burst for yield W_1 KT, h_2=the corresponding depth of burst for yield W_2 KT, d_1=distance to which given overpressure extends for yield W_1 KT, d_2=the corresponding distance to which given overpressure extends for yield W_2 KT.

Example.

Given: A 20 KT weapon burst 60 feet underground.

Find: The peak air overpressure 1,300 yards from surface zero.

Solution: Applying the above scaling to scale to 1 KT,

$$h_1=\frac{W_1^{1/3}\times h_2}{W_2^{1/3}}=\frac{1\times 60}{(20)^{1/3}}=22 \text{ ft},$$

$$\text{and } d_1=\frac{W_1^{1/3}\times d_2}{W_2^{1/3}}=\frac{1\times 1{,}300}{(20)^{1/3}}=480 \text{ yd}.$$

The 22-foot depth line and 480-yard distance line intersect on figure 2-18 at about 4 (± 1) psi. *Answer.*

Reliability. The reliability of pressures taken from figure 2-18 is estimated to be ± 25 percent.

Related material.

See paragraph 2.1*e*.

See also figures 2-9 and 2-10.

FIGURE 2-18

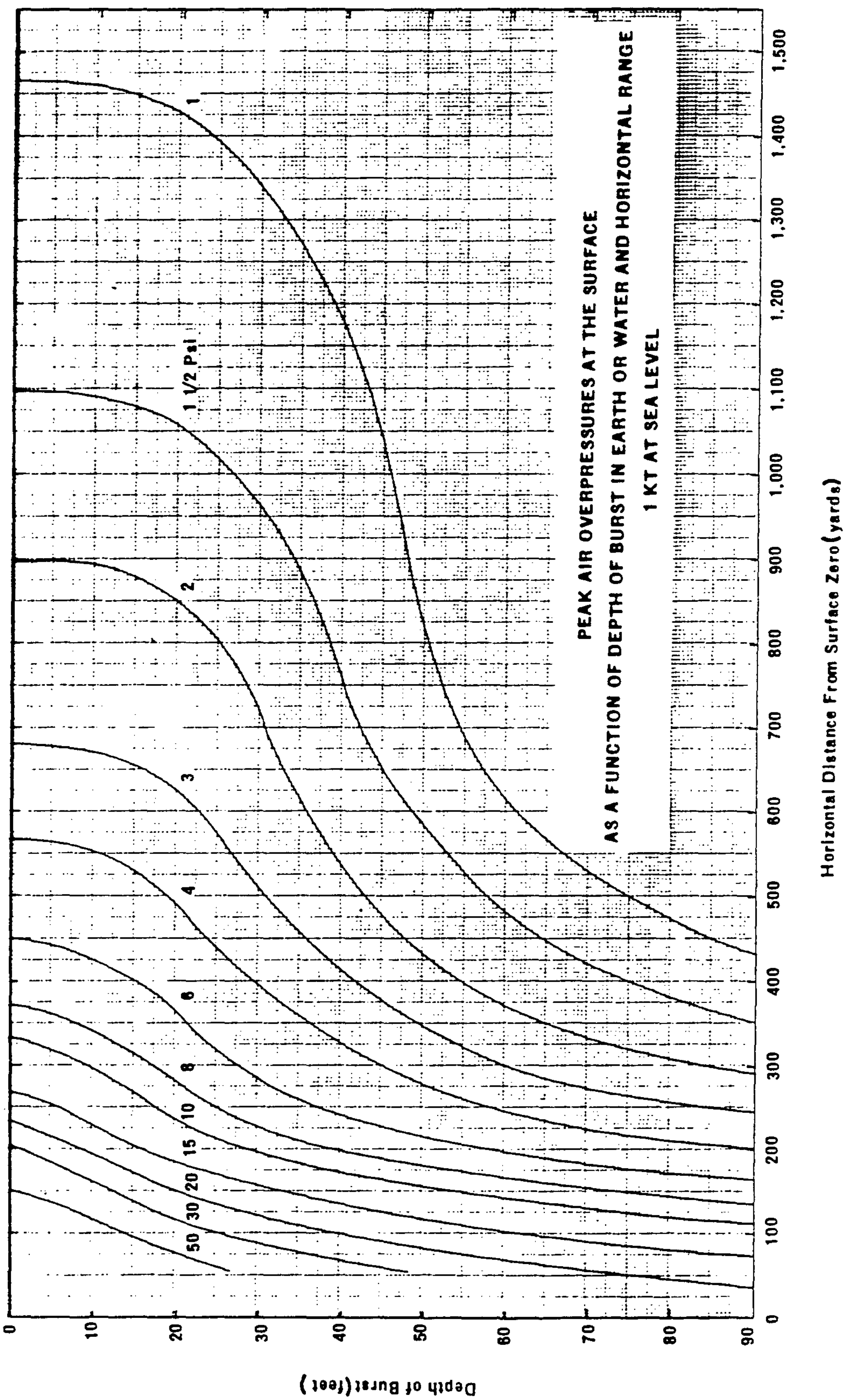
PEAK AIR OVERPRESSURES AT THE SURFACE
AS A FUNCTION OF DEPTH OF BURST IN EARTH OR WATER AND HORIZONTAL RANGE
1 KT AT SEA LEVEL
1
1 1/2 Psi
2
3
4
6
8
10
15
20
30
50
Horizontal Distance From Surface Zero (yards)
0
100
200
300
400
500
600
700
800
900
1,000
1,100
1,200
1,300
1,400
1,500
Depth of Burst (feet)
0
10
20
30
40
50
60
70
80
90

BLANK

Shock,
Craters

2.2 Ground Shock and Cratering Phenomena.

a. Cratering.

(1) *Land.*

(*a*) *General.* Land craters are pits, depressions or cavities formed in the surface of the earth by vaporizing, throwing, compressing and scouring the soil in an outward direction from a nuclear detonation. Usually they are further characterized as to apparent or true craters. The apparent crater is the visible crater remaining after a detonation, while the true crater is the crater excluding fall-back material. The true crater is bounded by a surface which represents the limiting distance from the explosion at which the original material surrounding the apparent crater was completely disassociated from the underlying material. The ensuing discussion of craters from underground bursts assumes weapons with no air space surrounding them, in locations that have been completely backfilled and tamped, and burst under a horizontal ground surface plane. Figure 2–19 shows schematically the dimensions used in describing a crater.

(*b*) *True and apparent craters.* The fall-back zone is the zone between the true and apparent craters as defined above. It contains both disassociated material that has fallen back into the crater and material that, even though disassociated, received insufficient energy to be thrown out of the crater. There is usually insignificant fall-back in craters from air or surface bursts, or bursts at depths less than 25 $W^{1/3}$ feet. Consequently, there is little difference between apparent and true craters from such bursts.

(*c*) *Crater radius and depth.* The crater radius is the average crater radius as measured at the original ground surface and scales as the cube root of the yield. The crater depth is the maximum depth of the crater as measured from the original ground surface and scales as the fourth root of the yield. Estimated crater radii and depths are given in figures 2–20 and 2–21 as functions of burst height and depth for 1 KT. Figures 2–22 and 2–23 are derived from figures 2–20 and 2–21, and present expected crater diameters and depths as functions of yield for specific burst conditions. All figures are directly applicable to dry soil or soft rock (rock that crumbles easily). For other types of soil or rock, crater dimensions may be estimated by multiplying the dimensions taken from figures 2–20 through 2–23 by the appropriate factors shown in the facing pages of these figures.

(*d*) *Crater lip.* The lip of the crater is formed both by fall-back and by the rupture of the soil surrounding the crater. For a deep underground burst, the resulting crater lip is formed primarily from fall-back. For a shallow underground or surface burst on the other hand, the crater lip is formed primarily by the ground nearest the burst shearing and piling up against the soil farther away from the crater. The approximate relative dimensions of the crater lip resulting from a surface burst are indicated in figure 2–19.

(*e*) *Rupture zone.* The rupture zone is characterized by extreme cracking. The zone surrounds the true crater and at the ground surface extends outward approximately 1.5 times the apparent crater. However, for bursts at large scaled depths, the zone at the ground surface extends outward only slightly beyond the true crater. When an explosion occurs in rock, it disturbs the rock in the ruptured zone by causing surface slabbing of local areas, by opening pre-existing cracks, and by developing new fractures tending to be radial from the point of burst. The rupture zone in sand may be difficult to define or may be non-existent.

~~CONFIDENTIAL~~

CRATER PROFILE

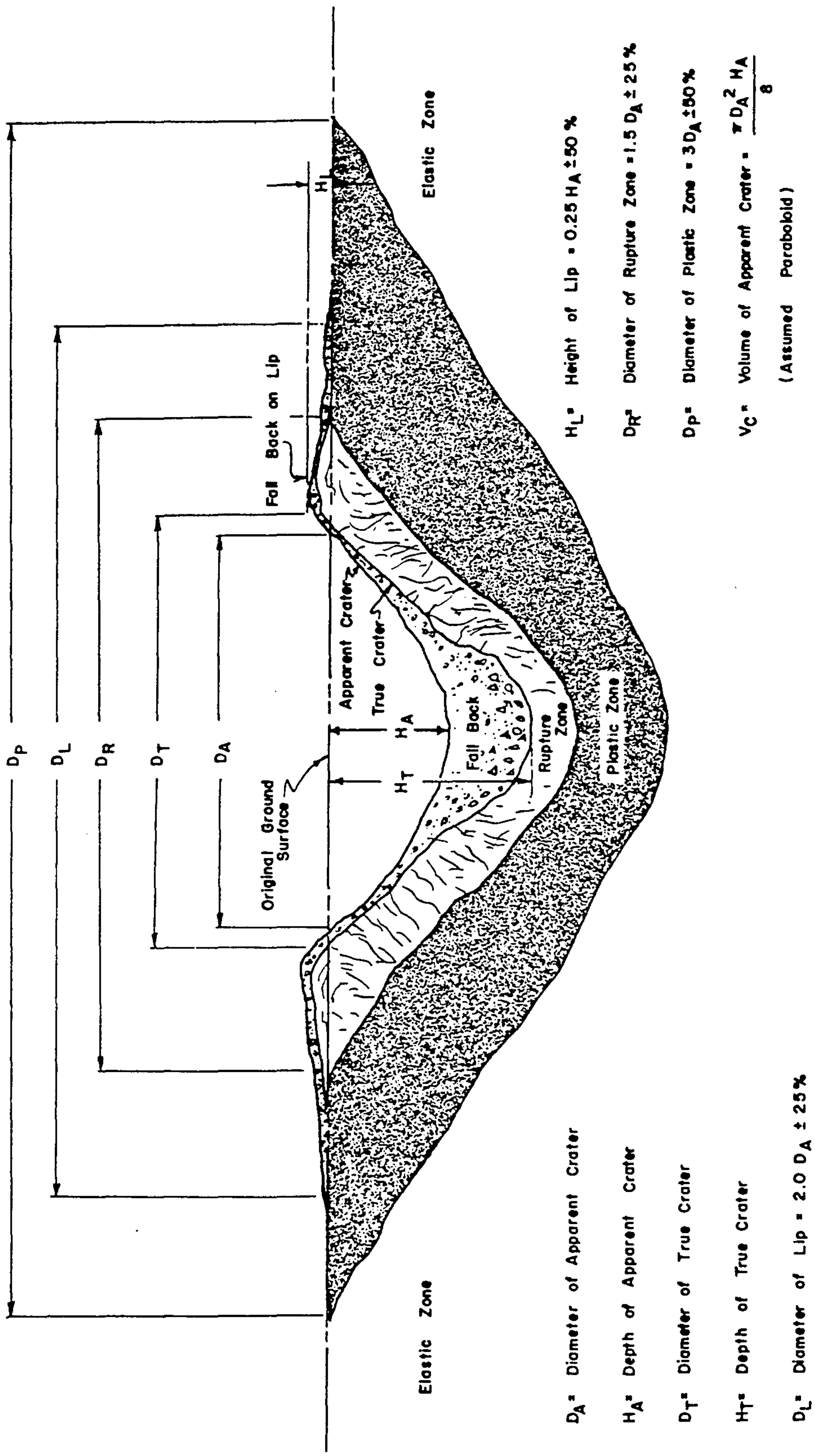

~~CONFIDENTIAL~~

(*f*) *Plastic zone*. In the plastic zone the soil is permanently displaced but without visible rupture. This zone surrounds the rupture zone and may extend outward at the ground surface approximately three times the apparent crater radius. Even for bursts at large scaled depths, where there is an appreciable difference between the true and apparent crater dimensions, the plastic zone still extends considerably beyond the true crater at the surface. In rock, little or no plastic deformation occurs.

(*g*) *Height and depth of burst*. At a height of burst less than about 10 $W^{1/3}$ feet, the expanding gases from a nuclear detonation form a land crater primarily by vaporizing, throwing and compressing the soil in an outward direction from the detonation. As the height of burst decreases from about 10 $W^{1/3}$ feet or the depth of burst increases, the crater radius continues to increase appreciably until a depth of burst of about 25 $W^{1/3}$ feet is reached. Below about 25 $W^{1/3}$ feet, however, the apparent crater radius increases only slightly with increasing depth of burst, and, below a depth of burst of approximately 70 $W^{1/3}$ feet, the apparent crater radius then decreases with increasing depth of burst.

As the height of burst is lowered from about 10 $W^{1/3}$ feet or the depth of burst is increased, the crater depth increases appreciably with increasing depth of burst, until a depth of burst of approximately 60 $W^{1/3}$ feet is reached. Below about 60 $W^{1/3}$ feet, the apparent crater depth increases but slightly with increasing depth of burst, until a depth of burst of about 90 $W^{1/3}$ feet is reached. Below this depth of burst, the fall-back material may form a crater with an apparent depth less than the depth of burst. The true depth of the crater, however, remains greater than the depth of burst by a constant value of approximately 57 $W^{1/3}$ feet when the depth of burst is below about 60 $W^{1/3}$ feet.

For bursts at heights greater than about 10 $W^{1/3}$ feet, the mechanism of cratering is primarily compression and scouring of soil. As indicated in figure 2–20, the crater radius increases for burst heights above 20 $W^{1/3}$ feet, reaching a maximum at about 60 $W^{1/3}$ feet. This results in a crossover of the 50, 100, and 300 foot burst height curves of figures 2–22A and 2–22B. However, this increase in radius is not considered significant, since the crater depth decreases very rapidly with increasing height of burst to relatively small values in the range of crossover. For bursts at heights above about 60 $W^{1/3}$, the crater may be difficult to detect.

(*h*) *Effect of slope*. Crater dimensions are not expected to change materially with ground slope, except for very steep terrain. On very steep slopes, craters will be somewhat elliptical in shape, with the downhill lip considerably wider than the uphill lip. The crater depth with respect to the surface plane of the terrain involved is not expected to be appreciably different from that of a burst under horizontal terrain conditions.

(2) *Underwater*.

(*a*) *General*. An underwater crater is considered to be the crater existing in the bottom material at a time shortly after the burst when conditions are no longer changing rapidly. Subsequent hydraulic wash action by the current, tides, etc. will tend to erode away any crater lip, while making the crater wider and shallower. The degree of this effect depends on the depth of water, type of bottom material, and current, wave, and tidal activity.

(*b*) *Burst geometry*. The size of the underwater crater is dependent upon burst depth, water depth, bottom composition and weapon yield. Figures 2–24 through 2–26 give the crater diameter, depth, and lip height for a burst on the surface and on the bottom in 25, 50, 100, and 200 feet of water. The figures show that the crater dimensions are greater for a bottom burst than for a surface burst. Also for a bottom burst, as the depth of water increases the crater dimensions increase, whereas for a surface burst, as the water depth increases the crater dimensions decrease.

b. Ground Shock.

(1) *General.* The production of ground shock by nuclear explosions is extremely complex, and, in some respects, not well understood. Basically, ground shock may be produced by two separate mechanisms. One mechanism is the sudden expansion of the bubble of gas from a surface or underground explosion which generates a pulse or oscillation in the ground. This is termed "direct ground shock". As this direct shock propagates through the ground, it may be modified by reflections and refractions from underlying bedrock or hard strata, or rarefaction from the air-ground interface. The second mechanism is the production of a ground shock by the air blast wave from a nuclear explosion striking and moving parallel to the ground surface. This is termed "air induced ground shock." For a given burst geometry, except at extremely short ranges, these two forms of ground shock are separated in time. Because the direct ground shock is usually attenuated very rapidly, induced ground shock is more important from the point of view of damage to underground installations, except for extremely close ranges and for deep underground bursts. Figure 2–27A shows in schematic form the relation of these two phenomena in the case of a surface burst. Since sonic velocity is generally higher in ground than in the air, the direct ground shock is indicated as moving faster than the air blast, and consequently faster than the air induced ground shock. Although the direct ground shock and the air blast of a surface or near-surface burst initially propagate approximately together, the velocity of the air blast decreases more rapidly with distance in the higher pressure region than the direct ground shock. Hence, the direct ground shock moves ahead.

Figure 2–27B shows the relation in idealized form of the vertical acceleration caused by the two different forms of ground shock. The direct vertical acceleration is initiated upon arrival of the direct ground shock. The "air blast slap acceleration" is initiated upon the arrival of the air blast which causes a sudden local increase in soil particle acceleration.

The physical mechanisms of major interest in regard to the production of ground shock damage are acceleration, displacement and pressure (or stress). Although extensive measurements have been made, no consistent correlation between these parameters has been found. Each is discussed for both direct ground shock and air induced ground shock in the following paragraphs.

(2) *Direct ground shock.*

(*a*) *Propagation.* The direct ground shock wave produced by a surface or underground burst propagates radially outward from the burst point. For a 1 KT surface or shallow underground burst, in Nevada type soil, propagation velocities on the ground surface are 4,600 feet per second approximately 300 feet from surface zero, and decrease to a more constant 3,500 feet per second approximately 2,500 feet from surface zero. The propagation velocity of ground shock at the surface may increase with distance from the burst due to refraction and reflection from underlying higher velocity strata; and, as the shock reduces to an acoustic wave, the velocity will approach the normal acoustic velocity of the medium near the surface. In sound rock and outside the zone of rupture, the propagation of shock obeys elastic formulae.

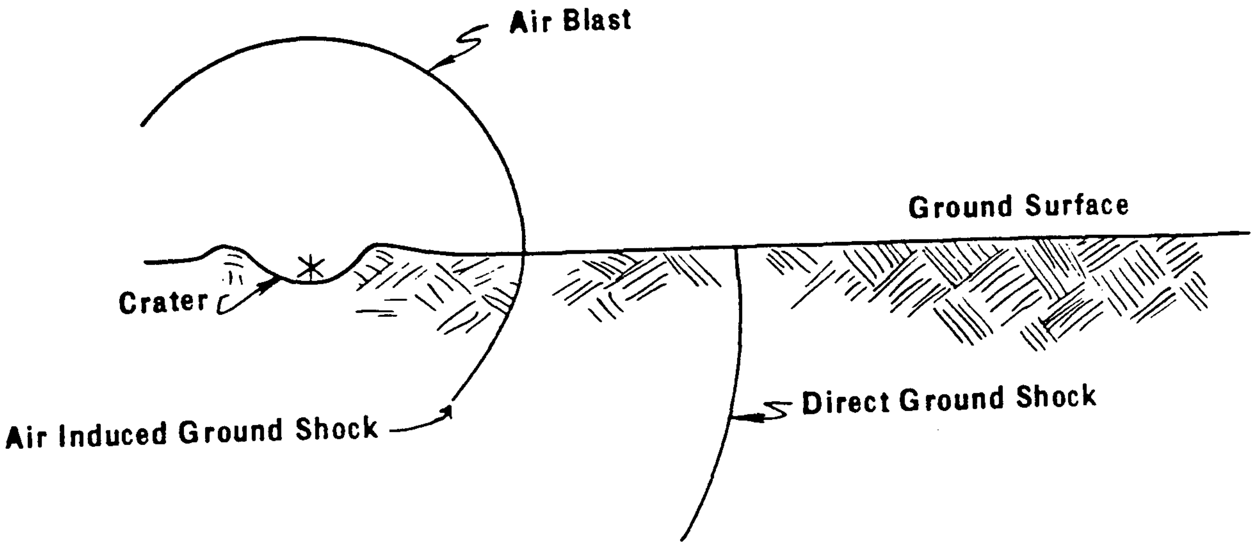

DIRECT AND AIR INDUCED GROUND SHOCK

GROUND ACCELERATION WAVE FORM WITH "SLAP"

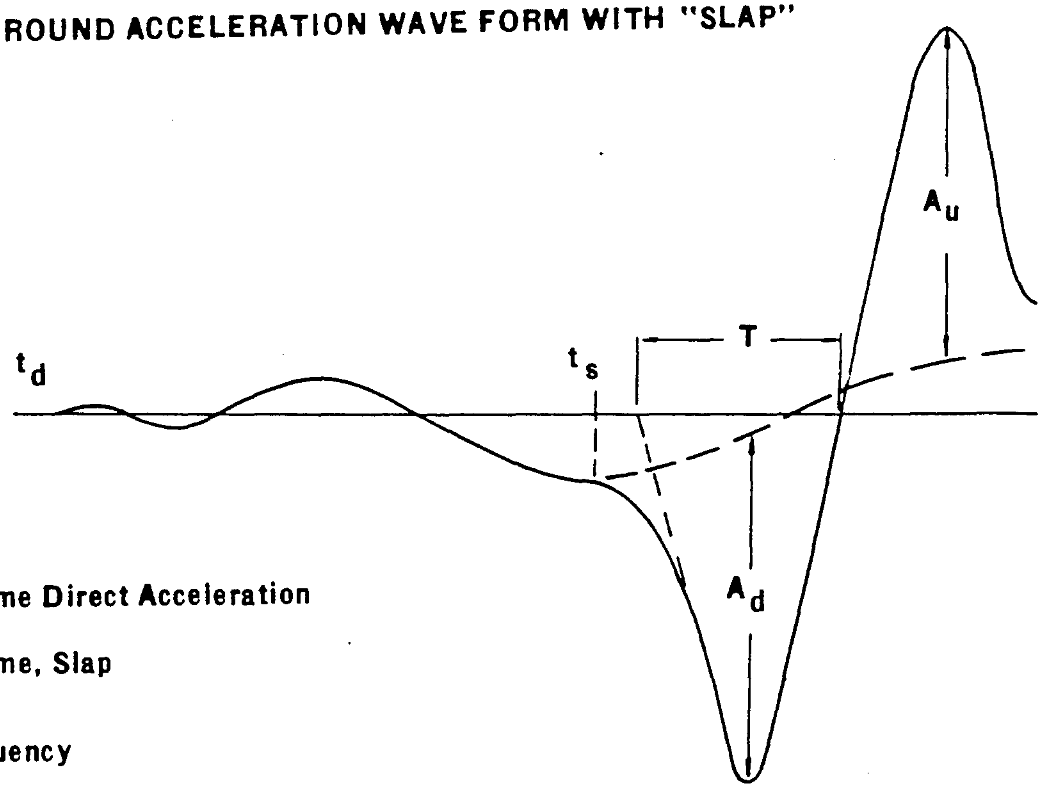

t_d = Arrival Time Direct Acceleration

t_s = Arrival Time, Slap

$\frac{1}{2T}$ = Slap Frequency

A_d = Max. Downward Slap Acceleration

A_u = Max. Upward Slap Acceleration

447555 O - 58 - 7

In such a homogeneous medium (not generally characteristic of surface conditions), there is little attenuation due to internal friction or plastic deformation. Ground shock (compression type wave) in rock is reflected from an air-rock interface as a tensile wave. The intensity of this tensile wave is dependent on shock strength, wave shape, and angle of incidence of the direct shock with the free surface.

(*b*) *Pressure* (*stress*). At any given point air blast or water shock overpressures resulting from a nuclear detonation are equal in all directions, but ground pressures are not. The shear and cohesive strength of the soil change the ground pressure into directional components which differ in magnitude depending upon the direction in which measured. These directional pressure components are termed stress. Under the dynamic loading from a nuclear explosion, the direct ground stresses rise most abruptly in the ground nearest the explosion, whereas at greater distances the peak stresses at any specific point are reduced and the rise times are increased. Stress pulses appear as various combinations of direct ground and air induced shock stresses, depending on arrival time and the range, depth and direction of the measurement. Direct and air induced ground shock stress pulses may coincide at close-in ranges outside the crater, as indicated in (1) above, but will gradually separate with increasing distance along the ground surface until two separate pulses may be detected a few feet beneath the ground surface. The peak stresses from direct ground shock usually attenuate rapidly with distance; however, in highly saturated soils the attenuation of these stresses is less, approaching the attenuation in water (approximately inversely as the range). The stress pulse from the direct ground shock is composed of vibrations of high and low frequencies, the period of which may vary from a few tenths of a second to several seconds. Two hundred feet from a 1 KT underground burst in Nevada type soil, the horizontal earth stress at a depth of 10 feet may be 125 psi; at 250 feet it may be 40 psi; while at 600 feet it may be only 3 psi. A rough comparison of peak stress intensities for various yields at the same distances may be made on the basis of relative crater size.

(*c*) *Acceleration of soil particles*. Acceleration of soil particles may be caused as a direct result of the explosion (direct acceleration), as a result of any shock reflection or refraction from underlying bedrock (indirect acceleration), or as a result of air blast (induced acceleration). Direct and indirect accelerations are generally indistinguishable and together are termed direct or fundamental acceleration. For acceleration values of 1 g or greater measured beyond a range of two crater radii from ground zero the frequency in soil will usually be less than 80 cycles per second for all yields, and for 1 KT the predominant frequencies will be from 3 to 15 cycles per second. In rock, the amplitude of accelerations may be considerably greater and the period may be less than in average soil.

(*d*) *Displacement of soil particles*. Displacement of soil particles is largely permanent within the plastic zone of a crater and transient beyond the plastic zone. For a small, near-surface burst, and at a range of three crater radii, the permanent displacement along the ground surface will probably be less than 0.0003 of a crater radius and the transient displacement will probably be less than 0.001 of a crater radius. A short distance beneath the ground surface, soil particle displacement is usually less than the displacement along the ground surface. Displacements are appreciably affected by soil types. In wet soils, for example, they may be of the order of ten times greater than the preceding values.

(3) *Air induced ground shock.*

(*a*) *Propagation.* Air induced ground shock propagates outward from the burst with the air blast. The air blast loading may be considered as a moving, non-uniform load that generates a ground shock. The air induced shock in soil quickly attains a velocity that may exceed the air blast velocity; however, the magnitude of any outrunning shock is small and its effects may be ignored. Consequently, as the air blast wave proceeds, the air induced ground shock propagates with a rather complex underground time-of-arrival contour depending on underground shock velocities; but, in general, the ground shock front slopes backward from the air blast shock front as shown in figure 2–27A. Air induced ground shock usually arrives with or after the direct ground shock.

(*b*) *Pressure* (*stress*). Air induced ground stress (pressure) is closely related to direct ground stress (pressure) discussed in (2)(*b*) above. Just below the surface, the air induced shock stresses and durations are approximately equal to the changing positive air blast pressure and duration. These induced ground stresses attenuate gradually with depth and the rise time of the stress pulse increases. The pulse of the air induced ground stress is composed of vibrations of high and low frequencies, the periods of which may vary from a few tenths of a second to several seconds. In general, air induced ground stress is larger than direct ground stress at distances greater than two crater radii for average soils, and for all heights and depths of burst down to about 75 feet for 1 KT.

(*c*) *Acceleration of soil particles.* Air blast induced acceleration maintains its identity in the acceleration pattern and can be separated from the direct shock acceleration. When interactions with other accelerations from reflection and refraction occur, the magnitude is affected markedly and separation is difficult. Upon its arrival, the air blast will cause a sudden local increase in soil particle acceleration termed "air blast slap acceleration" (see fig. 2–27B). For acceleration values of 1 g or greater measured away from ground zero, the predominant frequencies in soil of air blast induced acceleration are 20 to 120 cycles per second. Peak vertical accelerations are larger than peak horizontal (radial) accelerations by an amount approximating 50 percent. Peak accelerations attenuate with depth and are directly proportional to the overpressure and indirectly proportional to the rise time of the pressure pulse in the soil. See figure 2–28 for the relationship of peak accelerations to peak air blast overpressures at a depth of 10 feet.

(*d*) *Displacement of soil particles.* Air induced ground shock causes little permanent horizontal displacement of ground particles beyond two crater radii. When the shock is reflected from vertical soil-air interfaces, local displacement (spalling) of ground particles may occur. Air induced ground shock may cause a vertical displacement of soil particles. Dry Nevada type soil subjected to a peak overpressure of 250 psi has sustained a permanent downward displacement of approximately 2 inches and a transient downward displacement of approximately 8 inches.

c. Column and Base Surge. A general discussion of the column and base surge resulting from an underground burst has been given in paragraph 1.4*e*(4). The maximum column diameter is generally 2 to 3 times the apparent crater diameter and the maximum column height is roughly equal to 400 $W^{1/3}$. The characteristics of the base surge depend upon the depth and yield of burst. The shallowest burst depth at which an earth base

FIGURE 2-30

EFFECT OF CUT-OFF ON THE SHAPE OF THE POSITIVE PULSE

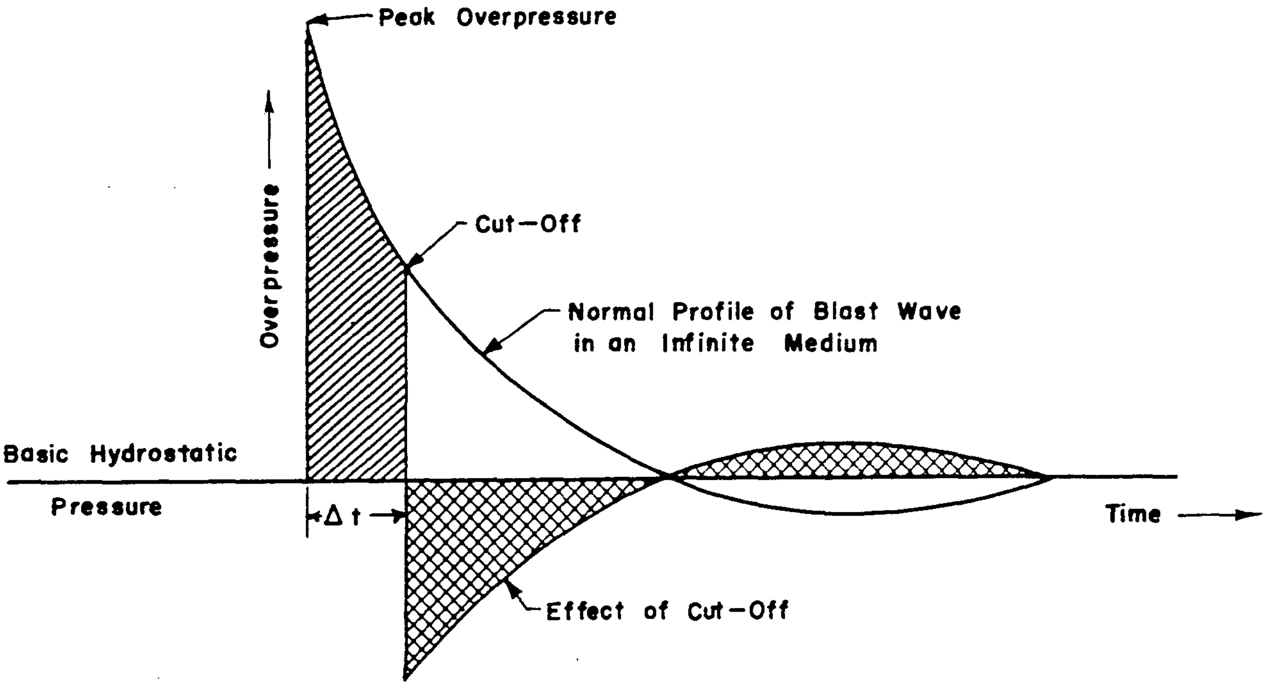

$$(\Delta t \text{ in msec} = \frac{0.4 \times (\text{Bomb Depth in Ft}) \times (\text{Target Depth in Ft})}{\text{Slant Range in Ft.}}$$

surge has been observed is 16 $W^{1/3}$ feet. As the burst depth is increased, the extent of the base surge is expected to increase until a burst depth of about 125 $W^{1/3}$ feet is attained. No further increase in base surge extent is expected below this depth of burst. Figure 2–29 shows the rate of growth of the base surge and maximum radii for various scaled depths of burst.

2.3 Water Shock and Surface Phenomena

a. *Water Shock.*

(1) *General.* The underwater detonation of a nuclear weapon at a distance from either the water surface or the bottom boundaries produces a shock wave early in the formation of the bubble. This shock wave propagates spherically at the rate of roughly 5,000 feet per second, and is characterized by an instantaneous rise in pressure followed by an exponential decay. In addition to this initial primary shock wave, several subsequent pressure pulses are produced within the water (see par. 1.4*f*(2) and (3)).

(2) *Burst geometry.*

(*a*) *Deep burst in deep water.* When the pressure wave is reflected from the water surface it is reflected as a rarefaction or tensile wave. This reflected rarefaction wave cuts off the tail of the primary compressional shock wave, thereby decreasing the duration of its positive phase. Figure 2–30 shows qualitatively the effect of the reflection wave upon the pressure-time history. The effect of this "cut-off" decreases rapidly with depth of the target in the water; that is, the deeper a target, the less the effect of cut-off for the same depth of detonation. Likewise, the greater the depth of detonation, the less the effect of cut-off for the same target location. The reflection of pressures from the bottom surface is similar to the reflection of pressures from the ground surface for an airburst. A crude approximation of the magnitude and shape of this

FIGURE 2-32

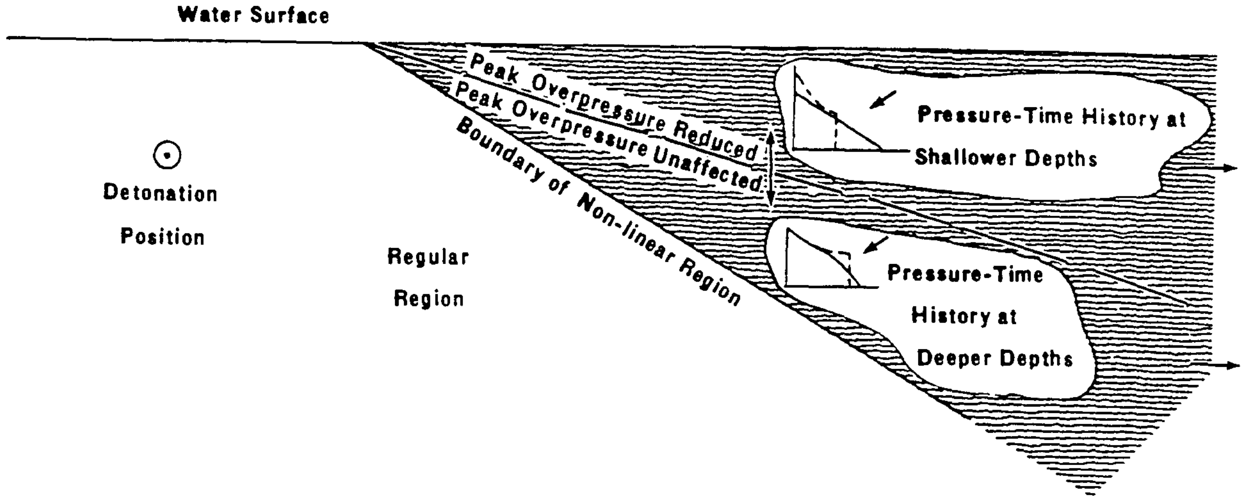

NON-LINEAR SURFACE REFLECTION EFFECTS

reflected water shock wave can be obtained by assuming that this wave is identical to an imaginary direct wave which has traveled a distance equal to the path distance of the reflected wave, i. e., that perfect reflection occurred. Estimated peak overpressure vs. slant range for various yields are shown in figure 2–31, where the order of magnitude of these pressures may be noted. However, the durations of these pressures are short, being measured in tens of milliseconds. They may even be shorter at points near the water surface, where the surface reflected wave arrives at the point before the complete passage of the primary compressional wave.

(*b*) *Shallow burst in deep water.* If the weapon is fired at shallow depths in deep water, the peak overpressure estimates of figure 2–31 overestimate actual overpressures for most regions of interest. For example, a 10 KT weapon fired at a depth of 200 feet in deep water would develop a peak overpressure of approximately 350 psi at a point which is at a range of 2,000 yards and at a depth of 50 feet, instead of the 550 psi predicted by the figure. This reduction is the result of the initial shock wave striking the water surface at a high obliquity and reflecting in an anomalous manner. The sharp cut-off from the reflected pressure does not occur; rather, the reflected tensile wave modifies the pressure-time history at early times and forms a nearly triangular pulse (see fig. 2–32). The region wherein this anomalous reflection affects the pressure history is termed the "non-linear" region. This non-linear region is in the form of a wedge, increasing in depth as the range from the burst point increases. At the shallower depths in this region, the anomalous behavior is sufficient to reduce the magnitude of the initial peak overpressure. At deeper depths the effect shades off, until only at the later times of the pressure history is there any reduction of overpressure. As the depth of burst is raised or the yield increased, the non-linear zone increases in scope and magnitude. Finally, for a surface burst, all points beneath the water surface (except those directly under the weapon) are in the non-linear region. Because the peak pressure in the non-linear region is a sensitive function of burst and target geometry, pressure-distance curves are not presented to account specifically for this effect. In the damage curves of part two, however, the non-linear effect is incorporated in the damage estimates for targets and bursts at shallow depths.

(c) *Shallow water burst.* When a nuclear weapon is detonated in shallow water, both the reflecting boundaries of the water surface and the bottom alter the peak pressure and duration of the primary underwater shock wave. In addition to the multiple reflections that occur, the shock wave is transmitted across these boundaries (i. e., propagated through the air and the bottom and then coupled back into the water). Hence, at a point distant from the source, there will be a direct water shock, water shocks induced by ground and air shocks, and water shocks reflected from the surface and the bottom. The order of arrival will be: first, the ground induced shock; then, the direct shock with the reflections; and finally, the air induced shocks (see fig. 2–33). At most scaled depths, the direct water shock is the greatest. As the direct shock travels outward, the rate of attenuation with distance is primarily determined by the depth of water and the relative position of the weapon within that depth. The shallower the depth of water and/or the closer the weapon to the water surface, the greater the rate of attenuation. This difference in attenuation can be attributed to the non-linear surface reflection and to the interference of multiple reflection waves with the direct shock wave. These effects far outweigh any apparent yield increase as a result of the weapon being detonated on the bottom, as occurs in the case of the land surface burst. Insufficient data exist for the preparation of water overpressure versus distance curves for detonations in shallow water, as is possible for deep water detonations. In the case of a 20 KT detonation at mid-depth in 180 feet of water, the peak overpressures at moderate ranges have been observed to be on the order of one-half those indicated for deep water. Pressures even less than these are expected for a mid-depth burst in more typical harbor conditions because of the shallower depths of water and bottom irregularities. On the other hand, a burst on the bottom will result in slightly higher peak overpressures than one at mid-depth in shallow water.

(3) *Cavitation collapse.* Since water has no tensile strength, the rarefaction resulting from a reflection at the water-air interface causes the water surface to cavitate. Thus, a "spray dome" is formed. When this collapses, an additional shock is induced in the water by an effect similar to water hammer. Little is known about the magnitude of the shock from this source; however, it is believed that it can generally be neglected.

(4) *Refraction.* The propagation of the underwater shock waves is distorted on passing through regions of sharp temperature changes within the water, with the result that the pressure wave form is affected. If the weapon is fired in close proximity to a region of temperature change, there is a shadow zone formed, wherein predictions based upon free water conditions overestimate the effectiveness of the shock wave. When the weapon is fired well above or below this temperature region, pressure histories at the normal ranges of interest are changed very little.

b. Waves.

(1) *General.* Surface waves generated by underwater explosions are the result of the emergence and collapse of the bubble. The first wave is generally a well defined breaking wave. (In the case of a deep burst in deep water, this wave was first observed at roughly 2,000 feet horizontal range.) The first wave is followed by a

WAVE FRONT PROPAGATION IN SHALLOW WATER

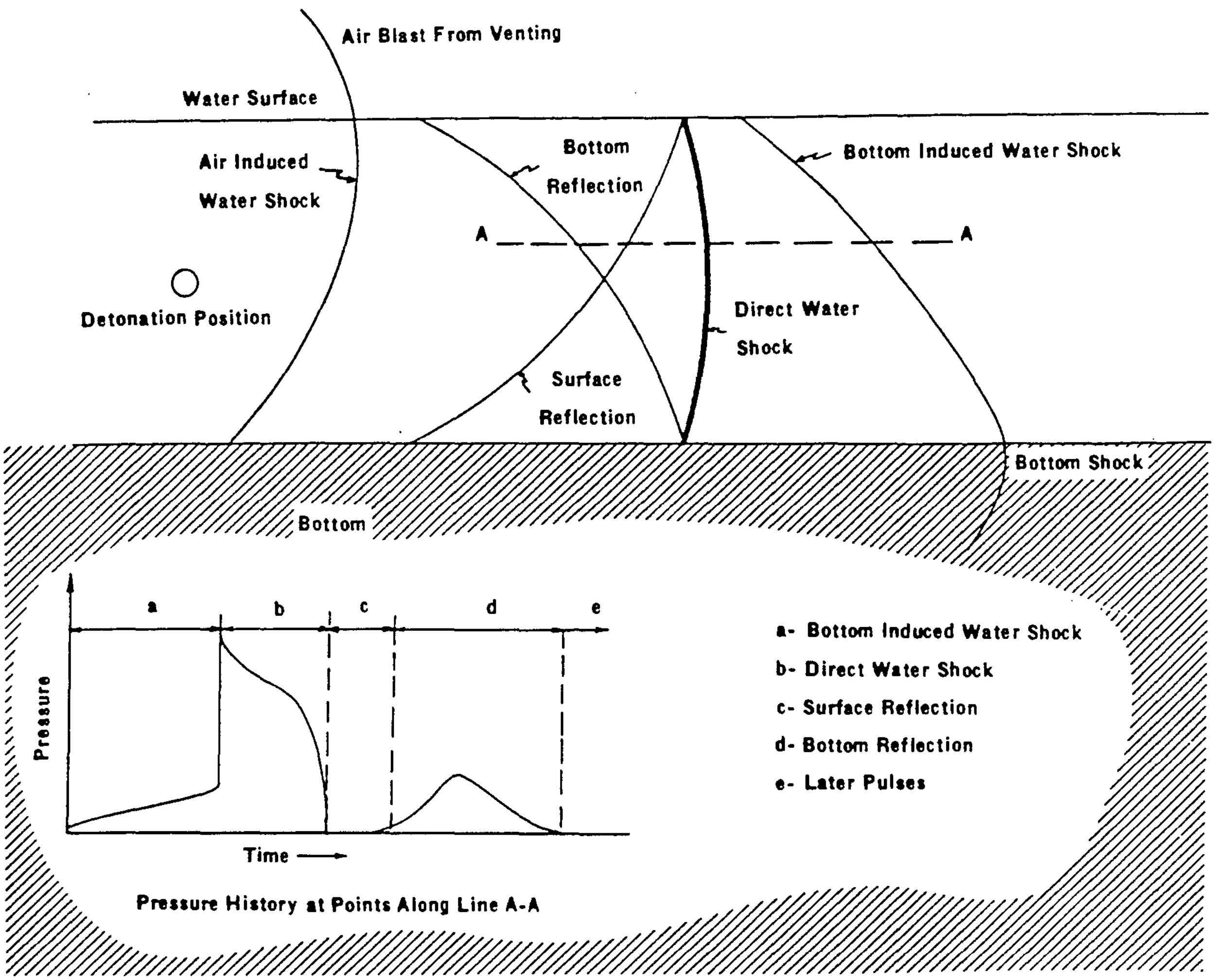

train of more stable oscillatory waves. As the disturbance moves outward, the number of waves in the wave train increases. At first, the initial wave of the group is the highest, but as the wave train progresses farther from the origin, the maximum wave height appears in successively later waves. It has been observed for a shallow water burst that by the time the wave train had progressed out to 22,000 feet the ninth wave was the highest of the group; while for a deep water burst at 10,000 feet the seventh wave was observed to have the largest amplitude. For the shallow water burst, the maximum wave height one mile from the detonation was about 20 feet; for the deep burst it was about 40 feet at the same distance, reflecting the greater depth of water and burst depth in the latter case. Figure 2–34 gives maximum wave heights as a function of range, under a number of stated conditions for a 1 KT underwater burst. These predictions are based upon the maximum wave passing the point of interest without regard to its position in the train. Thus, the maximum crest-to-trough amplitude decreases linearly as the reciprocal of distance, while the amplitude change with distance for any individual wave varies in a more complex manner. In a given depth of water, a wave no higher than about 0.7 times the water depth can propagate as a stable phenomenon. Higher waves are unstable and decrease in height until stability is attained.

(2) *Burst geometry.*

(*a*) *Shallow water burst.* The formation, propagation and magnitude of surface waves generated by an underwater burst in shallow water vary rapidly with the scaled depth of water and the configuration of the bottom. For prediction purposes in water shallower than 80 $W^{1/4}$ feet, the burst position has little effect on the wave generation.

(*b*) *Deep water burst.* For the underwater burst in deep water, the size of the surface waves generated is dependent upon the position of the weapon relative to the surface. For practical purposes, as the depth of burst is lowered from the surface to a depth of 180 $W^{1/4}$ feet, the maximum wave height can be considered to increase constantly. The scaled depth of 180 feet (two-thirds of the maximum bubble radius of a 1 KT burst) represents an optimum depth. With further increases in depth, the maximum height again drops off, approaching the scaled magnitude of waves observed from a burst at deep depth (scaled depth of burst of 850 $W^{1/4}$ feet).

(3) *Terminal waves.* Waves moving from deep into shallow water, or from open water into narrows, may be considerably increased in magnitude, but this increase is unpredictable unless the exact geometry of the bottom is known. Waves "break" on arriving at water depths about equal to the wave height, momentarily increasing in height by approximately 30 percent, then rapidly decreasing.

c. Column and Base Surge.

(1) *Shallow burst.* For depths of detonation less than 10 $W^{1/3}$ feet, the formation of a significant base surge is unlikely. When the detonation is at a greater depth, but one shallow enough that the gaseous explosion bubble vents the surface while it is still expanding to its first maximum radius, an extensive column of water is thrown into the air. The collapse of this column forms the base surge. An example of such a shallow shot is illustrated in figure 1–5. In this shot, a conical spray dome began to form about four milliseconds after the explosion. Its initial rate of rise was greater than 2,500 feet per second. A few milliseconds later, a hollow column began to form, rapidly overtaking the spray dome. The maximum height attained by the column of water was probably some 8,000 feet, and the greatest diameter was about 2,000 feet. The maximum thickness of the walls of the column was about 300 feet. Approxi-

mately 1,000,000 tons of water were thrown into the air. As the column fell back into the water, there developed on the surface, at the base of the column, a large doughnut-shaped cloud of dense mist. This cloud, called the base surge, formed about 10 seconds after detonation and traveled rapidly outward at an initial velocity greater than 100 feet per second, maintaining an ever-expanding doughnut-shaped form. In the first 100 seconds, the average velocity was 63 feet per second. In 180 seconds, the surge traveled 8,100 feet.

(2) *Deep burst.* If the detonation is at a depth such that the bubble goes through several oscillations prior to venting, a bushy, ragged plume-like mass of water is thrown into the air by the emerging bubble (see fig. 1–6). The collapse of these plumes generates the base surge. For this deep burst, the first visible surface phenomenon was a very flat spray dome some 7,000 feet in radius and 170 feet in height. Three seconds later a second spray dome emerged out of the first, sending spikes to a height of 900 feet. At 10 seconds the plumes appeared, reaching a height of 1,450 feet and a diameter of 3,100 feet. As the plumes collapsed, a base surge spread out laterally to a cross wind radius of 4,600 feet at 90 seconds and approximately 7,000 feet at 15 minutes.

(3) *Intermediate depths.* At intermediate depths of burst, such that the bubble vents after the first expansion is completed but before several oscillations are completed, the magnitude of the base surge varies in a manner dependent upon the phase of the bubble at venting, together with the motion of the water surrounding the bubble at venting. When the bubble vents in an expanding phase the surge phenomenon is similar to that described for a shallow burst. When the bubble vents in a contracting stage, a tall spire of water is jetted into the air. The base surge resulting therefrom is less dense and of a smaller final radius. However, lack of knowledge of bubble behavior permits only a coarse prediction of the maximum size of base surge.

(4) *Growth.* Figure 2–35A gives the radius of the base surge as a function of time for a 1 KT yield at various depths of burst. Figure 2–35B gives the maximum radius of base surge as a function of yield for several specific depths of burst. Winds cause the surge to travel faster in the direction in which the wind is blowing. Although relative humidity does not affect the initial formation of the base surge, it does influence its subsequent growth and duration. When the relative humidity is significantly less than 70 percent, the extent and duration of the base surge are apt to be less than predicted. A significant increase in extent and duration of the base surge is expected when the relative humidity is appreciably greater than 70 percent.

CRATER RADIUS VS. BURST POSITION IN DRY SOIL OR SOFT ROCK

Figure 2–20 gives the estimated apparent and true crater radius as a function of burst position for 1 KT bursts in dry soil or soft rock. For other soils, multiplication factors should be used as follows:

Relative crater radius factors

Soil type	*Factor*
Hard rock (granite and sandstone)	0.8
Saturated soil (water slowly fills crater)	1.5
Saturated soil (water rapidly fills crater)*	2.0

*Only for apparent craters with sloughing or washing action on the crater sides.

Scaling. The following relation can be used to estimate corresponding crater radii for a given burst yield and depth:

$$\frac{d_1}{d_2}=\frac{W_1^{1/3}}{W_2^{1/3}}=\frac{h_1}{h_2}$$

where d_1=crater radius produced by a yield W_1 at burst height or depth h_1, and d_2=crater radius produced by a yield W_2 at burst height or depth h_2.

Example.

Given: An 80 KT burst at a depth of 50 feet in dry sand.

Find: The apparent crater radius.

Solution: The burst depth for 1 KT is:

$$h_1=\frac{50\times 1}{(80)^{1/3}}=12 \text{ feet.}$$

From figure 2–20 the apparent crater radius (and also the true crater radius) for 1 KT is 93 feet. Hence, the crater radius for 80 KT is:

$$d_2=\frac{93\times(80)^{1/3}}{1}=400\ (\pm 120) \text{ feet.} \quad \textit{Answer.}$$

Reliability. The reliability of crater radii values obtained from figure 2–20 is estimated to be ±30 percent for burst heights of 5 $W^{1/3}$ feet to burst depths of 65 $W^{1/3}$ feet for all yields above 1 KT. For other burst conditions the reliability is estimated to be ±40 percent.

Related material.

See paragraphs 1.4*d*(4), *e*(6) and 2.2*a*(1).

See also figures 2–19 and 2–21 through 2–26.

FIGURE 2-20

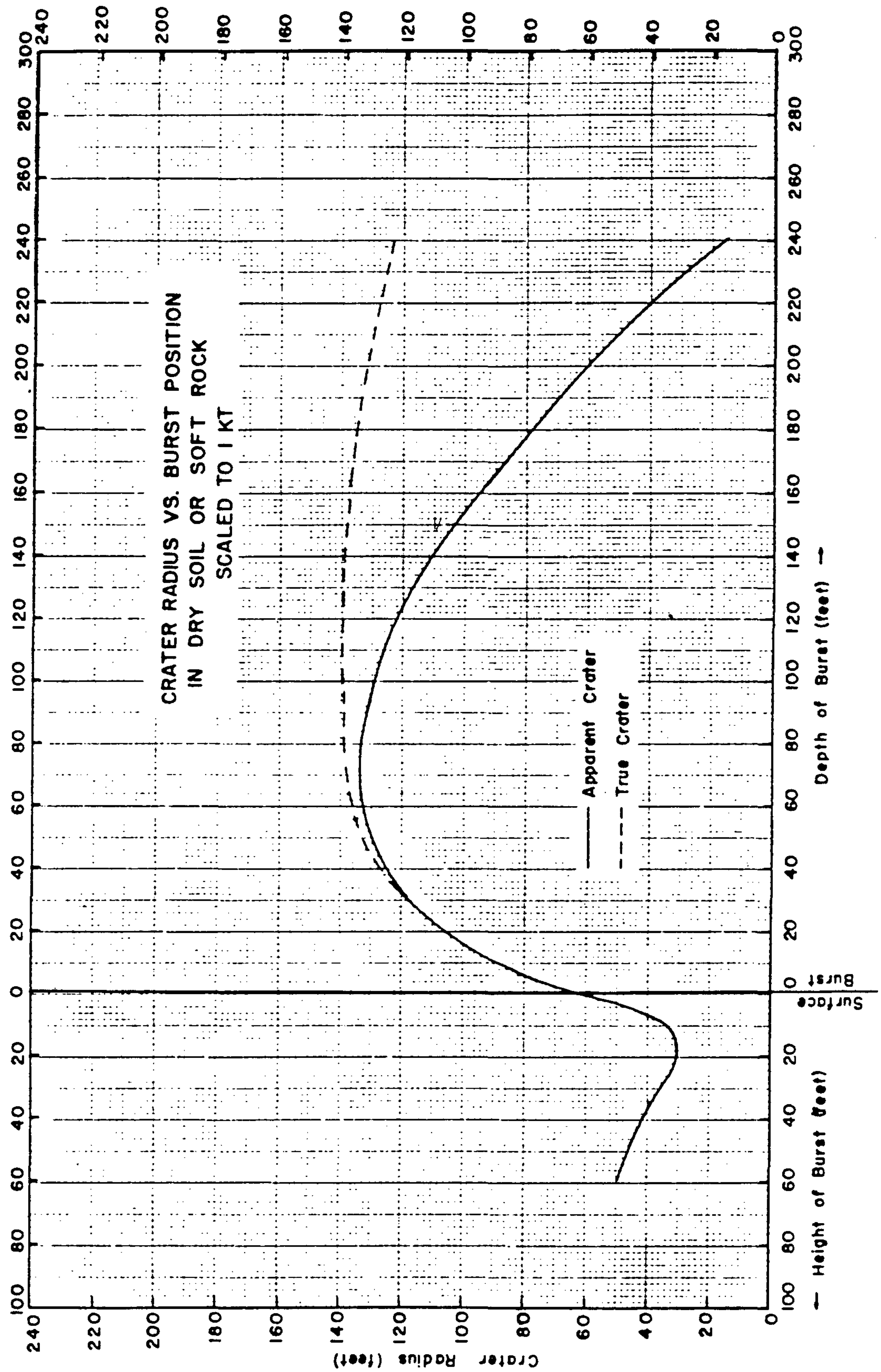
CRATER RADIUS VS. BURST POSITION
IN DRY SOIL OR SOFT ROCK
SCALED TO 1 KT
Apparent Crater
True Crater
Depth of Burst (feet)
Height of Burst (feet)
Surface
Burst
Crater Radius (feet)

CRATER DEPTH VS. BURST POSITION IN DRY SOIL OR SOFT ROCK

Figure 2–21 gives the estimated apparent and true crater depth as a function of burst position in dry soil or soft rock. Multiplication factors for other soils are as follows:

Relative crater depth factors

Soil type	*Factor*
Hard rock (granite and sandstone)	0.8
Saturated soil (water slowly fills crater)	1.5
Saturated soil (water rapidly fills crater)*	0.7

*Only for apparent craters with sloughing or washing action on the crater sides.

Scaling. For yields other than 1 KT, the following relations can be used to estimate corresponding crater depths for a given burst yield and depth:

$$\frac{h_1}{h_2}=\frac{W_1^{1/3}}{W_2^{1/3}} \text{ and } \frac{d_1}{d_2}=\frac{W_1^{1/4}}{W_2^{1/4}},$$

where d_1=crater depth produced by a yield W_1 at burst height or depth h_1, and d_2=crater depth produced by a yield W_2 at burst height or depth h_2.

Example.

Given: An 80 KT burst at a depth of 50 feet in wet sand of an ocean beach where water will rapidly fill the crater.

Find: Apparent crater depth.

Solution: Corresponding burst depth for 1 KT is:

$$h_1=\frac{50\times 1}{(80)^{1/3}}=12 \text{ feet.}$$

From figure 2–21 the crater depth for 1 KT at 12 feet=37 feet.

Crater depth (d_2) for 80 KT at 50 feet$=\frac{37\times(80)^{1/4}}{1}=111$ feet.

From the soil type table above, the factor for relative crater depth in saturated soil (where water rapidly fills crater) is 0.7. The crater depth is therefore $0.7\times 111=78$ (± 39) feet. *Answer.*

Reliability. The reliability of crater depths taken from figure 2–21 is estimated to be ± 50 percent for all yields and burst positions.

Related material.

See paragraphs 1.4*d*(4), *e*(6) and 2.2*a*(1).

See also figures 2–19, 2–20, and 2–22 through 2–26.

FIGURE 2-21

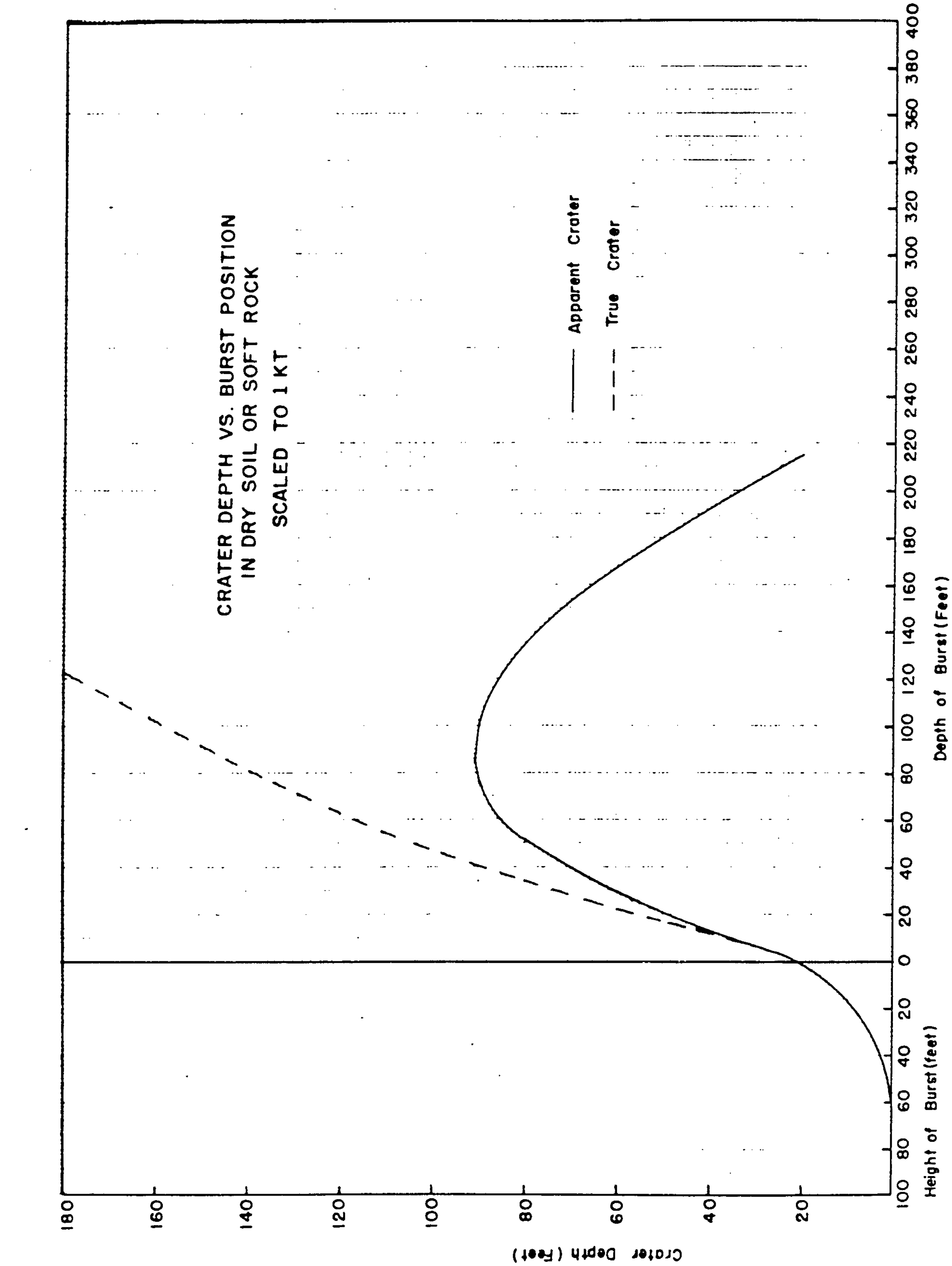
CRATER DEPTH VS. BURST POSITION
IN DRY SOIL OR SOFT ROCK
SCALED TO 1 KT
Apparent Crater
True Crater
Depth of Burst (Feet)
Height of Burst (feet)
Crater Depth (Feet)
180
160
140
120
100
80
60
40
20
400
380
360
340
320
300
280
260
240
220
200
180
160
140
120
100
80
60
40
20
0
20
40
60
80
100

BLANK

APPARENT CRATER DIAMETER VS. YIELD IN DRY SOIL OR SOFT ROCK

Figures 2–22A and 2–22B give values of apparent crater diameter vs. yield for various depths and heights of burst, derived by scaling from figure 2–20. No interpolation of depth or height of burst should be made for this figure. For values other than those given, use figure 2–20. Since there is little difference between true and apparent crater diameters from bursts at depths less than 25 $W^{1/3}$ feet or from above-ground bursts, these figures may be used also for true craters in that range. The assumed soil type is dry soil or soft rock (rock that will crumble or fall apart easily). For other soils, the diameter obtained from figure 2–22A or 2–22B should be multiplied by the relative crater dimension factor as follows:

Relative crater diameter factors

Soil type	*Factor*
Hard rock (granite and sandstone)	0. 8
Saturated soil (water slowly fills crater)	1. 5
Saturated soil (water rapidly fills crater)*	2. 0

*Only for apparent craters with sloughing or washing action on the crater sides.

Example.

Given: A 30 KT burst at a depth of 100 feet in dry clay.

Find: The apparent crater diameter.

Solution: The apparent diameter, taken directly from the 100 foot depth of burst curve of figure 2–22A for 30 KT is 750 (±225) feet. *Answer.*

Reliability. The reliability of crater diameters obtained from figures 2–22A and 2–22B for various yields is estimated to be ±30 percent for burst heights of 5 $W^{1/3}$ feet to burst depths of 65 $W^{1/3}$ feet for all yields above 1 KT. For other burst conditions, the reliability is estimated to be ±40 percent.

Related material.

See paragraphs 1.4*d*(4), *e*(6) and 2.2*a*(1).

See also figures 2–19 through 2–21 and 2–23 through 2–26.

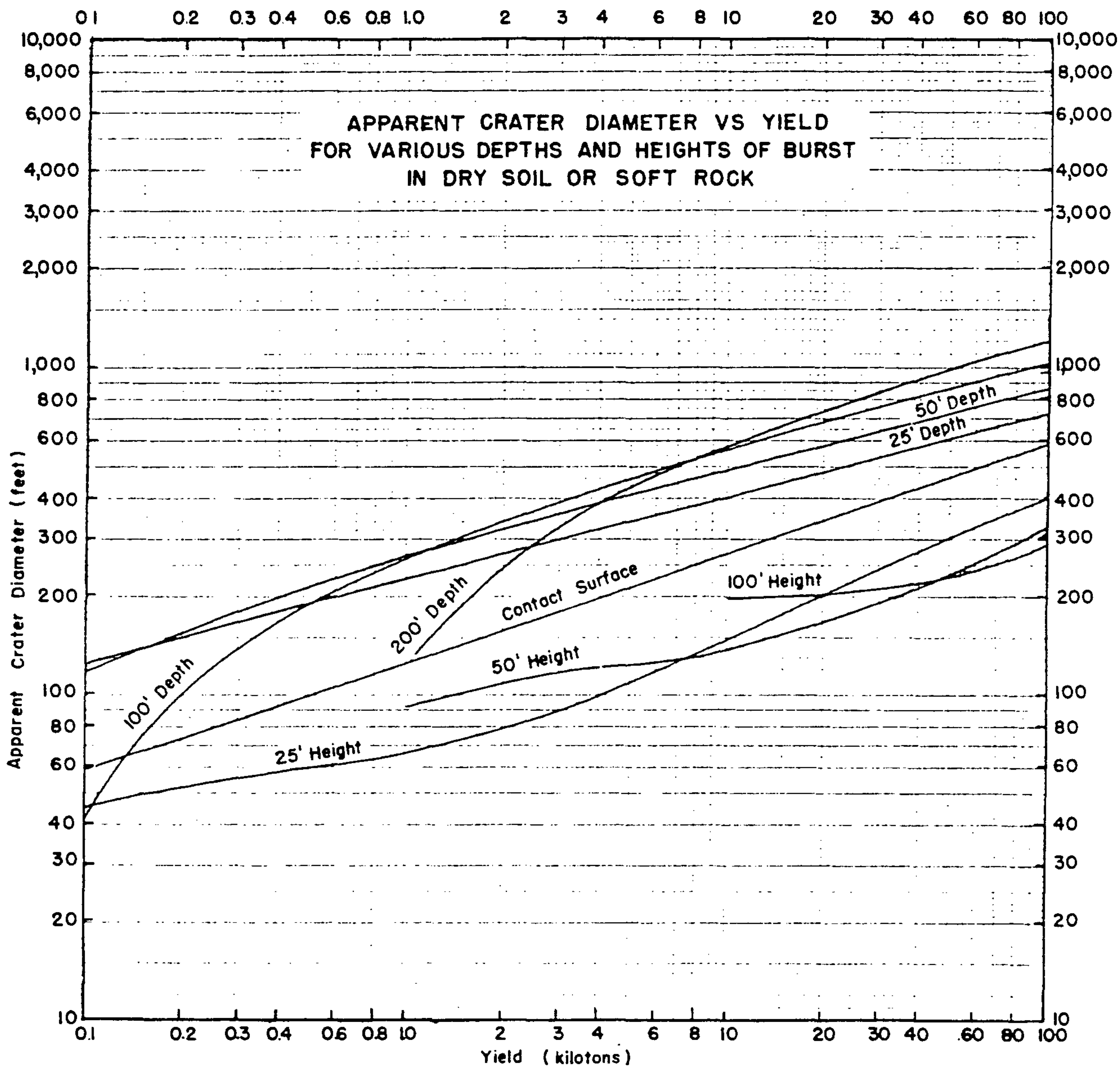
APPARENT CRATER DIAMETER VS YIELD
FOR VARIOUS DEPTHS AND HEIGHTS OF BURST
IN DRY SOIL OR SOFT ROCK
Apparent Crater Diameter (feet)
Yield (kilotons)
50' Depth
25' Depth
200' Depth
100' Depth
Contact Surface
100' Height
50' Height
25' Height
0.1
0.2
0.3
0.4
0.6
0.8
1.0
2
3
4
6
8
10
20
30
40
60
80
100
10,000
8,000
6,000
4,000
3,000
2,000
1,000
800
600
400
300
200
100
80
60
40
30
20
10

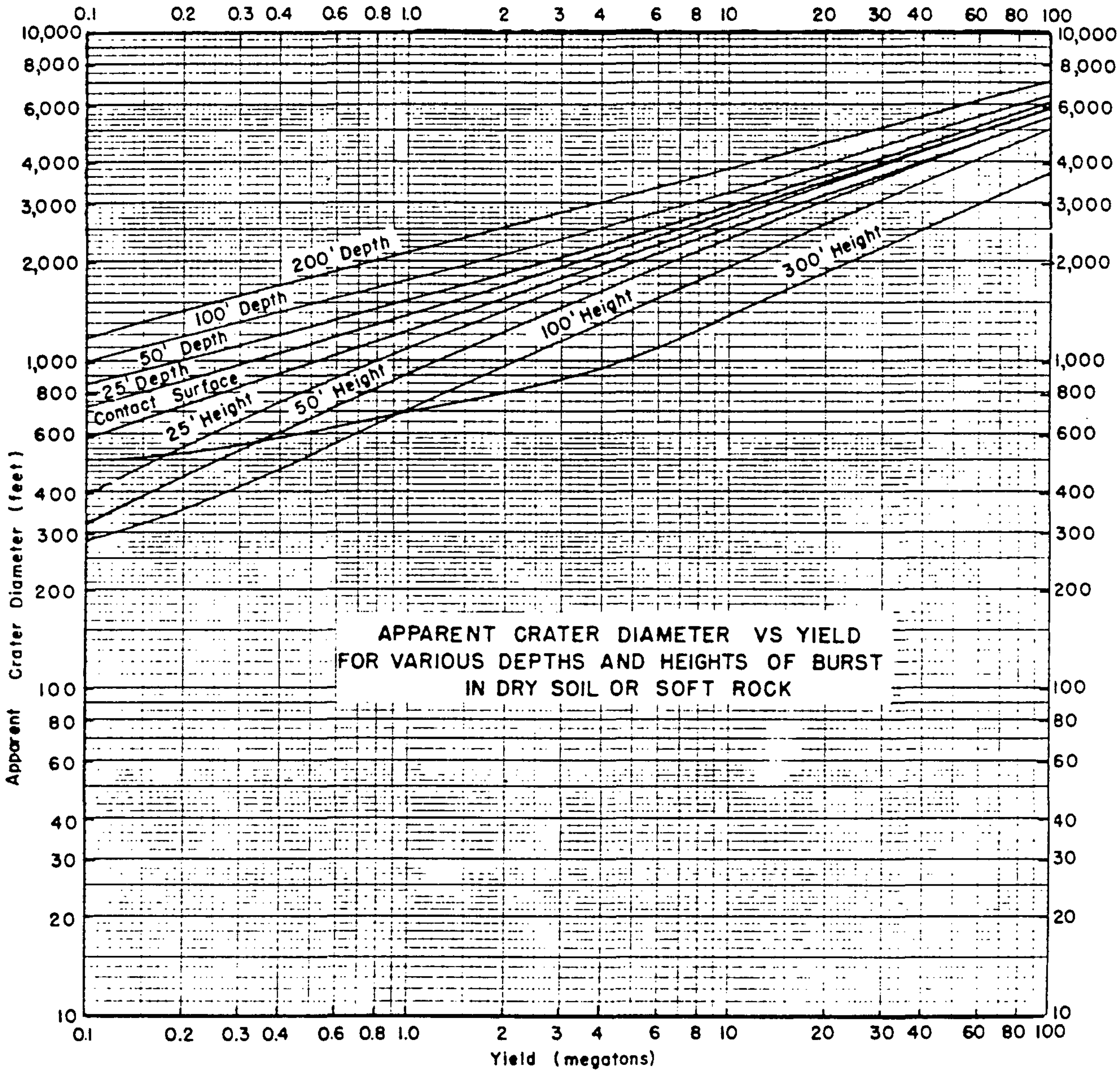
APPARENT CRATER DIAMETER VS YIELD
FOR VARIOUS DEPTHS AND HEIGHTS OF BURST
IN DRY SOIL OR SOFT ROCK
200' Depth
100' Depth
50' Depth
25' Depth
Contact Surface
25' Height
50' Height
100' Height
300' Height
Apparent Crater Diameter (feet)
Yield (megatons)
0.1
0.2
0.3
0.4
0.6
0.8
1.0
2
3
4
6
8
10
20
30
40
60
80
100
10,000
8,000
6,000
4,000
3,000
2,000
1,000
800
600
400
300
200
100
80
60
40
30
20
10

BLANK

APPARENT CRATER DEPTH VS. YIELD IN DRY SOIL OR SOFT ROCK

Figures 2-23A and 2-23B give values for apparent crater depth vs. yield for various depths and heights of burst, derived from figure 2-21 by scaling. No interpolation of depth or height of burst should be made from this figure. For values other than those given, use figure 2-21. Since there is little difference between true and apparent crater depths from bursts above ground or bursts at depths less than 10 $W^{1/3}$ feet, these figures may be used also for true craters in that range. The assumed soil type is dry soil or soft rock (rock that will crumble or pull apart easily). For other types of soil and rock, the depth obtained from figures 2-23A and 2-23B should be multiplied by the appropriate relative crater depth factor below:

Relative crater depth factors

Soil type	*Factor*
Hard rock (granite and sandstone)	0.8
Saturated soil (water slowly fills crater)	1.5
Saturated soil (water rapidly fills crater)*	0.7

*Only for apparent craters with a sloughing or washing action on the crater sides.

Example.

Given: An 80 KT burst at a depth of 100 feet in saturated clay containing water that will slowly fill the crater.

Find: The apparent crater depth.

Solution: From figure 2-23A the crater depth in dry soil is 158 feet. From the soil type table above, the factor for relative crater depth in saturated soil (water slowly fills crater) is 1.5. The crater depth is therefore $1.5 \times 158 = 237$ (± 119) feet. *Answer.*

Reliability. The reliability of crater depths obtained from figures 2-23A and 2-23B for all yields and burst positions is estimated to be ± 50 percent.

Related material.

See paragraphs 1.4d(4), e(6) and 2.2a(1).

See also figures 2-19 through 2-22 and 2-24 through 2-26.

FIGURE 2-23A

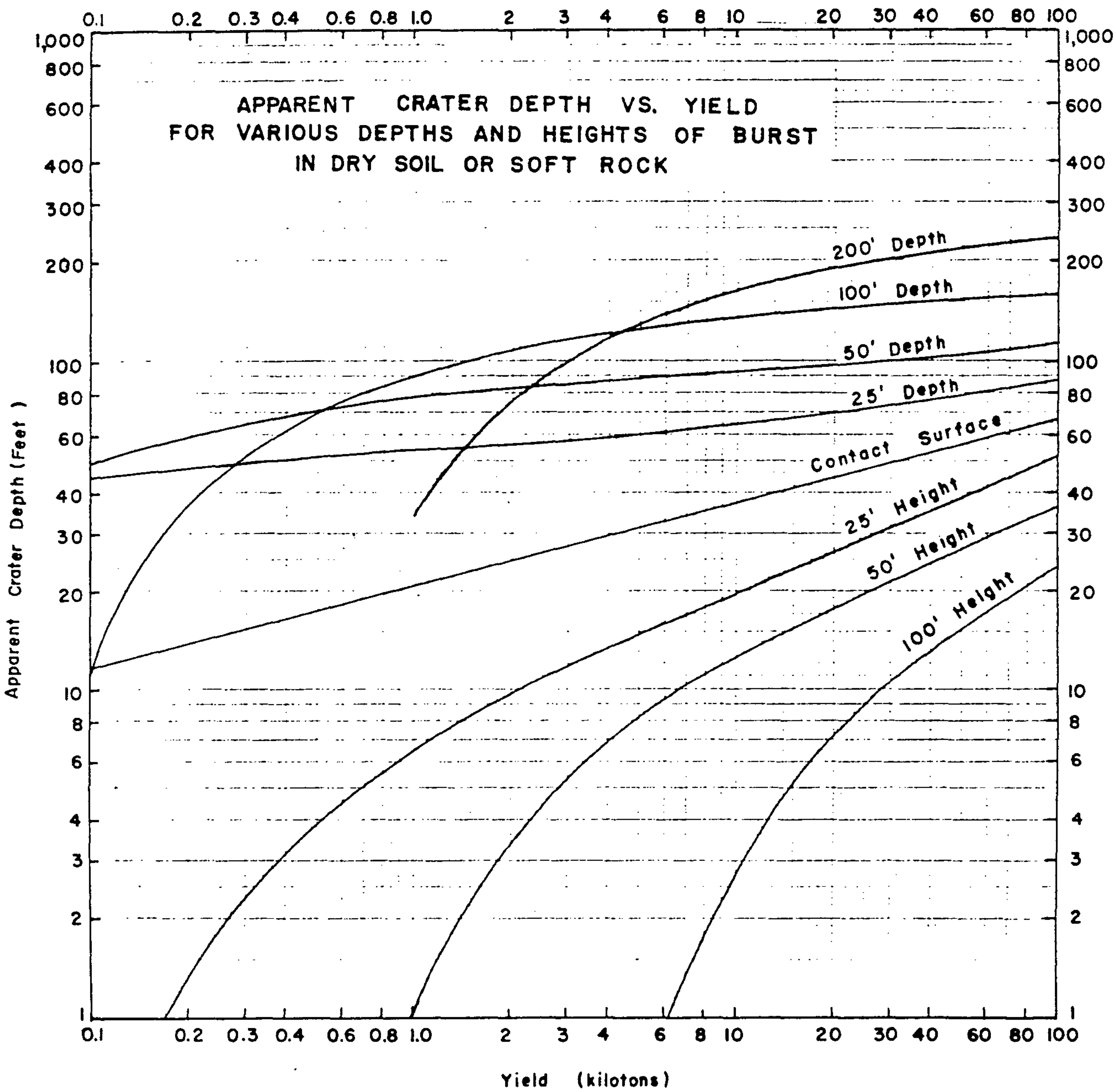
APPARENT CRATER DEPTH VS. YIELD
FOR VARIOUS DEPTHS AND HEIGHTS OF BURST
IN DRY SOIL OR SOFT ROCK
200' Depth
100' Depth
50' Depth
25' Depth
Contact Surface
25' Height
50' Height
100' Height
Apparent Crater Depth (Feet)
Yield (kilotons)
0.1
0.2
0.3
0.4
0.6
0.8
1.0
2
3
4
6
8
10
20
30
40
60
80
100
1,000
800
600
400
300
200
1

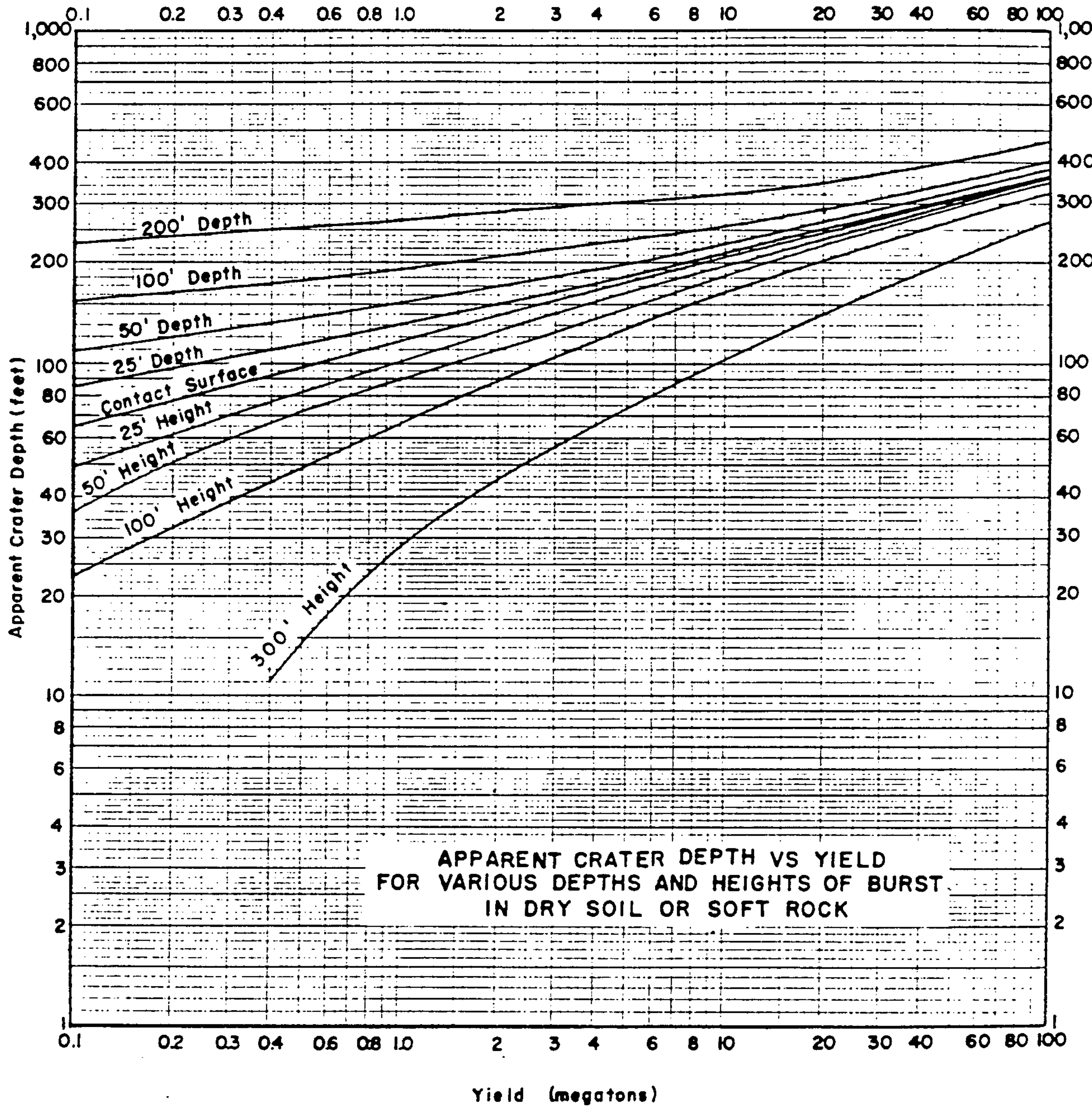

APPARENT CRATER DEPTH VS YIELD
FOR VARIOUS DEPTHS AND HEIGHTS OF BURST
IN DRY SOIL OR SOFT ROCK
200' Depth
100' Depth
50' Depth
25' Depth
Contact Surface
25' Height
50' Height
100' Height
300' Height
Apparent Crater Depth (feet)
Yield (megatons)
0.1
0.2
0.3
0.4
0.6
0.8
1.0
2
3
4
6
8
10
20
30
40
60
80
100
1,000
800
600
400
300
200
100
80
60
40
30
20
10
8
6
4
3
2
1

BLANK

UNDERWATER CRATERING

Figures 2–24 through 2–26 give underwater crater dimensions as a function of yield. These figures are given for both a surface and a bottom burst in 25, 50, 100, and 200 feet of water with bottom material of sand, sand and gravel, or soft rock. For burst positions between the surface and the bottom, linear interpolation may be used for approximate values. Figures 2–24A and 2–24B are for crater diameter; figures 2–25A and 2–25B are for crater depth; and figures 2–26A and 2–26B are for crater lip height.

For other bottom materials, the dimensions can be estimated by multiplying the values from figures 2–24 through 2–26 by the following:

Relative crater dimension factors

	Crater diameter	Crater depth	Crater lip height
Loess (fine grain soil)	1.0 (1.0)	1.7 (1.1)	0.7 (1.1)
Clay	1.0 (1.0)	2.3 (1.4)	2.3 (1.2)
Hard rock	0.7 (0.6)	0.5 (0.4)	0.4 (0.3)
Mud or muck	0.7 (1.4)	0.4 (0.4)	0.2 (0.4)

Example.

Given: A 70 KT burst on the bottom in 50 feet of water. The bottom is predominantly clay.

Find: The crater dimensions.

Solution: The dimensions from figures 2–24A, 2–25A, and 2–26A for a 70 KT burst at the bottom in 50 feet of water are:

Diameter, 1,500 feet;
Depth, 99 feet; and
Lip height, 12 feet.

The dimensions for a *clay* bottom are then:

Diameter $= 1{,}500 \times 1.0 = 1{,}500$ (± 600) feet;

Depth$=99 \times 2.3 = 226$ (± 90) feet; and

Lip height$=12 \times 2.3 = 28$ (± 11) feet.

Answers.

Reliability. Dimensions obtained from these curves are considered reliable within ±40 percent.

Related material.

See paragraph 2.2*a*(2).
See also figures 2–19 through 2–23.

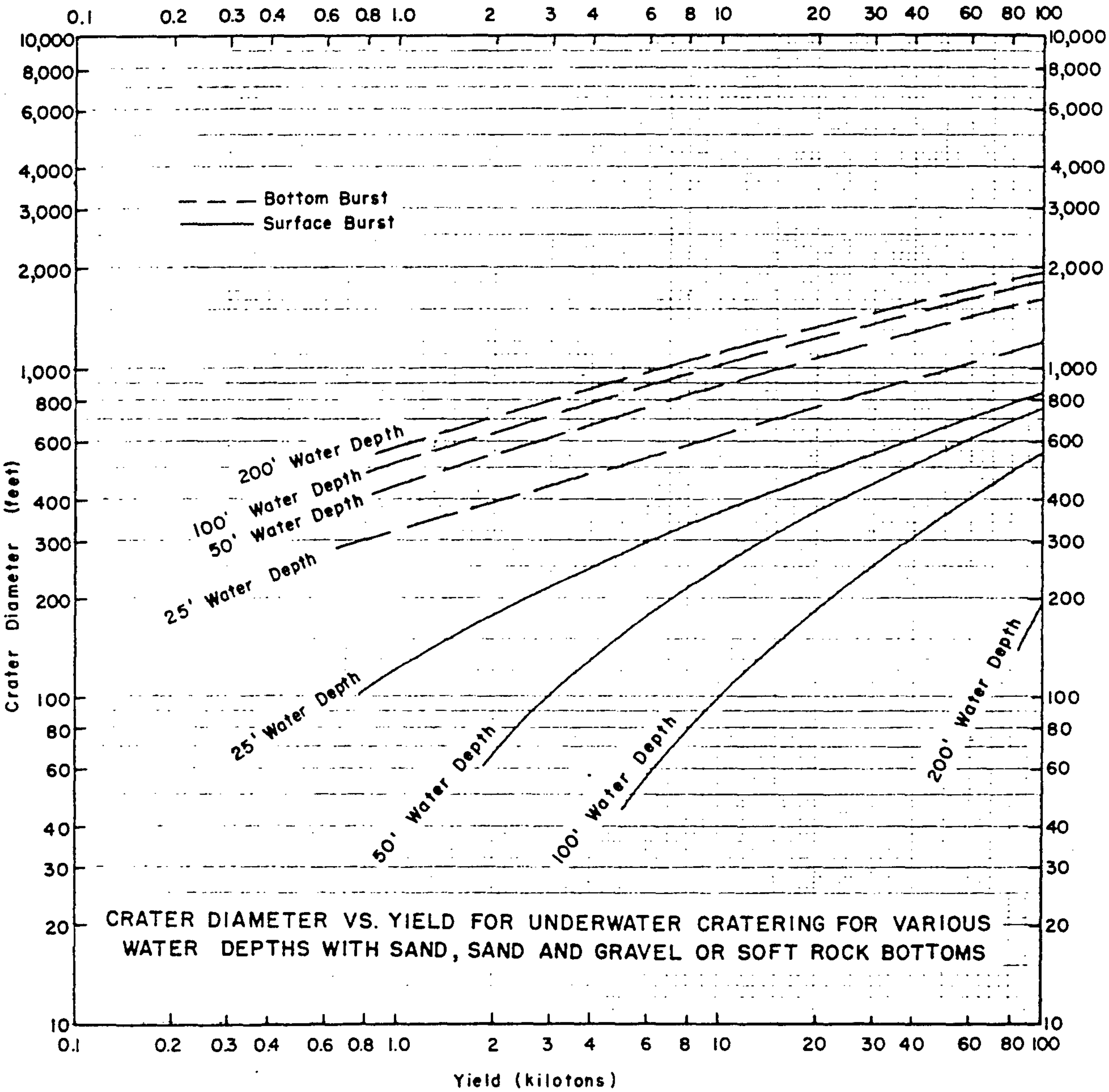

CRATER DIAMETER VS. YIELD FOR UNDERWATER CRATERING FOR VARIOUS WATER DEPTHS WITH SAND, SAND AND GRAVEL OR SOFT ROCK BOTTOMS

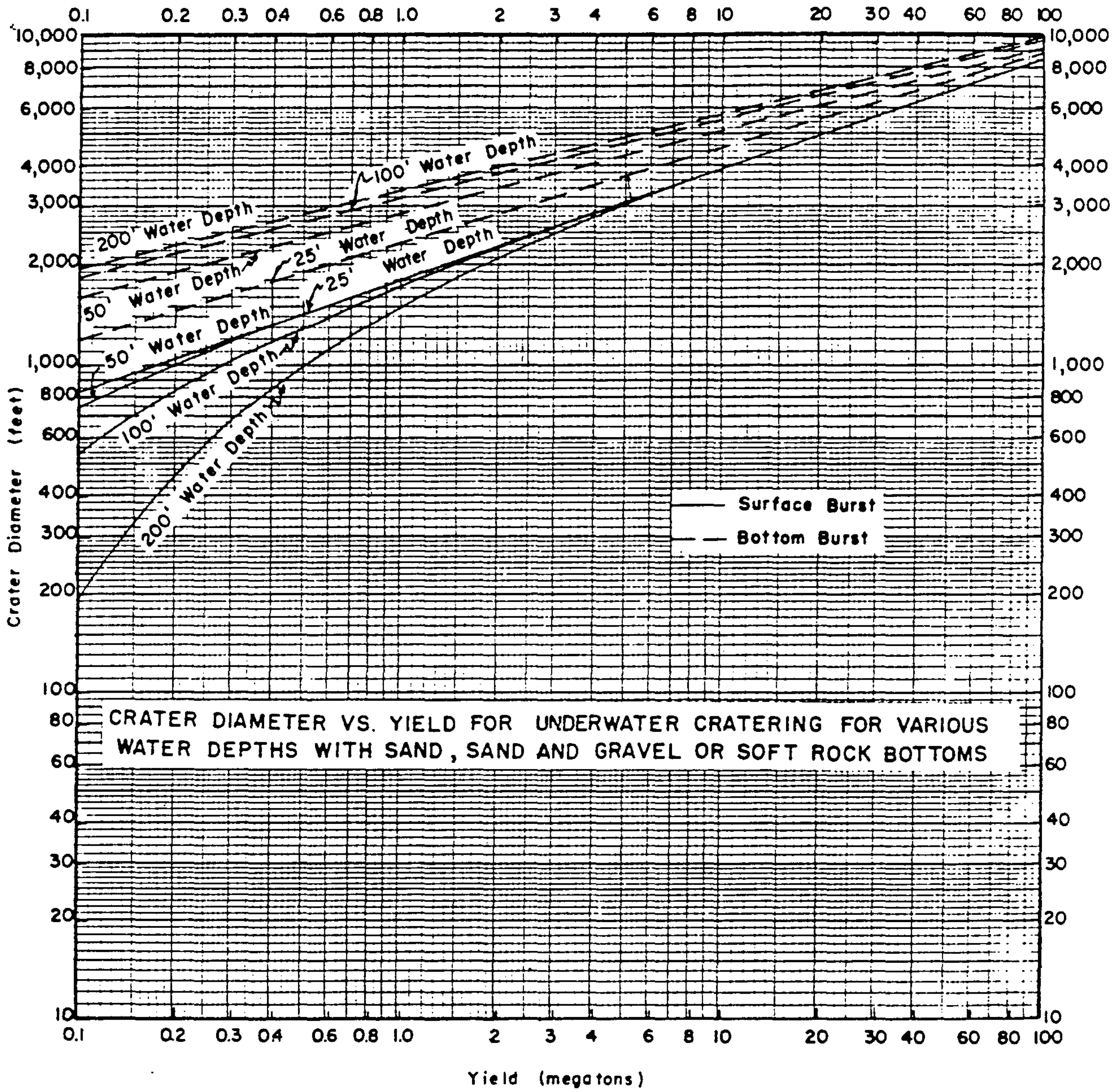

CRATER DIAMETER VS. YIELD FOR UNDERWATER CRATERING FOR VARIOUS WATER DEPTHS WITH SAND, SAND AND GRAVEL OR SOFT ROCK BOTTOMS

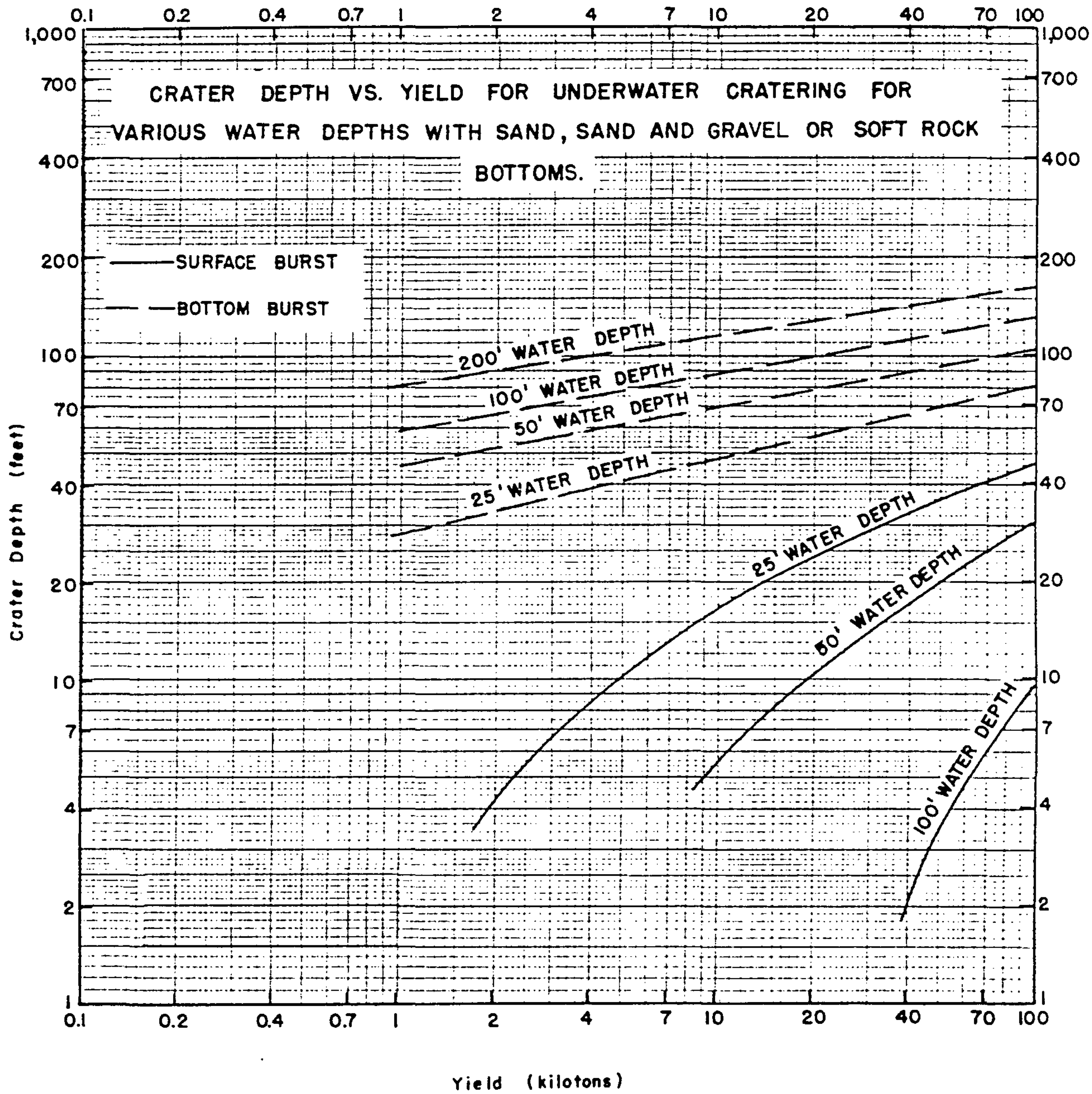
CRATER DEPTH VS. YIELD FOR UNDERWATER CRATERING FOR VARIOUS WATER DEPTHS WITH SAND, SAND AND GRAVEL OR SOFT ROCK BOTTOMS.
SURFACE BURST
BOTTOM BURST
200' WATER DEPTH
100' WATER DEPTH
50' WATER DEPTH
25' WATER DEPTH
25' WATER DEPTH
50' WATER DEPTH
100' WATER DEPTH
Crater Depth (feet)
Yield (kilotons)
0.1
0.2
0.4
0.7
1
2
4
7
10
20
40
70
100
1,000
700
400
200
100
70
40
20
10
7
4
2
1

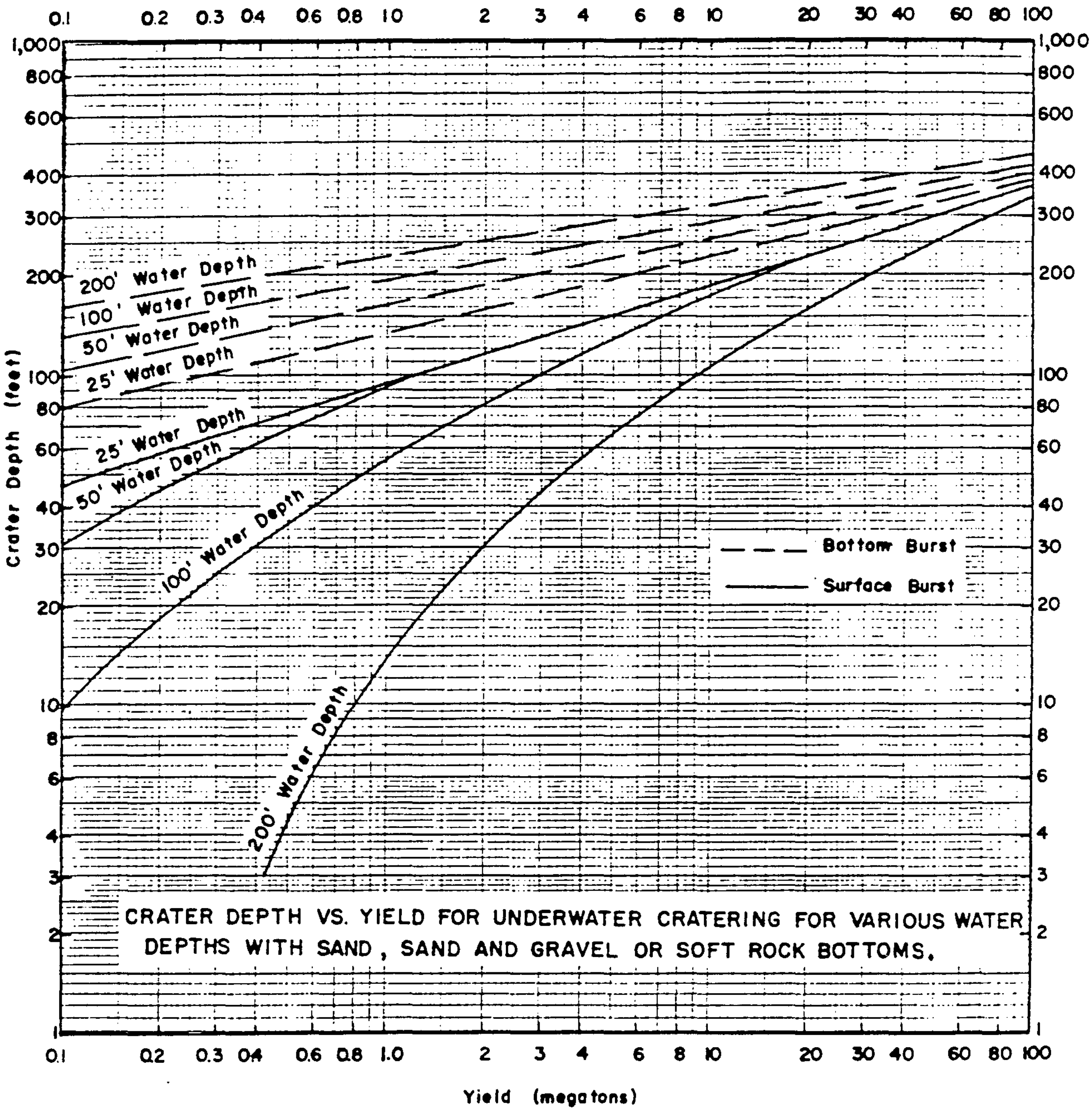

CRATER DEPTH VS. YIELD FOR UNDERWATER CRATERING FOR VARIOUS WATER DEPTHS WITH SAND, SAND AND GRAVEL OR SOFT ROCK BOTTOMS.

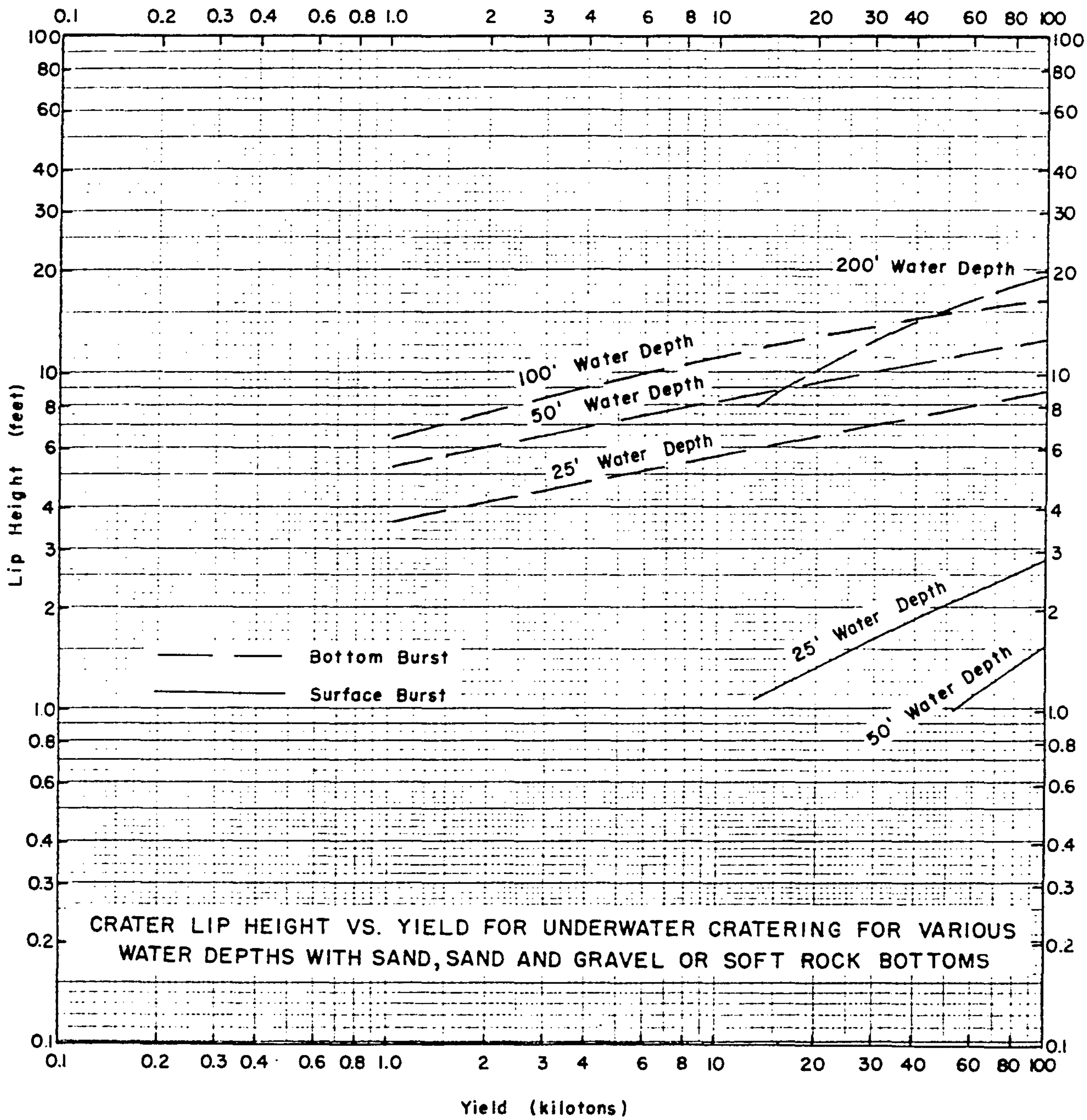

CRATER LIP HEIGHT VS. YIELD FOR UNDERWATER CRATERING FOR VARIOUS WATER DEPTHS WITH SAND, SAND AND GRAVEL OR SOFT ROCK BOTTOMS

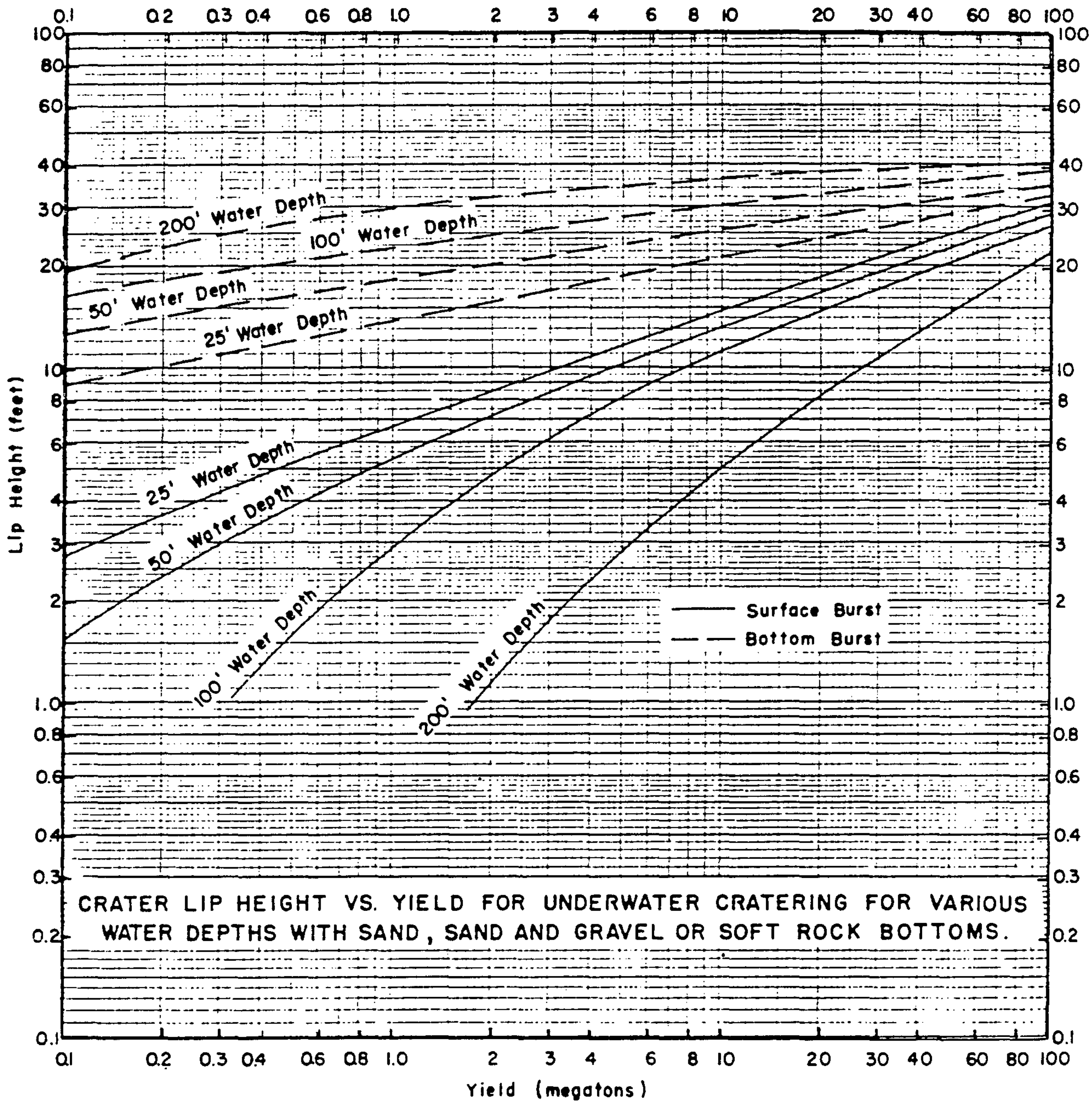

CRATER LIP HEIGHT VS. YIELD FOR UNDERWATER CRATERING FOR VARIOUS WATER DEPTHS WITH SAND, SAND AND GRAVEL OR SOFT ROCK BOTTOMS.

PEAK AIR BLAST INDUCED GROUND ACCELERATION (VERTICAL COMPONENT) VS. PEAK OVERPRESSURE

Figure 2–28 represents the relationship between overpressure and air blast induced ground acceleration. The acceleration shown is the maximum vertical acceleration (upward or downward) measured at a depth of approximately ten feet below the horizontal ground surface in Nevada type soil. Horizontal acceleration can be assumed to be approximately equal to 70 percent of the vertical acceleration. Accelerations measured at a depth of 5 feet may be roughly 150 percent of those indicated and accelerations measured at a depth of twenty feet may be roughly 50 percent of those indicated. Mediums denser than Nevada type soil may experience higher acceleration values and less dense mediums may experience less acceleration. The accelerations shown are applicable only to regions beyond the plastic zone of any crater produced.

Procedure. To determine the acceleration at any range, determine the peak overpressure at that range from figure 2–9 or figure 2–10, whichever is applicable, and read the acceleration directly from the curve.

Example.

Given: An 80 KT detonation at a height of burst of 2,580 feet over an "average" surface.

Find: The vertical ground acceleration at a range of 4,000 yards, 10 feet below the ground surface.

From figure 2–10B the overpressure from an 80 KT burst at 4,000 yards is 3 psi. Reading directly from figure 2–28, the acceleration is 0.2 g. *Answer.*

Reliability. The curve is based on full scale field tests in Nevada type soil. Accelerations obtained from the curve may be high by a factor of two or low by a factor of three even in Nevada type soil. When applied to other soils, the reliability of the curve is reduced.

Related material.

See paragraph 2.2*b*.

PEAK AIR BLAST INDUCED GROUND ACCELERATION VERTICAL COMPONENT Vs. PEAK OVERPRESSURE

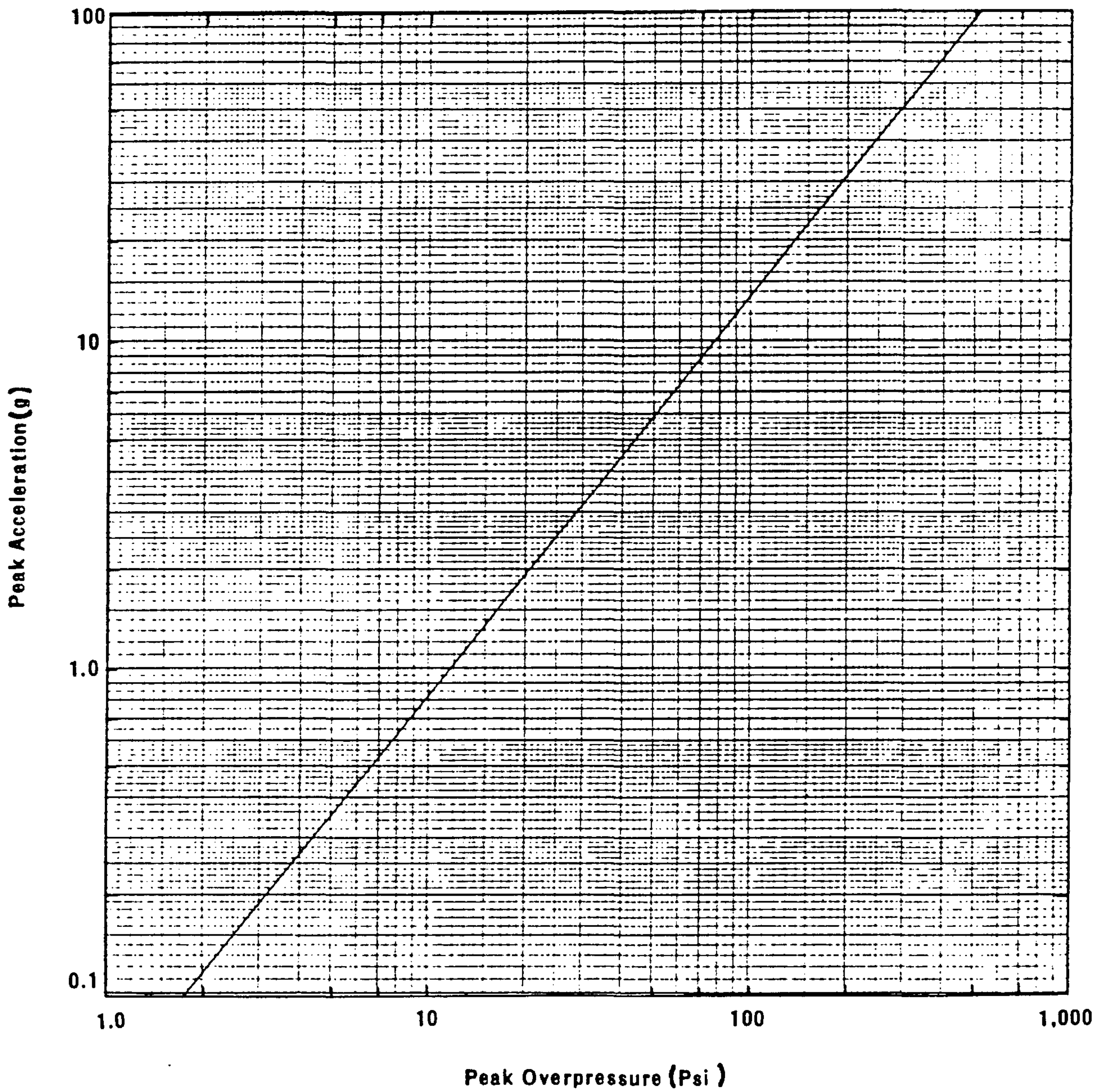

BLANK

BASE SURGE FOR UNDERGROUND BURSTS

Figure 2–29A gives the expected rate of radial growth of the earth base surge from a 1 KT underground burst; figure 2–29B gives the expected maximum base surge radius vs. yield. Figure 2–29B is based on extrapolation from the maximum base surge radii of the curves in figure 2–29A. Radii obtained from the figures assume no wind, or are crosswind radii. To compute *upwind* or *downwind* base surge radii at a specific time after detonation, add the distance traversed by the wind up to this time to the base surge radius obtained from the figures to obtain the downwind base surge radius, or subtract to obtain the upwind base surge radius.

Scaling. Depth of burst and the maximum radius of the base surge scale as the cube root of yield between scaled depths of burst of 16 $W^{1/3}$ and 125 $W^{1/3}$ feet, or:

$$\frac{h_1}{h_2}=\frac{r_1}{r_2}=\frac{W_1^{1/3}}{W_2^{1/3}}$$

where h_1 and r_1 are depth of burst and base surge radius for yield W_1, and h_2 and r_2 are the corresponding depth of burst and base surge radius for yield W_2.

Time to complete a given percentage of total radial growth of base surge scales as the one-sixth power of the yield for the same scaled depth of burst, or:

$$\frac{t_1}{t_2}=\frac{W_1^{1/6}}{W_2^{1/6}}$$

where t_1=time to complete a given percentage of total radial growth for yield W_1, and t_2=corresponding time to complete the same percentage of total radial growth for yield W_2.

Example.

Given: A 64 KT detonation 65 feet underground.

Find:

(*a*) The maximum base surge radius.

(*b*) The time at which the maximum radius occurs.

Solution: The corresponding depth of burst for 1 KT is:

$$h_1=\frac{W_1^{1/3}\times h_2}{W_2^{1/3}}=\frac{1\times 65}{(64)^{1/3}}=16 \text{ ft.}$$

From figure 2–29A the maximum radius for 1 KT at a 16 foot depth of burst is 2,010 feet and occurs at 180 seconds.

The corresponding radius for 64 KT is:

$$r_2=\frac{r_1\times W_2^{1/3}}{W_1^{1/3}}=\frac{2{,}010\times(64)^{1/3}}{1}=8{,}040 \text{ ft.} \quad \textit{Answer.}$$

This may also be read directly from figure 2–29B.

The time at which this maximum radius occurs is—

$$t_2=\frac{W_2^{1/6}\times t_1}{W_1^{1/6}}=\frac{(64)^{1/6}\times 180}{1}=360 \text{ sec.} \quad \textit{Answer.}$$

Reliability. The data presented in the figure are based on limited full scale testing and extensive HE reduced scale testing.

Related material.

See paragraphs 1.4*e*(4) and 2.2*c*.

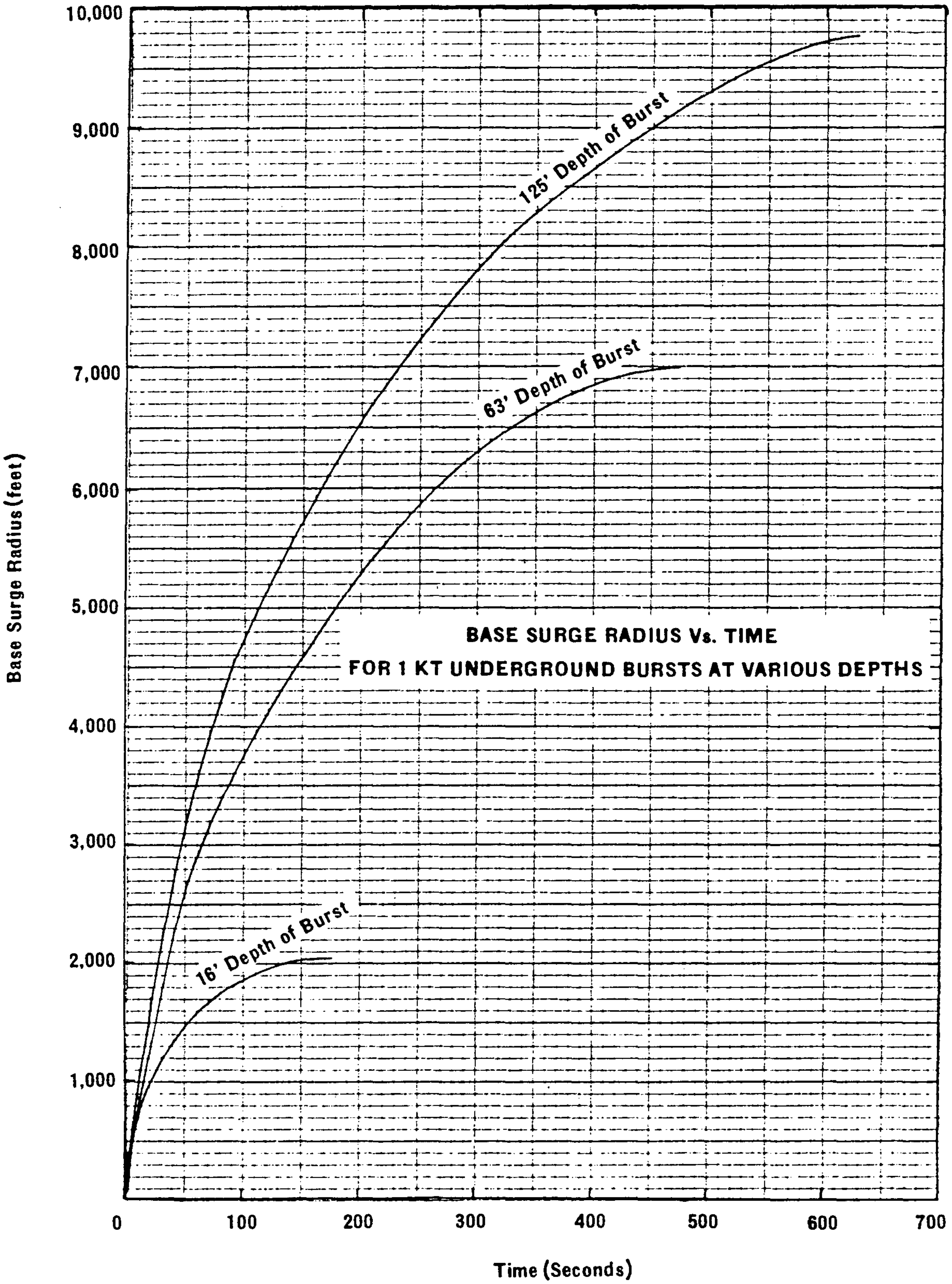
BASE SURGE RADIUS Vs. TIME
FOR 1 KT UNDERGROUND BURSTS AT VARIOUS DEPTHS
125' Depth of Burst
63' Depth of Burst
16' Depth of Burst
Base Surge Radius (feet)
10,000
9,000
8,000
7,000
6,000
5,000
4,000
3,000
2,000
1,000
0
100
200
300
400
500
600
700
Time (Seconds)

CONFIDENTIAL

FIGURE 2-29B

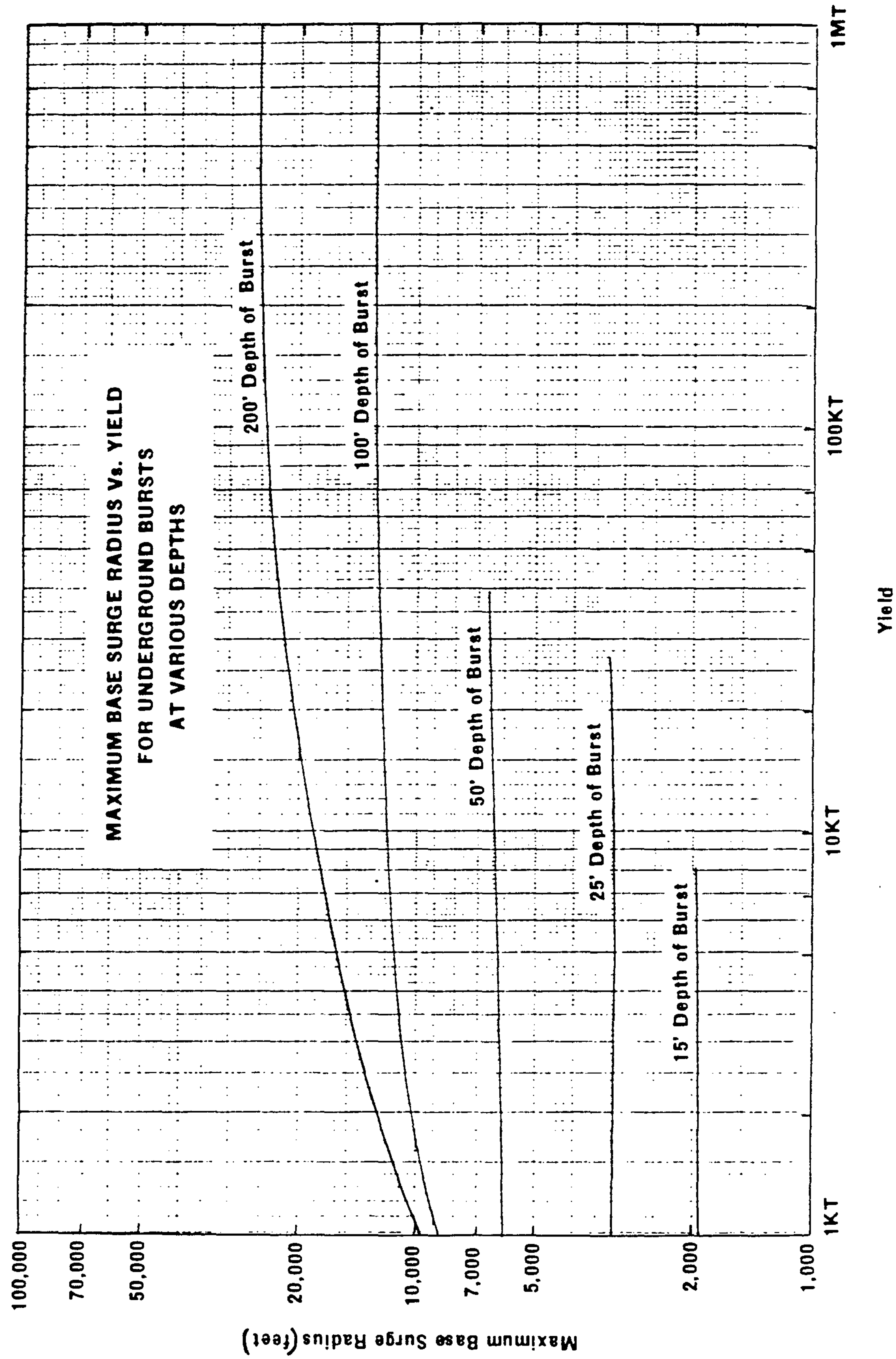

CONFIDENTIAL

PEAK WATER OVERPRESSURE FOR DEEP UNDERWATER BURSTS

Figure 2-31 gives the expected values for peak water overpressure versus slant range for various yields burst deep in deep water, where the effects of a reflecting surface are absent.

Scaling. Scaling for yields other than those shown may be done by linear interpolation between appropriate curves.

Example.

Given: A 40 KT weapon is burst at a depth of 1,000 feet in deep water.

Find: The peak water overpressure at a 1,000 foot depth 4,000 yards from the burst.

Solution: From figure 2-31, the peak water overpressure at a slant range of 4,000 yards for a 40 KT weapon can be read directly as 440 psi. *Answer.*

Reliability. Slant ranges obtained from figure 2-31 are estimated to be reliable within ±20 percent for the yield range shown.

Related material.

See paragraph 2.3*a*(2).

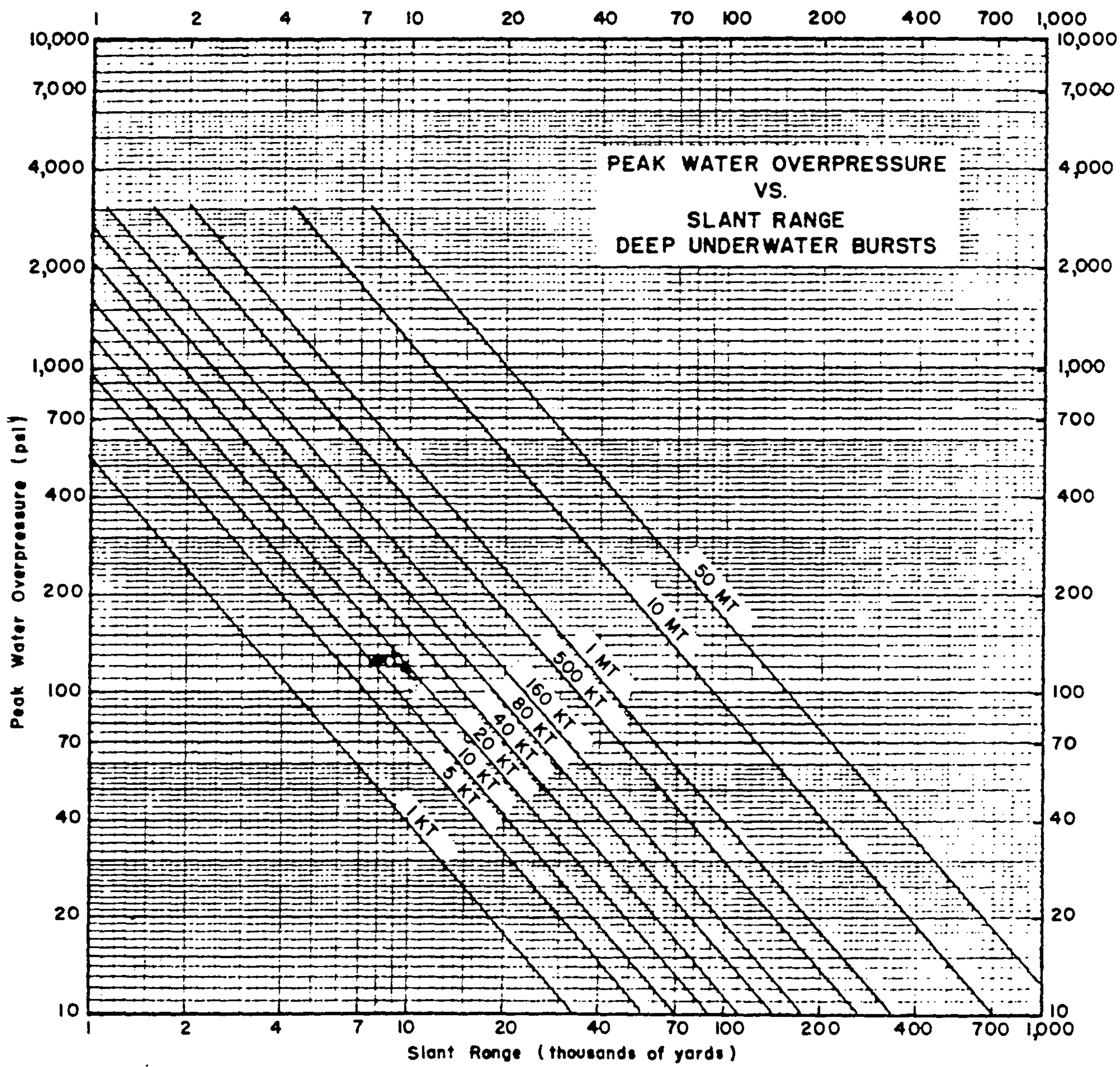
PEAK WATER OVERPRESSURE
VS.
SLANT RANGE
DEEP UNDERWATER BURSTS
Peak Water Overpressure (psi)
Slant Range (thousands of yards)
50 MT
10 MT
1 MT
500 KT
160 KT
80 KT
40 KT
20 KT
10 KT
5 KT
1 KT
10,000
7,000
4,000
2,000
1,000
700
400
200
100
70
40
20
10
1
2
4
7
10
20
40
70
100
200
400
700
1,000

MAXIMUM WAVE HEIGHT FOR WATER BURSTS

Figure 2–34 gives the approximate maximum crest-to-trough wave heights vs. horizontal distance to be expected from surface and underwater bursts of 1 KT weapons. These may be scaled to other yields as explained below. For burst depths greater than 180 $W^{1/4}$ feet but less than 850 $W^{1/4}$ feet, a linear interpolation between the values from the above limiting cases will provide a satisfactory prediction. Below 850 $W^{1/4}$ feet, the wave height is expected to decrease almost inversely with increasing depth.

Scaling. Use the following relations:

$$(a)\qquad \frac{W_1^{1/2}}{W_2^{1/2}}=\frac{h_1}{h_2},$$

where yield W_1 will give a wave height of h_1, and yield W_2 will give a corresponding wave height h_2 at the same scaled depth of burst.

$$(b)\qquad \frac{d_1}{d_2}=\frac{W_1^{1/4}}{W_2^{1/4}}=\frac{d_1'}{d_2'},$$

where yield W_1, burst at a depth d_1 in water of depth d_1', is equivalent to a burst of yield W_2 at a depth d_2 in water of depth d_2'.

Example.

Given: A 40 KT detonation at 450 feet in 1,500 feet of water.

Find: The expected maximum wave height at 10,000 yards from surface zero.

Solution: The corresponding burst depth for 1 KT is, from (*b*) above:

$$d_1=\frac{450}{(40)^{1/4}}=\frac{450}{2.5}=180\text{ feet.}$$

The corresponding water depth for 1 KT is:

$$d_1'=\frac{1,500}{(40)^{1/4}}=\frac{1,500}{2.5}=600\text{ feet.}$$

The curve of figure 2–34 for burst depth of 180 feet and water depths of 450 feet or greater is used. From this curve, the maximum wave height at 10,000 yards for a 1 KT burst is 2.2 feet. Therefore, for a 40 KT burst, the wave height at 10,000 yards is, from (*a*) above:

$$h_2=(2.2)\times(40)^{1/2}=(2.2)\times(6.3)=14\ (\pm 4)\text{ feet. } \textit{Answer.}$$

Reliability. The wave heights obtained from figure 2–34 are estimated to be reliable within ±30 percent.

Related material.

See paragraph 2.3*b*.

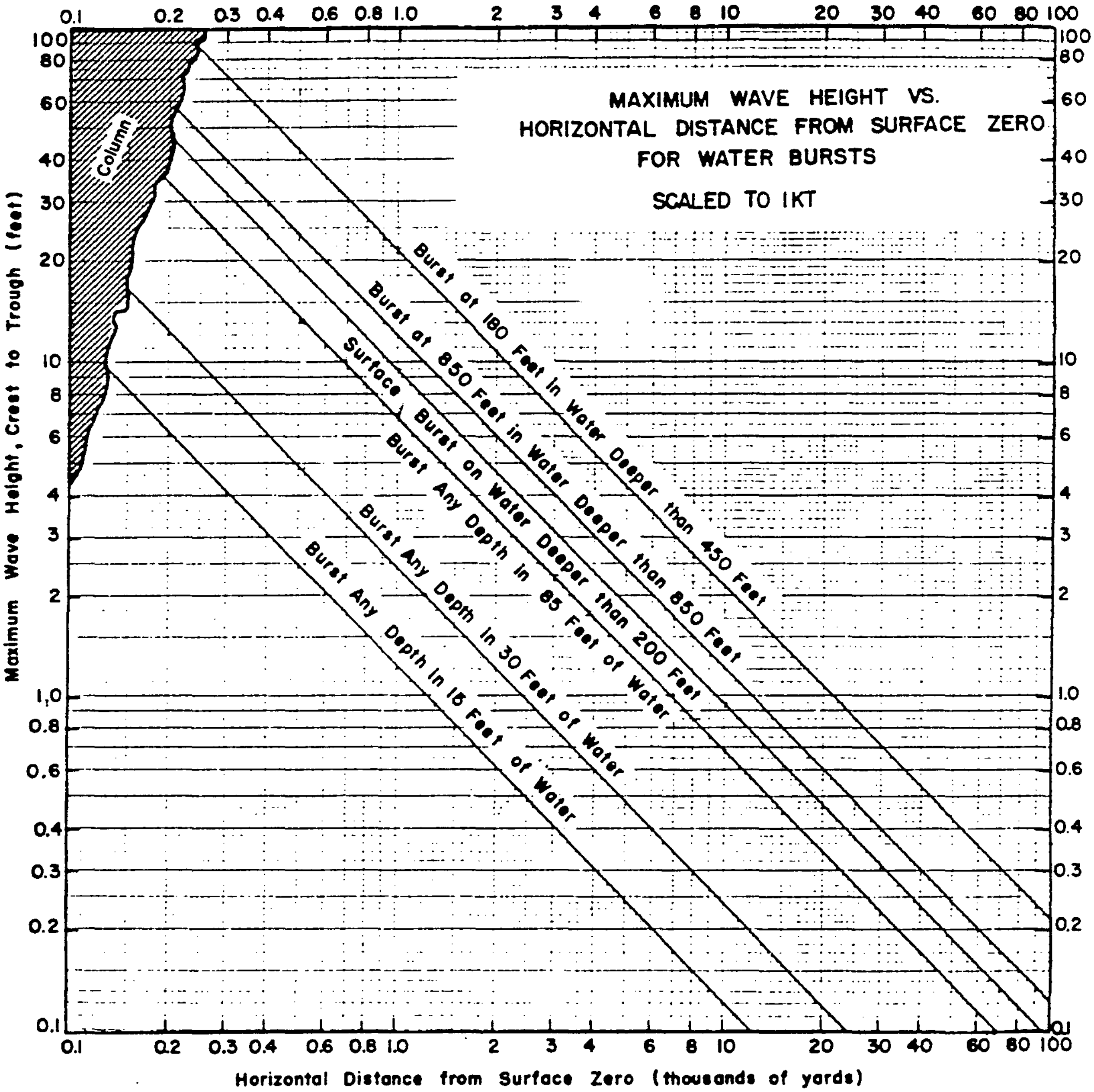
MAXIMUM WAVE HEIGHT VS.
HORIZONTAL DISTANCE FROM SURFACE ZERO
FOR WATER BURSTS
SCALED TO 1KT
Column
Burst at 180 Feet in Water Deeper than 450 Feet
Burst at 850 Feet in Water Deeper than 850 Feet
Surface Burst on Water Deeper than 200 Feet
Burst Any Depth in 85 Feet of Water
Burst Any Depth in 30 Feet of Water
Burst Any Depth in 15 Feet of Water
Maximum Wave Height, Crest to Trough (feet)
Horizontal Distance from Surface Zero (thousands of yards)
0.1
0.2
0.3
0.4
0.6
0.8
1.0
2
3
4
6
8
10
20
30
40
60
80
100

BASE SURGE FOR UNDERWATER BURSTS

Figure 2–35A gives the expected radial growth of the water base surge as a function of time after detonation for a 1 KT weapon at various depths of burst. Figure 2–35B gives the expected maximum base surge radius as a function of yield for several specific depth of burst conditions. The maximum base surge is developed from a weapon detonated at approximately the venting depth (250 $W^{1/4}$ ft.). For very shallow depths of burst, less than 10 $W^{1/3}$ feet, the occurrence of a base surge is improbable. Proximity of the bottom to the point of detonation has little effect upon the production of the base surge. For depths of burst between the limits 10 $W^{1/3}$ and 250 $W^{1/4}$ feet, the diameter of the water column producing the base surge is approximately one fourth of the resultant surge radius. With depths of burst below the venting depth of 250 $W^{1/4}$ feet, no such simple relation of the column or plume to the resultant surge exists. Little data or theory is available for base surge predictions at deep depths. A prediction can be made, however, by linear interpolation between the base surge radius of a burst at venting depth and one at a deep scaled depth (650 $W^{1/3}$ feet). A prediction thus made represents the maximum base-surge which could be expected.

Radii obtained from figures 2–35A and 2–35B assume "no wind" conditions. To compute upwind or downward base surge radii for a specific time after detonation, add the distance traveled by the wind up to this time to the "no wind" base surge radius to obtain the downwind base surge radius, or subtract to obtain the upwind base surge radius.

Scaling. Depth of burst and the accompanying maximum radius of the base surge scale as the cube root of yield for depths of burst between 25 $W^{1/3}$ and 250 $W^{1/4}$, or:

$$\frac{h_1}{h_2}=\frac{r_1}{r_2}=\frac{W_1^{1/3}}{W_2^{1/3}},$$

where h_1 and r_1 are depth of burst and base surge radius for yield W_1, and h_2 and r_2 are the corresponding depth of burst and base surge radius for yield W_2.

Time to complete a given percentage of total radial growth of the base surge scales as the one-sixth power of the yield for the same scaled depth of burst, or:

$$\frac{t_1}{t_2}=\frac{W_1^{1/6}}{W_2^{1/6}},$$

where t_1 = time to complete a given percentage of total radial growth for yield W_1 and t_2 = the corresponding time to complete the same percentage of total radial growth for yield W_2.

Time to reach the maximum base surge radius from a detonation at venting depth or less may also be computed by:

$$t_{max}=2.25r^{1/2}$$

where t_{max} = time to the maximum base surge radius in seconds,

and r = maximum base surge radius in feet.

Examples.

(1) *Given:* A 10 KT detonation at a depth of 150 feet below the water surface.

Find:

(*a*) The maximum base surge radius.

(*b*) Time to maximum base surge radius.

(*c*) The expected base surge radius 1 minute after detonation.

Solution:

(*a*) The maximum base surge radius is read directly from figure 2–35B as 7,200 feet. *Answer.*

(*b*) The venting depth is 250 $W^{1/4}$=440 feet. Since the depth of burst is less than venting, the simplified formula for time to maximum may be used. The time of maximum base surge radius is $t_{max}=2.25\ (7{,}200)^{1/2}=190$ seconds. *Answer.*

(*c*) A 10 KT detonation of 150 feet depth will complete the same percentage of its total radial growth in 60 seconds as a 1 KT detonation will complete at a corresponding scaled time and depth. Using the scaling above, the corresponding depth of burst for 1 KT is—

$$h_1=\frac{W_1^{1/3}\times h_2}{W_2^{1/3}}=\frac{1\times 150}{(10)^{1/3}}=70\text{ ft.}$$

The time that a 1 KT weapon burst at a depth of 70 feet will have completed the same percentage of its growth that a 10 KT burst will have completed in 60 seconds is:

$$t_1=\frac{t_2\times W_1^{1/6}}{W_2^{1/6}}=\frac{60\times 1}{(10)^{1/6}}=41 \text{ seconds.}$$

From figure 2-35A the maximum surge for a 1 KT at 70 feet is 3,400 feet and at 41 seconds the surge has a radius of 2,000 feet. Thus it has completed 60 percent of its growth. A 10 KT detonation at a depth of 150 feet will then complete in one minute 60 percent of its maximum radial growth or—

$0.60\times 7{,}200=4{,}300$ feet. *Answer.*

(2) *Given:* A 30 KT detonation at a depth of 1,000 feet below the water surface.

Find: The maximum base surge radius.

Solution: The venting depth for a 30 KT detonation is approximately 250 $W^{1/4}$ or 600 feet. Little data is available upon which to predict the maximum base surge radius at depths exceeding this. Hence, a prediction must be made by linear interpolation between the venting depth, 600 feet, and a depth of 650 $W^{1/3}$ or 2,000 feet.

From figure 2-35B the maximum base surge radius at venting depth is 12,000 feet. At 650 $W^{1/3}$ the maximum base surge radius is 7,000 feet. By interpolation the maximum base surge radius for a 30 KT detonation at 1,000 feet is

$$12{,}000-\left(\frac{400}{1{,}400}\times 5{,}000\right)=10{,}600 \text{ ft.}$$

Answer.

Reliability. Figures 2-35A and 2-35B are based upon limited full scale and extensive reduced scale testing.

Related material.

See paragraph 2.3*c*.

BASE SURGE RADIUS Vs. TIME
FOR 1 KT UNDERWATER BURSTS AT VARIOUS DEPTHS

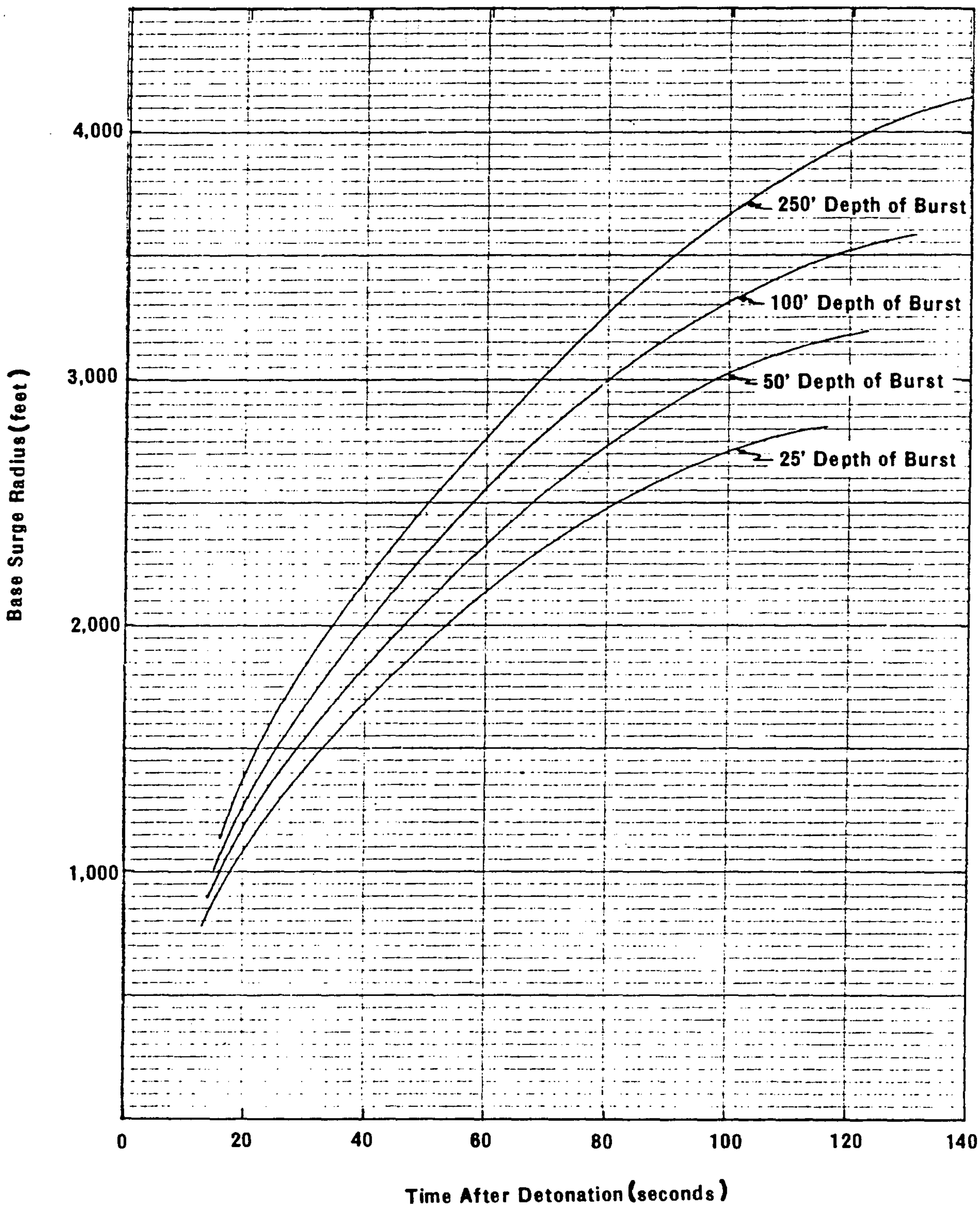

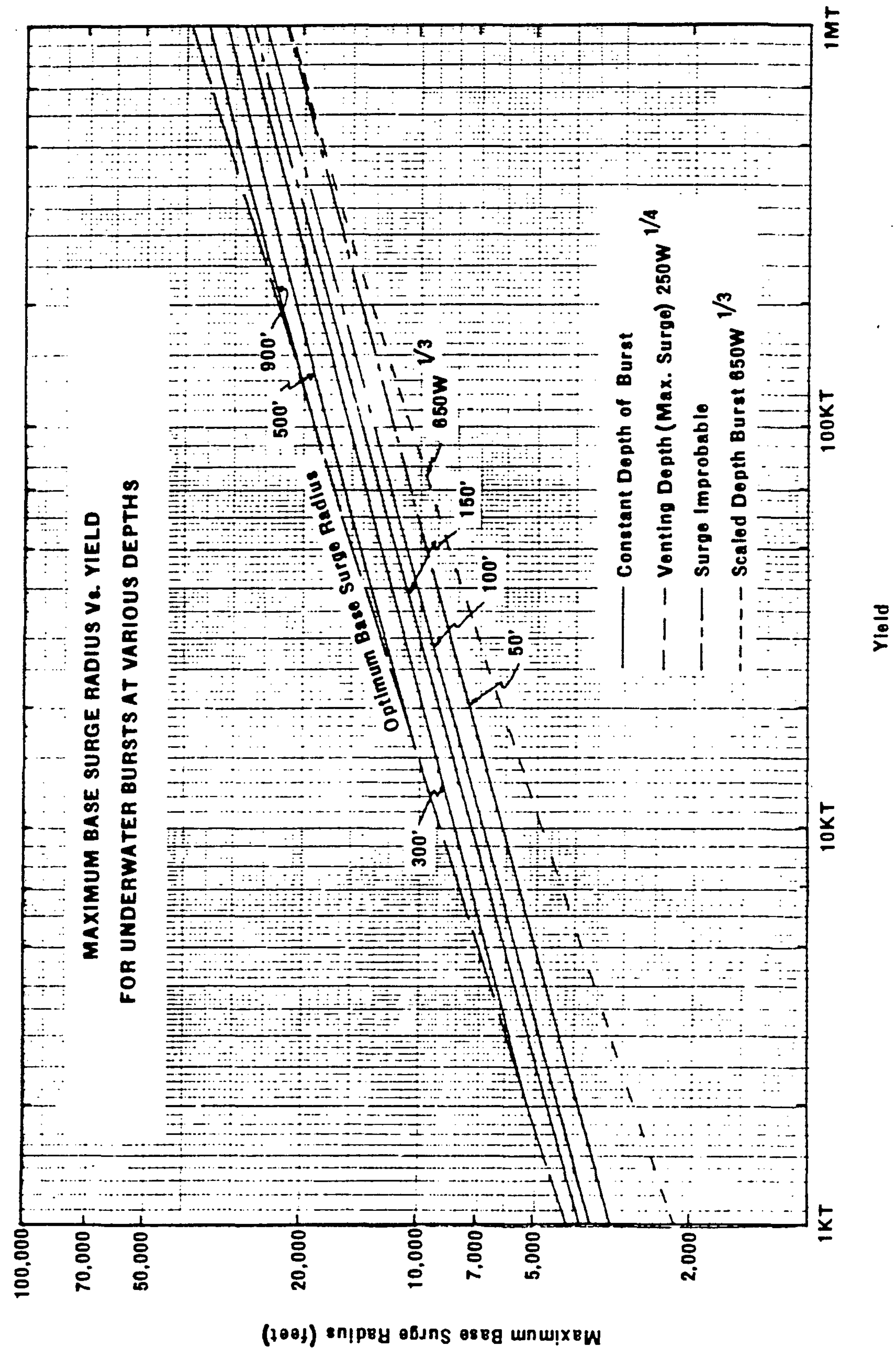
MAXIMUM BASE SURGE RADIUS Vs. YIELD
FOR UNDERWATER BURSTS AT VARIOUS DEPTHS
Optimum Base Surge Radius
900'
500'
300'
650W 1/3
150'
100'
50'
Constant Depth of Burst
Venting Depth (Max. Surge) 250W 1/4
Surge Improbable
Scaled Depth Burst 650W 1/3
1KT
10KT
100KT
1MT
Yield
100,000
70,000
50,000
20,000
10,000
7,000
5,000
2,000
Maximum Base Surge Radius (feet)

BLANK

3
Thermal

SECTION III
THERMAL RADIATION PHENOMENA

3.1 General

The extremely high temperatures in the fireball result in a large emission of thermal radiation. The relatively large fraction of the total energy of a nuclear detonation which is emitted as thermal radiation is one of its most striking characteristics. This radiant energy amounts to approximately one-third of the total energy of an air burst weapon; it is sufficient to cause serious burns to exposed personnel and to start fires in some combustible materials out to considerable distances. The duration of the thermal radiation emission depends upon the weapon yield, and is longer for the larger yields.

For a surface burst having the same yield as an air burst, the presence of the earth's surface results in a reduced thermal radiation emission and a cooler fireball when viewed from that surface. This is due primarily to heat transfer to the soil or water, the distortion of the fireball by the reflected shock wave, and the partial obscuration of the fireball by dirt and dust (or water) thrown up by the blast wave.

In underground bursts the fireball is obscured by the earth column, and therefore thermal radiation effects are negligible. Nearly all of the thermal radiation is absorbed in fusing and vaporizing the earth.

Thermal radiation from an underwater detonation is increasingly absorbed in vaporization and dissociation of the surrounding medium as the depth of burst is increased. Its direct effects are insignificant for most practical purposes; e. g., for a 20 KT burst in ninety feet of water, thermal effects are negligible.

3.2 Thermal Scaling

a. General. In paragraph 1.4*b*(2) the fireball was described as emitting thermal radiation in a pulse characterized by a rapid rise to a first maximum, a decline to a minimum, another rise to a second maximum and a subsequent final decline. The first phase of this pulse occurs so very rapidly that less than 1 percent of the total thermal radiation is emitted. Consequently, it is the second phase of the pulse which is of interest in weapons effects considerations at altitudes in the lower troposphere.

Throughout, the fireball may be considered to radiate essentially, though not ideally, as a black body, for which the radiant power is proportional to the radiating area and the fourth power of the temperature. After the minimum the radiating radius and area increase relatively slowly, so that the radiant power is predominately determined by the temperature cycle of the fireball. An illustration of the apparent temperature and fireball radius versus time for a 20 KT air burst is shown in figure 3–1. It should be emphasized, however, that the actual radiating area may vary substantially from that of the luminous fireball. Very little quantitative information is available concerning the rate of growth of the fireball following the time at which "breakaway" occurs (approximately 0.015 second for the 20 KT burst shown in figure 3–1). Up to the time of breakaway, however, the radius increases approximately as the 0.4 power of the time after detonation.

b. Thermal Pulse. The shape of the pulse after the radiant power minimum (t_{min}) is sufficiently similar for nuclear detonations that a single curve may represent the time distribution of radiant power emitted (fig. 3–2). This curve has been developed by using ratios. The ratio p/p_{max} is plotted against the ratio t/t_{max}, where p/p_{max} is the ratio of the radiant power at a given time to the maximum radiant power, and t/t_{max} is the ratio of time after detonation to the time to the second thermal maximum for that detonation.

The percent of the total thermal radiation emitted versus the ratio t/t_{max} is also shown on figure 3–2. From this figure it is seen that approximately twenty percent of the total emission occurs up to the time of the second power maximum, whereas approximately 82 percent is emitted prior to 10 times the time to the second maximum. By this time the rate of delivery has dropped to such a low value that the remaining energy is no longer of significance in damage production.

c. Time scaling. It has been found that both the time to the minimum and the time to the second maximum are proportional to the square root of the weapon yield. Thus, for airbursts at altitudes of burst below about 50,000 feet, the time to the minimum (t_{min}) is 0.0027 $W^{1/2}$ second. The time to the second maximum (t_{max}) is 0.032 $W^{1/2}$ second. (See figures 3–3A and 3–3B. These curves may also be used for surface bursts.) It should be noted that for weapon yields lower than 6 KT the actual values of t_{max} may be as much as 30 percent higher than those given by figure 3–3A. This is caused by the higher mass-to-yield ratio characteristic of low yield weapons. These relations indicate that a one megaton weapon delivers its thermal radiation over a period 32 times as great as does a one kiloton weapon. This can be expected to result in variations in total thermal energy required for a given effect. The significance of the dependence of delivery rate on weapon yield is discussed in the sections dealing with thermal injury and damage.

d. Thermal Yield. Measurements of the total thermal energy emitted for air burst weapons of low yield indicate that this energy is proportional to weapon yield and is about one-third of the total yield. From this and figure 3–2 a scaling procedure for maximum radiant power may be derived. Thus $p_{max} = 4W^{1/2}$KT/sec or $4 \times 10^{12} W^{1/2}$ cal/sec.

Measurements from the ground of the total thermal energy from surface bursts, although not as extensive as those for air bursts, indicate that the thermal yield is a little less than half that from equivalent air bursts. For a surface burst the thermal yield is assumed to be one-seventh of the total yield. For surface bursts, the scaling of the second radiant power maximum (p_{max}) cannot be determined on the basis of available data. Similarly, there are no data which show what the thermal radiation phenomena may be for detonation altitudes in excess of about 50,000 feet. It is expected that the thermal energy may increase with altitude of burst, and figure 3–4 gives a purely theoretical estimate of this increase.

3.3 Radiant Exposure vs. Slant Range

a. Spectral. Characteristics. At distances of operational interest, the spectral (wavelength) distribution of the incident thermal radiation, integrated with respect to time, resembles very closely the spectral distribution of sunlight. For each, slightly less than one-half of the radiation occurs in the visible region of the spectrum, approximately one-half occurs in the infrared region and a very small fraction (rarely greater than 10 percent) lies in the ultraviolet region of the spectrum. The color temperature of the sun and an air burst are both about 6,000° K. A surface burst, as viewed by a ground observer, contains a higher proportion of infrared radiation and a smaller proportion of visible radiation than the air burst, with almost no radiation in the ultraviolet region. The color temperature for a surface burst is about 3,000° K. A surface burst viewed from the air may exhibit a spectrum more nearly like an air burst.

b. Atmospheric Transmissivity. The atmospheric transmissivity ($\overline{T}$) is defined as the fraction of the radiant exposure received at a given distance after passage through the atmosphere, relative to that which would have been received at the same distance if no atmosphere were present. Atmospheric transmissivity depends upon several factors; among these are: water vapor and carbon dioxide absorption of infrared radiation, ozone absorption of ultraviolet radiation, and multiple scattering of all radiation. All of these factors vary with distance and with the composition of the atmosphere. Scattering is produced by the reflection and refraction of light rays by certain atmospheric constituents, such as dust, smoke and fog. Interactions such as scattering which divert the rays from their original paths result in a diffuse, rather than direct, transmission of the radiation. As a result, a receiver which has a large field of view (i. e., most military targets) receives radiation which has been scattered toward it from many angles, as well as the directly transmitted radiation. Since the mechanisms of absorption and scattering are wavelength dependent, the atmospheric transmissivity depends not only upon the atmospheric conditions, but also upon the spectral distribution of the weapon's radiation. In figures 3–5A and 3–5B the atmospheric transmissivity is plotted as a function of the slant range for air and surface bursts. For each type of burst three sets of atmospheric conditions are assumed. It is believed that these conditions represent the average and the extremes normally encountered in natural atmospheres. These conditions correspond to a visibility of 50 miles and a water vapor concentration of 5 grams/cubic meter; 10 miles visibility and 10 grams/cubic meter water vapor concentration; and 2 miles visibility and 25 grams/cubic meter of water vapor concentration. Curves are presented in appendix I to show under what conditions of ambient temperature and relative humidity the above water vapor concentrations are applicable. The curves of figures 3–5A and 3–5B are plotted to slant ranges equal to one-half the visibility for the three visibility conditions. The reason for this is that the empirical relationships used to obtain the transmissivity values have not been verified for ranges beyond one-half the visibility. As a result, the curves cannot be extrapolated to greater distances with any confidence. If the curves are extended beyond one-half the visibility, there is reason to believe that the values of transmissivity would be too high. Where cloud cover is appreciable or the air contains large quantities of fog or industrial haze, knowledge of the interactions with the radiation is too limited to provide estimates of atmospheric transmissivity.

c. Reflection. If a weapon is burst in the air below a large cloud, the thermal radiation is diffusely reflected downward from the cloud, resulting in greater radiant exposures at a given distance than would be received if no cloud were present. Similarly, if the weapon is burst near the earth's surface, the radiant exposure received at some altitude above the burst (as in the case of an aircraft flying above the detonation) will be greater than that which is received at the same distance on the ground. If the receiver is directly over the burst and the terrain has a high albedo, the reflected radiation from the terrain may be as much as twice the direct radiation. If a reflecting or scattering layer such as a cloud is between the detonation and the target, however, the radiant exposure received will be reduced considerably.

d. Calculation of Radiant Exposure. The radiant exposures at various slant ranges from air and surface burst weapons can be calculated from the following expressions:

$$Q=\frac{3.16\times10^6\ W\ (\overline{T})}{D^2}\ \text{cal/sq cm (air burst)}.$$

and

$$Q=\frac{1.35\times 10^6\ W\ (\overline{T})}{D^2}\ \text{cal/sq cm (surface burst)}.$$

where Q=radiant exposure (cal/sq cm)
$\overline{T}$=atmospheric transmissivity
W=weapon yield (KT)
D=slant range (yds).

The values of $\overline{T}$ for both air and surface bursts are obtained from the appropriate curves in figures 3–5A and 3–5B. Curves showing the radiant exposure (Q) as a function of slant range (D) for three atmospheric conditions for both air and surface bursts are shown in figures 3–6A and 3–6B. These curves are plotted for ranges up to one-half the visibility for the reasons explained in *b* above. The surface burst curves differ from the air burst curves for two reasons—the apparent thermal yield when viewed from the surface for a surface burst is lower than that for an air burst, and the spectral distribution of the surface burst is sufficiently different from that of an air burst to require the use of different atmospheric transmissivity curves. Radiant exposure for a burst in the transition zone may be estimated by interpolation between these curves as explained on the instruction page for figures 3–6A and 3–6B. It should be emphasized that these surface burst curves apply to the radiant exposure of *ground* targets. When the surface burst is viewed from the air, as from aircraft, the apparent radiating temperature and the thermal yield will be greater than when viewed from the ground. All of the curves plotted in figures 3–6A and 3–6B are for a total weapon yield of 1 KT. For weapon yields greater or less than 1 KT these radiant exposures should be multiplied by the yield of the weapon in question.

3.4 Other Influences on Thermal Radiation Propagation

a. Topography and Clouds. Propagation of thermal radiation from a nuclear detonation, like that from the sun, is affected by topography and the atmosphere. At close ranges, where the fireball subtends a relatively large angle, the shadowing effects of intervening objects such as hills or trees are less than are experienced with the sun. As discussed earlier, clouds in the atmosphere significantly affect the propagation of radiation through the atmosphere.

b. Fog and Smoke. Where the burst is in the air above a fog covering the ground, a significant fraction of the thermal radiation incident on the fog layer is reflected upward. That radiation which penetrates the fog is scattered. These two effects result in substantial reductions in thermal energy incident on ground targets covered by fog. White smoke screens act like fog in the attenuation of thermal radiation. Reductions as large as 90 percent of incident thermal energies are realized by dense fogs or smoke screens.

c. The Wilson Cloud. The Wilson Cloud, which is sometimes formed in a detonation, does not appreciably affect the thermal radiation incident on a target.

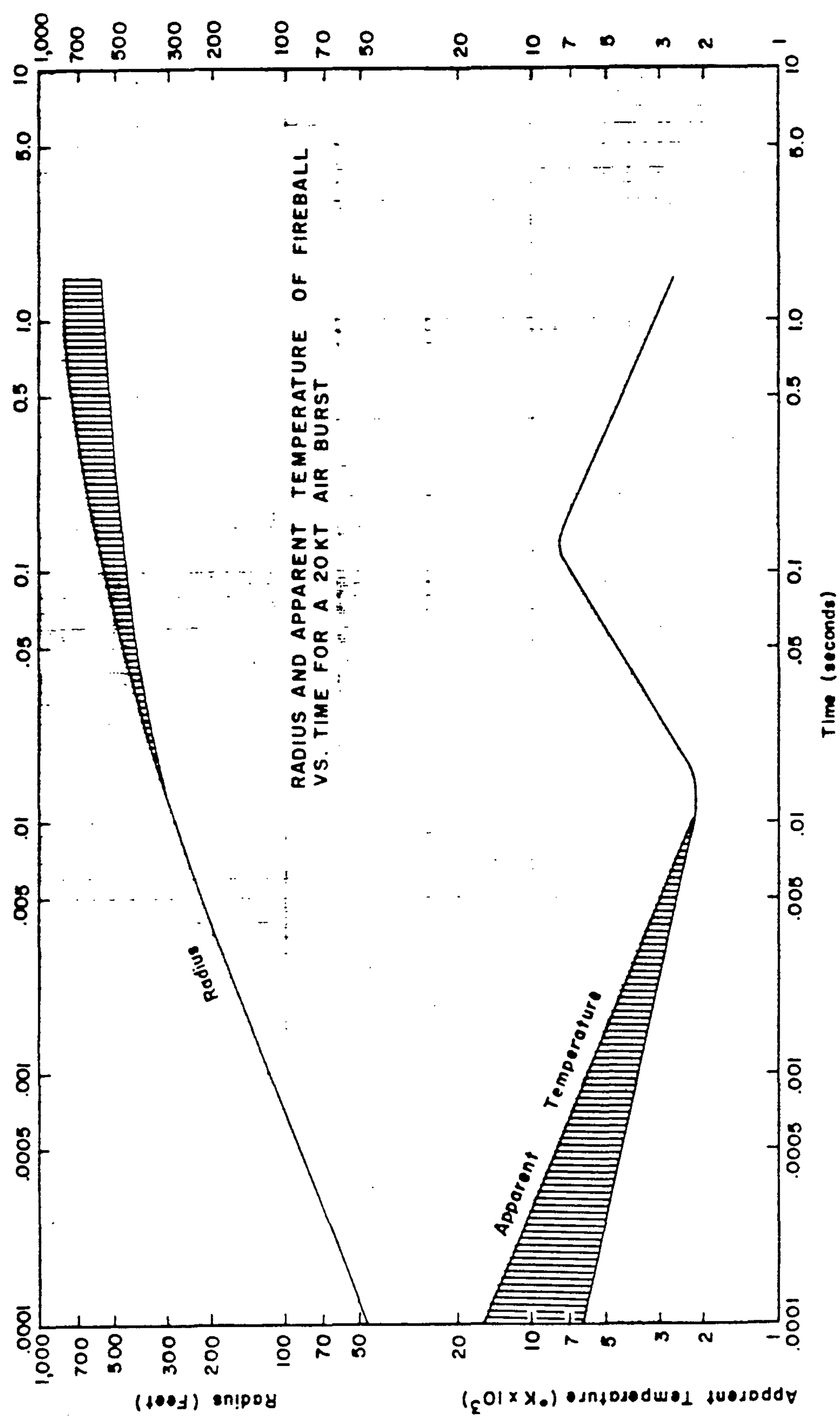
RADIUS AND APPARENT TEMPERATURE OF FIREBALL
VS. TIME FOR A 20KT AIR BURST
Radius
Apparent Temperature
Radius (Feet)
Apparent Temperature (°K x 10³)
Time (seconds)
1,000 700 500 300 200 100 70 50 20 10 7 5 3 2 1
.0001 .0005 .001 .005 .01 .05 0.1 0.5 1.0 5.0 10

GENERALIZED THERMAL PULSE

Figure 3-2 shows the radiant power relative to the second maximum and the percent of total thermal radiation emitted as functions of time after burst relative to the time of this maximum, for weapons burst at altitudes between 50,000 feet and the surface. Only the second phase of the pulse is shown, since the first phase includes less than one percent of the emitted thermal energy and is usually neglected in effects considerations.

Scaling. The second radiant power maximum and the time to this peak both scale as the square root of the yield. To determine any instantaneous level of radiant power and the corresponding time of this level after detonation for a weapon of yield "W" KT, the values obtained from figure 3-2 are multiplied by P_{max} and t_{max} respectively. The latter are determined by:

$$P_{max}=4\ W^{1/2}\ \text{KT/sec}=4\times 10^{12}\ W^{1/2}\ \text{cal/sec}.$$

$$t_{max}=0.032\ W^{1/2}\ \text{sec}.$$

Example.

Given: A 90 KT air burst.

Find: The radiant power at 2 seconds and the percent thermal radiation emitted up to 2 seconds.

Solution: From the scaling above, $t_{max}=0.032\times(90)^{1/2}=0.304$ second. For a 90 KT air burst, when $t=2.0$ seconds, $\frac{t}{t_{max}}=\frac{2.0}{0.304}=6.6.$

Reading from figure 3-2, for a value of $\frac{t}{t_{max}}=6.6$, one obtains a value for $\frac{P}{P_{max}}=0.06$.

From the scaling above, $P_{max}=4\times(90)^{1/2}$ KT/sec $=38.0$ KT/sec.

For a 90 KT air burst, when $t=2.0$ seconds, $P=P_{max}\times 0.06=38.0\times 0.06=2.28\ (\pm 0.68)$ KT/sec. *Answer.*

Reading from the percent emitted curve, when $\frac{t}{t_{max}}=6.6$, one finds the value of 76 percent. *Answer.*

Reliability. The radiant power values obtained from figure 3-2 are reliable to within ± 30 percent for air burst yields between 6 and 100 KT. The reliability decreases for air burst weapon yields lower than or above this range. Times are reliable to ± 15 percent for air burst weapons in the range 6 KT to 100 MT. For air burst weapon yields lower than 6 KT the times may be as much as 30 percent higher than those obtained from the above scaling relationship.

For other bursts, the reliability of the scaling of radiant power is expected to be lower than that shown for air bursts; nevertheless, the reliability cannot be estimated on the basis of available data.

Related material.

See paragraph 3.2.

FIGURE 3-2

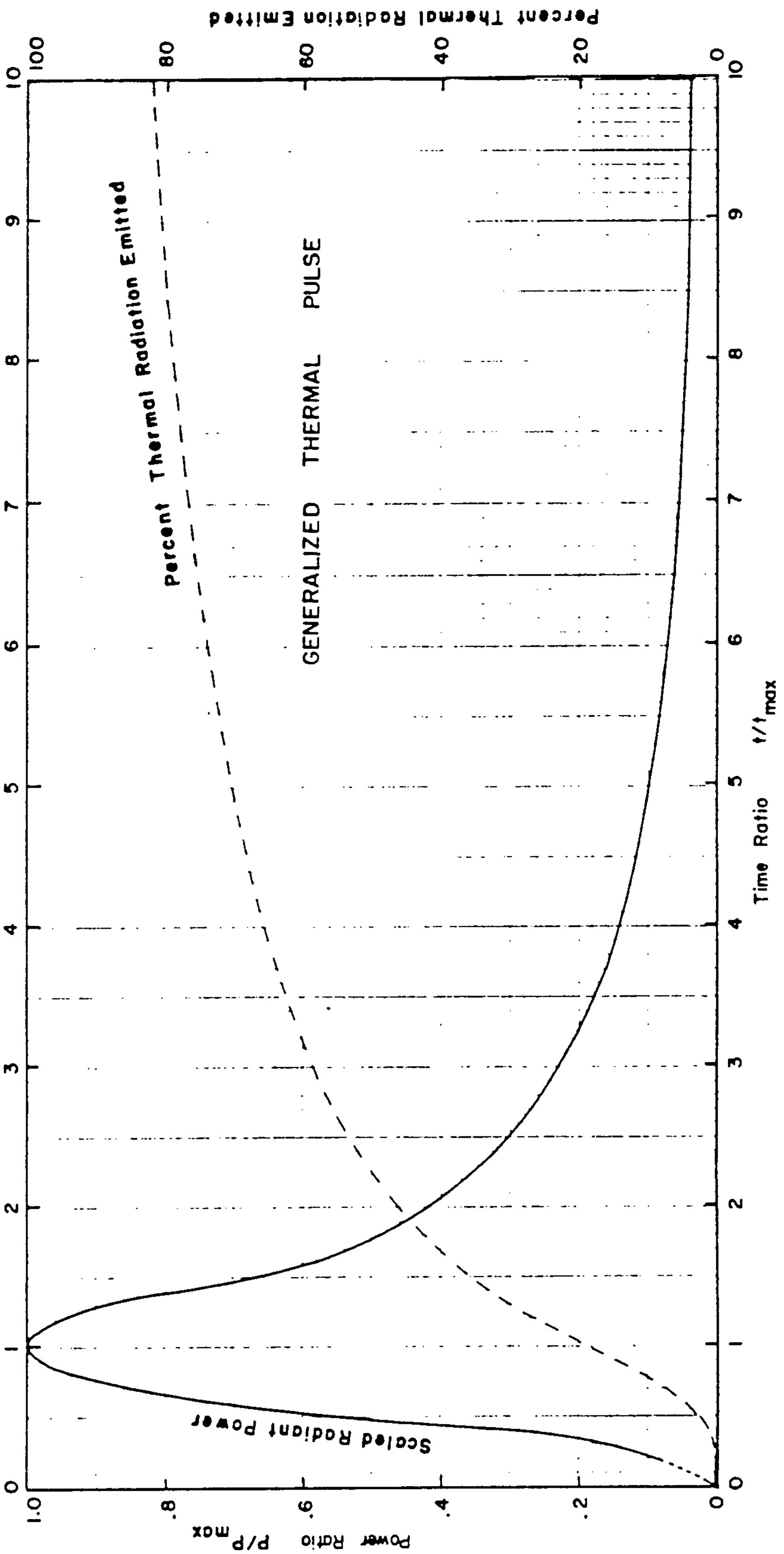
GENERALIZED THERMAL PULSE
Percent Thermal Radiation Emitted
Scaled Radiant Power
Time Ratio t/t max
Power Ratio P/P max
Percent Thermal Radiation Emitted

BLANK

TIME TO SECOND RADIANT POWER MAXIMUM AND TIME TO MINIMUM VS. YIELD

Figures 3-3A and 3-3B give the time to the second radiant power maximum (t_{max}) and the time to the radiant power minimum (t_{min}) as a function of weapon yield for air burst weapons at altitudes below 50,000 feet, and may also be used for surface bursts.

Example.

Given: The air burst of a 1 MT weapon.

Find: The time to the radiant power minimum and the time to the second radiant power maximum.

Solution: Find 1 MT on the abscissa of figure 3-3B and read from the two time curves $t_{min}=0.085$ (± 0.009) second. *Answer.*

and $t_{max}=1.1$ (± 0.2) second. *Answer.*

Reliability. The times read from the t_{min} curve of figures 3-3A and 3-3B are reliable to ± 10 percent. The times read from the t_{max} curves of figures 3-3A and 3-3B, in the range 6 KT to 100 MT are reliable to ± 15 percent. For weapon yields lower than 6 KT the values of t_{max} may be as much as 30 percent higher than those given by figure 3-3A.

Related material.

See paragraph 3.2*c*.

See also figures 3-1 and 3-2.

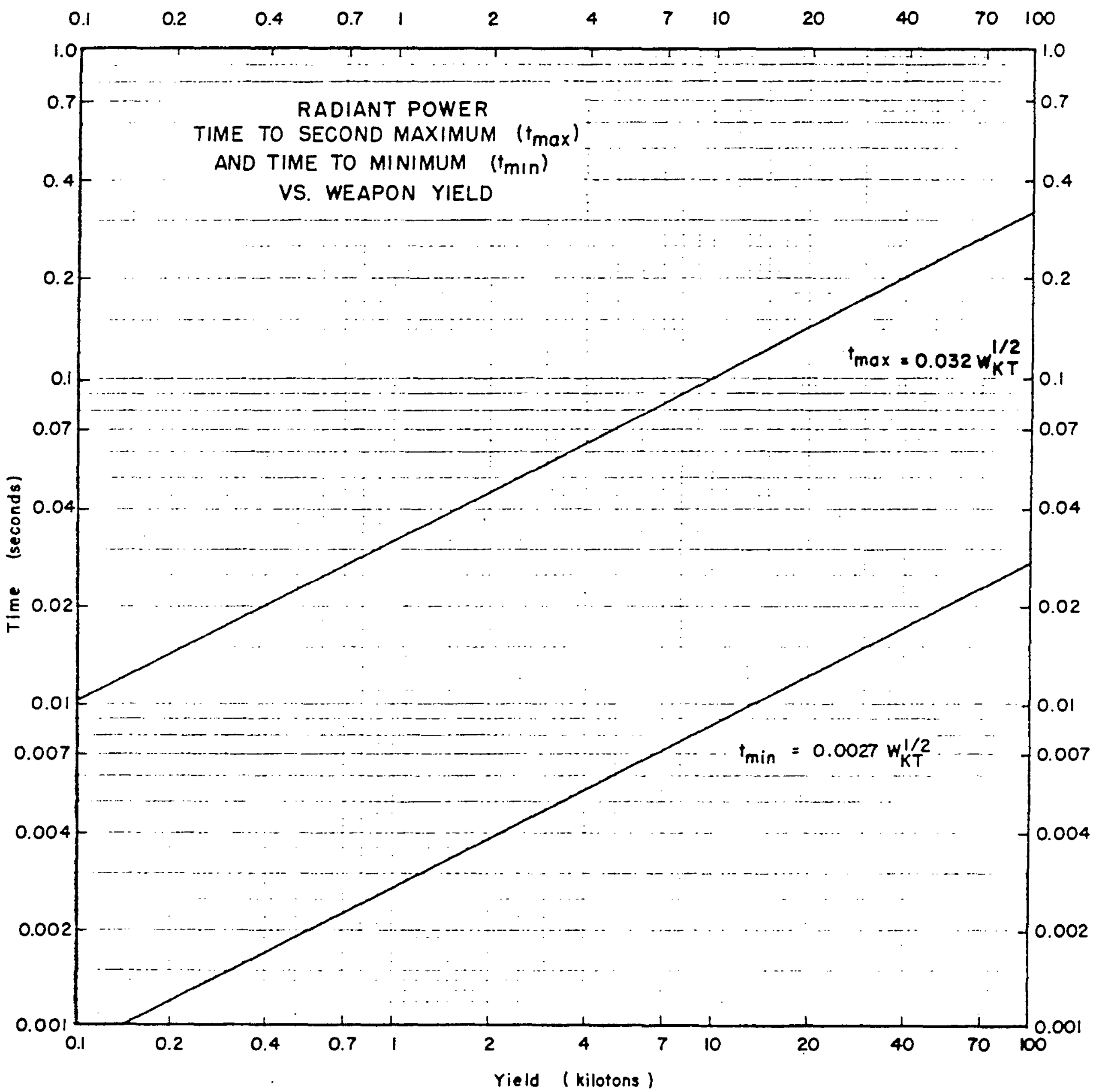
RADIANT POWER
TIME TO SECOND MAXIMUM (t_{max})
AND TIME TO MINIMUM (t_{min})
VS. WEAPON YIELD
$t_{max} = 0.032\,W_{KT}^{1/2}$
$t_{min} = 0.0027\,W_{KT}^{1/2}$
Time (seconds)
Yield (kilotons)
0.1
0.2
0.4
0.7
1
2
4
7
10
20
40
70
100
1.0
0.7
0.4
0.2
0.1
0.07
0.04
0.02
0.01
0.007
0.004
0.002
0.001

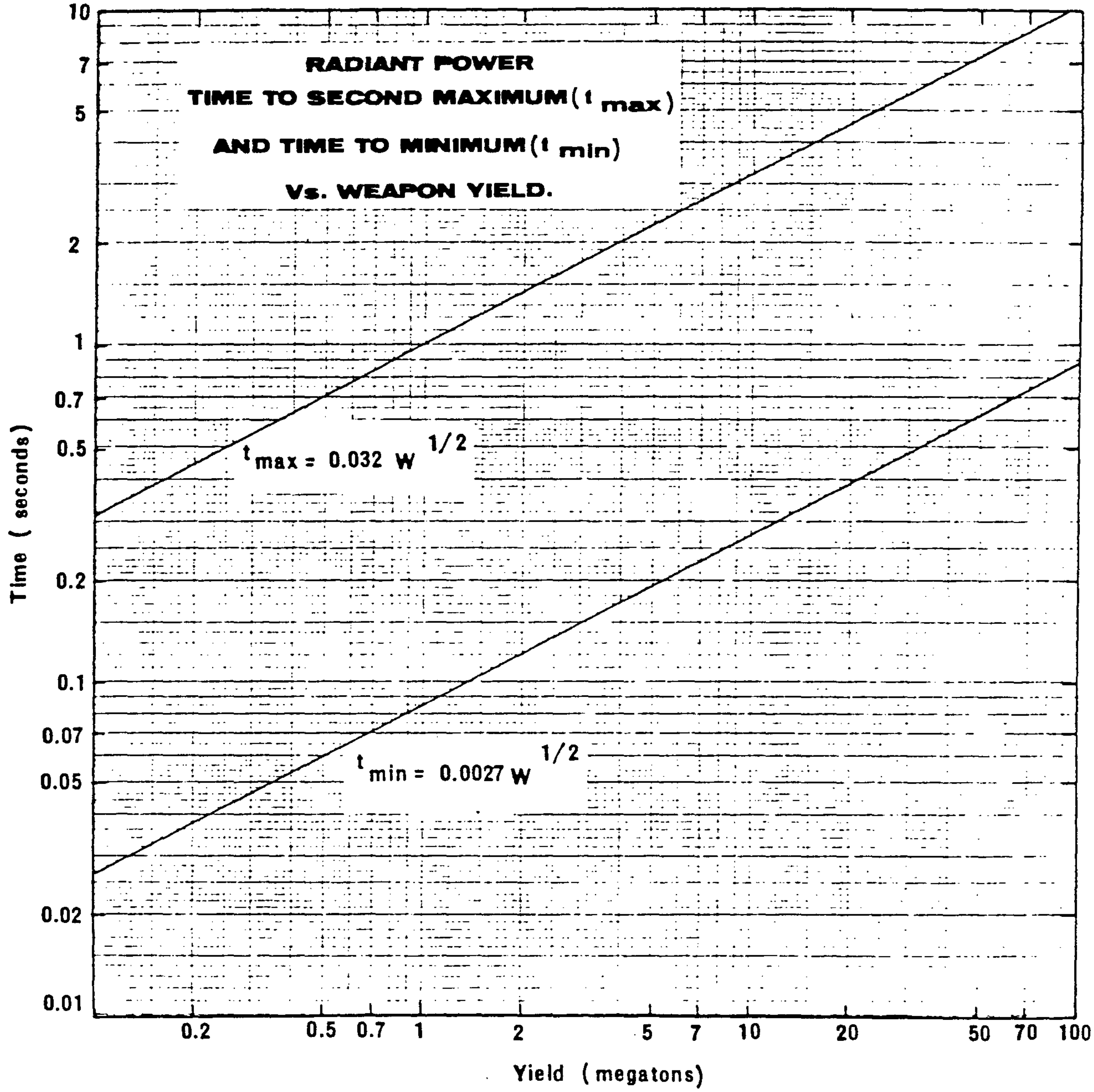
RADIANT POWER
TIME TO SECOND MAXIMUM (t_{max})
AND TIME TO MINIMUM (t_{min})
Vs. WEAPON YIELD.
$t_{max} = 0.032\ W^{1/2}$
$t_{min} = 0.0027\ W^{1/2}$
Time (seconds)
10
7
5
2
1
0.7
0.5
0.2
0.1
0.07
0.05
0.02
0.01
0.2
0.5
0.7
1
2
5
7
10
20
50
70
100
Yield (megatons)

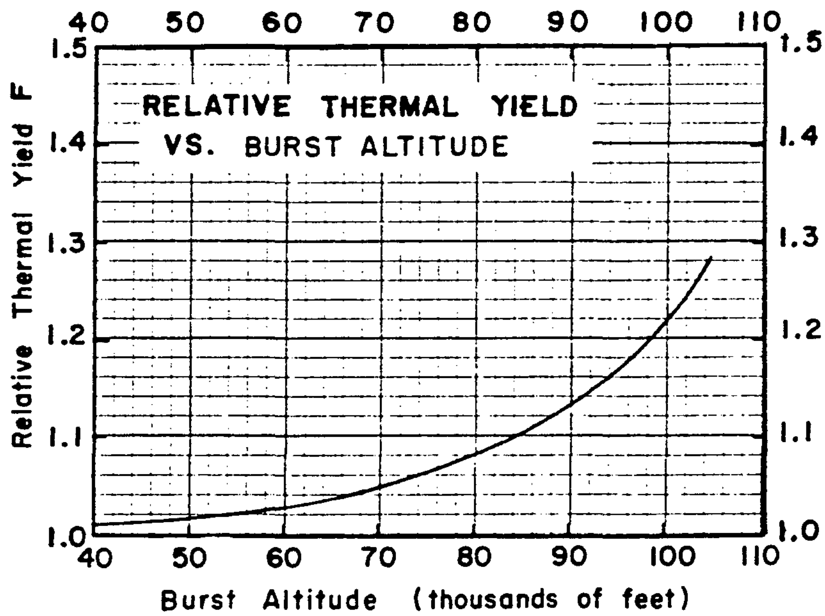

RELATIVE THERMAL YIELD VS. BURST ALTITUDE

Figure 3-4 gives an estimate of the relative thermal yield for various burst altitudes. The values of atmospheric transmissivity at very high altitudes are not known with any certainty, but are believed to be only slightly less than unity.

To calculate the radiant exposure, Q, at a given slant range from a high altitude burst, use the following equation:

$$Q=\frac{3.16\times10^6\ WF}{D^2}\ \text{cal/sq. cm.}$$

where W=weapon yield (in KT)

F=relative thermal yield (from figure 3-4)

D=slant range from detonation (yards)

Example.

Given: A 10 KT burst at 50,000 feet.

Find: Radiant exposure at 1,000 yards from the detonation.

Solution: From figure 3-4 the relative thermal yield, F, at 50,000 feet is 1.02. Therefore,

$$Q=\frac{3.16\times10^6\ (10)\ (1.02)}{(1{,}000)^2}=32.2\ (\pm4.8)$$

cal/sq cm. *Answer.*

Reliability. The values given for the relative thermal yield are subject to errors of ±15 percent at 50,000 feet and to increasingly larger errors at greater altitudes.

Related material.

See paragraph 3.2*d*.

See also figures 3-6A and 3-6B.

ATMOSPHERIC TRANSMISSIVITY

Figures 3–5A and 3–5B give the atmospheric transmissivity versus slant range for three sets of atmospheric conditions for both air and surface burst weapons. These curves are presented for illustrative purposes, since these were used to derive the radiant exposure vs. slant range curves of figures 3–6A and 3–6B.

The differences between the air burst and surface burst curves are caused by the difference in apparent radiating temperatures (when viewed from the ground) and the difference in geometrical configuration of the two types of burst. The three sets of atmospheric conditions represented are:

50 mile visibility and 5 gm/m^3 water vapor.

10 mile visibility and 10 gm/m^3 water vapor.

2 mile visibility and 25 gm/m^3 water vapor.

It is believed that these conditions pertain to the extreme and the average atmospheres which occur naturally.

Reference can be made to the atmospheric water vapor concentration curves in appendix I to ascertain under what conditions of relative humidity and ambient temperature a particular water vapor concentration will occur.

Reliability. The curves of figures 3–5A and 3–5B have not been verified at ranges beyond one-half the visibility and, as a result, are subject to considerably reduced reliability beyond these ranges.

Related material.

See paragraph 3.3*b*.

See also figures 3–6A and 3–6B.

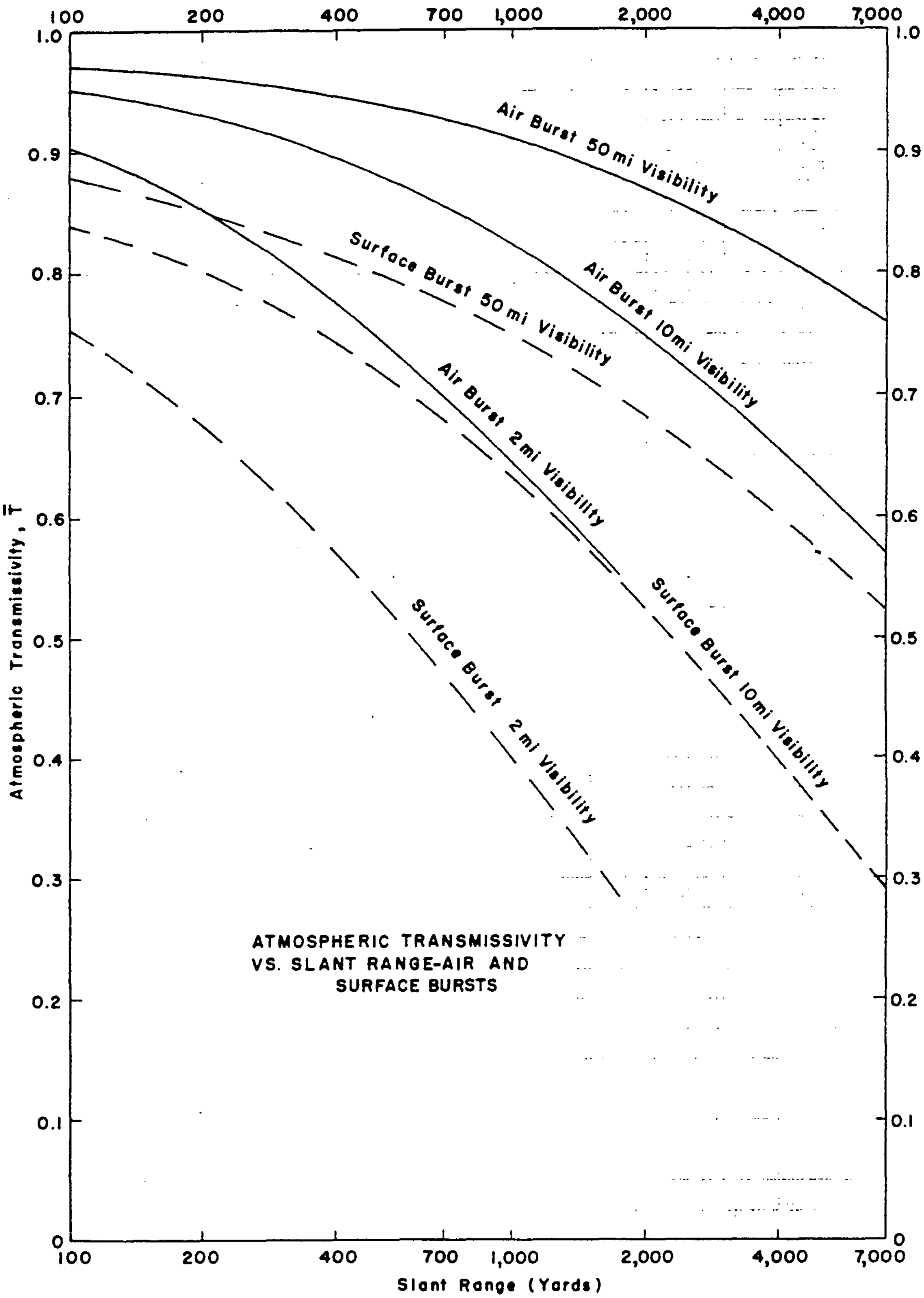
100
200
400
700
1,000
2,000
4,000
7,000
1.0
0.9
0.8
0.7
0.6
0.5
0.4
0.3
0.2
0.1
0
Atmospheric Transmissivity, T̄
Slant Range (Yards)
Air Burst 50 mi Visibility
Air Burst 10mi Visibility
Air Burst 2mi Visibility
Surface Burst 50 mi Visibility
Surface Burst 10mi Visibility
Surface Burst 2mi Visibility
ATMOSPHERIC TRANSMISSIVITY
VS. SLANT RANGE-AIR AND
SURFACE BURSTS

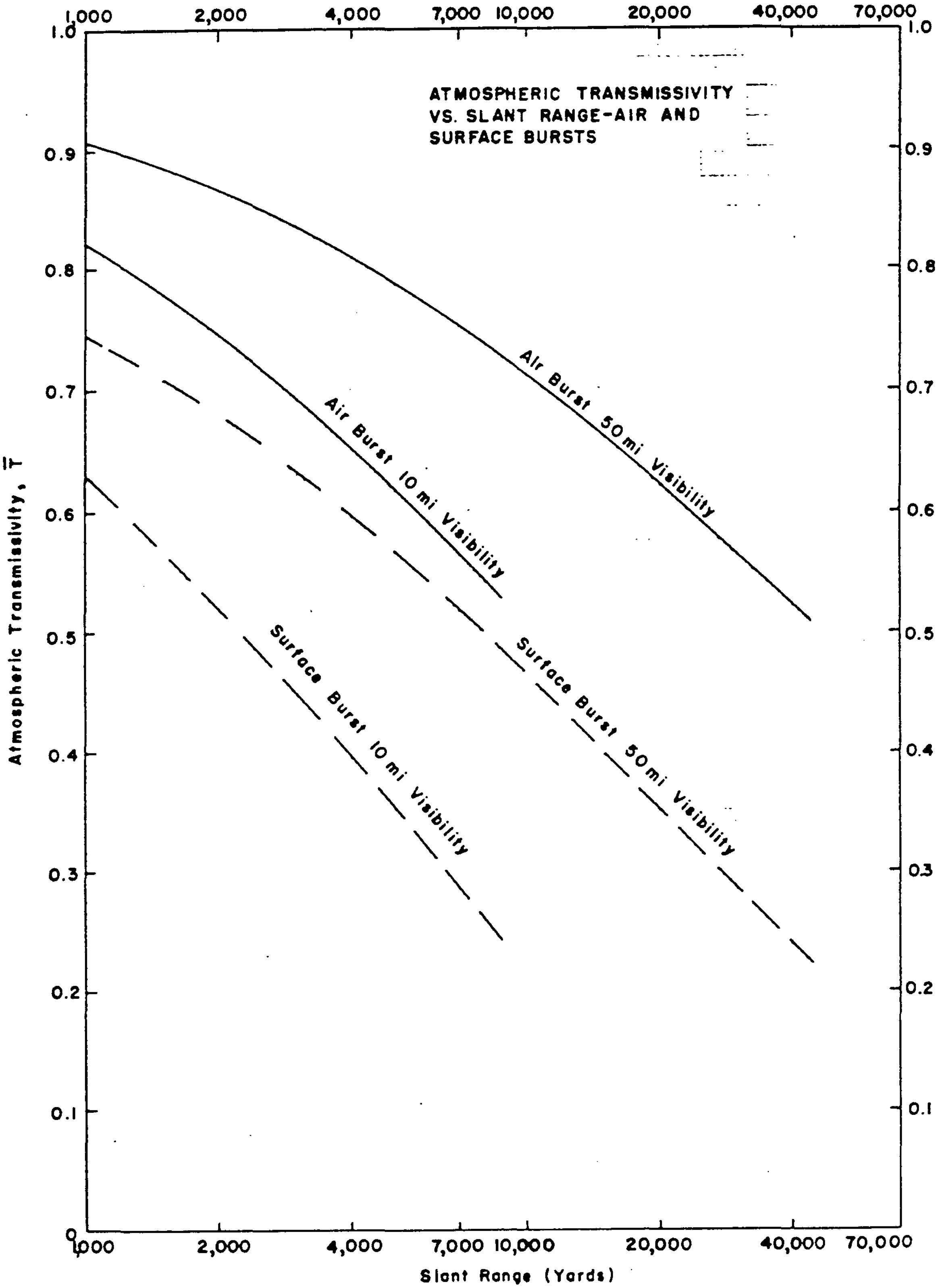
ATMOSPHERIC TRANSMISSIVITY
VS. SLANT RANGE-AIR AND
SURFACE BURSTS
1,000
2,000
4,000
7,000
10,000
20,000
40,000
70,000
1.0
0.9
0.8
0.7
0.6
0.5
0.4
0.3
0.2
0.1
0
Air Burst 50mi Visibility
Air Burst 10 mi Visibility
Surface Burst 50mi Visibility
Surface Burst 10 mi Visibility
Atmospheric Transmissivity, T̄
Slant Range (Yards)

BLANK

RADIANT EXPOSURE FROM AIR AND SURFACE BURSTS

Figures 3–6A and 3–6B present the radiant exposure (i. e., incident radiant energy per unit area) versus slant range curves for 1 KT air and surface bursts. The solid curves are for the air burst, those above 180 $W^{0.4}$ feet. For bursts at heights between 180 $W^{0.4}$ feet and the surface, the radiant exposure will lie between the corresponding solid and dashed curves. Until further data are obtained, a linear interpolation between the two curves should be made for bursts in the transition zone (see example 2). For each type of burst shown, three curves are presented: 50 mile visibility and 5 gm/m³ water vapor; 10 mile visibility and 10 gm/m³ water vapor; and 2 mile visibility and 25 gm/m³ water vapor.

Figures 3–6A and 3–6B are based on the air and surface burst thermal yields (par. 3.2*d*) and the atmospheric transmissivity curves of figures 3–5A and 3–5B.

Scaling. For a given slant range the radiant exposure, Q, is proportional to the weapon yield, W:

$$\frac{Q_1}{Q_2}=\frac{W_1}{W_2}$$

In figures 3–6A and 3–6B, Q_1 is given for $W_1=1$ KT.

Example 1.

Given: A 40 KT detonation at 3,000 feet height of burst and a 10 mile visibility.

Find: The slant range at which the radiant exposure is 10 cal/cm².

Solution: The scaled burst height is $\frac{3,000}{(40)^{0.4}}=$ 685 feet; therefore, the air burst curve should be used.

Then $Q_1=10\left(\frac{1}{40}\right)=0.25$ cal/cm². From figure 3–6B, the slant range at which 0.25 cal/cm² would be received from an air burst (visibility = 10 miles) is 3,000 yards. *Answer.*

Example 2.

Given: A 500 KT detonation at 1,200 feet height of burst and a 50 mile visibility.

Find: The slant range at which the radiant exposure is 25 cal/cm².

Solution: The scaled burst height is $\frac{1,200}{(500)^{0.4}}=$ 100 feet; therefore, for this transition burst, the range sought will lie $\frac{100}{180}$ of the distance between the surface and air burst values.

Then $Q_1=25\left(\frac{1}{500}\right)=0.05$ cal/cm².

From figure 3–6B, the ranges at which 0.05 cal/cm² would occur for surface and air bursts (visibility = 50 miles) are 4,100 and 7,000 yards, respectively. The answer is then:

$$4,100+\frac{100}{180}(7,000-4,100)=5,700 \text{ yards.}$$

Answer.

Reliability. Factors limiting the applicability of figures 3–6A and 3–6B are discussed in paragraphs 3.3*b* and 3.3*d*. In addition, the reliability is expected to decrease as the weapon yield is increased above 100 KT, and as the slant range is increased beyond one-half the visibility, as noted in figures 3–5A and 3–5B.

Related material.

See paragraphs 3.2 and 3.3.

See also figures 3–5A and 3–5B.

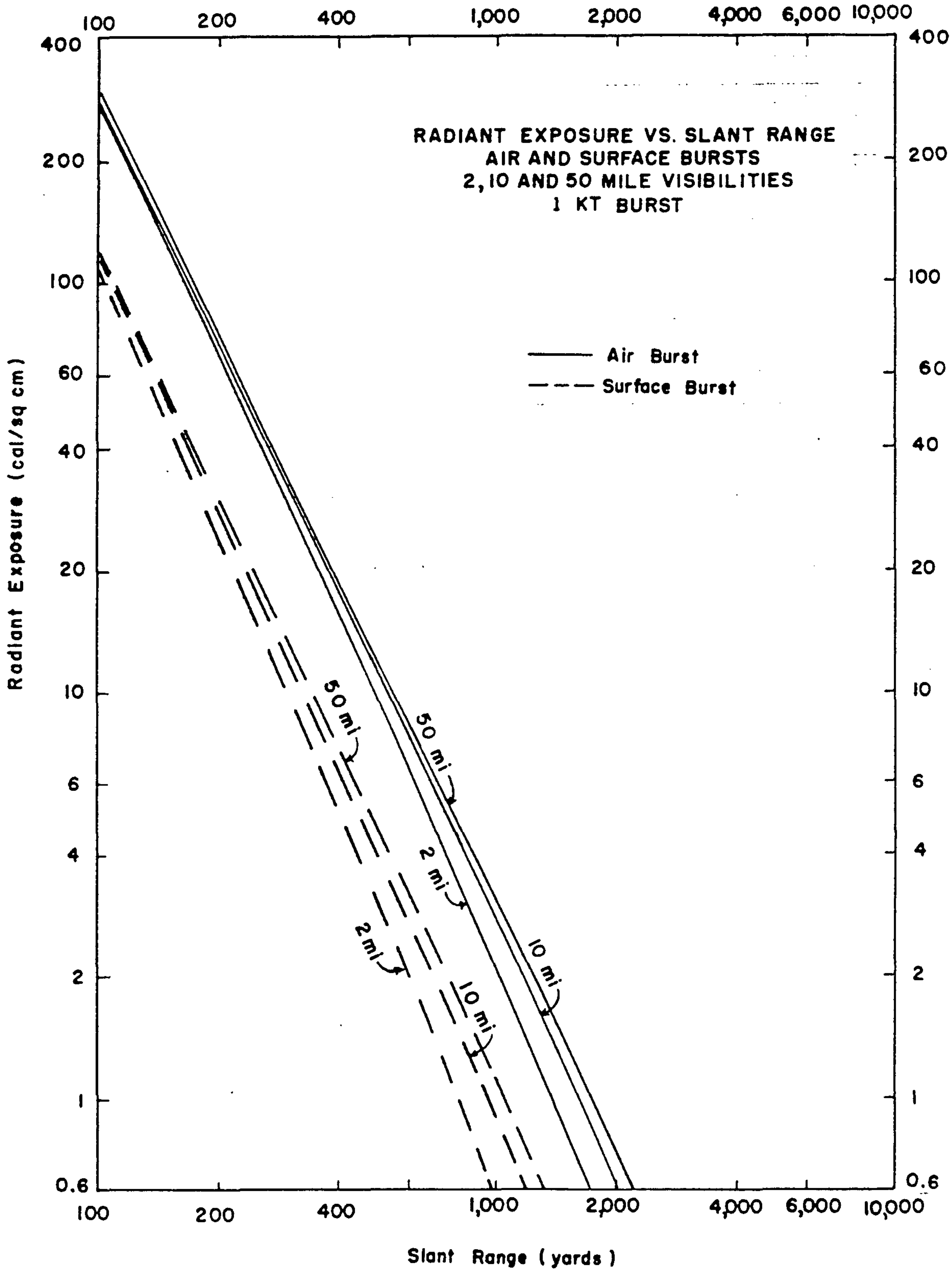
RADIANT EXPOSURE VS. SLANT RANGE
AIR AND SURFACE BURSTS
2, 10 AND 50 MILE VISIBILITIES
1 KT BURST
Air Burst
Surface Burst
50 mi
50 mi
2 mi
2 mi
10 mi
10 mi
Radiant Exposure (cal/sq cm)
Slant Range (yards)
100
200
400
1,000
2,000
4,000
6,000
10,000
400
200
100
60
40
20
10
6
4
2
1
0.6

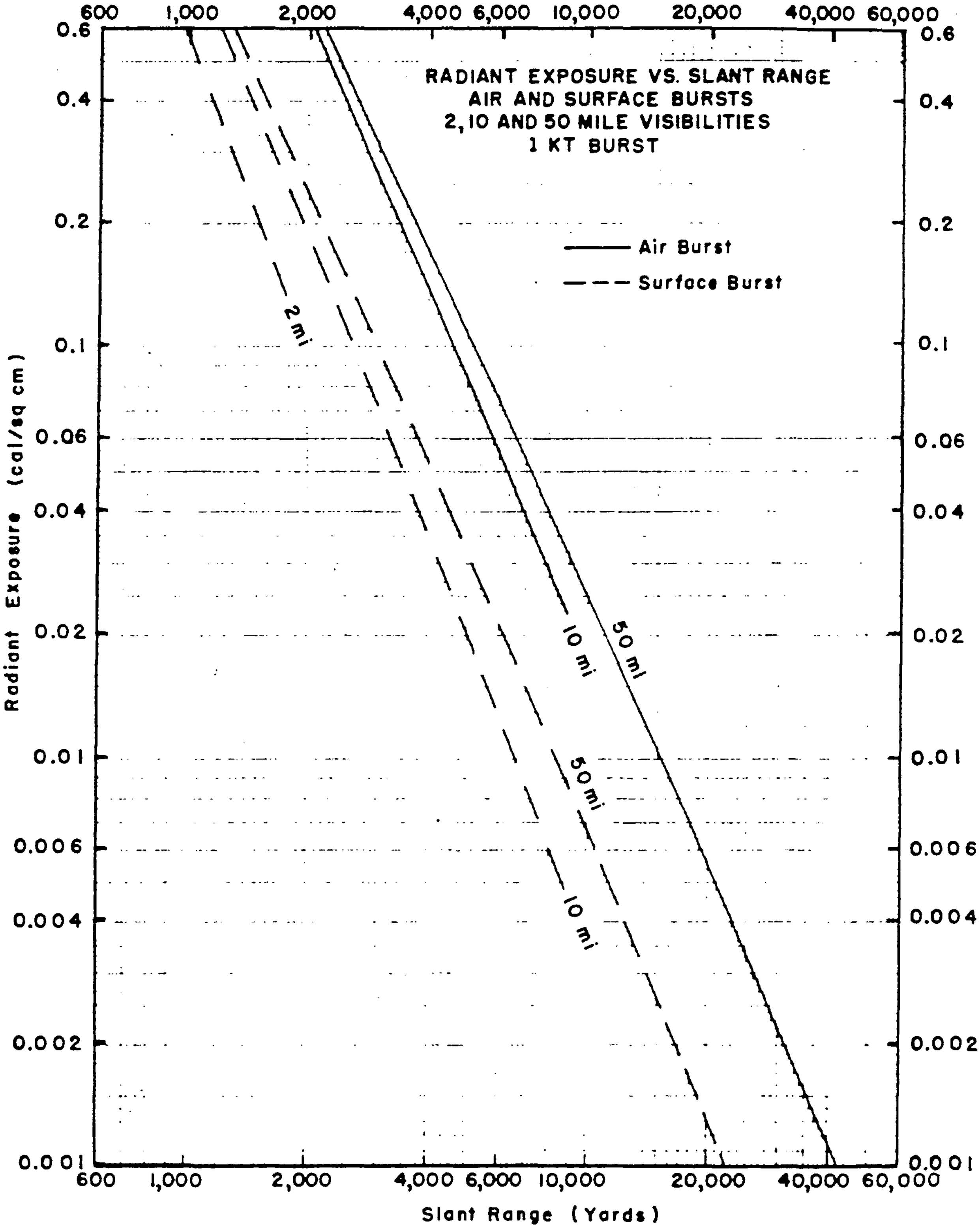
RADIANT EXPOSURE VS. SLANT RANGE
AIR AND SURFACE BURSTS
2, 10 AND 50 MILE VISIBILITIES
1 KT BURST
Air Burst
Surface Burst
2 mi
10 mi
50 mi
50 mi
10 mi
Radiant Exposure (cal/sq cm)
0.6
0.4
0.2
0.1
0.06
0.04
0.02
0.01
0.006
0.004
0.002
0.001
600
1,000
2,000
4,000
6,000
10,000
20,000
40,000
60,000
Slant Range (Yards)

BLANK

4
Nuclear
Initial

SECTION IV
NUCLEAR RADIATION PHENOMENA

4.1 General

a. Radiations Produced. When a nuclear weapon is exploded, part of the energy of the explosion appears in the form of nuclear radiations, consisting of gamma rays, neutrons, alpha particles and beta particles. For the purpose of discussing radiation effects, initial radiation is defined as that nuclear radiation which is delivered during approximately the first minute after detonation; while residual radiation is that radiation which is delivered thereafter, including that from bomb debris and from neutron induced activity in material which was outside the bomb case. The neutrons are released in the fission and fusion reactions; the gamma radiation arises from the fission products and from the capture of neutrons in bomb materials, nitrogen of the atmosphere or other materials; the beta particles are emitted by the radioactive fission products; and the alpha particles originate from any remaining plutonium or uranium. These general considerations apply to weapons using fusion principles in which a part of the energy arises from fission processes as well as to fission devices.

b. Relative Importance. The damaging effects of the nuclear radiations vary with the medium in which the bomb is detonated and will be discussed in detail under the specific burst conditions. In general, initial gamma radiation is more important than neutron radiation for weapons with relatively large amounts of neutron attenuating and absorbing material. Usually these weapons are of large physical size. However, for weapons of small physical size, neutron and gamma radiation may be of equal importance. Shielding can change the relative importance of gammas and neutrons at the target. Neutrons are almost all produced in the first second after detonation, while gamma radiation is emitted from the fireball, the cloud, fission products deposited on the ground, and from elements in which radioactivity has been induced by neutron irradiation. Because the ranges of alpha and beta particles are very limited in the air and the particles are readily absorbed in most materials, they are of little military importance when only the initial radiations are being considered. However, in the instances where significant amounts of bomb debris are concentrated or are in close proximity to the human skin, beta radiation may become a hazard.

c. Units. The total radiation dosage received by an individual is described in terms of the roentgen unit (r), and the rate at which the dose is received at a given time is given in roentgens per hour. The roentgen unit is an X- and gamma-radiation dose unit. As an illustration, one gram of radium will produce a dose rate of one roentgen per hour of gamma radiation at a distance of 3 feet. Neutron radiation dose may be measured in rem (roentgen-equivalent-mammal), which is a biological dose unit. The biological effect of 1 rem of neutrons equals that of 1 r of X-rays or 1 r of gamma rays. Combinations of these doses are treated in paragraph 6.3*b*. Neutron dose may also be measured in terms of a unit called the rep (roentgen-equivalent-physical); however, this unit will not be used in this manual since we are primarily concerned with the biological rather than the physical effects of radiation. Another unit which is important in many uses is the curie. A curie is that quantity of radioactive material which provides 3.7×10^{10} disintegrating atoms per second. One gram of radium decays at such a rate. The total amount of gamma-active fission products at 1 hour after the explosion of a 20 KT bomb is 6×10^{9} curies. One megacurie (10^{6} curies) of fission products per square mile distributed uniformly over an ideal flat surface produces a gamma radiation dose rate of about 4 r/hr at 3 feet above the surface.

4.2 Initial Radiation

a. Gamma Radiation.

(1) *General.* Air density is the controlling factor affecting attenuation of gamma radiation in the atmosphere; conse-

quently, gamma radiation dose varies with air density. Figures 4–1 through 4–7 reflect this variation. These figures are drawn for various relative air densities. Relative air density is the ratio of the density under a given condition to the density at a temperature of 0° C. and a pressure of 1,013 millibars (mb). (Standard pressure = 1 atmosphere = 1,013 mb = 14.7 psi = 29.9 inches of mercury.) Typical relative air densities at various altitudes are listed in table 4–1, while formulae and a chart for obtaining relative air density in various situations are given in appendix II. The contribution of relative humidity to the atmospheric density is negligible as compared with those changes which are due to temperature and pressure, and therefore its effect is not included in the gamma dose figures.

Table 4–1. Typical Relative Air Densities (R) at Various Altitudes

Altitude (ft)	P (mb)	t (° C.)	t (° F.)	R
0	1,013	15	59	0.95
2,000	940	10	50	.90
6,000	810	0	32	.80
10,000	690	−5	23	.70
14,000	580	−15	5	.60
20,000	460	−25	−13	.50
26,000	350	−35	−31	.40
34,000	250	−52	−62	.30
43,000	160	−55	−67	.20
56,000	80	−55	−67	.10

A considerable fluctuation of air density occurs after the shock front from a nuclear detonation has passed a given point. The reduced air density in the negative phase allows a heavy dose of gamma rays to arrive at the point before the air density returns to its ambient value. This "hydrodynamic enhancement" varies with weapon yield, range and height of burst. The enhancement factor increases with increasing yield and distance within the ranges of interest. From a burst close to the surface of the earth there will be a direct shock wave and reflected shock wave. As a result, the shock enhancement of the dose is greater for bursts on or near the surface than for higher altitude bursts where the magnitude of the reflected shock wave is small. The height of burst above which the enhancement due to the reflected shock wave becomes negligible is taken as the lower limit of an air burst for the initial gamma radiation effect, and, although a precise determination of this height is difficult or impossible with existing data, a scaled height of burst of 1,500 $W^{1/3}$ feet has been estimated as the point at which the changeover occurs.

(2) *Surface burst.* Figures 4–1 through 4–4 present the initial gamma radiation dose in roentgens versus slant range for various yields of nuclear weapons detonated on the surface of the earth. These curves are presented for four relative air densities selected to represent the usual atmospheric conditions for surface bursts. A method for treating the unusual case of lower relative air density on the surface is presented in (5) below. Instructions for interpolating for values of relative air density other than those presented are contained on the facing pages for these figures.

The curves of figures 4–1 through 4–4 are strictly applicable only to a receiver in close proximity to the earth's surface, such as a man standing on the ground. Since the gamma ray dose received by a man does not all arrive directly as a line-of-sight propagation from the source, owing to scatter by the atmosphere, elevation of the man to significant distances away from the surface permits a larger amount of radiation to reach him from all directions. To correct for this effect, the dose shown in figures 4–1 through 4–4 should be multiplied by 1.3 when the receiver is three hundred feet or more above the surface, as would be the case for personnel in aircraft.

(3) *Burst in the transition zone.* The shock enhancement of the gamma radiation dose from weapons detonated near the

surface will be about the same as that for a surface burst. This condition holds through most of the transition zone, with a rapid transition to the air burst condition near the top of the zone. For this reason, the dose from weapons detonated in the transition zone should be obtained from the surface burst curves (figs. 4–1 through 4–4) in the manner described in (2) above.

(4) *Air Burst.* As used in this paragraph, the term "air burst" refers to one above 1,500 $W^{1/3}$ feet. The shock enhancement factor of the initial gamma radiation from an air burst is about equal to that from a surface burst of half the yield. Thus, to find the initial gamma radiation dose received by a surface target from a particular air burst, one must first find the dose delivered during the surface burst of a weapon of half that yield (which will have the same enhancement factor as the weapon of interest). Since the gamma flux emitted is proportional to yield, one must then double the dose delivered during the surface burst of the smaller weapon to obtain the dose delivered by the weapon of interest in air (figs. 4–1 through 4–4). If the target is more than 300 feet above the surface of the earth, the dose thus calculated should once again be multiplied by 1.3.

To simplify the solution of problems where the nuclear detonation and the target are both at high altitude, figures 4–5 through 4–7 present the initial gamma radiation dose in roentgens versus slant range for air burst weapons of various yields for several low relative air densities. The doses obtained from these curves apply to targets which are more than 300 feet above the surface of the earth. To apply these curves to targets on the surface, the dose obtained from figures 4–5 through 4–7 must be divided by 1.3.

(5) *Exceptional cases.* For the exceptional case where a burst on the surface or in the transition zone occurs under atmospheric conditions such that the relative air density falls within the range of values presented in figures 4–5 through 4–7, the dose may be obtained from these air burst curves in the following manner. If the target is more than 300 feet above the surface, use the curve for the appropriate relative air density and for a yield equal to twice the yield of the burst in question in order to account for the increased enhancement. Divide the dose indicated for this higher yield by two to correct for the source strength.

If the target is on the surface, the dose is obtained as above and then divided by an additional factor of 1.3 to correct for target location. The complete procedure for such a condition is to read the dose for a yield equal to twice the yield in question and then divide this dose by three to correct for source strength and receiver location.

(6) *Subsurface bursts.* The initial gamma radiation dose from an underground nuclear explosion at a depth of 17 feet is given in figure 4–8 for a 1 KT detonation. For yields between 0.2 and 7.5 KT and depths between 12 and 22 feet, the dose is proportional to the yield. Extrapolation to higher yields is unreliable. For detonations at greater depths, the initial gamma dose is less than that indicated in figure 4–8. The magnitude of this reduction with increased depth is not known. The gamma radiation dose from an underwater burst is believed to be similar to that from an underground shot, though it may well be somewhat greater. The underground detonation curves of figure 4–8 may be used to estimate initial gamma radiation dose as a function of distance for underwater bursts.

b. Neutron Radiation. The neutron radiation dose delivered as a result of a nuclear detonation varies widely with different weapon configurations. Figure 4–10 presents the neutron radiation dose versus slant range in various air densities for a 1 KT detonation. These curves may be considered as representative of fission weapons. The doses predicted from figure 4–10 might be high by a factor of 10 for weapons containing large quantities of neutron attenuating material. A better estimate of neutron dose for many specific weapons may be obtained from the Nuclear Radiation Handbook (AFSWP-1100), published under a higher security classification. Figure 4-11 presents the neutron radiation dose versus slant range in various air densities for a 1 MT detonation of a thermonuclear weapon. The curves of figures 4-10 and 4-11 may be applied to all bursts except subsurface. Neutron radiation is not expected to be significant for subsurface bursts.

c. Delivery Rate. The rate of delivery of the militarily significant portion of the initial gamma radiation dose is governed by the rate of rise of the fireball, the magnitude of the changes in air density due to the blast wave, and the relative importance of the dose caused by gammas arising from neutron capture in nitrogen compared to the dose caused by gammas from the fission products. Thus the rate of delivery of initial gamma radiation varies both with weapon yield and with distance from the point of burst. Figure 4-9 gives examples of this, and shows the percentage of total initial gamma radiation dose received as a function of time after detonation. The rate of delivery of neutron radiation is quite large regardless of yield, and practically all of the neutron radiation is received within about 0.1 second.

BLANK

INITIAL GAMMA RADIATION DOSE FOR VARIOUS RELATIVE AIR DENSITIES

The curves of figures 4-1 through 4-7d present the initial gamma radiation dose as a function of range for various yields, with each figure representing a particular relative air density (R). From these curves can be determined the slant range at which a weapon of given yield will produce a specified dose, or conversely, the yield required to produce a given dose at a desired range.

Figures 4-1 through 4-4 are directly applicable to bursts on the surface or in the transition zone (heights of burst up to 1,500 $W^{1/3}$ feet), surface targets, and conditions of high (0.8 or greater) relative air density. Figures 4-5 through 4-7 are directly applicable to air bursts (heights of bursts greater than 1,500 $W^{1/3}$ feet), targets at heights of more than 300 feet above the surface, and conditions of low (0.6 or less) relative air density. Figures 4-7a, 4-7b, 4-7c, and 4-7d are applicable to sub-kiloton surface bursts. These are expected to be the most usual applications of the figures; however, the following chart summarizes the procedures to be followed to obtain the initial gamma radiation dose for these as well as other situations. The relative air density to be used is an average between burst point and receiver. Methods for obtaining the proper value are detailed in appendix II.

Interpolation to obtain the initial gamma radiation dose for conditions of relative air density other than those presented in figures 4-1 through 4-7d may be accomplished in the following manner. Obtain the dose for the burst height and target location of interest and for the two values of relative air density closest to the value of interest. Plot the doses so obtained opposite their respective relative air densities on the accompanying interpolation sheet and connect two points with a straight line. The desired dose is then read opposite the interesection of this line with the value of relative air density in question. When applying this method of interpolation, it must be borne in mind that the doses must be obtained for the same condition of burst height and target location.

Examples.

(1) *Given:* A 10 MT surface burst, with relative air density $R=0.9$.

Find: The dose at a point on the ground 5,000 yards from the burst.

Solution: From the 10 MT curve of figure 4-3 ($R=0.9$) the dose at 5,000 yards is 200*r*. *Answer.*

(2) *Given:* A 400 KT air burst, with relative air density $R=0.4$.

Find: The dose delivered to a target at the same altitude as the burst and at a slant range of 3,000 yards.

Solution: From the 0.4 MT curve of figure 4-6 ($R=0.4$), the dose at 3,000 yards is 4,000*r*. *Answer.*

(3) *Given:* A 10 MT surface burst, with relative air density $R=0.7$.

Burst height and R value	Target location	
	Surface	Air (over 300 ft)
Surface or transition zone—High R.	Read dose for actual weapon yield and appropriate R from figures 4-1 through 4-4 and 4-7a through 4-7d.	Read dose for actual weapon yield and appropriate R from figures 4-1 through 4-4, and 4-7a through 4-7d. Multiply dose so obtained by 1.3.
Surface or transition zone—Low R.	Read dose for yield equal to twice the actual yield and for appropriate R from figures 4-5 through 4-7. Divide the dose so obtained by 3.	Read dose for yield equal to twice the actual yield and for appropriate R from figures 4-5 through 4-7. Divide the dose so obtained by 2.
Air burst—Low R	Read dose for actual weapon yield and appropriate R from figures 4-5 through 4-7. Divide dose so obtained by 1.3.	Read dose for actual weapon yield and appropriate R from figures 4-5 through 4-7.
Air burst—High R	Read dose for yield equal to one-half the actual yield and for appropriate R from figures 4-1 through 4-4 and 4-7a through 4-7d. Multiply the dose so obtained by 2.	Read dose for yield equal to one-half the actual yield and for appropriate R from figures 4-1 through 4-4 and 4-7a through 4-7d. Multiply the dose so obtained by 3.

Find: The dose at a point on the ground 4,500 yards from the burst.

Solution: From the 10 MT curve of figure 4-4 ($R=0.8$), the dose at 4,500 yards is 1,900*r*.

From the 20 MT curve of figure 4-5 ($R=0.6$) the dose at 4,500 yards is 24,000*r*. This is the dose for an air borne target at 4,500 yards from a 20 MT air burst, with $R=0.6$.

$$\text{Then, } \frac{24{,}000}{3}=8{,}000r,$$

which is the dose for a surface target 4,500 yards from a 10 MT surface burst, with $R=0.6$.

The doses obtained above are plotted on the accompanying interpolation sheet opposite $R=0.8$ and $R=0.6$, respectively. These points are connected by a straight line, and, at the intersection of this line with the line representing $R=0.7$, the dose is read as 3,800*r*. *Answer.*

Reliability: The curves of figures 4-1 through 4-7d apply to surface burst weapons in the range of 0.01 KT to 20 MT, and to air burst weapons in the range of 0.01 KT to 40 MT. For yields from 0.01 KT to 100 KT the doses obtained are reliable within a factor of 2. For yields greater than 100 KT and less than 1 MT the doses obtained are reliable within a factor of 5. For yields above 1 MT the doses obtained are reliable within a factor of 10. Extrapolation to yields greater than 20 MT for surface bursts or 40 MT for air bursts is not recommended. The range obtained for a given dose will be reliable to within 10 percent for yields from 0.01 KT to 100 KT, 20 percent for yields greater than 100 KT and less than 1 MT, and 30 percent for yields greater than 1 MT.

Related Material

See paragraphs 4.2a (1) through (5).

See also figure 4-8 for subsurface bursts.

BLANK

RELATIVE AIR DENSITY INTERPOLATION SHEET

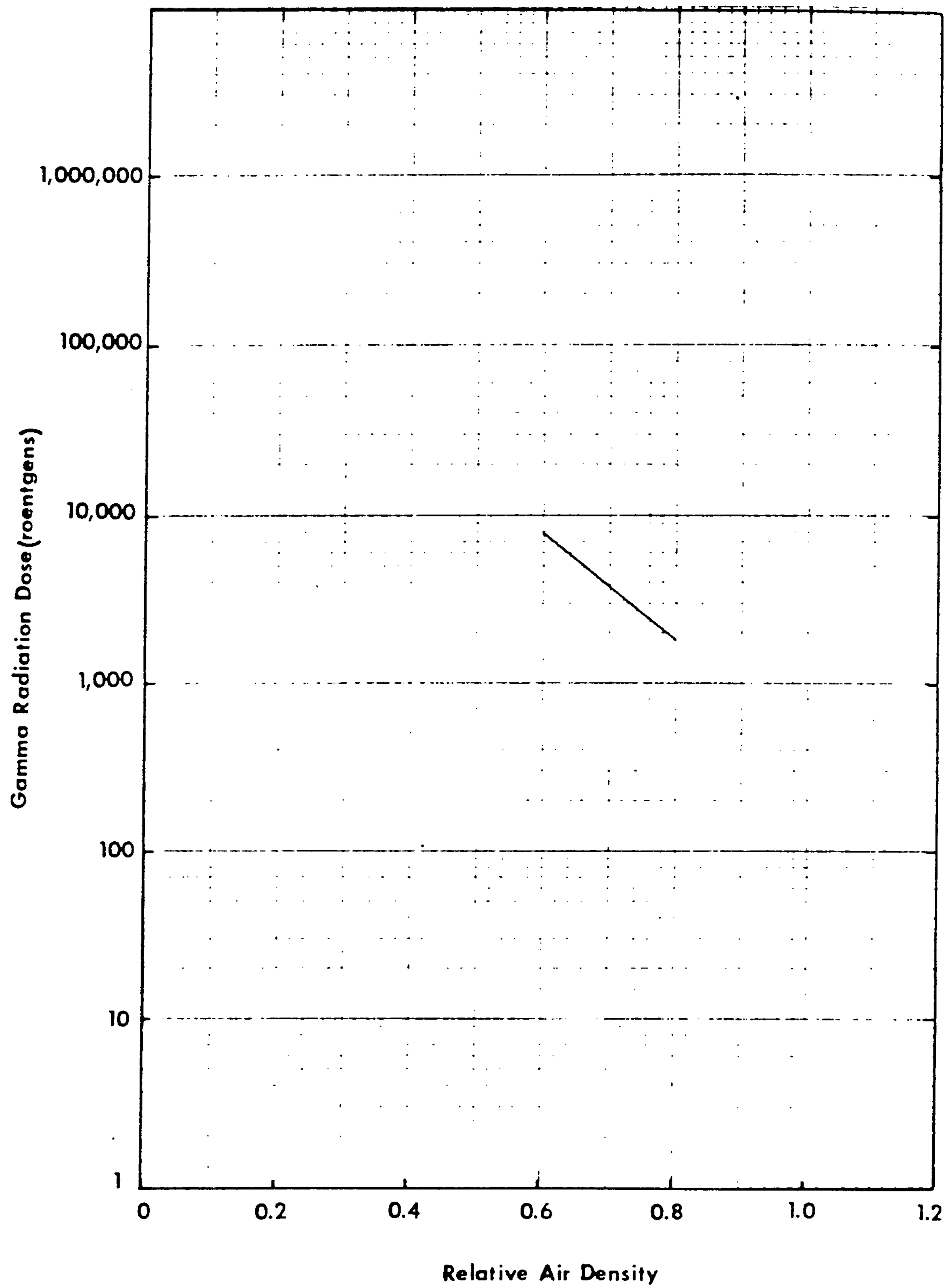

INITIAL GAMMA RADIATION DOSE Vs. SLANT RANGE
SURFACE BURST AND SURFACE TARGET
RELATIVE AIR DENSITY,1.1

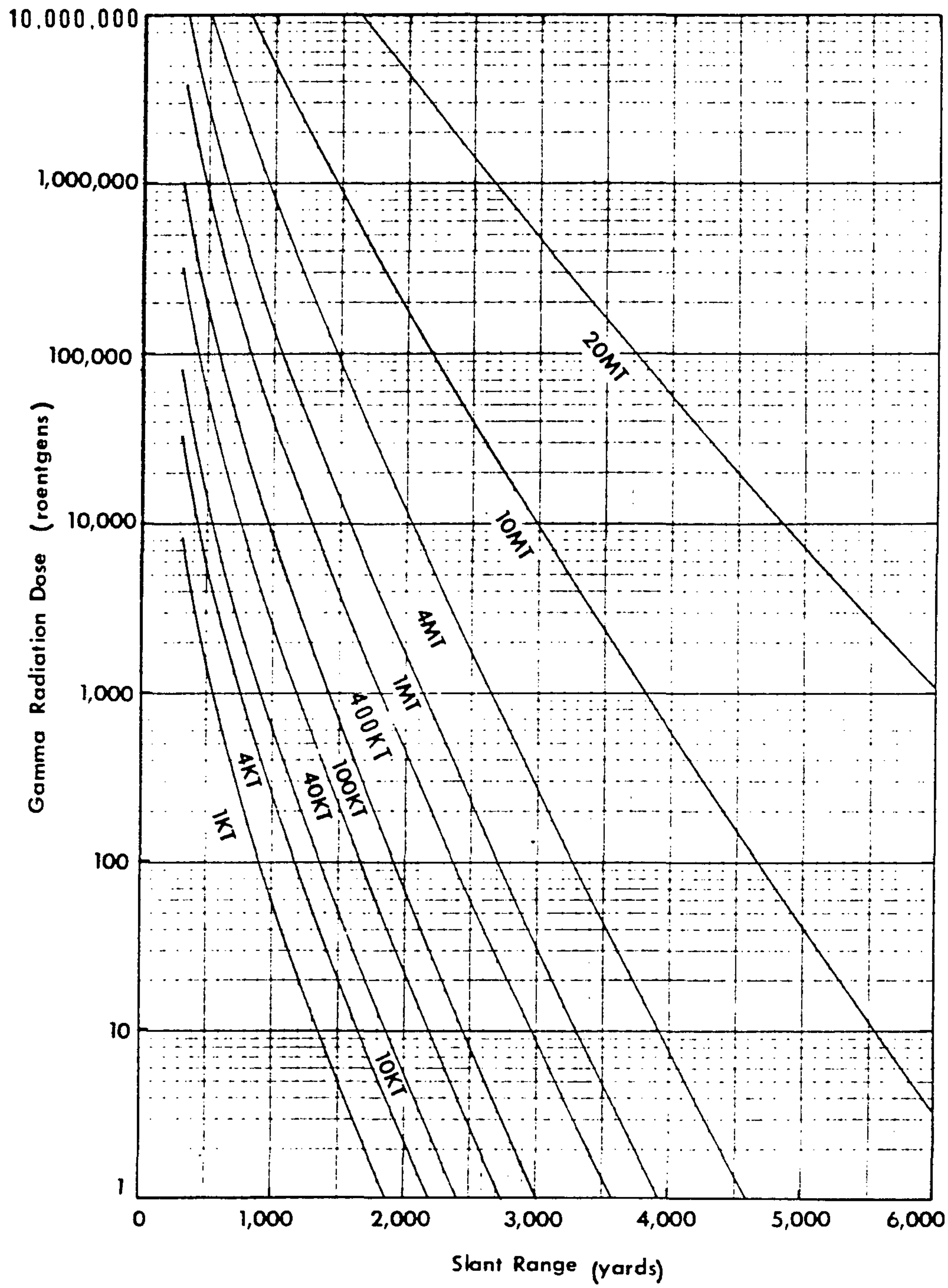

Note: Applicable to other situations as indicated on facing page.

INITIAL GAMMA RADIATION DOSE VS SLANT RANGE
SURFACE BURST AND SURFACE TARGET
RELATIVE AIR DENSITY, 1.0

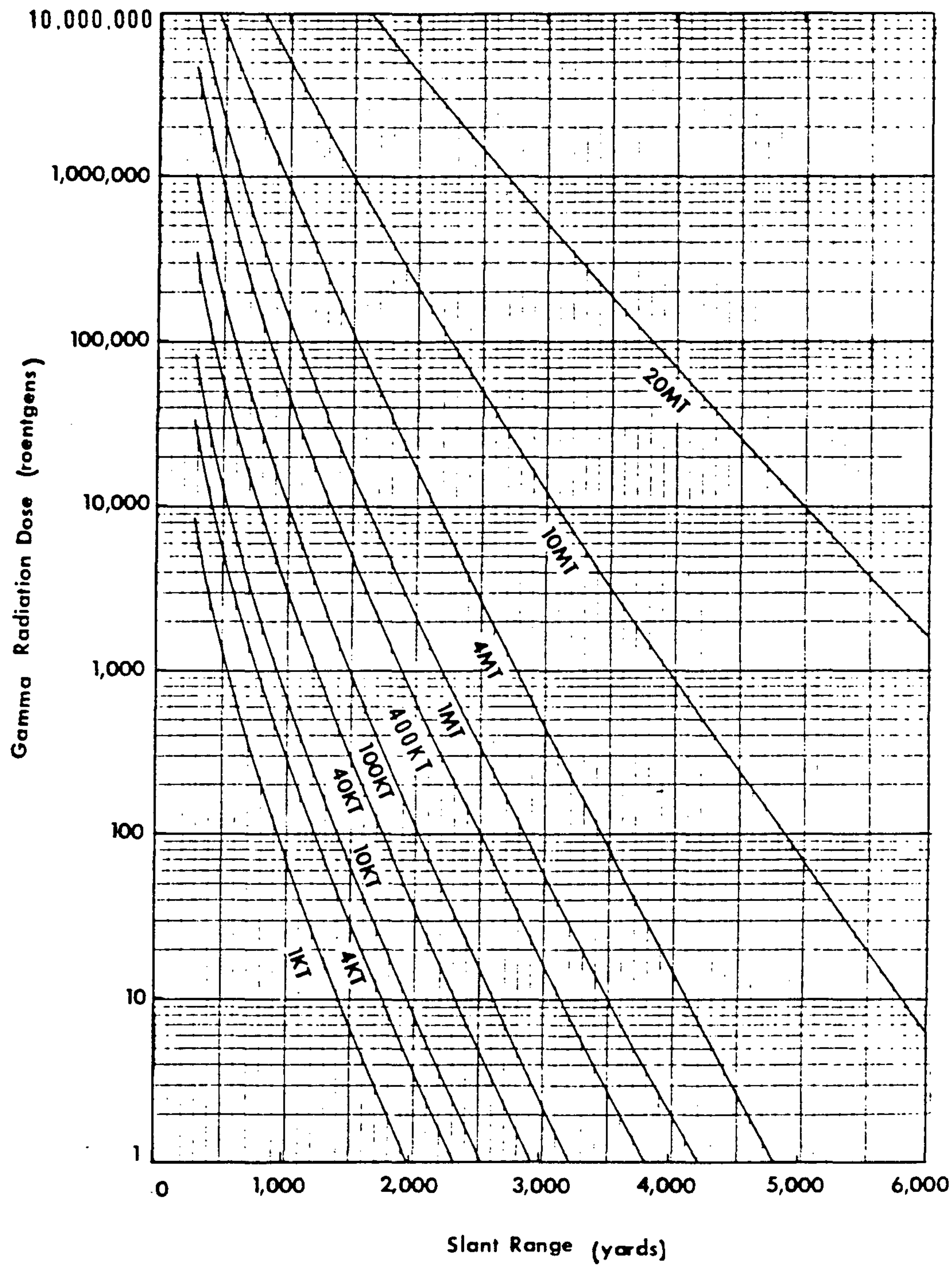

Note: Applicable to other situations as indicated on facing page.

INITIAL GAMMA RADIATION DOSE Vs. SLANT RANGE
SURFACE BURST AND SURFACE TARGET
RELATIVE AIR DENSITY, 0.9

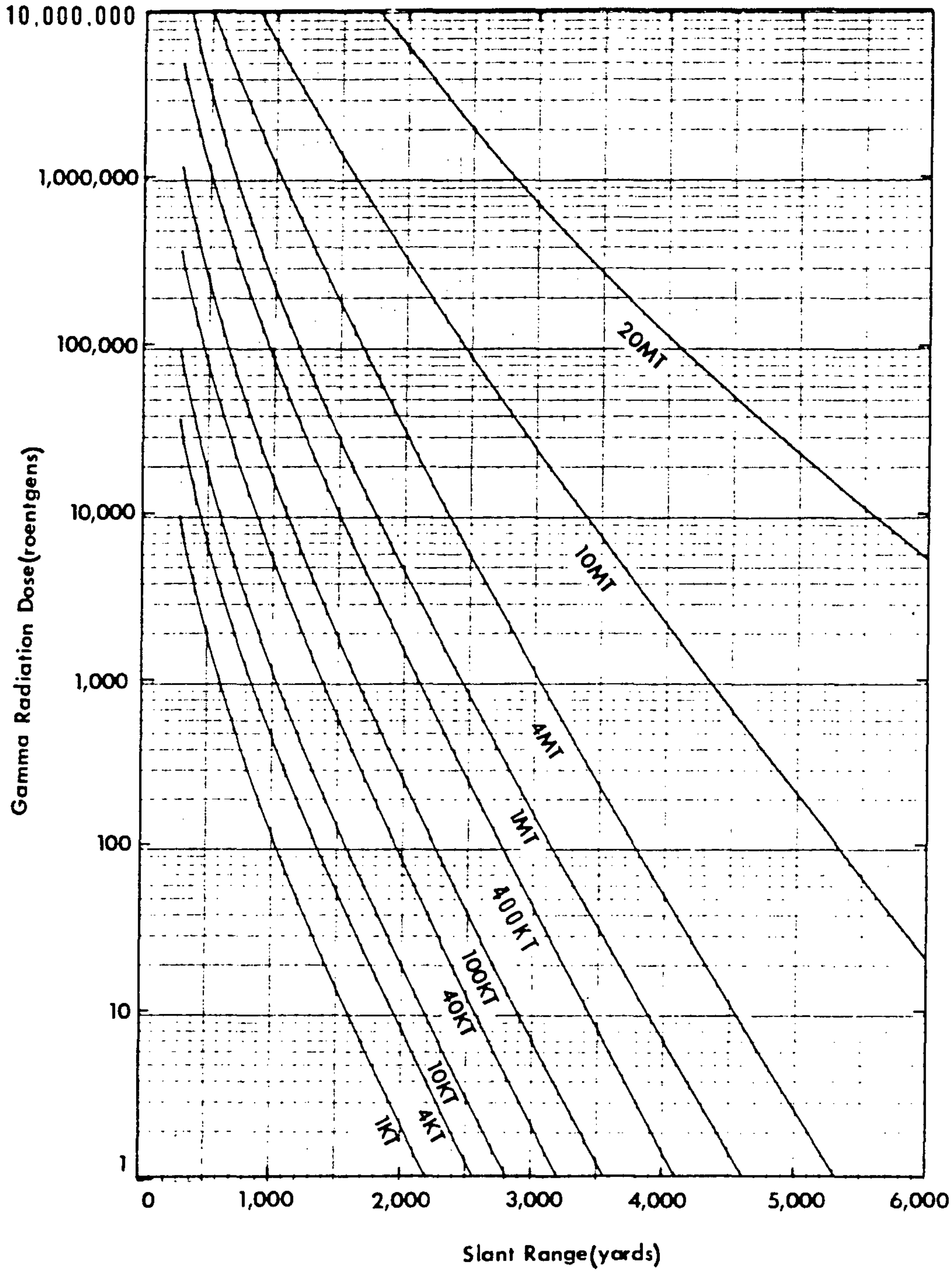

Note: Applicable to other situations as indicated on facing page.

INITIAL GAMMA RADIATION DOSE Vs. SLANT RANGE

SURFACE BURST AND SURFACE TARGET

RELATIVE AIR DENSITY, 0.8

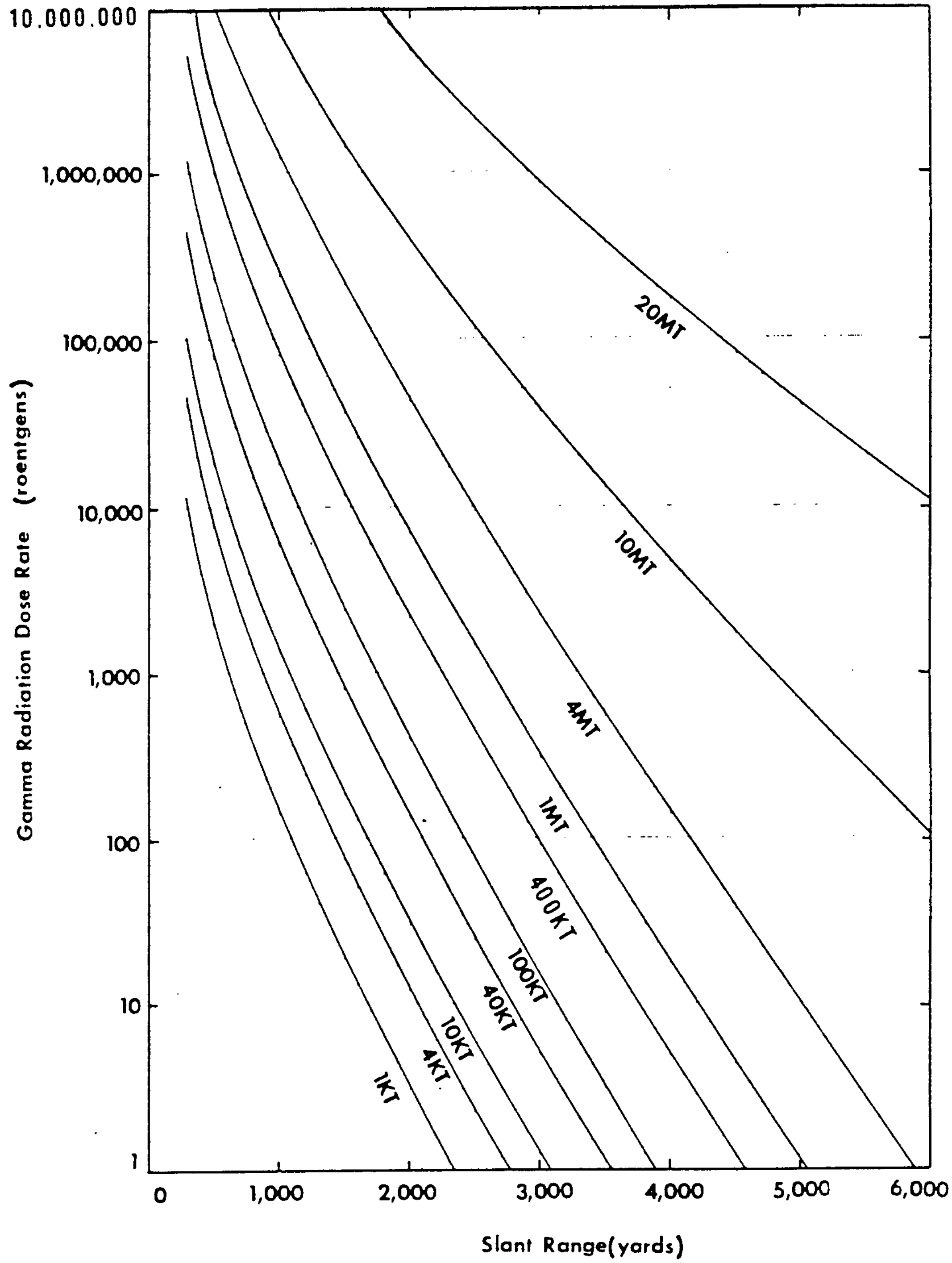

Note: Applicable to other situations as indicated on facing page.

INITIAL GAMMA RADIATION DOSE VS SLANT RANGE
AIR BURST AND AIR TARGET

RELATIVE AIR DENSITY, 0.6

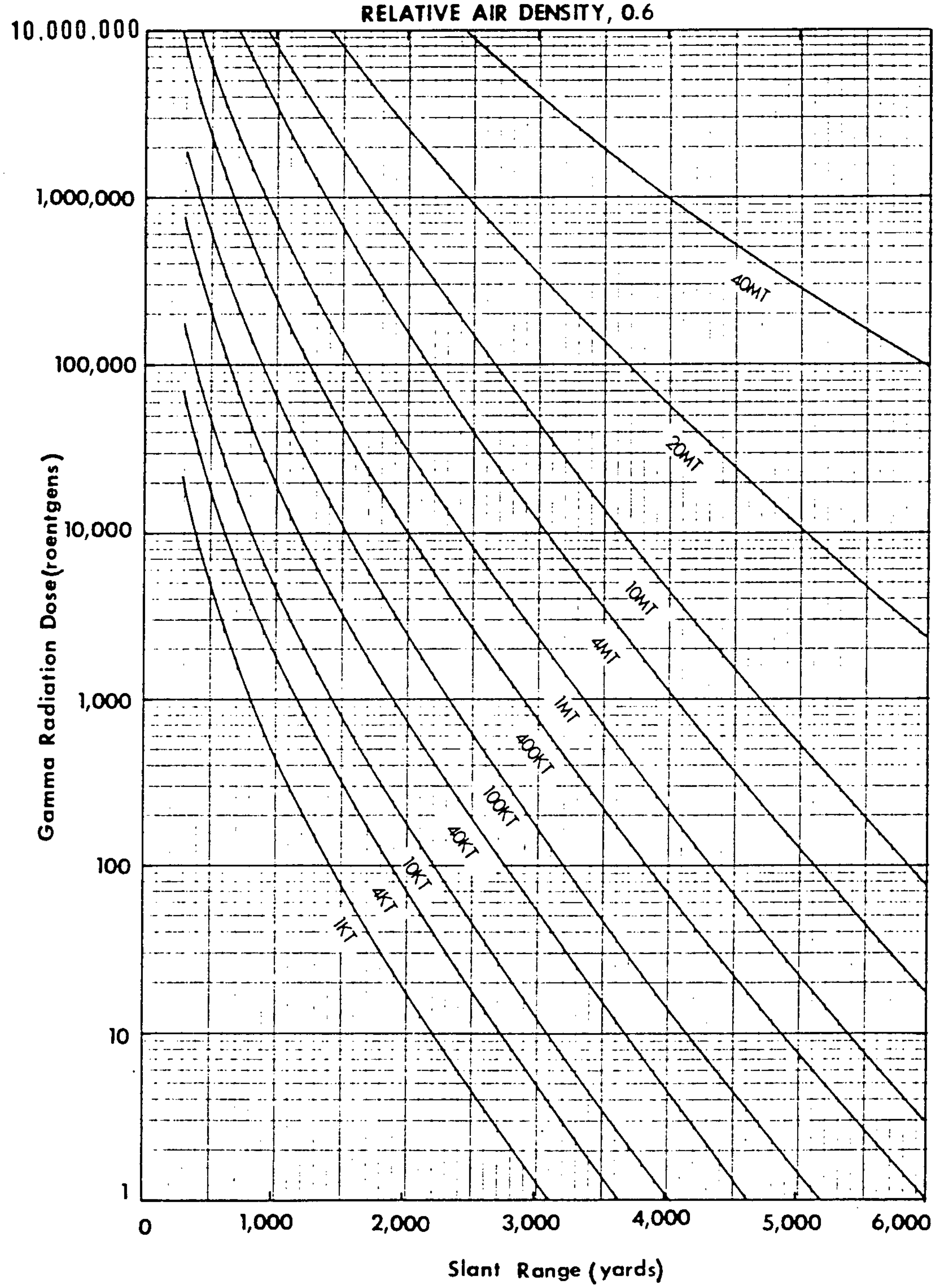

Note: Applicable to other situations as indicated on facing page.

INITIAL GAMMA RADIATION DOSE VS SLANT RANGE
AIR BURST AND AIR TARGET
RELATIVE AIR DENSITY, 0.4

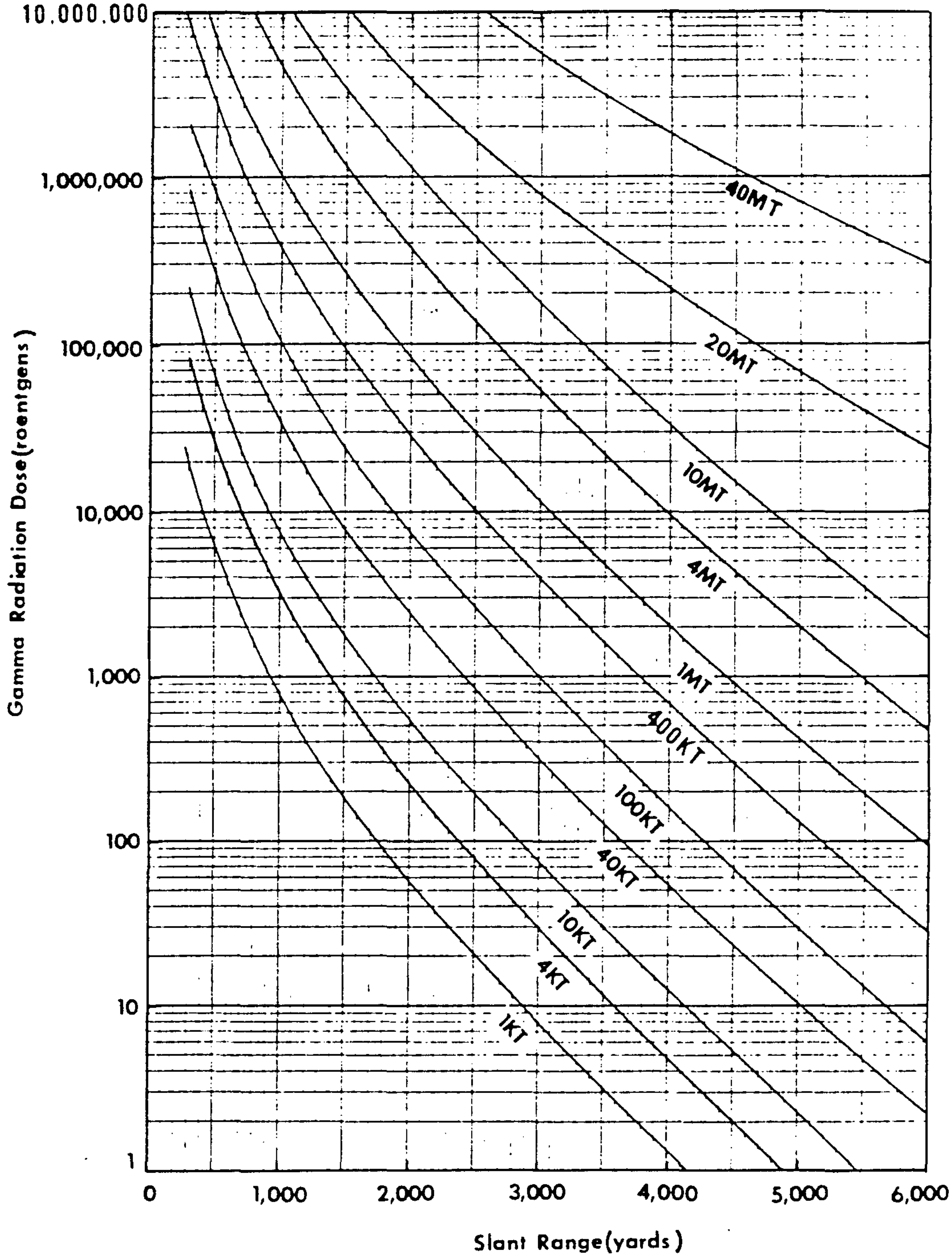

Note: Applicable to other situations as indicated on facing page.

INITIAL GAMMA RADIATION DOSE VS SLANT RANGE
AIR BURST AND AIR TARGET
RELATIVE AIR DENSITY, 0.2

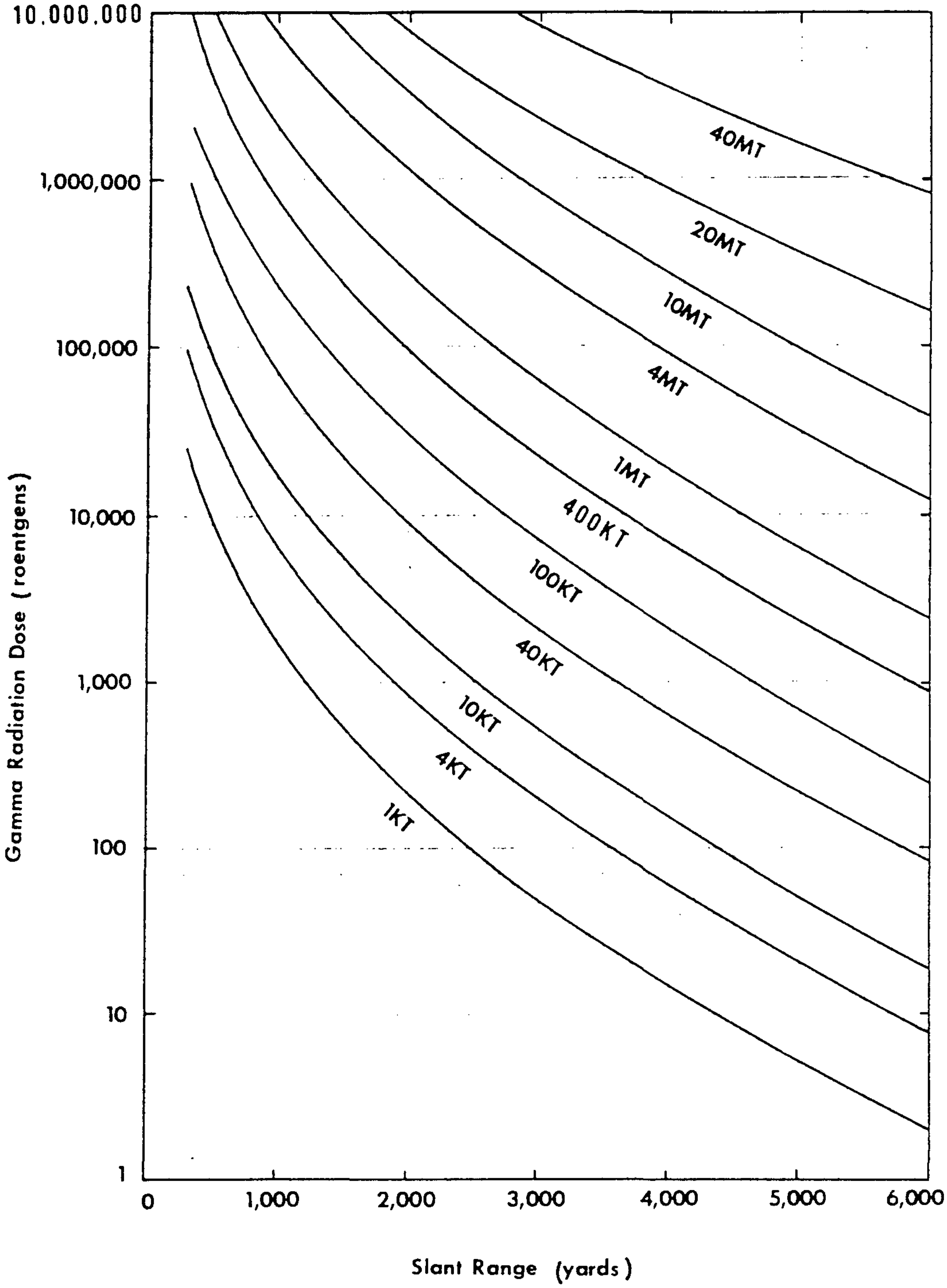

Note: Applicable to other situations as indicated on facing page.

INITIAL GAMMA RADIATION DOSE vs SLANT RANGE
SURFACE BURST AND SURFACE TARGET
RELATIVE AIR DENSITY 1.1

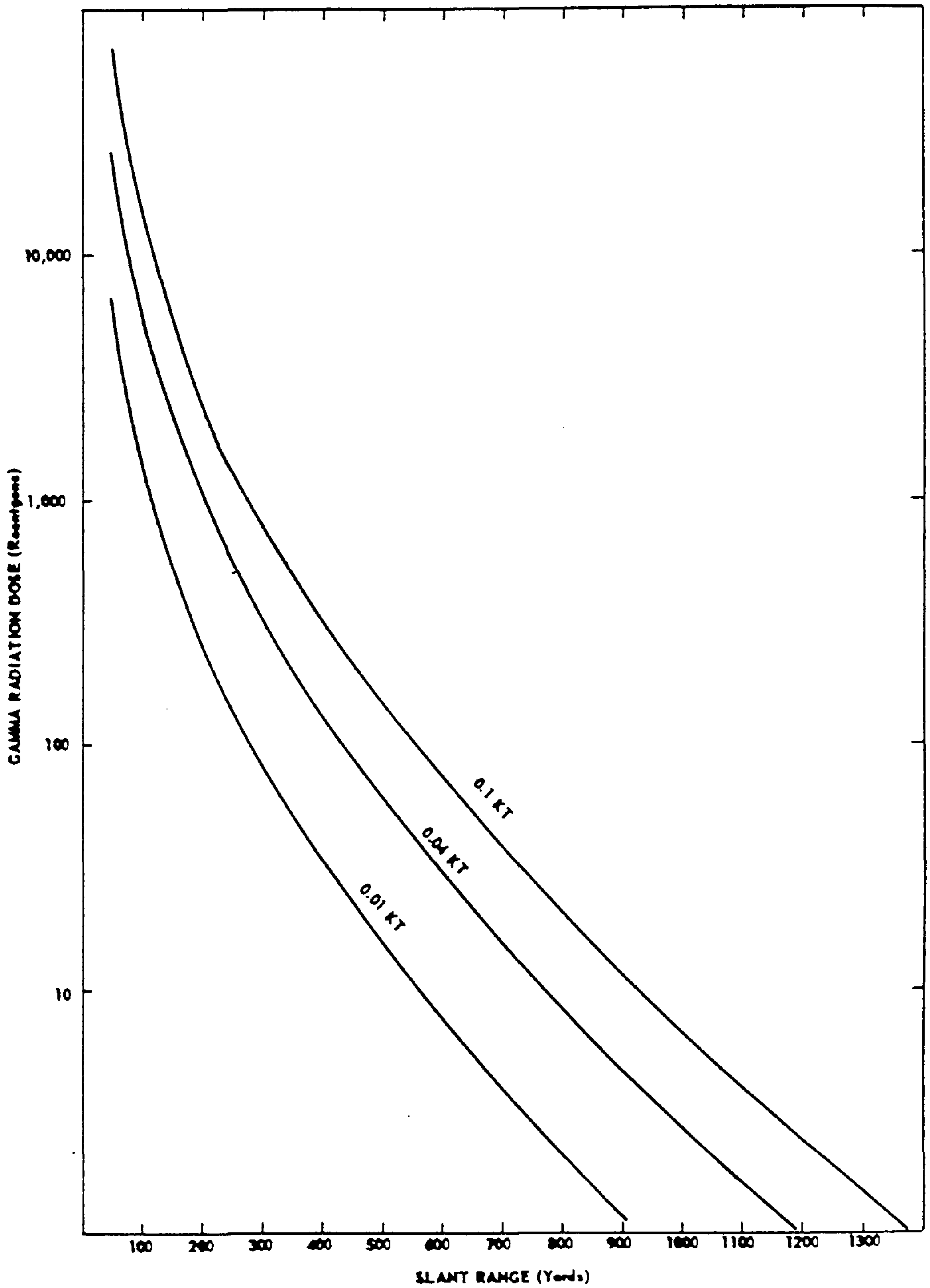

NOTE: Applicable to other situations as indicated on facing page.

INITIAL GAMMA RADIATION DOSE vs SLANT RANGE
SURFACE BURST AND SURFACE TARGET
RELATIVE AIR DENSITY 1.0

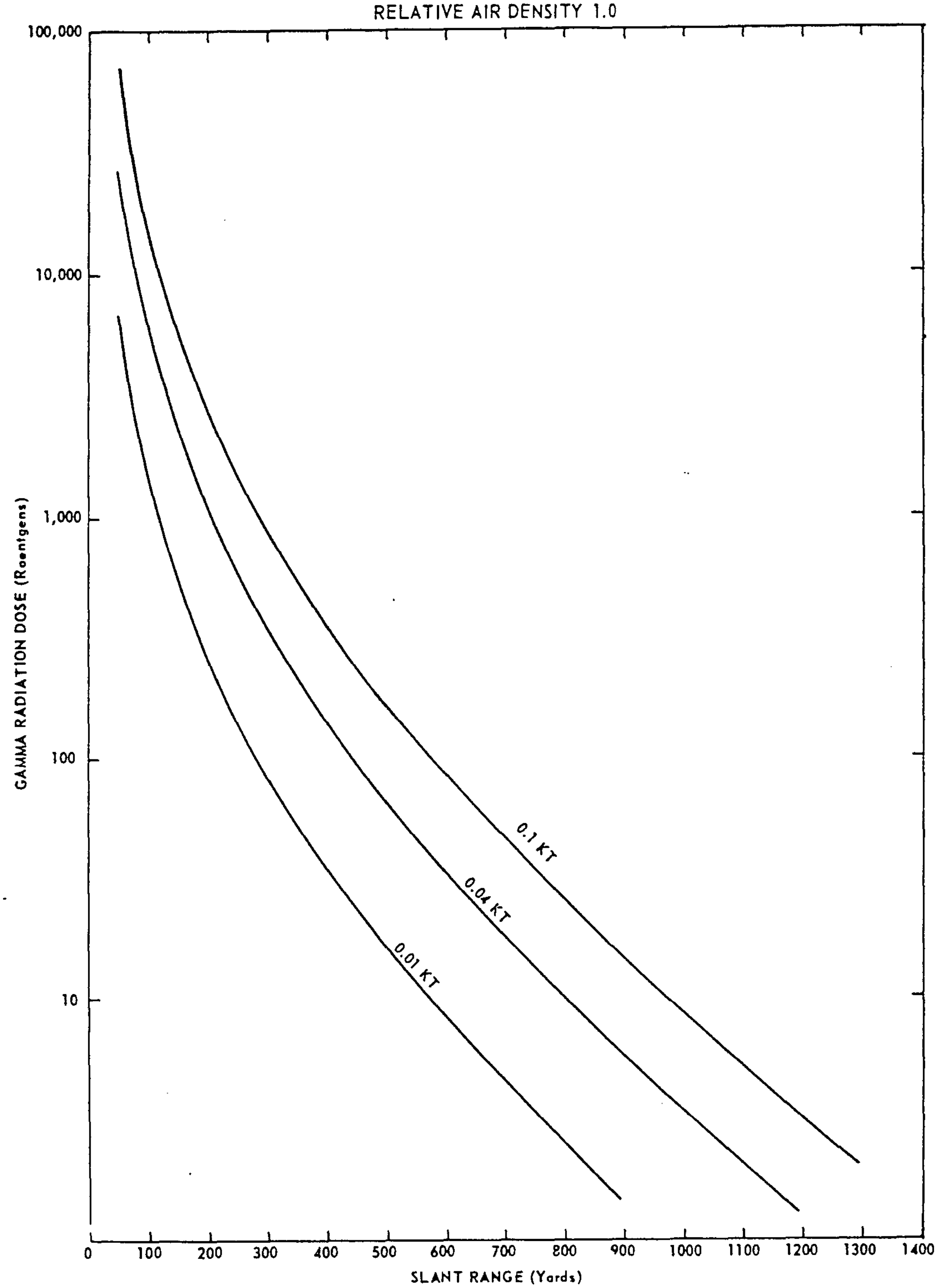

NOTE: Applicable to other situations as indicated on facing page.

INITIAL GAMMA RADIATION DOSE vs SLANT RANGE
SURFACE BURST AND SURFACE TARGET
RELATIVE AIR DENSITY 0.9

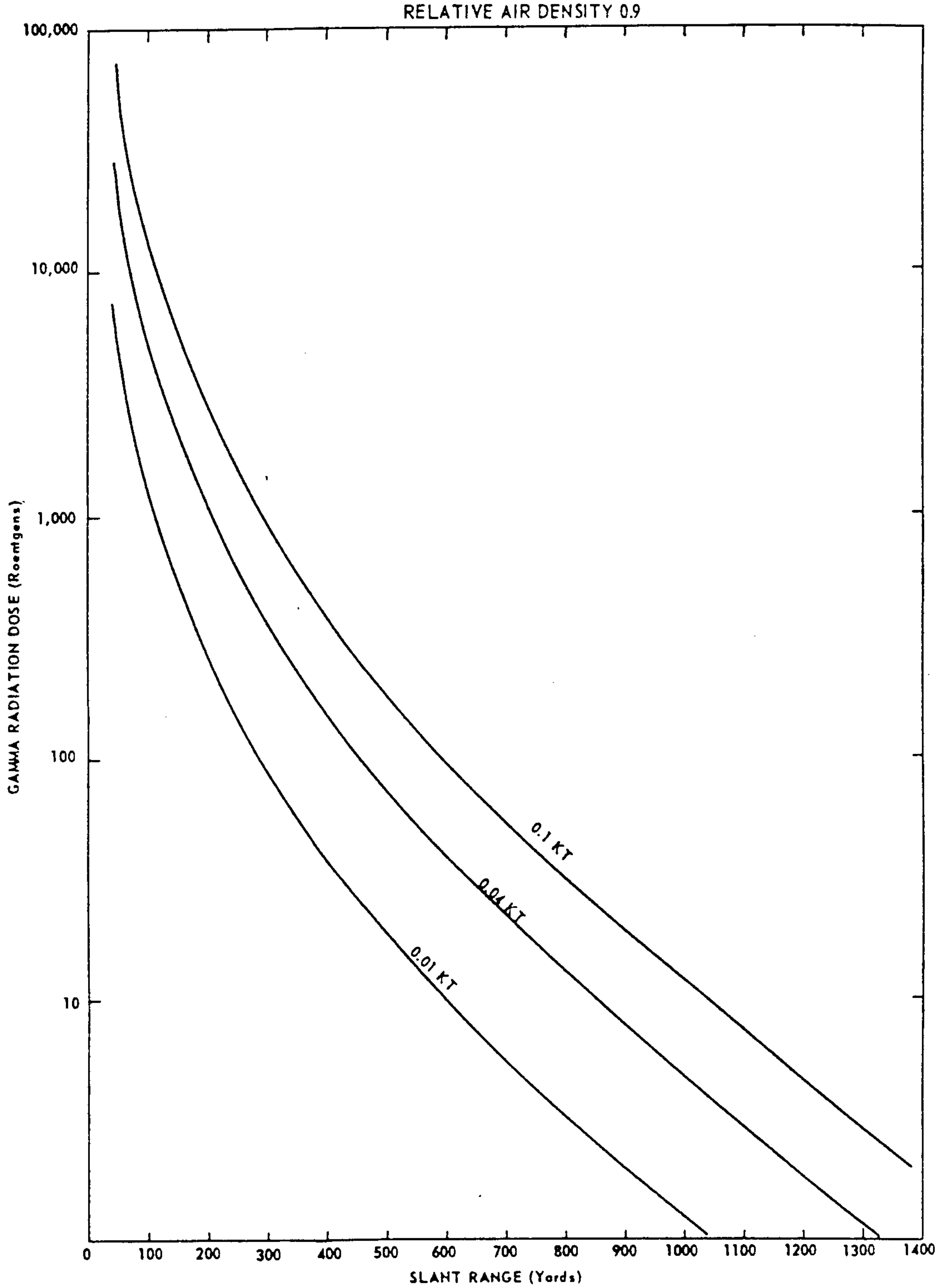

NOTE: Applicable to other situations as indicated on facing page.

INITIAL GAMMA RADIATION DOSE vs SLANT RANGE
SURFACE BURST WITH SURFACE TARGET
RELATIVE AIR DENSITY 0.8

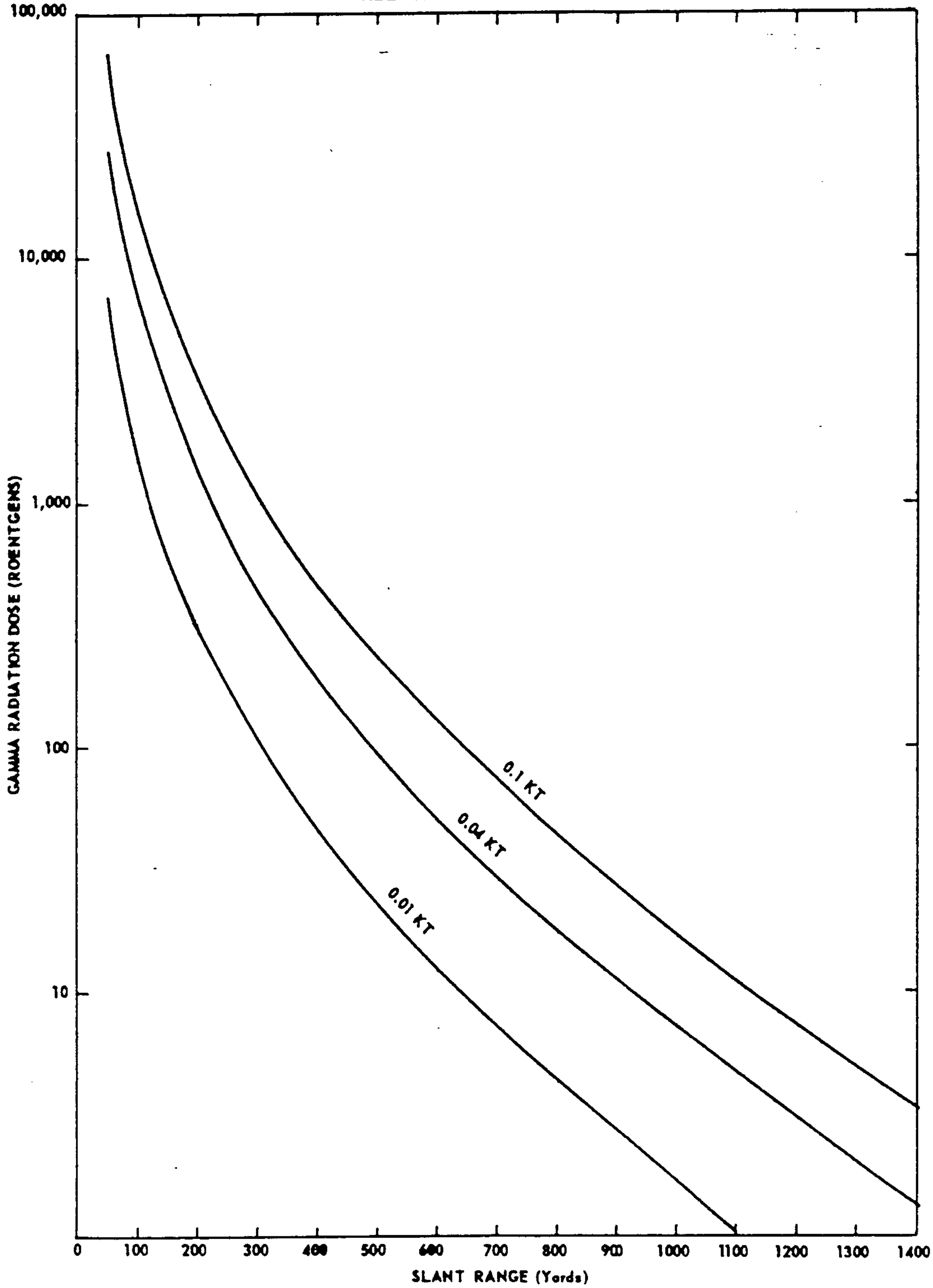

NOTE: Applicable to other situations as indicated on facing page.

BLANK

INITIAL GAMMA RADIATION DOSE FOR AN UNDERGROUND BURST

The curves of figure 4-8 present the initial gamma radiation dose as a function of distance for several air densities for a 1 KT underground detonation at 17 feet. They may also be used for underwater bursts.

Scaling. For other yields at about the same depth and the same relative air density, the dose at a given range is proportional to weapon yield. For relative air density see appendix II.

Example.

Given: A 5 KT burst 15 feet underground, with relative air density $R=0.9$.

Find: The distance at which 450*r* initial gamma dose is received.

Solution: The quotient $\frac{450}{5}=90r$ dose for 1 KT.

From the curve for $R=0.9$, the range at which 90*r* is received is 1,100 yards. *Answer.*

Reliability. The curves of figure 4-8 apply to weapons in the yield range from 0.2 KT to 7.5 KT and actual depths of burst from 12 to 22 feet. Used within the prescribed limits, results are good within a factor of two, provided the soil at the point of burst is not too different from the soil at the Nevada Test Site. The error that would be introduced by a very different soil type is similar in origin, but not necessarily in magnitude, to the error that would be expected from a distinctly different burial depth. At the present time the effect of soil type cannot be estimated. Extrapolation to other yields is unreliable.

Related material.

See paragraphs 4.2*a*(1) and (6).

See also figures 4-1 through 4-7 for air, transition, and surface bursts.

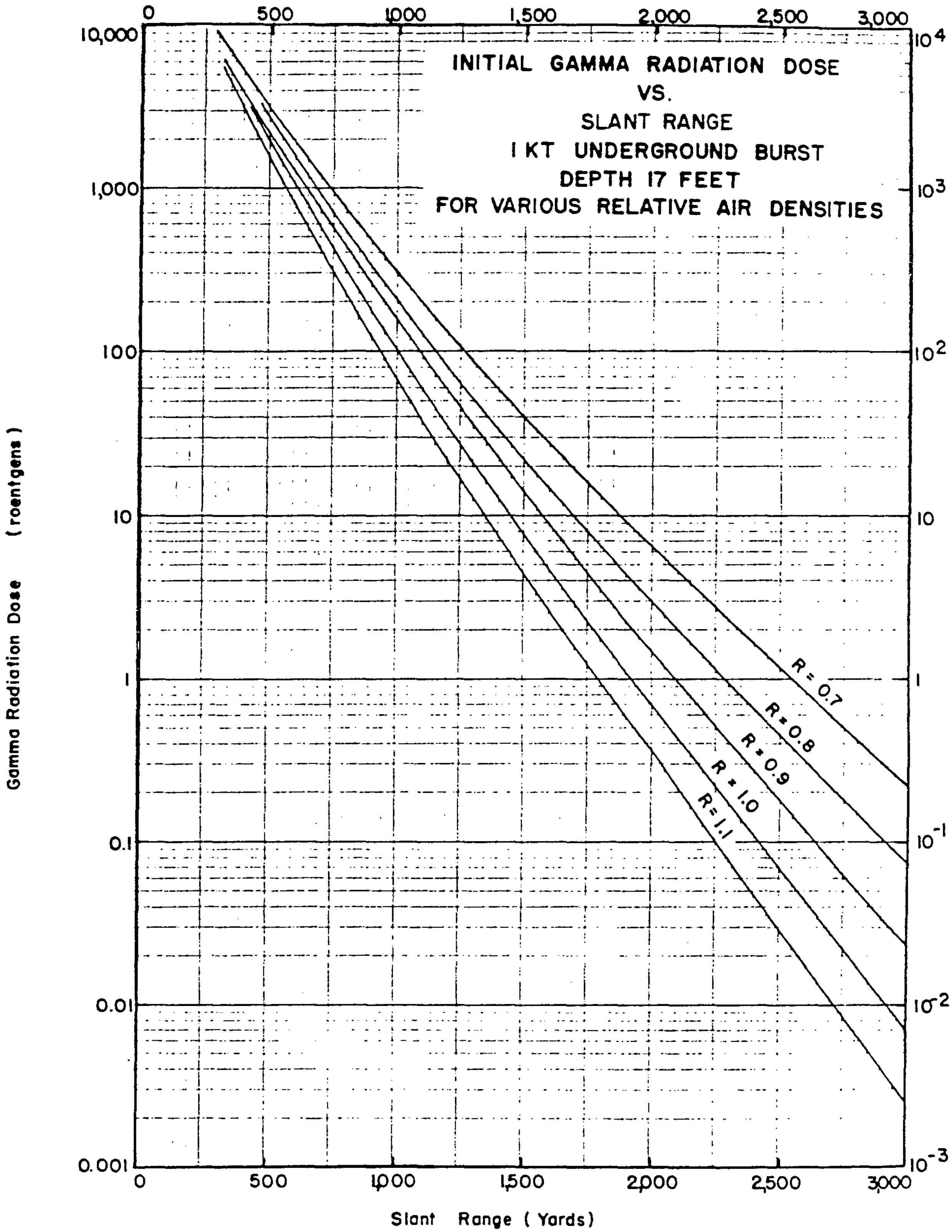
INITIAL GAMMA RADIATION DOSE
VS.
SLANT RANGE
1 KT UNDERGROUND BURST
DEPTH 17 FEET
FOR VARIOUS RELATIVE AIR DENSITIES
0
500
1,000
1,500
2,000
2,500
3,000
10,000
1,000
100
10
1
0.1
0.01
0.001
10^4
10^3
10^2
10
1
10^{-1}
10^{-2}
10^{-3}
R = 0.7
R = 0.8
R = 0.9
R = 1.0
R = 1.1
Gamma Radiation Dose (roentgens)
Slant Range (Yards)

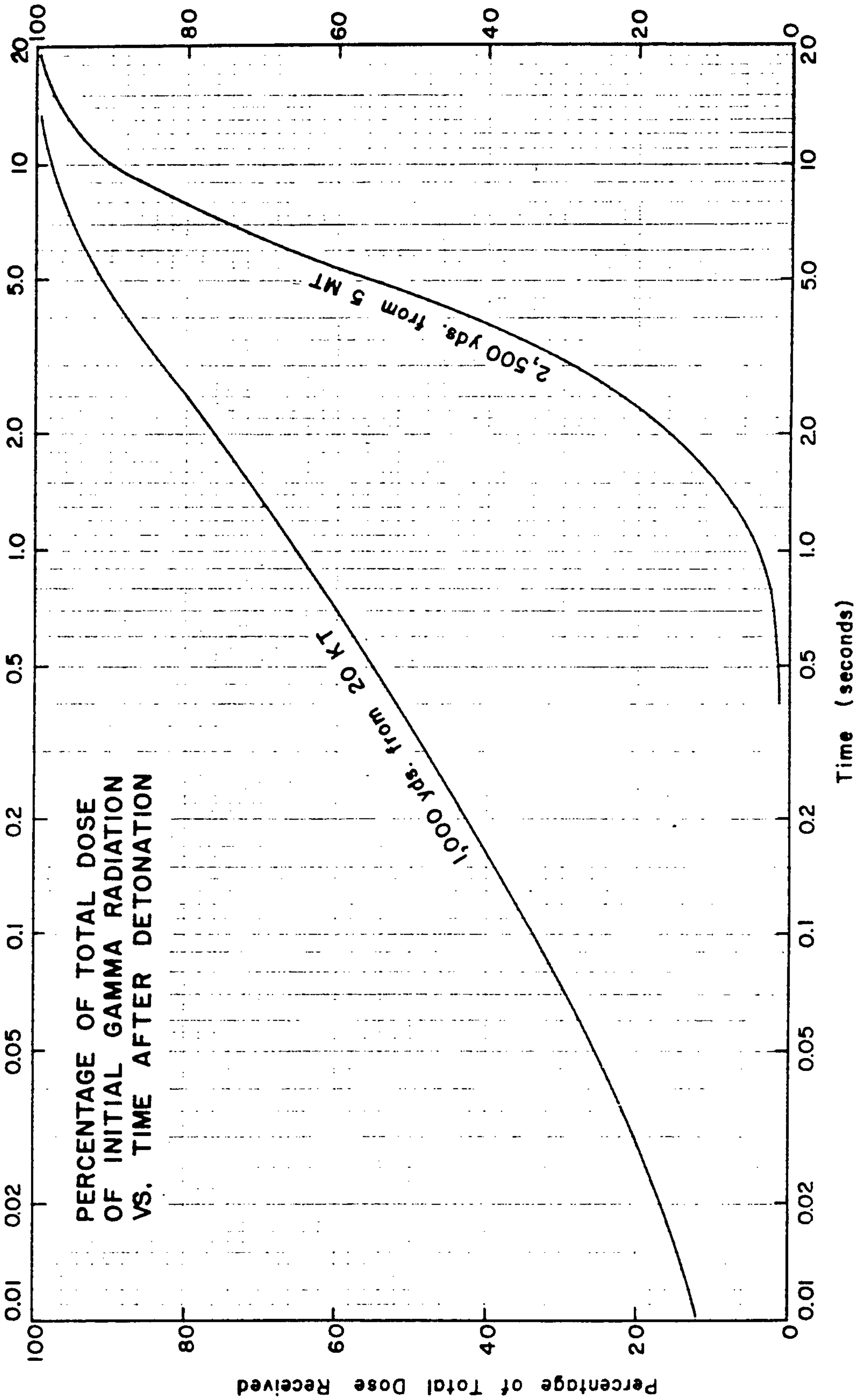
PERCENTAGE OF TOTAL DOSE
OF INITIAL GAMMA RADIATION
VS. TIME AFTER DETONATION
2,500 yds. from 5 MT
1,000 yds. from 20 KT
Time (seconds)
Percentage of Total Dose Received
0.01
0.02
0.05
0.1
0.2
0.5
1.0
2.0
5.0
10
20
100
80
60
40
20
0

BLANK

NEUTRON RADIATION DOSE

(Fission Weapons)

Neutron radiation is a function of bomb design. The curves presented in figure 4-10 may be regarded as representative of the neutron dose from fission weapons. The curves of figures 4-10a through 4-10d present the prompt neutron radiation dose as a function of range for various sub-kiloton yields, with each figure representing a particular relative air density. From these curves the slant range can be determined at which a weapon of given yield will produce a specified dose. Conversely, the yield required to produce a given dose at a desired range also can be found. A better estimate of neutron dose for many specific weapons may be obtained from the Nuclear Radiation Handbook (AFSWP-1100) published under a higher security classification.

Adjustment factors for receiver not on land surface	*Factor*
Water surface (or within 10 ft. thereof)	0. 9
Airborne, 300 ft. or more above land surface	1. 5

Scaling. At a given range and relative air density, the neutron dose is proportional to weapon yield. For relative air density, see appendix II.

Example.

Given: A 50 KT burst at 2,000 feet above a surface where, at the burst point, the pressure is 800 mb and, at the surface, the pressure is 860 mb.

Find: The maximum dose at a slant range of 1,750 yards.

Solution: From appendix II, the relative air density is 0.77.

From figure 4-10 for $R=0.8$, the dose for 1 KT at 1,750 yards is 6 rem. Therefore the maximum dose for 50 KT at 1,750 yards and $R=0.8$ is $6\times50=300$ rem. *Answer.*

Reliability. Depending upon weapon design, the dose values in figure 4-10 and figures 4-10a through 4-10d are estimated to be low by as much as a factor of 4 for certain experimental devices and can be high by a factor of 10 for other weapons.

Related material.

See paragraph 4.2b.

See also figure 4-11 for fusion weapons.

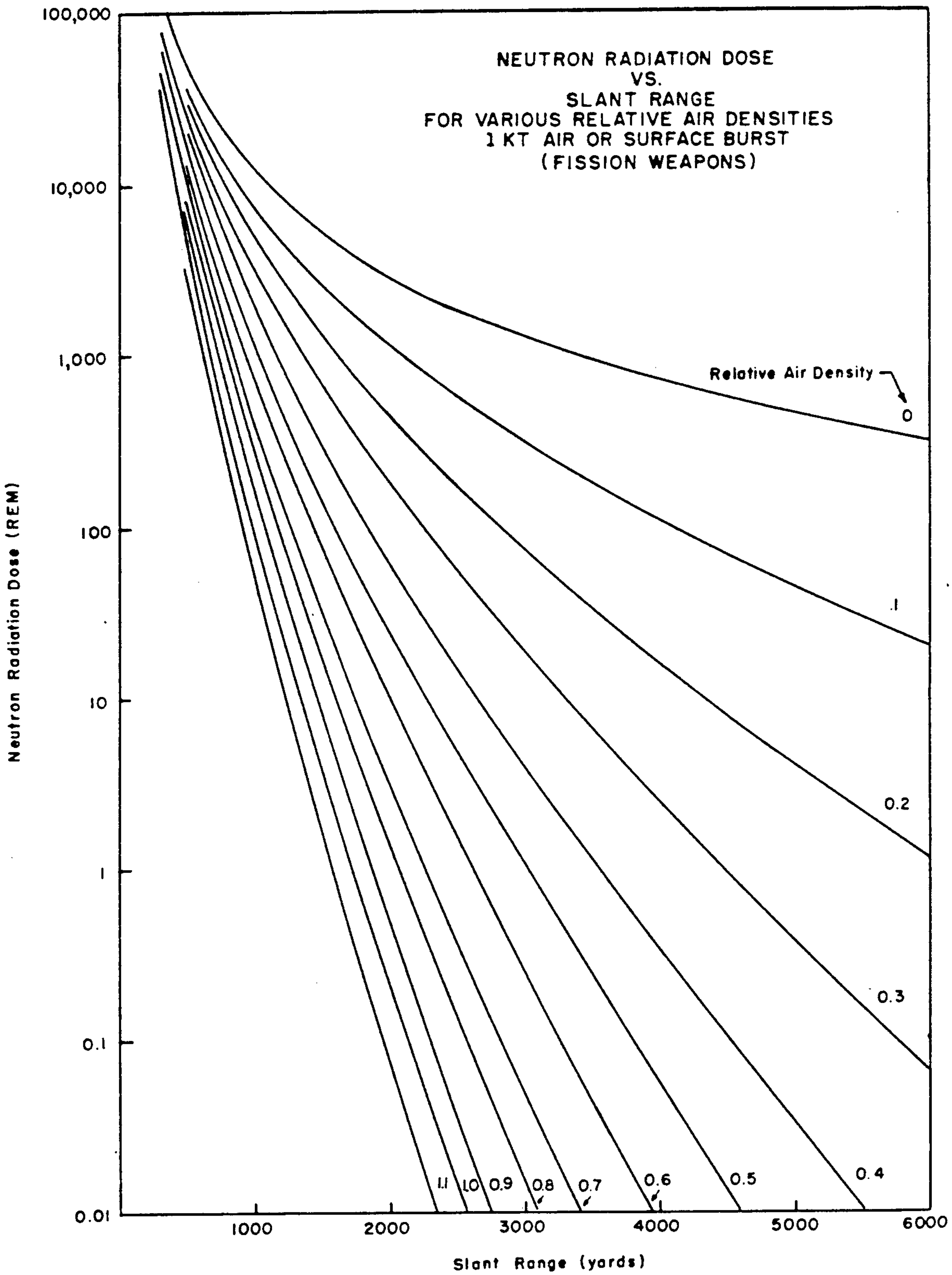
NEUTRON RADIATION DOSE
VS.
SLANT RANGE
FOR VARIOUS RELATIVE AIR DENSITIES
1 KT AIR OR SURFACE BURST
(FISSION WEAPONS)
Relative Air Density
0
.1
0.2
0.3
0.4
0.5
0.6
0.7
0.8
0.9
1.0
1.1
Neutron Radiation Dose (REM)
100,000
10,000
1,000
100
10
1
0.1
0.01
Slant Range (yards)
1000
2000
3000
4000
5000
6000

PROMPT NEUTRON DOSE vs SLANT RANGE
SURFACE BURST AND SURFACE TARGET
RELATIVE AIR DENSITY 1.1

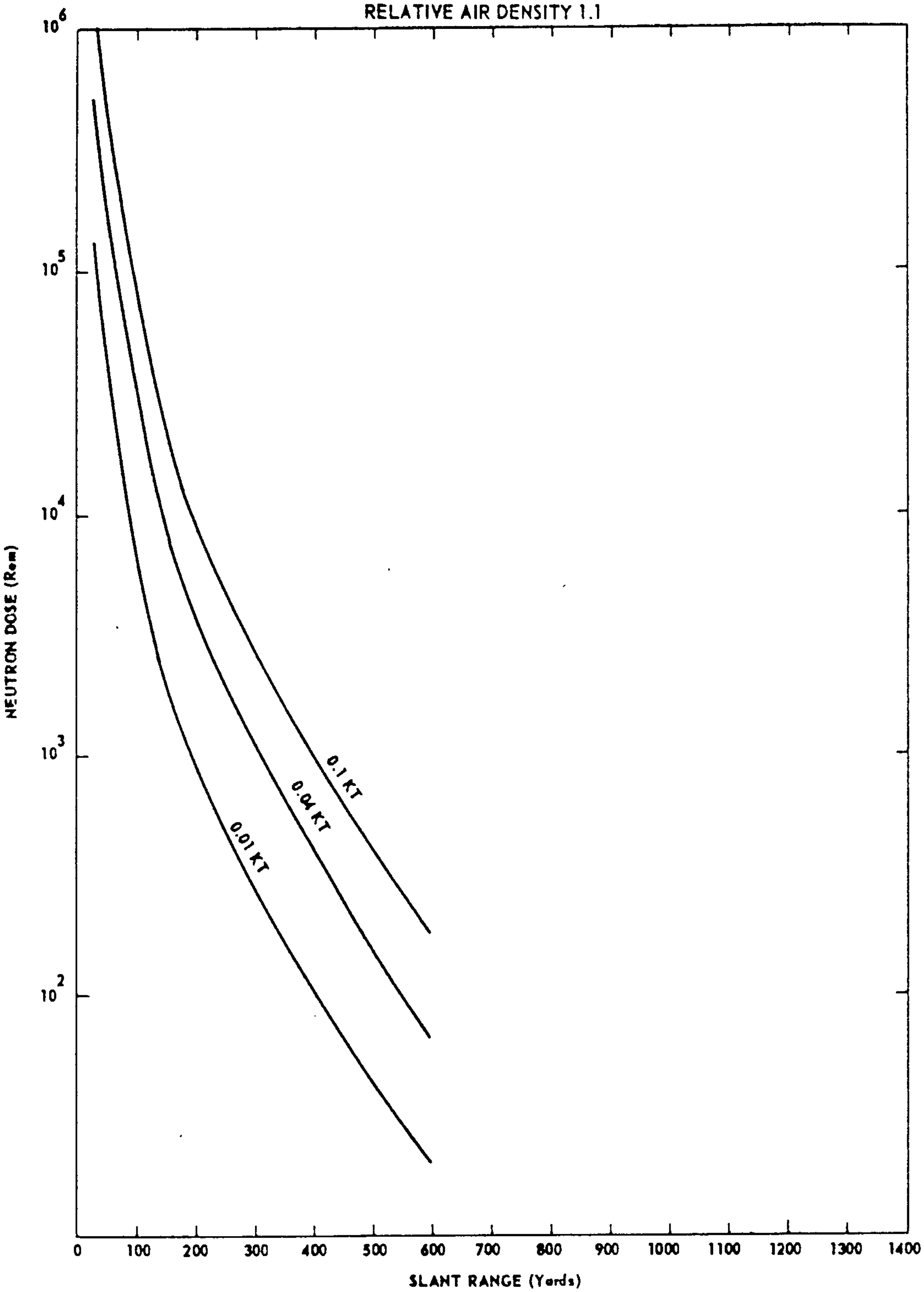

PROMPT NEUTRON DOSE vs SLANT RANGE
SURFACE BURST AND SURFACE TARGET
RELATIVE AIR DENSITY 1.0

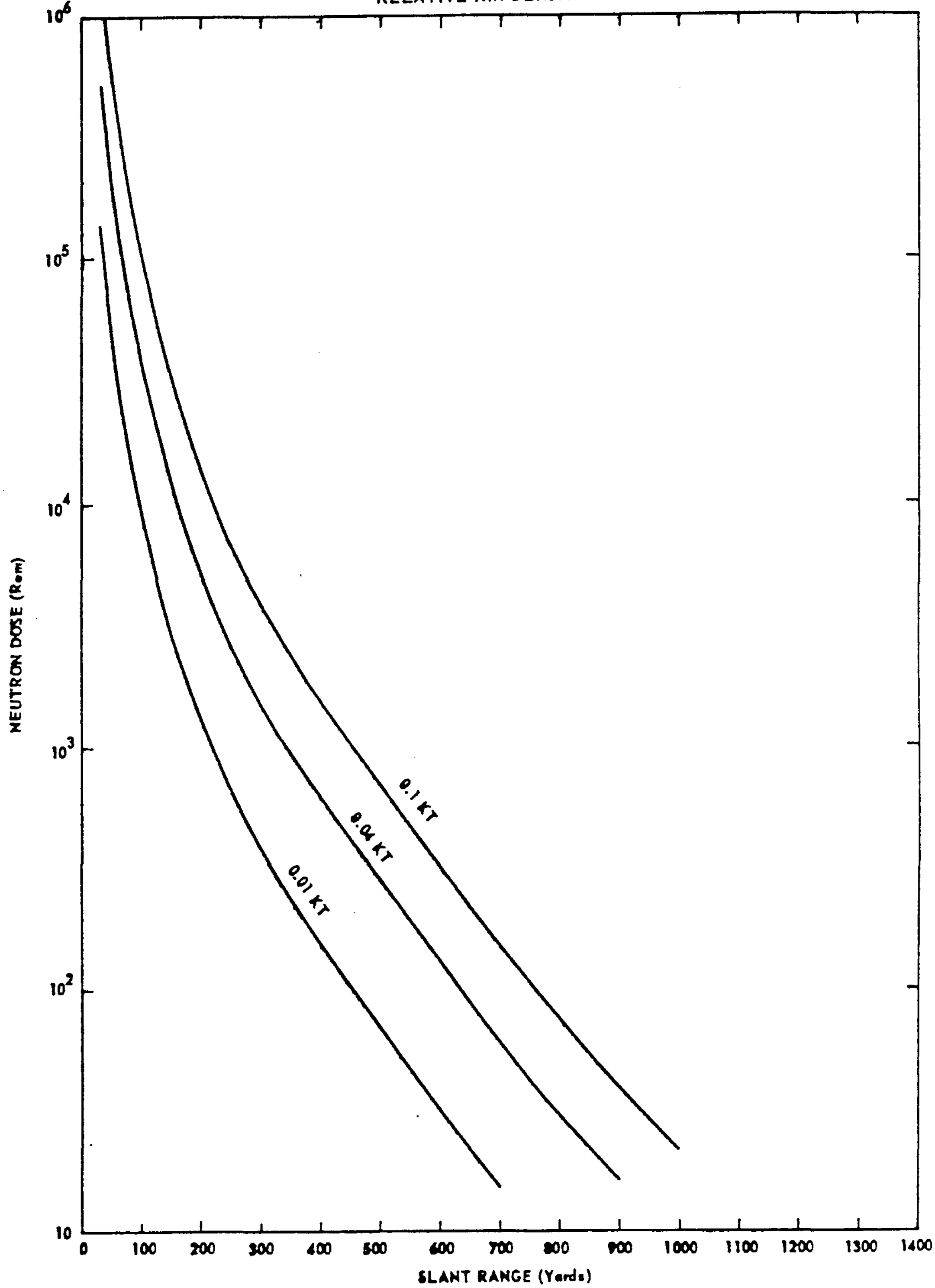

PROMPT NEUTRON DOSE vs SLANT RANGE
SURFACE BURST AND SURFACE TARGET
RELATIVE AIR DENSITY 0.9

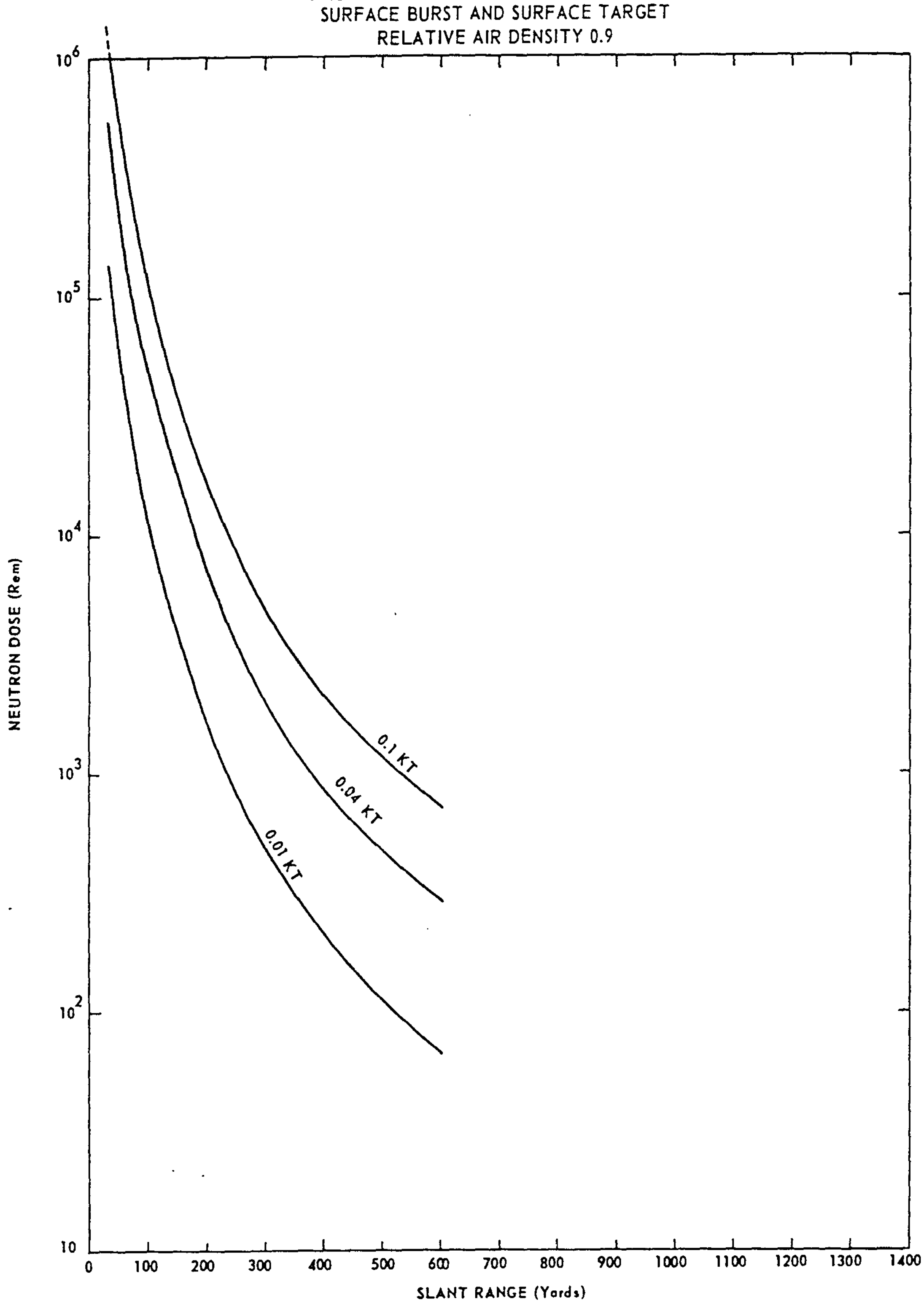

PROMPT NEUTRON DOSE vs SLANT RANGE
SURFACE BURST AND SURFACE TARGET
RELATIVE AIR DENSITY 0.8

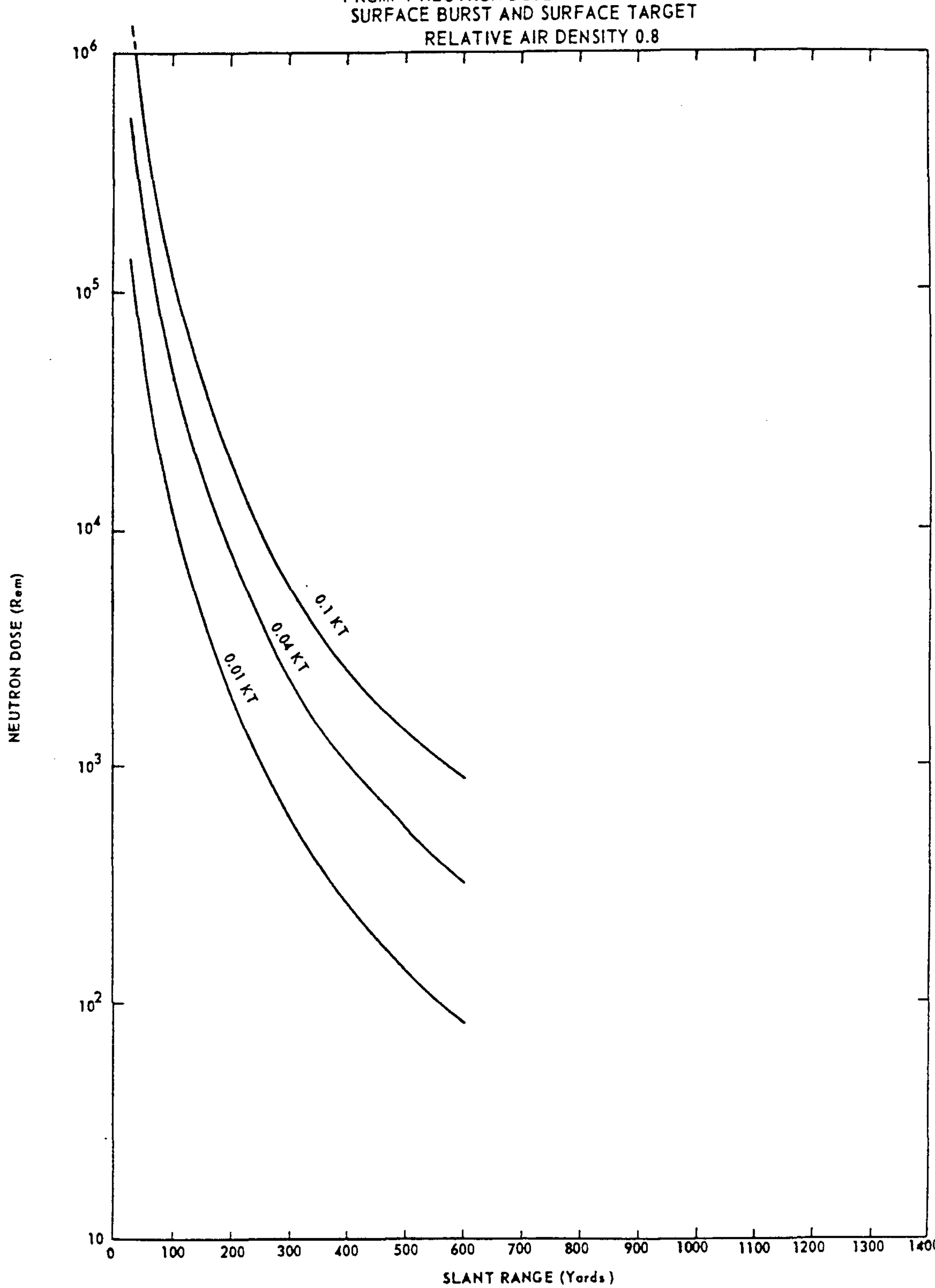

NEUTRON RADIATION DOSE

(Fusion Weapons)

The curves presented in figure 4-11 may be regarded as representative of weapons in the megaton yield range.

Adjustment factors for receiver not on land surface	*Factor*
Water surface (or within 10 ft. thereof)	0.9
Airborne, 300 ft. or more above land surface	1.5

Scaling. At a given range and relative air density the neutron dose is proportional to the yield of the weapon. See appendix II for determination of relative air density.

Example.

Given: A 2 MT burst at an altitude of 2,000 feet above the surface where, at burst point, the pressure is 800 mb and, at the surface, the pressure is 860 mb.

Find: The slant range at which a minimum neutron dose of 500 rem would be received by a surface target.

Solution: From appendix II, the relative air density is 0.77.

The corresponding dose for 1 MT is—

$$\frac{500}{2}=250 \text{ rem.}$$

From figure 4-11 for $R=0.8$ and a dose of 250 rem, read slant range=3,400 yards. *Answer.*

Reliability. Very poor, due to almost complete lack of data and sensitivity of neutron flux to weapon design. Actual dose may be within a factor of 10 of dose computed using figure 4-11. Extrapolation of curves to slant ranges less than 2,000 yards is not recommended.

Related material.

See paragraph 4.2b.

See also figures 4-10 through 4-10d for fission weapons.

NEUTRON RADIATION DOSE VS. SLANT RANGE
FOR VARIOUS RELATIVE AIR DENSITIES
1MT AIR OR SURFACE BURST (FUSION WEAPONS)

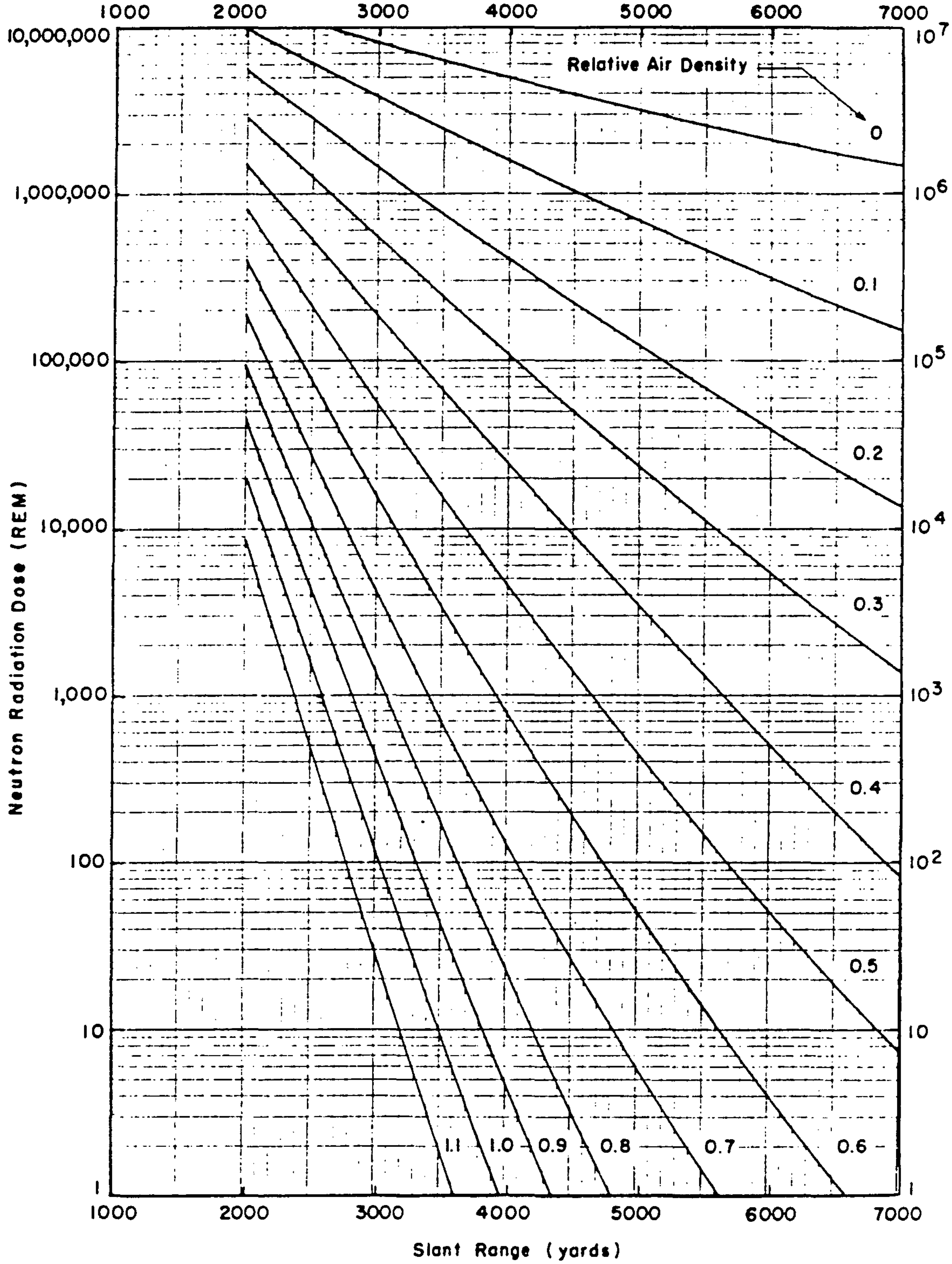

BLANK

Residual

4.3 Residual Radiation

a. General. Most of the damage caused by a nuclear explosion occurs within a few seconds after the detonation; however, there can be a further radiological hazard to personnel, extending over long periods of time. This hazard is most intense when the weapon is detonated at such an altitude that surface particles are drawn into the fireball. The resulting heat transfer changes the physical characteristics of the particles, causing them to become efficient scavengers of the finely divided radioactive remains of the weapon. These radioactive particles then fall under the action of gravity and are spread over a region which is determined by factors such as particle size, cloud height, and wind pattern. The dangerous area covered by this fallout can be of the order of thousands of square miles.

If the altitude of detonation is high enough, the above described interactions with the ground do not occur. The bomb materials will then remain suspended in the atmosphere for very long periods of time and, generally speaking, will settle out in low concentration over much of the earth's surface. This long range settling presents no significant military hazard.

For yields less than 100 KT, the height of burst at which fallout ceases to be a significant military hazard is about 100 $W^{1/3}$ feet. For yields in excess of 100 KT the height of burst at which fallout ceases to be a military hazard is not well defined; however, in the absence of data, the height of burst may be conservatively taken to be 180 $W^{0.4}$ feet.

b. Air Burst. The surface contamination effects of fallout from an air burst weapon are militarily insignificant in most cases, since the bomb cloud carries practically all the radioactive bomb debris to high altitudes. In general, by the time this material can fall back to earth, dilution and radioactive decay will decrease the activity to levels which are no longer important. An exception may occur in the case of a small yield weapon burst in the rain. In this case, the scavenging effect of the precipitation may cause a rain-out of radioactive material which will provide a hazard to personnel located downwind and downhill, and outside the hazard area of initial radiation and other effects. Although the range of weapon yields for which rain-out may become hazardous is not large, quantitative treatment of the problem is difficult. The contamination pattern on the ground depends upon two major dynamic processes, each of which is extremely sensitive to several factors. The major processes are—

(1) The scavenging effect of precipitation on suspended fission products in the atmosphere, and
(2) The flow and ground absorption of rain water after reaching the ground.

Some of the factors which influence the scavenging effect are—

(1) Height and extent of the rain cloud.
(2) Raindrop size and distribution.
(3) Rate of rainfall.
(4) Duration of precipitation.
(5) Position of the nuclear cloud relative to the precipitation.
(6) Hygroscopic character of the fission products.
(7) Solubility of the fission products.
(8) Size of the fission fragments.

The flow and ground absorption of the rain water will, in turn, depend upon such factors as—

(1) Soil porosity.
(2) Drainage features, including rate of drainage.
(3) Degree of soil saturation.

Even in extreme cases, the rainout from an air burst should not be a serious military problem for yields in excess of 20 KT, and for the average case, it should not be a serious problem for yields in excess of 8 KT. Although the weapons of greater yield produce more radioactive material, the updrafts carry the bulk of the material up through the weather to an altitude above the level of precipitation.

Thus, under some circumstances, a rain-out problem may exist; however, it must be evaluated with respect to local conditions. Ditches, puddles and low ground where water collects should be avoided unless survey indicates these areas are safe. Caution should be exercised for a considerable distance downwind and downhill from the burst. So long as drainage is taking place, the rate of decrease in intensity is likely to be greater than decay laws predict.

In addition to rain-out, another contamination mechanism assumes some importance in the case of a low air burst. This is the formation of radioactive elements in the soil by action of the neutrons emitted by the weapon. Activity induced in this manner is treated in paragraph 4.3*i*.

c. Surface Burst.

(1) *Land surface burst.*

(*a*) *General.* The activity available from weapon components at a reference time of one hour after the detonation is approximately that corresponding to 300 megacuries per kiloton of bomb yield.

For a burst exactly at the earth's surface, roughly fifty percent of the activity available is deposited in the general vicinity of the detonation, while the remainder is carried hundreds or perhaps thousands of miles from the point of detonation by the winds of the upper atmosphere.

(*b*) *Deposition patterns.* In a complete calm, the fall-out contamination forms a roughly circular pattern around the point of detonation. The existence of a wind leads to an elongated area, the exact nature of which depends upon the velocity and direction of the wind from the surface up to the altitude of the top of the stabilized cloud. If the direction of the wind does not vary excessively from the surface up to the top of the cloud, the ground fall-out contours may be characterized by a circular pattern around ground zero and an elliptical pattern extending downwind from ground zero. The circular pattern is formed by the rapid settling of the heavier particulate matter in the stem while the downwind elliptical pattern is formed by fall-out of smaller and lighter particles from the cloud.

The existence of complicated wind patterns (wind shear) as well as variations of the wind pattern in time and space may cause extreme departures from a simple elliptical pattern. In addition, the measured dose rate contours have frequently been observed to occur in patterns which are best described as a series of islands of relatively high activity surrounded by areas of lower activity. The most common pattern of this type has been one in which the higher dose rate contours appear around two major areas and one or more smaller areas. One of the larger areas is in the immediate vicinity of ground zero while the other is in the general downwind direction from ground zero. The locations of the smaller areas of high activity have not demonstrated patterns which can be described simply in terms of the wind structure. The dose rates observed within these high activity areas have been of comparable magnitude when extrapolated back to some early time after detonation, such as $H+1$ hour. However, due to the earlier arrival of the contaminant, the activities actually observed near ground zero have been higher than in the areas away from ground zero. It should be noted that these islands of relatively high activity generally cover areas considerably larger than those of the "hot spots" caused by local meteorological conditions discussed elsewhere. A quantitative treatment of such complicated deposition patterns would only be possible through use of a complex computational model together with time-consuming calculations. The simplified method for obtaining deposition patterns which is presented below will not predict these islands of relatively high activity.

The area covered and the degree of localization of the contamination also depend upon the character of the soil at the burst point. For example, a surface detonation over dry soil with small particle sizes results in a larger area enclosed by low dose rate contours and a smaller area enclosed by high dose rate contours than for the average case. A similar detonation over water-covered finely divided soil such as clay probably results in relatively high dose contours over larger areas close to the

GENERALIZED LOCAL CONTOURS FOR RESIDUAL RADIATION

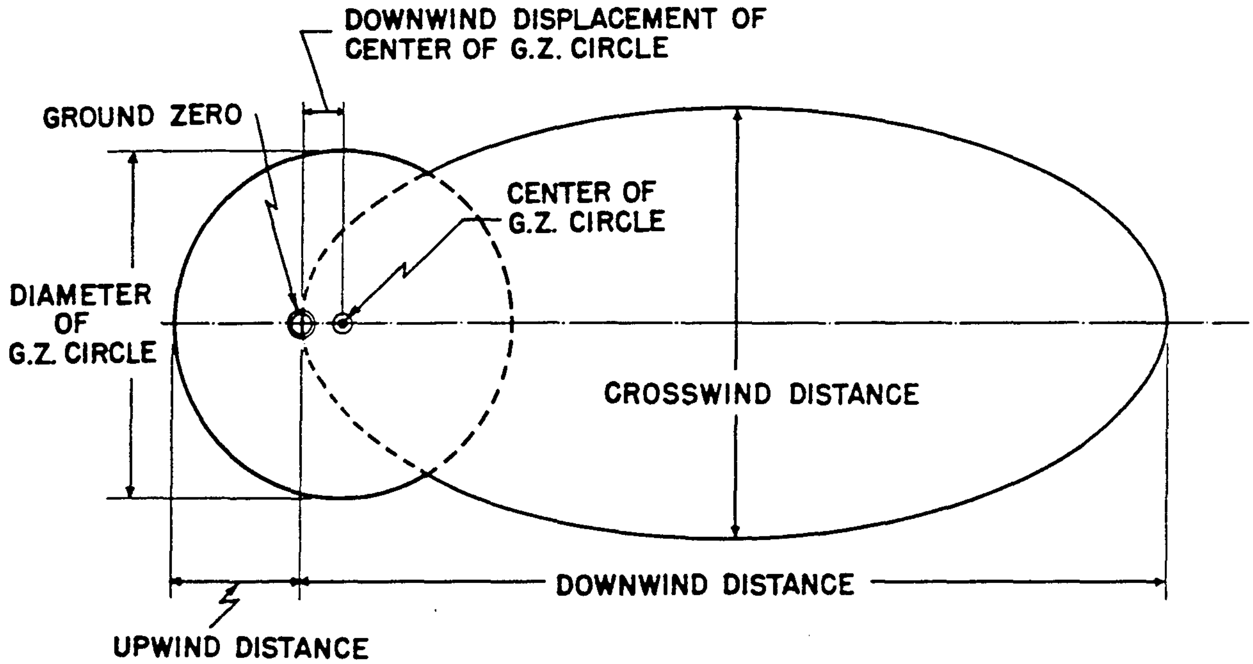

detonation, with a corresponding reduction in the areas of the lower dose rate contours farther out.

(c) *Idealized contours*. In any discussion of the areas affected by residual contamination from fallout, it is convenient to set up a system of contamination dose rate contours which, although simplified and idealized, fit actual contours measured in the field as closely as possible. Figure 4-12 illustrates such a contour system. The "idealized" contour shown consists necessarily of two parts—the ground zero circle, and an elliptical approximation to the downwind component of the fallout. The ground zero circle is formed quite soon after the detonation, largely from heavy particulate matter, throw-out, and soil made active by neutron capture reactions. The parameters which define it are its diameter and the downwind displacement of its center from ground zero. The idealized downwind component, consisting of the fallout proper, is elliptical in shape, and the parameters which define it are its major and minor axes (the downwind and crosswind extent respectively). One end of the ellipse is at ground zero. To define the downwind axis, a simplifying assumption is made—that the downwind direction and extent are determined by a single wind of constant velocity, the so-called "scaling wind." To obtain the scaling wind it is first necessary to obtain the "resultant wind vector" for each of an arbitrary number of equally spaced altitude zones between the top and bottom of the stabilized cloud. Each resultant wind vector is the vector average of all wind vectors for equally spaced altitude intervals from the altitude zone in question down to the surface. The scaling wind is then the vector average of all the resultant wind vectors for the various altitude zones within the cloud. As a rule wide discrepancy from the idealized elliptical pattern results if there are large directional shears in the resultant winds computed for the altitudes of the stabilized bomb cloud. Such shears can give rise to serious distortion of the idealized elliptical pattern, so that in practice radical distortions of these idealized patterns can be expected. However, contour areas will remain substantially unchanged. In such case, the close-in portions of the fallout pattern in general follow the direction of the resultant winds from the lower cloud altitudes, while the more distant downwind portions of the pattern tend to lie in the direction of the resultant winds from the upper cloud altitudes. The idealized contours described herein have a more general application.

(*d*) *Decay rate.* It is important to recognize that $H+1$ hour is used in the preparation of these contours as a *reference* time, and that only the contours from low yield weapons are complete one hour after burst time. For very high yield weapons, fallout over some parts of the vast areas indicated does not commence until many hours after the burst. In order to calculate the dose rates at times other than 1 hour after the detonation, decay factors may be taken from figure 4–13, which is a representation of the decay law. The factors are constants which are multiplied by the value of the dose rate at 1 hour to give the rate at any other time. These decay factors apply only to fission product contamination, such as predominates on the ground after a surface burst, and must not be used to estimate the decay of neutron-induced ground contamination resulting from an air burst. The $t^{-1.2}$ law, which approximates the decay of the mixture of fission products, holds reasonably well for actual contamination over long periods of time, but not as well over short periods of time because of the presence of weapon contaminants other than fission products.

(*e*) *Dose rate contour dimensions.* Families of curves (figs. 4–14 through 4–18) are given from which data may be obtained to draw idealized dose rate contours for land surface bursts of weapons with yields between 0.1 KT and 100 MT. A 15-knot scaling wind has been used in the preparation of these curves, since this is near the average of the scaling wind values most commonly encountered under field test conditions, and is probably a good average value for general application. Contour areas are substantially constant over the range of scaling winds likely to be experienced, but the linear contour dimensions, except for the diameter of the ground zero circle, must be scaled. Directions for scaling accompany the curves. Use of a true ellipse in the idealized contours results in idealized contour areas somewhat larger than those actually observed since the downwind contours observed in field tests in general have been thinner than true ellipses. For this reason true contour areas should be read directly from the area curves, rather than computed from the contour dimensions obtained.

(2) *Water surface burst.*

(*a*) *General.* Although detailed experimental confirmation is lacking, it is expected that there will be some difference in the character and distribution of residual radioactive contamination between a water and a land surface detonation. For a surface burst over water deep enough that particulate matter from the bottom is not carried aloft in the cloud and stem, it is expected that the contaminant is distributed as a very fine mist, and that, as a result, the lower dose rate contours would be larger and the higher dose rate contours smaller than for a corresponding burst over a land surface. There is also a somewhat greater probability that local meteorological conditions may cause condensation and rain-out of portions of this mist, resulting in localized "hot spots," the prediction of which would be a nearly impossible task. However, the total activity available for a given weapon burst under the two conditions is the same, and there are indications from limited test experience that the extent of the contaminated areas will be about the same as for land surface bursts. The contour parameters given in figures 4–14 through 4–18 for land surface bursts may be used also for water surface bursts to obtain dose rates over adjacent land masses.

(*b*) *Shallow water*. For the case of a burst over water so shallow that a significant portion of the contaminant is entrained in mud and particulate matter from the bottom and carried aloft, localization of the fallout may be expected to be greater than for the deep water case, with high dose rate contours of increased size in close to the burst point, and low dose rate contours of somewhat smaller size farther out. Quantitative estimates of contour parameters may be obtained from the land surface burst curves (figures 4–14 through 4–18) with the reservation that the values for contours of 300 r/hr or greater at $H+1$ hour should be thought of as minimum values, while those for contours of 100 r/hr or less at $H+1$ hour should be thought of as maximum values.

d. Burst in the Transition Zone. The deposition patterns and decay rate of the contamination from weapons which are detonated very close to the surface will be similar to those for a weapon of the same yield burst on the surface; however, a smaller quantity of the available activity will be deposited locally, resulting in lower dose rate values along contours derived for surface burst conditions. As the height of burst is increased, the activity deposited locally as fallout decreases, and the residual contamination due to neutron-induced activity becomes an increasingly more important part of the total contamination. The exact scaling of the fallout dose rate contour values with height of burst is uncertain. Residual contamination from tests at heights of burst immediately above or below 100 $W^{1/3}$ feet has been small enough to permit approach to ground zero within the first 24 to 48 hours after detonation without exceeding reasonable dosages. In these tests the mass of the tower, special shielding and other test equipment are considered to have contributed a considerable portion of the fallout actually experienced, and neutron induced activity in the soil has furnished an added contribution to the total contamination. Thus, for yields less than 100 KT and heights of burst of 100 $W^{1/3}$ feet or greater, it is considered that contamination from fallout will not be sufficiently extensive to materially affect military operations. It must not be assumed that weapons in the above yield range will never present a residual radiation problem when burst above 100 $W^{1/3}$ feet. The neutron-induced gamma activity can be very intense in a relatively small area around ground zero. However, a better idea of the contamination pattern, dose rate contour values, and decay rate of the residual radiation from the above types of detonations will be obtained by basing the predictions on the induced activity as discussed in *i* below.

Due to the uncertainties in the scaling, it is unsafe to extrapolate the above conclusions to weapons having yields greater than 100 KT. In the absence of data, a conservative estimate may be obtained by using a height of burst of 180 $W^{0.4}$ feet as the point above which fallout ceases to be militarily significant. Once again, the neutron-induced gamma activity may be intense for bursts above or below this height.

A rough estimate of the dose rate contour values for bursts in the transition zone may be obtained by applying an adjustment factor from figure 4–19 to the dose rate contour values obtained from figures 4–14 through 4–18. For bursts in the upper quarter of the fallout transition zone neutron-induced activity must also be considered. See *i*(2) below. For bursts in the lower three quarters of the transition zone the neutron-induced gamma activity can generally be neglected when compared to the fallout activity.

e. Subsurface Burst.

(1) *Underground burst.* A large amount of residual contamination is deposited in the immediate vicinity of the burst point after an underground detonation, because the major portion of the radioactive material falls quickly from the column and cloud to the surface. A very shallow underground burst conforms rather closely to the contamination mechanisms and patterns outlined previously for land surface bursts. As depth of burst is increased, however, a greater percentage of the total available contaminant is deposited as local fallout, until for the case of no surface venting, all of the contamination is contained in the volume of ruptured earth surrounding the point of detonation.

Families of curves are given in figures 4–20 through 4–23 by means of which idealized dose rate contours for a reference time of 1 hour after detonation can be drawn for underground bursts of weapons with yields between 1 KT and 1 MT at a depth of 17 $W^{1/3}$ feet with a 15 knot scaling wind. Multiplying factors are given in figure 4–24 by means of which contour parameters can be estimated for depths other than 17 $W^{1/3}$ feet, down to a limiting depth of 70 $W^{1/3}$ feet. As the depth of burst becomes greater, the contour shapes depart from the idealized pattern, and, particularly in the case of the higher dose rate contours, tend to become more nearly circular. For this reason, the areas obtained by use of the scaling factors from figure 4–24 for burst depths greater than 17 $W^{1/3}$ feet will more nearly represent the actual pattern than will the downwind and crosswind distances for the higher dose rate contours. A more precise scaling is not warranted on the basis of present understanding of the phenomena. For depths of burst greater than 70 $W^{1/3}$ feet, virtually all of the available contamination comes down in the vicinity of the burst point; as burst depth is increased, contours can be expected to decrease in size, with increase in dose rate values in and near the crater. Contours may be drawn for other wind values in the same manner as described for land surface bursts. The contour values given are for an unshielded, open area with substantially level terrain.

(2) *Underwater burst.*

(*a*) *General.* One test at mid-depth in shallow water provided some information on the residual radiation from an underwater detonation. The rather specialized burst conditions make application of the results to specific cases of interest of doubtful validity; however, certain guidelines were established which are applicable and useful in the general case. It was shown that for a ship subjected to fallout radiation, much of the contaminated fallout material drains off the ship into the water, and rapidly becomes relatively ineffective because of the dilution due to mixing in water. For adjacent land areas, residual radiation dose rates about four times as great as on board ship at the same relative position are expected soon after completion of fallout, because dilution and run-off do not occur. For adjacent land areas, the decrease in dose rate with time can be calculated from figure 4–13; however, this cannot be done for ships. As in the case of other types of contaminating bursts, the area of contamination varies considerably with meteorological conditions, particularly with wind.

(*b*) *Harbor burst.* In the case of a nuclear explosion in a comparatively shallow harbor, as in the hold of a ship, more than half of the available radioactivity associated with the device is deposited as local fallout, and large localized high dose rate contours are expected on the adjacent land masses. Although it does not appear feasible to attempt a detailed delineation of contour shapes for a harbor burst on the basis of information available, magnitudes of contour areas expected can be given with some confidence. Figure 4–25 indicates expected harbor burst contour areas on adjacent land masses for yields from 1 KT to 1 MT. For yields in the megaton range, contour areas should be estimated from the surface burst curves already presented (fig. 4–14B). To estimate dose rates on the weather decks of anchored ships in a harbor, divide the land-mass values given by four; and for ships alongside a wharf, divide the land-mass values by two.

f. Ground Zero Dose Rates. The residual dose rate curves presented herein make no provision for contours delineating dose rates greater than 3,000 roentgens per hour, except in the case of harbor bursts. Such dose rates occur in "hot spots" rather than over significant areas. The maximum residual radiation dose rates observed on the ground in such hot spots at a reference time of $H+1$ hour, regardless of weapon yield, have been more than 3,000 r/hr and less than 10,000 r/hr for surface burst nuclear weapons. The burst conditions for most of these shots were not truly representative of land shots; hence, there is a large degree of uncertainty regarding the maximum dose rates which may be expected at ground zero under true land surface burst conditions. Higher dose rates may be expected only under certain special circumstances, such as deep underground bursts and bursts in shallow harbors, and are not normally expected for land surface bursts.

g. Total Dose Received. To estimate the dose actually received at a point within an area contaminated by fallout, estimate the time of arrival of fallout at that point (using the scaling wind velocity and the distance from the burst point) and integrate the curve of dose rate as a function of time over the period the individual is within the area. The same procedure is used for the case of a person entering a contaminated area at some time after completion of fallout. Figure 4–26 is presented to facilitate this computation. and can be used to estimate total radiation dose received while in a contaminated area. If, at the time of the explosion, the individual is within the radius of effect of the initial radiation, the acute dose so received must be added to the cumulative residual radiation dose in the manner outlined in paragraph 6.3*b* to obtain the total dose received. If the individual is sheltered, the free field value so obtained should be multiplied by a reduction factor estimated from the degree of shielding involved, as described in paragraph 6.5.

h. Dose Contours. Approximate total dose contours for accumulated doses received during the 48 hours immediately following burst time can be estimated using the appropriate 1-hour dose rate contour curves in conjunction with a scaling factor obtained from figure 4–27. The scaling factor averages the time of arrival effect for 500 roentgen total dose contours using a 15 knot scaling wind, and gives results sufficiently accurate for planning purposes over a range of doses from 100 *r* to 1,000 *r*. This method may be used with somewhat less accuracy for accumulated doses outside this range. It should be recognized that dose and dose rate contours do not have the same shape, although the shapes are sufficiently alike to make this approximate method useful.

FISSION PRODUCT DECAY FACTORS FROM ONE HOUR AFTER DETONATION

From the dose rate at $H+1$ hour the dose rate at any other time is obtained by forming the product of the appropriate decay factor from figure 4-13 and the 1-hour dose rate.

Example.

Given: The dose rate at a given point at 1 hour after detonation is 500 r/hr.

Find: The dose rate at that point 12 hours after detonation.

Solution: From figure 4-13, the decay factor at 12 hours is 0.05. Therefore, the dose rate at 12 hours is $500 \times 0.05 = 25$ r/hr. *Answer.*

The decay curve may also be used to determine the value of the dose rate at 1 hour from the dose rate at a later time. In this case, the measured dose rate is divided by the appropriate decay factor.

Example.

Given: The dose rate at a given point 10 hours after detonation is 72 r/hr.

Find: The dose rate at the same point 1 hour after the detonation.

Solution: From the decay factor curve at 10 hours we have a factor of 0.06. Therefore, the dose rate at 1 hour is $\frac{72}{0.06} = 1{,}200$ r/hr. *Answer.*

Related material.

See paragraph 4.3*c*(1)(*d*).

See also figures 4-26 and 4-27.

FIGURE 4-13

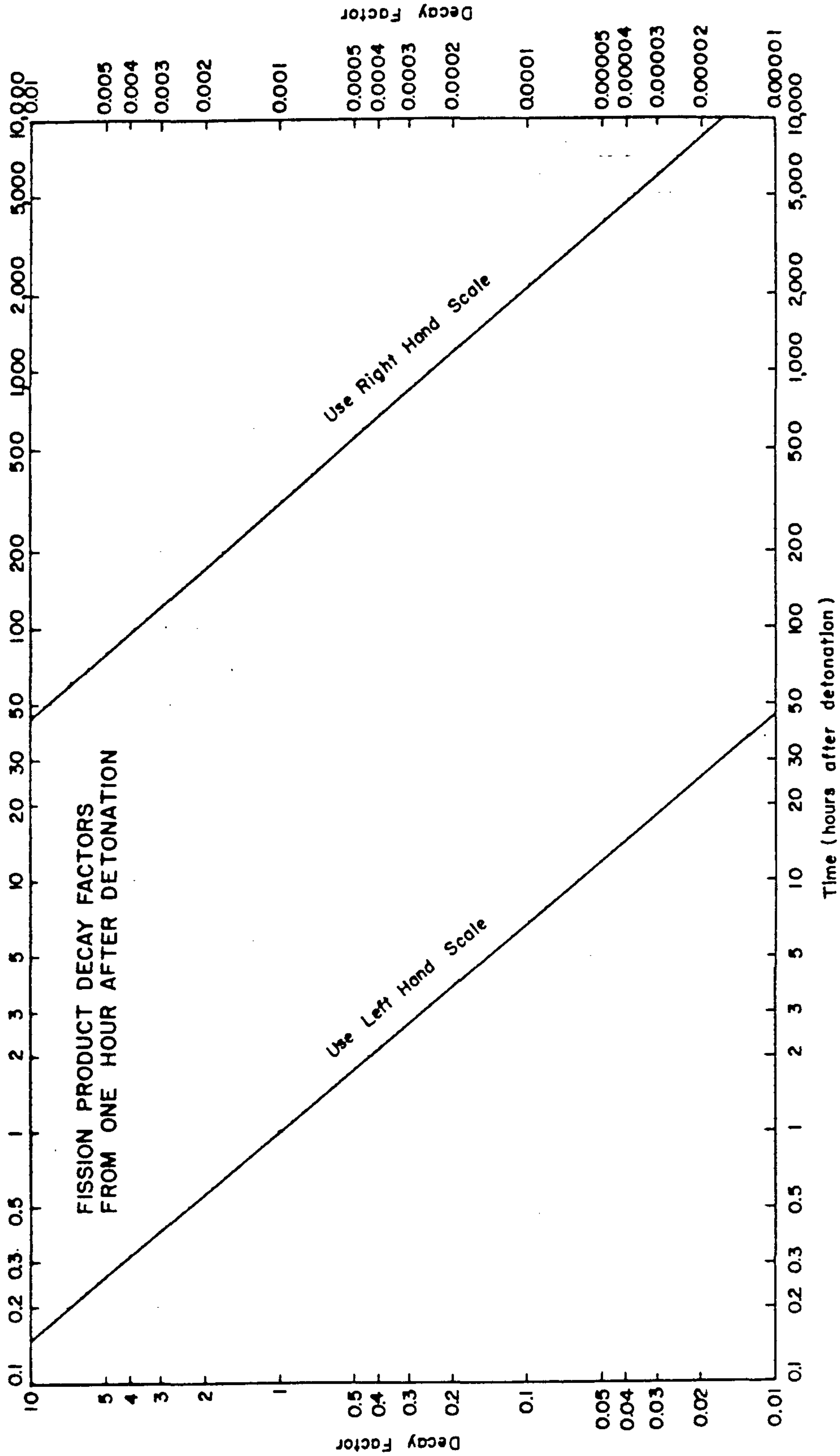
FISSION PRODUCT DECAY FACTORS
FROM ONE HOUR AFTER DETONATION
Use Right Hand Scale
Use Left Hand Scale
Decay Factor
Decay Factor
Time (hours after detonation)
0.1
0.2
0.3
0.5
1
2
3
5
10
20
30
50
100
200
500
1,000
2,000
5,000
10,000
10
5
4
3
2
1
0.5
0.4
0.3
0.2
0.1
0.05
0.04
0.03
0.02
0.01
0.005
0.004
0.003
0.002
0.001
0.0005
0.0004
0.0003
0.0002
0.0001
0.00005
0.00004
0.00003
0.00002
0.00001

RESIDUAL GAMMA RADIATION FROM SURFACE BURSTS

Dose Rate Contour Parameters vs. Yield for Various Dose Rates

Figures 4-14 through 4-18 present idealized dose rate contour parameters for residual fallout radiation from surface bursts of weapons with yields between 0.1 KT and 100 MT. The basic data are presented for weapons for which all of the yield is due to fission; however, as will be described below, the data can also be used to obtain fallout contours for weapons for which the fission yield is only a fraction of the total yield, and for which essentially all of the contamination produced (90 percent or more) is due to fission products. The dose rate values are given for a *reference* time of $H+1$ hour. It must be recognized that the more distant portions of the larger contours do not exist at $H+1$ hour, since the fallout which eventually reaches some of these more distant areas is still airborne at that time. The dose rate contours do exist at later times when fallout is complete, but with contour dose rate values reduced according to the appropriate decay factor from figure 4-13. Visual interpolation may be employed for dose rate contour values between those for which curves are given. Extrapolation to higher or to lower dose rate contour values than covered by the families of curves cannot be done accurately and should not be attempted.

To obtain dose rate values for times other than $H+1$ hour, decay factors from figure 4-13 should be used. To obtain contour values for scaling winds other than 15 knots, multiply downwind distance and downwind displacement of the ground zero circle by the appropriate factor given below, and divide crosswind distance by the same factor. Numerical values of contour areas and ground zero circle diameters are essentially wind-independent.

Adjustment Factors for Contour Parameters for Various Scaling Winds

Scaling Wind Velocity (knots)	5	10	15	20	25	30	40	50
Factor	0.7	0.9	1.0	1.1	1.2	1.3	1.4	1.5

For the special (and unusual) case of a zero scaling wind velocity, contours would be circular, centered at the burst point, with radii determined from the area curves by the formula:

$$\text{Contour Radius} = \sqrt{\frac{\text{Contour Area.}}{\pi}}$$

For a burst in the transition zone, a rough estimate of the resulting fallout contamination patterns may be made by multiplying the dose rate contour values for a contact surface burst weapon of the same yield by an adjustment factor obtained from figure 4-19 for the appropriate yield and height of burst.

Note that the contribution made by neutron-induced activity may be significant compared to the fallout activity in the area near ground zero for weapons burst in the upper quarter of the fallout transition zone. For guidance, a rough estimate of this contribution may be obtained using figures 4-28 through 4-33 together with the discussion in paragraph 4.3*i*(2).

It should be recognized that contour *shapes* and *sizes* are a function of the *total* yield of the weapon, whereas the dose rate contour *values* are determined by the amount of contaminant available; i. e., the *fission* yield. Thus, if only a fraction of the total yield of the weapon is due to fission, and this fraction is known, figures 4-14 through 4-18 may be used to estimate fallout contours resulting from the detonation of such a weapon. The dose rate for the dimension of interest as read from the figures opposite the total yield must be multiplied by the ratio of fission yield to total yield to obtain the true dose rate value for that dimension. Similarly, to obtain contour dimensions for a particular dose rate, the value of the desired dose rate must be divided by the ratio of fission to total yield, and the dimension of the resultant dose rate read from the figures opposite the total yield.

Example.

Given: A weapon with a total yield of 600 KT, of which 200 KT is due to fission, is detonated on a land surface under 10-knot scaling wind conditions.

Find:

(*a*) Contour parameters for a dose rate of 100 r/hr at $H+1$ hour reference time.

(*b*) If the weapon were burst at a height of 1,950 feet above the surface, what fallout contour would be represented by the 100 r/hr surface burst contour solved for in (*a*).

Solution:

(*a*) The 100 r/hr contour for a fission yield to total yield ratio of 200/600 is the same as the contour for $100 \div \frac{200}{600} = 300$ r/hr, for a weapon for which the total yield is fission yield. Figures 4-14B through 4-18B can therefore be applied together with wind factors from the table given above; i. e., the 300 r/hr contour values read from figures 4-14B through 4-18B (for fission yield = total yield = 600 KT) are also those for the 100 r/hr contour of the weapon described in the example. The problem solution is indicated in tabular form as follows:

Parameter (fig. 4-12)	Source figure	Basic value	Wind factor	Parameter value for 10-knot wind. *Answer*
Area	4-14B	190 sq. mi.	1.0	190 sq. mi.
Downwind distance	4-15B	38 mi.	0.9	34 mi.
Crosswind distance	4-16B	6.7 mi.	1/0.9	7.4 mi
Diameter of ground zero circle.	4-17B	4.5 mi.	1.0	4.5 mi.
Downwind displacement of ground zero circle.	4-18B	0.8 mi.	0.9	0.7 mi

(*b*) From figure 4-19, the adjustment factor for a 600 KT burst at a height of 1,950 feet is about 0.04, and the contour solved for in (*a*) corresponds for this burst condition to $0.04 \times 100 = 4$ r/hr at $H+1$ hour. *Answer.*

Reliability. The sensitive wind-dependence of the fallout distribution mechanism, and the degree to which wind and other meteorological conditions affect these contour parameters, cannot be overemphasized. The contours presented in these curves have been *idealized* in order to make it possible to present average, representative values for planning purposes. Recognizing these limitations, for average fair weather conditions, the curves can be considered reliable within ±50 percent.

Related material.

See paragraphs 4.3*a* through *h*.

See also figures 4-12, 4-13, and 4-26 through 4-33.

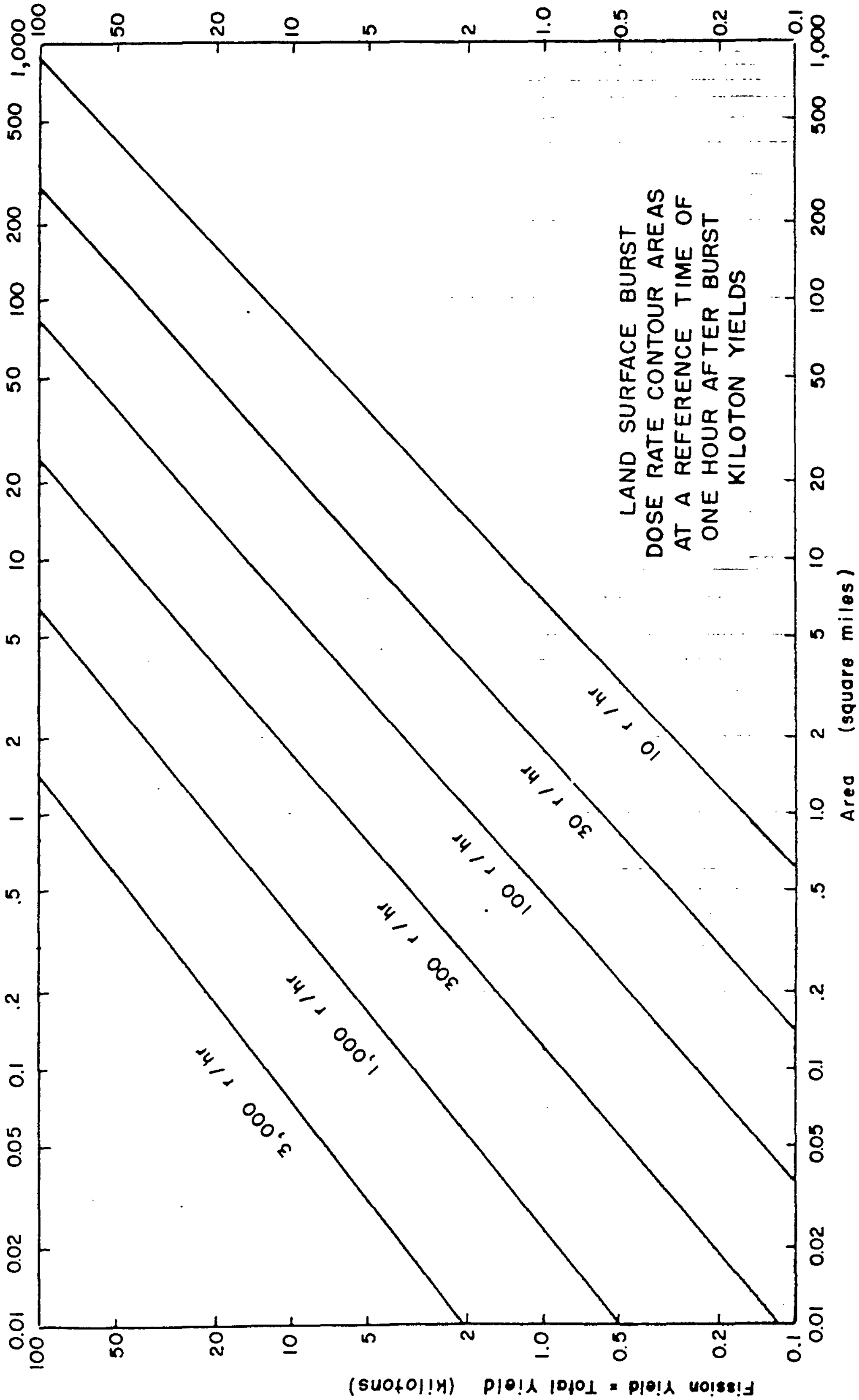
LAND SURFACE BURST
DOSE RATE CONTOUR AREAS
AT A REFERENCE TIME OF
ONE HOUR AFTER BURST
KILOTON YIELDS
10 r / hr
30 r / hr
100 r / hr
300 r / hr
1,000 r / hr
3,000 r / hr
Area (square miles)
Fission Yield = Total Yield (Kilotons)
0.01
0.02
0.05
0.1
.2
.5
1
2
5
10
20
50
100
200
500
1,000
100
50
20
10
5
2
1.0
0.5
0.2
0.1

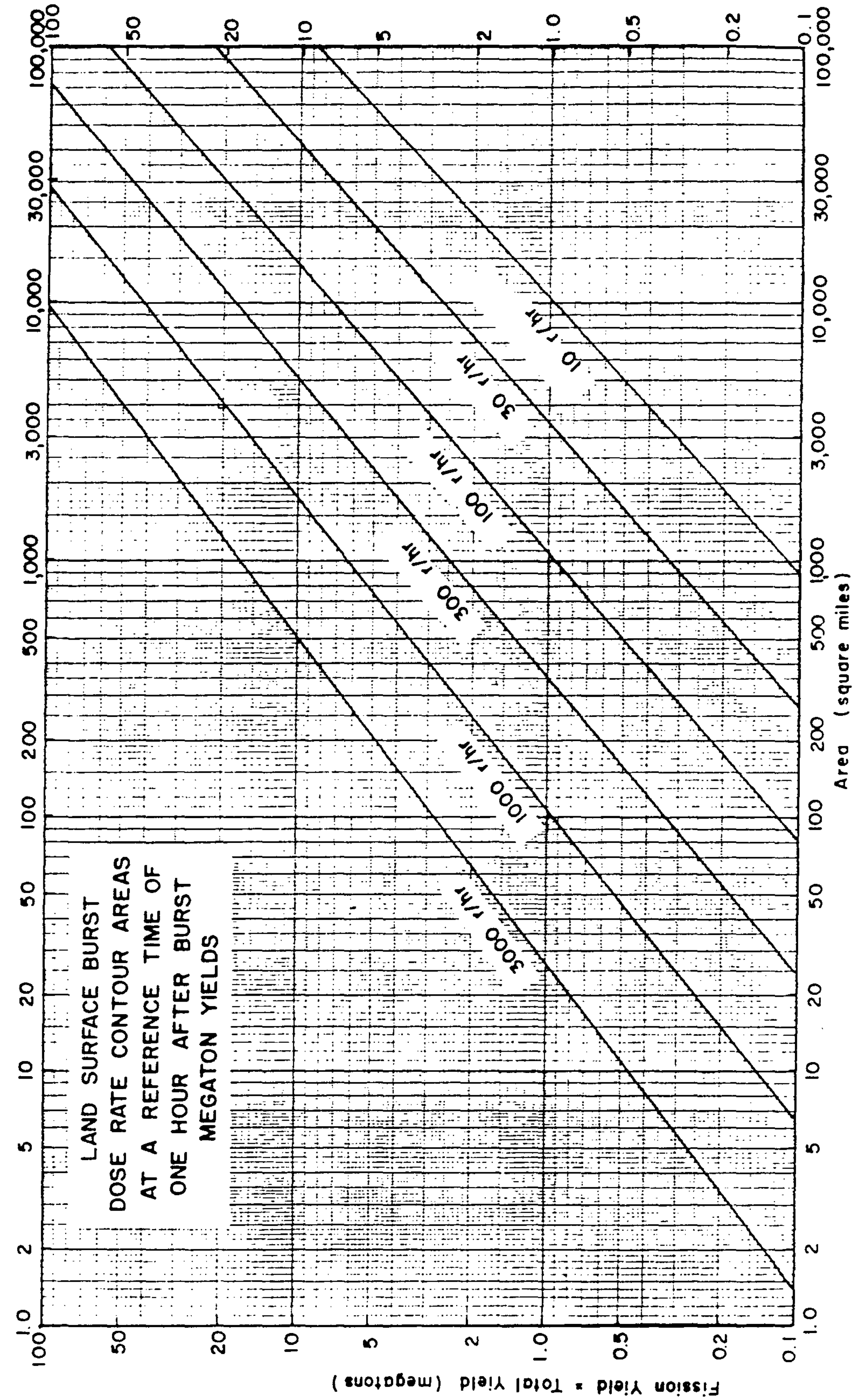
LAND SURFACE BURST
DOSE RATE CONTOUR AREAS
AT A REFERENCE TIME OF
ONE HOUR AFTER BURST
MEGATON YIELDS
10 r/hr
30 r/hr
100 r/hr
300 r/hr
1000 r/hr
3000 r/hr
Area (square miles)
1.0
2
5
10
20
50
100
200
500
1,000
3,000
10,000
30,000
100,000
Fission Yield = Total Yield (megatons)
100
50
20
10
5
2
1.0
0.5
0.2
0.1

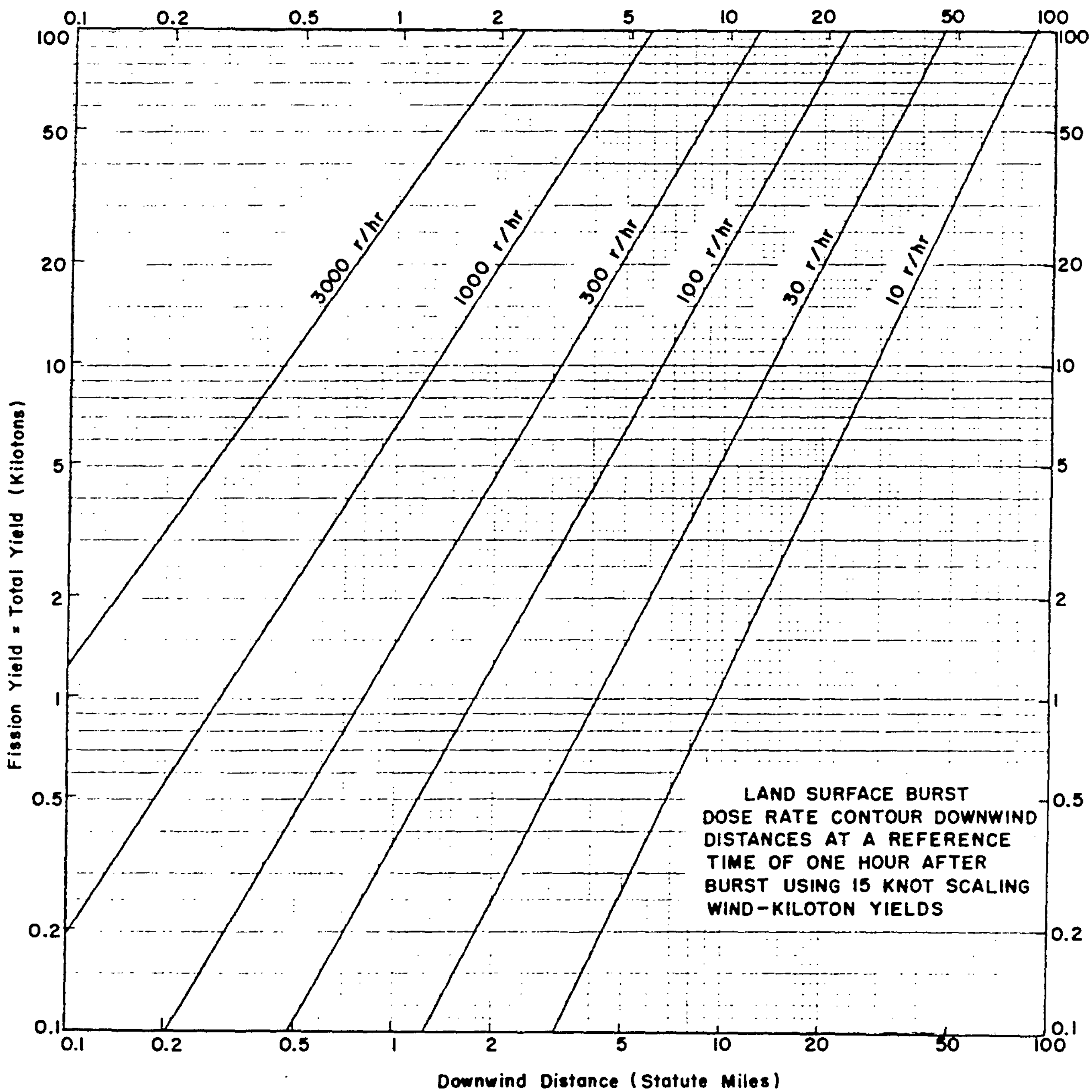
3000 r/hr
1000 r/hr
300 r/hr
100 r/hr
30 r/hr
10 r/hr
LAND SURFACE BURST
DOSE RATE CONTOUR DOWNWIND
DISTANCES AT A REFERENCE
TIME OF ONE HOUR AFTER
BURST USING 15 KNOT SCALING
WIND-KILOTON YIELDS
Fission Yield = Total Yield (Kilotons)
Downwind Distance (Statute Miles)
0.1
0.2
0.5
1
2
5
10
20
50
100

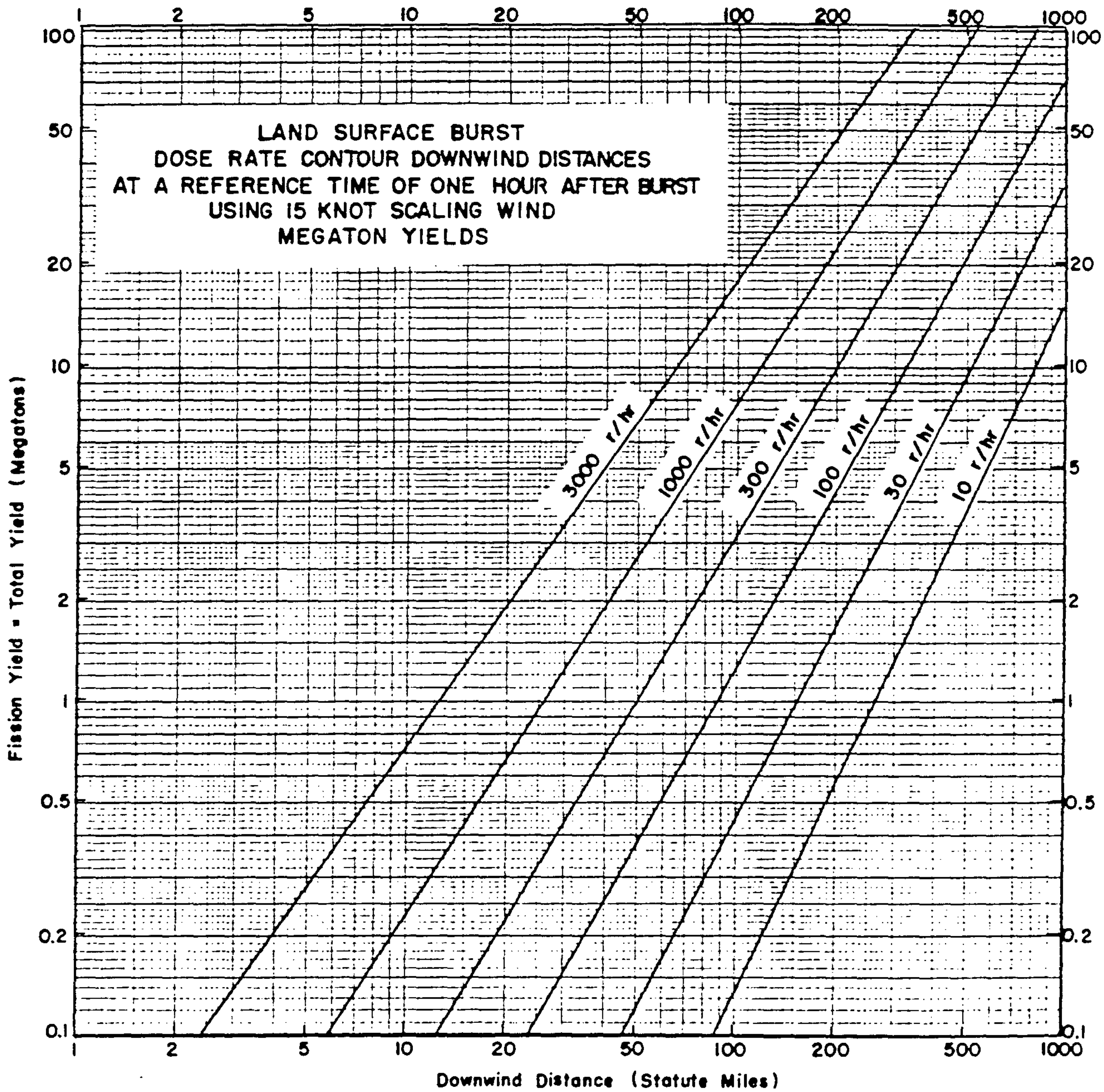
LAND SURFACE BURST
DOSE RATE CONTOUR DOWNWIND DISTANCES
AT A REFERENCE TIME OF ONE HOUR AFTER BURST
USING 15 KNOT SCALING WIND
MEGATON YIELDS
3000 r/hr
1000 r/hr
300 r/hr
100 r/hr
30 r/hr
10 r/hr
Fission Yield = Total Yield (Megatons)
Downwind Distance (Statute Miles)
1
2
5
10
20
50
100
200
500
1000
0.1
0.2
0.5
1
2
5
10
20
50
100

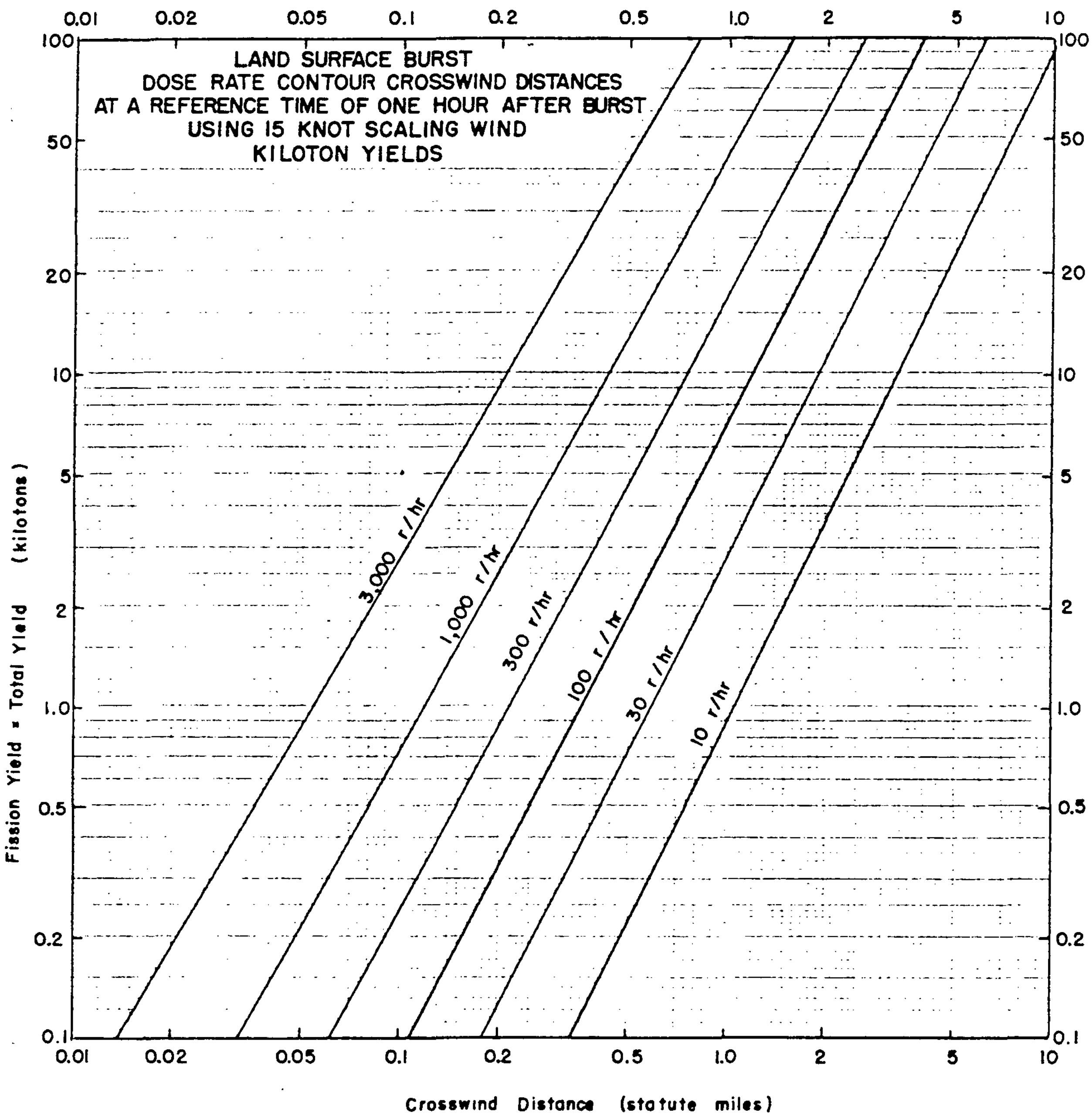
LAND SURFACE BURST
DOSE RATE CONTOUR CROSSWIND DISTANCES
AT A REFERENCE TIME OF ONE HOUR AFTER BURST
USING 15 KNOT SCALING WIND
KILOTON YIELDS
3,000 r/hr
1,000 r/hr
300 r/hr
100 r/hr
30 r/hr
10 r/hr
Fission Yield = Total Yield (kilotons)
100
50
20
10
5
2
1.0
0.5
0.2
0.1
0.01
0.02
0.05
0.1
0.2
0.5
1.0
2
5
10
Crosswind Distance (statute miles)

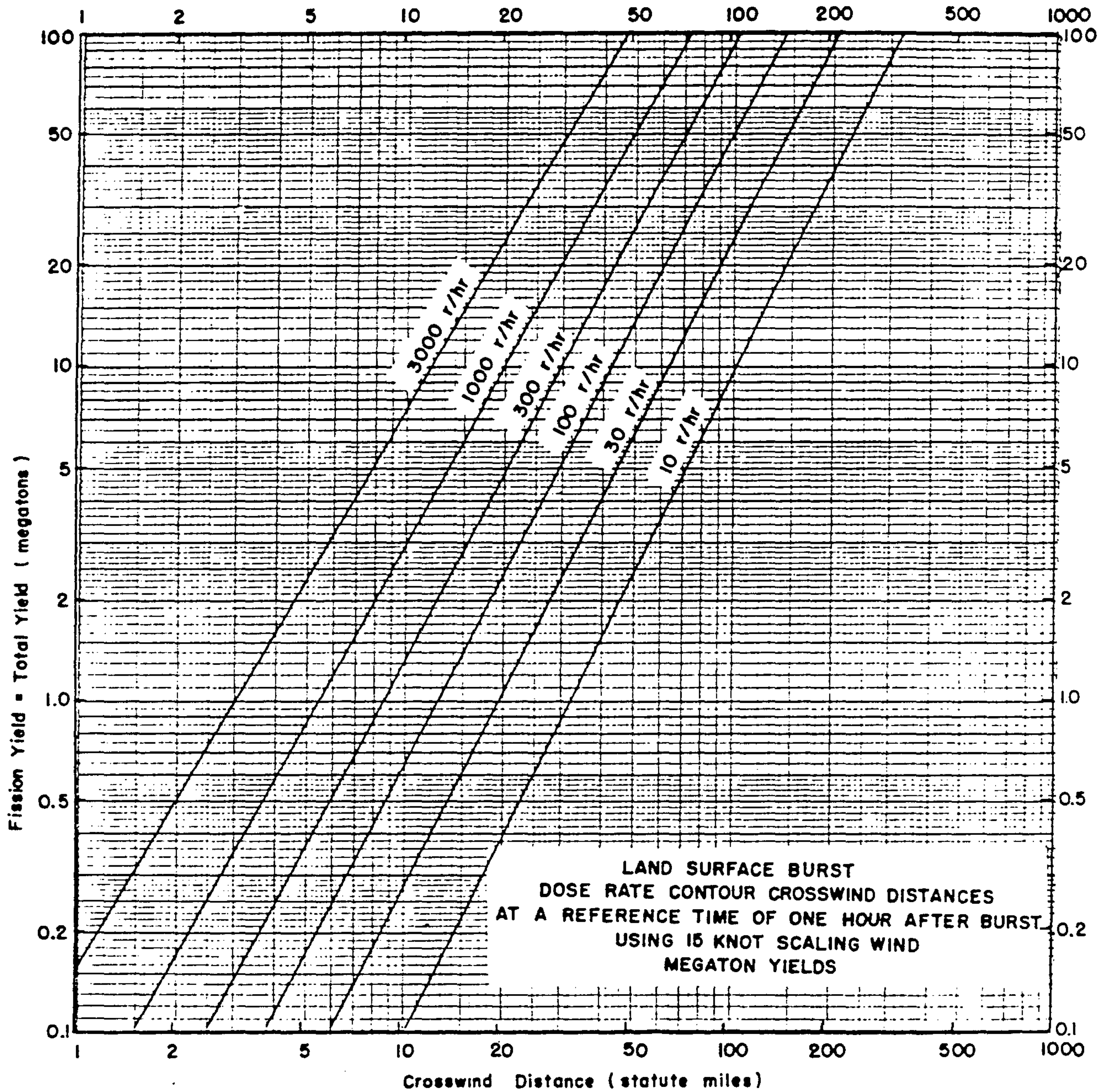
LAND SURFACE BURST
DOSE RATE CONTOUR CROSSWIND DISTANCES
AT A REFERENCE TIME OF ONE HOUR AFTER BURST
USING 15 KNOT SCALING WIND
MEGATON YIELDS
3000 r/hr
1000 r/hr
300 r/hr
100 r/hr
30 r/hr
10 r/hr
Fission Yield = Total Yield (megatons)
Crosswind Distance (statute miles)
1
2
5
10
20
50
100
200
500
1000
100
50
20
10
5
2
1.0
0.5
0.2
0.1

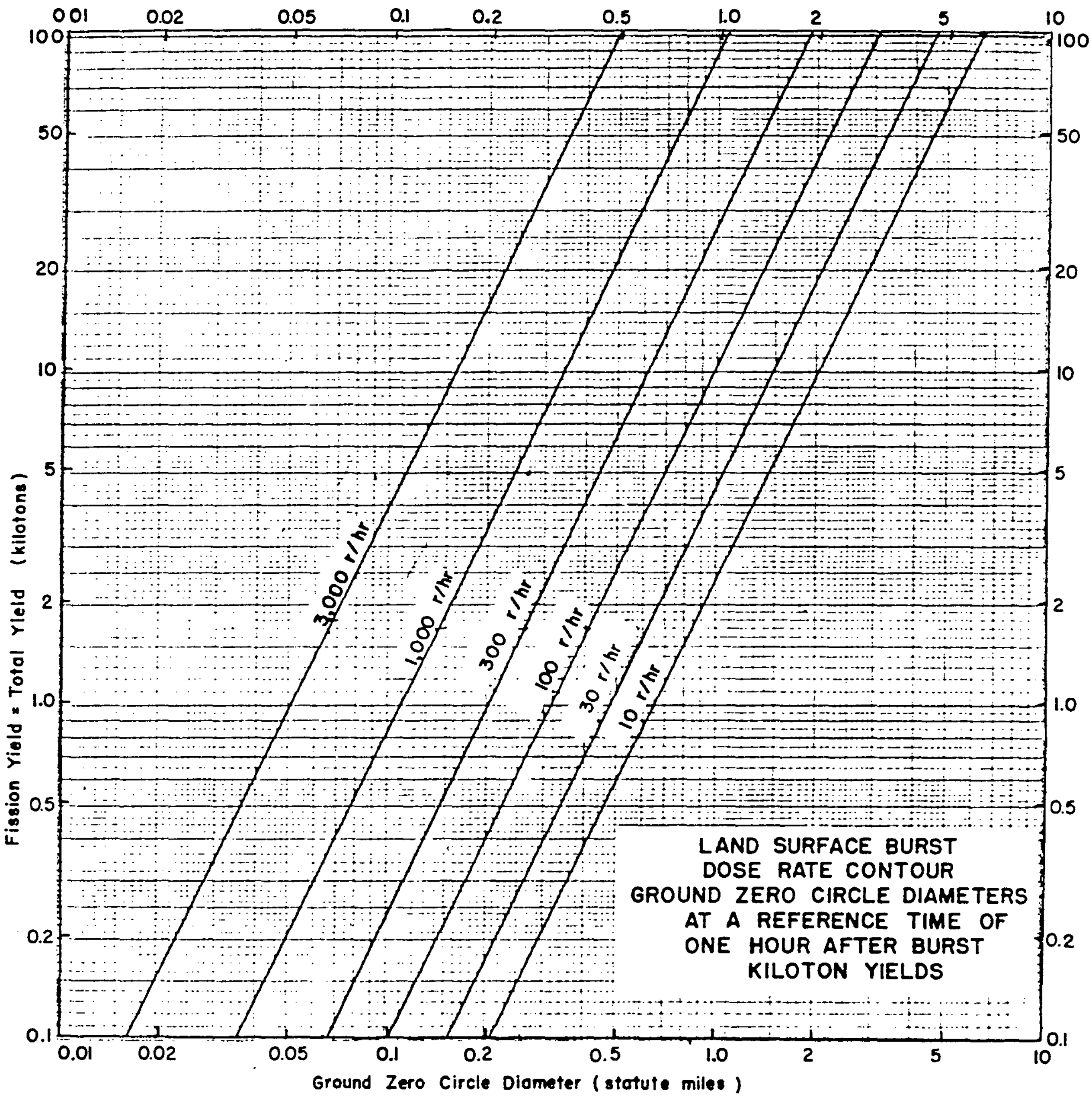

LAND SURFACE BURST
DOSE RATE CONTOUR
GROUND ZERO CIRCLE DIAMETERS
AT A REFERENCE TIME OF
ONE HOUR AFTER BURST
KILOTON YIELDS
3,000 r/hr
1,000 r/hr
300 r/hr
100 r/hr
30 r/hr
10 r/hr
Fission Yield = Total Yield (kilotons)
Ground Zero Circle Diameter (statute miles)
0.01
0.02
0.05
0.1
0.2
0.5
1.0
2
5
10
100
50
20
10
5
2
1.0
0.5
0.2
0.1

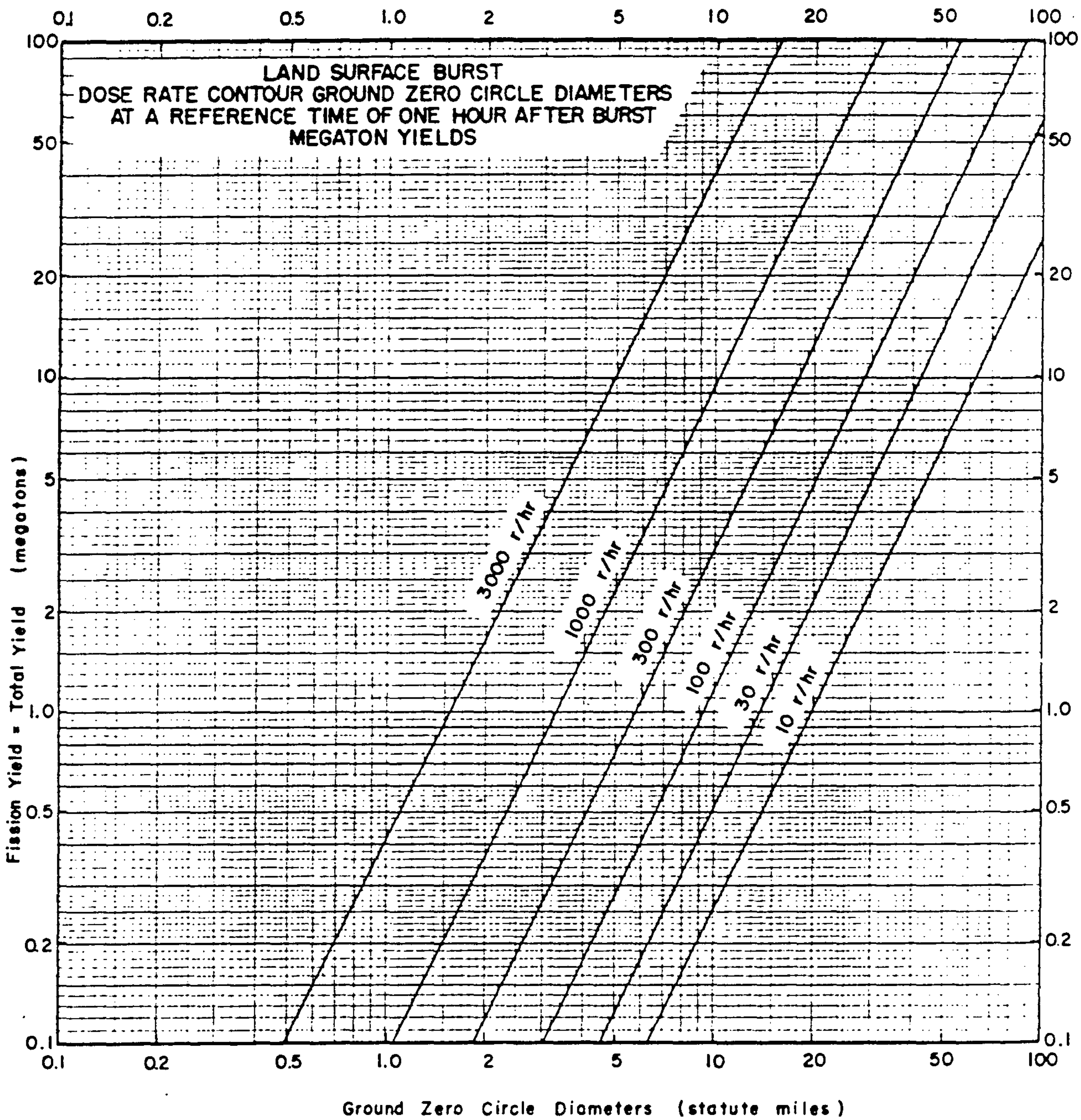
LAND SURFACE BURST
DOSE RATE CONTOUR GROUND ZERO CIRCLE DIAMETERS
AT A REFERENCE TIME OF ONE HOUR AFTER BURST
MEGATON YIELDS
3000 r/hr
1000 r/hr
300 r/hr
100 r/hr
30 r/hr
10 r/hr
0.1
0.2
0.5
1.0
2
5
10
20
50
100
Fission Yield = Total Yield (megatons)
Ground Zero Circle Diameters (statute miles)

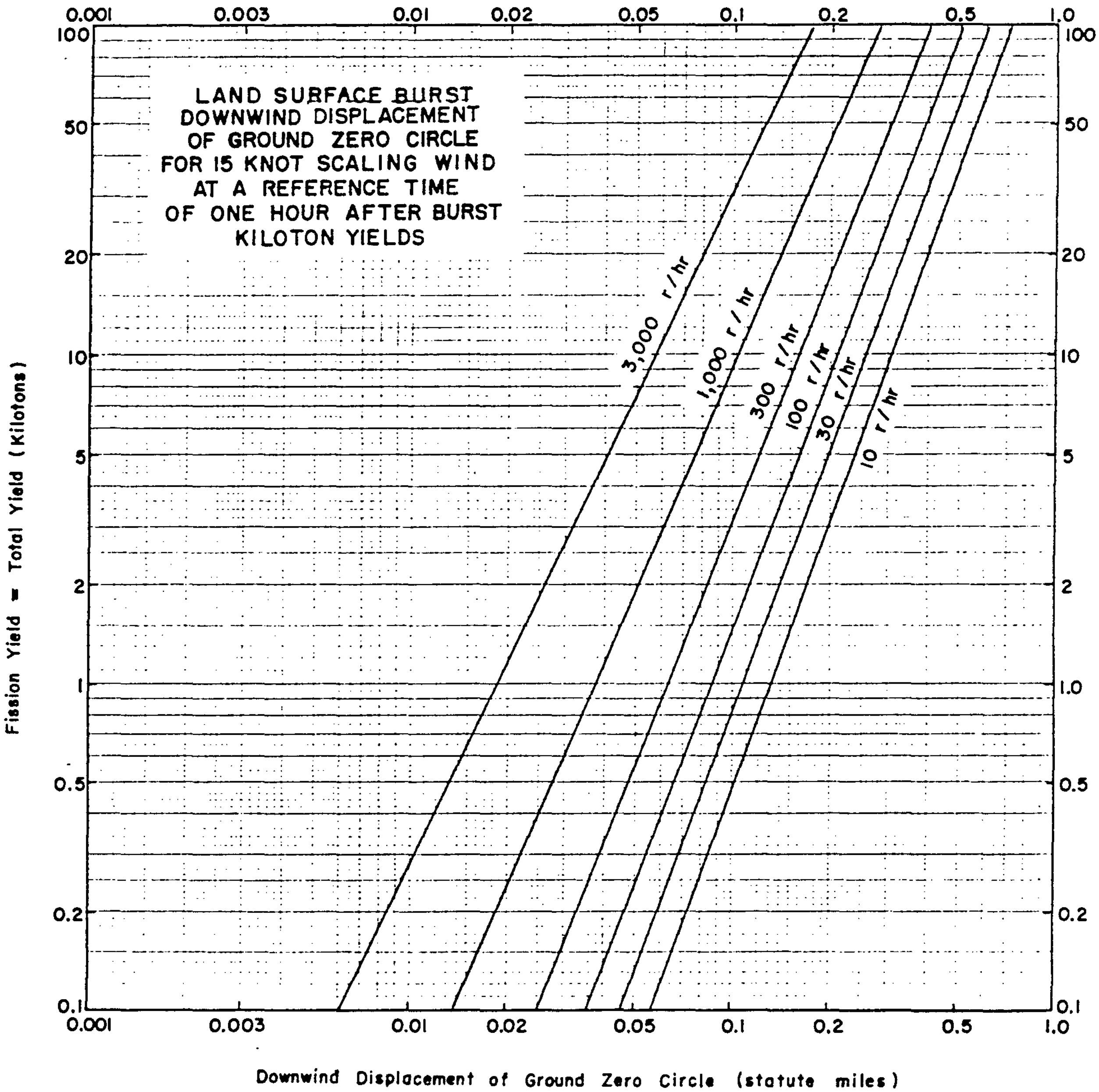
LAND SURFACE BURST
DOWNWIND DISPLACEMENT
OF GROUND ZERO CIRCLE
FOR 15 KNOT SCALING WIND
AT A REFERENCE TIME
OF ONE HOUR AFTER BURST
KILOTON YIELDS
3,000 r/hr
1,000 r/hr
300 r/hr
100 r/hr
30 r/hr
10 r/hr
Fission Yield = Total Yield (Kilotons)
Downwind Displacement of Ground Zero Circle (statute miles)
0.001
0.003
0.01
0.02
0.05
0.1
0.2
0.5
1.0
100
50
20
10
5
2
1
0.5
0.2
0.1

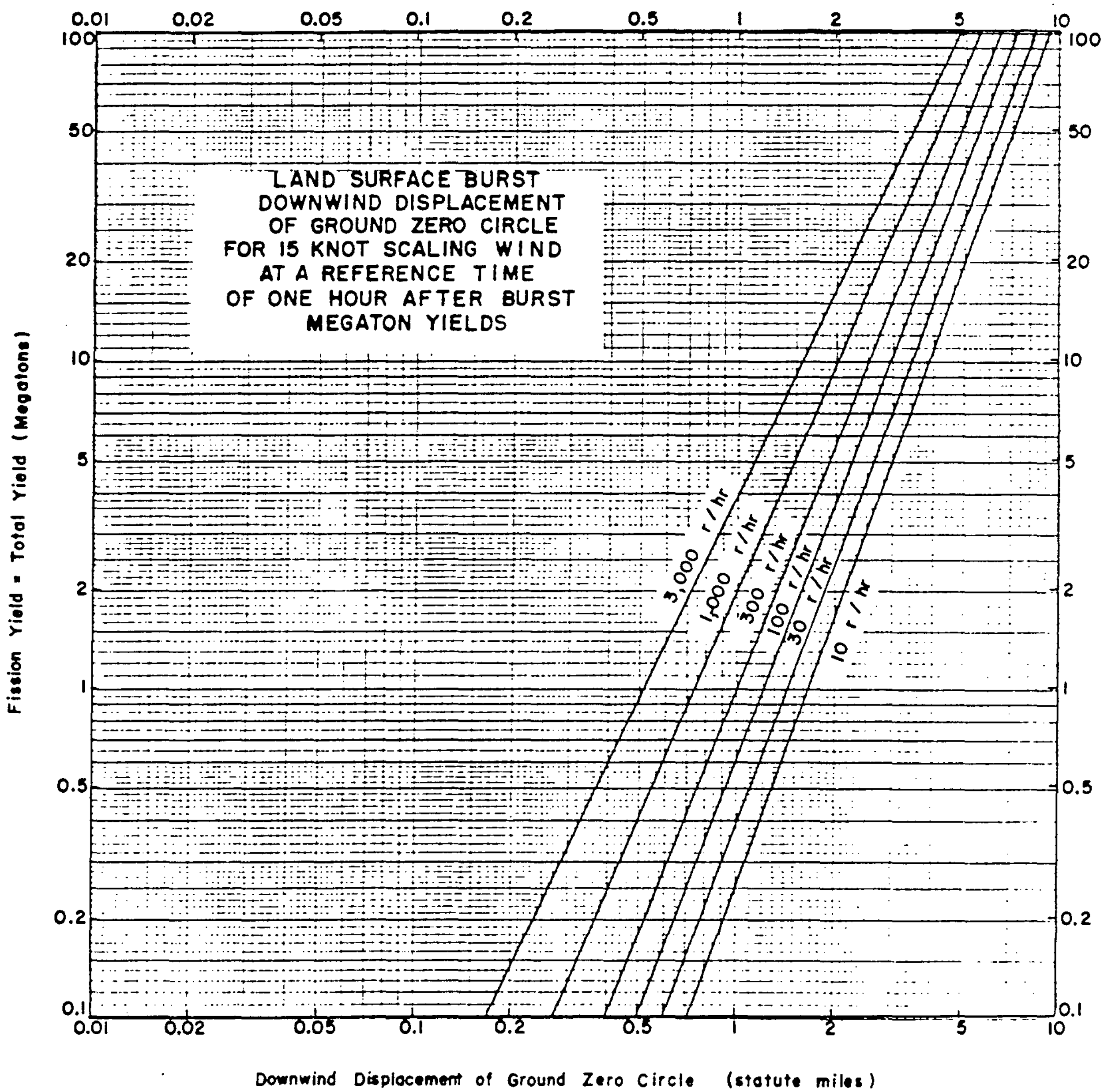
LAND SURFACE BURST
DOWNWIND DISPLACEMENT
OF GROUND ZERO CIRCLE
FOR 15 KNOT SCALING WIND
AT A REFERENCE TIME
OF ONE HOUR AFTER BURST
MEGATON YIELDS
3,000 r/hr
1,000 r/hr
300 r/hr
100 r/hr
30 r/hr
10 r/hr
Fission Yield = Total Yield (Megatons)
Downwind Displacement of Ground Zero Circle (statute miles)
0.01
0.02
0.05
0.1
0.2
0.5
1
2
5
10
20
50
100

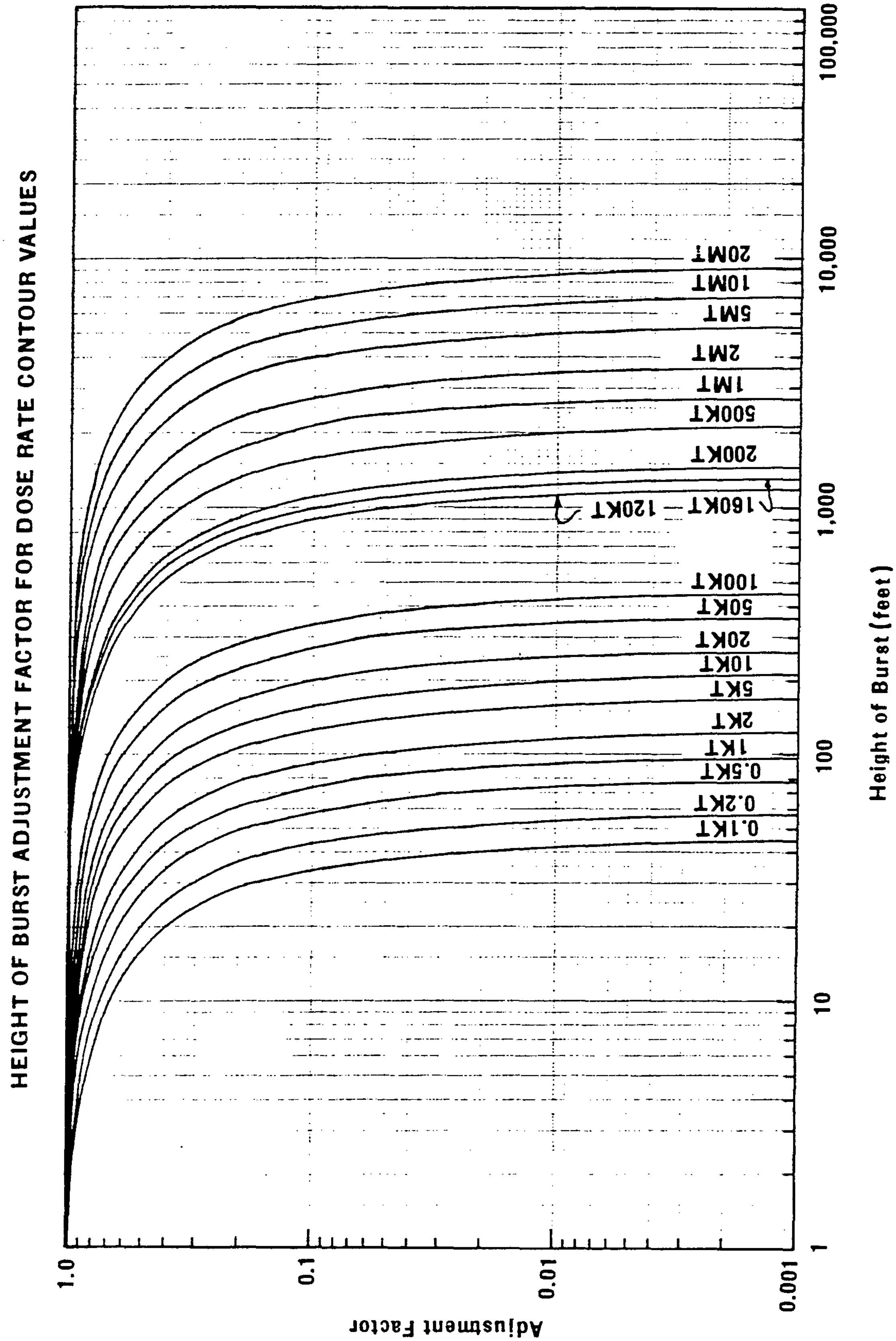
HEIGHT OF BURST ADJUSTMENT FACTOR FOR DOSE RATE CONTOUR VALUES
Height of Burst (feet)
Adjustment Factor
1.0
0.1
0.01
0.001
1
10
100
1,000
10,000
100,000
20MT
10MT
5MT
2MT
1MT
500KT
200KT
160KT
120KT
100KT
50KT
20KT
10KT
5KT
2KT
1KT
0.5KT
0.2KT
0.1KT

BLANK

RESIDUAL GAMMA RADIATION FROM UNDERGROUND BURSTS

Dose Rate Contour Parameters vs. Yield for Various Dose Rates

Figures 4–20 through 4–23 present idealized dose rate contour parameters for residual fallout gamma radiation from underground bursts of weapons with yields in the range between 1 KT and 1 MT. The fission yield of the weapon is assumed to be the total yield. If a portion of the yield is due to fusion, dose rate values read from the curves should be multiplied by the ratio of fission yield to total yield, as described for surface bursts (preceding fig. 4–14). The dose rate values given are for a *reference* time of $H+1$ hour. The more distant portions of the larger contours do not exist at $H+1$ hour, since the fallout which eventually reaches some of these more distant areas is still airborne at that time. Visual interpolation may be employed for dose rate contour values between those for which curves are given. Extrapolation to higher or to lower dose rate contour values than the range covered by the families of curves cannot be done accurately and should not be attempted.

To obtain dose rate values for times other than $H+1$ hour, decay factors from figure 4–13 should be used. Figure 4–27 may be used in conjunction with these curves to obtain approximate 48-hour total dose contours.

The contour parameters given by the curves are for a burst depth of 17 $W^{1/3}$ feet, and a scaling wind velocity of 15 knots. To obtain contour parameter values for other burst depths, multiply linear dimensions obtained from the curves by a depth multiplication factor read from figure 4–24, and multiply areas by the square of this factor. Figure 4–24 is plotted for a 1 KT yield. For yields other than 1 KT the depth of burst for a given multiplication factor scales as the cube root of the yield, i. e., $\frac{d_1}{d_2}=\frac{W_1^{1/3}}{W_2^{1/3}}$, where d_1 is the depth of burst for W_1 KT, and d_2 is the depth of burst for W_2 KT.

To obtain contour values for scaling winds other than 15 knots, multiply downwind distance and downwind displacement of the ground zero circle by the factors given below, and divide crosswind distance by the same factor. Numerical values of contour areas and ground zero circle diameters are essentially wind-independent.

Adjustment Factors for Contour Parameters for Various Scaling Winds

Scaling Wind Velocity (knots)	5	10	15	20	25	30	40	50
Factor	0.7	0.9	1.0	1.1	1.2	1.3	1.4	1.5

For the special (and unusual) case of a zero scaling wind velocity, contours would be circular, with radii determined from the area curves by the formula

$$\text{Contour Radius}=\sqrt{\frac{\text{Contour Area}}{\pi}}.$$

Example.

Given: A 20 KT weapon burst 115 feet underground under 20 knot scaling wind conditions.

Find:

(*a*) Contour parameters for a dose rate of 100 r/hr at one hour after the detonation.

(*b*) The approximate total accumulated dose up to 48 hours after burst time at this contour.

Solution:

(*a*) Figures 4–18A, 4–20 through 4–24, and 4–27 apply.

The corresponding depth for 1 KT is—

$$\frac{115}{(20)^{1/3}}=43 \text{ feet.}$$

Tabulating the solution:

Parameter (fig. 4-12)	Source figure	Basic value	Depth factor (fig. 4-24)	Wind factor	Parameter value for actual burst conditions. *Answer.*
Area	4-20	50 sq. mi.	0.8	1.0	40 sq. mi.
Downwind distance.	4-21	28 mi.	0.9	1.1	28 mi.
Crosswind distance.	4-22	2.8 mi.	0.9	1/1.1	2.3 mi.
Diameter of ground zero circle.	4-23	2.3 mi.	0.9	1.0	2.1 mi.
Downwind displacement of center of ground zero circle.	4-18A	0.28 mi	0.9	1.1	0.28 mi.

(*b*) From figure 4-27, the 48-hour dose scaling factor for a 20 KT weapon is 2.65. Thus, the approximate total dose accumulated up to 48 hours after burst time at the 100 r/hr contour is $100 \times 2.65 = 265$ roentgens. *Answer.*

Reliability. The sensitive wind-dependence of the fallout distribution mechanism, and the degree to which wind and other meteorological conditions affect these contour parameters, cannot be overemphasized. The contours presented in these curves have been *idealized* in order to make it possible to present average, representative values for planning purposes. Recognizing these limitations, for average fair weather conditions, values read from the curves can be considered reliable within ±50 percent.

Related material.

See paragraphs 4.3*a* through *h*.

See also figures 4-12 through 4-18, 4-26, and 4-27.

BLANK

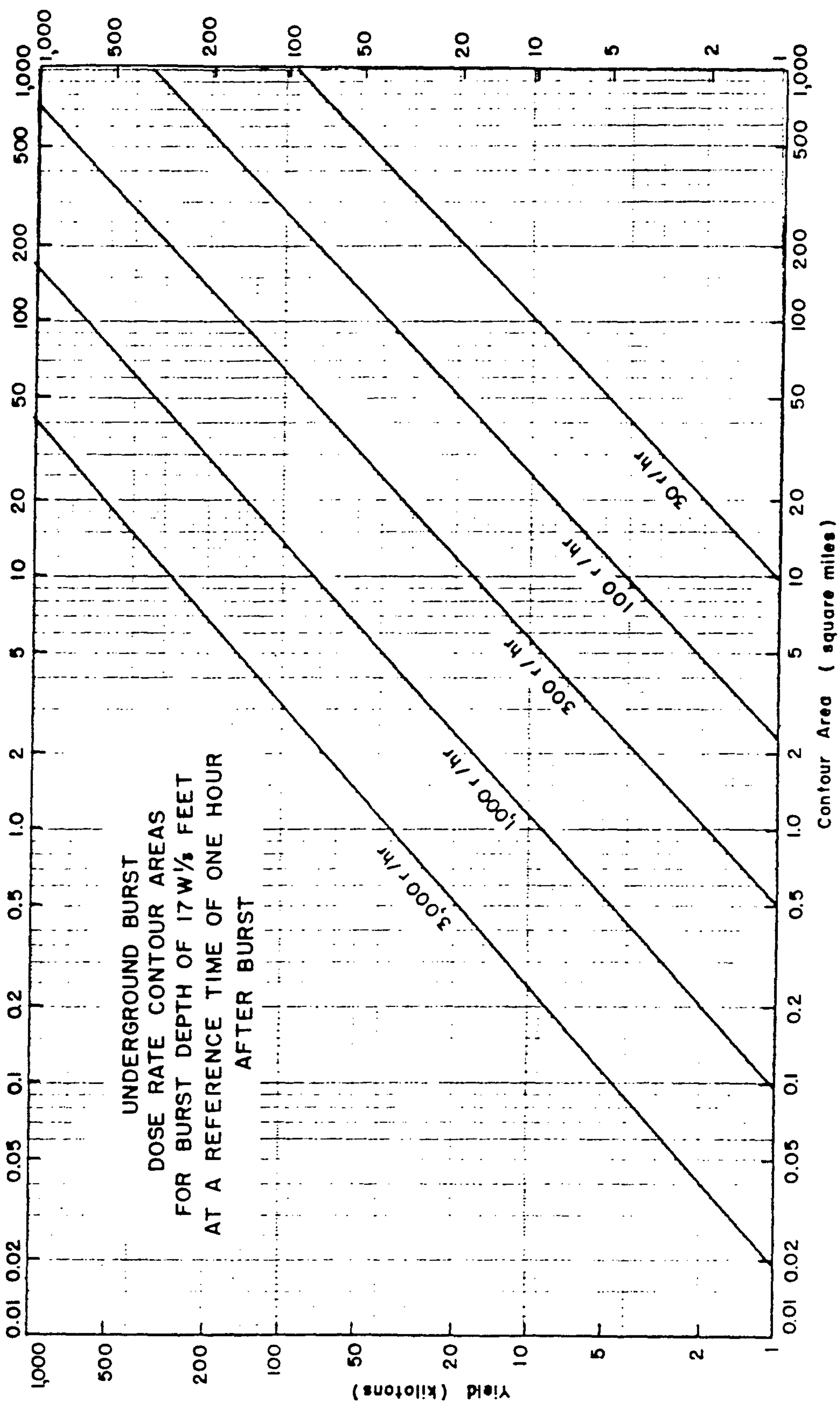
UNDERGROUND BURST
DOSE RATE CONTOUR AREAS
FOR BURST DEPTH OF 17 W1/3 FEET
AT A REFERENCE TIME OF ONE HOUR
AFTER BURST
30 r/hr
100 r/hr
300 r/hr
1,000 r/hr
3,000 r/hr
Contour Area (square miles)
Yield (kilotons)
0.01 0.02 0.05 0.1 0.2 0.5 1.0 2 5 10 20 50 100 200 500 1,000
1,000 500 200 100 50 20 10 5 2 1

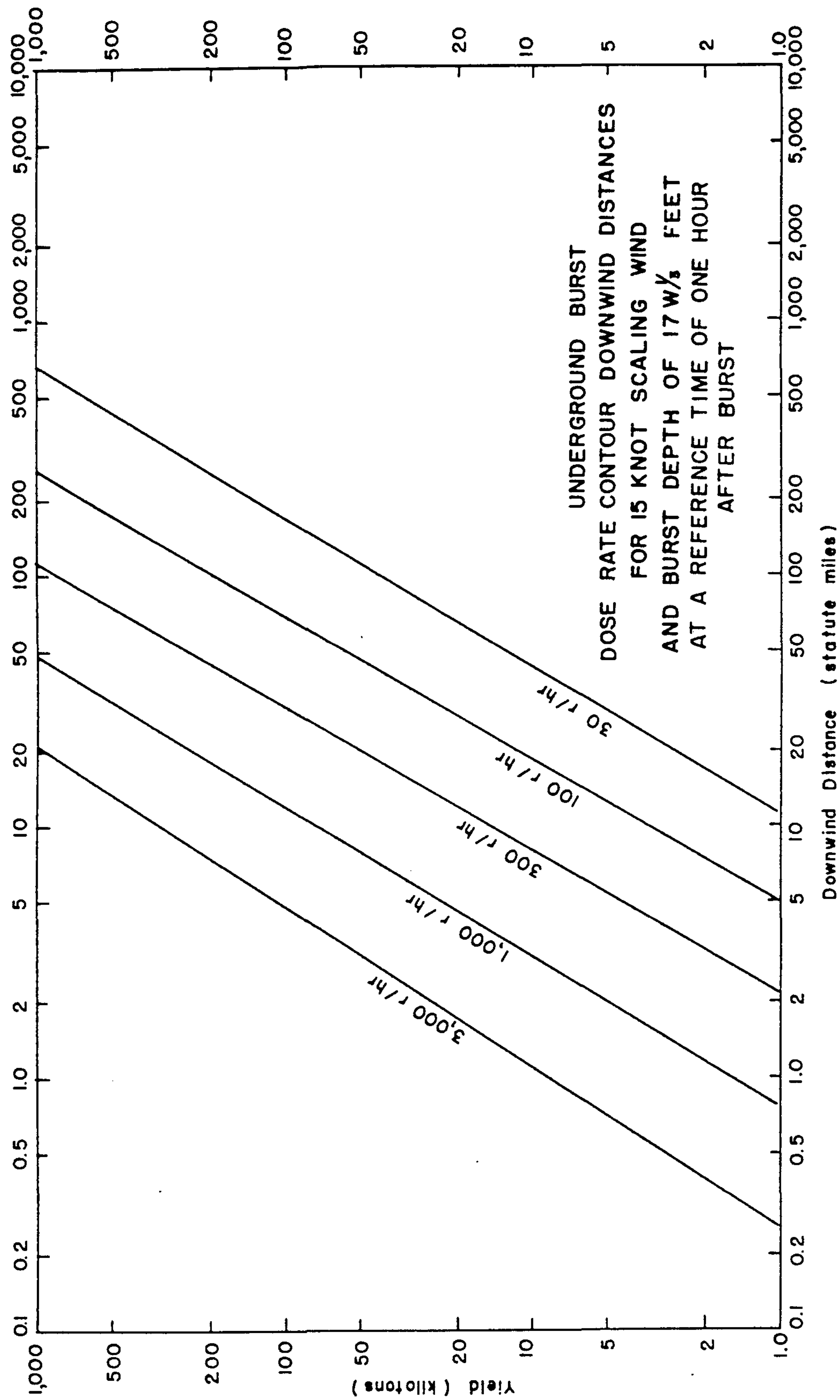
UNDERGROUND BURST
DOSE RATE CONTOUR DOWNWIND DISTANCES
FOR 15 KNOT SCALING WIND
AND BURST DEPTH OF 17 W^1/3 FEET
AT A REFERENCE TIME OF ONE HOUR
AFTER BURST
30 r/hr
100 r/hr
300 r/hr
1,000 r/hr
3,000 r/hr
Downwind Distance (statute miles)
Yield (kilotons)
0.1
0.2
0.5
1.0
2
5
10
20
50
100
200
500
1,000
2,000
5,000
10,000
1,000
500
200
100
50
20
10
5
2
1.0

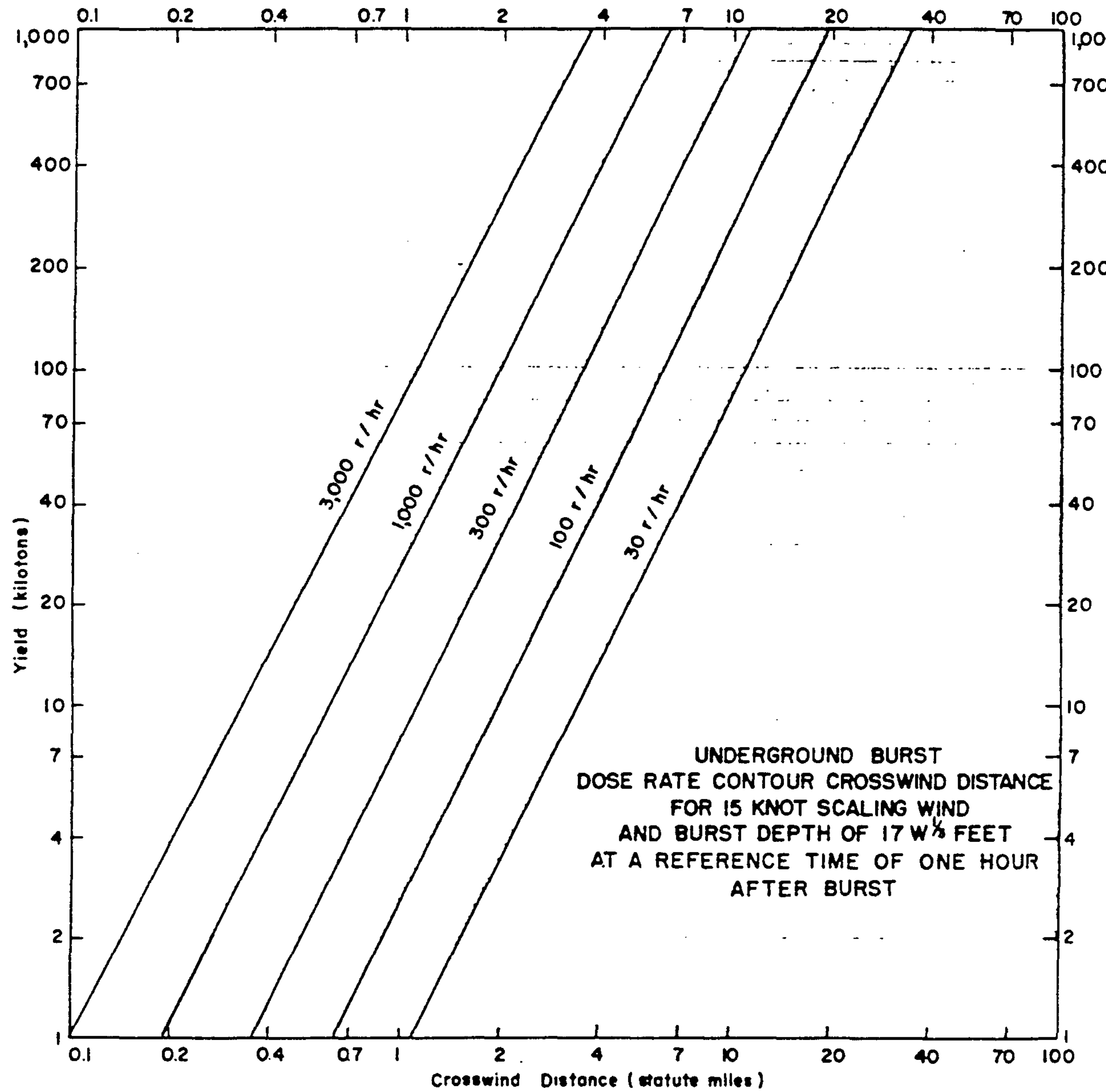
UNDERGROUND BURST
DOSE RATE CONTOUR CROSSWIND DISTANCE
FOR 15 KNOT SCALING WIND
AND BURST DEPTH OF $17 W^{1/3}$ FEET
AT A REFERENCE TIME OF ONE HOUR
AFTER BURST
3,000 r/hr
1,000 r/hr
300 r/hr
100 r/hr
30 r/hr
Yield (kilotons)
Crosswind Distance (statute miles)
0.1
0.2
0.4
0.7
1
2
4
7
10
20
40
70
100
1,000
700
400
200
100
70
40
20
10
7
4
2
1

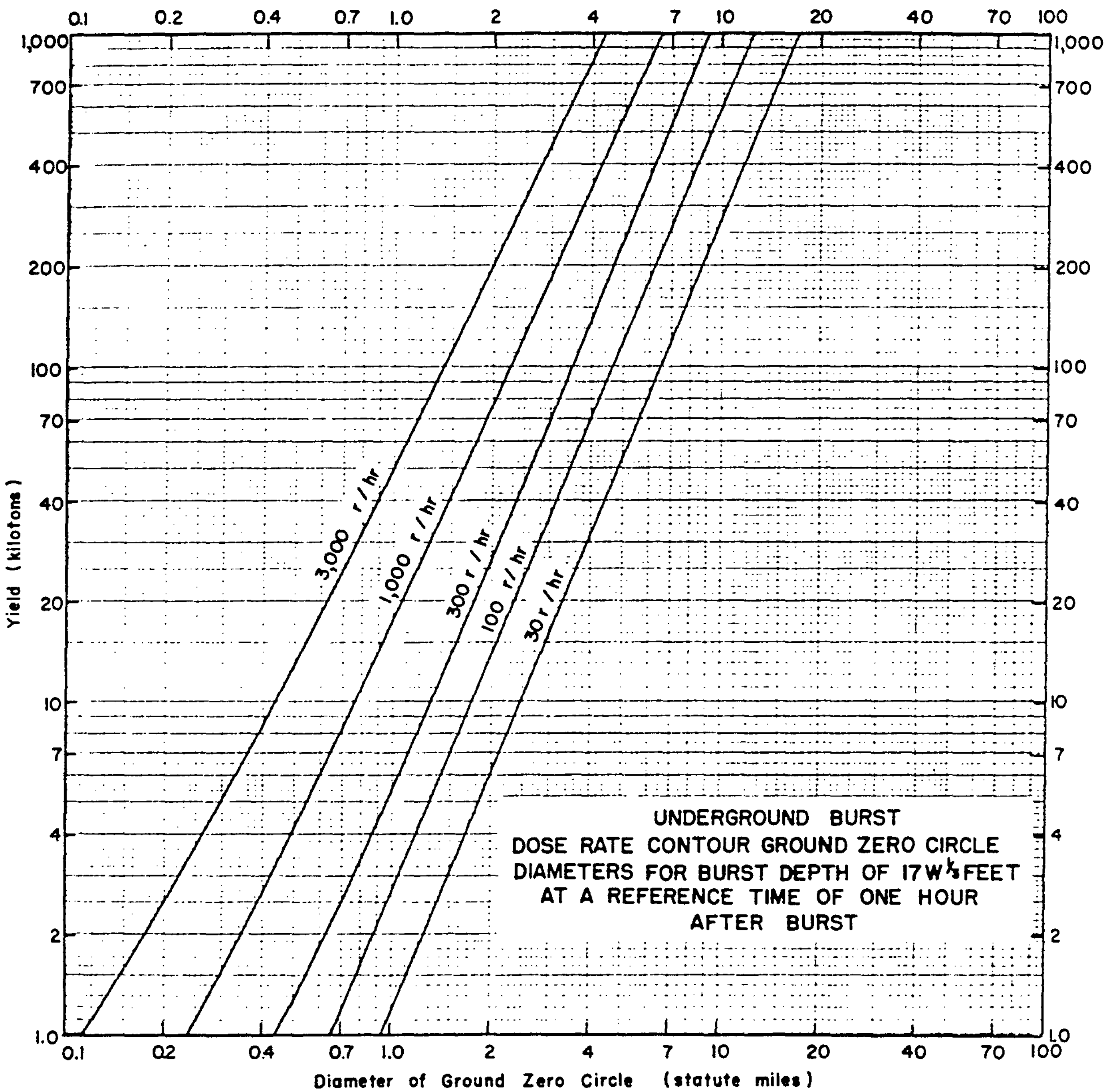
UNDERGROUND BURST
DOSE RATE CONTOUR GROUND ZERO CIRCLE DIAMETERS FOR BURST DEPTH OF 17W⅓ FEET AT A REFERENCE TIME OF ONE HOUR AFTER BURST
3,000 r/hr
1,000 r/hr
300 r/hr
100 r/hr
30 r/hr
Yield (kilotons)
Diameter of Ground Zero Circle (statute miles)
0.1
0.2
0.4
0.7
1.0
2
4
7
10
20
40
70
100
1.0
2
4
7
10
20
40
70
100
200
400
700
1,000

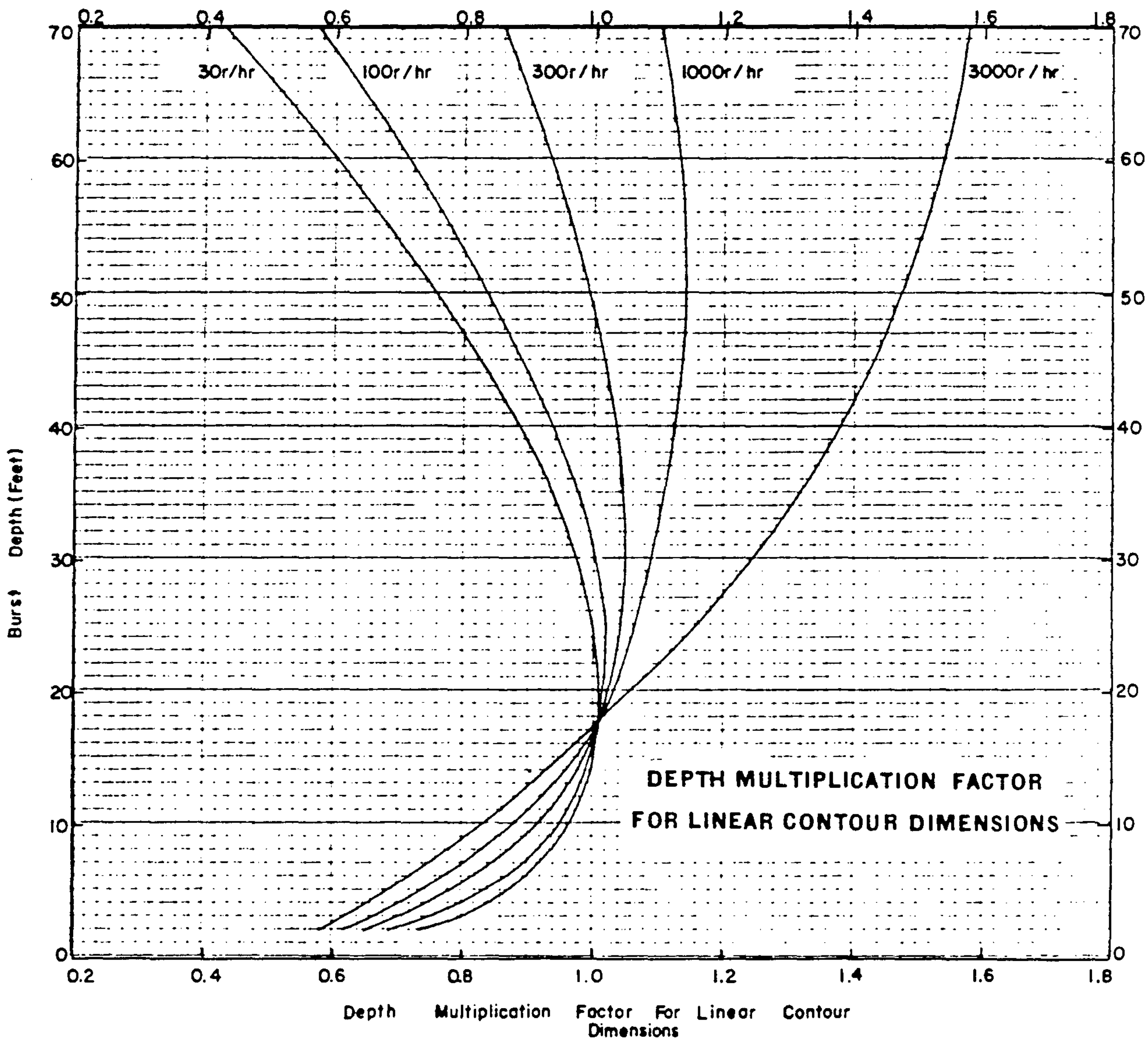
30r/hr
100r/hr
300r/hr
1000r/hr
3000r/hr
DEPTH MULTIPLICATION FACTOR
FOR LINEAR CONTOUR DIMENSIONS
Burst Depth (Feet)
0
10
20
30
40
50
60
70
0.2
0.4
0.6
0.8
1.0
1.2
1.4
1.6
1.8
Depth Multiplication Factor For Linear Contour Dimensions

HARBOR BURST DOSE RATE CONTOUR AREAS

Figure 4–25 presents dose rate contour areas to be expected over adjacent land masses at 1 hour after burst time due to residual radiation resulting from bursting nuclear weapons with yields from 1 KT to 1 MT in a shallow harbor. For this purpose, a harbor depth of 30 to 50 feet of water over a mud bottom is assumed, and the burst is assumed to take place a few feet below the water surface, such as in the hold of a ship. The areas given may be assumed to be independent of wind, although specific location of the contaminated areas with respect to the burst point is a sensitive function of wind and other meteorological conditions, as with other types of contaminating bursts. Area magnitudes may be read directly from the curves for those dose-rate values for which curves are provided. Extrapolation to higher or lower dose rate contour values than covered by the families of curves cannot be done accurately and should not be attempted. To obtain dose rate values for times other than $H+1$ hour, multiplying factors from figure 4–13 should be used.

Example.

Given: A 30 KT harbor burst.

Find: The area of effect for dose rates of 1,000 r/hr or greater at $H+1$ hour.

Solution: Reading directly from figure 4–25, the area for a dose rate of 1,000 r/hr or more at $H+1$ hour for a 30 KT harbor burst is 3.4 ($\pm$1.7) square miles. *Answer.*

Reliability. Area magnitudes obtained from these curves for a specific yield are considered reliable within $\pm$50 percent for the burst conditions indicated.

Related material.

See paragraph 4.3*e*.

See also figure 4–13 and figure 4–26.

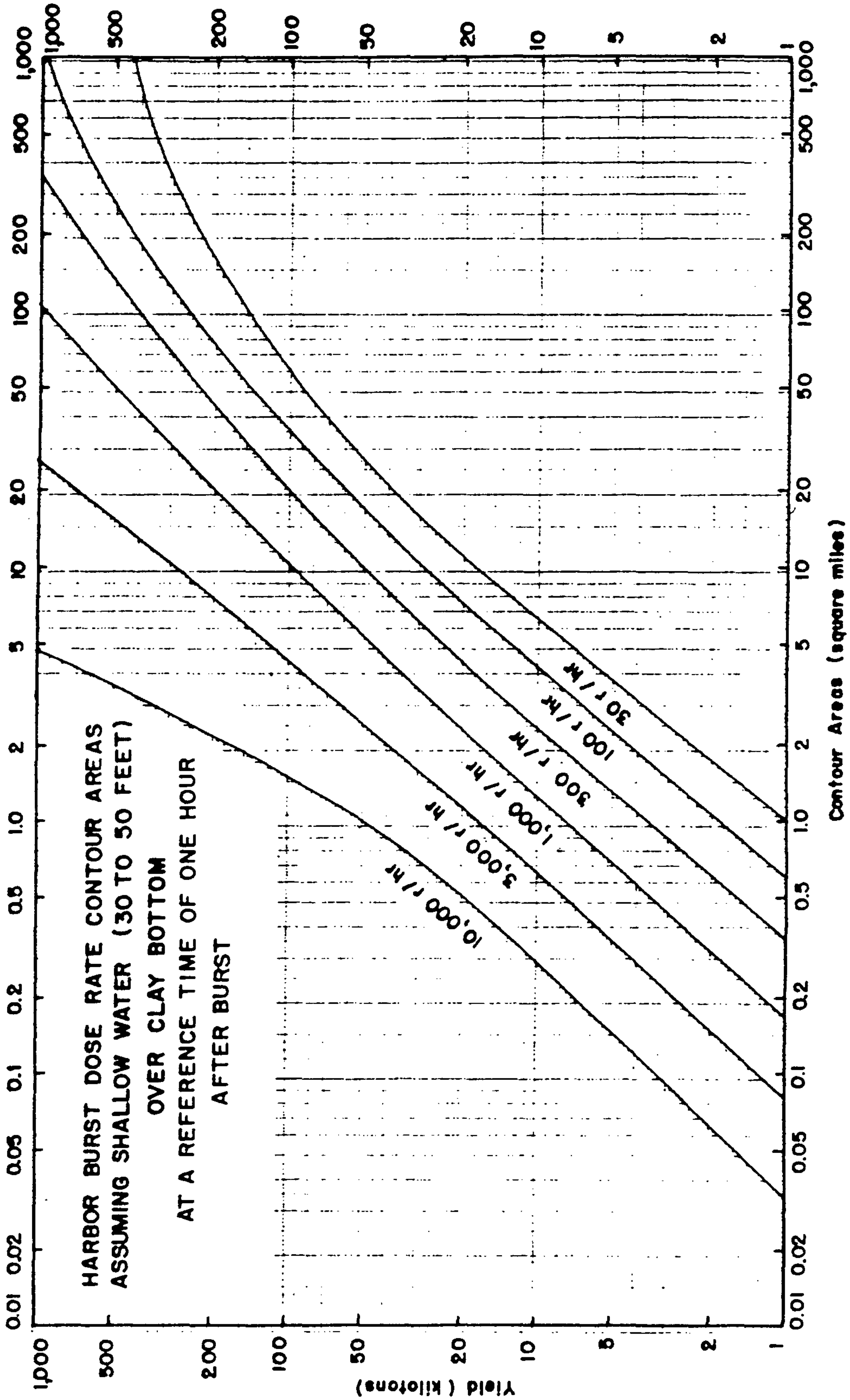
HARBOR BURST DOSE RATE CONTOUR AREAS
ASSUMING SHALLOW WATER (30 TO 50 FEET)
OVER CLAY BOTTOM
AT A REFERENCE TIME OF ONE HOUR
AFTER BURST
30 r/hr
100 r/hr
300 r/hr
1,000 r/hr
3,000 r/hr
10,000 r/hr
Yield (kilotons)
Contour Areas (square miles)
1,000
500
200
100
50
20
10
5
2
1
1.0
0.5
0.2
0.1
0.05
0.02
0.01

TOTAL RADIATION DOSE RECEIVED IN A CONTAMINATED AREA

From figure 4–26 can be obtained the total dose received on entering a given contaminated area at a specified time and remaining for a specified interval of time. The vertical axis gives the accumulated dose for each unit (r/hr) of dose rate at one hour after the detonation. The various curves represent times of stay in the contaminated area. To get the accumulated dose, a factor is taken from the vertical axis corresponding to the time of entry and the time of stay. The product of this factor and the dose rate at one hour gives this accumulated dose.

Example.

Given: The dose rate in a given area at one hour after detonation is 500 r/hr.

Find: The total dose received by a man entering the area two hours after detonation and remaining 4 hours.

Solution: From figure 4–26 the intersection of the line for a time of entry of two hours after detonation with the 4-hour curve gives a factor of 0.80. Therefore, the accumulated dose is—

$500 \times 0.80 = 400\ r.$ *Answer.*

Related material.

See paragraphs 4.3*c*(1)(*d*) and 4.3*g*.

See also figures 4–13 and 4–27.

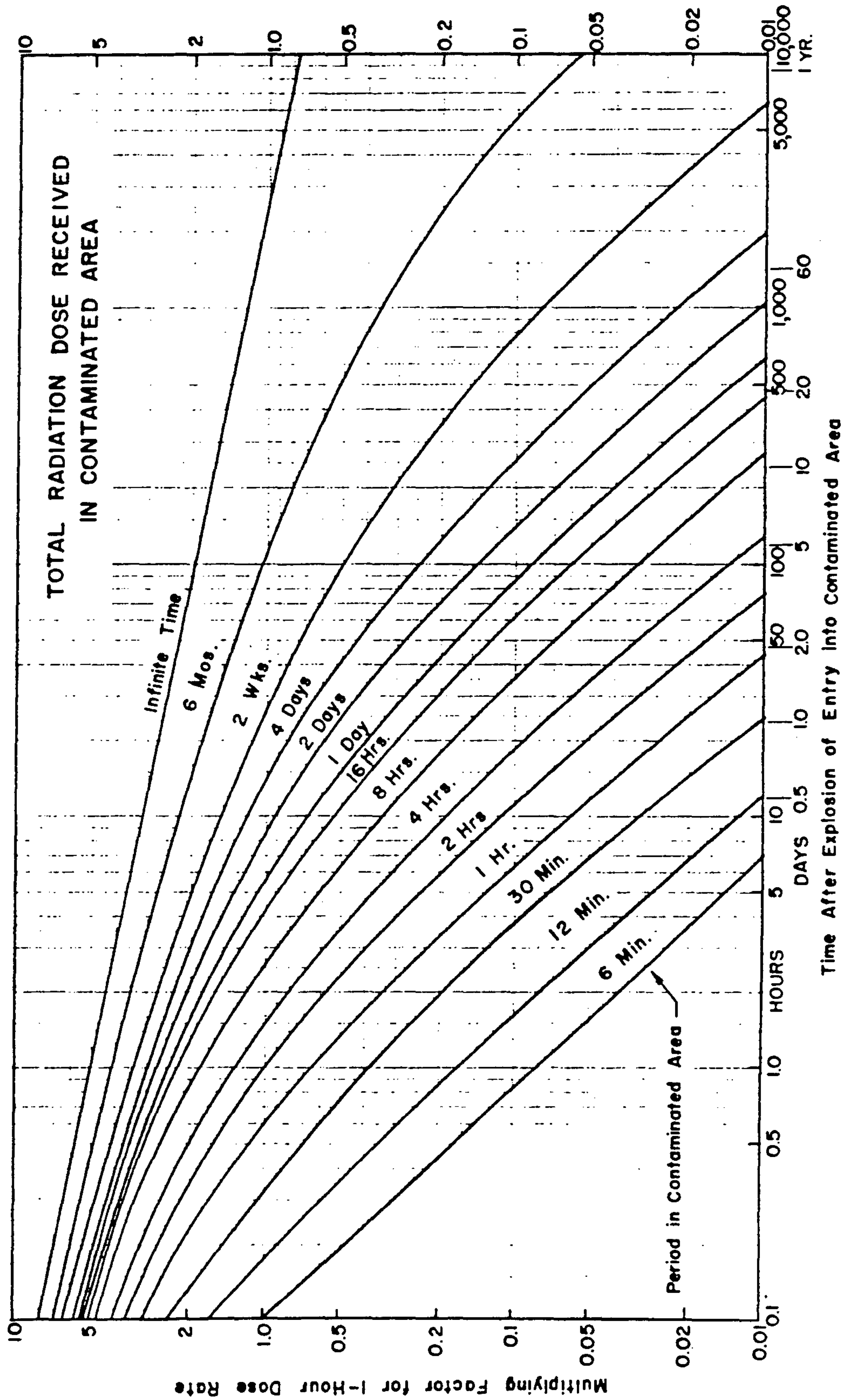

TOTAL RADIATION DOSE RECEIVED IN CONTAMINATED AREA
Multiplying Factor for 1-Hour Dose Rate
10
5
2
1.0
0.5
0.2
0.1
0.05
0.02
0.01
Time After Explosion of Entry Into Contaminated Area
HOURS
0.1
0.5
1.0
5
10
50
100
500
1,000
5,000
10,000
DAYS
0.5
1.0
2.0
5
10
20
60
1 YR.
Infinite Time
6 Mos.
2 Wks.
4 Days
2 Days
1 Day
16 Hrs.
8 Hrs.
4 Hrs.
2 Hrs
1 Hr.
30 Min.
12 Min.
6 Min.
Period in Contaminated Area

48-HOUR DOSE SCALING FACTOR

Figure 4–27 gives scaling factors for weapon yields from 0.1 KT to 100 MT by means of which approximate contours can be obtained for residual gamma radiation doses accumulated during the 48 hours immediately following burst time. Given a 1-hour dose rate contour, the dose rate value can be multiplied by the appropriate scaling factor from this curve to give an approximate total dose value received over the 48-hour period following the burst by personnel in the open within that contour. If it is desired to construct a particular 48-hour dose contour, the desired 48-hour dose value should be divided by the scaling factor obtained from figure 4–27 to obtain a preliminary dose rate value. For a surface burst this value may be used to enter the appropriate figures 4–14 through 4–18 to obtain the desired contour dimensions for the 1-hour dose rate which will result in the desired 48-hour dose value. For a burst in the transition zone, divide the preliminary dose rate value by the appropriate height of burst adjustment factor obtained from figure 4–19 before entering figures 4–14 through 4–18 to obtain the desired contour parameters for the necessary 1-hour dose rate. For an underground burst, the preliminary dose rate value is used to enter the appropriate figures 4–20 through 4–23 to obtain initial contour dimensions. Linear dimensions must then be multiplied by the appropriate depth multiplication factor from figure 4–24 (area dimensions by the square of the appropriate factor) to obtain the final contour dimensions. If the fission yield is less than the total yield, the values for each burst condition used as described above to enter the appropriate figures 4–14 through 4–18 or 4–20 through 4–23 are not used but are further divided by the fission yield to total yield ratio to obtain the actual value for use in entering the appropriate figure.

Example.

Given: A 400 KT surface burst under 15-knot scaling wind conditions.

Find: Approximate contour parameters for 500 roentgens total dose accumulated up to 48 hours after burst time.

Solution: From figure 4–27, the scaling factor for a 400 KT weapon is 2.0. Hence, the dose rate contour for $\frac{500}{2.0}=250$ r/hr at $H+1$ hour approximates the 48-hour total dose contour for 500 *r*. Using figures 4–14 to 4–18, the approximate total dose contour parameters for 500 roentgens accumulated during the 48 hours following the burst are—

Contour area	160 square miles
Downwind distance	34 miles
Crosswind distance	6 miles
Ground zero circle diameter.	4 miles
Downwind displacement of the ground zero circle.	0.7 mile

Answer.

Reliability. Recognizing the idealized nature of the basic contours, total dose contours obtained in the manner described above are considered reliable within a factor of two for doses between 100 *r* and 1,000 *r*, for scaling winds up to about 15 knots. The method may be applied for other dose conditions with somewhat less confidence in the results, but should not be applied for scaling wind conditions significantly greater than 15 knots.

Related material.

See paragraphs 4.3*c* through *h*.

See also figures 4–14 through 4–23, and figure 4–26.

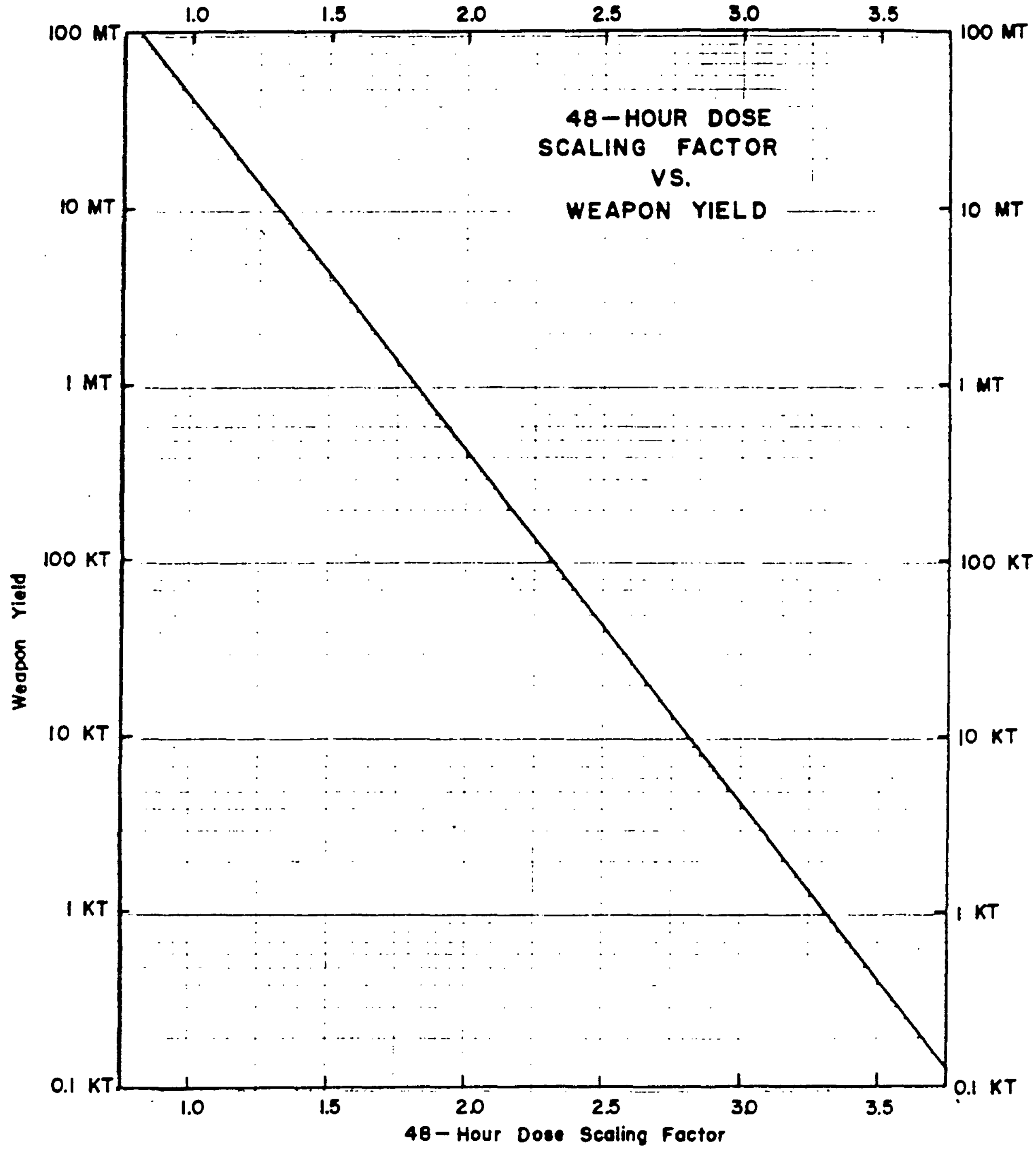
1.0
1.5
2.0
2.5
3.0
3.5
100 MT
10 MT
1 MT
100 KT
10 KT
1 KT
0.1 KT
48—HOUR DOSE
SCALING FACTOR
VS.
WEAPON YIELD
Weapon Yield
48—Hour Dose Scaling Factor

BLANK

Induced

i. Neutron-Induced Activity.

(1) *Air burst.* The neutron-induced gamma activity will depend on soil type as well as weapon type and yield. It is therefore impractical to attempt to define a height of burst above which this effect ceases to be militarily significant.

(2) *Burst in the transition zone.* If a nuclear weapon is detonated at a height of burst above that at which fallout is expected to be a hazard, the radioactivity which is induced in the soil by neutrons can give rise to dose rates of military importance in the vicinity of ground zero. The type, intensity, and energy distribution of the residual activity produced will depend on which isotopes are produced and in what quantity. This, in turn, depends on the number and energy distribution of the incident neutrons and the chemical composition of the soil. Induced contamination contours are independent of wind, except for some wind redistribution of the surface contaminant, and can be expected to be roughly circular.

Four soils have been chosen to illustrate the extent of the hazard which may be expected from induced activity. These soils were selected so as to show wide variations in predicted dose rates; the activity from most other soils should fall within the range of activities presented for these soils. The chemical composition of the selected soils is shown in table 4–2.

The elements which may be expected to contribute most of the induced activity are sodium, manganese and aluminum and small changes in the quantities of these materials can change the activity markedly; however, other elements which capture neutrons can also influence the magnitude of the activity. The elements are listed in table 4–2 in the order of probable importance so far as induced activity is concerned.

Figures 4–28A and 4–28B indicate the manner in which the induced activity is expected to vary with slant range and weapon type. $H+1$ hour dose rates for the four soils may be obtained by multiplying the dose rate obtained from figure 4–28A or 4–28B by the multiplying factor for that soil shown on the facing page of these figures.

In order to calculate the dose rates at times other than one hour after the detonation, decay factors may be taken from figure 4–29 which represents the decay characteristics of the four soils. The decay factors are constants which are multiplied by the value of the dose rate at one hour to give the rate at any other time.

Figures 4–30 through 4–33 are presented to facilitate computation of total dose. Multiplying factors may be obtained from these figures which, when applied to the one hour dose rate for the particular soil, will give the dose accumulated over any of several periods of time for various times of entry into the contaminated area.

When applying the data presented in this section to soils other than the four chosen for illustrative purposes, the activity should be estimated by using the data for the illustrative soil which most closely resembles the soil in question in chemical composition. If none of the illustrative soils resembles the soil in question very closely, the following remarks should be kept in mind. For times less than $H+1/2$ hour aluminum is the most important contributor. For times between $H+1/2$ hour and $H+5$ hours, manganese is generally the most important element. In the absence of manganese, the sodium content will probably govern the activity for this period. Between $H+5$ hours and $H+10$ hours, sodium and manganese content are both important. After $H+10$ hours, sodium will generally be the only large contributor. In the absence of sodium, manganese and aluminum, the activity will probably be low, and will generally be governed by the silicon content. Soil type IV is an example of this latter type.

Table 4–2. Chemical Composition of Illustrative Soils

Element	Percentage (by weight)			
	Soil type I (Liberia, Africa)	Soil type II (Nevada desert)	Soil type III (lava clay, Hawaii)	Soil type IV (beach sand, Pensacola, Fla.)
Sodium	----------	1. 30	0. 16	0. 001
Manganese	0. 008	0. 04	2. 94	----------
Aluminum	7. 89	6. 90	18. 79	0. 006
Iron	3. 75	2. 20	10. 64	0. 005
Silicon	33. 10	32. 00	10. 23	46. 65
Titanium	0. 39	0. 27	1. 26	0. 004
Calcium	0. 08	2. 40	0. 45	----------
Potassium	----------	2. 70	0. 88	----------
Hydrogen	0. 39	0. 70	0. 94	0. 001
Boron	----------	----------	----------	0. 001
Nitrogen	0. 065	----------	0. 26	----------
Sulfur	0. 07	0. 03	0. 26	----------
Magnesium	0. 05	0. 60	0. 34	----------
Chromium	----------	----------	0. 04	----------
Phosphorus	0. 008	0. 04	0. 13	----------
Carbon	3. 87	----------	9. 36	----------
Oxygen	50. 33	50. 82	43. 32	53. 332

Thus, it may be possible to obtain better data for a given soil by using data from a different illustrative soil at each of several times of interest.

If a weapon is burst at such a height as to be in the transition zone from the fallout standpoint, the neutron-induced activity generally can be neglected if the burst height is in the lower three quarters of the fallout transition zone. For weapons burst in the upper quarter of the fallout transition zone the neutron-induced activity may not be negligible compared to fallout. For the cases where fallout dose rate contour parameters, as determined from figures 4–14 through 4–18, are much smaller than those for a burst on the surface, an idea of the magnitude of induced activity may be obtained from figures 4–28 through 4–33. The overall contour values may then be obtained by combining the induced activity and fallout activity. For these cases it must be remembered that fission products and induced activity will decay at different rates. This necessitates a determination of the magnitude of each type of activity for each time of interest.

(3) *Surface and subsurface bursts.* For surface and subsurface bursts, the residual radioactive contamination from fission products is vastly greater than the neutron-induced activity. As a result, neutron-induced activity generally can be neglected for surface and subsurface bursts.

j. Residual Beta Radiation. The discussion of residual radiation has thus far considered only gamma radiation. In general, the hazard due to residual gamma radiation exceeds the beta hazard for all cases except those in which intimate contact with beta-active materials occurs, as in the case of a soldier lying prone in a contaminated area, or for particles falling out directly upon the skin or scalp. For such cases, superficial burns may result, the effect of which is discussed in paragraph 6.3*b*(3).

k. Shielding. The dose rates obtained from the contours described, and the total doses derived therefrom, are free field values which must be reduced if the individual concerned is protected by some degree of shelter. Shielding factors can be estimated from the shielding information given in paragraph 6.5. For example, personnel in the open in a built-up city area would receive 0.7 of the free field dose, while personnel in the best average shelter available in a city (such as the basement of a dwelling) would receive about one-tenth the free field dose.

l. Cloud Contamination. Since much of the radioactive material is airborne, the radiation hazard produced by the nuclear cloud to personnel in aircraft flying through it may be great for some time. The cloud size and rate of rise vary with the yield of the bomb and the prevailing meteorological conditions. For detonations in fair weather, except where meteorological conditions such as high wind velocities are involved, the top and bottom of the mushroom head of the cloud have been observed to stabilize in altitude at a time of approximately 6 to 10 minutes after detonation independent of yield. The altitude above burst point of this portion of the cloud increases with weapon yield when other factors remain the same. Figure 4–34 illustrates this for yields between 0.1 KT and 100 MT. The height of a nuclear cloud is influenced by atmospheric conditions, which include the temperature gradient, winds, relative humidity, and the height of the tropopause. Since these atmospheric effects are very complex and also because it would be most difficult to consider all possible weather variations, a quantitative treatment of the effect of atmospheric conditions on cloud heights is not included in this manual. The percentage of maximum cloud height reached by the cloud at any time after a detonation and before stabilization is relatively independent of the yield and is shown in figure 4–35. From the curves shown in figure 4–34, the height of the top or bottom of the nuclear cloud as a function of yield may be determined for the stabilization condition. Then, by use of figure 4–35, intermediate heights at any time prior to stabilization can be determined. The diameter of the cloud increases rapidly at times earlier than 1 minute after a detonation. After about 1 minute, the width of the cloud from all but extremely large yield weapons increases more slowly until the cloud reaches its maximum altitude. If the yield is large enough for the cloud to reach the tropopause, the cloud upon reaching this level rises more slowly and increases in lateral dimension more rapidly, as though flattening out against a ceiling. The rate of lateral growth of the cloud during this time is about three times the rate before reaching the tropopause. After reaching maximum altitude, the diameter slowly increases as the cloud drifts downwind. These diameter versus time relationships are illustrated in figure 4–36. The dose received by personnel in aircraft flying through an atomic cloud at various times after the detonation can be obtained from figure 4–37. This figure gives the dose that is received for several times of entry for various transit times through the cloud.

BLANK

NEUTRON-INDUCED GAMMA ACTIVITY

Given the weapon type and the slant range from the point of burst to the point of interest, the induced gamma dose rates in the vicinity of ground zero at $H+1$ hour can be estimated using figures 4-28A and 4-28B for bursts over soils similar in composition to any of the soils illustrated in table 4-2. To estimate the dose rate, enter the slant range axis with the slant distance in yards, read the dose rate for the appropriate weapon type, and multiply this dose rate by the appropriate factor for the soil type of interest from the following:

Soil type	Multiplying factor
I	0.11
II	1.0
III	12.0
IV	0.0026

Scaling. For yields other than 1 KT multiply the dose rate read from the curve by the yield in KT.

Example.

Given: An average neutron flux 50 KT weapon is burst at a height of 900 feet above soil of type III.

Find: The $H+1$ hour dose rate at ground zero and at 600 yards from ground zero.

Solution: From the average neutron flux weapon curve of figure 4-28A the dose rate at $H+1$ hour at ground zero (300 yd. slant range) is 9 r/hr per KT of weapon yield. The multiplying factor for soil type III is 12. Therefore, the dose rate at ground zero one hour after detonation of a 50 KT weapon over soil type III is:

$50 \times 12 \times 9 = 5{,}400$ r/hr. *Answer.*

At 600 yards from ground zero the slant range is 670 yards. From the curve, the induced gamma intensity is 0.35 r/hr per KT of weapon yield at this distance. Therefore, the dose rate 600 yards from ground zero one hour after detonation of a 50 KT weapon over soil type III is:

$50 \times 12 \times 0.35 = 210$ r/hr. *Answer.*

Reliability. Dose rate values taken from the curves for the soils presented are correct to within a factor of 5 for the conditions indicated. For other soils, the data will merely furnish an estimate of the magnitude of the hazard.

Related material.

See paragraph 4.3*i*.

See also figures 4-29 through 4-33.

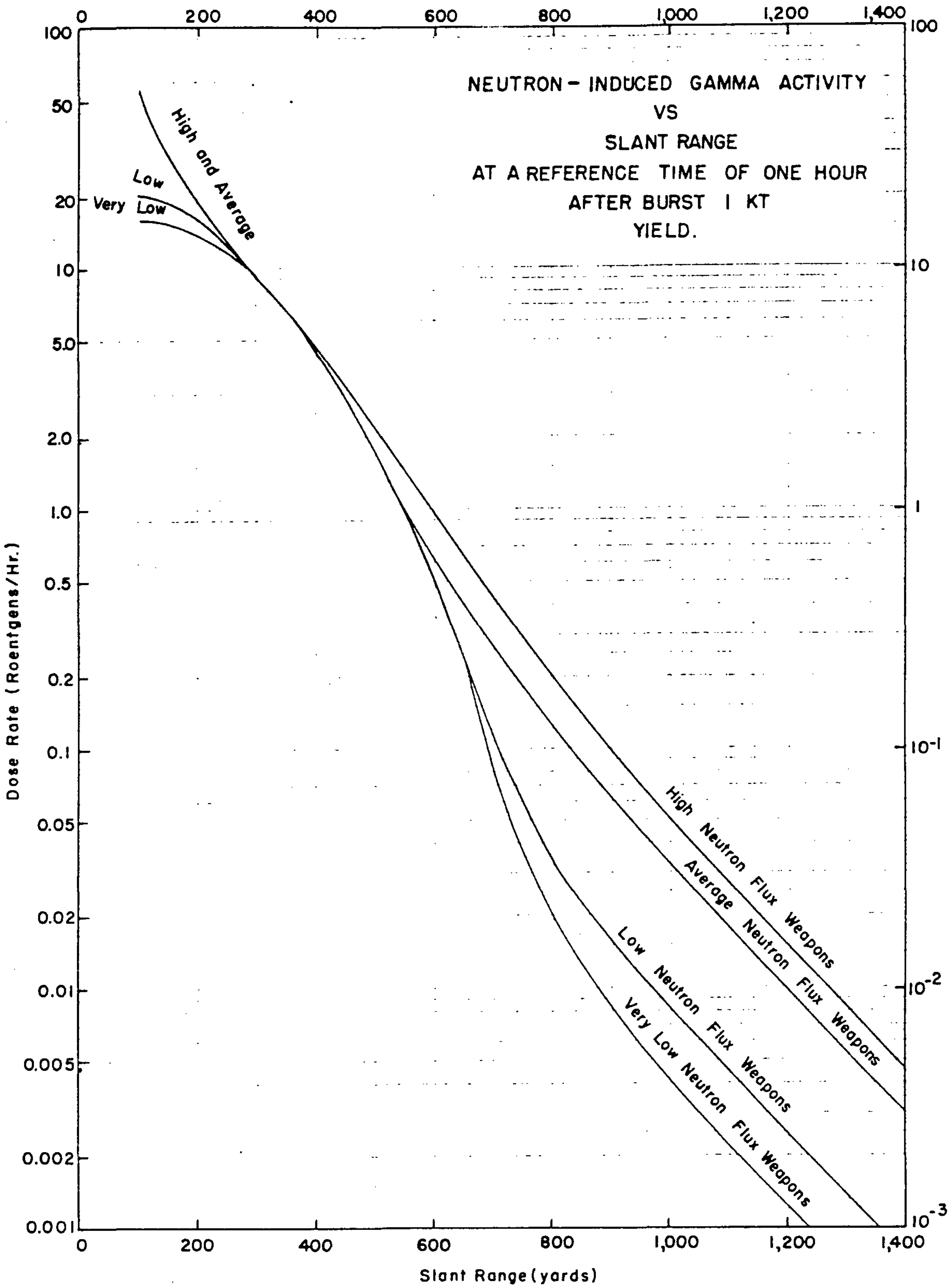
NEUTRON – INDUCED GAMMA ACTIVITY
VS
SLANT RANGE
AT A REFERENCE TIME OF ONE HOUR
AFTER BURST 1 KT
YIELD.
High and Average
Low
Very Low
High Neutron Flux Weapons
Average Neutron Flux Weapons
Low Neutron Flux Weapons
Very Low Neutron Flux Weapons
Dose Rate (Roentgens/Hr.)
Slant Range (yards)
0
200
400
600
800
1,000
1,200
1,400
100
50
20
10
5.0
2.0
1.0
0.5
0.2
0.1
0.05
0.02
0.01
0.005
0.002
0.001
1
10^{-1}
10^{-2}
10^{-3}

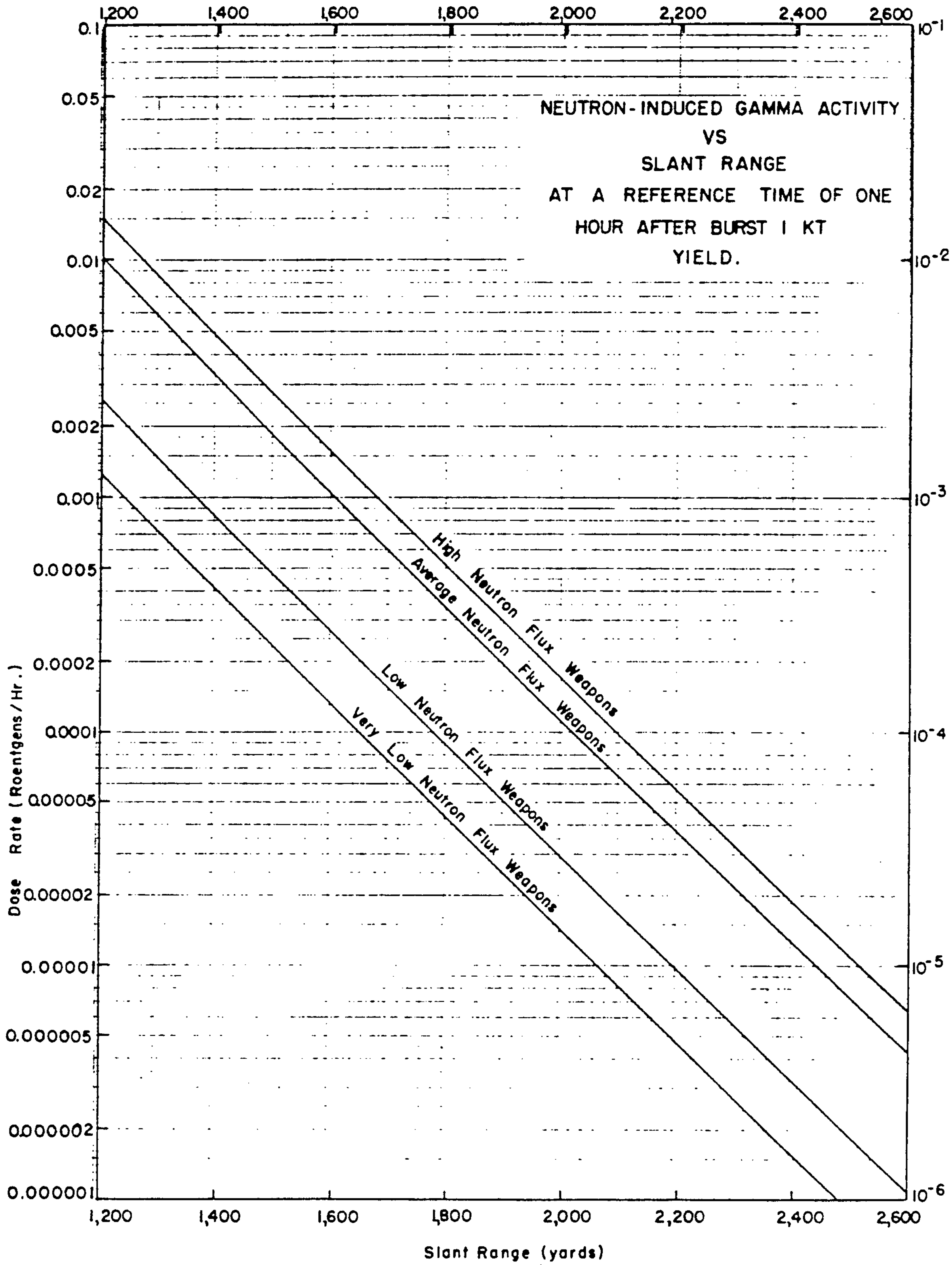
NEUTRON-INDUCED GAMMA ACTIVITY
VS
SLANT RANGE
AT A REFERENCE TIME OF ONE
HOUR AFTER BURST I KT
YIELD.
High Neutron Flux Weapons
Average Neutron Flux Weapons
Low Neutron Flux Weapons
Very Low Neutron Flux Weapons
Dose Rate (Roentgens/Hr.)
Slant Range (yards)
1,200
1,400
1,600
1,800
2,000
2,200
2,400
2,600
0.1
0.05
0.02
0.01
0.005
0.002
0.001
0.0005
0.0002
0.0001
0.00005
0.00002
0.00001
0.000005
0.000002
0.000001
10^{-1}
10^{-2}
10^{-3}
10^{-4}
10^{-5}
10^{-6}

DECAY FACTORS FOR NEUTRON-INDUCED GAMMA ACTIVITY

From the dose rate at $H+1$ hour, the dose rate at any other time is obtained by computing the product of the appropriate decay factor from figure 4-29 and the 1-hour dose rate.

Example.

Given: The dose rate at a given point on soil type I is 30 r/hr at $H+1$ hour.

Find: The dose rate at that point at $H+1/2$ hour and at $H+10$ hours.

Solution: From figure 4-29 the decay factors for soil type I for 1/2 hour and 10 hours are 3.0 and 0.083 respectively. The dose rate at 1/2 hour is—

$30 \times 3.0 = 90$ r/hr. *Answer,*

and the dose rate at 10 hours is—

$30 \times 0.083 = 2.5$ r/hr. *Answer.*

The decay curves may also be used to determine the value of the dose rate at $H+1$ hour from the dose rate at a later time. In this case, the measured dose rate is divided by the appropriate decay factor.

Example.

Given: The dose rate at a given point on soil type II 20 hours after detonation is 100 r/hr.

Find: The dose rate at the same point 1 hour after the detonation.

Solution: From figure 4-29, the decay factor at 20 hours is 0.24. Therefore, the dose rate at 1 hour is

$\frac{100}{0.24} = 417$ r/hr. *Answer.*

Reliability. The reliability is the same as for figures 4-28A and 4-28B.

Related material.

See paragraph 4.3*i*.

See also figures 4-28A, 4-28B and 4-30 through 4-33.

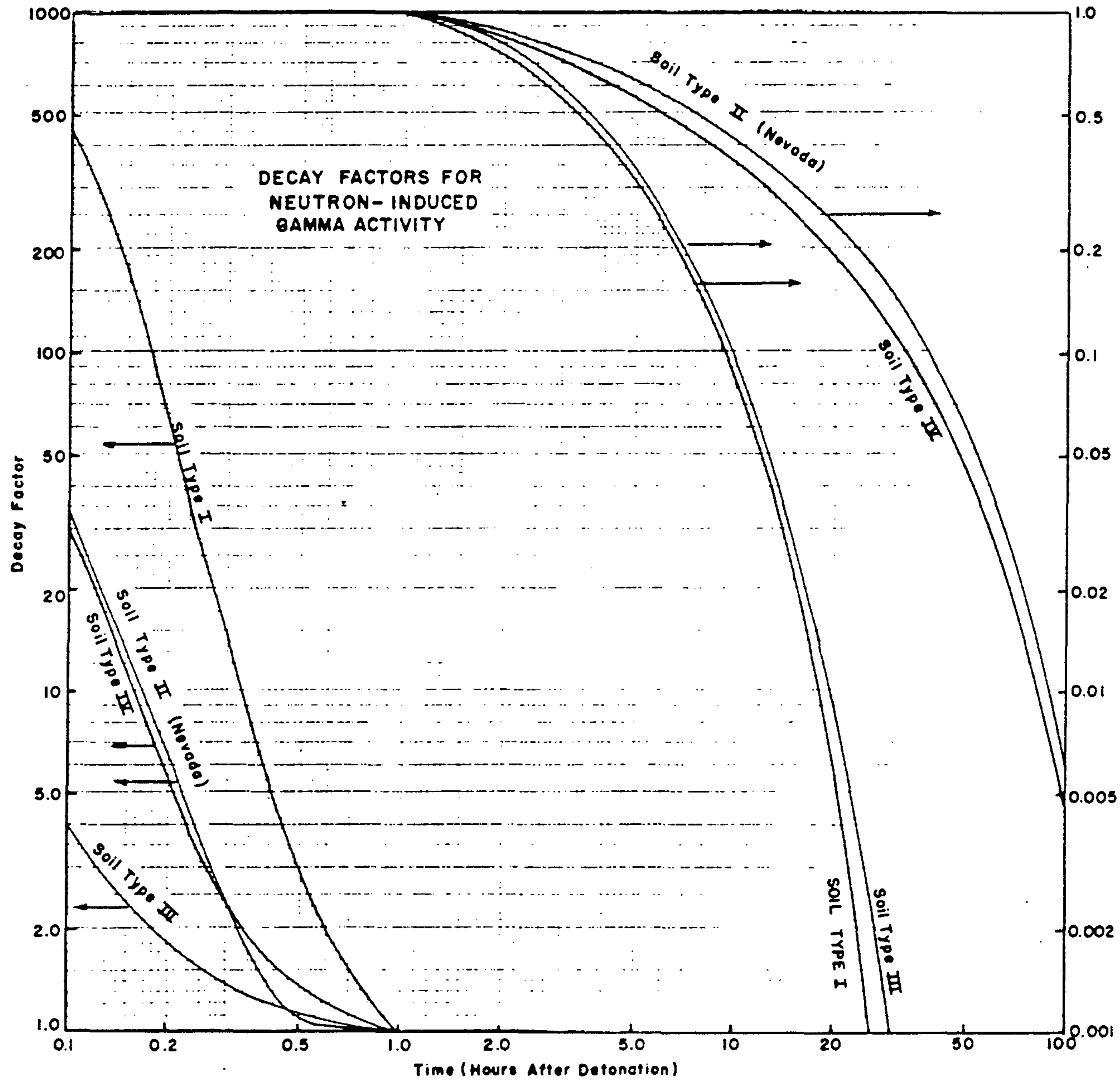
DECAY FACTORS FOR
NEUTRON- INDUCED
GAMMA ACTIVITY
Decay Factor
1000
500
200
100
50
20
10
5.0
2.0
1.0
1.0
0.5
0.2
0.1
0.05
0.02
0.01
0.005
0.002
0.001
0.1
0.2
0.5
1.0
2.0
5.0
10
20
50
100
Time (Hours After Detonation)
Soil Type I
Soil Type II (Nevada)
Soil Type IV
Soil Type III
Soil Type II (Nevada)
Soil Type IV
SOIL TYPE I
Soil Type III

TOTAL-NEUTRON INDUCED GAMMA DOSE FOR VARIOUS SOIL TYPES

From figures 4–30 through 4–33 can be obtained the total dose received on entering a given contaminated area at a specified time and remaining for a specified interval of time. The vertical axes give the accumulated dose for each unit of dose rate (r/hr) at one hour after a detonation over that soil. The various curves represent times of stay in the contaminated area. To get the accumulated dose, a factor is taken from the vertical axis corresponding to the soil type, time of entry and the time of stay. The product of this factor and the dose rate at one hour gives the accumulated dose.

Example.

Given: The dose rate in a given area over soil type III at one hour after detonation is 300 r/hr.

Find: The total dose received by a man entering the area 5 hours after detonation and remaining 1 hour.

Solution: The proper curves for soil type III are found on figure 4–32. From this figure the intersection of the line for a time of entry of 5 hours after detonation with the 1 hour curve gives a factor of 0.30. Therefore, the accumulated dose is:

$$300 \times 0.30 = 90\ r.$$

Related material.

See paragraph 4.3*i*.

See also figures 4–28A, 4–28B and 4–29.

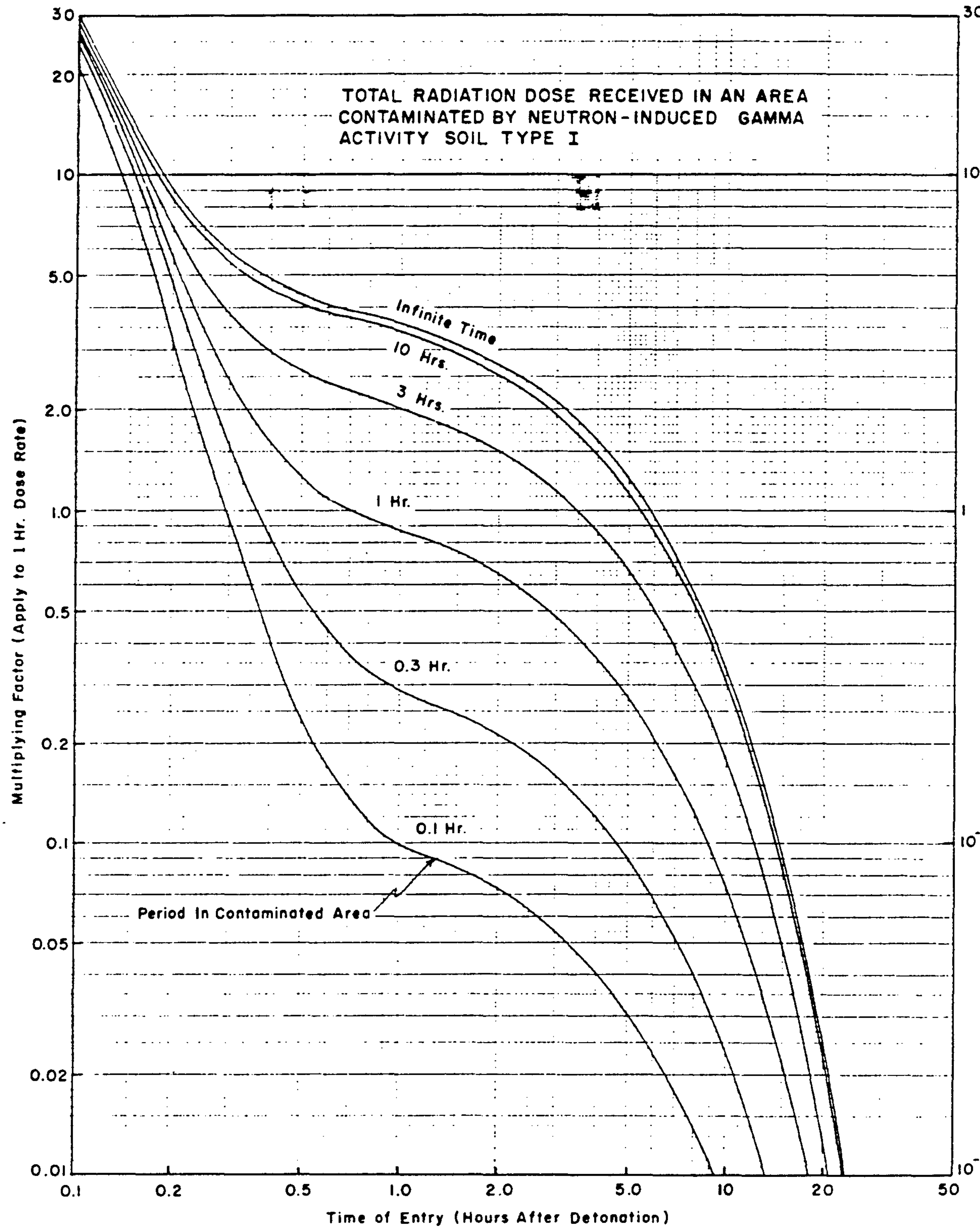
TOTAL RADIATION DOSE RECEIVED IN AN AREA CONTAMINATED BY NEUTRON-INDUCED GAMMA ACTIVITY SOIL TYPE I
Infinite Time
10 Hrs.
3 Hrs.
1 Hr.
0.3 Hr.
0.1 Hr.
Period In Contaminated Area
Multiplying Factor (Apply to 1 Hr. Dose Rate)
Time of Entry (Hours After Detonation)
30
20
10
5.0
2.0
1.0
0.5
0.2
0.1
0.05
0.02
0.01
1
10^-1
10^-2
0.1
0.2
0.5
1.0
2.0
5.0
10
20
50

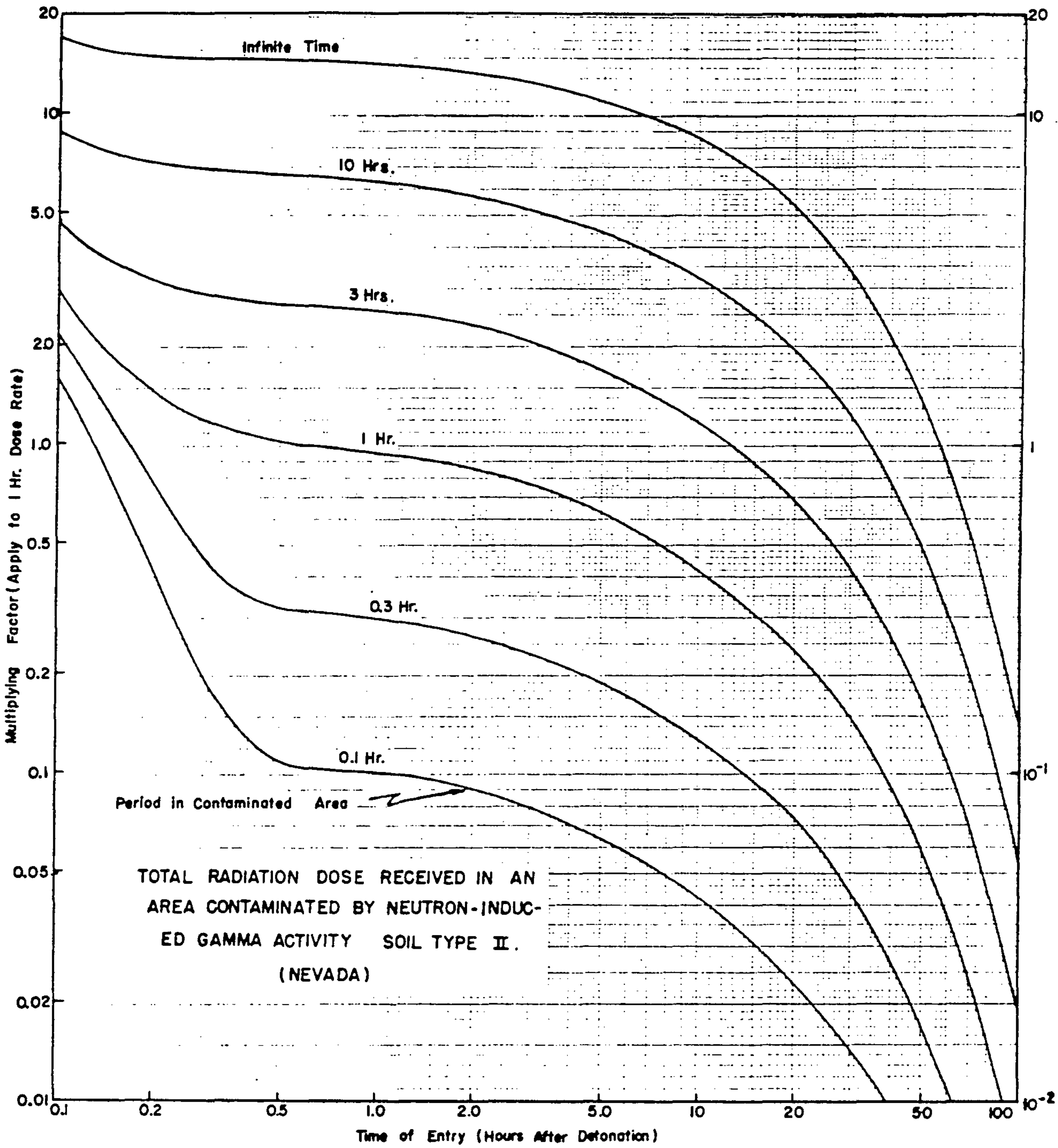
Infinite Time
10 Hrs.
3 Hrs.
1 Hr.
0.3 Hr.
0.1 Hr.
Period in Contaminated Area
TOTAL RADIATION DOSE RECEIVED IN AN AREA CONTAMINATED BY NEUTRON-INDUCED GAMMA ACTIVITY SOIL TYPE II. (NEVADA)
Multiplying Factor (Apply to 1 Hr. Dose Rate)
Time of Entry (Hours After Detonation)
20
10
5.0
2.0
1.0
0.5
0.2
0.1
0.05
0.02
0.01
0.1
0.2
0.5
1.0
2.0
5.0
10
20
50
100
1
10^{-1}
10^{-2}

FIGURE 4-32

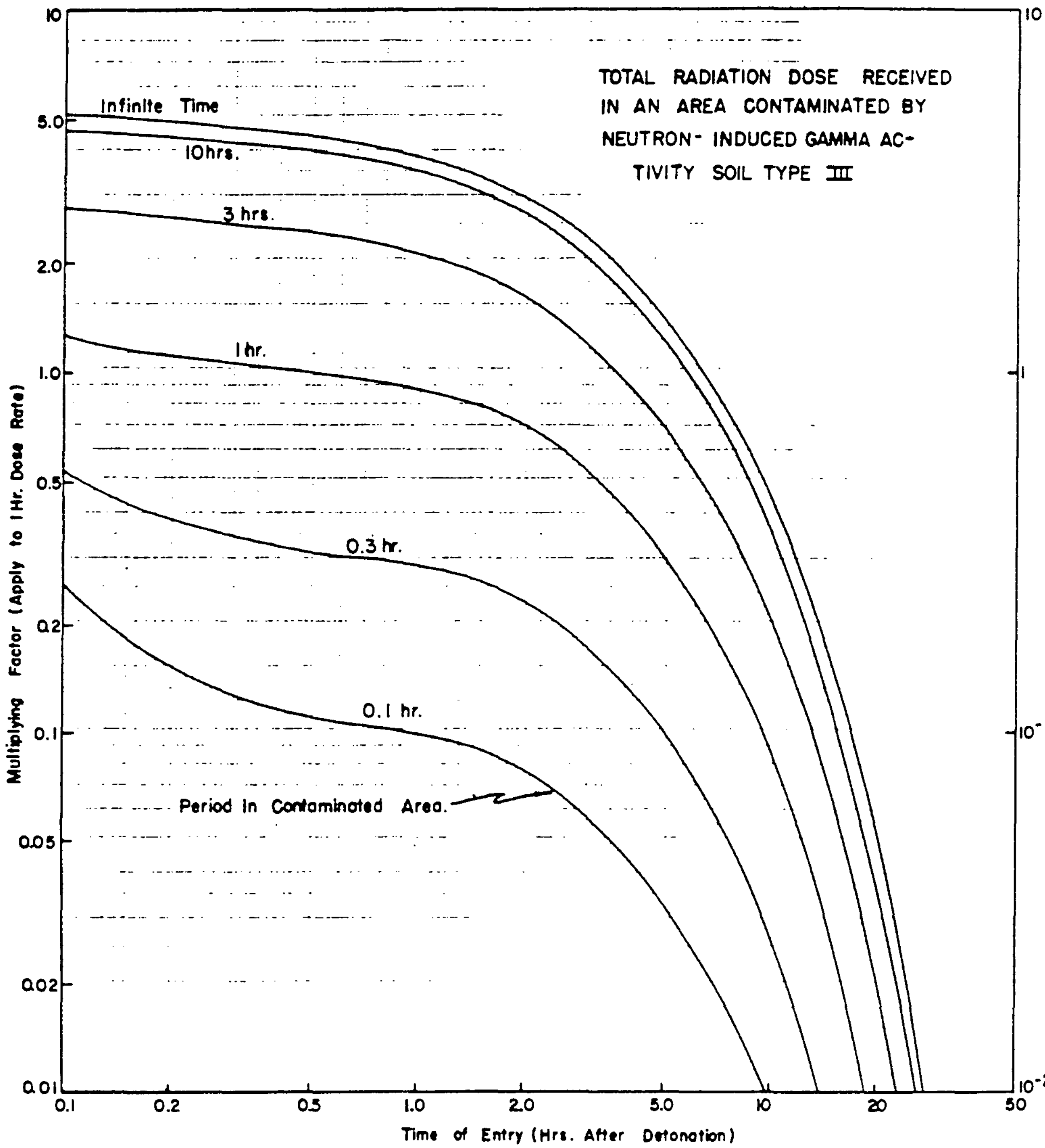
TOTAL RADIATION DOSE RECEIVED IN AN AREA CONTAMINATED BY NEUTRON- INDUCED GAMMA ACTIVITY SOIL TYPE III
Infinite Time
10hrs.
3 hrs.
1 hr.
0.3 hr.
0.1 hr.
Period in Contaminated Area.
Multiplying Factor (Apply to 1 Hr. Dose Rate)
Time of Entry (Hrs. After Detonation)
10
5.0
2.0
1.0
0.5
0.2
0.1
0.05
0.02
0.01
1
10^{-1}
10^{-2}
0.1
0.2
0.5
1.0
2.0
5.0
10
20
50

TOTAL RADIATION DOSE RECEIVED IN AN AREA CONTAMINATED BY NEUTRON-INDUCED GAMMA ACTIVITY
SOIL TYPE IV

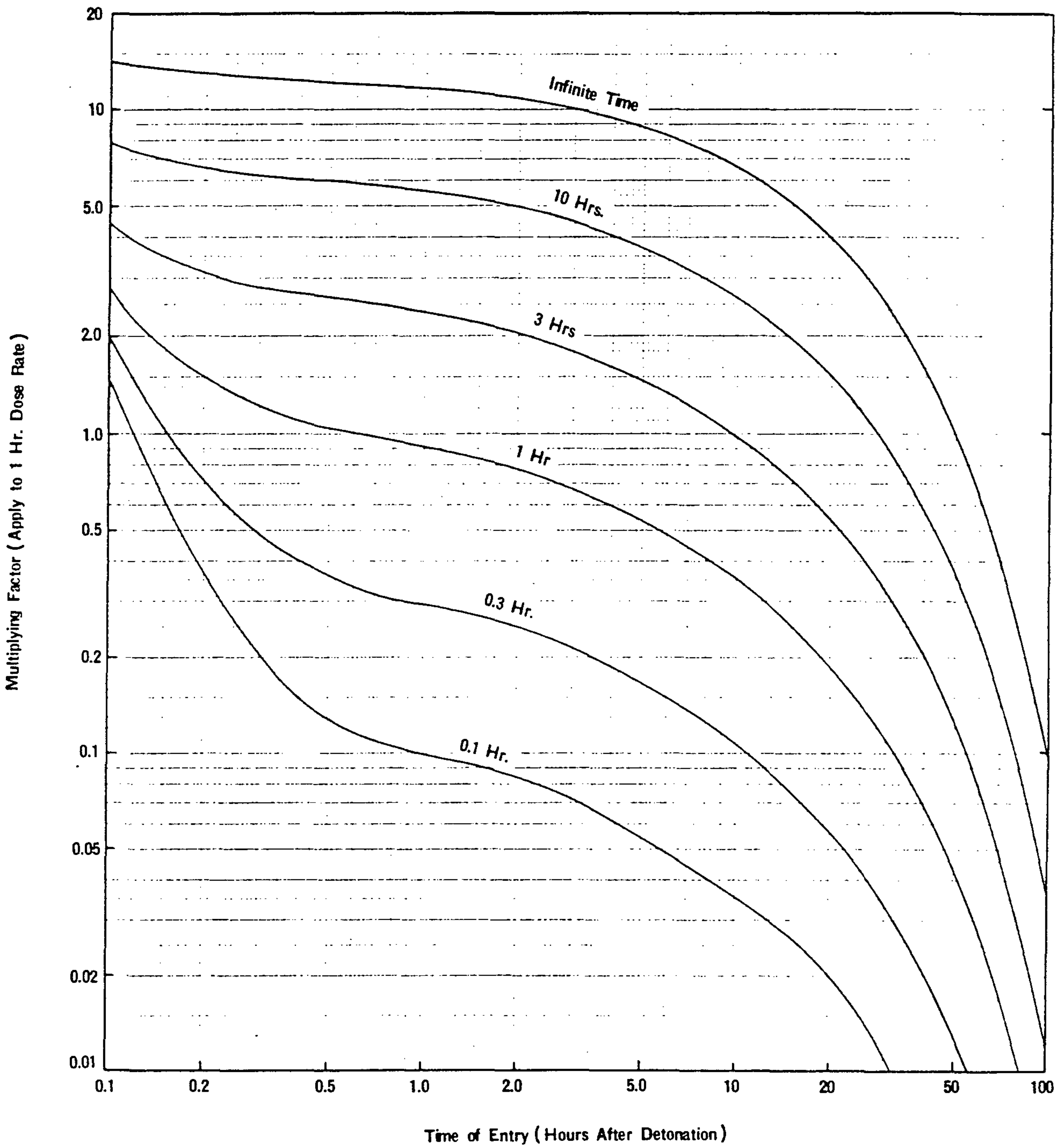

BLANK

STABILIZED CLOUD ALTITUDES

The curves of figure 4-34 give the altitudes of the top and bottom of a nuclear cloud above the burst point after it has ceased to rise in the atmosphere.

Example.

Given: An 80 KT burst at 3,000 feet above terrain.

Find: The altitude above terrain of the top and bottom of the stabilized cloud.

Solution: From figure 4-34 an 80 KT cloud stabilizes above the burst point at:

top---------- 52,000 feet
bottom------ 38,000 feet

Therefore, the altitude above terrain is:

top---------- 52,000+3,000=55,000 feet
bottom------ 38,000+3,000=41,000 feet.
Answer.

Reliability. Figure 4-34 applies to clouds from surface and air bursts with yields between 0.1 KT and 100 MT. The reliability is such that clouds are not expected to rise above the burst point more than 20 percent higher than indicated. However, extremes in meteorological conditions, such as winds of 50 knots or greater, can cause clouds from weapon yields less than 100 KT to rise only half as high as indicated. For yields greater than 100 KT, meteorology is less important in limiting the altitude given under almost all conditions.

Related material.

See paragraph 4.3*l*.

See also figures 4-35 through 4-37.

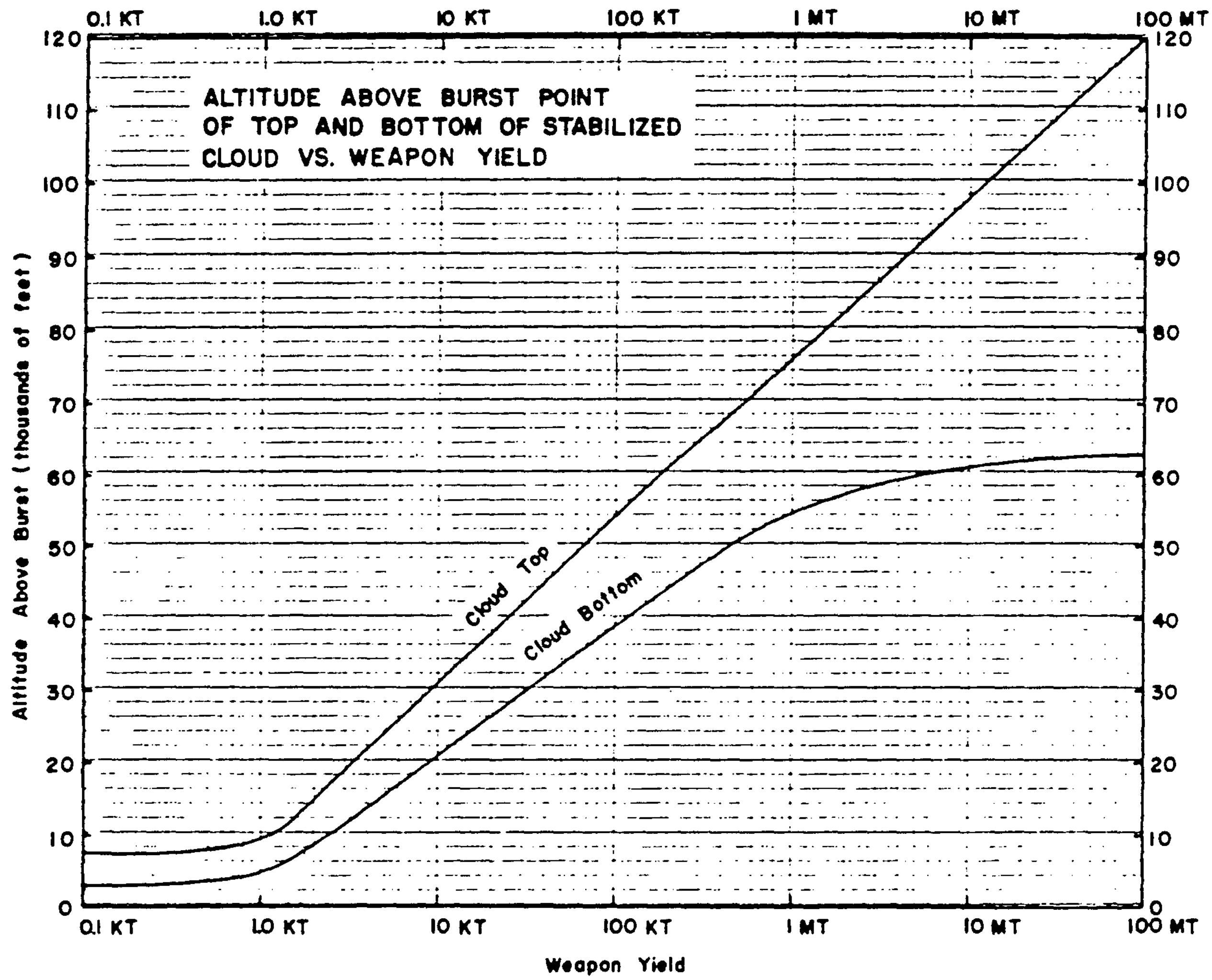
ALTITUDE ABOVE BURST POINT
OF TOP AND BOTTOM OF STABILIZED
CLOUD VS. WEAPON YIELD
0.1 KT
1.0 KT
10 KT
100 KT
1 MT
10 MT
100 MT
0
10
20
30
40
50
60
70
80
90
100
110
120
Altitude Above Burst (thousands of feet)
Cloud Top
Cloud Bottom
Weapon Yield

CLOUD HEIGHT GROWTH

Figure 4–35 gives the percentage of the maximum height reached by a nuclear cloud as the cloud moves up into the atmosphere for times after detonation up to about 7 minutes.

Example.

Given: A 5 MT nuclear detonation.

Find: The altitude above burst point of the cloud top 3 minutes after detonation.

Solution: From figure 4–35, at 3 minutes after burst time the cloud has reached 62 percent of its maximum altitude. From figure 4–34 the cloud top maximum altitude is 92,000 feet. Therefore, the cloud top at 3 minutes is:

$92,000 \times 0.62 = 57,000$ feet above the burst point. *Answer.*

Reliability. Figure 4–35 applies to clouds from surface and air bursts of weapons with yields between 0.1 KT and 100 MT. The time to reach a given percentage of the maximum altitude is believed to be accurate within ±30 percent.

Related material.

See paragraph 4.3*l*.

See also figures 4–34, 4–36 and 4–37.

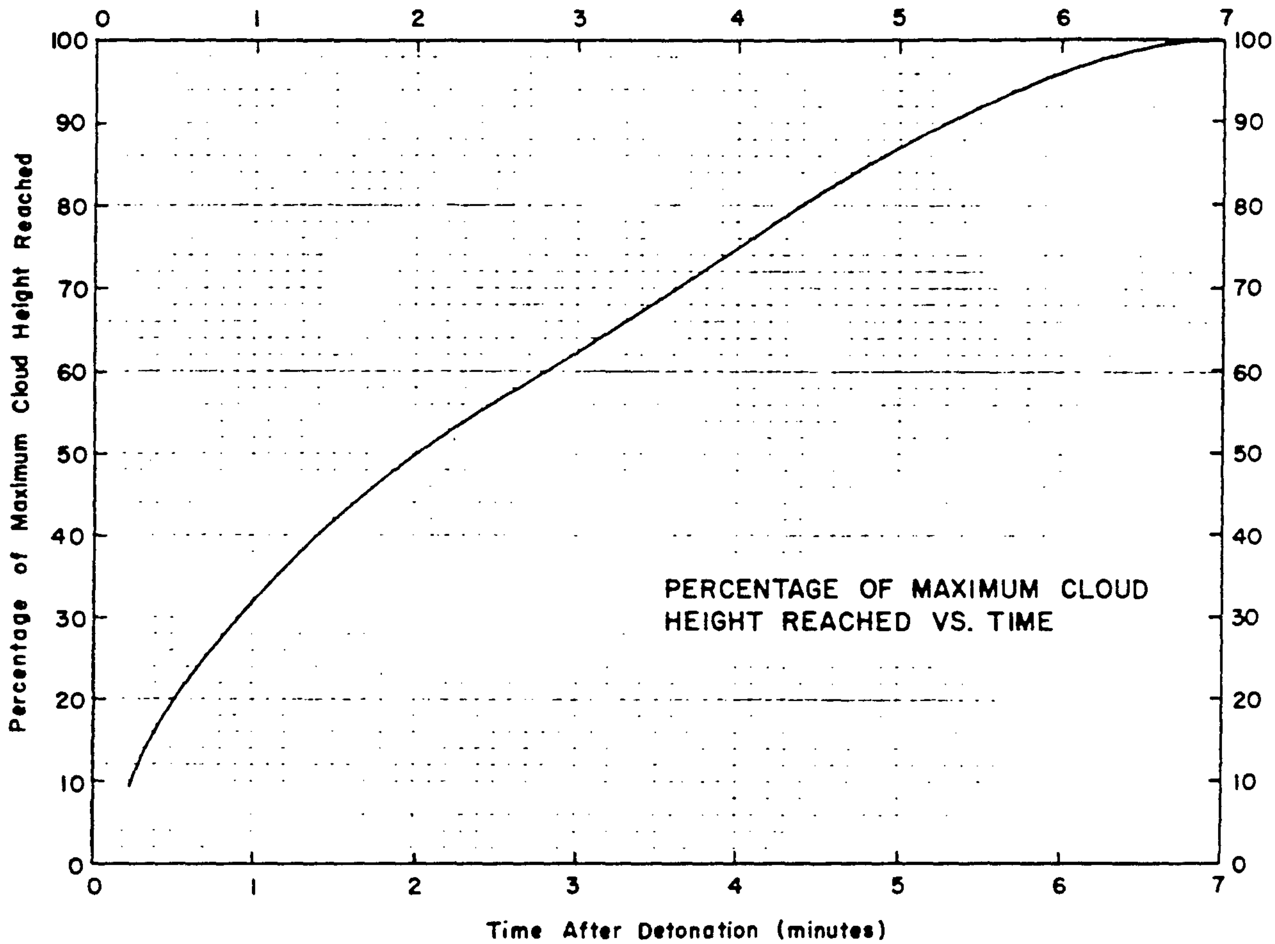
PERCENTAGE OF MAXIMUM CLOUD HEIGHT REACHED VS. TIME
Percentage of Maximum Cloud Height Reached
Time After Detonation (minutes)
0 1 2 3 4 5 6 7
0 10 20 30 40 50 60 70 80 90 100

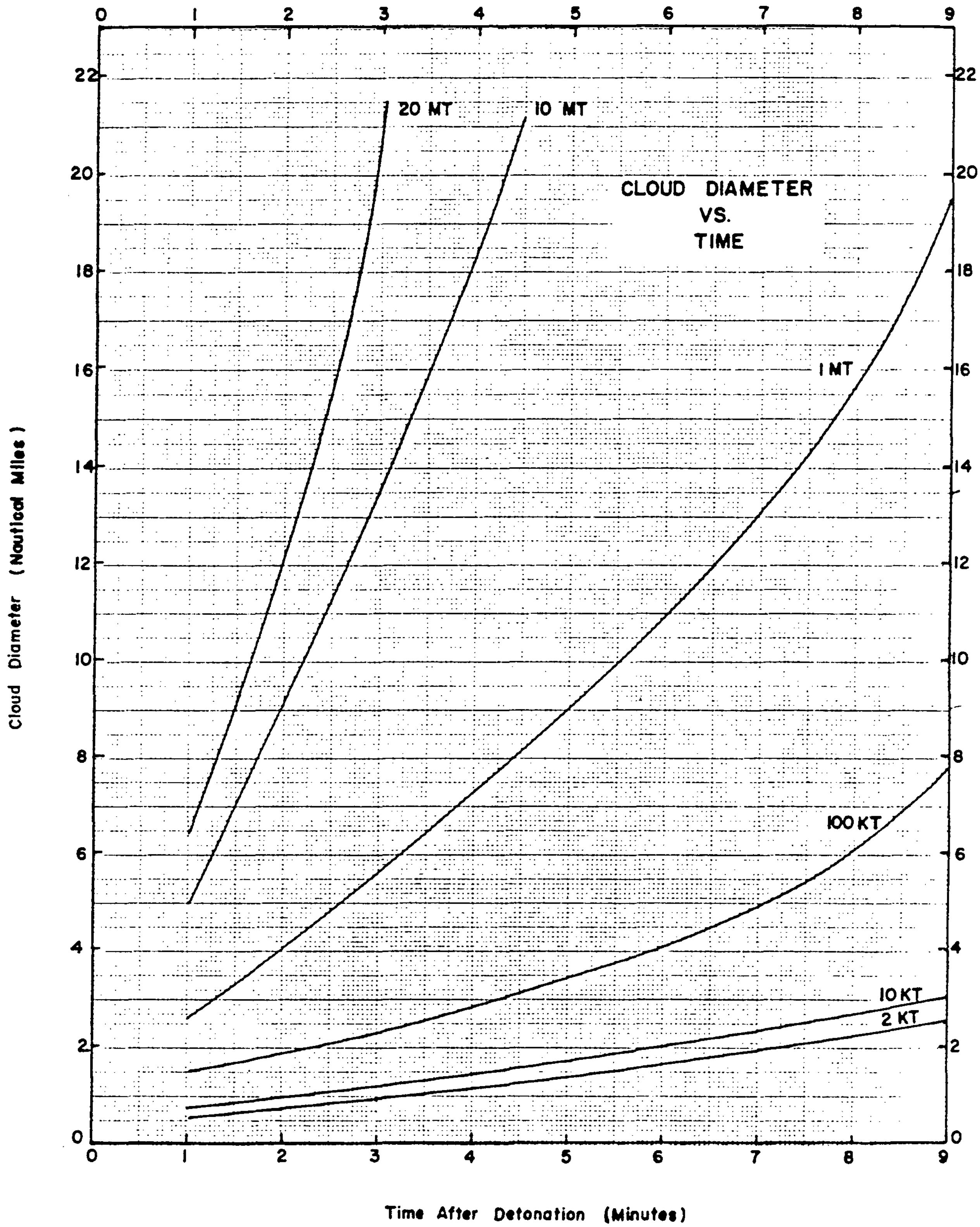
CLOUD DIAMETER
VS.
TIME
20 MT
10 MT
1 MT
100 KT
10 KT
2 KT
0
1
2
3
4
5
6
7
8
9
0
2
4
6
8
10
12
14
16
18
20
22
Cloud Diameter (Nautical Miles)
Time After Detonation (Minutes)

BLANK

DOSE RECEIVED WHILE FLYING THROUGH A NUCLEAR CLOUD

The curves of figure 4-37 give the total dose received from passage through nuclear clouds at various times after burst. The relative hazard for flight through the stem is not definitely known; however, flight through the stem is considered somewhat less hazardous than flight through the center of the cloud.

Example.

Given: An aircraft flying at 25,000 feet at a speed of 200 knots is to pass through the center of the cloud from a 50 KT bomb exploded on the surface, which is 1,000 feet above sea level.

Find: The dose which the crew will receive.

Solution: The aircraft will intercept the cloud at—

25,000 − 1,000 = 24,000 feet above the burst point.

From figures 4-34 and 4-35 the center of the cloud will reach this altitude above the burst point in 2.8 minutes. At this time after detonation the diameter of the cloud from a 50 KT weapon is 1.5 nautical miles (fig. 4-36). The time spent in the cloud is—

$$\frac{1.5}{200} = 0.0075 \text{ hours or } 0.45 \text{ minutes}$$

From figure 4-37 the dose accumulated in the cloud for an entry time of 2.8 minutes and a transit time of 0.45 minutes is 110 *r*. *Answer*.

Reliability. The doses indicated are considered accurate within a factor of two for flight paths which pass near the cloud center. For paths close to the cloud boundaries, the predicted dose will probably be higher than the actual dose, although the magnitude of the error is unknown.

Related material.

See paragraph 4.3*l*.

See also figures 4-34 through 4-36.

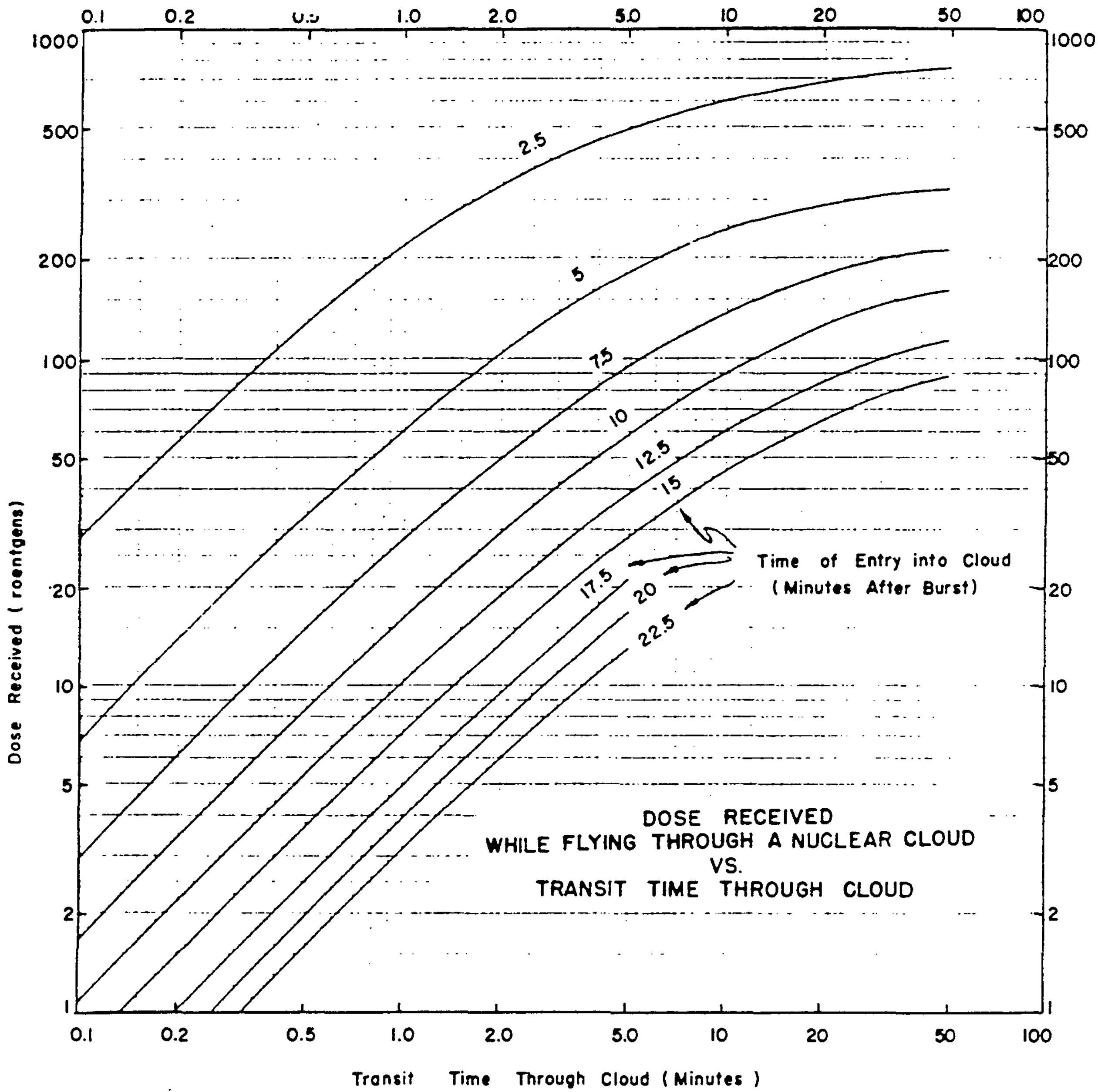

DOSE RECEIVED
WHILE FLYING THROUGH A NUCLEAR CLOUD
VS.
TRANSIT TIME THROUGH CLOUD
Time of Entry into Cloud
(Minutes After Burst)
2.5
5
7.5
10
12.5
15
17.5
20
22.5
Dose Received (roentgens)
Transit Time Through Cloud (Minutes)
0.1
0.2
0.5
1.0
2.0
5.0
10
20
50
100
1000
500
200
100
50
20
10
5
2
1

BLANK

447555 O - 58 - 17

PART TWO—DAMAGE
5. Introduction

PART TWO
DAMAGE CRITERIA

SECTION V
INTRODUCTION

5.1 General

In part one, the phenomena associated with a nuclear explosion are described for various burst conditions. It remains to express the numerical values of these phenomena in terms of damage in varying degree to targets of military interest. Part two is a summary of the aggregate knowledge of nuclear weapons effects on personnel and materiel, and includes statistical and theoretical treatment of the large amount of data from tests of nuclear explosions, results of the bombs dropped on Japan, and laboratory work. Where check points are not available, some extrapolation of data is made where reasonable accuracy can be expected. An attempt is made to present the information in a form suitable for use by the atomic weapons staff officer. Graphical presentation is used in preference to tabular presentation wherever possible. Part two is divided into sections according to classes of targets which can be considered as a group because of similar response characteristics. Further subdivisions within the sections are generally by the phenomena causing the damage. The damage curves presented in part two are drawn for a probability of 50 percent of inflicting the degree of damage indicated, with curves of 90 percent and 10 percent probability included where the amount and quality of data available are sufficient to justify it.

5.2 Blast and Shock Damage

a. General. When a blast or shock wave strikes a target, the target may be damaged (distorted by an amount sufficient to impair usefulness) by the blast or shock wave itself, being translated by the blast wave and striking another object or the ground, or by being struck by another object translated by the blast wave. For example, the air blast wave itself can shatter windows, dish in walls, collapse roofs, deflect structural frames of buildings, and bend or rupture aircraft panels and frames. Vehicles, tanks, artillery pieces, and personnel can strike other objects or the ground while being hurled through the air or tumbled on the ground by the blast wave. Ship hulls may be split or crushed by the water shock wave. Buried structures or structural foundations can be displaced, collapsed or ruptured by the ground shock wave. Usually, the degree of damage sustained by a particular target cannot be specifically correlated to a single blast or shock parameter. The total damage received by the target may be dependent upon a combination of air blast and ground or water shock parameters, the manner in which the target is oriented with respect to the blast or shock wave, and the type of surface (the topography and/or the type of soil) associated with the target. In *b* and *c* below, the relationship between loading, response and damage of various targets is discussed briefly. In the introductory paragraphs of sections VI through XI, a detailed discussion of blast and shock damage criteria is given.

b. Loading. The blast loading on an object is a function not only of the blast characteristics of the incident wave (rise time, peak overpressure, peak dynamic pressure, decay and duration), but also of the size, shape, orientation, and response of the object. The manner in which the loading is influenced by the target characteristics is discussed below with emphasis on air blast loading.

(1) *Air blast loading.* The loading on an object exposed to air blast is a combination of the forces exerted by the overpressure and the dynamic pressure of the

incident blast wave. The loading at any point on a surface of an object can be described as the sum of the dynamic pressure, multiplied by a local drag coefficient, and the overpressure after any initial reflections have cleared the structure. Since the loading changes rapidly during the time the blast wave is reflecting from the front surfaces and diffracting around the object, loading generally comprises two distinct phases—first, loading during the initial diffraction phase, and second, loading after the diffraction is complete (i. e., the object is completely engulfed by the blast wave). This latter phase approaches a steady state and is usually referred to as the drag phase, because during this phase the drag forces (i. e., forces resulting from the dynamic pressures) predominate in producing a net translational force on the object. The generalized discussion of the loading process given below is based primarily on an ideal blast wave as described in section II. Where non-ideal blast waves (with slow rise time, irregular shapes and high dynamic pressures) introduce complications into the loading process, further explanation is given.

(*a*) *Diffraction loading.* As the shock front of an air blast wave strikes an object, the shock is reflected from the side facing the blast, creating overpressures on this face up to several times that of the incident overpressure. In the Mach reflection region the overpressure incident on the object is actually that of the original free air blast wave which has been reflected from the ground surface to a higher value; therefore, the reflection off the object constitutes a second reflection process. In the regular reflection region, the incident overpressure is that of the free air blast wave (see (*e*) below). The magnitude of this reflected overpressure depends principally on the angle between the shock front and the face of the object, the rise time of the incident blast wave, and the initial incident shock strength. The greatest reflected overpressures occur when the direction of propagation of the shock front is normal to the face of the object, when the rise to the peak overpressure is essentially instantaneous, and when the incident shock strength is very high. As the blast wave progresses, it bends or diffracts around the object, eventually exerting overpressures on all sides. Before the object is entirely engulfed in the pressure region, however, overpressure is exerted on the front side of the object, while only ambient air pressure exists on the back side. During the diffraction phase this pressure differential produces a translational force on the object in the direction of blast wave propagation. When the blast wave has completely surrounded a small object, the differential pressure is reduced essentially to zero, since the pressures on the front and on the back are almost equal. In the case of long objects or for short duration blast waves, the net force may actually reverse, since the overpressure on the front face may decay to a value lower than that on the rear face. The importance of this translational loading in the production of damage to the target depends on the duration of the loading or on the time required for the shock front to traverse the target, and therefore, on the size of the target. For the same overpressure, the effects of the translational load decrease as the duration of the load is decreased, until in certain cases such loading can be ignored. The overpressures continue on all sides of the object until the positive phase of the blast wave has passed. These pressures may be sufficient to crush an object (a 55-gallon drum may be so damaged in addition to damage incurred by translation). Thus the diffraction phase translational loading depends primarily on the object size and on increases in differential overpressures resulting from reflection on the front face. Upon completion of the diffraction phase, crushing pressures continue on all sides due to the blast wave overpressures. Loading as a consequence of the negative phase is considered negligible.

(*b*) *Drag loading*. During the time of diffraction and until the blast wave has passed, dynamic pressures, caused by the high wind behind the shock front, are also exerted on the object. These pressures, except for high shock strengths, are much lower than the reflected overpressures but produce a translational force on a target component during the entire duration of the blast wave. For a given blast wave, the loading resulting from dynamic pressures depends principally on the shape and orientation of the object, ranging from less than four-tenths the dynamic pressures in the case of a cylinder (when normal to the cylindrical axis) to over twice the dynamic pressures for an irregular, sharp-edged object. This loading is called drag loading.

(*c*) *Net loading*. Figures 5–1A and 5–1B give representative net loadings on two structural elements or objects, one small and one large, for two weapon yields. The term "net loading" is used to denote the combined load on the element that tends to translate it in the direction of propagation of the blast wave. Thus the back face loading has been subtracted from the front face loading; the loads on the sides are of no effect. The terms "small element" and "large element" are relative, but the general sizes to keep in mind are—for "small", an object of about the size of a telephone pole or a jeep, and for "large", an object of the size of a house or larger. The loadings display an initial peak value, due to the overpressure being reflected up to more than twice the incident pressure on the front face of the element. The reflected pressure decays or clears the front face at a time dependent on the size of the element. The rapid decay for the small element may make the reflected pressure spike of no significance, whereas the slow decay for the large element creates a load which may entirely govern the response of the target. For the representative cases indicated, the diffraction phase is shown to terminate at time t_{diff}, the time at which the reflected pressure has decayed to the incident pressure. At this time the drag phase begins, and continues until the end of the positive phase of the incident blast wave. The load during the drag phase is shown as equal to the dynamic pressure (i. e., the drag coefficients of the elements are equal to 1.0). The characteristics of the target element determine whether the response of the element is governed primarily by the diffraction phase or the drag phase. Figures 5–1A and 5–1B show that for medium and high yield weapons and small elements, a much greater impulse (the area under the loading curve) occurs during the drag phase than during the diffraction phase. As the yield increases the drag phase impulse increases in predominance. For large elements and medium yield weapons, a much greater impulse occurs during the diffraction phase than during the drag phase. In this instance, as yield decreases the diffraction phase impulse increases in predominance. For large elements and large yield weapons, the diffraction phase and drag phase impulses are about equal. In this latter case the drag phase impulse may still be of no importance, since the significant target response may occur during the diffraction phase. Note that the diffraction phase impulses are not changed by the yield of the weapon (this remains true for all but very large structures exposed to low yield weapons), while the drag phase impulses are directly related to the weapon yield (for the same peak dynamic pressures).

(*d*) *Target motion.* When air blast loading is considered, except for aircraft in flight, the movement of the target component during loading is assumed to have negligible effect on the loading itself. For the case of aircraft in flight, speed, orientation, and movement during loading assume increased importance. (See sec. IX.)

(*e*) *Regular and Mach reflection.* In computing the loading on a target, specific aspects of the blast wave propagation must be considered. The loading of a surface target in the regular reflection region is complicated by the vertical component of the incident blast wave, causing multiple reflections between the ground and the target and additional reflected pressures on horizontal surfaces. In the Mach reflection region the loading is simplified because the blast wave propagation is horizontal. Since near the surface of the ground the vertical component of the drag forces in the regular reflection region is quickly cancelled by the reflected wave, the brief vertical drag loading is ignored except when the target is very near the ground zero of an air burst. For aircraft in flight, the loading may be a single horizontal shock from a Mach stem or two separate shocks, the first from the free air wave and the second from the ground reflected wave. In establishing the damage curves for surface targets, the loadings on targets in the regular reflection region during the diffraction phase are considered separately from the loadings on similar targets in the Mach reflection region, and the surface conditions are assumed to be average unless otherwise indicated. Objects which are susceptible primarily to horizontal drag loading if in the Mach region may become primarily susceptible to crushing action if they are in the early regular reflection region.

(*f*) *Non-ideal wave forms.* As discussed in paragraphs 2.1*c*(3)(*c*) and (4)(*c*), ideal wave forms are seldom found along the surface for overpressure levels above 6 psi. The description above of the diffraction and drag phases no longer holds true in regions of non-ideal wave forms. If the overpressure wave has a long rise time (30 or 40 msec) to a peak value, full reflection of the wave off the surface of a structure will not occur. At the same time, the relationship between dynamic pressure and overpressure is very much different from that described for the ideal blast wave, so that during the diffraction phase the drag forces due to high dynamic pressures may predominate as the damage producing criteria. Since many conventional surface structures sustain severe damage at low peak overpressure levels and since non-ideal wave forms occur only in the higher overpressure regions, such wave forms have not been considered in determining damage criteria for these structures. For protective shelters that are designed to withstand high pressures, however, careful consideration must be given to non-ideal wave forms and the dynamic pressures which are even higher than would be expected if the wave forms were ideal. Accurate prediction of blast loading in the high pressure regions is further complicated by inadequacy of data.

(2) *Water shock loading.* Water shock loading is not as well understood as air blast loading. As with an air blast shock front, when the water shock front strikes an object the pressure is reflected from the front face and, consequently, attains a higher pressure than in the incident shock front. The

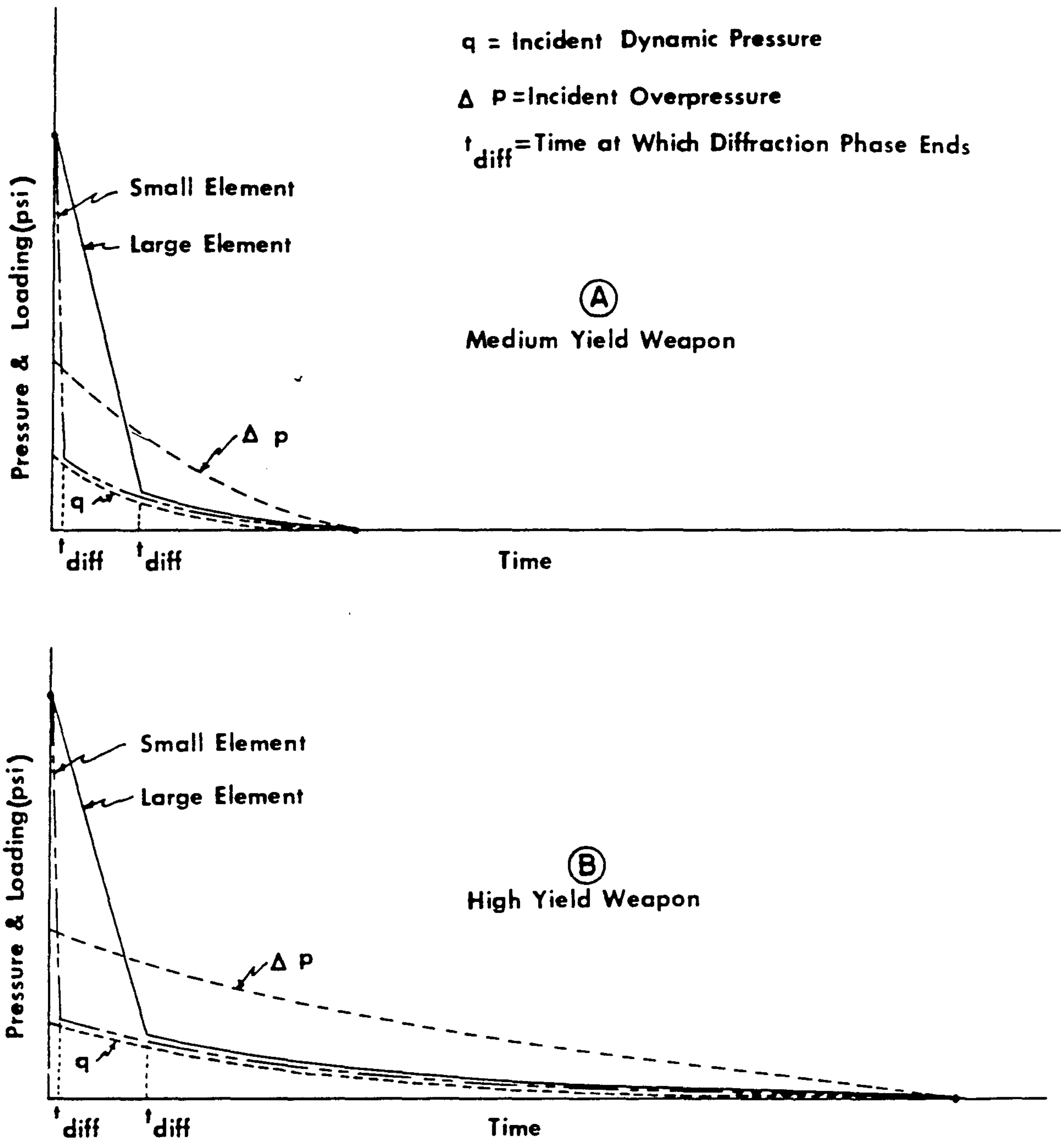

NET BLAST LOADING ON REPRESENTATIVE STRUCTURES loading following the initial shock, however, is altered considerably by reflections from the surface of the water and by movement of the object.

(3) *Ground shock loading.* The loading of buried objects by ground shock is intimately tied to the response of the objects. Ground shock has to be so intense in order to cause serious damage to underground structures or foundations of aboveground structures that the damage area for these structures is confined closely to the crater area of a surface or underground burst. Therefore, the ground shock damage is given in terms of the crater radius and not in terms of the shock phenomena of stress (pressure), particle velocity, acceleration, or displacement. However, air blast induced ground shock, transmitted with little attenuation to a depth as great as 8 feet, may cause significant loading pressures on the roofs of shallow buried structures (with less than 15 feet cover) outside of the crater. Loading pressures are numerically equal to the ground stress normal to the structure. Such pressures do not produce detectable reflected pressures. The pressures exerted on the sides of such structures vary from 15 percent of the air blast pressures for dry soil up to nearly 100 percent for saturated soil. Internal equipment of a structure may be subjected to accelerations resulting from ground shock that will severely damage the equipment but may not damage the structure. For a discussion of accelerations resulting from ground shock see paragraph 2.2*b*.

c. Response and Damage. Damage to a target is closely related to its response and is a direct derivative thereof. For targets anchored to the ground, damage is most often the result of displacement of one part of the target with respect to another part, resulting in permanent distortion, collapse or toppling. For movable targets, however, the target may be moved by the loading with or without damage resulting. In these cases the damage to the target is governed primarily by the manner in which the moving target comes to rest. Depending on the yield of the weapon, target characteristics and the damage level considered, either drag phase loading or diffraction phase loading assumes the greater importance.

For large targets such as buildings having small window areas and walls which either support the structure or are as strong as the structural frames, the reflected overpressure loading during the diffraction phase is predominant in causing failure of the structure. The failure occurs because the pressure differential between the front and rear face exists over a relatively long period of time. If the window area is large, the pressure on each wall is quickly equalized by the entry of the blast wave through the windows. The pressures exerted on the inside of the wall thus reduce the translational force on the wall. This translational force is also reduced because of a smaller wall area on which the pressures can act; however, the force exerted on interior partitions and rear walls tends to offset the reduction in front face loading in production of total damage. When the overpressures causing translational force on the structural component are quickly equalized because of the geometry or construction of the building, the primary damaging forces are those produced by the dynamic pressures or drag forces. Drag forces are the significant damaging forces when the structural components have fairly small cross sections, such as columns and beams. Structures normally damaged by drag forces are smoke stacks, telephone poles, truss bridges, and steel or reinforced concrete frame buildings with light walls. These buildings are drag sensitive because the light walls of corrugated steel, asbestos or cinder block fail at low reflected pressures, transmitting little load to the structure frame. Then only the frame itself is exposed to the blast and, being composed of small cross section structural elements, is distorted primarily by drag forces. These buildings are not considered severely damaged unless the structural frame has collapsed or is near the point of collapse. A tree is a good example of a drag sensitive target, since the duration of the diffraction phase is extremely short and there is considerable force applied by the high wind velocity drag loading. Most military field equipment is drag sensitive, because damage generally results from the tumbling or overturning caused by the drag forces.

If the target is shielded from the drag forces or lies within the early regular reflection region, high overpressures may become the damage-producing criteria. For blast resistant aboveground structures designed to resist more than 5 to 10 psi overpressure, the distinction between diffraction and drag sensitivity cannot be well defined primarily because full reflection from the surface of the structure does not occur and dynamic pressures greatly exceed those expected in the ideal wave form case. As a result, drag forces may predominate even during the diffraction phase in producing damage.

Aircraft may be damaged by the forces developed in the diffraction phase, in the drag loading phase, or in both. Parked aircraft can receive light, moderate, or often severe degrees of damage as a result of diffraction or crushing forces corresponding to low overpressures. For example, light skins and frames are easily dished and buckled at relatively low overpressures. At higher overpressure levels, drag loading (referred to as "gust loading" with respect to aircraft) adds to the damage. At these levels, much of the damage may result from translation and overturning of the aircraft. For aircraft in flight, the diffraction and drag forces combine with the existing aerodynamic forces to develop destructive loads on airfoils at low overpressure levels. The diffraction or crushing overpressure effects on the fuselage and other thin skinned components, however, are usually of secondary importance for the in-flight aircraft.

Severe water shock damage to ships or submarines results when the hull is split or crushed by the shock pulse. Generally, severe damage to surface ships is related to hull deformation, certain values of which are used empirically for damage criteria. For submarines, the damage to the hull is related to the impulse in the shock. Interior machinery damage is related to the bottom plate velocity for surface ships, and to the hull velocity for submarines. Water wave action produced by surface or subsurface bursts also may contribute to surface ship damage. In addition, waves striking shore installations may cause serious damage to the components of such installations.

5.3 Thermal Radiation Damage

a. General. The two most important effects of thermal radiation on ground targets are injury (burns) to personnel and the setting of fires in the target area. Depending upon the yield and detonation conditions of the weapon, and upon target characteristics, blast effects or nuclear radiation effects may override the thermal effects in importance. Predictions of thermal damage to targets are limited by the precision with which thermal energy may be scaled with yield, height of burst and slant range. The factors of target geometry, previous precipitation history, prevailing meteorology and seasonal effects introduce additional uncertainties. The criteria for thermal damage, set forth in part two in terms of specific radiant exposures required to produce the damage of interest, should be applied with the understanding that significant deviations from the mean values quoted may be experienced in individual cases because of variations in the factors mentioned above.

b. Energy and Rate Dependence. The damage produced by thermal radiation is dependent upon the energy per unit area incident on the target and the rate at which the energy is delivered. For convenience, the incident thermal energy per unit area (or *radiant exposure*) has been adopted as the damage criterion. Since the emission period for the thermal pulse increases with increasing yield of the detonation, the thermal radiation from the larger yield weapons is delivered over a longer period of time. For a given total amount of thermal energy received by each unit area of exposed material, the damage will be greater if the energy is delivered rapidly than if it were delivered slowly. For example, it takes 4 cal/cm^2 to produce a second degree burn on bare skin for the rapid pulse of a 1 KT detonation, whereas direct sunlight produces this amount of radiation in a little over 2 minutes with no effect. This means that, in order to produce the same thermal effect in a given material, the total amount of thermal energy received per unit area must be larger for a nuclear explosion of high yield than for one of lower yield, because the energy is delivered over a longer period of time, i. e., more slowly, in the former case. Therefore, thermal damage criteria in part two are given for specified yields, or factors for scaling the criteria with yield are given.

c. Damage Mechanisms. Except for thin materials such as fabrics, newspaper, and leaves, thermal damage to materials is largely confined to changes at shallow depths in the exposed surface. Damage to materials results from raising the temperature of the surface, which, in the case of organic materials, brings about permanent chemical changes or induces ignition of the material. Only the portion of the energy which is absorbed (i. e., neither reflected nor transmitted) by the material is effective in producing thermal damage. Highly reflecting materials or transparent materials are relatively resistant to thermal damage. Light colored objects of a given thickness are more resistant than dark colored objects of the same material and thickness because they reflect more of the incident energy. However, color has little effect on the response of materials which blacken readily upon exposure early in the thermal pulse, since the energy delivered during the remainder of the pulse is largely absorbed by the blackened surface. The effect of absorptivity has been included in the derivation of damage criteria.

d. Effect of Thickness. Thick organic materials such as wood, plastics, and heavy fabrics do not support combustion, but only char as the result of exposure to thermal radiation. During the delivery of the pulse, the surfaces of these materials may flame, but the combustions are not sustained once the radiant pulse has died out. Materials such as light fabrics, newspaper, dried leaves and grass, and dry rotted wood may ignite at energies as low as 3 cal/cm^2 from a 1 KT detonation. The subsequent arrival of the blast wave at distances corresponding to these low ignition energies frequently fails to extinguish the ignitions and they become possible sources of primary fires. Charring and flaming or disintegration is typical of organic substances. Many of these substances emit jets of flame or smoke during exposure but do not actually ignite. Bare metals are unchanged unless structurally weakened or melted by heat action. The thicker the metal, the more resistant it is to thermal effects.

e. Effect of Orientation. Orientation of material is an important factor affecting the thermal damage produced by a weapon detonated in clear atmospheres, since the radiant exposure of a plane surface depends on the angle between the perpendicular to the surface and the direction of the burst. The maximum effect is produced when the incident radiation is perpendicular to the surface. Surfaces which do not receive direct radiation may be exposed to the lesser amounts of radiation reflected from the ground or from clouds or scattered by haze in the atmosphere. Under hazy conditions at slant ranges greater than half the visibility, much of the energy received is scattered by particles in the atmosphere and comes from all directions. References in table 12–2 to the exposures required to produce various types of damage are based on an alignment perpendicular to the incident beam. For other orientations of the target surface, greater exposures will be required to produce the same degree of damage.

f. Effect of Shielding. Except under hazy conditions at greater slant ranges, when the incident radiation is received from all angles, the geometry of the target of interest with respect to nearby objects is of importance, particularly within buildings or in complex target areas. Trees, buildings, foxholes, hills, etc., if in a position to shield the target from the fireball, are effective as thermal shields. The shielding effect of deciduous trees, once the leaves have been shed, is greatly reduced. Reflection of thermal radiation from exposed walls of foxholes is about 5 percent.

g. Moisture Content. Thermal damage to materials which absorb moisture is dependent upon the percentage of water in such materials. Usually, the moisture content varies with the prevailing relative humidity. However, exposure to recent rain may greatly alter the moisture content. Scorching or charring of an organic surface by radiant energy is preceded by vaporization of the water. Because of this effect, more energy is required to produce a given damage effect to wet surfaces or to targets in highly humid atmospheres. Materials located within structures during the latter part of the heating season (late winter and early spring) are more readily damaged by thermal radiation, largely due to decreased interior humidities. On the other hand, materials exterior to structures are more readily damaged during the summer and fall. Vegetation at the end of the growing season and fallen leaves are classed as ignition sources of greatest potential in the summer and fall. (See sec. XII.)

5.4 Nuclear Radiation

a. Relative Effects. With only a few exceptions, which are discussed in paragraph 12.2, significant radiation damage is limited to living organisms, so that for all practical purposes it is an antipersonnel effect. Basic nuclear radiation data are presented in previous sections, subdivided within burst types as to initial radiation and residual radiation. The penetrating radiations (neutrons and gamma rays) are the most dangerous, and the effect of these penetrating radiations in nearly every case exceeds that of the less penetrating residual alpha and beta radiations. The latter two may, however, become an internal hazard if taken into the lungs or digestive system, or an external hazard to skin in the case of beta rays. The ultimate effect of each of these radiations on living tissue is the same, and involves the damage of individual living cells. The modes of interaction with cellular matter differ, but these differences are not important in assessing the end result. The nature of the radiation determines whether the resultant injury is localized or diffuse. Thus beta rays, with their low penetrating power, are stopped within the first few hundredths of an inch of tissue, and may produce localized surface burns of varying degrees of severity; whereas gamma rays and neutrons can penetrate deeply (or may even pass completely through the body) before giving up some or all of their energy by interaction with body tissue.

b. Cumulative Effects. Ultimate body damage resulting from nuclear radiation is necessarily a summation of the several separate radiation effects involved. Thus, roentgens of initial gamma radiation received must be added to the roentgen equivalent dose for man (rem) of neutron radiation received, plus the roentgens of residual gamma radiation received, to obtain total dose. Beta radiation dose received must be evaluated separately, since it is a localized surface effect rather than a diffuse type of injury. If a significant portion of the total dose is received over an extended period of time, some biological recovery or repair occurs (see par. 6.3*a*).

c. Shielding. It is important to recognize that the basic nuclear radiation data presented in part one of this manual pertain to completely open and unshielded regions. Reductions in dosage actually received by an individual will occur from shielding afforded by surrounding structures and terrain elevations. Shielding factors and transmission curves by means of which actual doses behind certain shields can be estimated are given in paragraph 6.5.

5.5 Selection of Burst

a. General Considerations. Many factors enter into the selection of burst height or depth, and yield for a particular weapon. Among these factors are fuzing limitations, delivery systems available, the extent and vulnerability of the target, and the degree of damage which is desired. From an effects standpoint, the basic criteria which govern burst height or depth and yield selection are peak blast wave overpressure, peak dynamic pressure, duration of the positive phase, crater extent, initial nuclear radiation, residual fission product fallout and induced ground contamination, and thermal radiation. In the majority of cases, one of these criteria is present which, commensurate with troop safety, clearly indicates the type of burst to be employed, thus eliminating the time and effort necessary to make a detailed comparison of types of burst for a specific target. Some generalized statements on the relative importance of various effects for different burst conditions, which are useful in making such a decision, are as follows:

(1) *Surface bursts.* A surface burst will increase the range at which peak overpressures occur for pressures greater than about 12 psi; reduce thermal radiation received by ground targets compared to that received from an airburst at the same slant range; produce large areas of fallout contamination; and produce significant cratering and ground shock.

(2) *Air bursts (depending on the applicable criterion).* An airburst will increase the range on the ground at which overpressures of about 10 psi or less are obtained; maximize areas of thermal radiation received on the ground; elimi-

nate significant fallout contamination; and may increase the importance of neutron-induced activity.

(3) *Subsurface bursts*. Peak air overpressures, thermal radiation, and initial nuclear radiation will decrease as the depth of burst is increased. Cratering, ground or water shock, and fallout contamination will increase with depth of burst up to a maximum—the optimum depth depending on the effect being considered—and then decrease. Maximum water waves will be produced at certain critical depths of burst.

b. Estimation of Phenomena Extent. Figures 5–2A, B, and C show the horizontal range to which various physical phenomena extend as a function of yield for scaled heights of burst of 0 $W^{1/3}$ feet (surface), 250 $W^{1/3}$ feet (in the transition zone with respect to some phenomena), and 650 $W^{1/3}$ feet (air burst), respectively. Figures 5–3A, B, and C are nomograms for the same scaled burst heights and conditions, from which the slant range of given levels of any phenomenon may be estimated with reasonable accuracy.

The curves and nomograms are presented to allow a rapid visual comparison of the extent of the various physical phenomena and to permit a rapid determination of the controlling damage mechanism at a particular distance for a given yield. The conditions for which the curves and nomograms are drawn are given on the figures. For other conditions, or to obtain maximum accuracy, the basic data curves of part one must be utilized.

The parameter values selected are not intended to imply equally damaging effects on a given target. Blast and thermal curves are not related directly to damage, since this depends on blast duration and rate of delivery of thermal energy, which in turn are related to yield. A discussion of this point is given in the facing page of figure 5–2. Areas of effect generated from this data would generally be circular, except in the case of fallout, the major portion of which is elliptical, and the horizontal component of the peak dynamic pressure, which may take the form of a hollow circle or annular ring (note fig. 5–2C).

BLANK

PHENOMENA AT VARIOUS SCALED BURST HEIGHTS

Figures 5–2A, B, and C show the range from ground zero of various physical phenomena when a burst is on the surface, at a scaled height of 250 $W^{1/3}$ feet, and at a scaled height of 650 $W^{1/3}$ feet, respectively. They are presented primarily for rapid visual comparison of the distance to which the various physical phenomena will extend, and secondarily for a rapid determination of the controlling mechanism of damage at any distance for any yield. From data presented in part one, a similar illustration could be prepared for any scaled or actual burst height.

The significance of the various phenomena curves presented varies with the target being considered. The initial and residual radiation curves are the most significant ones for human targets in the open or in shelters. The values chosen for plotting represent the following:

- 5 *r*—No obvious effect on personnel.
- 100 *r*—Non-lethal dose causing sickness in a few personnel, but permitting a unit to remain operationally effective.
- 450 *r*—Dose lethal within 30 days to 50 percent of personnel exposed.
- 10,000 *r*—Free field dose which will produce a dose of 100 *r* for personnel within a shelter having a dose transmission factor of 0.01.

The blast and thermal radiation curves cannot be related directly to damage, because of the increasing duration of blast and thermal phenomena with increasing yield and the dependence of the degree of damage sustained on the duration of the damage-producing effect. To assist in relating the curves presented to expected damage, the following table shows the variation with yield of the magnitude of weapon phenomena required to cause various degrees of damage to certain selected targets. (Refer to secs. VI through XII for a more detailed presentation of damage criteria.)

	1 KT	*100 KT*	*10 MT*
Thermal effects:		(cal/cm²)	
Second degree bare skin burn	4	5.1	9.1
Newspaper ignition	2.9	5.1	9.1
White pine charring	10	18	32
Army khaki summer uniform destruction	18	31	56
Navy white uniform destruction	34	60	109
Blast effects (in the Mach region):			
Severe damage to overpressure sensitive structures:		(PSI overpressure)	
Blast-resistant designed buildings	50	40	35
Reinforced concrete buildings	10.5	9.5	9
Monumental wall bearing buildings	20	15	15
Wood frame housing	3	3	3
Window pane breakage	0.5	0.5	0.5
Severe damage to dynamic pressure sensitive structures:		(PSI dynamic pressure)	
Light steel frame single story buildings	4.5	2	0.9
Heavy steel frame single story buildings	6	3	1.5
Steel frame multistory buildings	7.5	2.5	0.9
150′–250′ span truss bridges	50	8	5.5

Some curves are extrapolated beyond data presented in part one, since it is felt that the relationships between phenomena as shown will hold in those regions where there is little supporting knowledge, even though the actual values may be questionable. Since thermal curves are extended beyond one-half the visibility, their interpretation in that region must be approached with caution. In figures B and C, the relative air density would decrease as the actual height of burst is increased in a real case. However, it is held constant for illustrative purposes here. The conversion from slant range to ground range, plus the variation in enhancement of gamma radiation, causes the change in the shape of the radiation curves with change of burst height. Fallout contours are elliptical; only the downwind extent is shown.

Reliability. Varies with the phenomenon of interest. See part one.

Related material.

See paragraph 5.5.

FIGURE 5-2

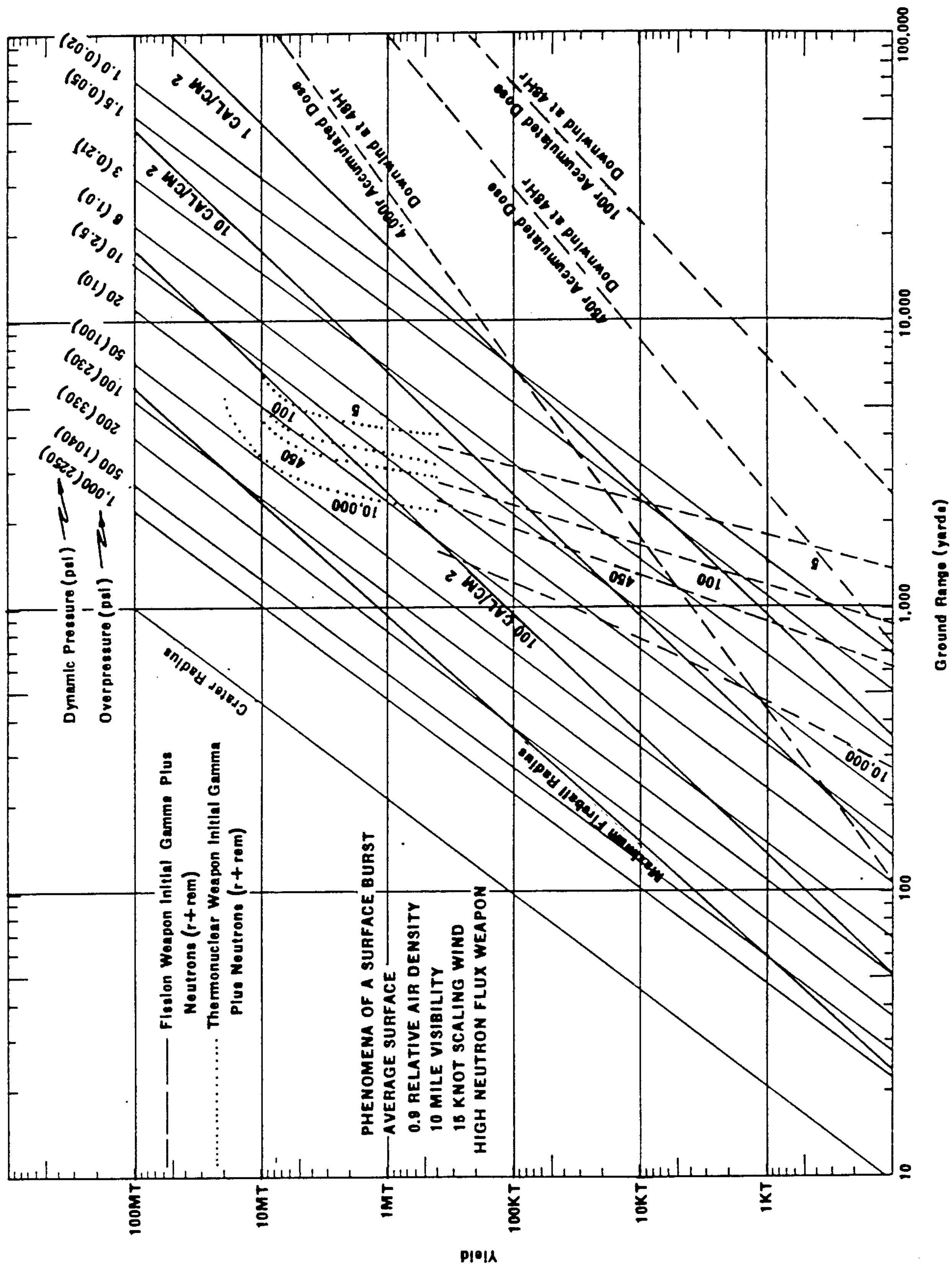
Dynamic Pressure (psi)
Overpressure (psi)
1.0 (0.02)
1.5 (0.05)
3 (0.21)
6 (1.0)
10 (2.5)
20 (10)
50 (100)
100 (230)
200 (330)
500 (1040)
1,000 (2250)
1 CAL/CM 2
10 CAL/CM 2
100 CAL/CM 2
Downwind at 48Hr
4,000r Accumulated Dose
Downwind at 48Hr
400r Accumulated Dose
Downwind at 48Hr
100r Accumulated Dose
5
100
450
10,000
Crater Radius
Maximum Fireball Radius
— Fission Weapon Initial Gamma Plus Neutrons (r+rem)
..... Thermonuclear Weapon Initial Gamma Plus Neutrons (r+rem)
PHENOMENA OF A SURFACE BURST
AVERAGE SURFACE
0.9 RELATIVE AIR DENSITY
10 MILE VISIBILITY
15 KNOT SCALING WIND
HIGH NEUTRON FLUX WEAPON
100MT
10MT
1MT
100KT
10KT
1KT
Yield
10
100
1,000
10,000
100,000
Ground Range (yards)

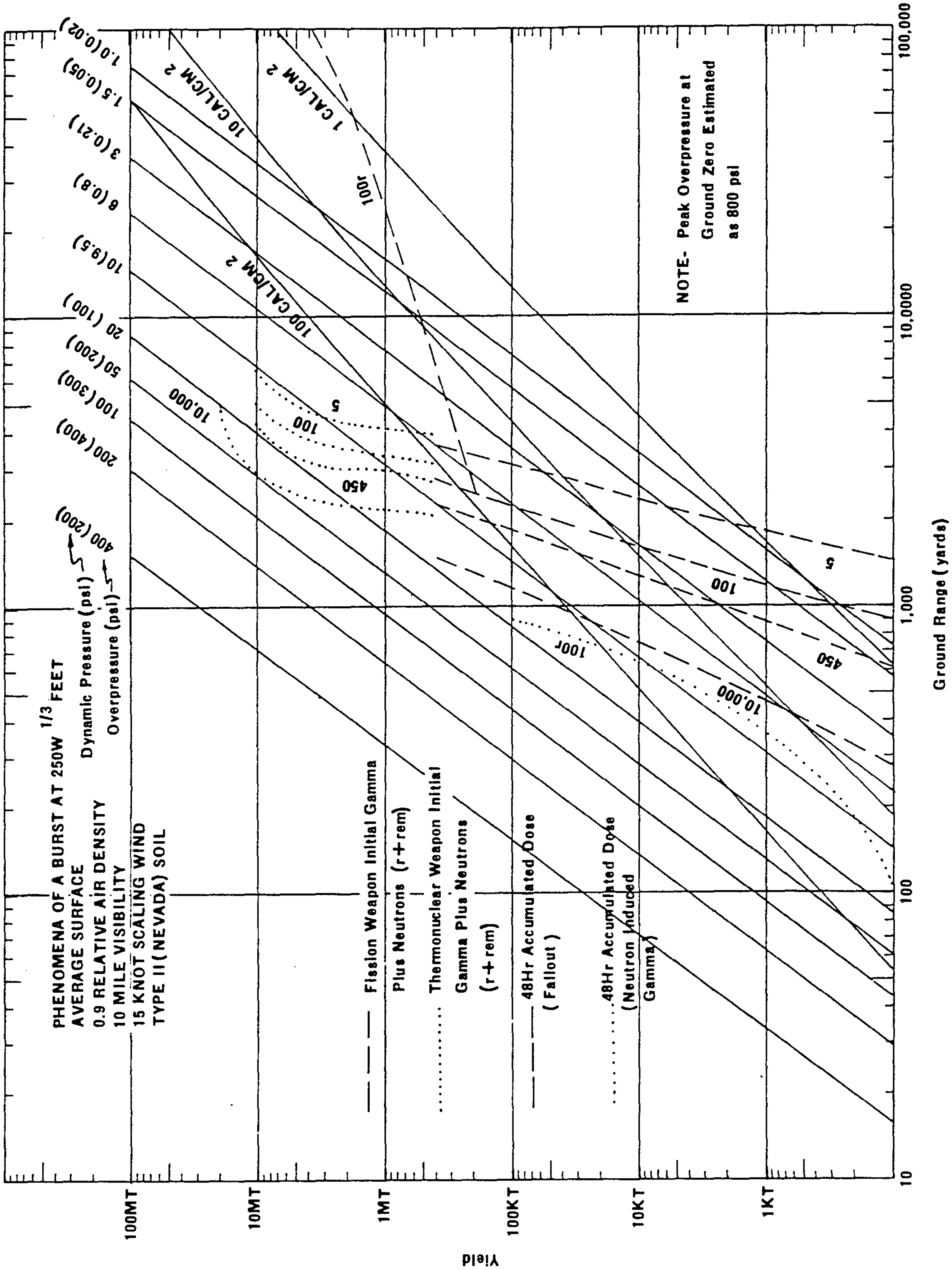
PHENOMENA OF A BURST AT 250W 1/3 FEET
AVERAGE SURFACE
0.9 RELATIVE AIR DENSITY
10 MILE VISIBILITY
15 KNOT SCALING WIND
TYPE II (NEVADA) SOIL
Dynamic Pressure (psi)
Overpressure (psi)
1.0 (0.02)
1.5 (0.05)
3 (0.21)
6 (0.8)
10 (9.5)
20 (100)
50 (200)
100 (300)
200 (400)
400 (200)
10 CAL/CM 2
1 CAL/CM 2
100 CAL/CM 2
NOTE- Peak Overpressure at Ground Zero Estimated as 800 psi
Fission Weapon Initial Gamma Plus Neutrons (r+rem)
Thermonuclear Weapon Initial Gamma Plus Neutrons (r+rem)
48Hr Accumulated Dose (Fallout)
48Hr Accumulated Dose (Neutron Induced Gamma)
10,000
100
5
450
100r
10,000
Ground Range (yards)
10
100
1,000
10,0000
100,000
Yield
100MT
10MT
1MT
100KT
10KT
1KT

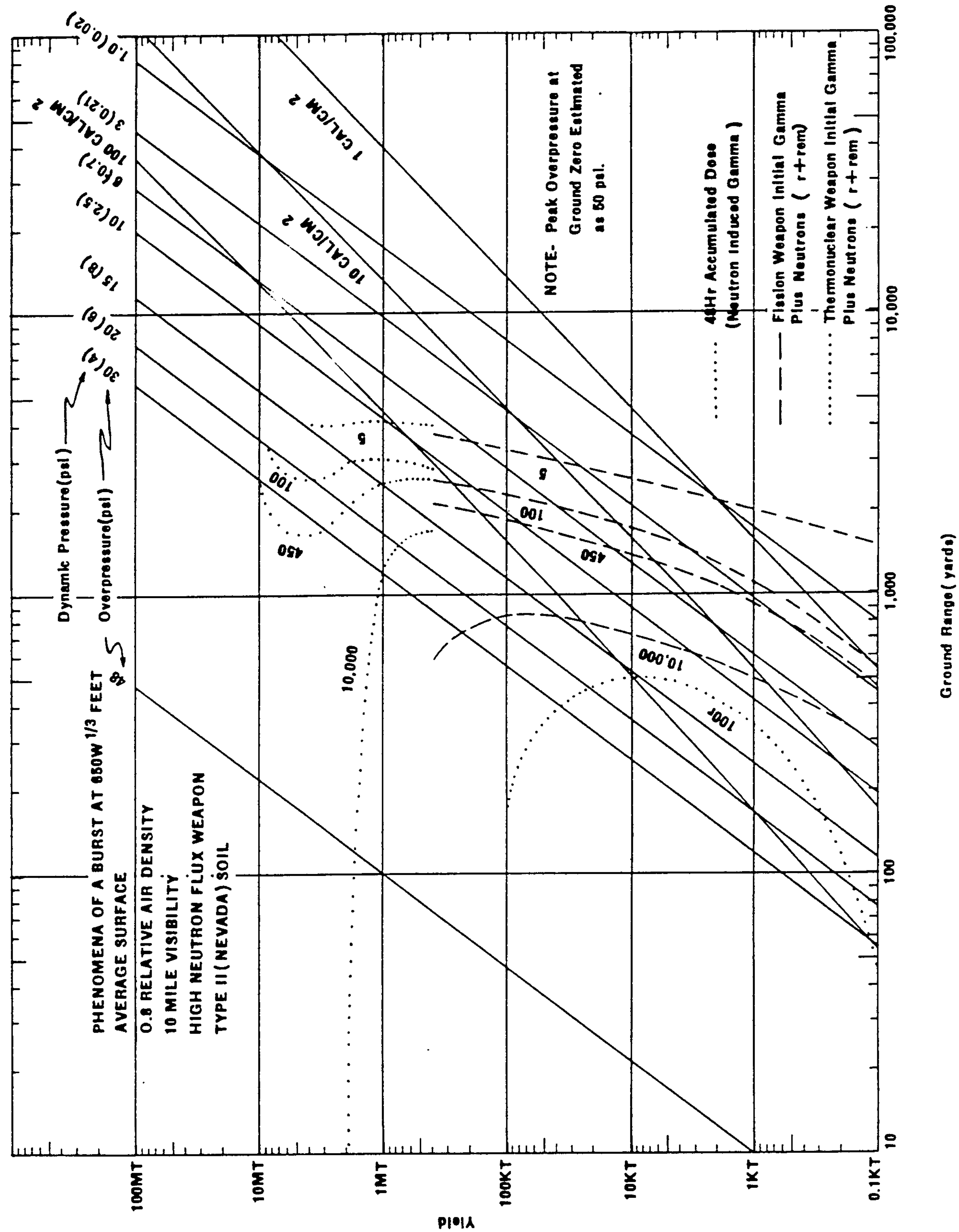
PHENOMENA OF A BURST AT 650W 1/3 FEET
AVERAGE SURFACE
0.8 RELATIVE AIR DENSITY
10 MILE VISIBILITY
HIGH NEUTRON FLUX WEAPON
TYPE II (NEVADA) SOIL
NOTE- Peak Overpressure at Ground Zero Estimated as 50 psi.
48Hr Accumulated Dose (Neutron Induced Gamma)
Fission Weapon Initial Gamma Plus Neutrons (r+rem)
Thermonuclear Weapon Initial Gamma Plus Neutrons (r+rem)
Dynamic Pressure(psi)
Overpressure(psi)
1.0(0.02)
3(0.21)
6(0.7)
10(2.5)
15(8)
20(6)
30(4)
48
100 CAL/CM 2
10 CAL/CM 2
1 CAL/CM 2
5
100
450
10,000
Ground Range (yards)
10
100
1,000
10,000
100,000
Yield
100MT
10MT
1MT
100KT
10KT
1KT
0.1KT

PHENOMENA NOMOGRAMS FOR VARIOUS SCALED BURST HEIGHTS

Figures 5-3A, B, and C are nomograms which present various physical phenomena as a function of yield and slant range for a burst on the surface, at a scaled height of burst of 250 $W^{1/3}$ feet, and at a scaled height of burst of 650 $W^{1/3}$ feet, respectively. These nomograms afford a means of quick comparison of the slant ranges to which various phenomena extend under certain fixed conditions. It will rarely occur that all of these conditions are satisfied in a given situation. Thus, the answers to specific problems should normally be derived from the curves of part one. In addition, it is possible to generate some information from the nomograms which is outside the reliability criteria specified for the curves in part one from which the nomograms were derived. In these cases the reliability cannot be stated, but it may be assumed to be poor. Figure 5-3D is furnished to facilitate the conversion of slant range to horizontal distance for the specific heights of burst used in the phenomena nomograms.

Figures 5-3A, B, and C contain a range scale for each of the phenomena; a common scale on which is read initial gamma dose (roentgens), initial neutron dose (rem), or thermal exposure (cal/cm^2); peak pressure scales which give peak dynamic pressure and peak overpressure in psi; and scales of yield in KT. On figures 5-3A and 5-3C one yield scale is common to all phenomena except initial gamma radiation, while on figure 5-3B thermal exposure and initial gamma radiation both require separate yield scales.

To find the level of phenomena for a given yield, scaled height of burst, and slant range, select the appropriate nomogram for the height of burst, then connect the yield on the appropriate yield scale with the range on the appropriate range scale by a straight line. This line extended will intersect the appropriate phenomenon line at the level sought. The process is then repeated for all phenomena of interest. Conversely, a line connecting a particular level of any phenomenon with a yield on the yield scale for that phenomenon will intersect the range scale for that phenomenon at the range to which that particular level will extend.

In addition to the various scales described above, figure 5-3A contains two tick marks which may be used in conjunction with the yield and range scales for blast phenomena to determine crater dimensions (radius and depth) for a surface burst. A straight line connecting either of these marks with the proper yield on the blast phenomena yield scale will intersect the blast phenomena range scale at a point at which that particular dimension may be read.

Figure 5-3D contains a yield scale to be used for a scaled height of burst of 250 $W^{1/3}$ feet and one to be used for a scaled height of burst of 650 $W^{1/3}$ feet. It also contains a slant range scale, a horizontal distance scale, and two auxiliary scales. To obtain a horizontal distance corresponding to a given yield, scaled height of burst, and slant range, connect the yield on the appropriate yield scale and the slant range on the slant range scale with a straight line. Note the value at which this line, extended, crosses auxiliary scale number 1. Locate the value read from auxiliary scale number 1 on auxiliary scale number 2 and connect this point on auxiliary scale number 2 with the slant range on the slant range scale by a straight line. This line will cross the horizontal distance scale at the desired horizontal distance. If the line connecting yield and slant range goes off scale on the auxiliary scale number 1 in a direction such that the reading would be less than 1, the horizontal distance may be taken to be equal to the slant range. If the same line goes off scale such that the reading on auxiliary scale number 1 would be equal to or greater than 10, the height of burst is equal to or greater than the slant range being used and horizontal distance is zero or meaningless. It should be noted that figure 5-3D does not provide an easy method for obtaining a slant range for a given yield, height of burst and horizontal distance. This can be accomplished only through trial and error on figure 5-3D.

Example.

(1) *Given:* A 40 KT typical fission weapon is burst on an average surface. The visibility is 10 miles and relative air density is 0.9.

Find:

(*a*) The values of thermal exposure, initial gamma dose, initial neutron dose, peak overpressure, and peak dynamic pressure on the surface 2,000 yards from the burst.

(b) The radius and depth of the crater.

Solution: (a) From figure 5-3A, the desired values are—

Thermal exposure	*7.5 cal/cm²*	*Answer.*
Initial gamma dose.	*85 r*	*Answer.*
Initial neutron dose.	*23 rem*	*Answer.*
Peak overpressure	*4 psi*	*Answer.*
Peak dynamic pressure.	*0.4 psi*	*Answer.*
(b) Crater radius	*72 yds*	*Answer.*
Crater depth	*18 yds*	*Answer.*

(2) *Given:* A 4 MT thermonuclear weapon is burst at a height of 250 $W^{1/3}$ feet above an average surface. Visibility is 10 miles and relative air density is 0.9.

Find: The values of thermal exposure and initial nuclear radiation dose at a point where the peak overpressure is 15 psi.

Solution: From figure 5-3B the slant range at which this burst causes an overpressure of 15 psi is 3,600 yards. At this range the values of the other phenomena are—

Thermal exposure	*610 cal/cm²*	*Answer.*
Initial gamma dose.	*170 r*	*Answer.*
Initial neutron dose.	*105 rem*	*Answer.*

(3) *Given:* A 100 KT fission weapon is burst at a height of 650 $W^{1/3}$ feet above an average surface.

Find: The horizontal distance to which 15 psi peak overpressure extends.

Solution: From figure 5-3C, the slant range at which this burst causes a peak overpressure of 15 psi is 1,500 yards.

On figure 5-3D, the line connecting 100 KT on the 650 $W^{1/3}$ height of burst yield scale with 1,500 yards on the slant range scale intersects the auxiliary scale number 1 at a value of 6.8. The line connecting the value of 6.8 on the auxiliary scale number 2 with 1,500 yards on the slant range scale intersects the horizontal distance scale at *1,100 yards. Answer.*

Reliability. The same as for the various curves in part one from which these nomograms were derived, except where the limits of the reliability criteria for any curve are exceeded, in which case the reliability is unknown but may be assumed to be poorer than when the limits are not exceeded.

Related material.

See paragraph 5.5.

See also figures 5-2A, B, and C.

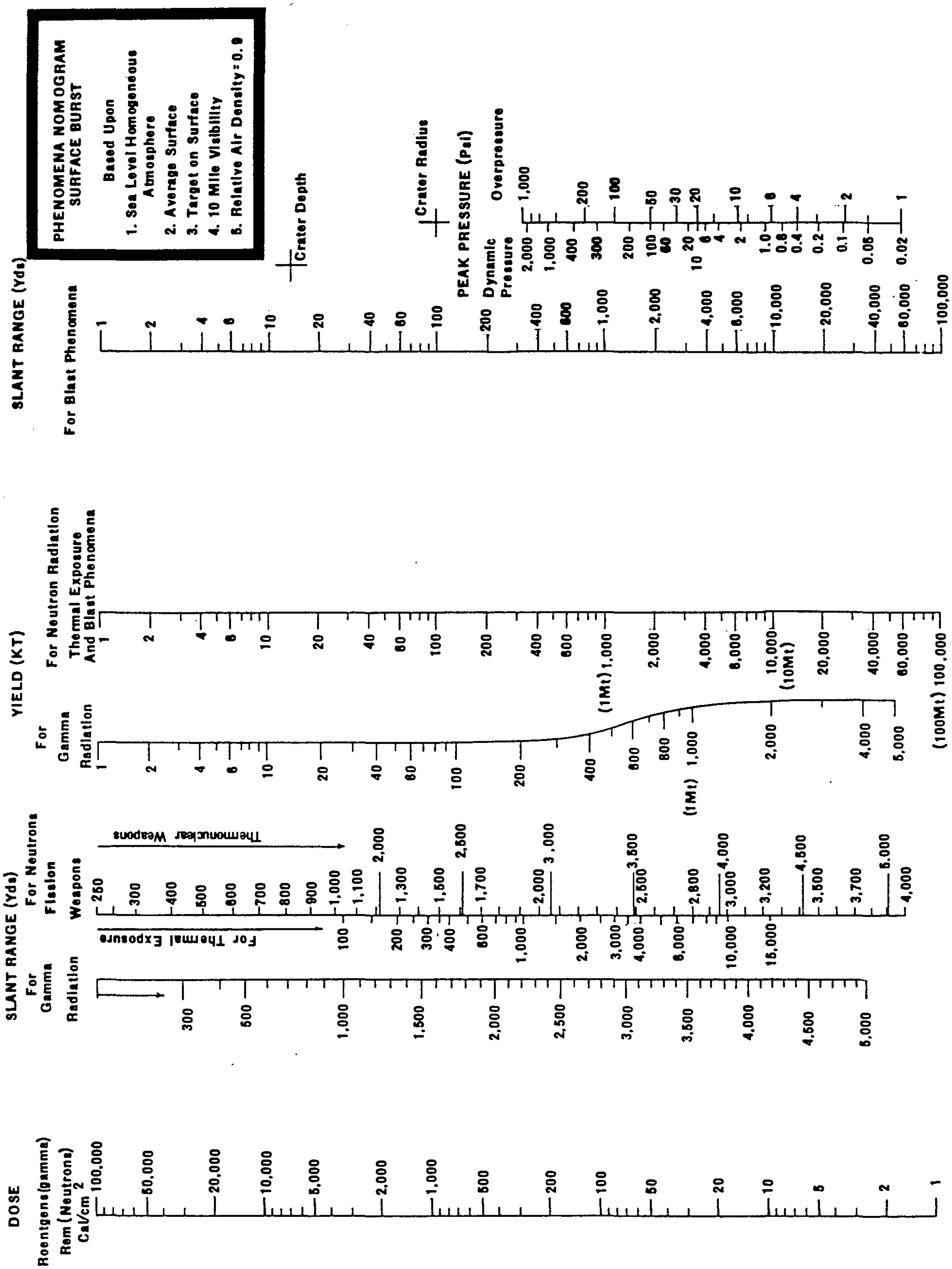
PHENOMENA NOMOGRAM
SURFACE BURST
Based Upon
1. Sea Level Homogeneous Atmosphere
2. Average Surface
3. Target on Surface
4. 10 Mile Visibility
5. Relative Air Density = 0.9
SLANT RANGE (Yds)
For Blast Phenomena
Crater Depth
Crater Radius
PEAK PRESSURE (Psi)
Dynamic Pressure
Overpressure
YIELD (KT)
For Neutron Radiation Thermal Exposure And Blast Phenomena
For Gamma Radiation
(1Mt)
(10Mt)
(100Mt)
SLANT RANGE (Yds)
For Neutrons Fission Weapons
Thermonuclear Weapons
For Thermal Exposure
For Gamma Radiation
DOSE
Roentgens (gamma)
Rem (Neutrons)
Cal/cm 2

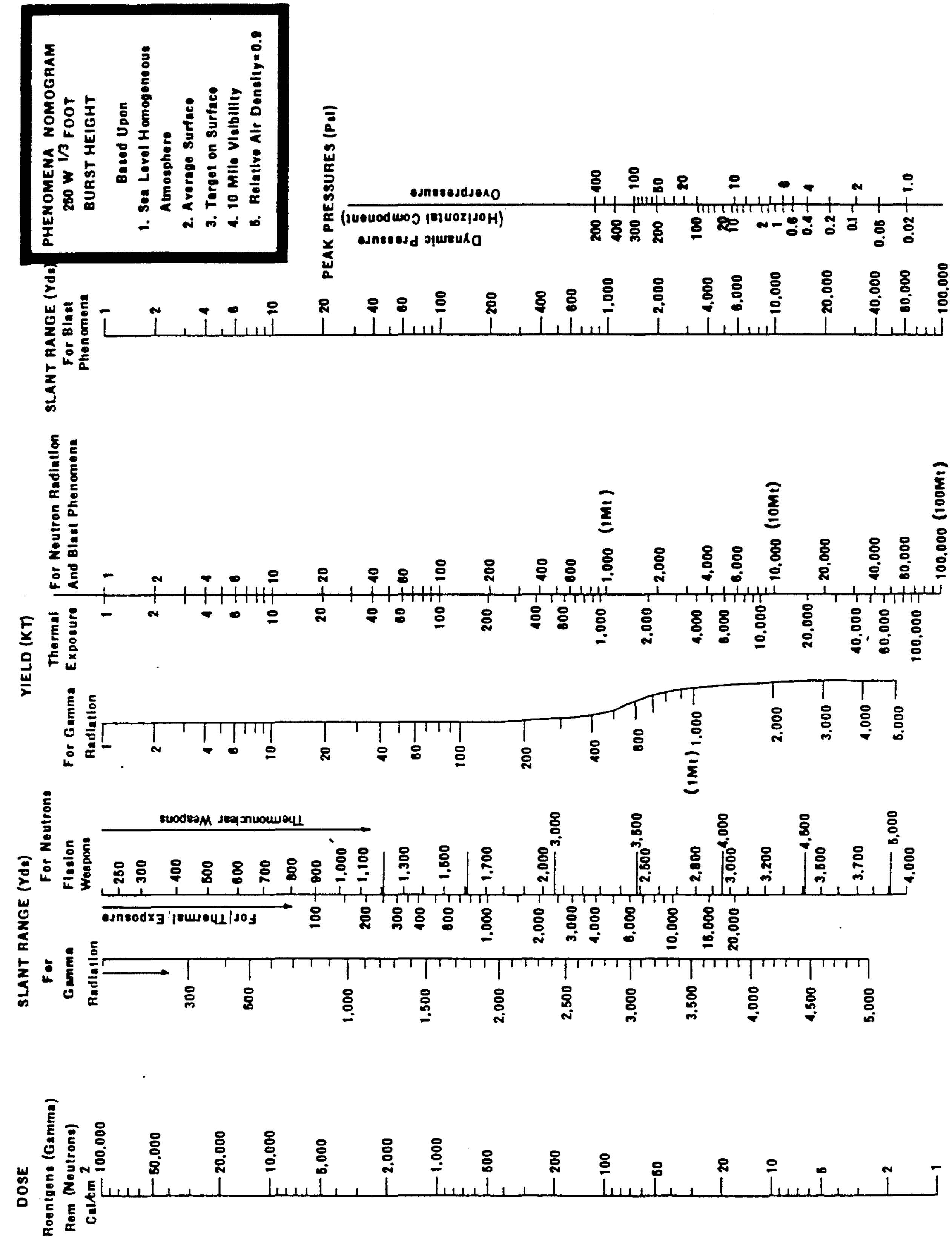
PHENOMENA NOMOGRAM
250 W 1/3 FOOT
BURST HEIGHT
Based Upon
1. Sea Level Homogeneous Atmosphere
2. Average Surface
3. Target on Surface
4. 10 Mile Visibility
5. Relative Air Density=0.9
PEAK PRESSURES (Psi)
Overpressure
Dynamic Pressure (Horizontal Component)
SLANT RANGE (Yds) For Blast Phenomena
YIELD (KT)
For Neutron Radiation And Blast Phenomena
Thermal Exposure
For Gamma Radiation
SLANT RANGE (Yds)
For Neutrons
Fission Weapons
Thermonuclear Weapons
For Thermal Exposure
For Gamma Radiation
DOSE
Roentgens (Gamma)
Rem (Neutrons)
Cal/cm 2

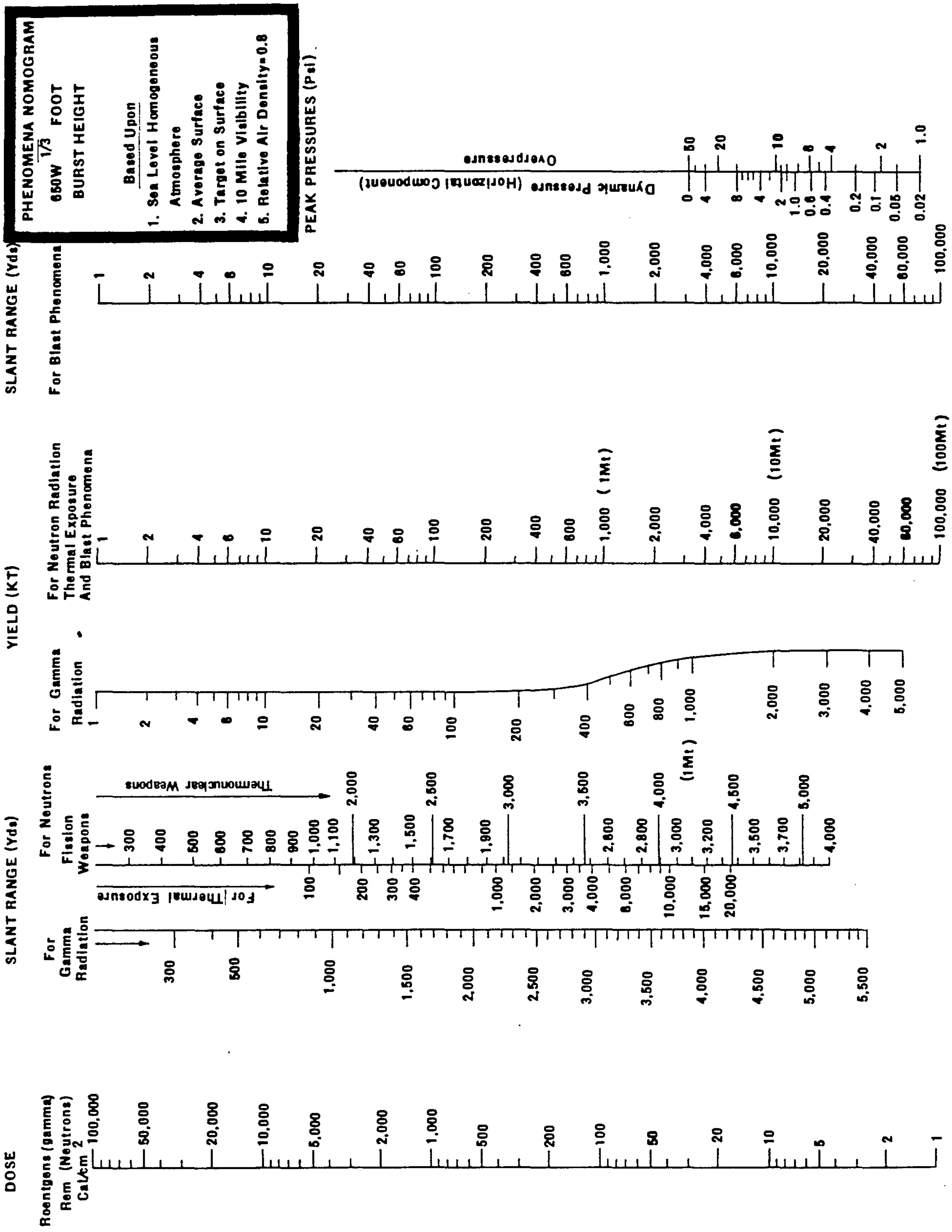
PHENOMENA NOMOGRAM
650W 1/3 FOOT
BURST HEIGHT
Based Upon
1. Sea Level Homogeneous Atmosphere
2. Average Surface
3. Target on Surface
4. 10 Mile Visibility
5. Relative Air Density=0.8
PEAK PRESSURES (Psi)
Overpressure
Dynamic Pressure (Horizontal Component)
SLANT RANGE (Yds)
For Blast Phenomena
YIELD (KT)
For Neutron Radiation Thermal Exposure And Blast Phenomena
(1Mt)
(10Mt)
(100Mt)
For Gamma Radiation
SLANT RANGE (Yds)
For Neutrons
Thermonuclear Weapons
Fission Weapons
For Thermal Exposure
For Gamma Radiation
DOSE
Roentgens (gamma)
Rem (Neutrons)
Cal/cm 2

RANGE CONVERSION NOMOGRAM

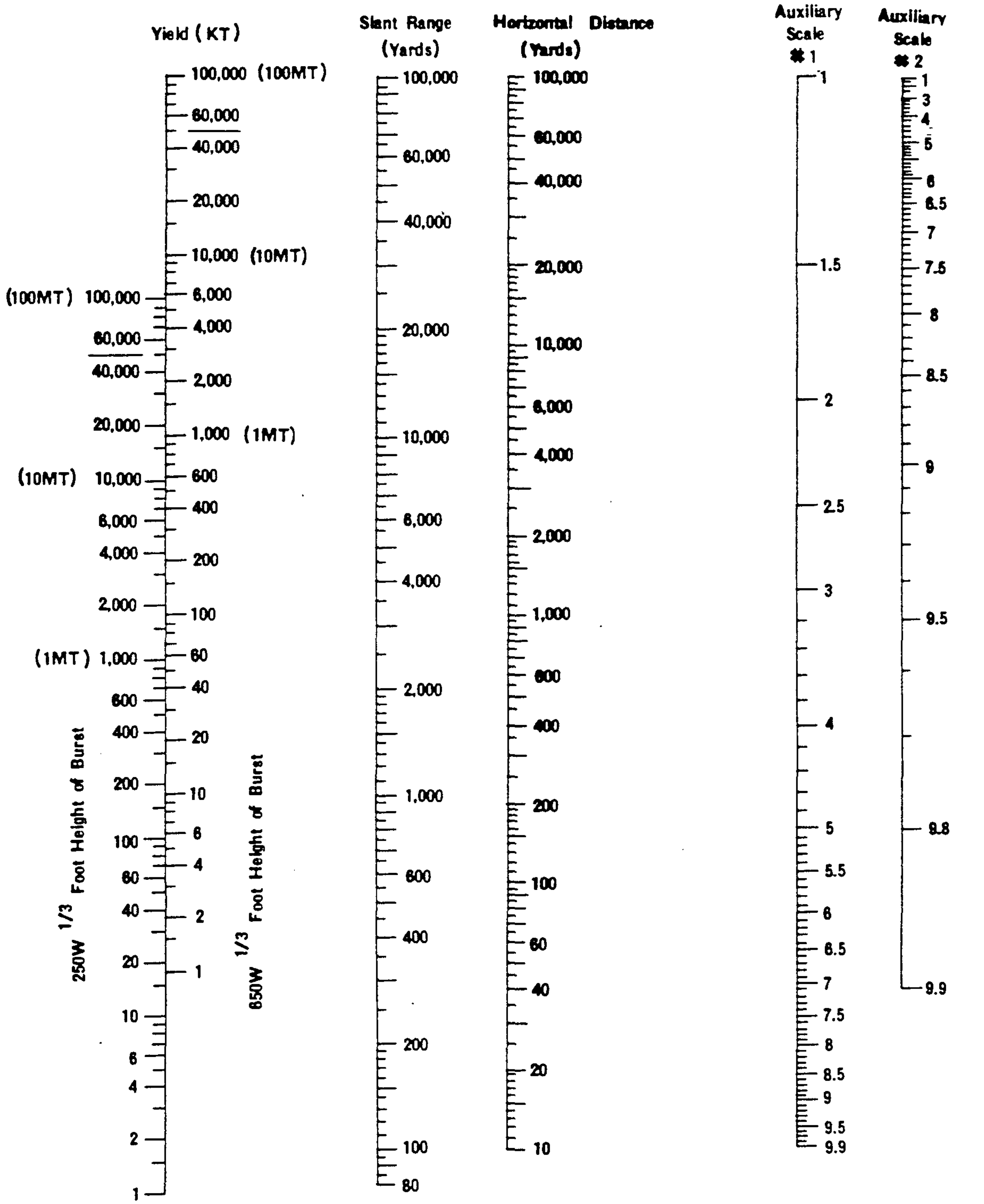

BLANK

6
Personnel

SECTION VI
PERSONNEL CASUALTIES

6.1 Air Blast and Mechanical Injury

a. General. The air blast from a nuclear detonation may cause casualties among human beings in two ways—direct blast injury and indirect blast injury.

b. Direct Blast Injury.

(1) *Crushing forces.* Although the human body is relatively resistant to the crushing forces which result from air blast loading, large pressure differences resulting from blast wave overpressures may cause damage to lungs, abdominal organs and other gas-filled body organs. Based on data obtained from high explosive detonations, it is estimated that on the order of 200 to 300 psi peak overpressure is required to cause death in humans, provided no translational motion occurs. However, the long duration of the overpressure from a nuclear explosion may appreciably lower this peak overpressure criterion. In any event, no crushing injury other than ear drum rupture occurs for a peak overpressure of less than 35 psi. Although ear drum rupture may result from peak overpressures of 7 to 15 psi, this is not considered a disabling injury, and the overall effectiveness of a unit will not be hampered by the occurrence of these injuries. Therefore, since other damage producing effects are overriding at pressures above 35 psi, crushing forces as such need not be considered as a primary mechanism of producing casualties to personnel in the field.

In structures of certain types, such as bomb shelters or permanent type gun emplacements, where adequate shielding exists against thermal and nuclear radiation, the design of the structure may permit the build-up of blast pressure due to multiple reflections. Blast injuries may therefore occur inside even though the free air overpressure outside the structure would not be sufficient to cause injury.

Both ear drum rupture and other bodily damage which may result from overpressure are largely dependent upon the characteristics of the shock front. If the rise time is long, the body organs are subjected to less severe pressure differences and also are able to better adapt themselves to high overpressure. Consequently, the probability of injury is reduced.

(2) *Translational Forces.*

(*a*) *Mechanisms.* The translational force to which an individual exposed to a blast wave is subjected depends primarily on drag forces. Since the human body is relatively small and the blast wave almost immediately envelops it, the diffraction process is short. The translational force may be predicted with reasonable accuracy if the burst position, yield, terrain, and the orientation of the human body are known. Since the translational force applied depends on the exposed frontal surface area of the human body, an individual standing in the open is subjected to much larger translational forces than an individual lying on the ground surface. Thus, assuming a prone position at the instant a nuclear bomb flash is detected is quite effective in reducing the likelihood of injuries resulting from bodily translation. In addition, the translational forces are appreciably reduced for an individual who is behind a building or in a shelter which is sufficiently blast resistant. The degree of protection afforded by a foxhole against injury resulting from translation is not too well known at present. However, appreciable protection should be provided if the foxhole is deep enough to prevent lifting therefrom.

(*b*) *Criteria for injury.* Although no direct correlation is known between translational motion parameters and injury, it is reasonable to assume that some relationship exists. The initial rate of acceleration, the motions of various parts of the body while being translated, and the nature of the impact, all certainly contribute to injury. Probably most injuries will result from impact. The severity of injury will depend on the nature of the object or objects with which the translated body collides, the nature of the impact, whether glancing or solid, and the velocity at impact. Some individuals may survive a large translation, whereas others may be severely injured or killed by a relatively small translation. Because increased yield results in increased positive phase duration, attainment of velocities sufficient to cause injury on impact will occur for lower peak pressures. The manner of impact likewise depends on the nature of the terrain and surface configuration. If solid impact occurs, it is estimated that body velocities of about 12 feet per second will produce serious injury approximately 50 percent of the time, while collision at about 17 feet per second will result in approximately 50 percent mortality. Figure 6–1 is a plot of burst height vs. ground range at which 50 percent of standing and prone personnel in the open are expected to become direct blast casualties. The curves are drawn for 1 KT and may be scaled to other yields by multiplying the burst heights by the cube root of the yield and the ground distance by the four-tenths power of the yield.

c. Indirect Blast Injury.

(1) *General.* Indirect blast casualties result from burial by debris from collapsed structures with attendant production of fractures and crushing injuries, from missiles placed in motion by the blast wave, or from fire or asphyxiation where individuals are prevented from escaping the wreckage.

(2) *Personnel in structures.* A major cause of personnel casualties in cities is structural collapse and damage. The number of casualties in a given situation may be reasonably estimated if the structural damage is known. Table 6–1 shows estimates of casualty production in two types of buildings for several damage levels. Data from Section VII may be used to predict the ranges at which specified structural damage occurs. Demolition of a brick house is expected to result in approximately 25 percent mortality, with 20 percent serious injury and 10 percent light injury. On the order of 60 percent of the survivors must be extricated by rescue squads. Without rescue they may become fire or asphyxiation casualties, or in some cases be subjected to lethal doses of residual radiation. Reinforced concrete structures, though much more resistant to blast forces, produce almost 100 percent mortality on collapse. The figures of table 6–1 for brick homes are based on data from British World War II experience. It may be assumed that these predictions are reasonably reliable for those cases where the population is in a general state of expectancy of being subjected to bombing and that most personnel have selected the safest places in the buildings as a result of specific air raid warnings. For cases of no prewarning or preparation, the number of casualties is expected to be considerably higher. To make a good estimate of casualty production in structures other

than those listed in table 6–1, it is necessary to consider the type of structural damage that occurs and the characteristics of the resultant missiles. Glass breakage extends to considerably greater ranges than almost any other structural damage, and may be expected to produce large numbers of casualties at ranges where personnel are relatively safe from other effects, particularly for an unwarned population.

Table 6–1. Estimated Casualty Production in Structures for Various Degrees of Structural Damage

	Killed outright	Serious injury (hospitalization)	Light injury (No hospitalization)
1–2 story brick homes (high explosive data):	*Percent*	*Percent*	*Percent*
Severe damage	25	20	10
Moderate damage	<5	10	5
Light damage	------	<5	<5
Reinforced-concrete buildings (Japanese data, nuclear):			
Severe damage	100	------	------
Moderate damage	10	15	20
Light damage	<5	<5	15

Note. These percentages do not include the casualties which may result from fires, asphyxiation, and other causes from failure to extricate trapped personnel. The numbers represent the estimated percentage of casualties expected at the maximum range where the specified structural damage occurs. For the distances at which these degrees of damage occur for various yields, see section VII.

(3) *Personnel in vehicles.* Personnel in vehicles may be injured as a result of the response of the vehicle to blast forces. Padding where applicable and the use of safety belts, helmets, and harnesses virtually eliminates this source of casualties, at least within armored vehicles. In the absence of these protective devices, serious lacerations may result from impact with sharp projections within the vehicle interiors. Comparative numbers of casualties are almost impossible to assess in this respect due to the many variables which are involved.

(4) *Personnel in the open.* Missiles translated by the blast wave may be a significant source of injury to exposed personnel. Missiles having low velocities, if of sufficient size, may cause crushing injuries. In contrast, penetrating wounds may be caused by high velocity missiles. The missile density and characteristics are largely a function of the target. Where the target area is relatively clean and there is little material present subject to fragmentation and displacement, fewer injuries from missiles are expected in the open than from debris within structures at comparable distances. When the target complex presents many possible sources of missiles this may not be the case. Personnel in a prone position are less likely to be struck by flying missiles than those who remain standing. Those who succeed in getting into bunkers, foxholes, or in defilade probably will achieve almost complete protection from the flying missile hazard.

6.2 Thermal Injury

a. Introduction. Before attempting to predict the number of thermal casualties which occur in a given situation, it is necessary to recognize the factors which influence the number and distribution of casualties to be expected. These factors include—the distribution or deployment of personnel within the target area, whether proceeding along a road, in foxholes, standing or prone, in the open or under natural cover; orientation with respect to the bomb; clothing, including number of layers, color, weight, and whether the uniform includes helmets, gloves, or other devices which might protect the bare skin, such as flash creams; and natural shielding. These parameters which define the target must be considered along with the factors which define the source of radiation such as yield of the weapon, height of burst, and visibility, as discussed in section III. In many target complexes, a large percentage of thermal casualties may be due to secondary burns. This is particularly true in cities and industrial areas where a major part of the direct radiation may be shielded by intervening structures. Because of the number of factors involved, it is necessary to analyze each particular target situation in order to make realistic predictions of the thermal casualties to be expected.

b. Primary Radiant Energy Burns. Damage to bare skin through the production of burns may be directly related to the radiant exposure and the rate of delivery of the thermal radiation, both of which are yield dependent. For a given total exposure, as the weapon yield increases, the thermal radiation is delivered over a longer period of time and thus at a lower rate. This allows energy loss from the skin surface by conduction to the deeper layers of the skin and by convection to the air. Thus, a given level of damage also is yield dependent. Critical radiant exposures for the production of two degrees of burn on bare skin as a function of yield are presented in figure 6–2 for normal incidence of radiation. Although the data are presented as a single curve, it must be recognized that there will be variations due to factors such as skin color (i. e., darker skin requires a lesser exposure to produce a given severity of burn) and skin temperature (i. e., colder skin as is found in winter or in arctic climates requires a greater exposure to produce the given burn). The curves represent those radiant exposures which will burn 50 percent of any group, including these variants. A first degree burn is defined as one which shows redness; a second degree burn exhibits partial skin destruction or blistering.

c. Burns Under Clothing. Clothing reflects and absorbs much of the thermal radiation incident upon it and thereby protects the wearer against flashburn. In some cases, the protection is complete, but in many cases it is partial in that clothing merely reduces the severity of injury rather than preventing it. At large radiant exposures, there is the additional possibility that the glowing or ignition of the clothing could deliver additional energy to the skin, thereby causing a more severe injury than bare skin would have suffered. There are many factors which contribute to the degree of protection which clothing affords the underlying skin. The thermal resistance of the clothing material itself is probably the most important, as skin burns under undamaged cloth are rarely seen unless the cloth is in close contact with the skin. Other factors are the weight and weave of the fabric; the number of clothing layers worn; the spacing between layers and between the inner layer and the skin; the moisture content, initial temperature, and color of the cloth; the amount and kind of dirt in the cloth; the wind velocity and direction across the surface of the cloth; etc.

The complexity of the interrelations among the above factors makes an accurate prediction extremely difficult. Table 6–2 lists various estimates of radiant exposures required to effect burns under clothing. These values are considered representative of some field conditions, within the limitations due to the varying factors described above.

Table 6–2. Critical Radiant Exposures for Burns Under Clothing

(Expressed in cal/cm² incident on outer surface of cloth)

Clothing	Burn	1 KT	100 KT	10 MT
Summer Uniform	1°	8	11	14
(2 layers)	2°	20	25	35
Winter Uniform	1°	60	80	100
(4 layers)	2°	70	90	120

Note. These values are sensitively dependent upon many variables which are not easily defined (see text), and are probably correct within a factor of two.

d. The Combat Ineffective. A useful term in the discussion of effects of thermal radiation on personnel is "the combat ineffective." A combat ineffective is defined as a person who, because of his injuries, is no longer capable of carrying out his assigned tasks. This is differentiated from the more common term "casualty," which is defined as an individual whose injuries require medical attention. Damage to certain areas of the body produces a greater number of combat ineffectives than damage to other areas. Burns in the area surrounding the eyes which eventually cause the eyes to swell shut, and burns to the hands which lead to loss of mobility are particularly apt to cause ineffectiveness.

If a sufficient portion of the total body area is burned, physiological shock follows and the individual becomes a casualty. When more than 10 to 15 percent of the total body area receives second degree burns or worse, shock may be expected. The efficacy of injuries to the hands and eyes in producing combat ineffectives, coupled with the vulnerability of these parts due to lack of protection under ordinary circumstances, indicates the importance of providing protection for these areas when nuclear attack is likely. Table 6–3 presents estimates of the production of combat ineffectives by various degrees of thermal injury.

Table 6-3. Combat Ineffectives Due to Thermal Injury

	1° burns	2° burns
Both eyes	Combat effective*	Combat ineffective.
Both hands	Combat effective	Combat ineffective.
15% burns excluding hands and eyes.	Combat effective	A few ineffectives (10–15%).
25% burns excluding hands and eyes.	Combat effective	Up to 50% ineffective.

*Some lowering of effectiveness may be expected; however, all should be able to perform combat duties.

e. Thermal Shielding.

(1) *General.* In addition to the protection provided to troops by clothing as discussed above, other possible sources of protection should be considered. Almost any nontransparent material withstands the thermal radiation long enough to afford some shielding to an object behind it. Heavy smoke screens are excellent energy absorbers as described in section III.

Because of the ease of complete shielding from thermal radiation, the amount of forewarning, if any, is of utmost importance to exposed personnel. Covered foxholes or bunkers are excellent thermal shields. The degree to which uncovered foxholes afford protection is related to the height of burst and the distance from ground zero as well as the position of the man within the foxhole. The nearer foxholes offer less protection, since the shadowed portion is a smaller fraction of the total volume. At greater distances from low yield weapons, burns are produced only on those areas subjected to the direct radiation, since reflection from the exposed surfaces of the foxholes may be neglected. Under high megaton burst conditions, a sufficient amount of thermal radiation may be reflected and produce casualties. In highly scattering atmospheres, such as fog or haze, scatter of the radiation into the foxholes could become an important factor. It is important to note than many targets contain openings such as windows in buildings and aircraft, and ports in tanks and ships. While the general target may not be damaged by external thermal radiation, openings in these targets may allow damaging amounts of thermal radiation to fall on personnel inside.

(2) *Evasive action.* Figure 6–3 demonstrates that evasive action against thermal radiation following the detonation of weapons up to 100 KT is not expected to be successful due to the rapid delivery of the thermal pulse. For weapons in the megaton range, the thermal pulse is delivered over a period of seconds. Significant portions of this pulse may be avoided by simple evasive action such as covering exposed hands and face, or dropping to the ground.

f. Specific Effects on the Eye. Effects of thermal radiation on the eye may be divided into two categories—flash blindness, which is a transitory loss of vision; and retinal burns, which constitute permanent injuries to the retina of the eye. In general, under daylight conditions, flash blindness is not an important factor in estimating effects on personnel. If the flash occurs during daylight in the forward field of vision, impairment to precise vision does not persist for more than 2 or 3 minutes. If not in the forward field of vision, no impairment is expected. During darkness, impairment of vision persists for 5 to 10 minutes if the detonation is in the forward field of view, and for 1 to 2 minutes if not. Loss of dark adaptation persists for longer periods. When the fireball is in the forward field of vision and in clear atmospheres, retinal burns and some degree of permanent loss of visual acuity may occur at relatively great distances from the detonation. Retinal burns have occurred in a few individuals located at distances of 2 to 10 miles from the point of detonation and are theoretically possible at distances where the other immediate effects of the weapon are minimal. This loss of vision is more severe if the eye is focused directly on the point of detonation. As with flash blindness, this effect is likely to be more severe in situations where the eye is dark-adapted.

g. Secondary Flame Burns and Conflagration Effects may be a source of casualties. Secondary flame burns of the hands and face may occur from ignition of clothing. In areas where conflagrations are likely to result from the detonation, large numbers of burn casualties may occur among individuals trapped in the wreckage of burning buildings or structures, or in forest fires. Under circumstances where conflagrations can occur, individuals in shelters may die of asphyxiation, even though otherwise protected from the other casualty producing effects of the nuclear detonation. After a firestorm or a large scale conflagration begins, it is virtually impossible for an individual to leave the shelter and reach safety through the streets of a burning city.

6.3 Nuclear Radiation Injury

a. General. The radiation effects of a nuclear explosion may be divided into two categories; external radiation (from gamma rays, beta particles, and neutrons) and internal radiation (from gamma rays, alpha and beta particles). The end result in cells receiving doses of these nuclear radiations is qualitatively the same. The effects may be acute or delayed. *Only acute effects will be considered here.* Delayed effects, while important, may not be manifest for years and thus will not affect the immediate military situation.

The essential criterion for injury from ionizing radiation is delivery of the radiation to sensitive body tissues. Thus, external beta radiation affects only the skin, while the penetrating gamma rays and neutrons affect critical tissues within the body. With penetrating radiation from external sources the relationship of the free field dosage to biological effect varies according to the amount of shielding interposed between the source and the critical tissues. In fact, the body itself may shield internal organs from external radiation of low energy or from a single direction.

Radiation can be received in a short time or over an extended period. When received in a short time (i. e., in a few days) the effect is essentially independent of dose rate except for extremely large doses of radiation. (See par. 6.3*d* on immediate incapacitation.) When received over a long period of time, either continuously or in repeated doses, biological recovery takes place. This recovery may not be complete, however. It is not possible to specify for the whole body a definite biological recovery rate or a percentage of irreparable damage, since different tissues have different repair rates and different sensitivities to radiation. As an example, the tissue producing one type of white blood cell may repair at the rate of from 2 to 10 percent per day and incur permanent damage of from 10 to 20 percent of the total injury. The skin on the other hand, unless damaged throughout its thickness, may recover functionally 100 percent. Since in the mid-lethal range the state of the blood forming tissues is directly related to survival, it is perhaps reasonable to consider these tissues as representing the whole body response. This is the reason that studies to measure recovery rates and irreparable damage using LD50/30 (the dose lethal to 50 percent of the test population by the end of a 30-day period) as an end point seem to fit an exponential-type function. What is really being measured is a single critical tissue.

b. External Radiation Hazard. The only external radiations of any consequence are gamma rays and neutrons, and under special circumstances, beta particles. During a nuclear explosion the gamma rays and neutrons alone are important, while in a residual fallout field gamma rays and sometimes beta particles must be considered.

(1) *Gamma radiation* received at the time of detonation is biologically instantaneous. It is from an essentially point source, so is less effective than a corresponding free field dose received from an infinite plane source, such as a residual radiation field. The difference may be expressed thus—in humans an acute free field dose of about 600 roentgens from a point source may be equivalent to about 400 roentgens acute free field dose from a bilateral or an extended source. This dose is currently thought to be the amount required to cause about 50 percent of exposed personnel to die within a month. The best estimates of the effects of various dose ranges in humans are presented in table 6–4.

Table 6-4. Probable Effects of Acute Whole Body Radiation Doses

Acute dose (roentgens)*	Probable effect
0 to 50	No obvious effect except possibly minor blood changes.
80 to 120	Vomiting and nausea for about 1 day in 5 to 10 percent of exposed personnel. Fatigue but no serious disability.
130 to 170	Vomiting and nausea for about 1 day, followed by other symptoms of radiation sickness in about 25 percent of personnel. No deaths anticipated.
180 to 220	Vomiting and nausea for about 1 day, followed by other symptoms of radiation sickness in about 50 percent of personnel. No deaths anticipated.
270 to 330	Vomiting and nausea in nearly all personnel on first day, followed by other symptoms of radiation sickness. About 20 percent deaths within 2 to 6 weeks after exposure; survivors convalescent for about 3 months.
400 to 500	Vomiting and nausea in all personnel on first day, followed by other symptoms of radiation sickness. About 50 percent deaths within 1 month; survivors convalescent for about 6 months.
550 to 750	Vomiting and nausea in all personnel within 4 hours from exposure, followed by other symptoms of radiation sickness. Up to 100 percent deaths; few survivors convalescent for about 6 months.
1,000	Vomiting and nausea in all personnel within 1 to 2 hours. Probably no survivors.
5,000	Incapacitation almost immediately. All personnel will be fatalities within 1 week.

*(1) And/or rem in the case of neutrons. See discussion in paragraph 6.3b(2).
*(2) Continuing investigations indicate that these ranges may be low for corresponding effects by a factor of 2.

(2) *Neutrons*, like the gamma rays, are delivered essentially instantaneously at the time of a nuclear explosion. There is some evidence that in animals the size of a man, neutrons are less effective than hitherto supposed because of rapid attenuation in superficial tissues. The following discussion will depend on an understanding of certain units and terms used in the evaluation of biologically hazardous doses of radiation.

The roentgen equivalent physical (rep) is defined as that dose, of any ionizing radiation, which will produce in a unit volume of the irradiated substance, the same energy absorption which would be produced in the same substance by a roentgen of gamma or X-rays. Inasmuch as different radiations, even though producing the same energy absorption per unit volume, have different effectiveness in producing biological injury, the relative biological effectiveness (RBE) of these various radiations must be taken into account. If, for example, it is found that a rep of neutrons causes 30 percent more damage than a rep of gamma rays, it is said that such neutrons have an RBE of 1.3. X-rays produced at 250 KVP (kilo-volt peak) are assigned an RBE of 1.0, and the hazard of the other radiations is measured in terms relative to the effectiveness of X-rays for producing injury. One can then multiply the reps of any other ionizing radiation by the appropriate RBE to get another unit of dose which is directly proportional to the biological damage, i. e., the roentgen equivalent mammal (rem)—

$$(rep) \times (RBE) = (rem).$$

Rem, correctly measured for each type of ionizing radiation, may be added to obtain the total dose. See paragraph 5.4.

Physical dosimetry of neutrons, however, is difficult. The most consistent indicator which responds to the largest biologically important portion of the bomb neutron spectrum is reduction in weight of the spleen and thymus of mice. This measure serves as a basis for comparing gamma rays and neutrons in a biological system in terms of rem. This rem unit applies strictly to this effect, and it may well be that acute effects in man are not predictable on the basis of presently available data.

The curves of neutron dose given in part one, figures 4-10 and 4-11, give the dose directly in rem, an RBE of 1.3 for whole body neutron radiation

447555 O - 58 - 19

having been assumed in preparing the curves. Therefore, the neutron dose in rem determined from figure 4–10 or 4–11 may be added directly to the gamma dose in roentgens obtained from one of the figures 4–1 through 4–8, and the total dose so determined used in conjunction with table 6–4 to estimate the probable overall effects of the immediate nuclear radiations.

(3) *Beta particles.*

(*a*) *General.* Beta particles, as well as gamma rays, constitute an external hazard from residual contamination. In an extended field of fallout radiation the gamma hazard generally far outweighs that from beta particles. However, the beta hazard may become quite important in certain circumstances, such as—

A person receives fallout particles directly on the body, or lies on a contaminated surface.

Personnel are located in a relatively confined area which has been subjected to fallout, and surrounding structures provide shielding from much of the gamma radiation, as would be the case in a narrow city street.

Fallout particles are removed from the extended field into a new environment, but remain in close proximity to personnel.

(*b*) *Effect.* Beta particle penetration is quite limited and may be partially blocked by thin absorbers such as clothing. Due to the limited range of beta radiation, the skin is the only structure directly affected. Mammals may be killed by total surface beta radiation, however. The amount required for an LD50/45 is inversely proportional to the area/mass ratio (i. e., the amount of skin in relationship to the rest of the body). Small mammals are quite sensitive, there being a good correlation between species in this regard. On this basis man *might* require about 40,000 rep over his whole body surface before entering the mid-lethal range.

It should be pointed out, however, that the LD50 is a poor end point for evaluation of a skin damaging process, and that large area injuries would be highly incapacitating, though not necessarily lethal, within a short period of time. A total surface beta injury is an extremely unlikely possibility. The typical human beta injuries from residual contamination are multiple ones, on surfaces directly exposed to the material. These indicate that direct contact is usually necessary for this type of "beta burn".

(*c*) *Decontamination.* Where personnel have been exposed to direct contact with radioactive fallout particles, a few simple measures greatly reduce the probability of development of beta burns. Immediate showering, bathing, or simple removal by brushing off the particulate matter, accompanied by securing shelter and donning clothing of a protective nature (long-sleeved shirts, cover-alls, shoes, etc.) affords sufficient protection against the beta burn hazard. The longer the fallout remains in contact with the skin, the more severe and extensive the beta burn is likely to be.

c. Internal Radiation Hazard.

(1) *General.* The hazard associated with the intake of radioactive material into the body is present only in cases where fallout occurs. In such instances radioactive elements may be breathed into the lungs or may be swallowed and absorbed from food and water. The vast majority of the radioactive elements which are inhaled do not remain in the lung, because particles must be within a limited size range to be retained. Only a small fraction of the retained particles are likely to be concentrated and fixed in the lung. Swallowed and inhaled elements must be soluble to become absorbed. Once absorbed, these elements are handled in exactly the same manner as are the cor-

responding non-radioactive elements. Thus, they are eliminated from the body at various rates, with some being concentrated in certain locations for long periods of time. It is this prolonged retention of some radioactive fission products that characterizes the internal hazard.

(2) *Importance.* The significance of internal radiation in terms of *immediate* effects is negligible, since the external gamma hazard in the residual field of fallout contamination is the controlling factor in determining the danger to personnel. The same condition holds for the passage of aircraft through a radioactive cloud. Following the contaminating incident in the Marshall Islands in March 1954, a great quantity of data regarding the hazard associated with internal sources was obtained. In spite of the facts that the Marshallese people lived under conditions where the maximum probability of contamination of food and water supplies existed, and that they took no steps to protect themselves in any way, the degree of internal hazard due to fallout was small.

(3) *Protective measures.* Gas masks, air filters, or even handkerchiefs are effective in removing the particulate matter from inhaled air. Various methods of water decontamination have been proposed and evaluated, resulting in certain effective processes. Distillation, coagulation, filtration, adsorption and ion exchange may all be used advantageously. The Army Engineers' Erdlator units are of particular value. This equipment, which utilizes the processes of coagulation, diatomite filtration and disinfection, is ordinarily used to treat and purify surface waters in the field. When used for radioactive decontamination, a 50–85 percent removal of dissolved gross fission products may be expected when the unit is operated in conventional fashion. The removal can be increased to 93 percent with a clay pre-treatment and to over 99.9 percent with an ion exchange post-treatment. The Mobile Water Purification Unit (Erdlator) may be expected to remove essentially all of the radioactivity present in the form of turbidity or particulates. Canned and covered food and water are not contaminated by fallout. Directly contaminated food may be used when necessary by cutting or scraping off the outer layers.

d. Immediate Incapacitation. There are direct effects of massive, rapidly administered doses of radiation on the vital organs which result in early nausea, vomiting, and loss of ability to perform purposeful actions due to lack of coordination and imbalance. These symptoms may be sufficiently severe to result in immediate incapacitation of an individual to such a degree that he is not able to perform his duties. Experimental animal data indicate the onset of incapacitation by the end of 3 to 7 minutes, but the delay may be even less in the case of very high dose exposures from a nuclear explosion. Extrapolation of experimental data to man in this case is extremely difficult. It appears that on the order of 5,000 roentgens or rem from initial radiation may be sufficient to cause immediate incapacitation, but experimental evidence suggests the possibility of a temporary partial recovery from such doses after about 15 minutes. It is not known whether this partial recovery would result in the individual again becoming combat effective. With doses on the order of 15,000 to 20,000 roentgens, even the transient recovery period is unlikely and death may occur within a few hours.

6.4 Combined Injury

Any combination of moderate but sublethal exposures to thermal or nuclear radiations and/or mechanical injury is expected to produce more casualties or greater lethality than any effect considered singly, due either to additive effects or even to mutually reinforcing (synergistic) effects. Figure 6–4 represents a comparison of the ranges of the three effects considered individually in one situation. Insufficient data precludes the presentation of any summation curve at this time.

6.5 Nuclear Radiation Shielding

a. General. The gamma radiation dosage actually received by an individual is reduced if absorbing material is located between the individual and the point of detonation. Thus, the dose received by a person behind a building, in a field fortification, in a tank, or in a ship is less, and in some cases much less, than that which would be received in an exposed position at the same distance from the detonation. The shielding under such circumstances is generally discussed in terms of a "dose transmission factor", defined as the ratio of the dose received behind shielding material to the dose which would be received in the absence of the shielding.

b. Initial Radiation. The determining factors in the effectiveness of shielding are the mass of the material between the source of radiation and the target; the energy distribution of the gamma radiation at the target; the distance from the source, which partly determines the gamma energy distribution; the angle of the incident radiation; and the geometry of the shielding itself. Some of these parameters are combined in figure 6–5 to give a series of curves of the dose transmission factor as a function of shielding thickness for various materials. The curves are based on the assumption that the radiation is perpendicular to the slab of shielding material. Since gamma rays are scattered considerably in air, the resultant dose transmission factor holds strictly only for slab shields so large that no radiation can get around the edges. To insure sufficient protection against radiation scattered from all directions, shielding material should be used for all exterior surfaces. The curves of figure 6–5 are applicable for yields between 0.1 KT and 100 KT. For yields above 100 KT, the curves are considered to be a conservative estimate of attenuation of initial gamma radiation (i. e., the transmission is even less than indicated), because the initial spectrum received at the target contains a higher proportion of low energy gamma rays, and is therefore less penetrating. Dose transmission factors are given in table 6–5 for particular situations, such as personnel in tanks, foxholes, houses, buildings, and basements.

c. Residual Radiation. Residual radiation is somewhat less penetrating than initial radiation, as can be seen from the dose transmission curves for residual radiation in figure 6–6. In the case of residual radiation from a contaminated ground surface, the most effective location for shielding material is between the receiver and the contaminated ground, such as the floor of a tank, or the ceiling of an underground shelter. Some shielding against residual radiation is afforded by walls also, since a portion of the radiation received can come horizontally from points up to several hundred yards from the receiver.

Table 6–5. Dose Transmission Factors (Interior Dose/Exterior Dose)

Geometry	Gamma rays		Neutrons [a]
	Initial	Residual	
Foxholes [b]	0.05–0.10	0.02–0.10	0.3
Underground—3 feet	0.04–0.05	0.0002	0.002–0.01
Built-up city area (in open)	....	0.7	....
Frame house	0.9	0.3–0.6	0.9–1.0
Basement	0.05–0.5	0.05–0.10	0.1–0.8
Multistory building:			
Upper	0.9	0.01	0.9–1.0
Lower	0.3–0.6	0.1	0.9–1.0
Blockhouse walls:			
9 inches	0.1	0.05	0.3–0.5
12 inches	0.05–0.09	0.01–0.02	0.2–0.4
24 inches	0.01–0.03	0.001–0.002	0.1–0.2
Factory, 200 x 200 feet	....	0.10–0.20	....
Shelter, partly above grade:			
With earth cover—2 feet	0.02–0.04	0.005–0.02	0.02–0.08
With earth cover—3 feet	0.01–0.02	0.001–0.005	0.01–0.05
[redacted]			
LVT (Landing Vehicle Tracked)	0.5–0.9	....	1.0
Battleships and large carriers [c]:			
15% of crew	1.0	1.0	0.8–1.0
25% of crew	0.2	0.1	0.2–0.8
10% of crew	0.05	0.03	0.05–0.2
50% of crew	0.0005–0.005	0.0003–0.003	0.001–0.05
Cruisers and carriers [c]:			
10% of crew	1.0	1.0	0.8–1.0
20% of crew	0.5	0.3	0.4–0.8
30% of crew	0.1–0.3	0.1	0.1–0.4
40% of crew	0.005–0.1	0.003–0.05	0.01–0.1
Aircraft	1.0	....	1.0
Destroyers, transports, and escort carriers [c]:			
10% of crew	1.0	1.0	0.8–1.0
20% of crew	0.7	0.5	0.6–0.8
30% of crew	0.4	0.2	0.3–0.6
40% of crew	0.1–0.4	0.1	0.1–0.3

ARMY (b)(1)

[a] Estimated values.
[b] No line-of-sight radiation received.
[c] Crew at General Quarters.

DIRECT BLAST CASUALTIES FOR PERSONNEL IN THE OPEN

Figure 6-1 is a plot of burst height vs. ground range for 50 percent probability of producing direct blast casualties to personnel in the open as a result of translational motion. The curves are drawn for a 1 KT detonation.

Scaling.

$$\frac{h_1}{h_2}=\frac{W_1^{1/3}}{W_2^{1/3}} \text{ and } \frac{d_1}{d_2}=\frac{W_1^{0.4}}{W_2^{0.4}},$$

where

h_1 and d_1 are the burst height and ground distance for yield W_1,

and h_2 and d_2 are the burst height and ground distance for yield W_2.

Example:

Given: A 20 KT weapon burst at a height of 500 feet over open terrain.

Find: The distance at which there is a 50 percent probability of producing direct blast casualties to standing personnel as a result of translational motion.

Solution: The corresponding burst height for 1 KT is $\frac{500}{(20)^{1/3}}=185$ feet.

From figure 6-1 at a burst height of 185 feet, ground distance for 50 percent probability of direct blast casualties to standing personnel as a result of translational motion is 434 yards. The corresponding ground distance for 20 KT is $434\times(20)^{0.4}=1{,}440$ yards. *Answer.*

Reliability. Based primarily upon observed results of disasters involving humans and experiments with small animals, together with theoretical calculations.

Related material.

See paragraph 6.1*b*.

See also figure 6-2 and table 6-2 for thermal casualty data; and table 6-4 for nuclear radiation casualty data.

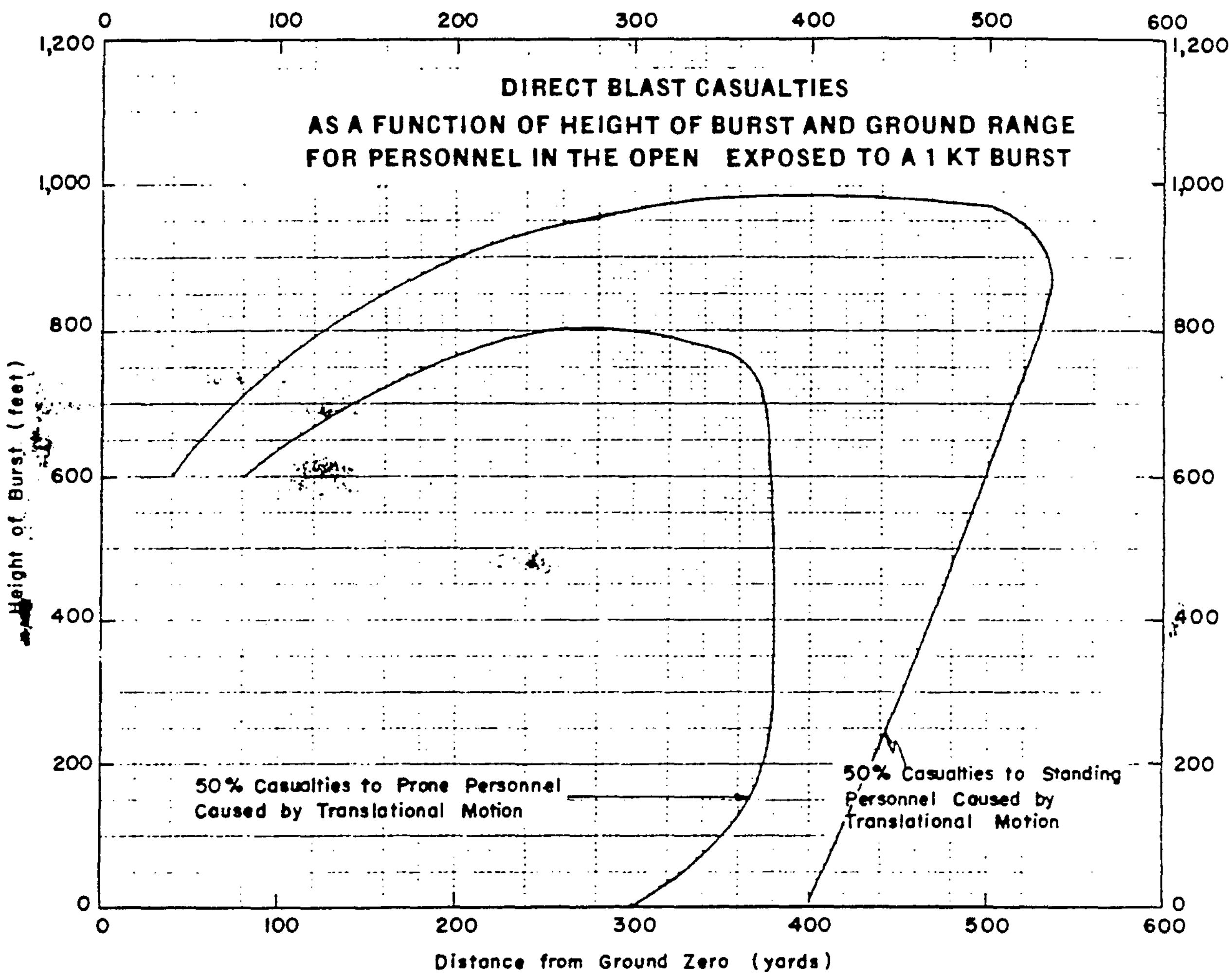
DIRECT BLAST CASUALTIES
AS A FUNCTION OF HEIGHT OF BURST AND GROUND RANGE
FOR PERSONNEL IN THE OPEN EXPOSED TO A 1 KT BURST
50% Casualties to Prone Personnel Caused by Translational Motion
50% Casualties to Standing Personnel Caused by Translational Motion
Height of Burst (feet)
Distance from Ground Zero (yards)
0
100
200
300
400
500
600
1,200
1,000
800
600
400
200
0

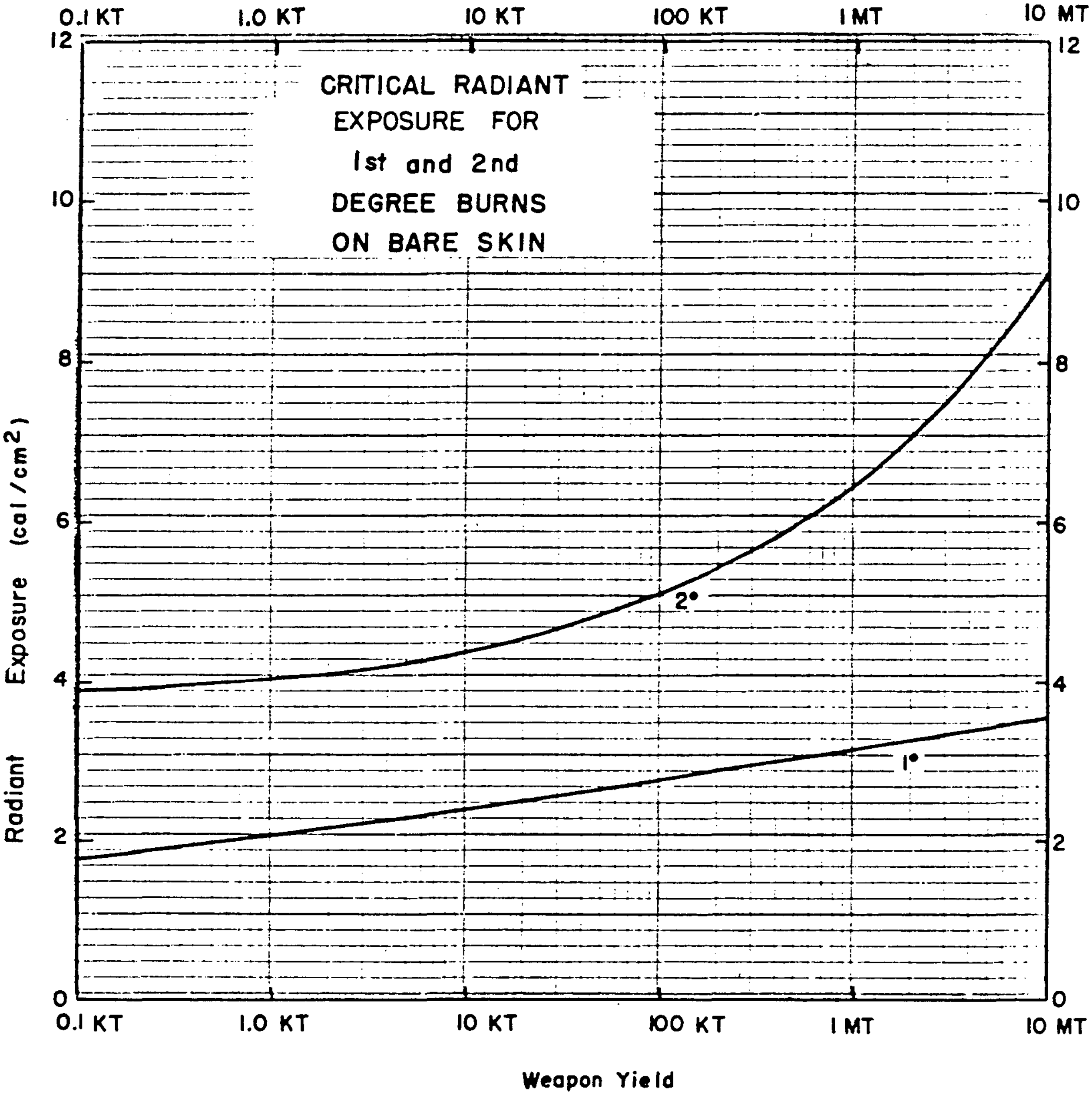
CRITICAL RADIANT EXPOSURE FOR 1st and 2nd DEGREE BURNS ON BARE SKIN
0.1 KT
1.0 KT
10 KT
100 KT
1 MT
10 MT
0
2
4
6
8
10
12
2°
1°
Radiant Exposure (cal/cm²)
Weapon Yield

FIGURE 6-3

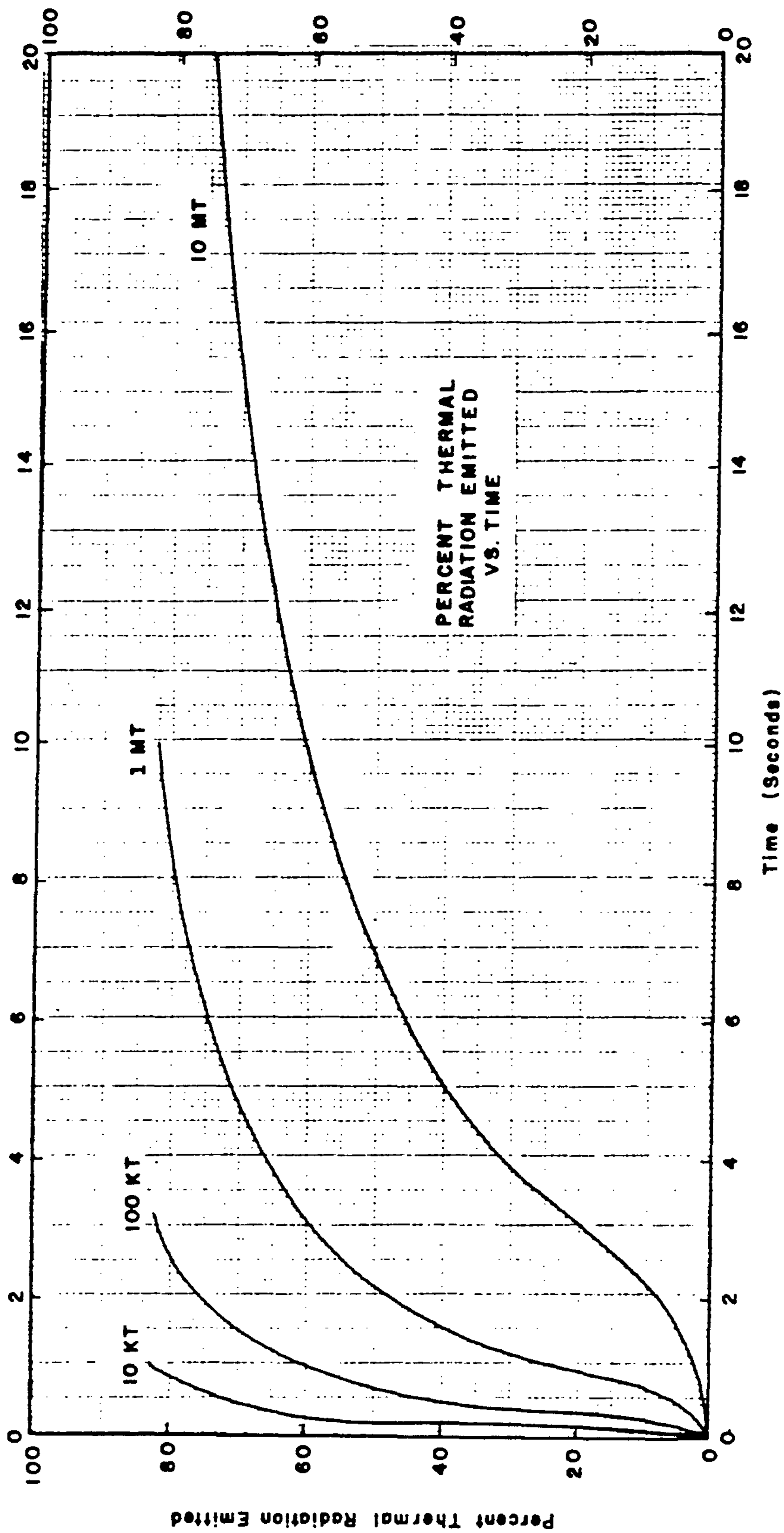
PERCENT THERMAL
RADIATION EMITTED
VS. TIME
10 MT
1 MT
100 KT
10 KT
Time (Seconds)
Percent Thermal Radiation Emitted
0
2
4
6
8
10
12
14
16
18
20
100
80
60
40
20
0

IMMEDIATE CASUALTY PRODUCTION BY VARIOUS PHYSICAL PHENOMENA

Figure 6-4 represents a comparison of the ranges of the three casualty-producing effects of various nuclear weapons when detonated at a scaled height of burst of 300 feet in a clear atmosphere in which the visibility is 50 miles. It should be emphasized that these casualty predictions are based on the assumption, which will not be true in the majority of cases, that personnel receive a given dose or amount of a single effect only, and that this single effect will produce casualties without assistance from the other effects. Actually, there is some reason for believing that ionizing radiation and thermal radiation are synergistic, that is to say, that sub-injury levels of each, delivered simultaneously to the same person, could easily cause serious injury or death. However, there is no satisfactory way, at present, of estimating the extent to which combined injuries can cause ineffectiveness, and figure 6-4 is designed as illustrative of the relative injury-producing capacities of the separate effects acting independently.

Related Material. See paragraph 6.4.

FIGURE 6-4

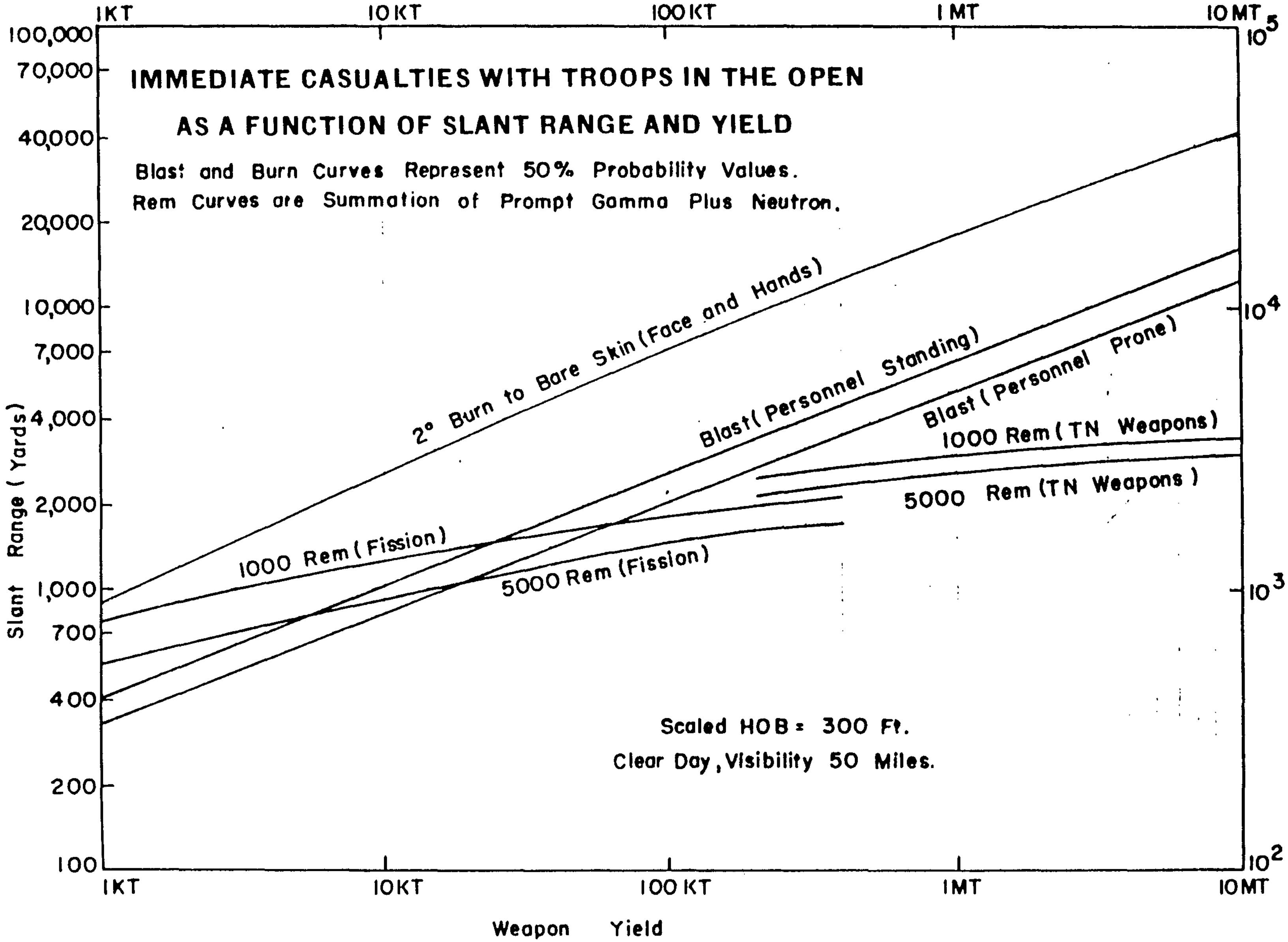
IMMEDIATE CASUALTIES WITH TROOPS IN THE OPEN
AS A FUNCTION OF SLANT RANGE AND YIELD
Blast and Burn Curves Represent 50% Probability Values.
Rem Curves are Summation of Prompt Gamma Plus Neutron.
2° Burn to Bare Skin (Face and Hands)
Blast (Personnel Standing)
Blast (Personnel Prone)
1000 Rem (TN Weapons)
5000 Rem (TN Weapons)
1000 Rem (Fission)
5000 Rem (Fission)
Scaled HOB = 300 Ft.
Clear Day, Visibility 50 Miles.
Slant Range (Yards)
100,000
70,000
40,000
20,000
10,000
7,000
4,000
2,000
1,000
700
400
200
100
10^5
10^4
10^3
10^2
1KT
10KT
100KT
1MT
10MT
Weapon Yield

SHIELDING FROM INITIAL AND RESIDUAL GAMMA RADIATION

The curves in figures 6-5 and 6-6 indicate dose transmission factors for bomb initial and residual gamma radiation, respectively, perpendicularly incident upon various thicknesses of earth, water, concrete, iron, and lead. For other materials of known density, the transmission factor may be estimated by interpolation, on a density basis, between the curves given.

Example.

Find: How much concrete would be required to reduce the dose from initial radiation to one one-hundredth the unshielded dose?

Solution: Examine the curve for concrete of figure 6-5. It is seen that the thickness of a slab of concrete required to reduce the dose to 0.01 of its former value is 34 inches. *Answer.*

Reliability. Thicknesses indicated for a given transmission factor are considered reliable within ±20 percent, for conditions outlined in paragraph 6.5.

Densities of Certain Materials
(Expressed in pounds per cubic foot)

Brick, common	120
Clay, dry	63
Clay, damp, plastic	110
Clay and gravel, dry	100
Coal, piled	40-50
Earth, dry, loose	76
Earth, dry, packed	95
Earth, moist, loose	78
Earth, moist, packed	96
Earth, mud, packed	115
Fuel oil	54
Granite	175
Limestone	165
Masonry, stone	150
Sand, gravel, dry packed	100-120
Fir	34
Hemlock	29
Oak	46
Pine, white	26
Pine, yellow	40

Related Material.

See paragraph 6.5. For radiation input data, see figures 4-1 through 4-7 for air and surface burst initial gamma. Figures 4-28 through 4-33, neutron induced gamma activity. Figures 4-14 through 4-19, surface burst residual gamma. Figure 4-8, underground burst, initial gamma. Figures 4-20 through 4-23, underground residual gamma. Figure 4-25, harbor burst, residual gamma.

FIGURE 6-5

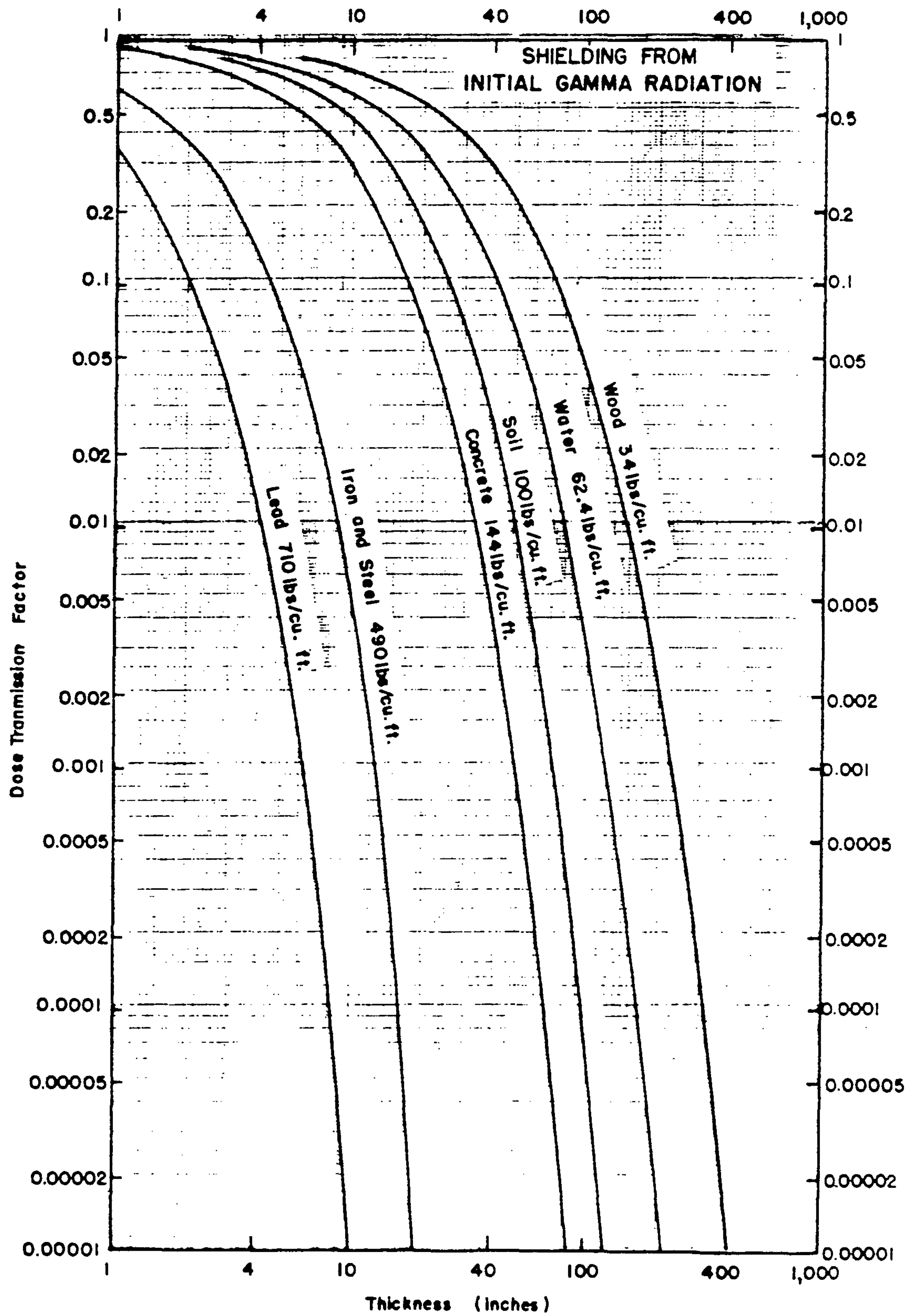
SHIELDING FROM
INITIAL GAMMA RADIATION
Dose Tranmission Factor
Thickness (inches)
Lead 710lbs/cu. ft.
Iron and Steel 490lbs/cu. ft.
Concrete 144lbs/cu. ft.
Soil 100lbs/cu. ft.
Water 62.4lbs/cu. ft.
Wood 34lbs/cu. ft.
1
4
10
40
100
400
1,000
0.5
0.2
0.1
0.05
0.02
0.01
0.005
0.002
0.001
0.0005
0.0002
0.0001
0.00005
0.00002
0.00001

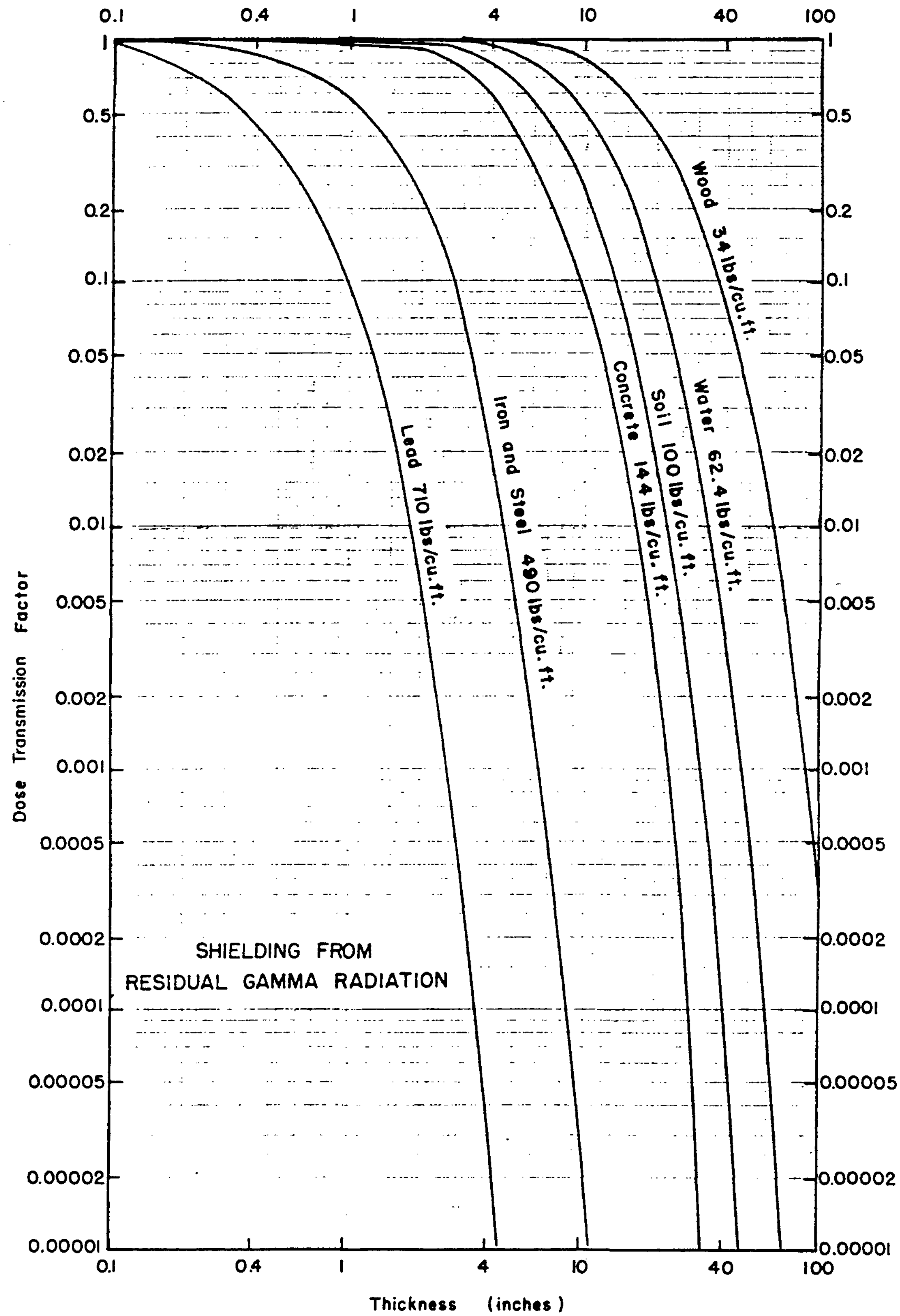
SHIELDING FROM
RESIDUAL GAMMA RADIATION
Lead 710 lbs/cu.ft.
Iron and Steel 490 lbs/cu.ft.
Concrete 144 lbs/cu. ft.
Soil 100 lbs/cu. ft.
Water 62.4 lbs/cu.ft.
Wood 34 lbs/cu.ft.
Dose Transmission Factor
Thickness (inches)
0.1
0.4
1
4
10
40
100
0.5
0.2
0.05
0.02
0.01
0.005
0.002
0.001
0.0005
0.0002
0.0001
0.00005
0.00002
0.00001

7
Structures

SECTION VII
DAMAGE TO STRUCTURES

7.1 General

a. Comparison of Effects. Of the blast, thermal and nuclear energy produced by a nuclear detonation, only the first two are important in producing damage to structures. Air blast causes damage to surface structures ranging from breaking of windows to complete destruction. Blast may also damage structures by secondary effects such as fires initiated by short circuits, ruptured gas mains and overturned stoves and furnaces. Direct thermal radiation causes fires by ignition of kindling fuels such as wastepaper, rags, curtains, upholstery and rotted wood. These ignitions to kindling fuels occur well beyond the limits of significant blast damage.

b. Air Blast Damage. For a given height of burst and yield, structural characteristics such as mass, strength, ductility, design detail and wall composition including openings, are the major influences on structural response. Values of the vertical and horizontal loading components vary with the angle of elevation of the burst. Directly underneath the burst, the roofs of structures may be dished in or destroyed and the walls collapsed, but there is no tendency to displace the structure laterally. Farther out, the horizontal component of the loading becomes more important. Damage under these circumstances may be greater because of the small lateral resistance of structures in comparison with their vertical resistance. Generally, damage at the same overpressure increases with yield because loading duration increases with increasing yield.

c. Ground Shock Damage. The effect of an underground explosion on underground structures differs from the air blast case in that the medium through which the shock passes has approximately the same density as the underground structure itself. In such a case, the behavior of the ground and the structure located in it are closely related. Damage is generally limited to the radius of rupture of the soil or the distance to which permanent displacements occur. The underground portions of surface structures are affected in a similar manner; but since the air blast damage to the above ground portions of surface structures extends out to a much greater distance than the ground shock damage, air blast is the controlling damage mechanism. Underground utilities are damaged primarily by differential movement at the point where the lines enter structures. Tunnels in solid rock are difficult to destroy by explosions of nuclear weapons. In this case, the shock wave is transmitted through the rock. When it reaches the tunnel the wave is reflected as a tensile wave, and there is a tendency for the rock to spall or become detached from the rock-tunnel interface. Use of tunnel linings materially reduces this spalling. Mass crushing of the rock and filling of the tunnel occurs closer to the burst point.

d. Water Shock Damage. Water shock damage is particularly effective in causing structural damage to dams and canal locks. Rupture of the dam or lock releases the impounded water so as to cause the maximum flood damage downstream in addition to the destruction of the plant and its equipment. Other possible land targets subject to underwater shock damage are graving dock caissons and certain shore installations.

7.2 Surface Structures

a. Air Blast.

(1) *General.* The discussion in paragraph 5.2 applies to the air blast loading of structures in general. The following discussion of loading applies primarily to regions in which ideal wave forms occur. It is also applicable to loading in regions of non-ideal wave forms but the differentiation between drag and diffraction sensitivity becomes less distinct as the blast wave forms become non-ideal and dynamic pressures become proportion-

ately greater. The effect of non-ideal wave forms on air blast loading is described in paragraph 5.2*b*(1)(*f*).

(2) *Loading during the diffraction phase.* An essentially closed large structure with walls that remain intact throughout most of the load duration is primarily sensitive during the diffraction phase, since most of the translational load is applied during this period. As the blast wave strikes this type structure it is reflected, creating overpressures greater than those incident thereon. Subsequently, the reflected overpressure decays to that of the blast wave. As the blast wave progresses, it diffracts around the structure, eventually exerting overpressures on all sides. Before the blast wave reaches the rear face, overpressures on the front exert translational forces in the direction of blast wave propagation. After the blast wave reaches the rear face, the overpressures on the rear tend to counter the overpressures on the front. For smaller structures, the blast wave reaches the rear face more quickly, so that the pressure differential exists for a shorter time. Thus, the net translational loading resulting from overpressures during the diffraction phase depends primarily on structural dimensions. For some structures where wall failure takes place early in the diffraction phase, only the structural frame may remain during the remainder of the diffraction process, and essentially no load is transmitted to the structural frame through the walls. A longer duration blast wave does not materially change the magnitude of the net translational loading during the diffraction phase or the damage resulting therefrom. In other words, the structure is primarily sensitive to the peak blast wave overpressure. Table 7–1 lists those types of structures which are generally affected primarily by blast wave overpressure during the diffraction phase.

(3) *Loading during the drag phase.* During the diffraction phase, and until the blast wave has passed, dynamic pressures are also exerted on structures. Dynamic pressure loading is commonly called drag loading. In the case of a closed large structure the drag phase loading is small relative to the overpressure loading during the diffraction phase. For smaller structures, the drag phase assumes greater relative importance. For small area components such as the frame of a structure after removal of siding, the translational load applied as a result of the drag phase is much greater than the net translational loading from overpressures during the diffraction phase. For frame buildings with siding removed during the diffraction phase, the drag phase is the predominant factor in producing further damage. Likewise for bridges, the net load during the diffraction phase is applied for an extremely short time, while the drag phase continues until the entire blast wave passes the structure. Because the drag phase duration is closely related to the duration of the blast wave rather than to the overall dimensions of the structure, damage is dependent not only on peak dynamic pressure but also on the duration of the positive phase of the blast wave. Thus damage to this type of structure is dependent on yield as well as peak loading. Table 7–2 lists those types of structures which are primarily sensitive during the drag phase.

(4) *Damage to structures.*

(*a*) *Structural characteristics.* The cases discussed above represent extremes in structural loading. Most structures have characteristics which cause them to be affected by the loading during both the diffraction phase and the drag phase. Some elements of a structure may be damaged more by loading during the diffraction phase; other elements of the same structure may be damaged more by the drag phase. The dimensions and orientation of a structure, together with the number and area of the openings and the rapidity with which wall and roof

Table 7-1 Damage to Types of Structures Primarily Affected by Blast Wave Overpressure During the Diffraction Phase

Figure	Description of structure	Description of damage		
		Severe	Moderate	Light
[a] 7-1	Multistory reinforced concrete building with reinforced concrete walls, blast resistant designed, no windows, three story.	Walls shattered, severe frame distortion, incipient collapse of first floor columns.	Walls cracked, building slightly distorted, entranceways damaged, doors blown in or jammed. Some spalling of concrete.	
7-2	Multistory reinforced concrete building, with concrete walls, small window area, five story.	Walls shattered, severe frame distortion, incipient collapse of first floor columns.	Exterior walls badly cracked. Interior partitions badly cracked or blown down. Structural frame permanently distorted; spalling of concrete.	Windows and doors blown in. Interior partitions cracked.
7-3	Multistory wall bearing building, brick apartment house type, up to three stories.	Bearing walls collapse, resulting in total collapse of structure.	Exterior walls badly cracked, interior partitions badly cracked or blown down.	Windows and doors blown in. Interior partitions cracked.
[b] 7-4	Multistory wall bearing building, monumental type, four story.	Bearing walls collapse, resulting in collapse of structure supported by these walls. Some bearing walls may be shielded enough by intervening walls so part of structure may receive only moderate damage.	Exterior walls facing blast badly cracked, interior partitions badly cracked, although toward far end of building damage may be reduced.	Windows and doors blown in. Interior partitions cracked.
7-5	Wood frame building, house type, one or two stories.	Frame shattered so that structure is for the most part collapsed.	Wall framing cracked. Roof badly damaged. Interior partitions blown down.	Windows and doors blown in. Interior partitions cracked.
7-6	Oil tanks, 30 feet in height, 50 feet in diameter. (Tanks considered full; more vulnerable if empty.)	Large distortion of sides, seams split, so that most of contents are lost.	Roof collapsed, sides above liquid buckled, some distortion below liquid level.	Roof badly damaged.

[a] Designed to withstand 20 psi overpressure in the Mach stem from a 20 KT weapon without any impairment of facilities.
[b] Large structure (over 200 ft x 200 ft plan dimensions). In this case the side facing the blast may be severely damaged while the interior remains relatively undamaged.

Table 7–2. Damage to Types of Structures Primarily Affected by Dynamic Pressure During the Drag Phase

Figure	Description of structure	Description of damage		
		Severe	Moderate	Light
7–7	Light steel frame industrial building, single story, with up to 5-ton crane capacity. Lightweight, low strength walls fail quickly.	Severe distortion of frame (one-half column height deflection).	Some distortion of frame; cranes, if any, not operable until repairs made.	Windows and doors blown in. Light siding ripped off.
7–8	Heavy steel frame industrial building, single story, with 50-ton crane capacity. Lightweight, low strength walls fail quickly.	Severe distortion of frame (one-half column height deflection).	Some distortion of frame; cranes, if any, not operable until repairs made.	Windows and doors blown in. Light siding ripped off.
7–9	Multistory steel frame office type building, five story. Lightweight, low strength walls fail quickly.	Severe frame distortion. Incipient collapse of lower floor columns.	Frame distorted moderately. Interior partitions blown down.	Windows and doors blown in. Light siding ripped off. Interior partitions cracked.
7–10	Multistory reinforced concrete frame office type building, five story. Lightweight, low strength walls fail quickly.	Severe frame distortion. Incipient collapse of lower floor columns.	Frame distorted moderately. Interior partitions blown down. Some spalling of concrete.	Windows and doors blown in. Light siding ripped off. Interior partitions cracked.
7–11	Highway and railroad truss bridges, spans of 150 feet to 250 feet. (See facing page of figures 7–1 through 7–17 for effect of orientation.)	Total failure of lateral bracing, collapse of bridge.	Some failure of lateral bracing such that bridge capacity is reduced about 50 percent.	Capacity of bridge unchanged. Slight distortion of some bridge components. (Use $q=0.6$ psi curve scaled to weapon yield.)
7–12	Highway and railroad truss bridges, spans of 250 feet to 550 feet. (See facing page of figures 7–1 through 7–17 for effect of orientation.)	Total failure of lateral bracing, collapse of bridge.	Some failure of lateral bracing such that bridge capacity is reduced about 50 percent.	Capacity of bridge unchanged. Slight distortion of some bridge components. (Use $q=0.6$ psi curve scaled to weapon yield.)
7–13	Floating bridges, U. S. Army standard M–2 and M–4, random orientation.	All anchorages torn loose, connections between treadways or balk and floats twisted and torn loose, many floats sunk.	Many bridle lines broken, bridge shifted on abutments, some connections between treadways or balk and floats torn loose.	Some bridle lines broken, bridge capacity unimpaired.
7–14	Earth covered light steel arch with 3 feet minimum cover (10 gauge corrugated steel with 20–25 foot span).	Total collapse of arch section.	Slight permanent deformation of arch.	Deformation of end walls, possible entrance door damage.
7–15	Earth covered light reinforced concrete structures with 3 feet minimum cover (2 to 3 inch panels with beams on 4-foot centers).	Total collapse	Deformation, severe cracking and spalling of panels.	Cracking of panels, entrance door damage.

panels fail, determine which type of loading is predominant in causing damage. Structural characteristics determining response and damage are ultimate strength, period of vibration, ductility, dimensions and mass. Ductility increases the ability of a structure to absorb energy and increases its resistance to failure. Brittle structures, such as those of masonry construction, have little ductility and fail after relatively small deflections. Ductile structures, such as steel frame buildings, have the ability to withstand large and even permanent deflections without failure. For each representative structural type listed in tables 7–1 and 7–2, structural characteristics are similar enough that structures of a given type are considered to respond to approximately the same degree under identical loading conditions despite a recognized variability of unknown amount for each type. The direction of the imposed load may have considerable effect on response as discussed in paragraph 5.2. Most structures are designed to withstand much larger vertical than horizontal loads. Consequently, they are more resistant to a load imposed on the top of a structure than an equal load imposed against a side. Thus in the early regular reflection region, damage from the same peak loading is likely to be less than damage to a similar structure in the Mach reflection region. Figures 7–1 through 7–17 are damage curves constructed for average characteristics of each of the selected structural types under average surface conditions. The curves incorporate current knowledge of the loading influences of Mach and regular reflection, positive phase duration, peak overpressure and dynamic pressure. The figures apply for random structure orientation unless specifically stated to the contrary, as in figures 7–11 and 7–12 for truss bridges. For truss bridges the distances given are for orientations of blast propagation of 45° to 90° from the longitudinal bridge axis. The distances given in figure 7–11 are reduced to 60 percent for an orientation of 0° for all span lengths. The assumed loading is that which occurs at sea level over a surface of average characteristics; i. e., the blast wave peak overpressures, durations and dynamic pressures of figures 2–10, 2–11, and 2–13 are used to deduce the air blast loading. In the case of earth covered surface structures the earth mounding reduces the reflection factor and improves the aerodynamic shape of the structure. This results in a large reduction in both horizontal and vertical translational forces. It is estimated that the peak force applied to the structural elements is reduced by a factor of at least 2 by the addition of earth cover. The structure is somewhat stiffened against large deflections by the buttressing action of the soil when the building is sufficiently flexible.

(*b*) *Shallow underground bursts.* Air blast is the determining factor for damage to surface structures from relatively shallow underground bursts, but the distances for a given degree of damage are reduced from those for a surface burst. The surface burst values from figures 7–1 through 7–17 may be used to predict damage to surface structures from such underground bursts if the distances obtained are reduced in accordance with figure 7–18. This figure is also applicable to other damage data (See pars. 9.2*a*, 10.1*d*, and 11.2*b*).

(*c*) *Damage classification.* A major factor to consider in assessing structural damage is the effect of the damage on continued operations within the structure. If rugged equipment is mounted on a foundation at ground level, major distortion or even collapse of a structure may not preclude operation of the equipment. Conversely, if the equipment is tied in with the structural frame, distortion of the structure may prevent or seriously affect operability. No satisfactory general method has been developed for relating damage of structures to the operational equipment contained in them. This relationship may be established for particular cases of interest on an individual basis. In general, severe structural damage approaching collapse entails a major reduction in operating capability. Damage to structures has been divided into three major categories as follows:

1. *Severe damage.* That degree of structural damage which precludes further use of a structure for the purpose for which it is intended without essentially complete reconstruction. Requires extensive repair effort before usable for any purpose.
2. *Moderate damage.* That degree of structural damage to principal load carrying members (trusses, columns, beams and load carrying walls) that precludes effective use of a structure for the purpose for which it is intended until major repairs are made.
3. *Light damage.* That degree of damage which results in broken windows slight damage to roofing and siding, blowing down of light interior partitions, and slight cracking of curtain walls in buildings, and as described in tables 7-1 and 7-2 for other structures.

The figures of this section may be used to predict the conditions under which the degrees of damage listed above may be expected. These predictions are made as functions of yield, height of burst and distance from ground zero. Figures 7-1 through 7-17 show the distances at which nuclear detonations of various yields are expected to cause severe damage to different types of structures. Figures 7-1 through 7-15 are for various heights of burst, while figures 7-16 and 7-17 are for surface bursts only.

The curves are drawn for a 50 percent probability of attaining severe damage. 90 percent and 10 percent probabilities may be determined as follows:

1. *90 percent probability.* Use a curve of one-half the yield to determine distance at the same burst height.
2. *10 percent probability.* Use a curve of twice the yield to determine distance at the same burst height.
3. *50 percent probability of moderate damage.* For structures damaged primarily during the diffraction phase (figures 7-1 through 7-6 and 7-16) use a curve for a yield four times that of the desired yield at the same burst height. For structures damaged primarily during the drag phase (figures 7-7 through 7-15 and 7-17) use a curve of twice the selected yield.
4. *50 percent probability of light damage.* Use 1 psi (blast wave peak overpressure) for practically all types of structures except bridges, blast resistant structures without windows, and earth covered surface structures. This range may be determined from figure 2-10 for various burst heights and scaled to various yields as discussed on the facing page of this figure. Light damage is not pertinent to blast resistant structures without windows.

b. Ground Shock and Cratering. The air blast from surface bursts or underground bursts at a depth less than 35 $W^{1/3}$ feet causes severe damage to most surface structures at ranges where damage from ground shock and cratering is insignificant. In cases where the burst depth is greater than $35 \cdot W^{1/3}$ feet, ground shock may become the controlling damage producing mechanism.

c. Thermal Radiation Damage. Primary thermal radiation is seldom a factor in damage to structures. However, since surfaces of the exteriors and interiors of many structures are covered with protective coatings (paint), these coverings may be scorched at moderate levels of thermal radiation when subjected to direct radiation from the fireball. All structures, whether principally of steel and concrete construction or of wood, contain some combustible material. It is considered improbable that kindling fuels (discussed in par. 12.1) will ever be entirely absent. Therefore, the possibility that fire may be initiated in kindling fuels and spread from these ignitions must always be considered. A more complete treatment of fire in built-up areas appears in paragraph 12.1. Certain classes of surface structures such as badly weathered or rotted wooden buildings with thatched roofs, houses with lacquered paper windows, etc., may be ignited by direct thermal radiation with resultant self-sustaining fires.

7.3 Underground Structures

a. Air Blast. Air blast is the controlling damage mechanism for light, shallow buried underground structures. For depths of cover less than 8 feet in most soils there is little attenuation of pressure applied to the horizontal, top surface of an underground structure. No increase in pressure exerted on the structure appears to arise from ground shock reflection at the interface between the earth and the structure, partially accounting for a reduction factor of 2 in peak force as discussed in paragraph 7.2*a*(4)(*a*). The lateral pressures exerted on vertical faces of a buried structure have been found to be about 15 percent of the pressures on the roof in dry, silty soil: This lateral pressure is likely to be somewhat higher in general and may approach 100 percent in a porous saturated soil. The pressures exerted on the bottom of a buried structure in which the bottom slab is a structural unit integral with the walls may be as low as 75 percent of the roof pressure but may range up to 100 percent of that pressure.

b. Ground Shock and Cratering. The mechanism of damage to underground structures from ground shock and cratering is dependent upon several more or less unrelated variables such as the size, shape, flexibility and orientation of the structure with respect to the explosion, and the characteristics of the soil or rock. The shock parameter causing damage is not defined theoretically or empirically. However, considerable experimental evidence from studies using high explosives indicates that the parameters involved in producing damage can be related to the crater radius, except for burst heights greater than 5 $W^{1/3}$ feet. Therefore, except for burst heights greater than 5 $W^{1/3}$ feet, the criteria for structural damage from ground shock are given in terms of apparent crater diameter, which can be obtained from figure 2–22. For purposes of estimating earth shock damage from surface or subsurface bursts, underground structures are divided into various categories as follows:

(1) *Relatively small highly resistant targets in soil.* This type, which includes reinforced concrete fortifications, can probably be damaged only by acceleration and displacement of the structure in its entirety.

(2) *Moderate size, moderately resistant targets.* These targets are damaged by soil pressure as well as acceleration and bodily displacement.

(3) *Long, relatively flexible targets.* These include buried pipes and tanks, which are likely to be damaged in regions where large soil strains exist.

(4) *Orientation sensitive targets.* Targets such as gun emplacements may be susceptible to damage from small permanent displacements or tilting.

(5) *Rock tunnels.* Damage to such targets from an external explosion is caused by the tensile reflection of the shock wave from the rock-air interface, except when the crater breaks through into the tunnel. Larger tunnels are more easily damaged than smaller ones. However, no correlation between damage and tunnel size or shape is known.

(6) *Large underground installations.* Such installations can usually be treated as a series of smaller structures.

c. Damage Criteria.

(1) *Air blast damage.* Peak overpressures given in figures 2–9, 2–10, and 2–18 may be used as applicable to predict damage to relatively shallow buried underground structures located more than 2 crater radii from the burst point. For most of these structures, the response time and the period of the structural elements is short.

(2) *Ground shock and cratering damage.*

(*a*) *Structures in soil.* Heavy, well designed underground structures are not damaged by air blast. These structures are likely to be damaged only by ground shock and cratering from surface and underground bursts. The

Table 7–3. Damage Criteria for Underground Structures

Structure	Damage	Damage distance	Remarks
Relatively small, heavy, well designed underground targets.	Severe	$1\frac{1}{4}R_a$	Collapse.
	Light	$2R_a$	Slight cracking, severance of brittle external connections.
Relatively long, flexible targets, such as buried pipelines, tanks, etc.	Severe	$1\frac{1}{2}R_a$	Deformation and rupture.
	Moderate	$2R_a$	Slight deformation and rupture.
	Light	$2\frac{1}{2}$ to $3R_a$	Failure of connections. (Use higher value for radial orientation of connections.)

Note. R_a=Apparent Crater Radius. (See fig. 2–20 or 2–22).

isodamage contour for structures at depths less than 20 $W^{1/3}$ feet can be approximated by a segment of a hemisphere with center at ground zero and a radius which is the damage distance given in table 7–3. For structures deeper than 20 $W^{1/3}$ feet, the damage distances are somewhat less than the values given.

(*b*) *Tunnels in rock.* Figure 7–19 presents isodamage contours for tunnels of average size in sound rock from a 1 KT surface burst or shallow subsurface burst.

(*c*) *Utility connections.* Underground structures may also be damaged by shearing off connecting services, such as those for ventilation, water, power and access. In this case, relative earth displacement is an important factor in producing damage. Damage of this type may extend out to about 2½ crater radii in some soils if the connections are of brittle material and are rigidly attached to the structure.

(*d*) *Displacement-sensitive targets.* Heavy machinery and other items susceptible to small displacements located in underground structures receive moderate damage out to about 2½ crater radii, and are likely to be unusable without realignment.

(3) *Crater and missile damage.* A nuclear explosion, either on the surface or underground, creates a crater of considerable size. Structures within the crater, including massive permanent installations of the concrete and steel type, are almost certain to be destroyed. The area in and around the crater will be highly contaminated with radioactive material. An additional source of damage from surface and underground bursts is the throwout associated with crater formation. Because portions of damaged targets have better ballistic properties than the soil, they may be thrown for large distances and are apt to cause missile damage. Since the number of missiles falling on a given area is low at long ranges, serious missile damage does not extend beyond the range of severe air blast damage except in isolated cases.

7.4 Field Fortifications

a. Air Blast. Air blast is the controlling damage-producing mechanism for destruction of field fortifications, including those reinforced, revetted or covered. Definitions of severe, moderate, and light damage levels to various types of field fortifications are given in table 7–4. These damage levels are based upon various degrees of collapse and structural failure except for unrevetted trenches and foxholes, which have damage levels based on degree of filling caused by collapse of the walls and by filling with dust and debris. Areas covered with loose material, such as sand and gravel, may provide sufficient dust and debris to completely fill a trench or foxhole, whereas areas with stable vegetation or areas of dry silty soil may not provide significant quantities of dust and debris to appreciably fill a trench

Table 7–4. Damage Criteria for Field Fortifications

Figure	Description	Description of damage: Severe	Description of damage: Moderate	Description of damage: Light
7–20	Command post and personnel shelter, modular sections 6′ x 8′ with top 3′–5′ below ground surface, earth covered, and with covered trench entrance.*	Caps and posts broken, large displacement and disarrangement of timbers, revetment failure.	Some caps and posts broken, moderate displacement, some revetment failure.	Damage to minor components only, slight displacement, occasional revetment failure.
7–21	Machine gun emplacement, 7′ x 7′, framework extends 2′ above original ground surface, has open firing ports and open trench entrance. 3′–5′ mound of earth covers framework and extends down to the ground surface except at openings.*	Caps and posts broken, large displacement and disarrangement of timbers, revetment failure.	Some caps and posts broken, moderate displacement, some revetment failure.	Damage to minor components only, slight displacement, occasional revetment failure.
7–22	Unrevetted trenches and foxholes with or without light cover.	The trench or foxhole is at least 50 percent filled with earth.	The trench or foxhole is at least 10 percent but less than 50 percent filled with earth.	The trench or foxhole is less than 10 percent filled with earth.

*Post, cap, and stringer construction, timber approx. 6″ x 8″, or 12″ diameter.

or foxhole. Collapse of the walls of foxholes and trenches by air blast and air induced ground shock is usually not significant except at ranges less than those shown for severe damage in figure 7–22. Figures 7–20 through 7–22 give ranges at which severe, moderate, and light damage levels may be expected for 1 KT as a function of height of burst. The range for a given damage level is reduced in more cohesive soils and increased in less cohesive soils.

(1) *Revetments.* The resistance of unrevetted trenches and foxholes to air blast is primarily dependent upon the soil characteristics, particularly the cohesive qualities of the soil. Revetted emplacements resist collapse at considerably greater overpressures than unrevetted emplacements. Light revetting materials such as chicken wire and burlap or pasteboard, light timber, plywood and corrugated sheet metal, when well supported, are fairly resistant to air blast.

(2) *Overhead cover.* Covered fortifications that have their cover flush with grade level are subject primarily to downward pressures on the roof, whereas those fortifications having their cover above grade level are subject also to drag loading, which tends to remove loose earth and disarrange and remove the cover structures. Entrances are usually the weakest point of blast resistance.

b. Ground Shock and Cratering. Damage from air blast and air induced ground shock to revetted field fortifications occurs at ranges where damage due to direct ground shock and cratering alone is insignificant. However, for unrevetted foxholes and trenches in most soils, the direct ground shock produced by an underground burst contributes somewhat to the collapse. Ground shock and cratering are of importance for predicting damage to heavy, deliberate fortifications. (See par. 7.3*c*.)

c. Thermal Radiation Damage. Superficial scorching of the wooden portions of field fortifications subject to direct thermal radiation from the fireball may occur. Sandbags fail at 10 cal/cm^2 from a 1 KT detonation.

7.5 Dams and Harbor Installations

a. Air Blast.

(1) *Concrete gravity dams.* A concrete gravity dam with the water depth less than

about half the dam height is most vulnerable to a surface burst upstream from the dam. An air burst on the downstream side of the dam is the least effective method of producing breaching of concrete gravity dams. Air blast from such a burst or from a burst on top of the dam is a primary damaging agent against powerhouse structures; these should be analyzed according to structural type as in paragraph 7.2.

(2) *Harbor installations.* Air blast is the most important damaging mechanism for most structures around a harbor. Air blast damage to surface structures is discussed in paragraph 7.2. For canal or river locks, where the water level around the gates is low, air blast is effective in making the locks inoperable by damage to the gates.

b. Water Shock. A concrete gravity dam with the reservoir water level higher than about half the dam height is most vulnerable to an underwater burst. As the depth of water increases, the vulnerability of the dam to an underwater burst increases. This is because underwater shock impulse for a given yield weapon at a given distance is greater for greater depths. Only a limited amount of information is available on dam destruction, and scaling laws are not fixed. The following are estimated ranges for damage by a 20 KT underwater burst at mid-depth to full concrete gravity dams (straight or slightly curved in plan):

60 ft. high dam

Cracks are produced at a range of about 300 yards; portions are cracked loose and displaced small distances at a range of about 200 yards.

150-foot high dam

Cracks are produced at a range of about 500 yards; portions are cracked loose and displaced sizable distances at a range of about 200 yards.

500-foot high dam

Cracks are produced at a range of about 1,300 yards; portions are cracked loose and displaced large distances at a range of about 200 yards.

Canal and river locks, where there is a high water level around the gates, are most vulnerable to damage from an underwater burst.

c. Cratering. For earth dams and causeways, the primary damaging mechanism is cratering; for breaching, the dam or causeway should be within the crater. The crater lip formed by an underwater burst in a harbor may create a navigational hazard; however, water erosion may make this hazard temporary. For structures on shore around a harbor, the range for air blast damage is greater than the range of cratering damage to these structures from an underwater burst near the shore. Cratering is the most important damaging mechanism for concrete quay walls and canal and river locks if the structure is within the rupture zone. The crater dimensions formed by an underwater burst can be computed using the procedure given with figures 2–24 through 2–26. Craters from ground surface and underground bursts can be computed from the procedures given in paragraph 2.2. Weapons detonated on the top or at the toe of a concrete gravity dam produce damage to the dam by cratering. The extent of the rupture can be computed by the method given in paragraph 2.2. For a burst on the top of the dam, the extent of rupture determines the amount the water level drops. When the burst is at the toe of the dam the extent of rupture also determines whether the dam loses its stability against overturning. For a detonation in a dam gallery, the extent of damage can be computed as for an underground burst by the method given in paragraph 2.2. Radius of rupture should be taken as 1.5 times the crater depth computed for rock.

d. Water Waves. The many variables involved in predicting damage from wave action require an individual analysis of each target. Among the variables involved are water depth, bottom slope, wave height, wave length, target response characteristics, orientation of target to the wave front, location of target relative to the point of wave breaking, and variation in width of the channel or harbor. Figure 2–34 gives estimated maximum wave height as a function of water depth and burst position. These figures are for a constant depth of water. As the water depth or width of the wave front varies, the wave height also changes. Wave action may cause additional damage to structures which have already been damaged by air blast. Wave damage may result from the following:

(1) *Impact and hydrostatic pressure.* The magnitude of the impact force depends upon the wave velocity and mass and whether the wave has broken or is breaking. The hydrostatic pressure depends upon the wave height against the structure. Since the lower limiting velocity for damage to light structures by impact is obtained by very low amplitude waves and the velocity increases with amplitude, a wave with a height sufficient to reach inland structures should be considered as a probable damaging agent.

(2) *Drag force.* Objects around which a wave may easily pass such as piling, are also subject to drag forces. A wave passing by a ship may cause displacement due to drag forces and damage may occur as a result of the ship colliding with some other object, such as a pier.

(3) *Inundation.* When a long duration wave from a nuclear explosion reaches a sloping beach, the wave tends to increase in height and run inland. Large areas may be temporarily inundated.

e. Thermal Radiation Damage. Dams, whether of earthen or concrete construction, are not affected significantly by thermal radiation. Many waterfront areas contain a high incidence of kindling fuels and large amounts of highly combustible materials. Consequently, large fires might result in these areas from ignitions in kindling fuels such as excelsior, oily rags or sails, and rotted piling.

DAMAGE TO SURFACE STRUCTURES

The families of curves presented in figures 7-1 through 7-17 show the distances and heights of burst at which there is a 50 percent probability of a nuclear detonation causing severe damage to various types of surface structures. Figures 7-1 through 7-15 present damage distance as a function of height of burst for various yields from 1 KT to 10 MT. Data for yields not indicated may be found by interpolation. Figures 7-16 and 7-17 apply to surface bursts only for yields from 0.1 KT to 100 MT.

To obtain a damage curve of 90 percent probability of severe damage for a selected yield and burst height, use a curve of one-half the selected yield to determine distances at the same height of burst. To obtain a damage curve of 10 percent probability of severe damage, use a curve of twice the selected yield at the same burst height. To obtain a damage curve of 50 percent probability of *moderate* damage for a selected yield and burst height, use a curve of four times the selected yield to determine distance at the same height of burst for structures damaged primarily during the diffraction phase (figures 7-1 through 7-6 and 7-16). For structures damaged primarily during the drag phase (figures 7-7 through 7-15 and 7-17) use a curve of twice the selected yield. Fifty percent probability *light* damage curves for buildings may be obtained by scaling the 1 psi peak overpressure contour of figure 2-10B to the desired yield. The range for light damage to truss bridges can be obtained by scaling the 0.6 psi dynamic pressure contour of figure 2-13 to the desired yield.

The curves presented are for random orientation except the curves for truss bridges given in figures 7-11 and 7-12. These figures give distances of severe damage when the direction of blast wave propagation varies between 45° and 90° from the longitudinal bridge axis. To determine distances for an orientation of 0°, use figure 7-11 for all span lengths by reducing the distances to 60 percent of those given. For orientations between 0° and 45°, a linear interpolation is to be used.

Example 1.

Given: (*a*) Heavy steel frame building.

(*b*) 100 KT burst at 1,000 feet burst height.

Find: Distances at which 90 percent, 50 percent, and 10 percent probability of severe damage occur and the distances at which moderate and light damage occur with 50 percent probability.

Solution: From figures 7-8A and 7-8B:

(*a*) 90 percent probability of severe damage—read the 50 KT curve at 1,000 feet height of burst. 1,375 yards. *Answer.*

(*b*) 50 percent probability of severe damage—read the 100 KT curve at 1,000 feet height of burst. 1,800 yards. *Answer.*

(*c*) 10 percent probability of severe damage—read the 200 KT curve at 1,000 feet height of burst. 2,290 yards. *Answer.*

(*d*) 50 percent probability of moderate damage—read the 200 KT curve at 1,000 feet height of burst. 2,300 yards. *Answer.*

(*e*) 50 percent probability of light damage—1,000 feet height of burst for 100 KT corresponds to—

$$\frac{1,000}{(100)^{1/3}} = 215 \text{ feet for a 1 KT burst.}$$

From figure 2-10B the scaled distance at 215 feet burst height is equal to 1,550 yards for 1 psi. Therefore, the actual distance for light damage is $(1,550)(100^{1/3}) = 7,200$ yards. *Answer.*

Example 2.

Given: A 125 KT detonation at 50 feet depth.

Find: The distance to which there is a 50 percent or better probability of producing *moderate* damage to a multistory, blast-resistant, reinforced concrete building.

Solution: Since the curves are for severe damage, use the curve of four times the yield (i. e., 4×125 KT$=$500 KT) to find moderate damage. From figure 7-1, a 500 KT burst at the surface will produce severe damage to 1,400 yards; therefore, 125 KT will produce moderate damage to the same distance.

Figure 7-18 must be used to find the reduction in distance due to the burst being underground.

Scaling. $h_1=\frac{h_2\,W_1^{1/3}}{W_2^{1/3}}=\frac{50\times 1}{(125)^{1/3}}=10$ feet.

From figure 7-18, lowering a burst of 1 KT to a depth of 10 feet will reduce the damage-producing distance by 30 yards. Scaling this to the given burst,

$$d_2=\frac{d_1\times W_2^{1/3}}{W_1^{1/3}}=\frac{30\times(125)^{1/3}}{1}=150 \text{ yards.}$$

This is to be subtracted from the previously determined distance: 1,400 − 150 = 1,250 yards. *Answer.*

Reliability. Based on full scale field test data extended by establisbed physical laws. Variables in both air-blast loading and structural characteristics prevent an exact prediction of damage to a given structure in a particular case.

Related material. See paragraph 7.2*a*(4).

See also tables 7-1 and 7-2.

See also figures 7-18 through 7-22.

SEVERE DAMAGE TO MULTISTORY BLAST RESISTANT DESIGNED REINFORCED CONCRETE BUILDINGS BY VARIOUS YIELDS AS A FUNCTION OF HEIGHT OF BURST AND GROUND RANGE

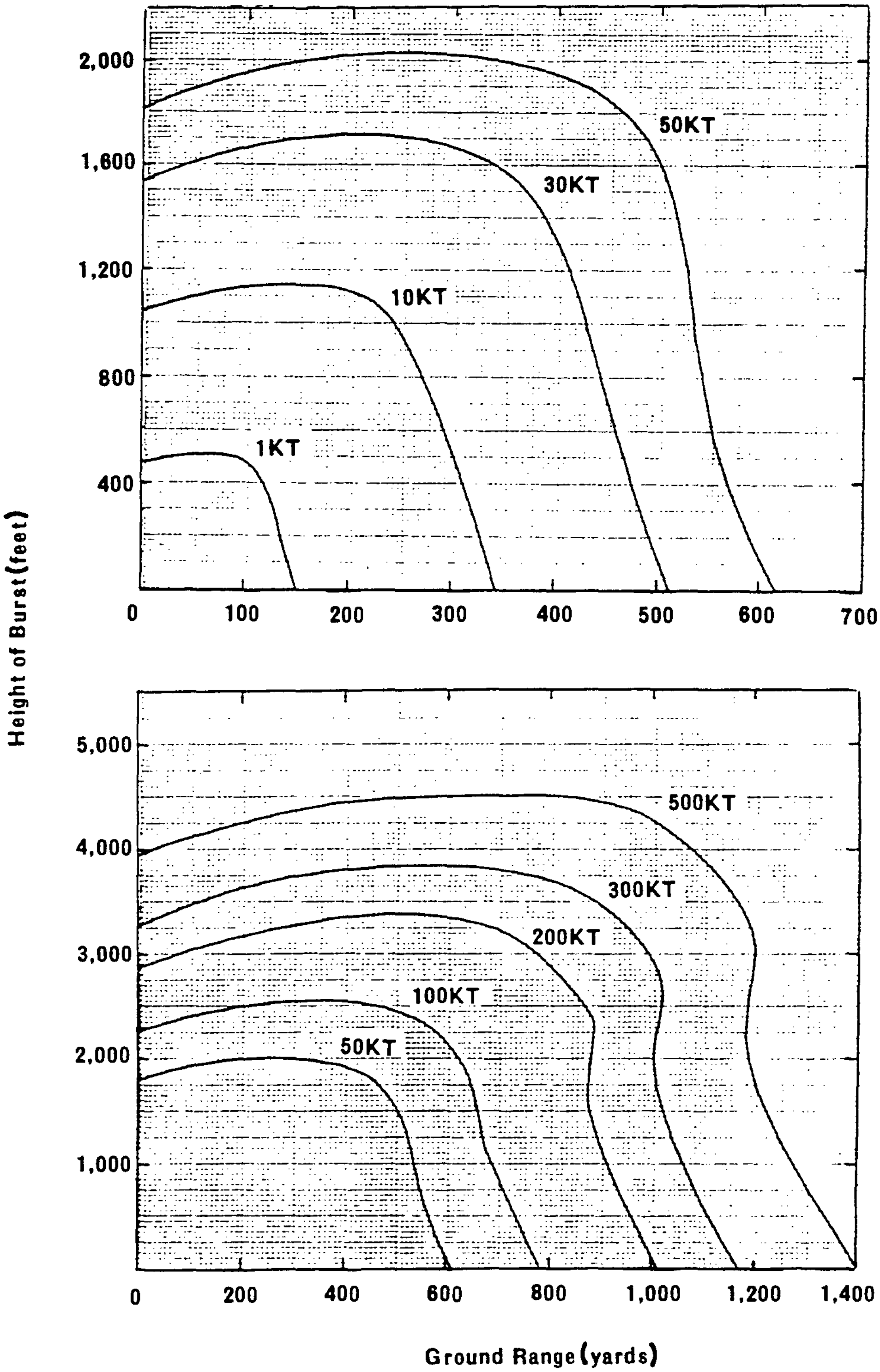

SEVERE DAMAGE TO MULTISTORY BLAST RESISTANT DESIGNED REINFORCED CONCRETE BUILDINGS BY VARIOUS YIELDS AS A FUNCTION OF HEIGHT OF BURST AND GROUND RANGE

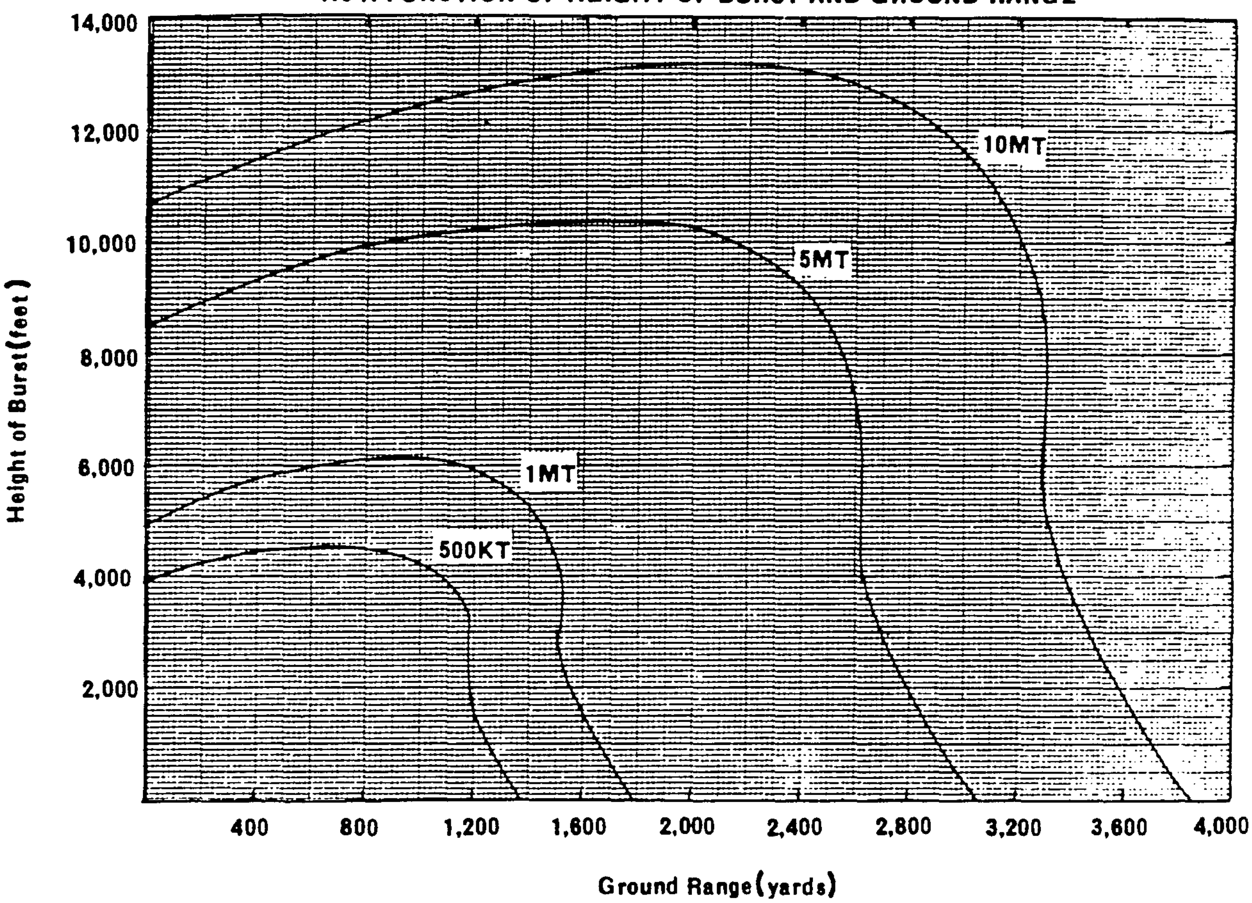

SEVERE DAMAGE TO MULTISTORY REINFORCED CONCRETE BUILDINGS WITH CONCRETE WALLS AND SMALL WINDOW AREA BY VARIOUS YIELDS AS A FUNCTION OF HEIGHT OF BURST AND GROUND RANGE

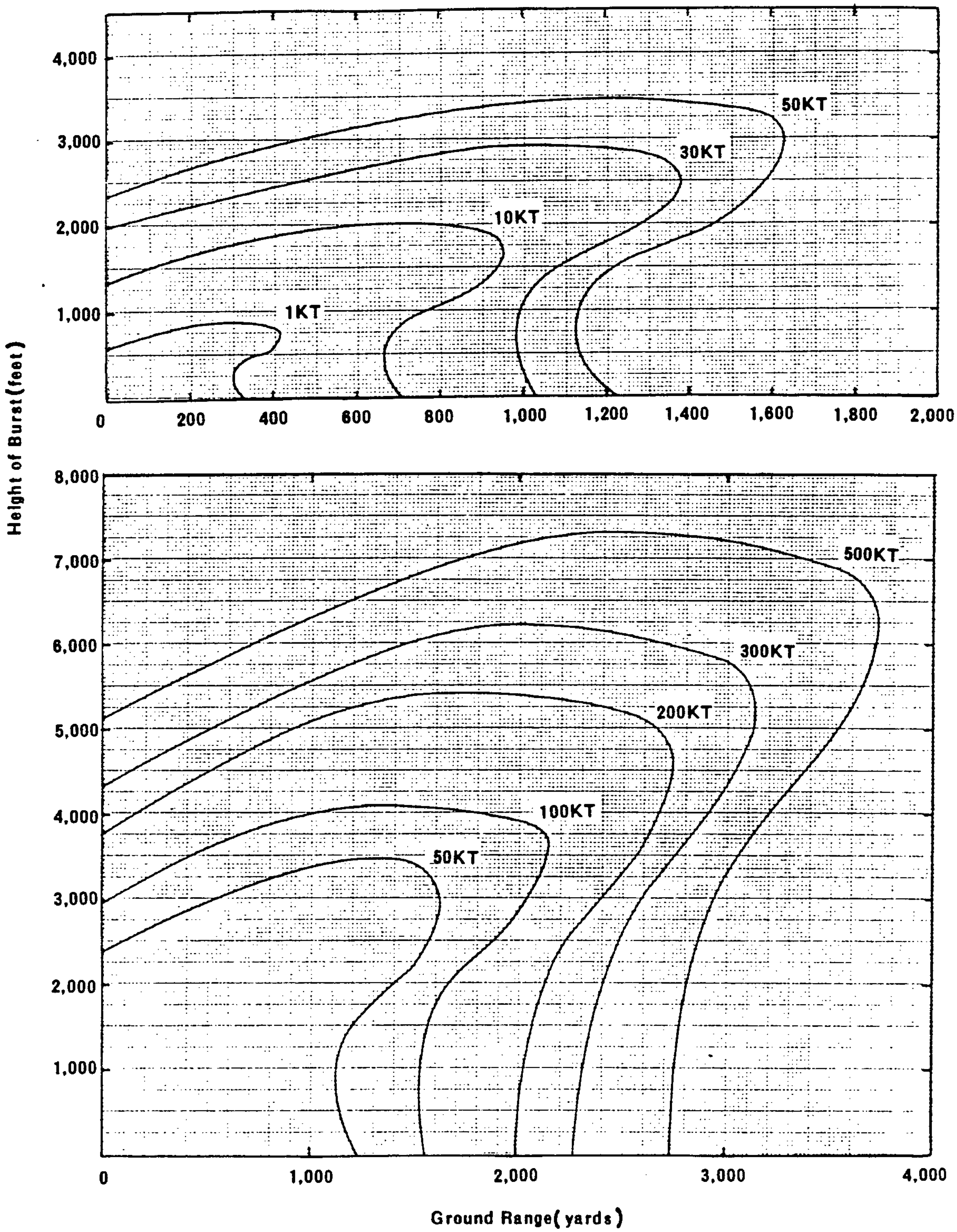

FIGURE 7-2C

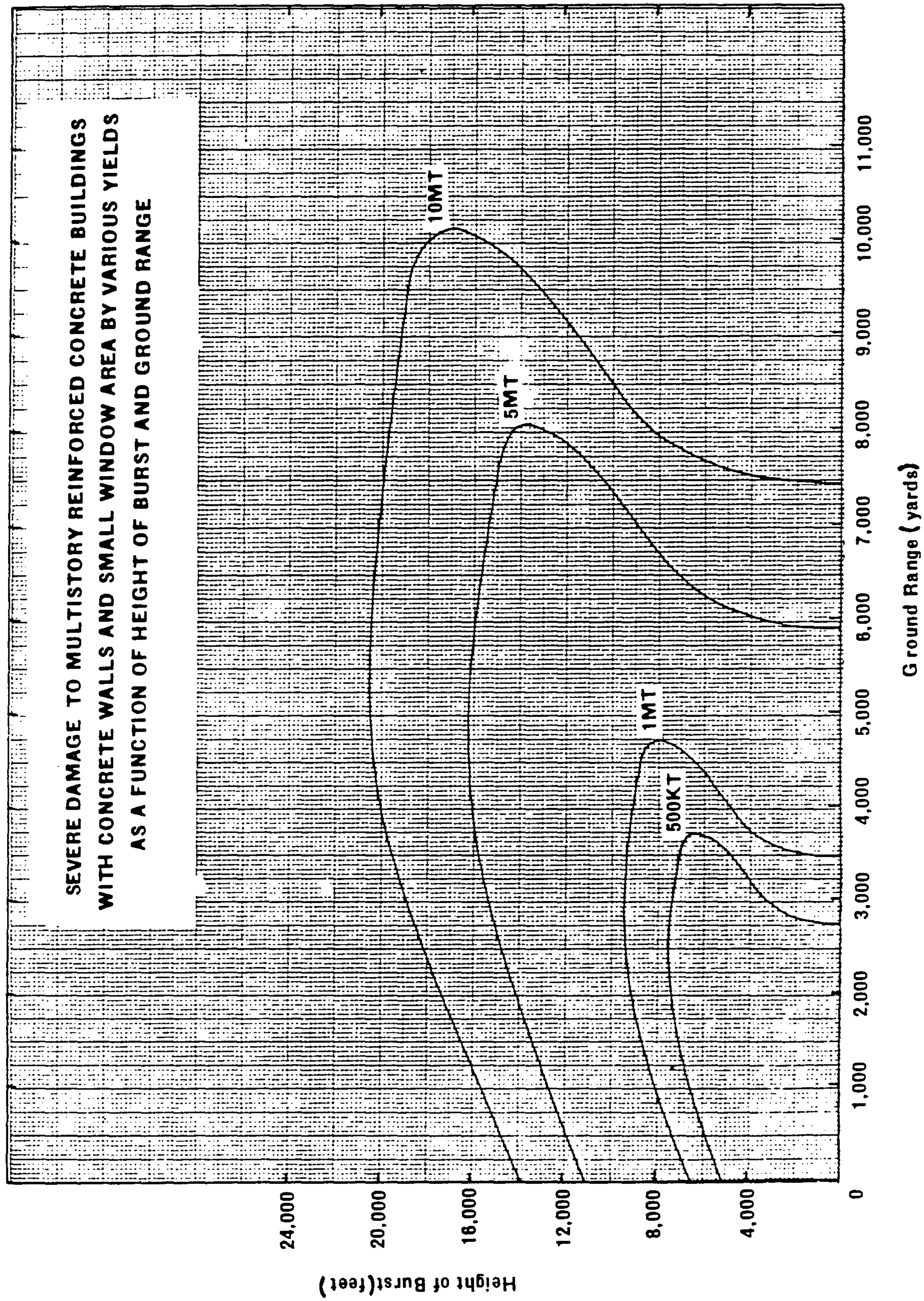
SEVERE DAMAGE TO MULTISTORY REINFORCED CONCRETE BUILDINGS
WITH CONCRETE WALLS AND SMALL WINDOW AREA BY VARIOUS YIELDS
AS A FUNCTION OF HEIGHT OF BURST AND GROUND RANGE
10MT
5MT
1MT
500KT
0
1,000
2,000
3,000
4,000
5,000
6,000
7,000
8,000
9,000
10,000
11,000
Ground Range (yards)
4,000
8,000
12,000
16,000
20,000
24,000
Height of Burst (feet)

SEVERE DAMAGE TO MULTISTORY WALL BEARING BUILDINGS

BRICK APARTMENT HOUSE TYPE WITH SMALL WINDOW AREA

BY VARIOUS YIELDS AS A FUNCTION OF HEIGHT OF BURST AND GROUND RANGE

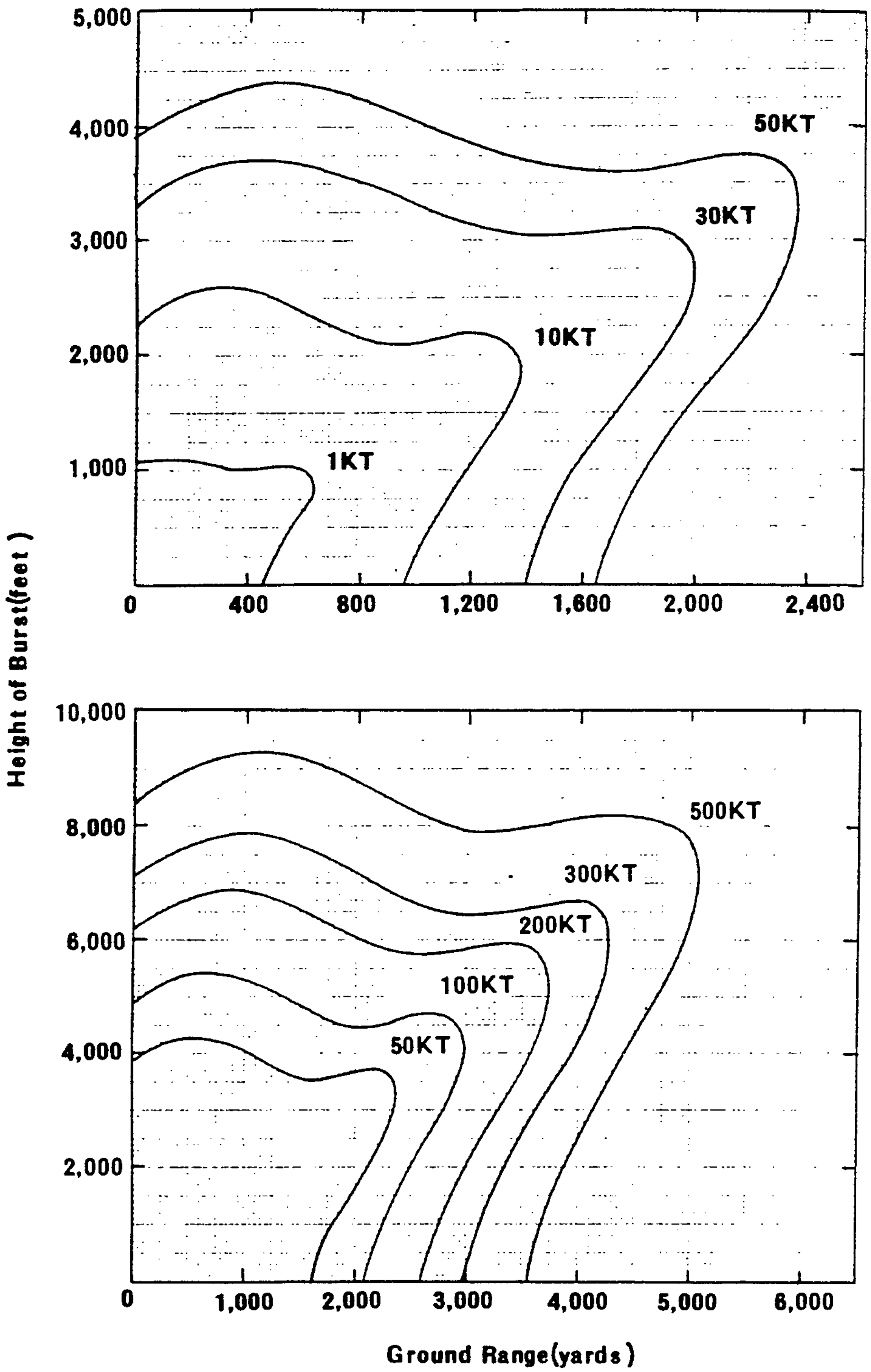

SEVERE DAMAGE TO MULTISTORY WALL BEARING BUILDINGS
BRICK APARTMENT HOUSE TYPE WITH SMALL WINDOW AREA
BY VARIOUS YIELDS AS A FUNCTION OF HEIGHT OF BURST AND GROUND RANGE

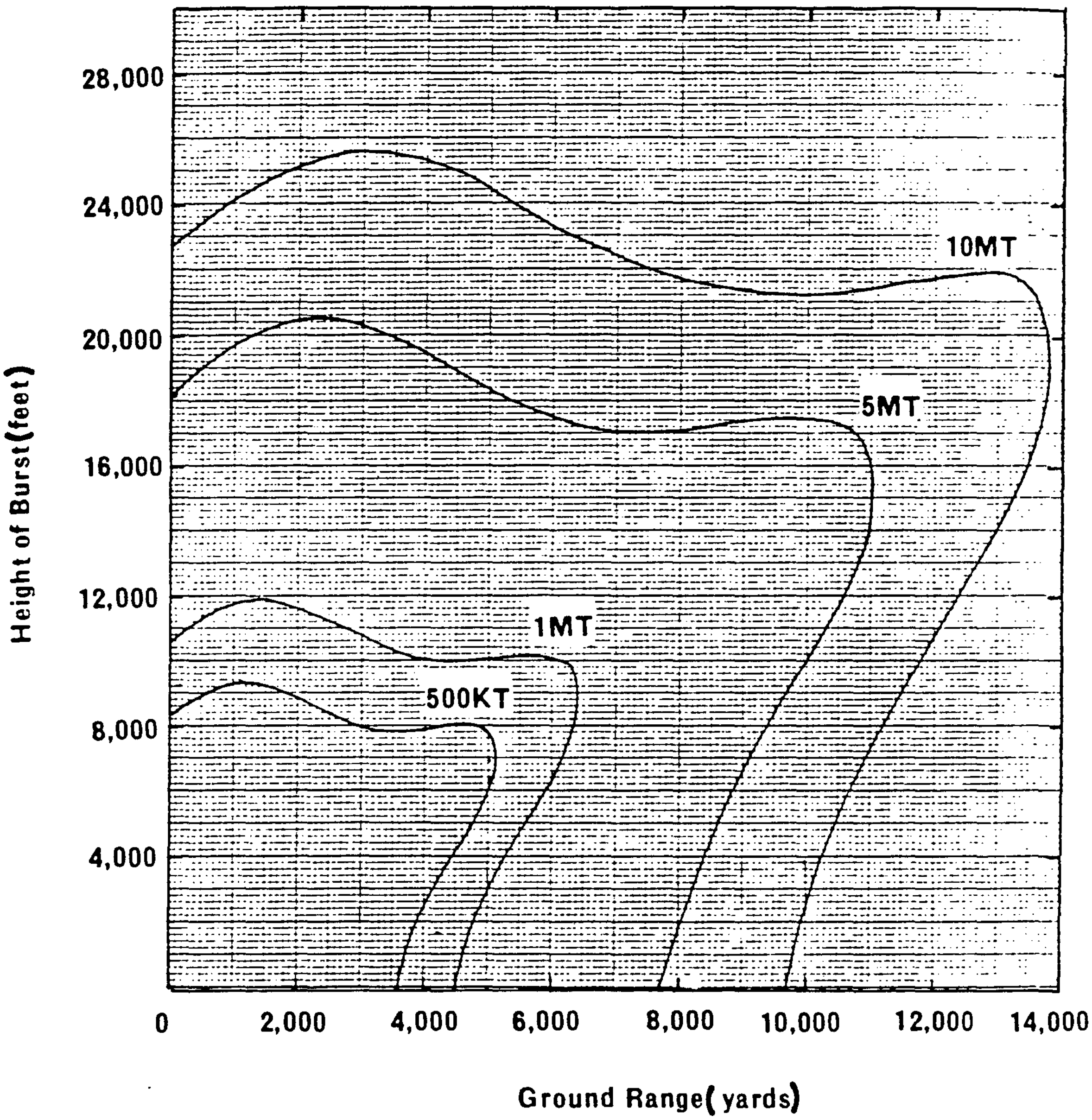

FIGURE 7-4A
FIGURE 7-4B

SEVERE DAMAGE TO MONUMENTAL TYPE MULTISTORY
WALL-BEARING BUILDINGS BY VARIOUS YIELDS
AS A FUNCTION OF HEIGHT OF BURST AND GROUND RANGE

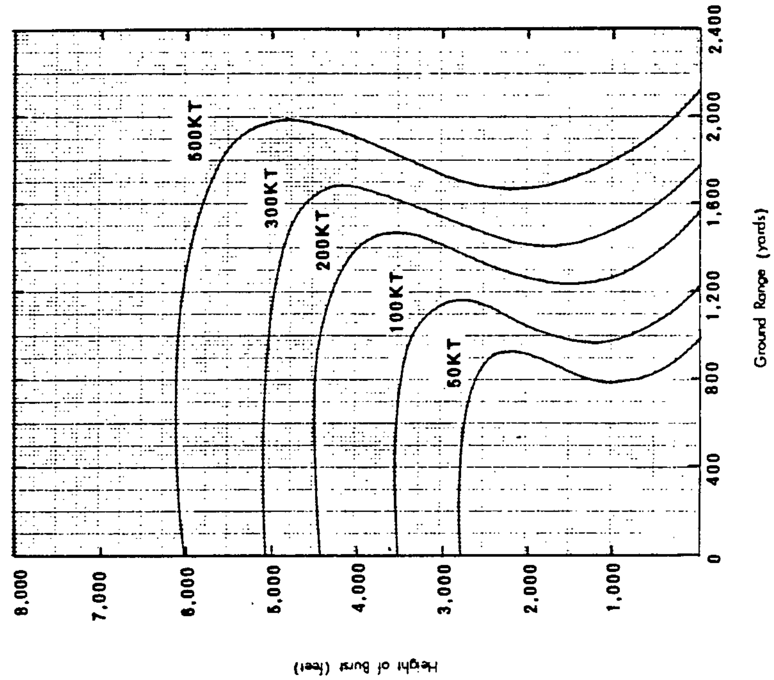

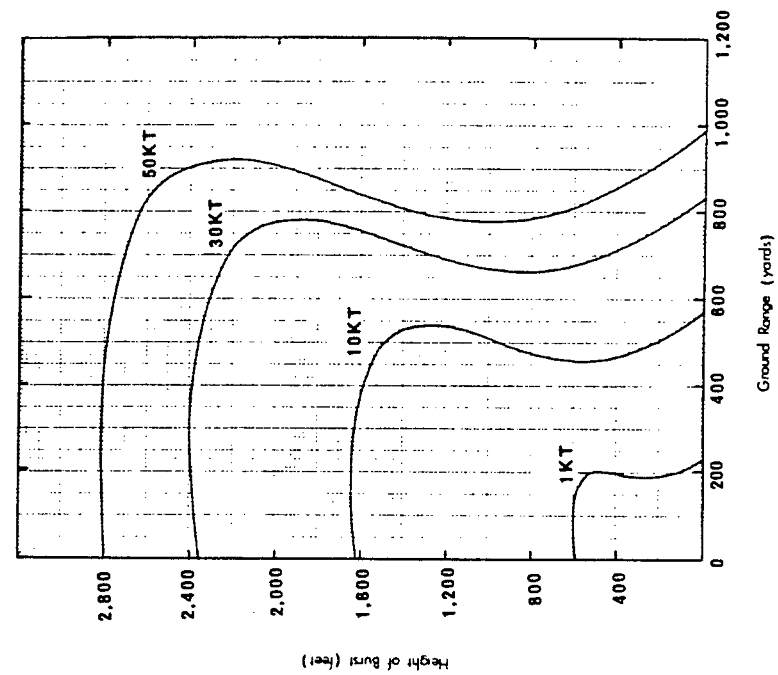

SEVERE DAMAGE TO MONUMENTAL TYPE MULTISTORY WALL-BEARING BUILDINGS BY VARIOUS YIELDS AS A FUNCTION OF HEIGHT OF BURST AND GROUND RANGE

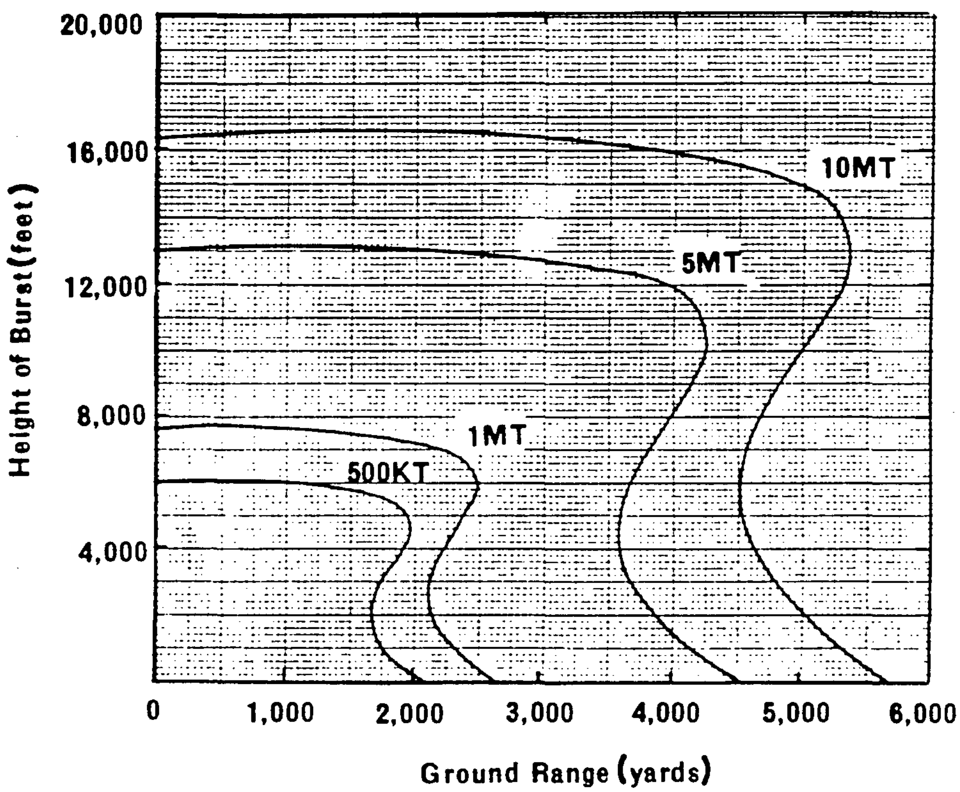

FIGURE 7-5A
FIGURE 7-5B

SEVERE DAMAGE TO WOOD FRAME BUILDINGS BY VARIOUS YIELDS
AS A FUNCTION OF HEIGHT OF BURST AND GROUND RANGE

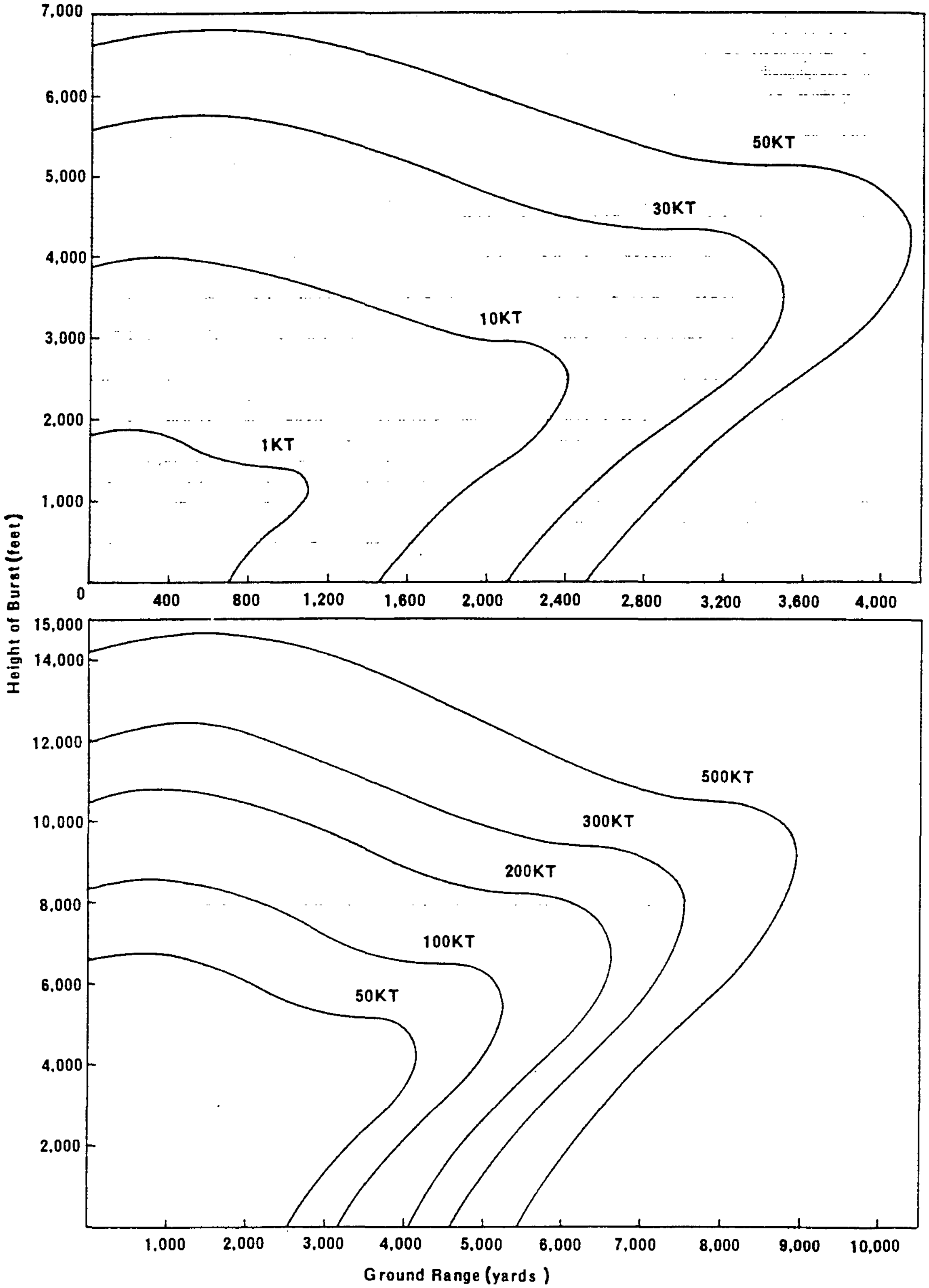

SEVERE DAMAGE TO WOOD FRAME BUILDINGS BY VARIOUS YIELDS AS A FUNCTION OF HEIGHT OF BURST AND GROUND RANGE

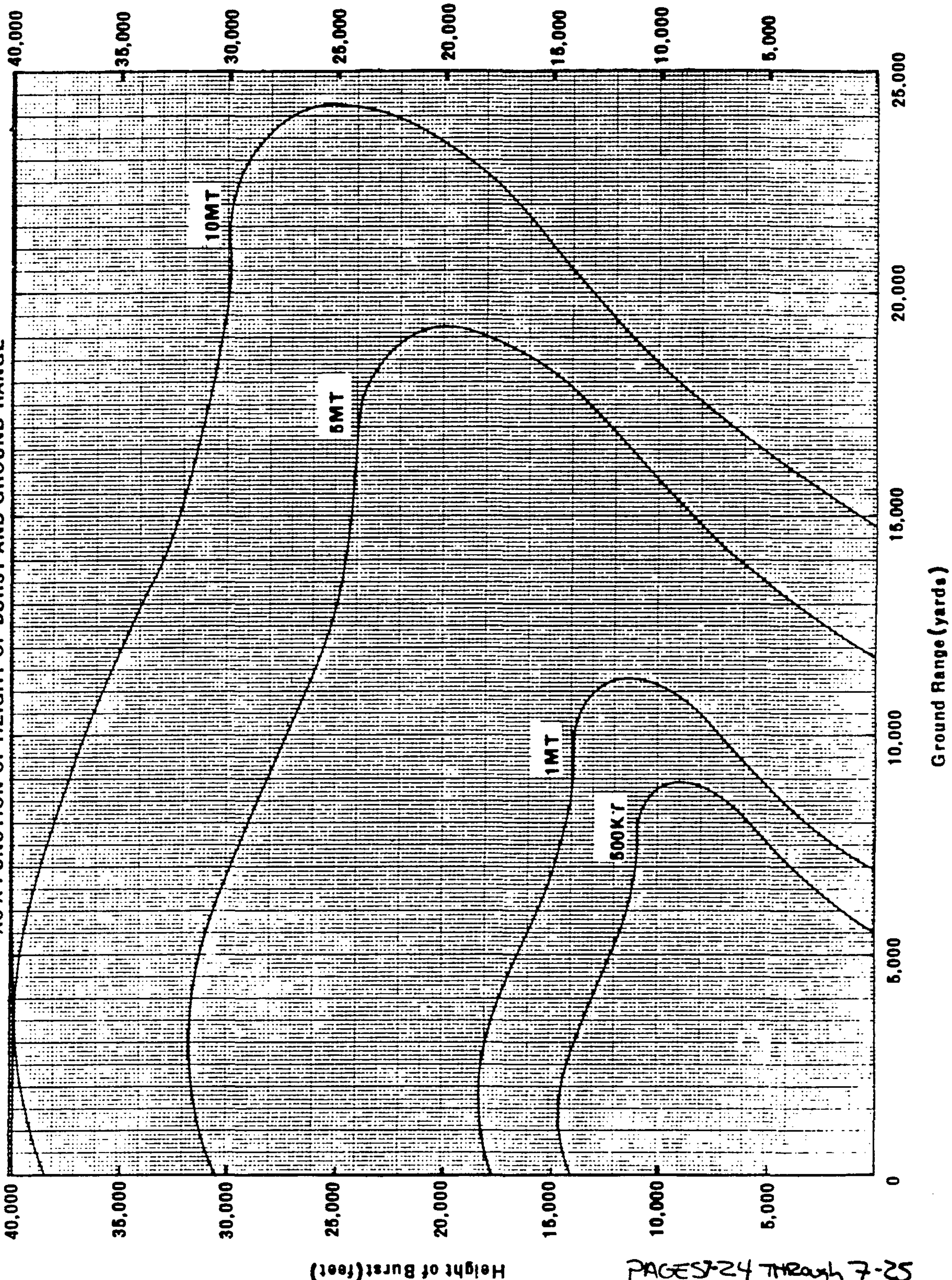

PAGES 7-24 Through 7-25 WITHHELD IN THEIR ENTIRETY (ARMY (b)(1))

FIGURE 7-7A
FIGURE 7-7B

[redacted]

SEVERE DAMAGE TO LIGHT STEEL FRAME INDUSTRIAL BUILDINGS
BY VARIOUS YIELDS AS A FUNCTION OF HEIGHT OF BURST AND GROUND RANGE

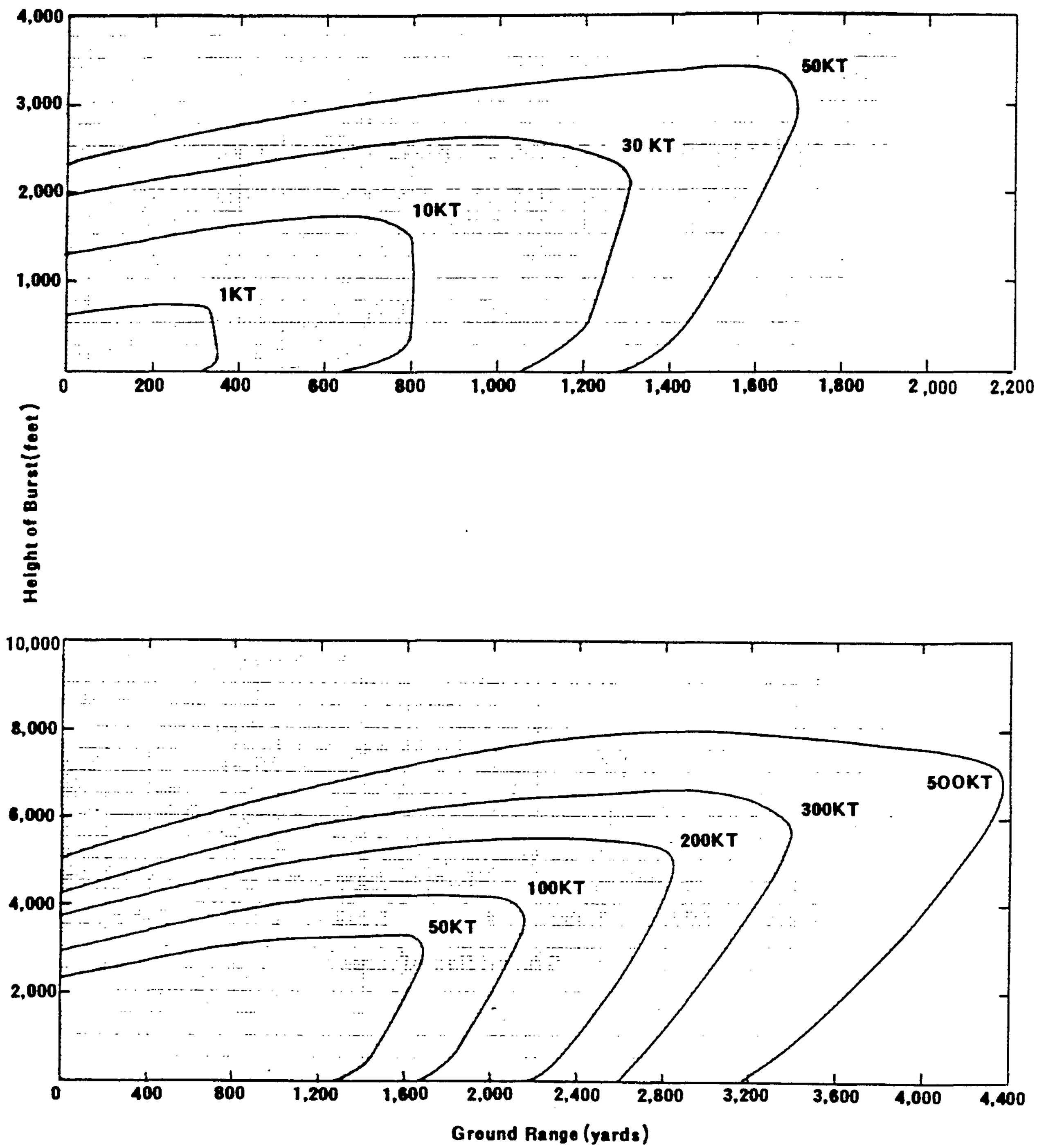

[redacted]

SEVERE DAMAGE TO LIGHT STEEL FRAME INDUSTRIAL BUILDINGS BY VARIOUS YIELDS AS A FUNCTION OF HEIGHT OF BURST AND GROUND RANGE

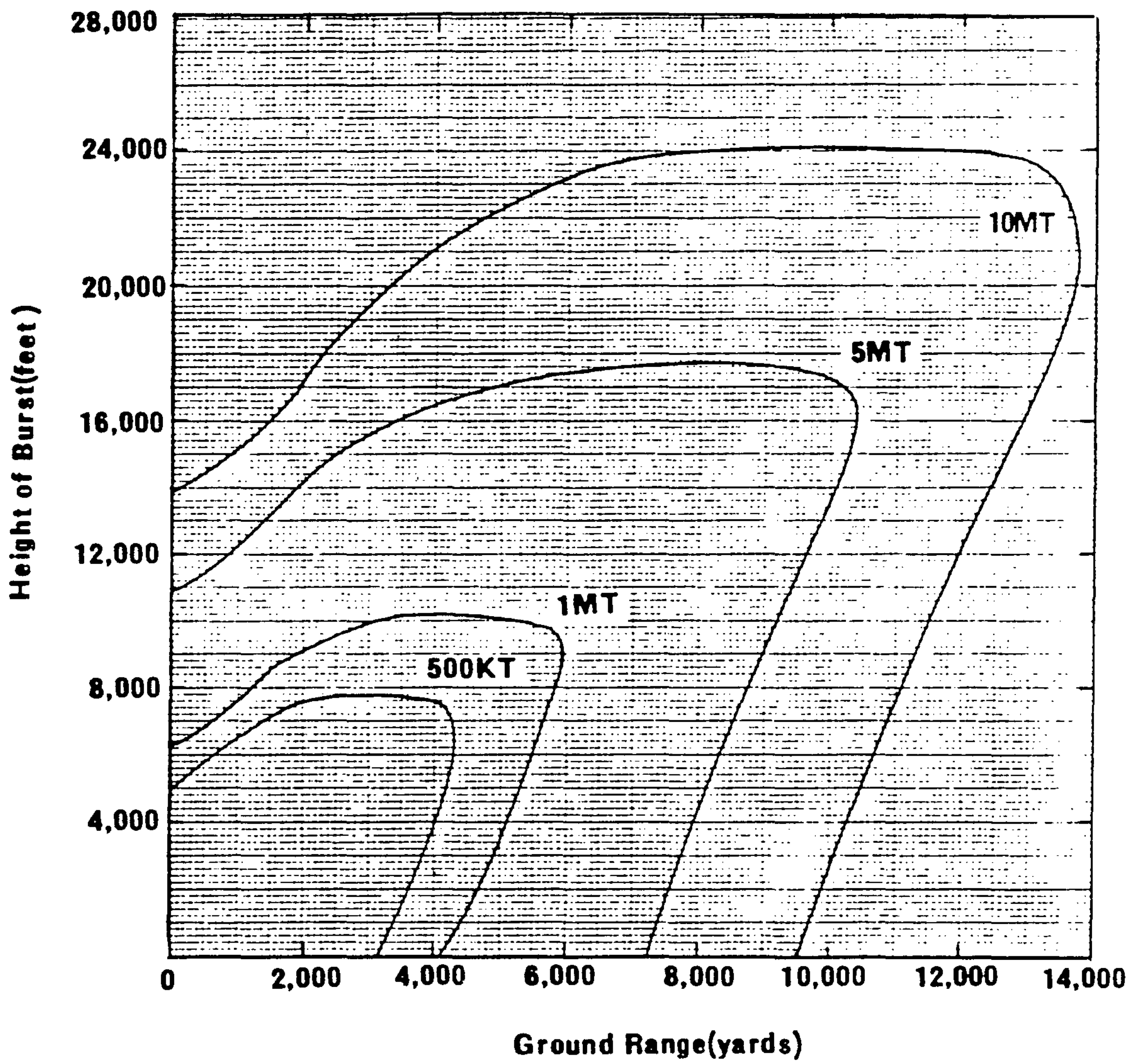

SEVERE DAMAGE TO SINGLE STORY HEAVY STEEL FRAME INDUSTRIAL BUILDINGS BY VARIOUS YIELDS AS A FUNCTION OF HEIGHT OF BURST AND GROUND RANGE

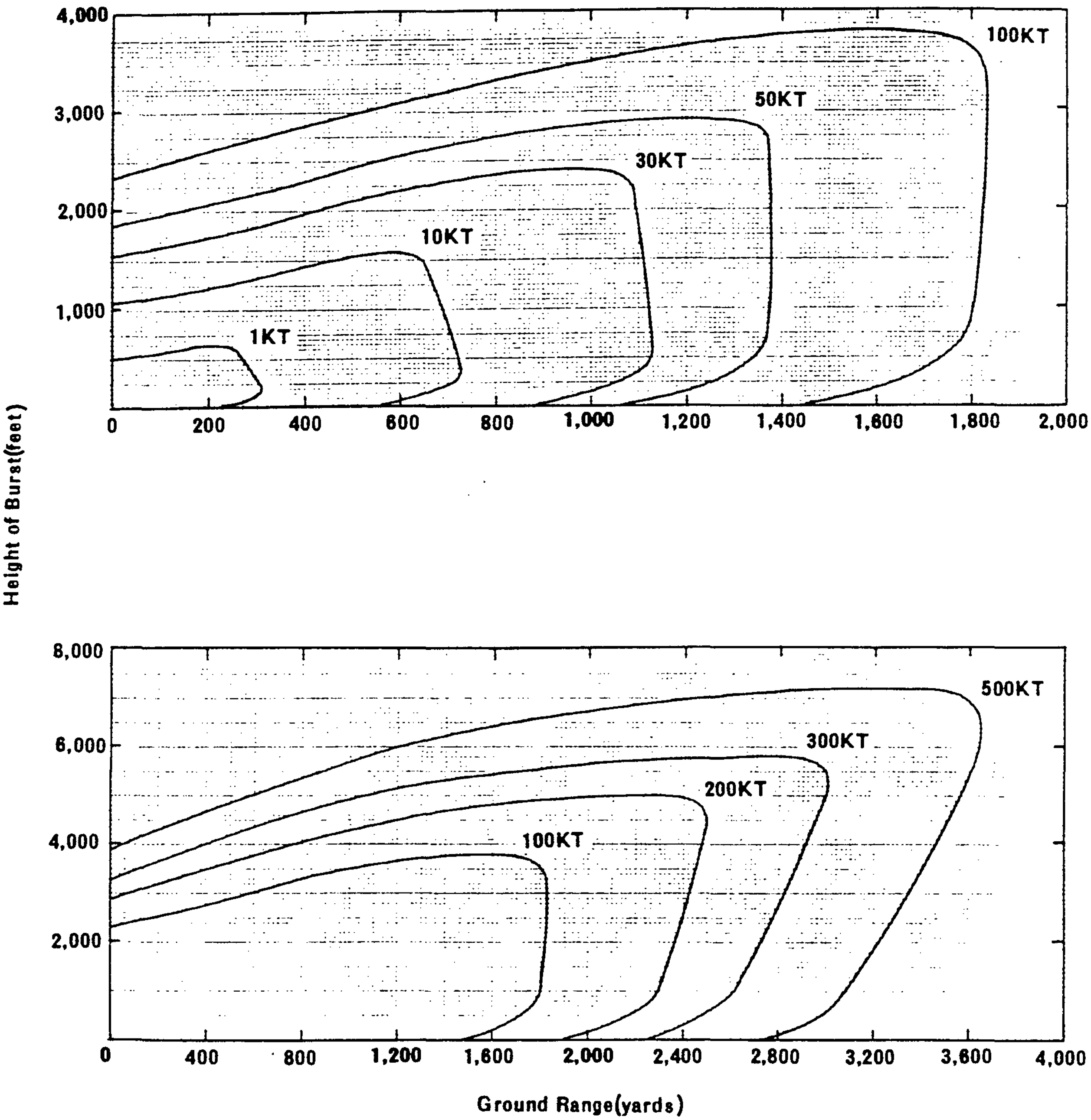

SEVERE DAMAGE TO SINGLE STORY HEAVY STEEL FRAME INDUSTRIAL BUILDINGS BY VARIOUS YIELDS AS A FUNCTION OF HEIGHT OF BURST AND GROUND RANGE

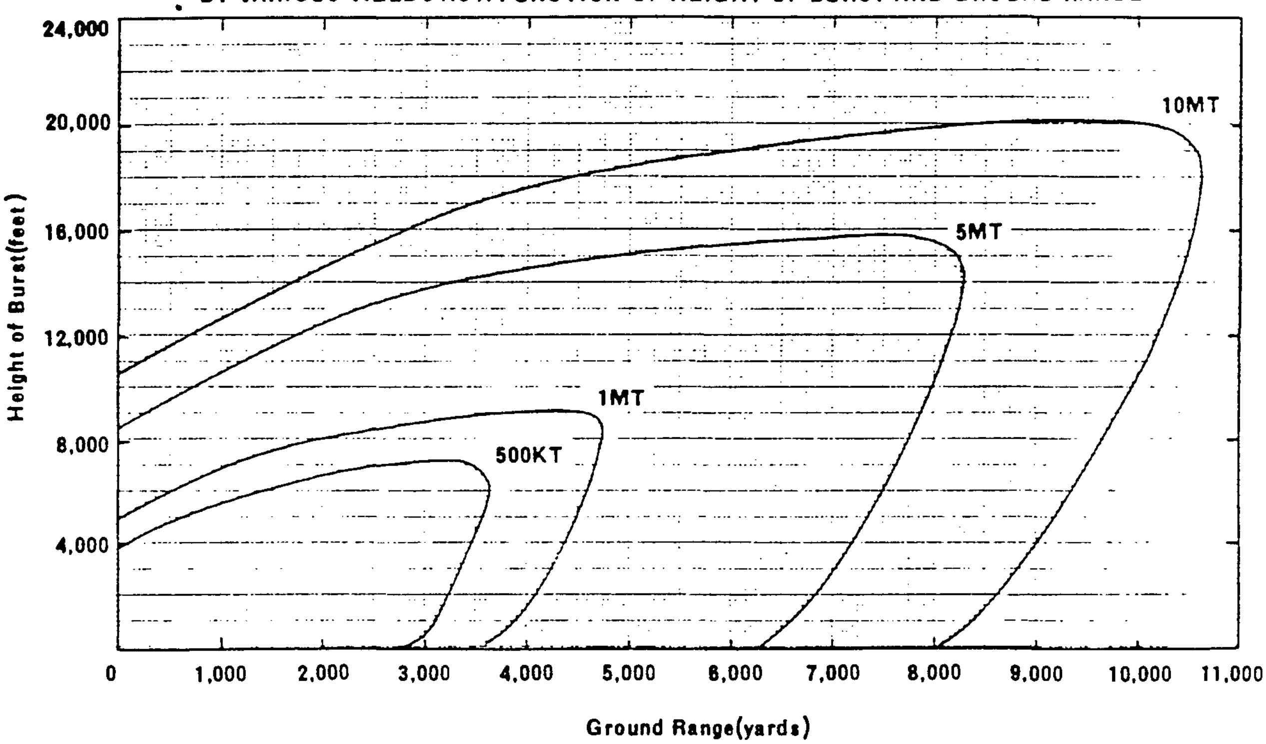

FIGURE 7-9A
FIGURE 7-9B

SEVERE DAMAGE TO MULTISTORY STEEL FRAME OFFICE BUILDING BY VARIOUS YIELDS AS A FUNCTION OF HEIGHT OF BURST AND GROUND RANGE

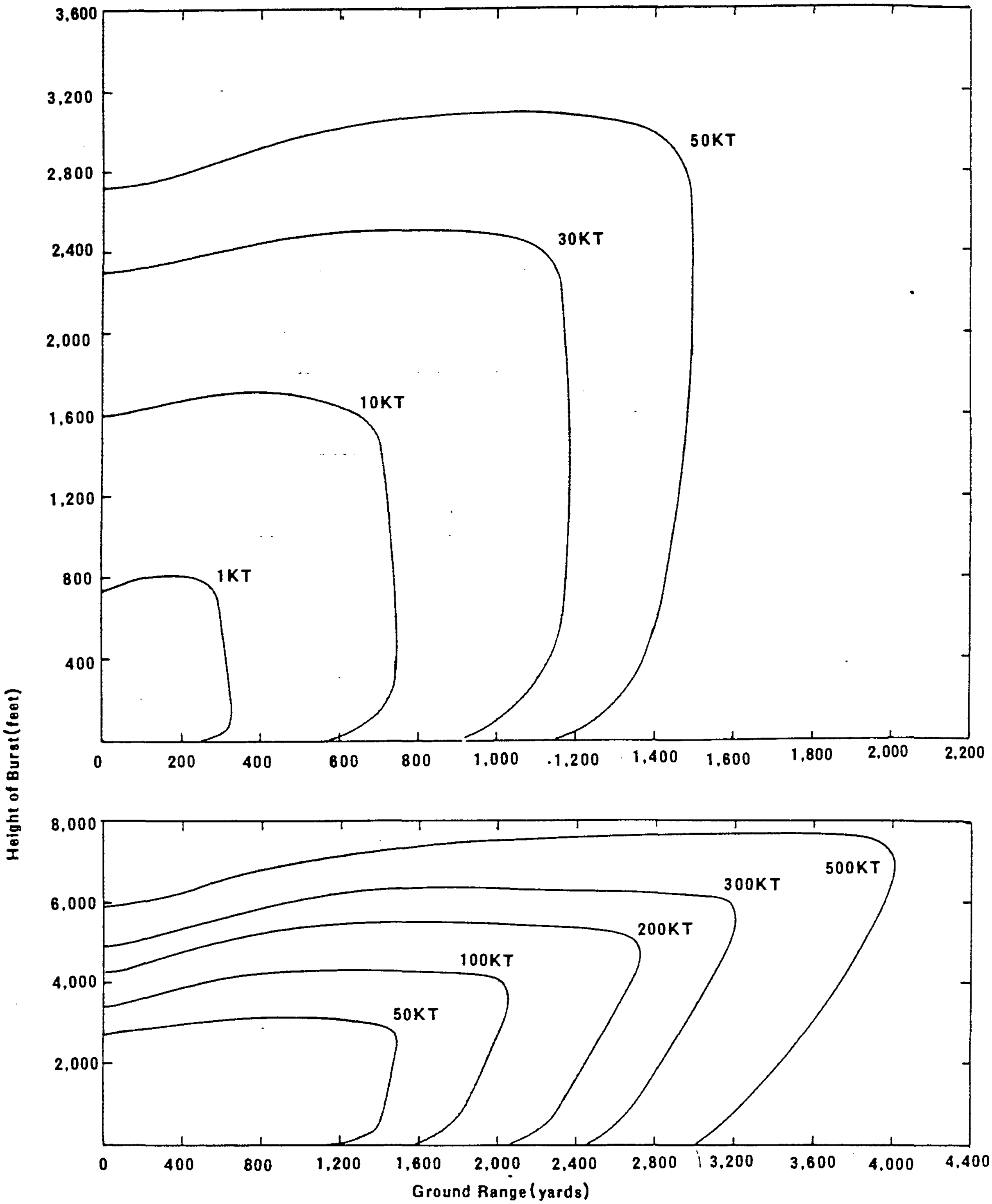

SEVERE DAMAGE TO MULTISTORY STEEL FRAME OFFICE BUILDING
BY VARIOUS YIELDS AS A FUNCTION OF HEIGHT OF BURST AND GROUND RANGE

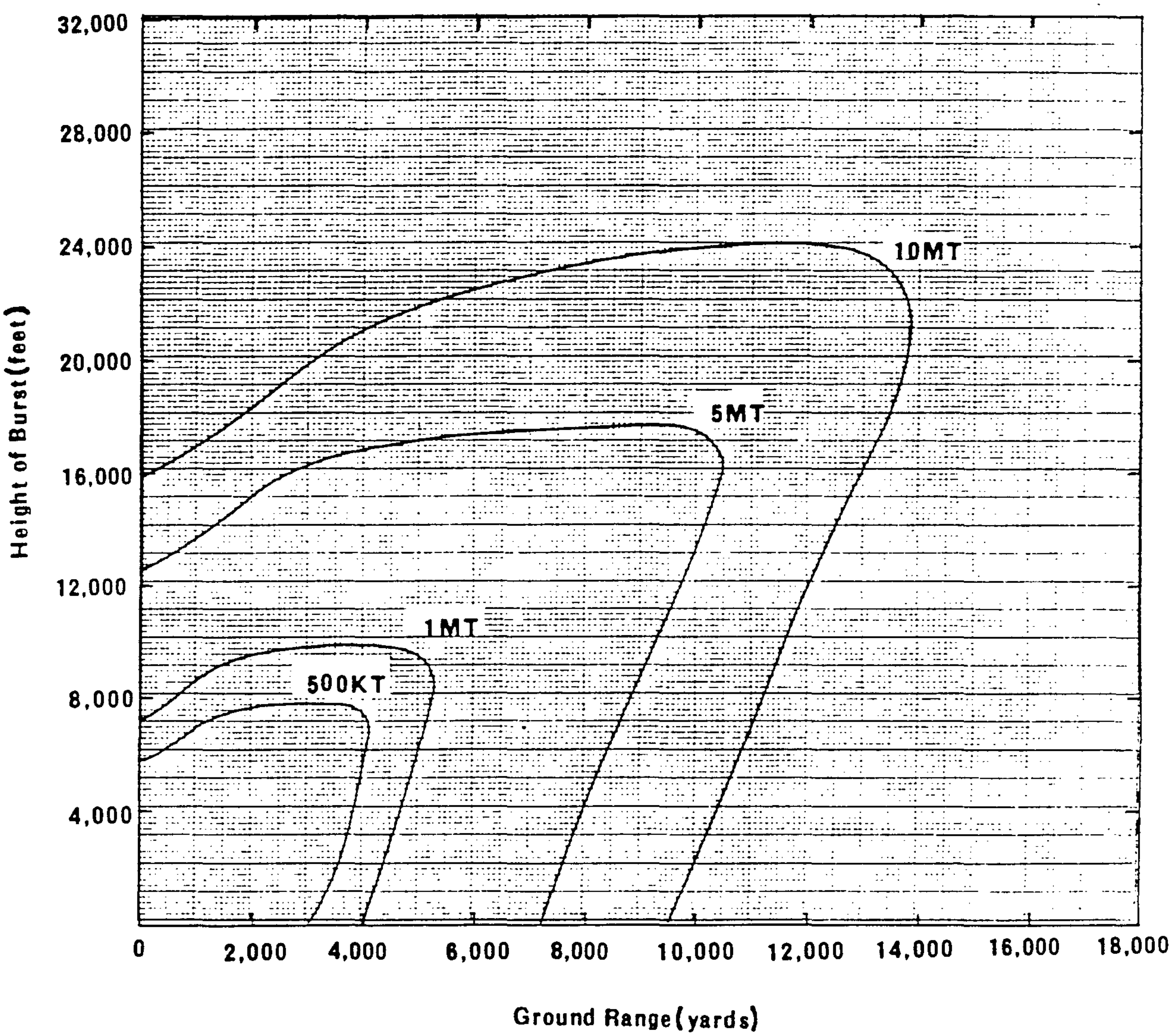

SEVERE DAMAGE TO REINFORCED CONCRETE FRAME OFFICE BUILDINGS
BY VARIOUS YIELDS AS A FUNCTION OF HEIGHT OF BURST AND GROUND RANGE

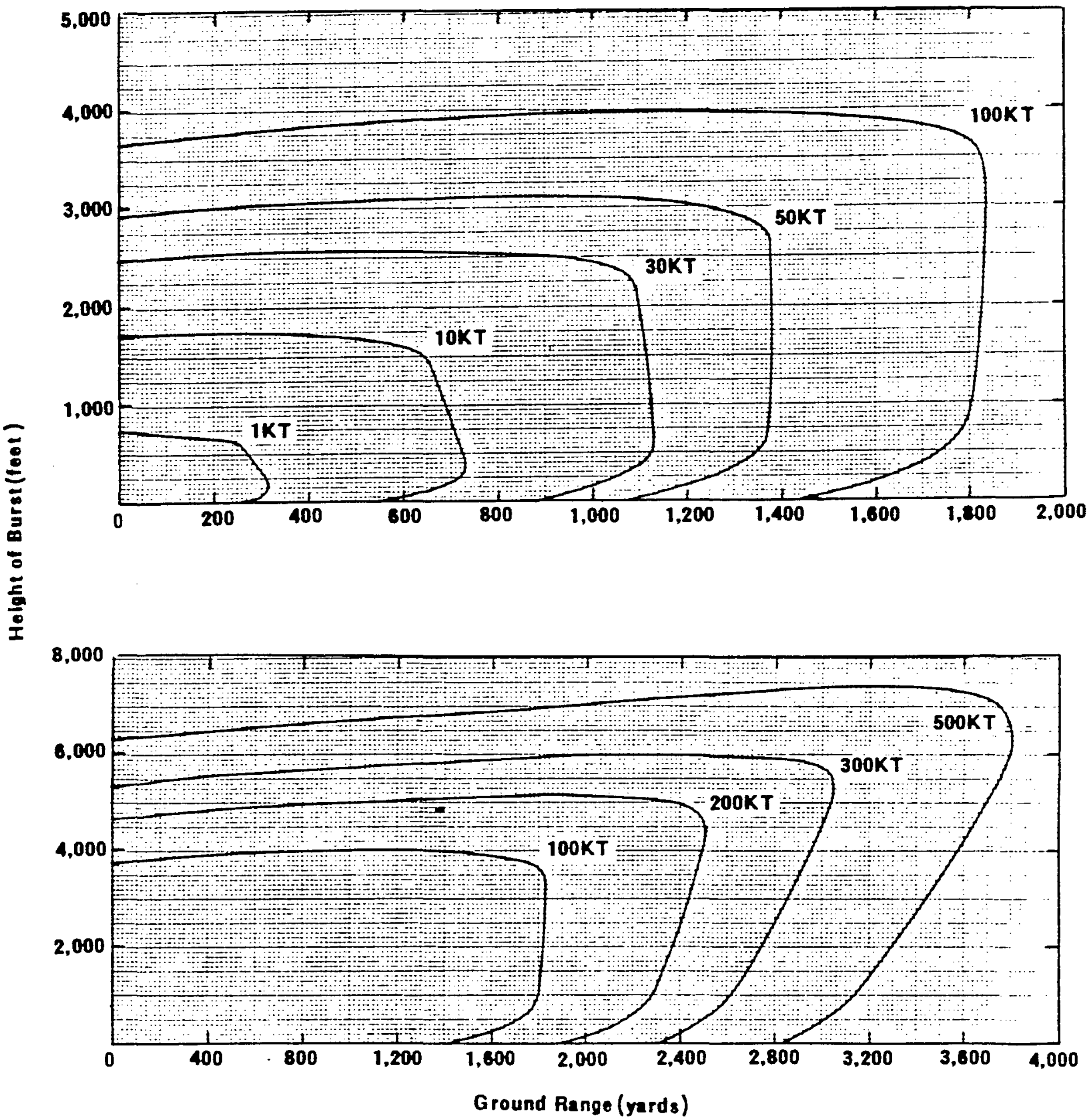

SEVERE DAMAGE TO REINFORCED CONCRETE FRAME OFFICE BUILDINGS
BY VARIOUS YIELDS AS A FUNCTION OF HEIGHT OF BURST AND GROUND RANGE

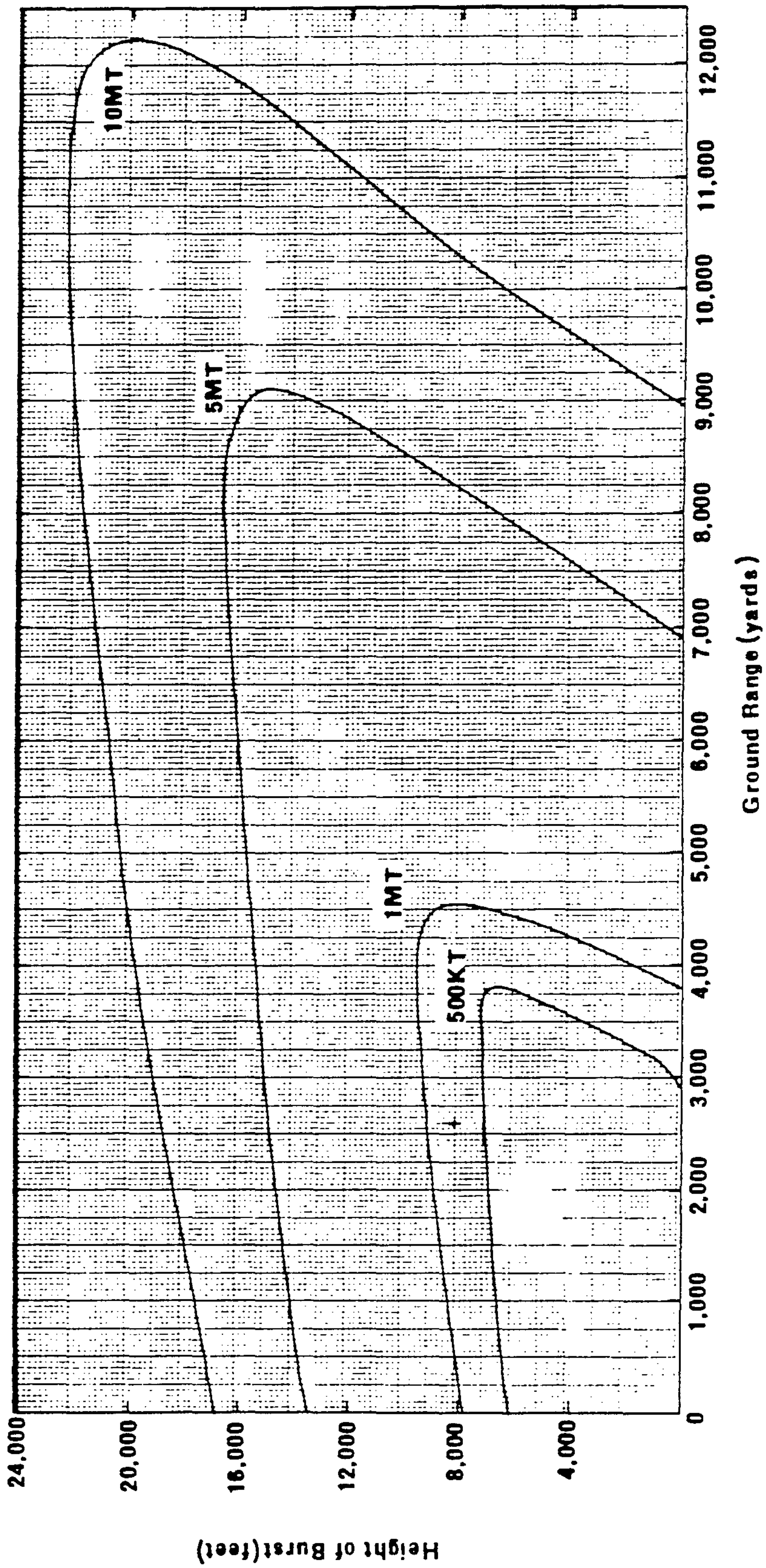

SEVERE DAMAGE TO HIGHWAY AND RAILWAY TRUSS BRIDGES OF 150 TO 250 FOOT SPAN
(BLAST NORMAL TO LONGITUDIONAL BRIDGE AXIS)
BY VARIOUS YIELDS AS FUNCTIONS OF HEIGHT OF BURST AND GROUND RANGE

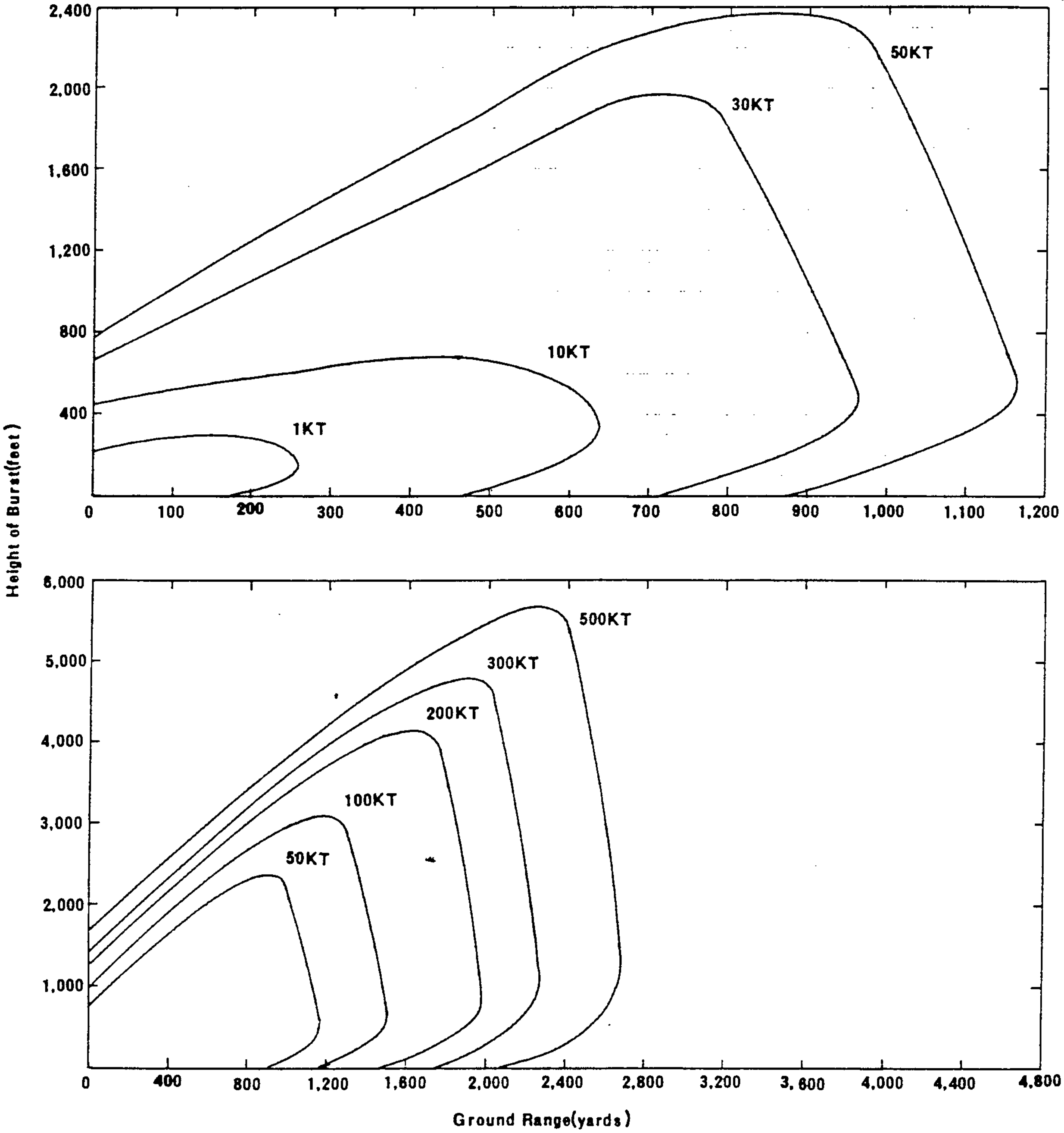

SEVERE DAMAGE TO HIGHWAY AND RAILWAY TRUSS BRIDGES OF 150 TO 250 FOOT SPAN
(BLAST NORMAL TO LONGITUDINAL BRIDGE AXIS)
BY VARIOUS YIELDS AS A FUNCTION OF HEIGHT OF BURST AND GROUND RANGE

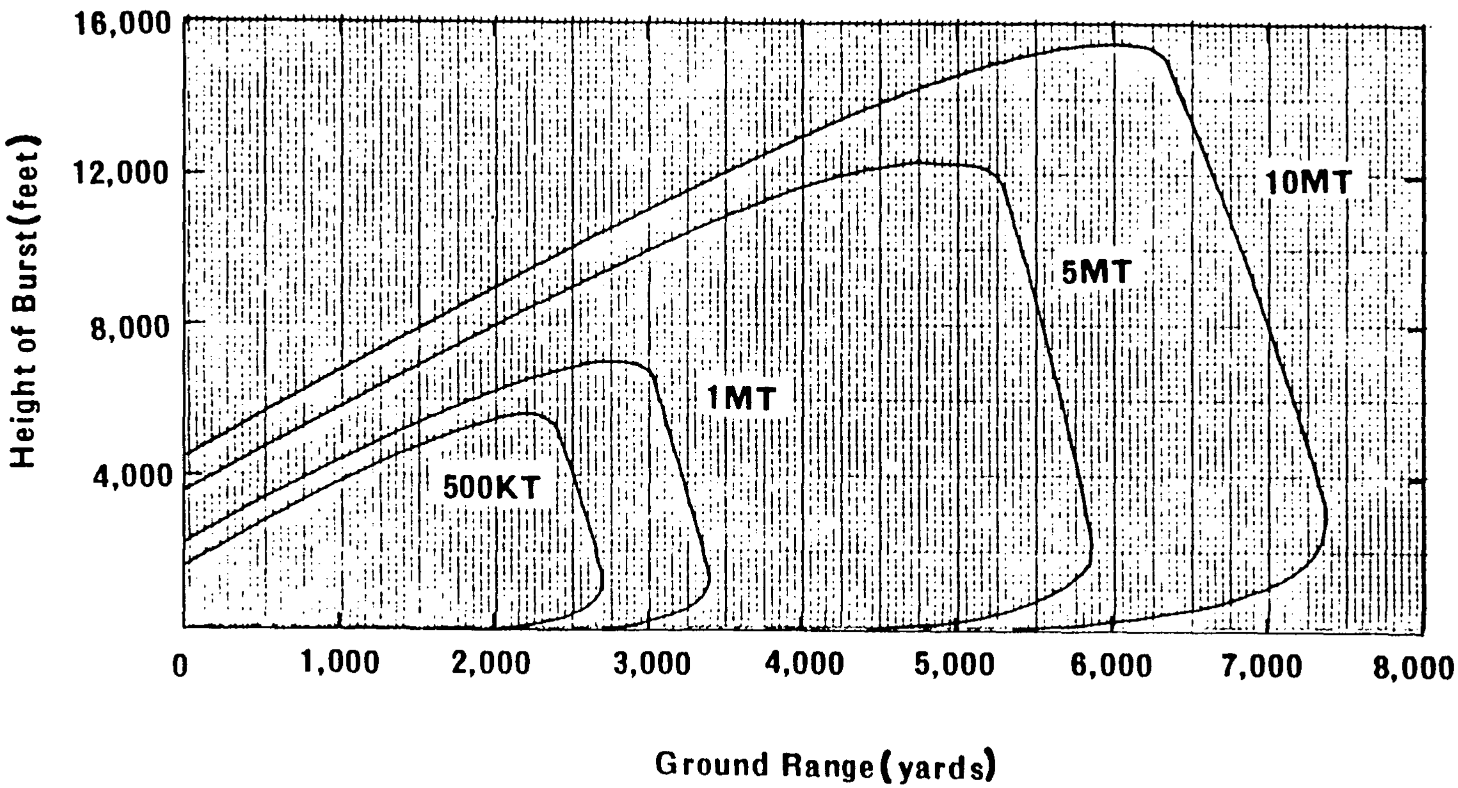

SEVERE DAMAGE TO HIGHWAY AND RAILWAY TRUSS BRIDGES OF 250 TO 550 FOOT SPAN (BLAST NORMAL TO LONGITUDINAL BRIDGE AXIS) BY VARIOUS YIELDS AS A FUNCTION OF HEIGHT OF BURST AND GROUND RANGE

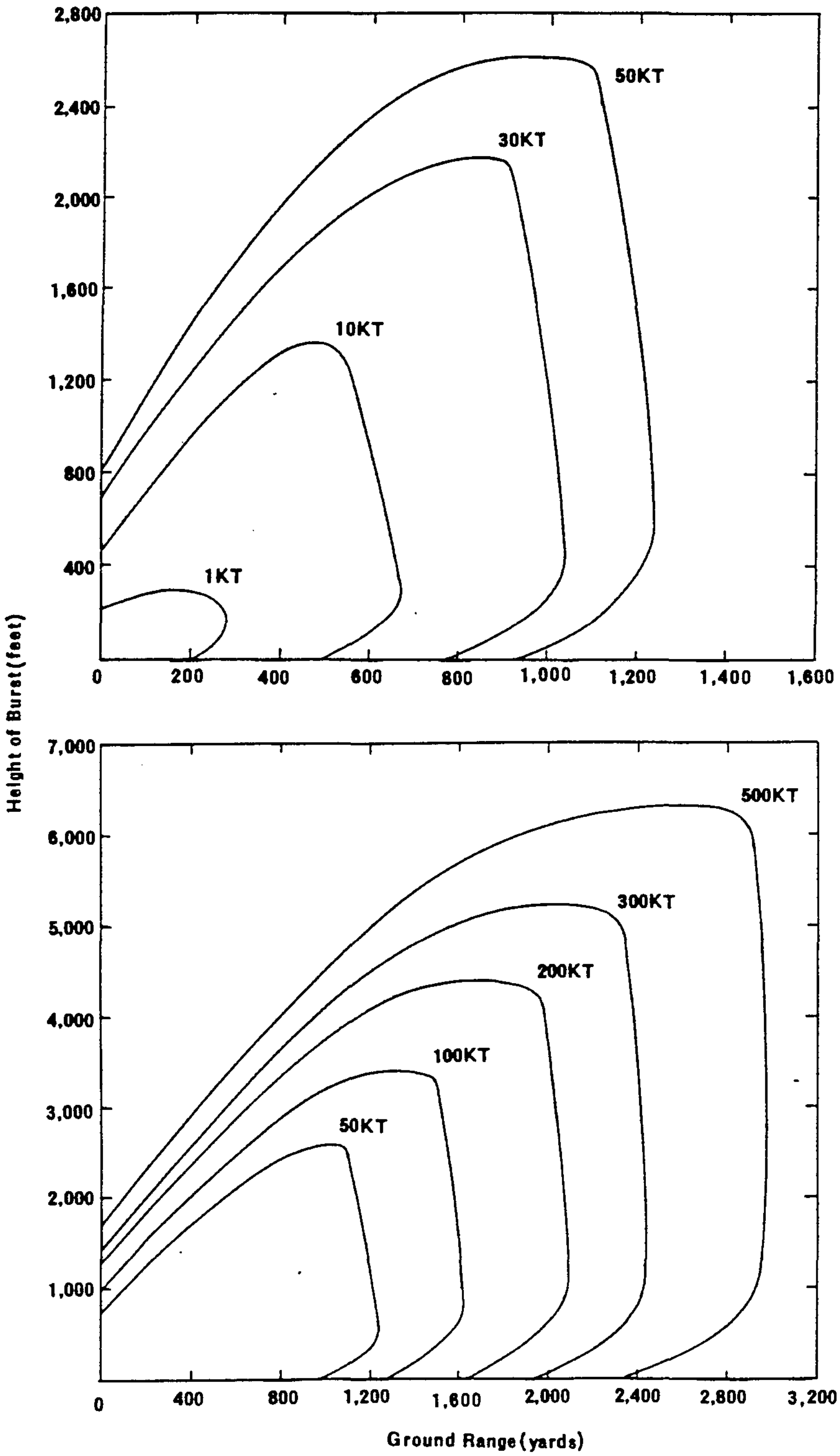

SEVERE DAMAGE TO HIGHWAY AND RAILWAY TRUSS BRIDGES OF 250 TO 550 FOOT SPAN
(BLAST NORMAL TO LONGITUDINAL BRIDGE AXIS)
BY VARIOUS YIELDS AS A FUNCTION OF HEIGHT OF BURST AND GROUND RANGE

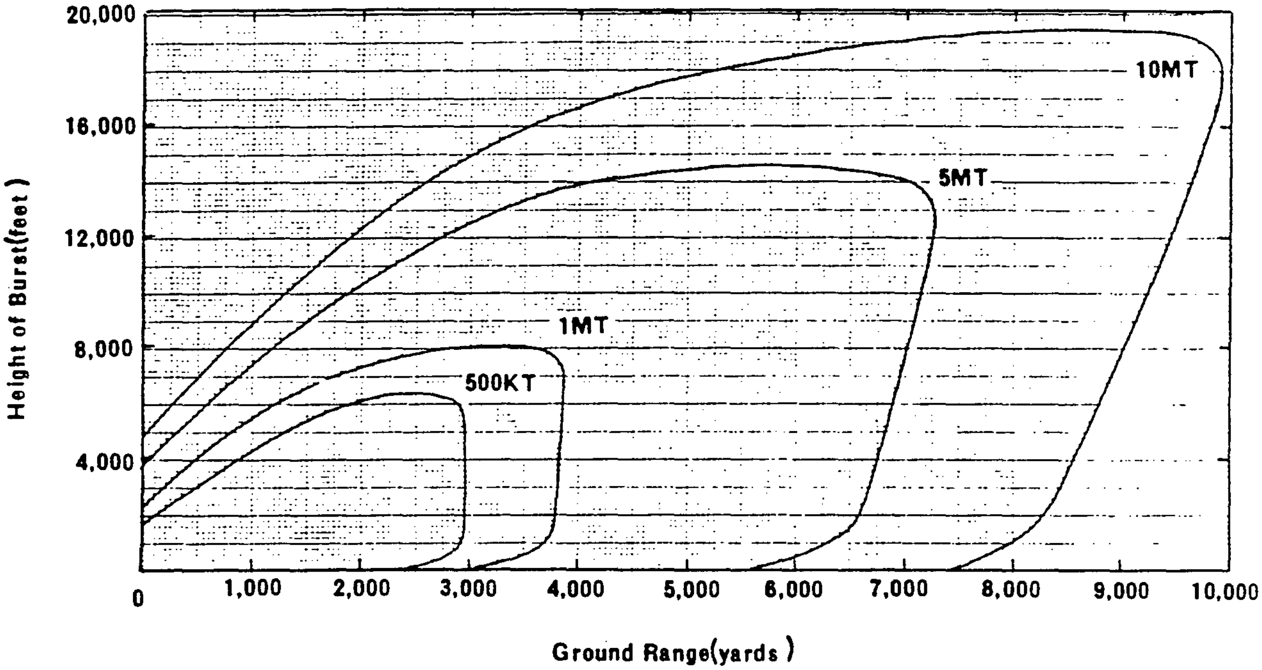

FIGURE 7-13A
FIGURE 7-13B

SEVERE DAMAGE TO M2 OR M4 FLOATING BRIDGES (RANDOM ORIENTATION) FOR VARIOUS YIELDS AS A FUNCTION OF GROUND RANGE AND HEIGHT OF BURST

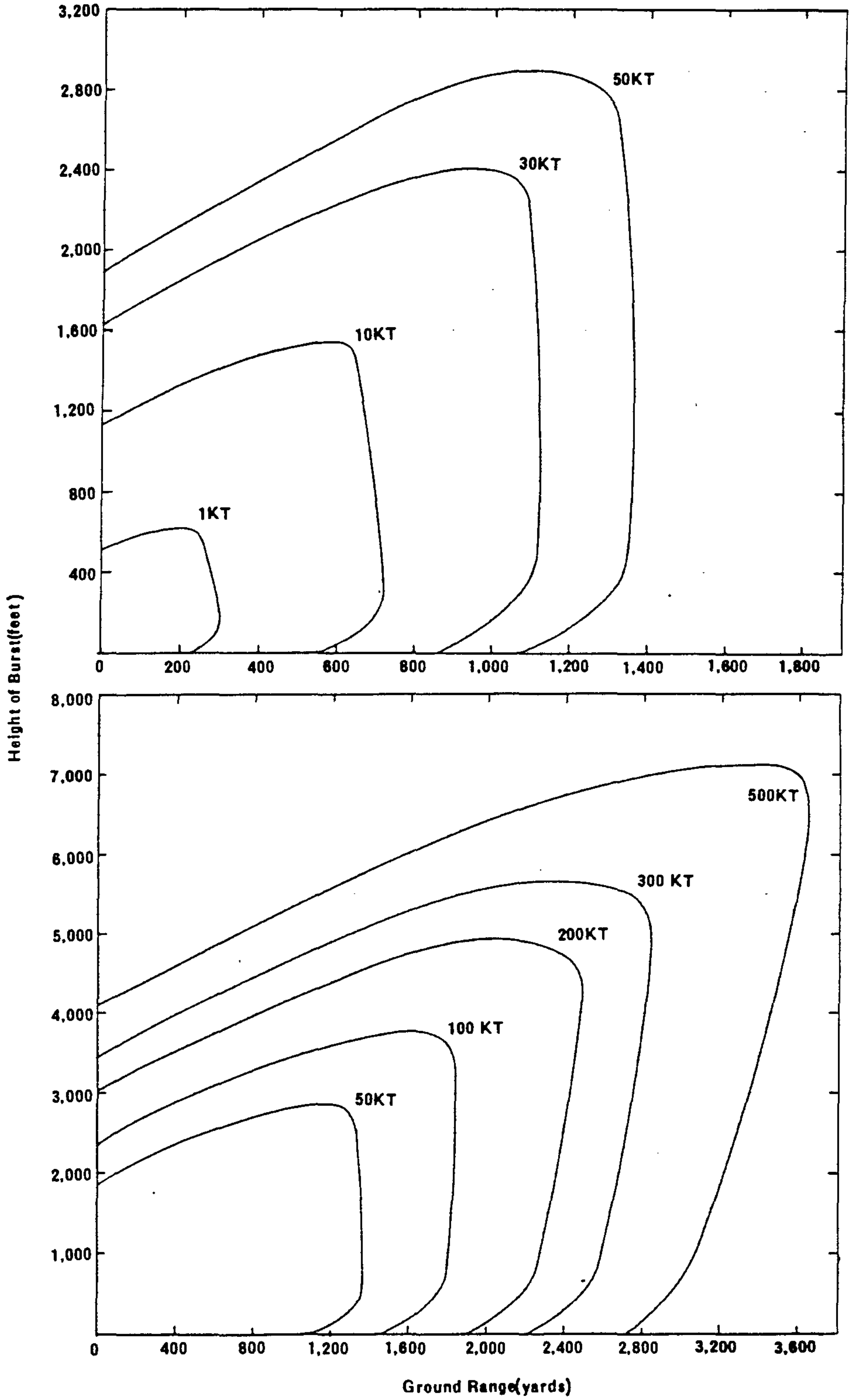

SEVERE DAMAGE TO M2 OR M4 FLOATING BRIDGES (RANDOM ORIENTATION)
FOR VARIOUS YIELDS AS A FUNCTION OF GROUND RANGE AND HEIGHT OF BURST

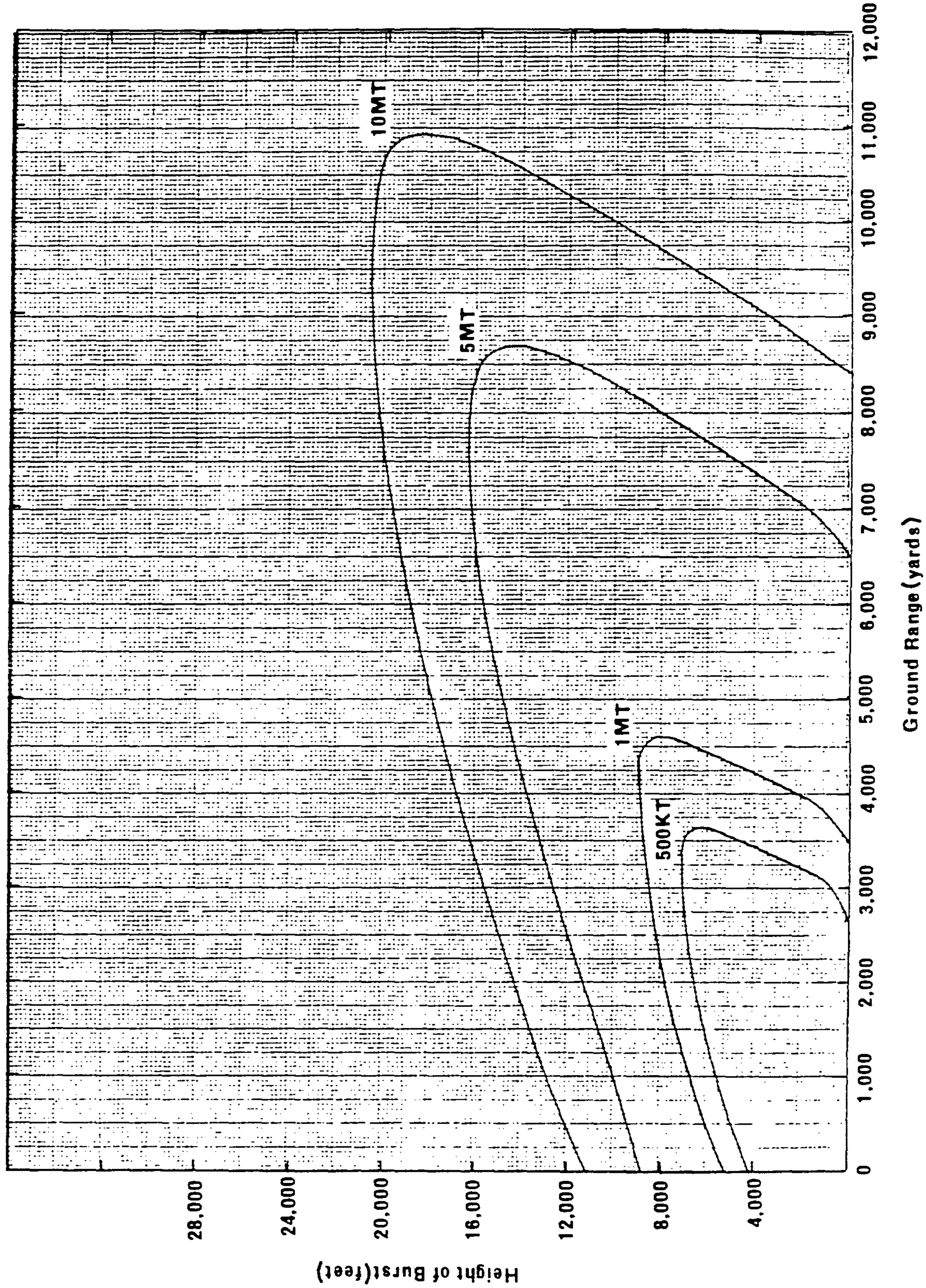

[redacted]

SEVERE DAMAGE TO EARTH COVERED LIGHT STEEL ARCH SHELTER
(10 GAUGE CORRUGATED STEEL WITH 20 TO 25 FOOT SPAN)
BY VARIOUS YIELDS AS A FUNCTION OF HEIGHT OF BURST AND GROUND RANGE

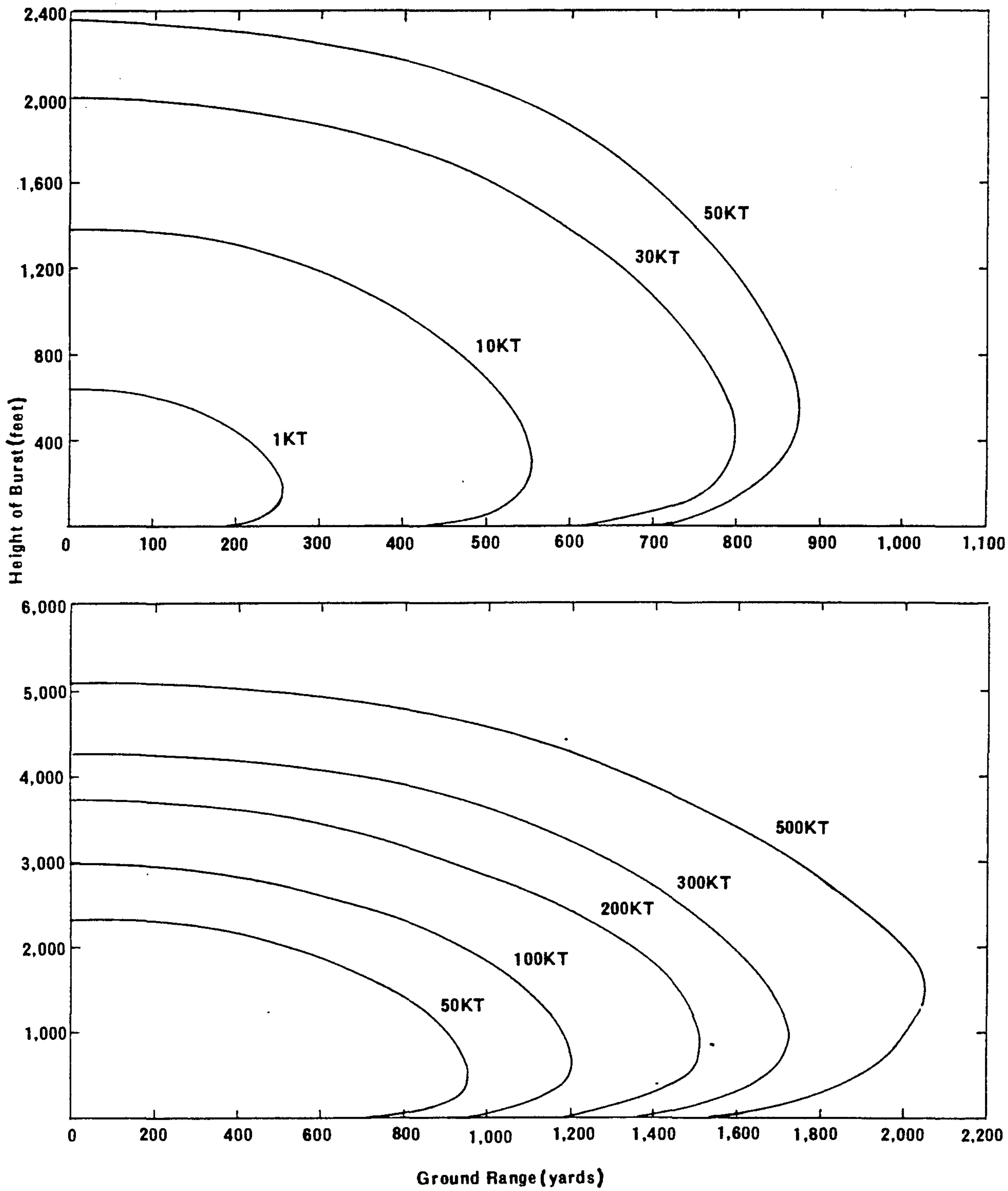

SEVERE DAMAGE TO EARTH COVERED LIGHT STEEL ARCH SHELTER (10 GAUGE CORRUGATED STEEL WITH 20 TO 25 FOOT SPAN) BY VARIOUS YIELDS AS A FUNCTION OF HEIGHT OF BURST AND GROUND RANGE

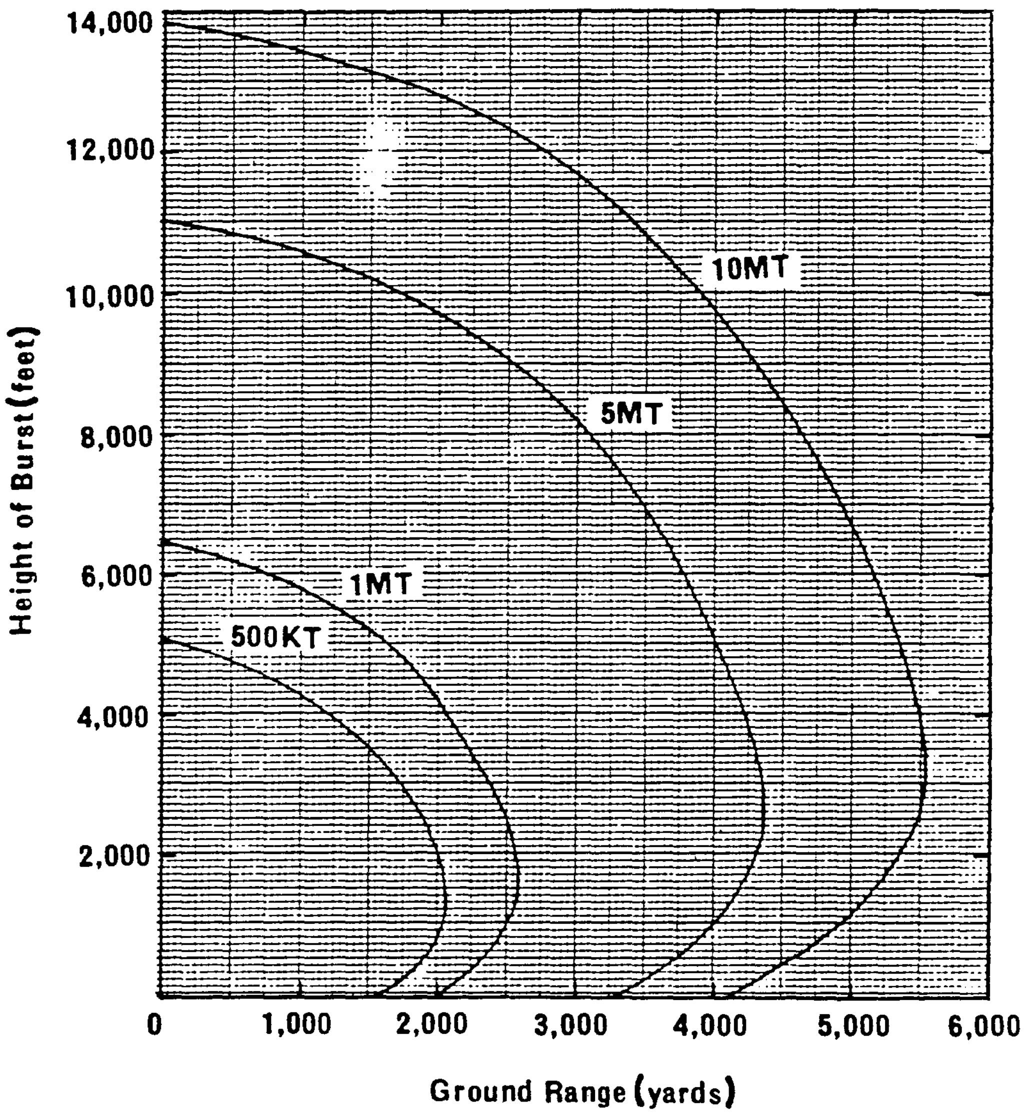

SEVERE DAMAGE TO EARTH COVERED LIGHT REINFORCED CONCRETE STRUCTURE BY VARIOUS YIELDS AS A FUNCTION OF HEIGHT OF BURST AND GROUND RANGE

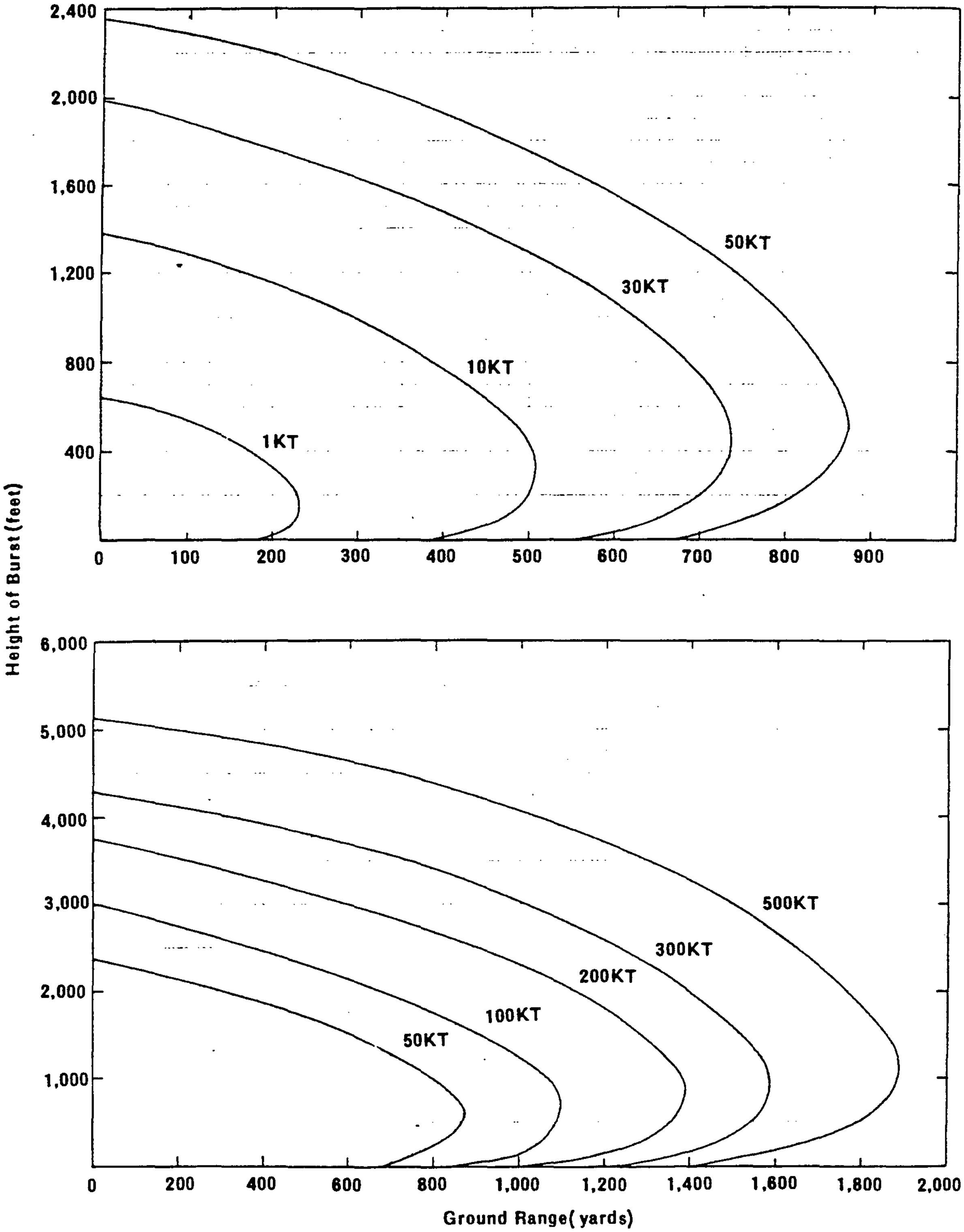

SEVERE DAMAGE TO EARTH COVERED LIGHT REINFORCED CONCRETE STRUCTURE BY VARIOUS YIELDS AS A FUNCTIONS OF HEIGHT OF BURST AND GROUND RANGE

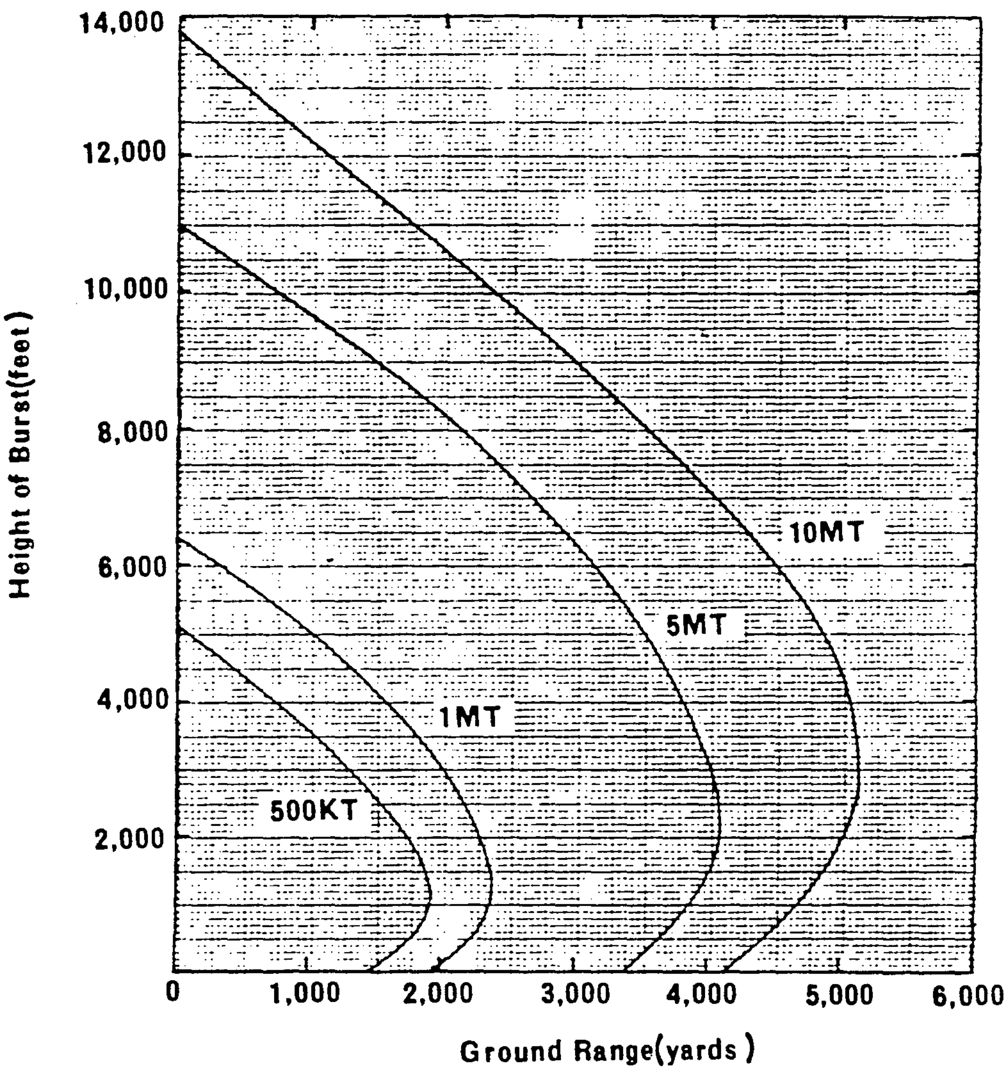

BLANK

SEVERE DAMAGE TO VARIOUS STRUCTURES PRIMARILY OVERPRESSURE -SENSITIVE BY SURFACE BURST OF VARIOUS YIELDS

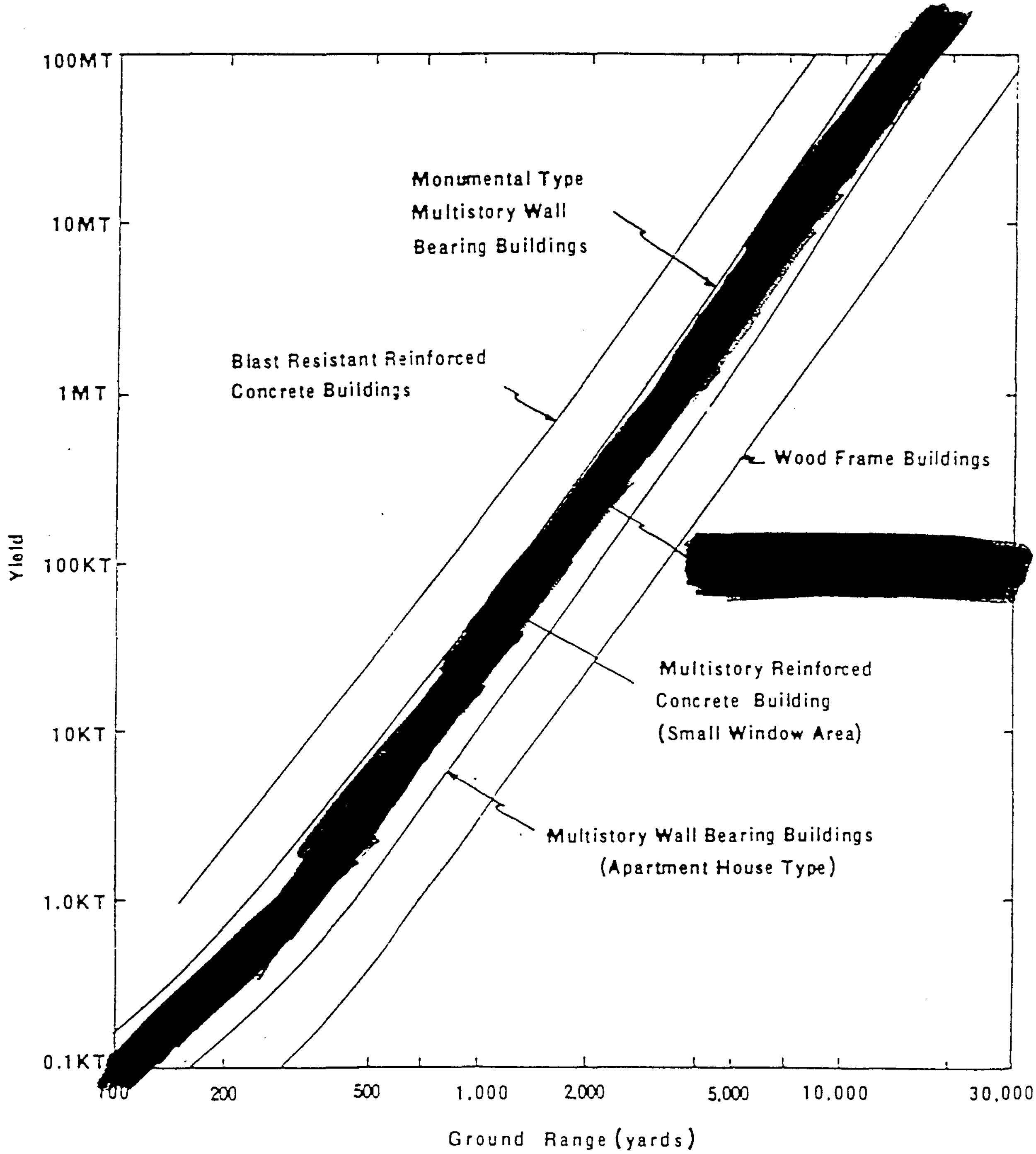

ARMY (b)(1)

SEVERE DAMAGE TO VARIOUS STRUCTURES PRIMARILY DYNAMIC PRESSURE-SENSITIVE
BY SURFACE BURST OF VARIOUS YIELDS

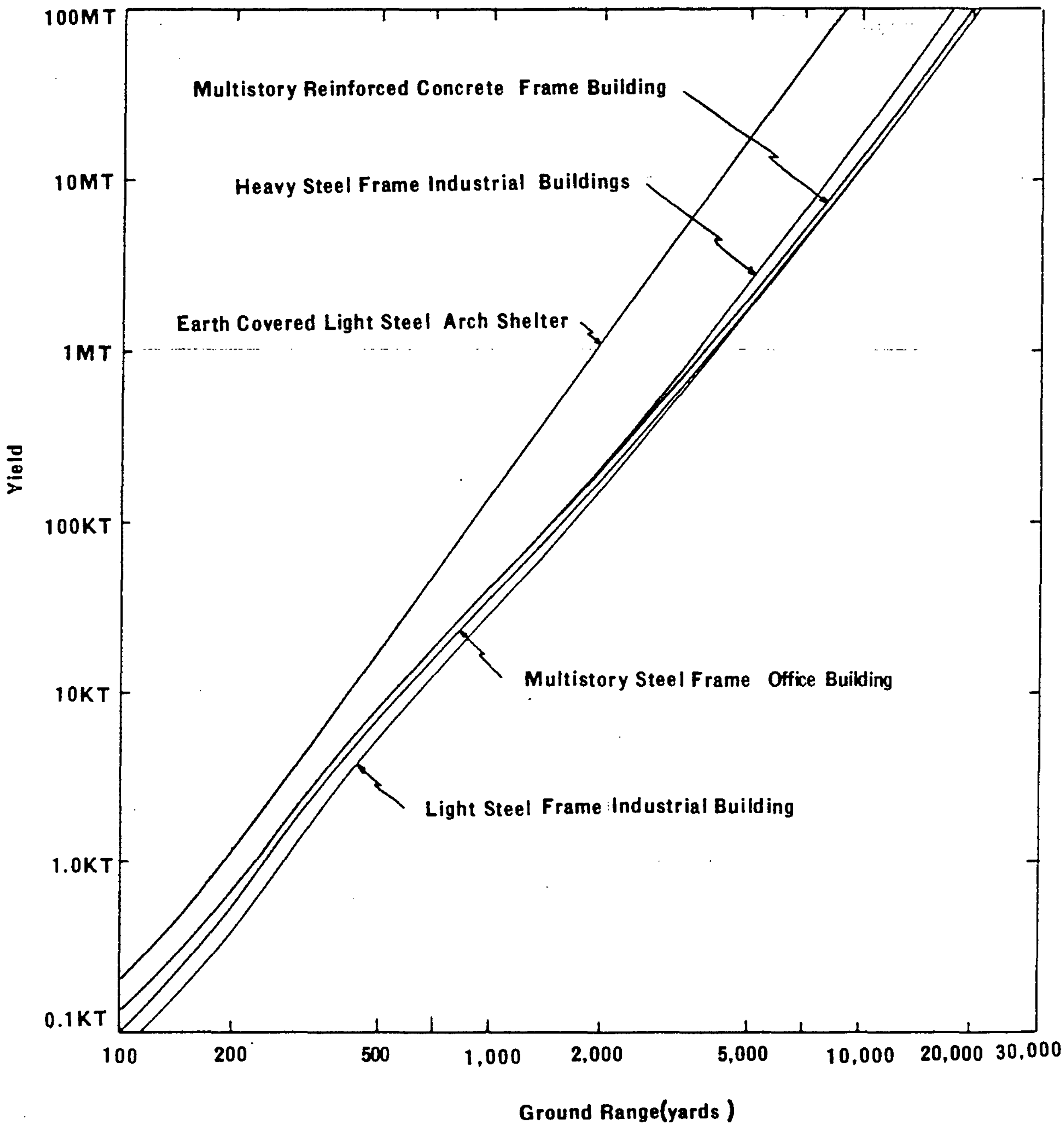

SEVERE DAMAGE TO VARIOUS STRUCTURES PRIMARILY DYNAMIC PRESSURE-SENSITIVE BY SURFACE BURST OF VARIOUS YIELDS

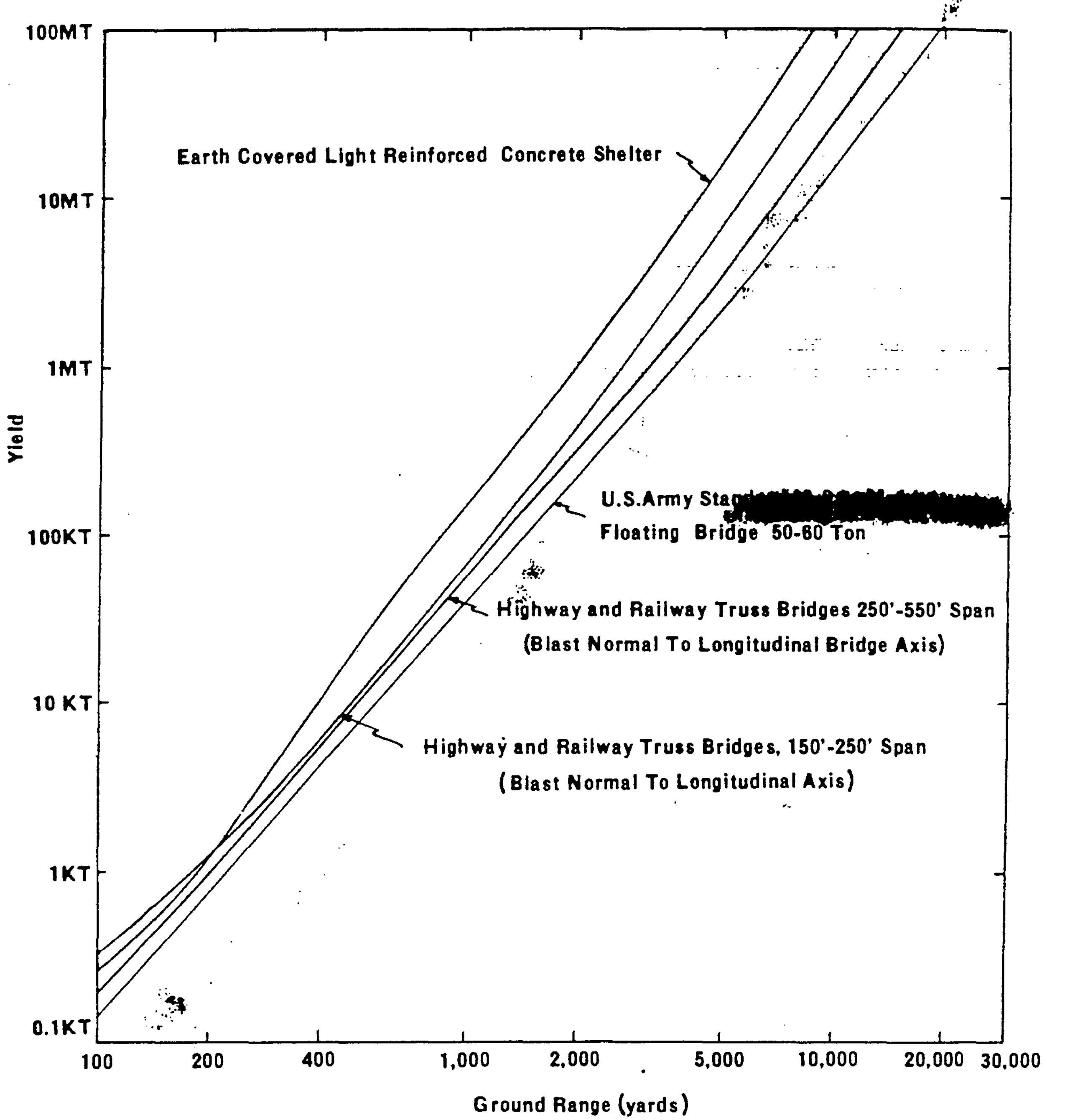

SUBSURFACE BURST DAMAGE DISTANCE REDUCTION FOR SURFACE TARGETS

As shown by the curves of figure 2–18, the peak air overpressures experienced on the surface are reduced below those resulting from a surface burst if the detonation is below the surface. Since the damage to many surface targets is directly related to these overpressures, the distance from the burst at which a given level of damage occurs will be similarly reduced as the burst depth is increased. The amount of this reduction may be derived from figure 7–18, which presents data for a shallow subsurface burst of 1 KT yield, and which is applicable to data derived from sections VII (except tunnels and field fortifications), IX, X, and XI. Since the data presented in section VIII includes subsurface bursts, this figure is not applicable there.

Scaling. For yields other than 1 KT, use:

$$\frac{h_1}{h_2}=\frac{W_1^{1/3}}{W_2^{1/3}}=\frac{d_1}{d_2},$$

where lowering a burst of yield W_1 to depth h_1 will reduce the distance on the surface to which a given degree of damage will be produced by d_1 yards, and lowering a burst of yield W_2 to depth h_2 will reduce the surface damage distance by d_2 yards.

Example.

Given: A 125 KT burst at a 50-foot depth.

Find: The distance at which there is a 50 percent probability of severe damage to a heavy steel frame building on the surface.

Solution: Applying the scaling above,

$$h_1=\frac{h_2\times W_1^{1/3}}{W_2^{1/3}}=\frac{50\times 1}{(125)^{1/3}}=10 \text{ feet}$$

From figure 7–18, the damage distance reduction produced by lowering the depth of a 1 KT burst 10 feet underground will be 30 yards. Then, for a 125 KT burst at 50 feet, the damage distance reduction will be:

$$d_2=\frac{W_2^{1/3}\times d_1}{W_1^{1/3}}=\frac{(125)^{1/3}\times 30}{1}=150 \text{ yards.}$$

Answer.

This value, then, is subtracted from the damage-producing distance found from curve 7–8B, 1,600 yards: 1,600−150=1,450 yards. *Answer.*

Reliability. Based on full scale field tests.

Related material.

See paragraphs 7.2*a*(4)(*b*), 9.2*a*, 10.1*d*, and 11.2*b*.

See also figures 7–1 through 7–17, 9–1 through 9–3, 10–1 through 10–8, and 11–1 through 11–6.

SUBSURFACE BURST
DAMAGE DISTANCE REDUCTION
FOR SURFACE STRUCTURES (1KT)

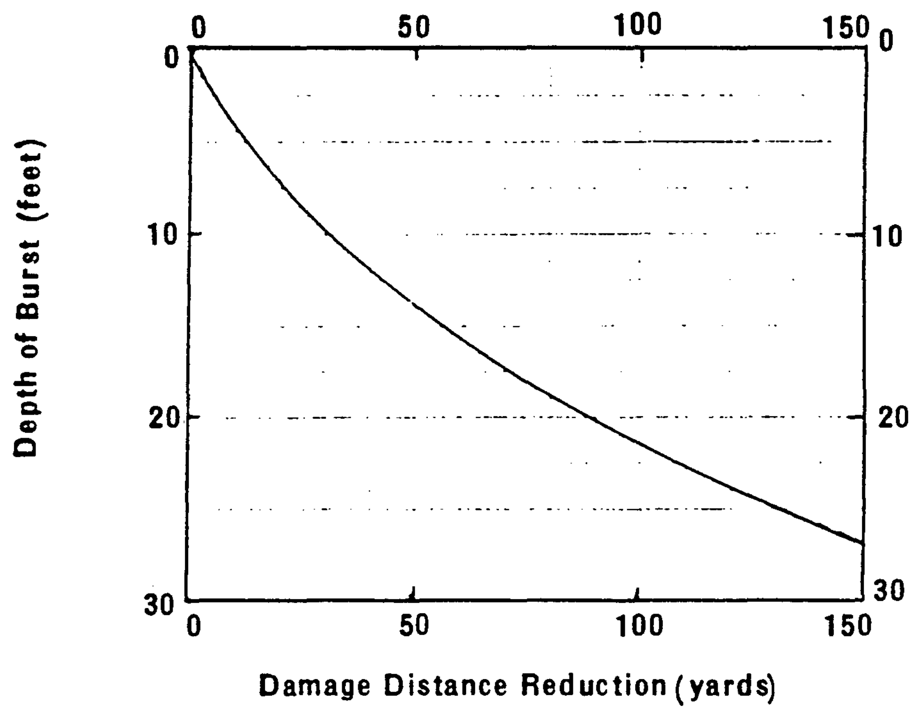

DAMAGE TO UNLINED TUNNELS IN SOUND ROCK

Figure 7-19 presents isodamage contours for tunnels in sound rock from a 1 KT surface burst.

Scaling. The shock front in sound rock is assumed to be spherically symmetrical around the burst point. For yields other than 1 KT, use:

$$\frac{h_1}{h_2}=\frac{W_1^{1/3}}{W_2^{1/3}}=\frac{d_1}{d_2},$$

where a burst of yield W_1 at the surface will produce a given damage level at distance d_1 to a tunnel at depth h_1, and a burst of yield W_2 at the surface will give the same damage level at distance d_2 to a tunnel at depth h_2. To predict the horizontal distance to a certain zone of damage to tunnels from underground bursts of the same yield, multiply the distance obtained from figure 7-19 by the ratio:

$$\frac{\text{crater diameter for weapon yield and burst depth used}}{\text{crater diameter for weapon used, burst at the surface}}$$

Crater diameters for surface bursts and various depths of burst may be obtained from figure 2-20 or 2-22.

Example.

Given: A 20 KT burst 25 feet below the surface.

Find: To what horizontal distance average zone 3 damage may be expected to occur to a 100-foot deep tunnel in sound granite.

Solution: Tunnel depth for 1 KT=

$$\frac{\text{actual tunnel depth}}{W^{1/3}}=\frac{100}{(20)^{1/3}}=37 \text{ feet.}$$

From figure 7-19, the horizontal distance from a 1 KT surface burst to the average of zone 3 damage to a 37-foot deep tunnel is 103 feet. The horizontal distance from a 20 KT surface burst to the average of zone 3 damage = the distance for 1 KT $\times W^{1/3}=103\times(20)^{1/3}=280$ feet.

From figure 2-36A,

$$\frac{\text{crater diameter, 20 KT at 25 feet}}{\text{crater diameter, 20 KT at surface}}=\frac{450}{290}=1.55.$$

The horizontal distance for 20 KT burst at 25 feet $=1.55\times280=435$ feet. *Answer.*

Reliability. Based on scaled field test data.

Related material.

See paragraphs 7.1*c*, 7.3*b*(5) and 7.3*c*(2)(*b*).

See also figures 2-20 and 2-22.

FIGURE 7-19

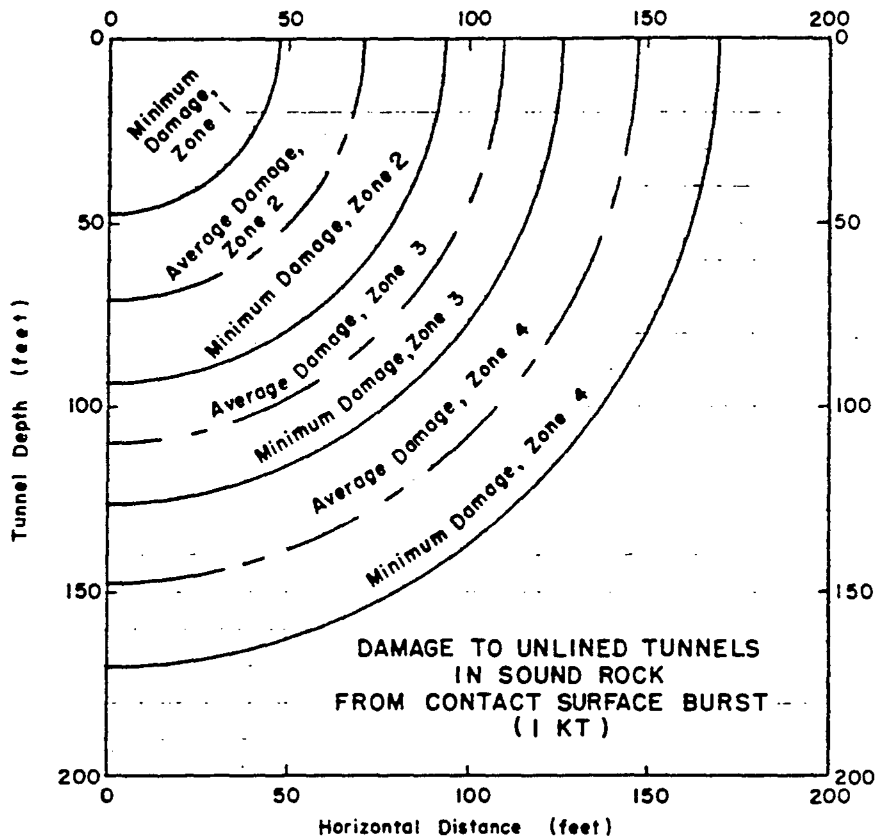

Zones of Damage to Unlined Tunnels in Sound Rock :

Zone 1. Crater opening into tunnel.
Zone 2. Increasing thickness of spalling.
Zone 3. Continuous spalling of about constant thickness.
Zone 4. Intermittent light spalling.

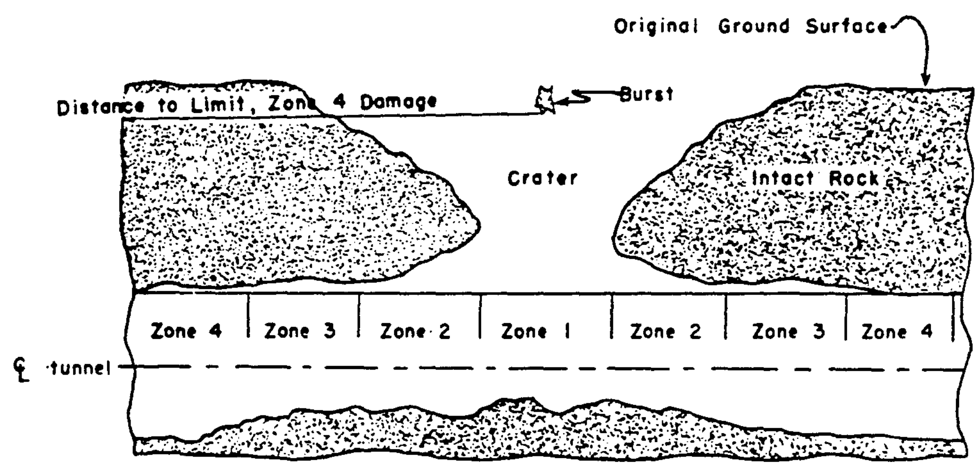

DAMAGE TO FIELD FORTIFICATIONS

Figures 7–20 through 7–22 are a series of plots of height of burst vs. scaled ground range for 50 percent probability of severe, moderate, or light damage to various field fortifications in Nevada type soil scaled to 1 KT. To determine 90 percent or 10 percent probability of damage to structures, lines of probability should be drawn between the indicated 50 percent probability lines. For example, because there is little difference between a line indicating approximately 10 percent probability of severe damage and one indicating 90 percent probability of moderate damage, a single line can represent both and should be drawn midway between the indicated lines for 50 percent probability of severe and moderate damage. To determine the range for 90 percent probability of severe damage use one-half the yield at the same burst height.

The curves in figure 7–22 are based on results of tests run in a *consolidated dry sand and gravel soil*. Trenches and foxholes in damp soil with stable vegetation or dry silty soil will receive moderate and severe damage at ranges less than those shown in figure 7–22. The curves of figure 7–22 are for average rectangular foxholes with the longitudinal axis perpendicular to the direction of air blast propagation. Damage will be equal or less for other orientations.

Scaling. To obtain heights of burst and distances for yields other than 1 KT, use the scaling procedure—

$$\frac{d_1}{d_2}=\frac{h_1}{h_2}=\frac{W_1^{1/3}}{W_2^{1/3}},$$

where d_1 and h_1 are ground distance and height of burst for yield W_1 KT, and d_2 and h_2 are the corresponding ground distance and height of burst for yield W_2 KT.

Example.

Given: A 50 KT burst at an altitude of 1,000 feet.

Find: To what horizontal distance there is a 50 percent probability of severe damage to an unrevetted foxhole in a dry, consolidated sand and gravel soil.

Solution:

$$h_1=\frac{h_2\times W_1^{1/3}}{W_2^{1/3}}=\frac{1{,}000\times 1}{(50)^{1/3}}=270 \text{ feet},$$

the corresponding burst height for 1 KT. From figure 7–22 the ground range for severe damage is 185 yards. To obtain the corresponding ground range for 50 KT:

$$d_2=\frac{d_1\times W_2^{1/3}}{W_1^{1/3}}=\frac{185\times(50)^{1/3}}{1}=680 \text{ yards.}$$

Answer.

Reliability. This figure is based on results of a limited number of full scale tests at which severe, moderate and light damage were observed.

Related material.

See paragraph 7.4.

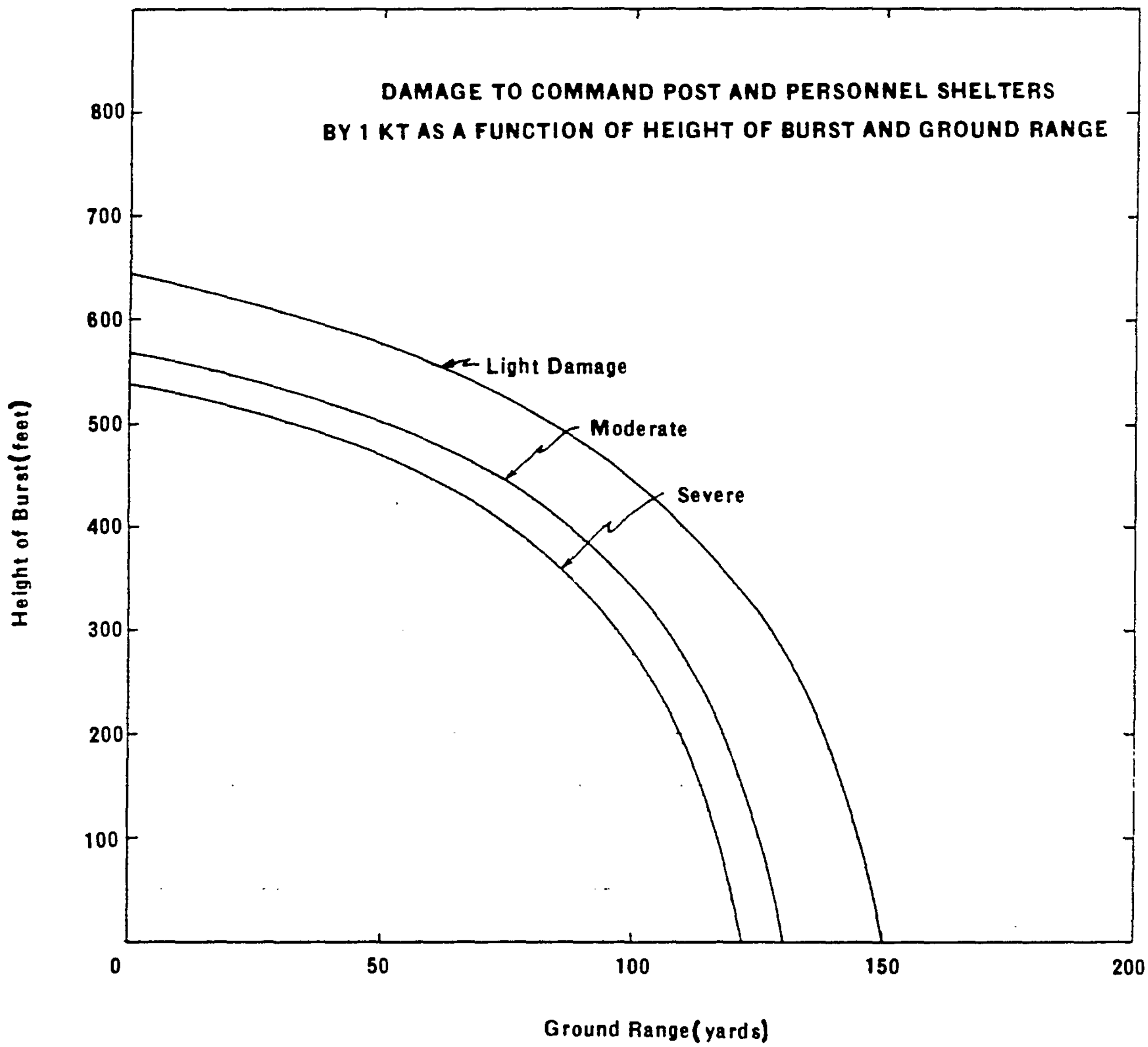
DAMAGE TO COMMAND POST AND PERSONNEL SHELTERS
BY 1 KT AS A FUNCTION OF HEIGHT OF BURST AND GROUND RANGE
Height of Burst(feet)
800
700
600
500
400
300
200
100
Light Damage
Moderate
Severe
0
50
100
150
200
Ground Range(yards)

FIGURE 7-21

CONFIDENTIAL

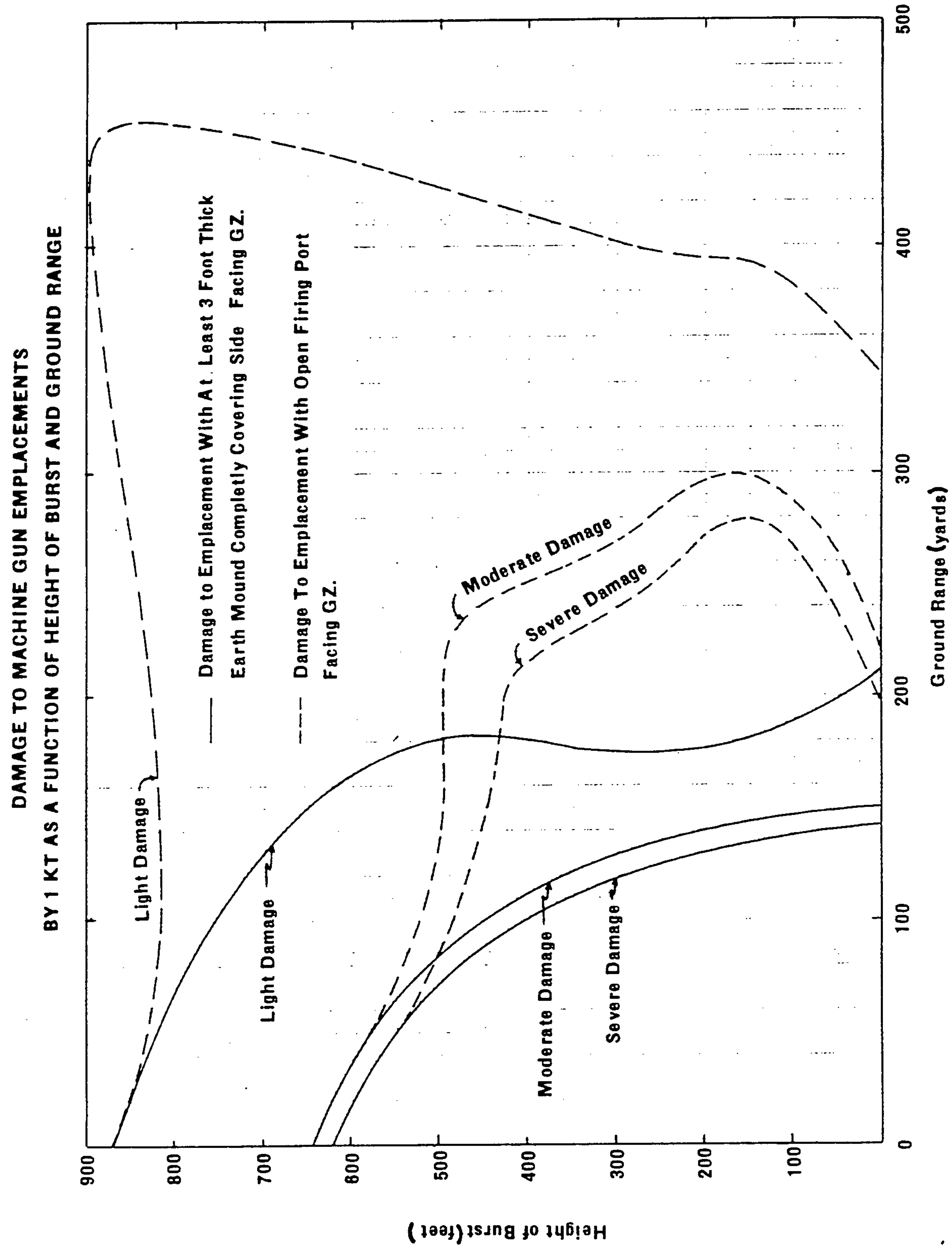

PAGE 7-55 WITHHELD IN ITS ENTIRETY

CONFIDENTIAL

BLANK

8
Naval

SECTION VIII
DAMAGE TO NAVAL EQUIPMENT

8.1 General

a. Damage Mechanisms. Mechanical damage to surface ships may be caused by air blast, water shock, and surface wave action. Submerged submarines may be damaged by water shock. Thermal damage to naval vessels and topside equipment is not considered a significant factor, in that it does not of itself cause sinking or immobilization.

b. Damage Classification for Surface Ships. The degree of damage to surface ships and surfaced submarines is separated into three categories—

(1) *Severe damage (probable sinking).* The ship is sunk or is damaged to an extent requiring rebuilding.

(2) *Moderate damage (immobilization).* The ship requires extensive repairs. This includes damage to certain shock sensitive components or their foundations, such as propulsion machinery, boilers, and damage to interior equipment.

(3) *Light damage.* This category includes damage to electronic, electrical, and mechanical equipment; however, the ship may still be able to operate effectively.

c. Damage Classification for Submarines. For submerged submarines two degrees of damage are specified—

(1) *Lethal hull damage.* Pressure hull rupture occurs.

(2) *Interior shock damage (surfacing damage).* Extensive interior damage to equipment, machinery, and piping occurs with immobilization probable. Submarines are forced to surface.

8.2 Surface Ship Damage

a. Water Shock Damage. Water shock is the principal cause of damage to surface ships from underwater explosions. The directly transmitted shock, however, is not the sole damaging mechanism. When the water depth is of the order of 3,000 feet or less for a 1 KT underwater burst, it is possible that the shock wave reflected from the bottom may produce more severe equipment damage at a given range than the direct shock wave, even though the peak pressure of the reflected wave is less. This phenomenon results from the reflected wave propagating in a more vertical direction and hence being more effective in producing vertical velocities in the hull. In addition, certain bottom formations may focus the reflected wave, resulting in local areas of much higher pressures. It is therefore not possible to predict accurately the effects in a given case without extensive knowledge of the bottom structure in the vicinity of the detonation. To estimate the effects of the reflected shock wave in the absence of such knowledge, it is necessary to assume the bottom to be flat and a perfect reflector, and to use the image of the actual burst point as the apparent source of the reflected shock wave.

Refraction of the water shock wave, discussed in paragraph 2.3*a*(4), may act to reduce the range at which a given level of damage occurs. This reduction is not significant, however, except at the ranges for light damage, and the actual magnitude of the reduction depends upon the individual circumstances. Since this range reduction is of a small magnitude when considering severe and moderate damage levels and is in the conservative direction when considering possible effects against weapon delivery vessels, the influence of water shock wave refraction has not been included in the damage curves.

Water shock damage curves for surface ships are presented in figures 8-1 through 8-3. These curves are based upon several criteria. Severe damage to ships with multi-plate side protective systems (cruisers, carriers, etc.) is defined by bottom deflection, while for those with thin skin shells (transports, destroyers, etc.), it is defined by side deflection. Moderate and light damage to all types is related to the bottom plate velocity.

b. Air Blast Damage. As the depth of a burst is decreased, a transition from water shock to air blast as the primary damage-producing mechanism occurs. Peak overpressure is considered a satisfactory parameter for estimating damage to ships from air blast. Peak overpressures of 5 psi cause light damage to most types of surface ships, while overpressures required for severe damage vary from 25 psi for destroyers to 45 psi for battleships. Figures 8–1 and 8–2 present damage ranges for a 1 KT detonation for heights of burst less than 600 feet and depths of burst less than 800 feet, with means of scaling to other yields. A tabulation of peak overpressure required to cause ship damage is given in table 8–1 for use with burst heights greater than those shown in figures 8–1 and 8–2. For such burst heights, distances to which overpressures extend can be obtained from figure 2–17.

Table 8–1. Surface Ship Peak Air Overpressure Damage Criteria

Type of ship	Peak air overpressure (psi)		
	Severe	Moderate	Light
Aircraft carriers	30	20	5
Battleships	45	25	5
Cruisers (heavy)	40	20	5
Cruisers (light) (AA)	30	20	5
Destroyers	25	15	5
Pontoons (for pier construction)	60	------	------
Transports	30	20	5
LST's, landing craft and landing vehicles	25	15	5
Submarines (surfaced)	80	60	------

c. Water Wave Damage. Water waves are a contributing factor in causing damage to surface ships. Wave action may add to the damage to a ship which has already been weakened by air and water shock. The waves may also cause "hogging" damage to ships oriented end-on to the burst, and may cause ships oriented beam-on to the burst to capsize. Small craft may be overturned and sunk or destroyed by wave action.

d. Thermal Damage. Thermal damage to naval vessels and topside equipment is probably limited to superficial scorching of exposed organic surfaces (including paint). Fires are unlikely to originate aboard vessels as the result of thermal radiation from a nuclear explosion, except in cases where severe and probably overriding damage due to blast is also sustained.

8.3 Subsurface Target Damage

a. Submarines.

(1) *Air blast damage.* Air blast damage to surfaced submarines is significant only for the case of surface, transition zone or air bursts. Peak air overpressures of 80 and 60 psi are expected to cause severe and moderate damage, respectively, to surfaced submarines.

(2) *Water shock damage.* Water shock is the controlling damage-producing mechanism for a submerged submarine for any burst position, and also for a surfaced submarine subjected to an underwater burst. The criterion used for estimating lethal hull damage is a function of "excess impulse." This excess impulse is defined as the impulse delivered by that portion of the shock overpressure which is in excess of the static collapse pressure minus the hydrostatic pressure. In deep water when a sharp change in water temperature with depth exists (thermocline) and the weapon is fired in close proximity to this region, refraction may reduce the range for a given degree of damage on the order of perhaps 20 percent. This reduction will only occur when the weapon and the submarine are on opposite sides of the thermocline. For weapons fired well below or above the thermocline, there should be no reduction. Isodamage curves for the hull lethal range and interior shock damage range are presented in figures 8–4 and 8–5 for a submarine with a 600 psi static collapse pressure subjected to a 10 KT and a 30 KT surface or underwater detonation, with methods for scaling to other yields. No account of refraction has been taken in the damage curves presented. Non-linear effects as described in paragraph 2.3 have been incorporated. Initial translational

velocity is the criterion used for prediction of shock damage to submarine equipment.

b. Underwater Mines. Underwater mines are expected to be neutralized when the peak pressure acting on the mines is equal to or greater than the mine case static collapse pressure, or when the mines are within the crater. Figures 8–6 through 8–8 show the neutralization ranges for mines with hydrostatic collapse pressures of 250, 500, and 1,000 psi in depths of water of 50, 100, and 200 feet and for a range of yields from 1 to 100 KT. These curves are computed for mines and burst both on the bottom.

BLANK

SURFACE SHIP DAMAGE

Figure 8–1 gives estimated ranges for severe damage (probable sinking) plotted as a function of burst height and depth for surface ships for a 1 KT detonation. Figure 8–2 gives the ranges for moderate (immobilization) damage and for light damage as functions of burst height and shallow depths. Figure 8–3 is an extended plot of light damage vs. depth of burst. This latter figure enables an estimate to be made for the effect of the bottom reflection pressures on the predicted light damage range using the assumptions given in paragraph 8.2*a* (i. e., a flat perfect reflector bottom and a burst depth at the image of the actual burst point). For evaluation of light damage, a value should be found for both the direct shock wave and the bottom reflected shock wave and the larger value chosen.

Scaling. For yields other than 1 KT the following relations can be used to estimate ranges for a given degree of damage:

$$\frac{d_1}{d_2}=\frac{W_1^{1/3}}{W_2^{1/3}}=\frac{h_1}{h_2},$$

where d_1=range for a given degree of damage for yield W_1 KT at a depth h_1, and d_2=range for a given degree of damage for yield W_2 KT at depth h_2.

Example.

Given: A 30 KT burst at a depth of 2,000 feet in 5,000 feet of water.

Find:

(*a*) The range at which an aircraft carrier suffers severe damage.

(*b*) The range at which a destroyer suffers light damage.

Solution:

(*a*) The depth of 2,000 feet for a 30 KT burst corresponds for a 1 KT to

$$\frac{h_1}{h_2}=\frac{W_1^{1/3}}{W_2^{1/3}} \text{ or } h_1=\frac{h_2\times(W_1^{1/3})}{W_2^{1/3}}$$

$$h_1=\frac{2{,}000(1)}{(W_2)^{1/3}}=\frac{2{,}000}{(30)^{1/3}}=640 \text{ feet.}$$

From figure 8–1 the range at which an aircraft carrier suffers severe damage from a 1 KT burst 640 feet below the surface is 320 yards.

The range of severe damage to an aircraft carrier for a 30 KT detonation at a depth of 2,000 feet is then

$$\frac{d_1}{d_2}=\frac{W_1^{1/3}}{W_2^{1/3}} \text{ or } d_2=\frac{(d_1)\times(W_2)^{1/3}}{W_1^{1/3}}=$$

$$\frac{(320)\times(30)^{1/3}}{1}=1{,}000 \text{ yards.} \quad \textit{Answer.}$$

(*b*) From either figure 8–2 or 8–3 the range at which a destroyer suffers light damage from the direct shock wave of a 1 KT burst at 640 feet below the surface is 990 yards.

The imaginary burst point from which the bottom reflected shock waves are assumed to come is equal to the depth of the water plus the height of the weapon above the bottom, or 5,000+3,000=8,000 feet for the 30 KT weapon. The corresponding depth for a 1 KT is

$$\frac{h_1}{h_2}=\frac{W_1^{1/3}}{W_2^{1/3}} \text{ or } h_1=\frac{h_2\times W_1^{1/3}}{W_2^{1/3}},$$

$$h_1=\frac{8{,}000\times(1)}{(W_2)^{1/3}}=\frac{8{,}000}{(30)^{1/3}}=2{,}560 \text{ ft.}$$

From figure 8–3 the range at which a destroyer suffers light damage from the shock wave of a 1 KT burst at 2,560 feet is 1,300 yards. Since this is greater than the range noted above (990 yards), the bottom reflected shock wave governs. Hence the range of light damage to a destroyer from a 30 KT burst at a depth of 2,000 feet in 5,000 feet of water is then,

$$\frac{d_1}{d_2}=\frac{W_1^{1/3}}{W_2^{1/3}} \text{ or } d_2=\frac{(d_1)\times(W_2)^{1/3}}{W_1^{1/3}}=$$

$$\frac{(1{,}300)\times(30)^{1/3}}{1}=4{,}000 \text{ yards.} \quad \textit{Answer.}$$

Reliability. Based on limited data. Predictions become less reliable as depth of burst decreases.

Related Material.

See paragraphs 8.1 and 8.2.

See also figures 8–4 and 8–5 for submarine damage.

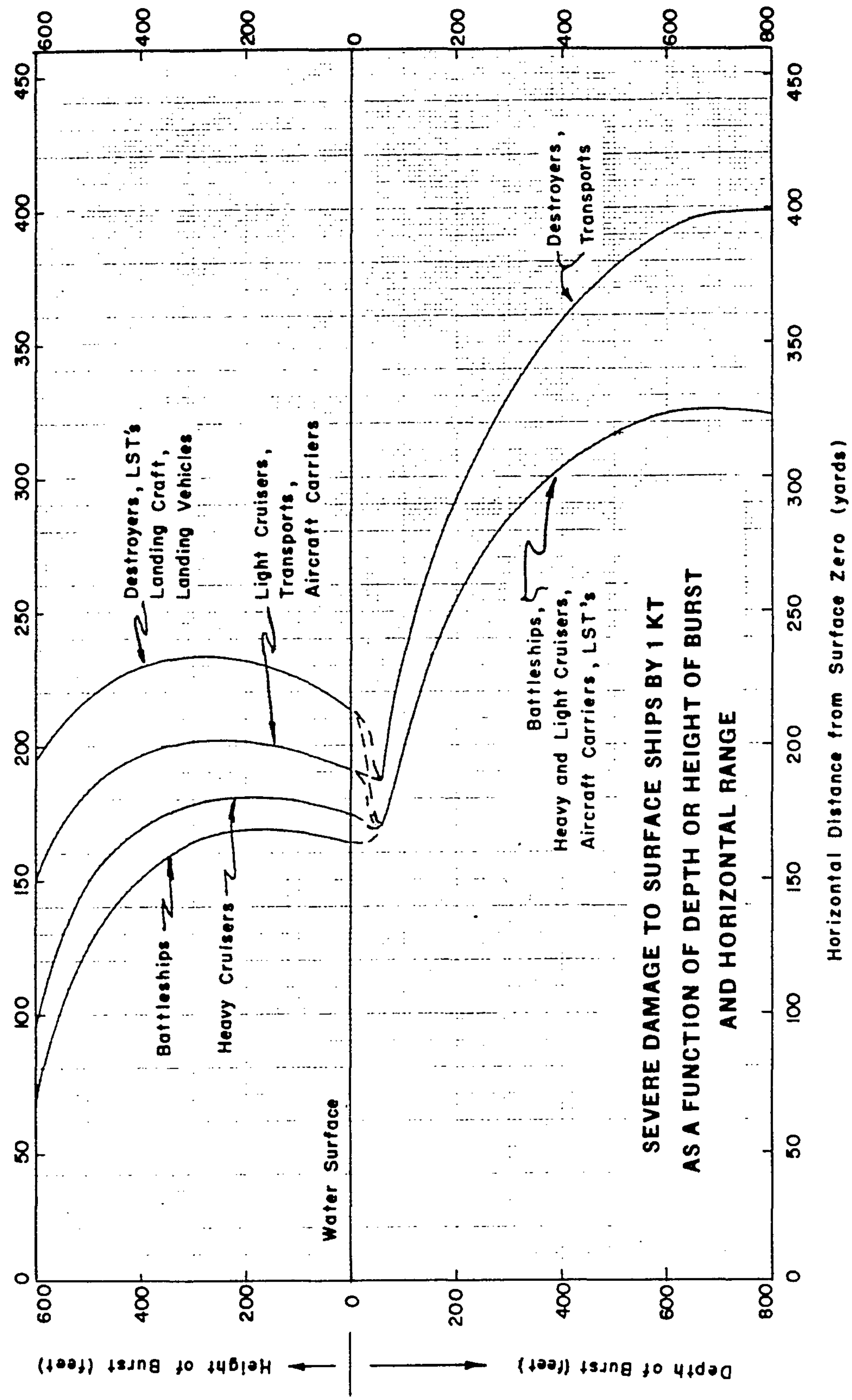
SEVERE DAMAGE TO SURFACE SHIPS BY 1 KT
AS A FUNCTION OF DEPTH OR HEIGHT OF BURST
AND HORIZONTAL RANGE
Horizontal Distance from Surface Zero (yards)
Height of Burst (feet)
Depth of Burst (feet)
Water Surface
Destroyers, LST's, Landing Craft, Landing Vehicles
Light Cruisers, Transports, Aircraft Carriers
Battleships
Heavy Cruisers
Destroyers, Transports
Battleships, Heavy and Light Cruisers, Aircraft Carriers, LST's
0
50
100
150
200
250
300
350
400
450
600
400
200
0
200
400
600
800

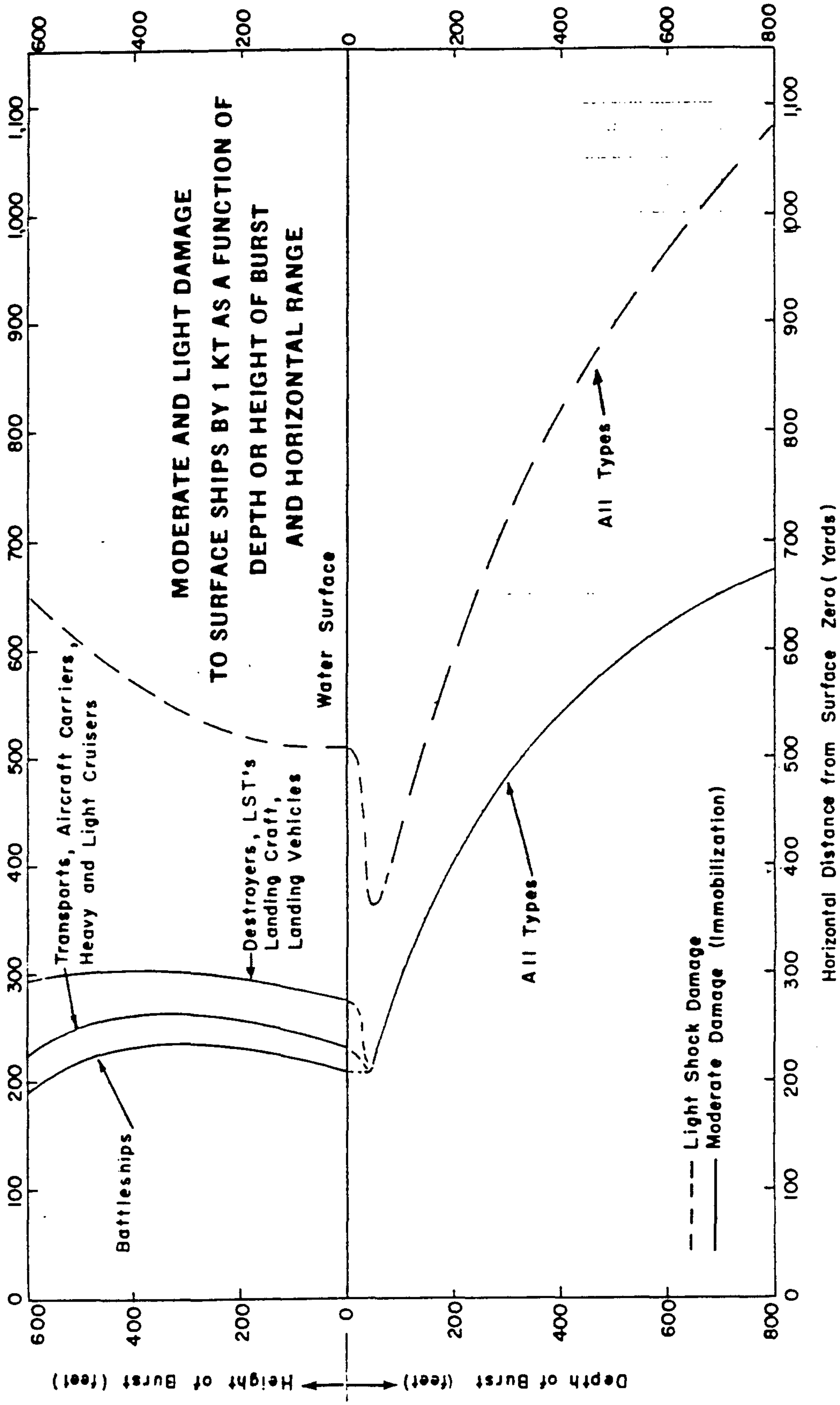
MODERATE AND LIGHT DAMAGE
TO SURFACE SHIPS BY 1 KT AS A FUNCTION OF
DEPTH OR HEIGHT OF BURST
AND HORIZONTAL RANGE
Water Surface
Transports, Aircraft Carriers, Heavy and Light Cruisers
Destroyers, LST's, Landing Craft, Landing Vehicles
Battleships
All Types
All Types
Light Shock Damage
Moderate Damage (Immobilization)
Horizontal Distance from Surface Zero (Yards)
Height of Burst (feet)
Depth of Burst (feet)
0
100
200
300
400
500
600
700
800
900
1,000
1,100
600
400
200
0
200
400
600
800

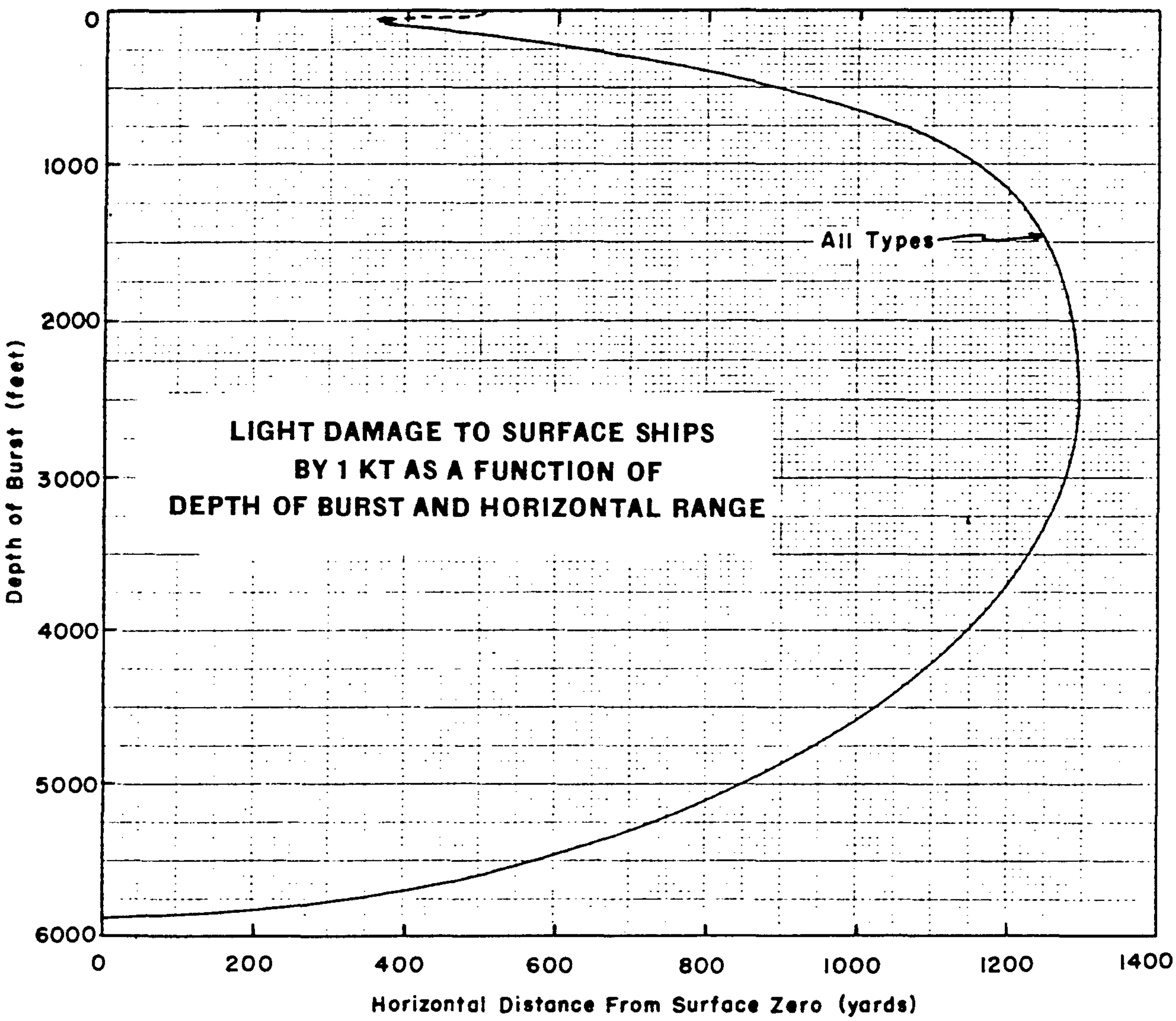
LIGHT DAMAGE TO SURFACE SHIPS
BY 1 KT AS A FUNCTION OF
DEPTH OF BURST AND HORIZONTAL RANGE
All Types
Depth of Burst (feet)
0
1000
2000
3000
4000
5000
6000
Horizontal Distance From Surface Zero (yards)
0
200
400
600
800
1000
1200
1400

SUBMARINE DAMAGE

Figure 8-4 presents isodamage curves of lethal hull range for a submarine with a static collapse pressure of 600 psi when subjected to a 10 KT or a 30 KT burst. For submarines of other structural strengths, the lethal range is assumed to be inversely proportional to the pressure hull thickness. For depths of submergence between those presented in the curves a linear interpolation may be used. Figure 8-5 presents isodamage curves for interior shock damage. While the ranges given in figure 8-4 are dependent upon hull strength, those in figure 8-5 are independent of hull strength. For shallow submarine submergence the range for interior shock damage is greater than the lethal hull range. However, for a depth of submergence greater than about 350 feet the lethal hull range predominates.

Scaling. Although direct scaling techniques are not applicable, useful data with sufficient accuracy may be obtained by these approximate procedures.

(1) For yields in the range of 30 to 100 KT, a given depth of burst and a given submarine depth, the following relation can be used with the 30 KT curves to estimate ranges for a given degree of damage:

$$\frac{d_1}{d_2}=\frac{W_1^{1/3}}{W_2^{1/3}},$$

where d_1=range for a given degree of damage for a yield of W_1 KT, and d_2= range for a given degree of damage for a yield of W_2 KT.

(2) A similar relation should be used for yields in the range of 3 to 10 KT using the 10 KT curves. For yields between 10 and 30 KT, compute a range using the 10 KT curves as the basis for cube root scaling and a second range using the 30 KT curves as the basis for cube root scaling, then linearly interpolate between these two computed ranges.

Example.

Given: A 20 KT weapon burst at a depth of 400 feet.

Find: The lethal hull range for a submarine (600 psi static collapse pressure) submerged to a depth of 100 feet.

Solution: From figure 8-4, the lethal hull range for a 10 KT burst at 400 feet is 1,040 yards. The scaled range is then,

$$\frac{d_1}{d_2}=\frac{W_1^{1/3}}{W_2^{1/3}} \text{ or } d_2=\frac{W_2^{1/3}\times d_1}{W_1^{1/3}},$$

$$d_2=\frac{(20)^{1/3}}{(10)^{1/3}}\times 1{,}040=1{,}300 \text{ yards.}$$

The lethal range for a 30 KT bomb burst at 400 feet is 1,300 yards. The scaled range is then,

$$d_2=\frac{W_2^{1/3}\times d_1}{W_1^{1/3}}$$

or

$$d_2=\frac{(20)^{1/3}}{(30)^{1/3}}\times 1{,}300=1{,}100 \text{ yards.}$$

The lethal hull range for a 20 KT bomb burst at a depth of 400 feet is then d_2=1,300−½(1,300−1,100)=1,200 yards. *Answer.*

Reliability. Based on limited data.

Related Material.

See paragraphs 8.1*c* and 8.3*a*.

See also figures 8-1 through 8-3 for surface ship damage.

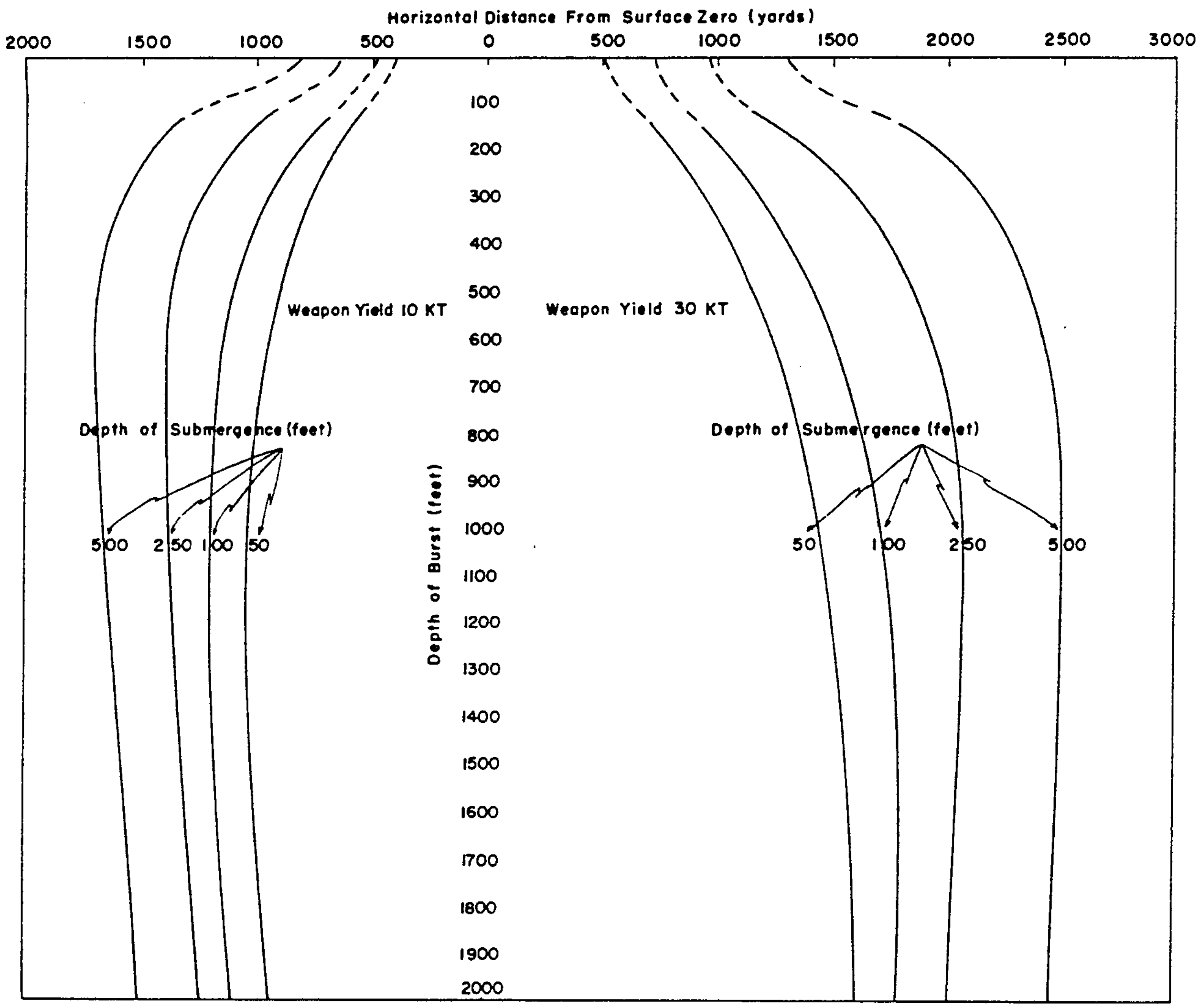

SUBMARINE LETHAL HULL DAMAGE BY 10KT AND 30KT
AS A FUNCTION OF DEPTH OF BURST AND HORIZONTAL RANGE

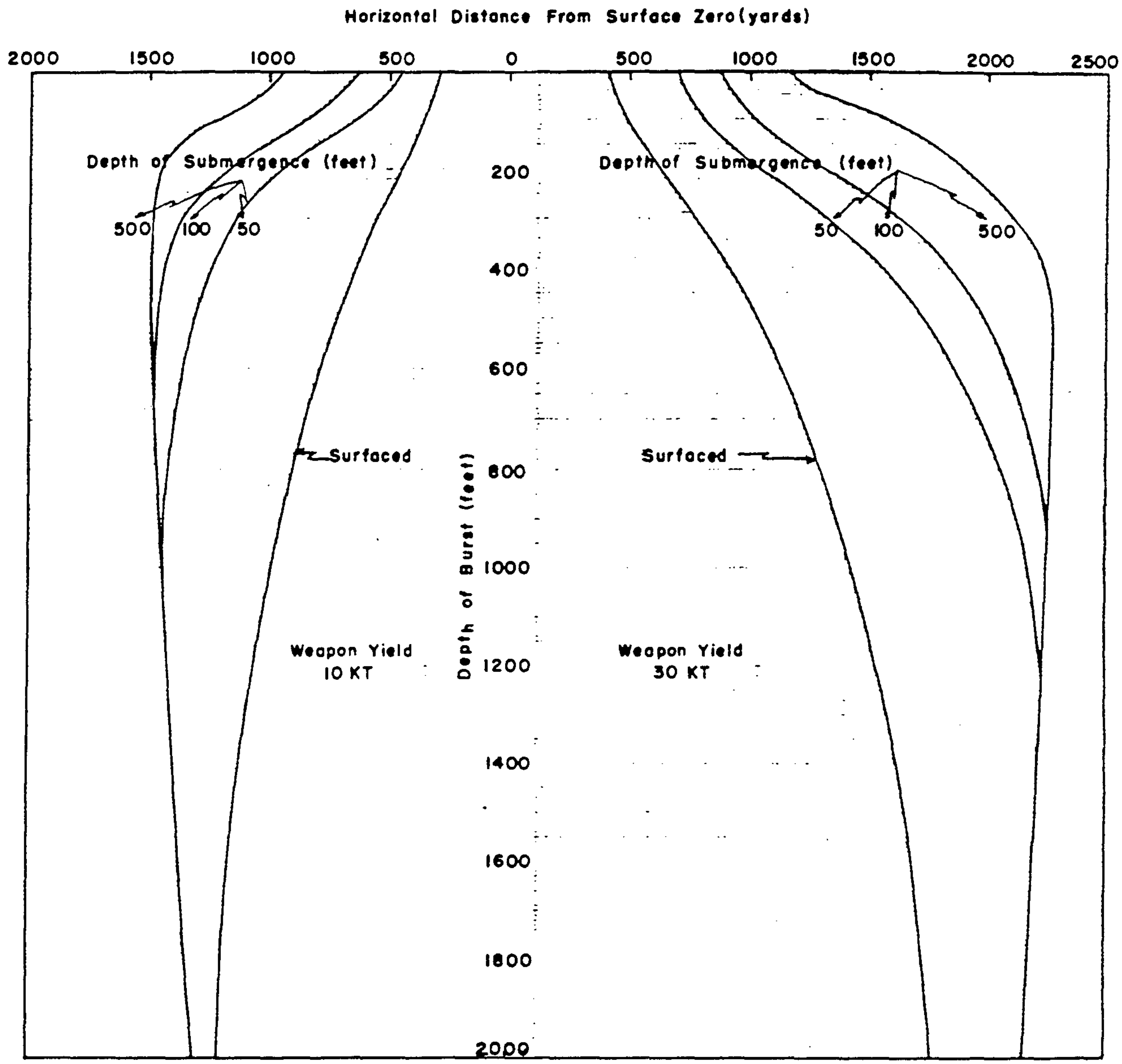

SUBMARINE INTERIOR SHOCK DAMAGE BY 10 KT AND 30 KT
AS A FUNCTION OF DEPTH OF BURST AND HORIZONTAL RANGE

UNDERWATER MINEFIELD NEUTRALIZATION

Figures 8–6 through 8–8 give ranges for underwater minefield neutralization as a function of yield for collapse pressures of 250, 500 and 1,000 psi with both the burst and mines on the bottom. Figure 8–6 is for a 50-foot water depth, figure 8–7 for 100 feet, and figure 8–8 for 200 feet. Linear interpolation between these curves can be used for intermediate water depths and mine case static collapse pressures.

Example.

Given: A 30 KT burst on the bottom in 100 feet of water.

Find: The range at which mines with a 500 psi static case collapse pressure located on the bottom are neutralized.

Solution: The range at which the mines are neutralized is taken directly from figure 8–7 to be 400 yards. *Answer.*

Reliability. Based on limited data.

Related Material.

See paragraph 8.3*b*.

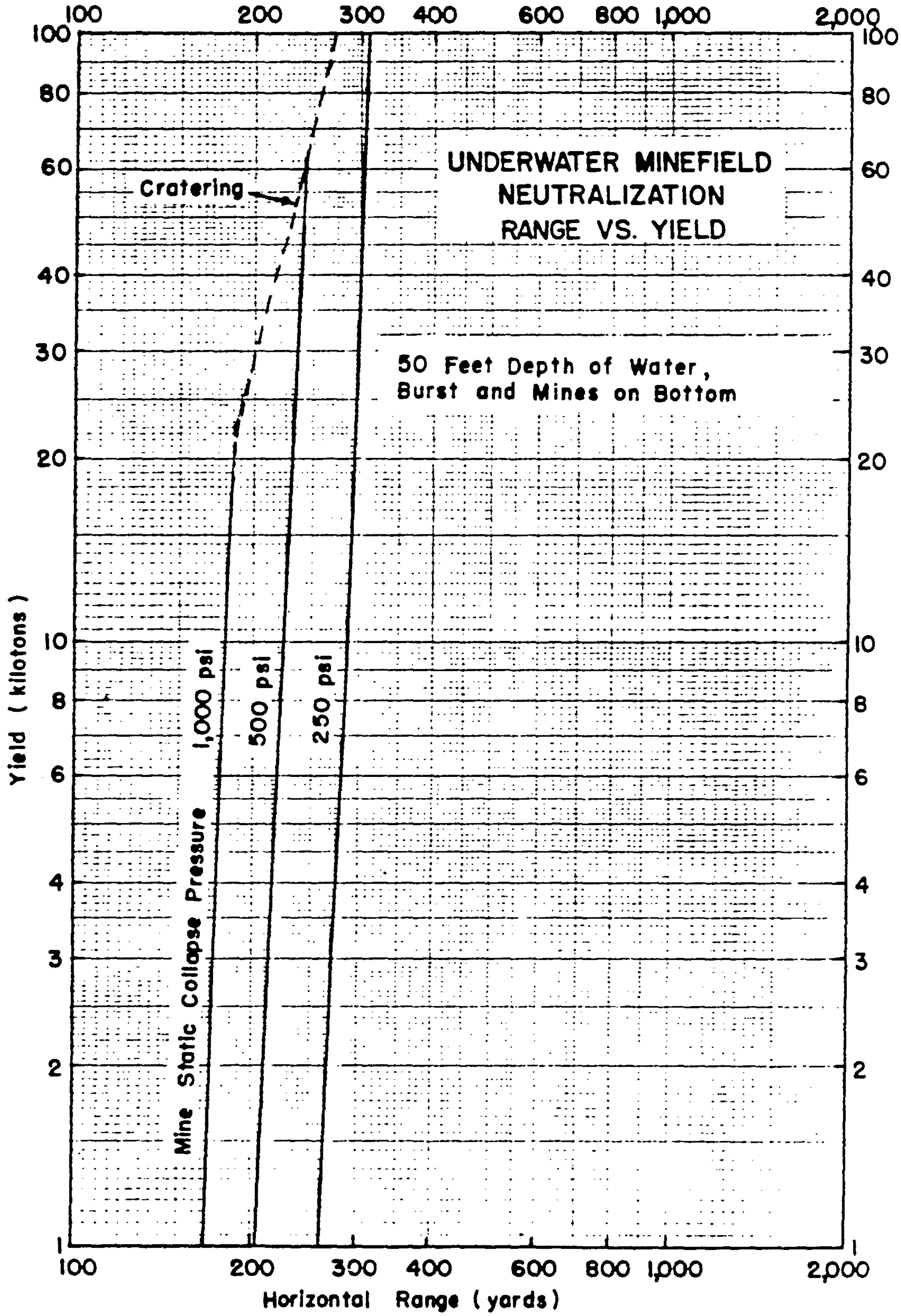
UNDERWATER MINEFIELD
NEUTRALIZATION
RANGE VS. YIELD
50 Feet Depth of Water,
Burst and Mines on Bottom
Cratering
Mine Static Collapse Pressure
1,000 psi
500 psi
250 psi
Yield (kilotons)
Horizontal Range (yards)
100
200
300
400
600
800
1,000
2,000
1
2
3
4
6
8
10
20
30
40
60
80
100

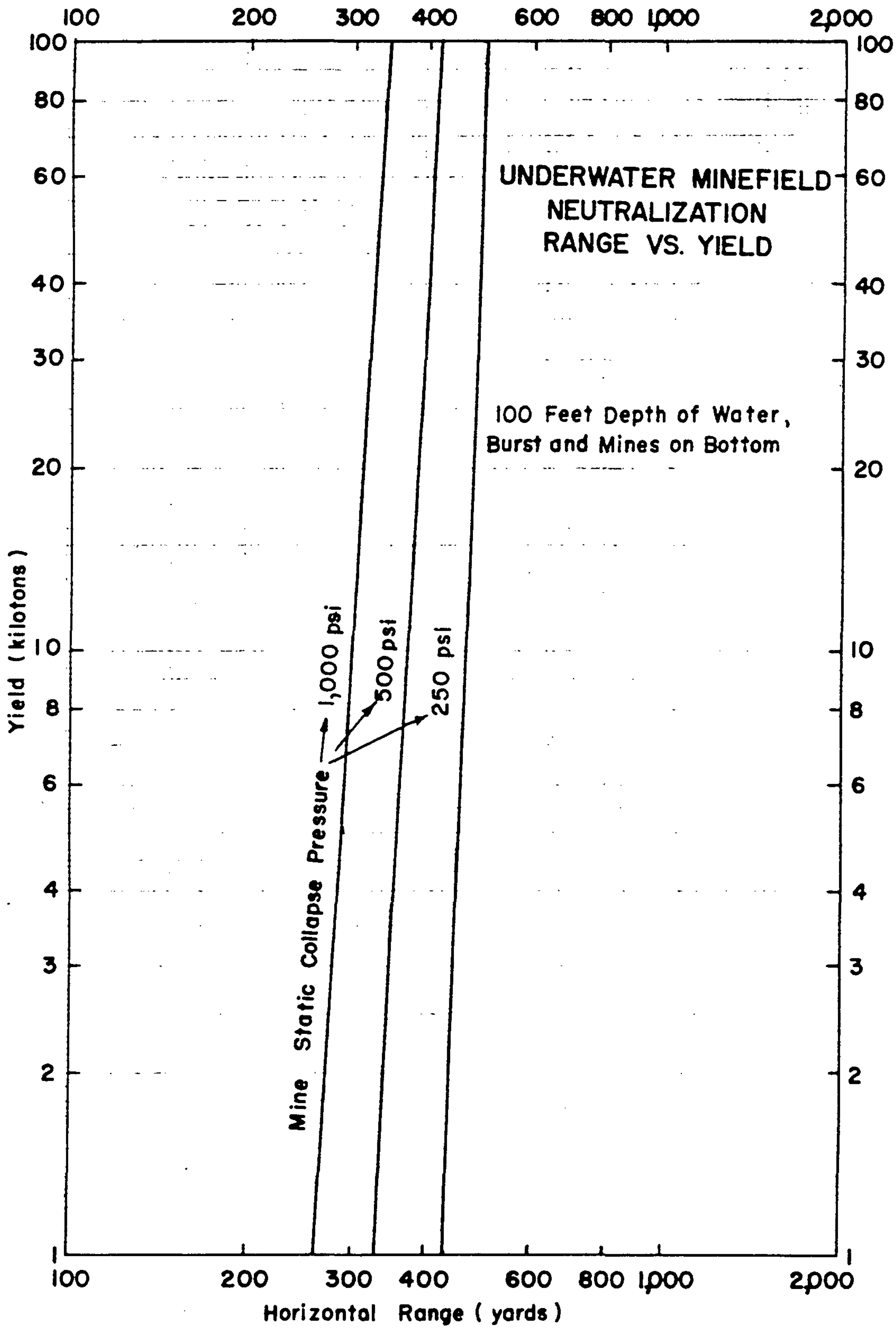
UNDERWATER MINEFIELD NEUTRALIZATION RANGE VS. YIELD
100 Feet Depth of Water, Burst and Mines on Bottom
Mine Static Collapse Pressure
1,000 psi
500 psi
250 psi
Yield (kilotons)
Horizontal Range (yards)
100
200
300
400
600
800
1,000
2,000
1
2
3
4
6
8
10
20
30
40
60
80
100

~~CONFIDENTIAL~~

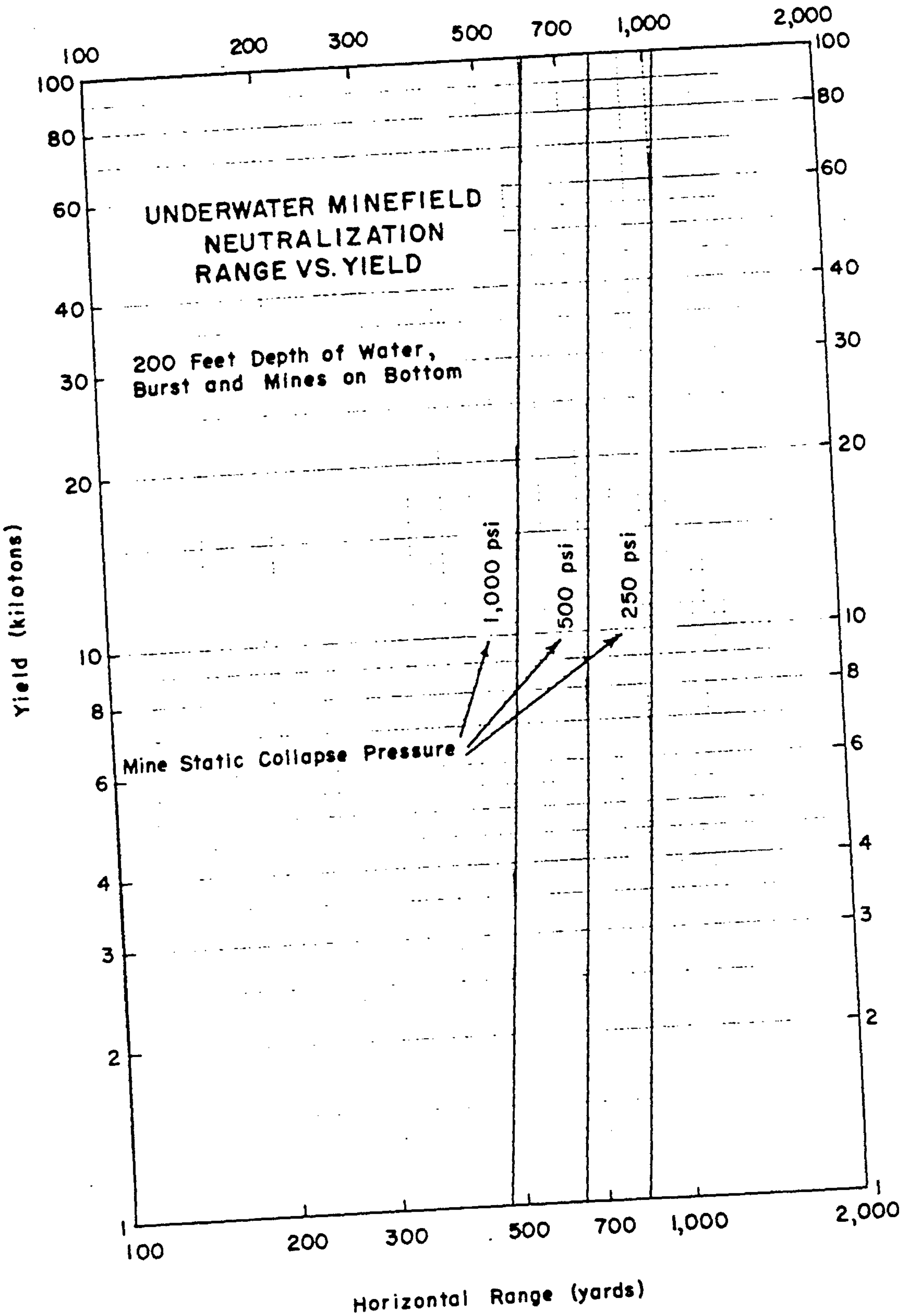

~~CONFIDENTIAL~~

BLANK

9
Aircraft

SECTION IX
DAMAGE TO AIRCRAFT

9.1 General

Aircraft are relatively vulnerable to the blast and thermal effects of nuclear detonations. Since aircraft are designed within narrow limits for flight and landing loads, the structure can withstand only small additional loads imposed by weapon effects. Blast overpressure on striking an aircraft surface may cause dishing of panels and buckling of stiffeners and stringers. On the side struck by the blast wave, the pressure is increased above the incident intensity by reflection and a diffractive force of short duration is generated. As the wings, empennage, and fuselage are completely enveloped by the blast, further dishing and buckling of skins and structure may result from the crushing effect of the differential pressure between the outside and inside of the aircraft components. Additional damaging loads are also developed by the particle velocity accompanying the blast wave. This particle velocity results in drag loading, which is usually termed "gust loading" with reference to aircraft. The duration of the gust loading is many times that of the diffractive loading, and it develops bending, shear, and torsion stresses in the airfoil and fuselage structures. For aircraft in flight, these stresses are usually the major effect on the aircraft.

The weapon thermal energy which is absorbed by aircraft components can also produce damaging effects. Very thin skins are rapidly heated to damaging temperatures by exposure to the short period thermal flux, because the energy is absorbed by the skin so much more rapidly than it can be dissipated by conduction and convective cooling. Exposed fabric, rubber, and similar materials with low ignition and charring temperatures are vulnerable items which may also initiate extensive fire damage at very low levels of radiant exposure. In recent years, designers of military aircraft have reduced aircraft vulnerability to thermal effects by coating thin skinned materials with low absorptivity paints, by eliminating ignitable materials from exposed surfaces, and by substitution of thicker skins for very thin skins. With these protective measures and design modifications, aircraft can be safely exposed at radiant exposure levels several times those which formerly caused serious damage.

9.2 Parked Aircraft

a. Air Blast. The diffraction phase loading and the drag phase loading have varying relative importance in producing damage to parked aircraft. In general, the diffraction phase is of primary importance in the zones of light and moderate damage. In the zone of severe damage the drag phase assumes more importance. Orientation of the aircraft with respect to the point of burst affects vulnerability considerably. With the nose of the aircraft directed toward the burst, higher weapon effects inputs can be absorbed without damage than for any other orientation. The longer duration of the positive phase of the blast from a large yield weapon may result in some increase in damage over that expected from small yields at the same overpressure level. This increase is likely to be significant at input levels producing severe damage but is not likely to be important at the levels of moderate and light damage. Experiments have shown that revetments provide only slight shielding against blast overpressure and under some conditions reflected pressures within the revetment are higher than corresponding incident pressures. Revetments do provide significant shielding from damage due to flying debris borne by the blast wave. Damage to various types of parked aircraft may be estimated from the curves of figures 9–1, 9–2 and 9–3. Distances to which a given level of damage from a subsurface burst occurs may be derived from figure 7–18 in conjunction with these figures. Quantitative data with respect to high yield influence on damage is not available. Therefore this influence has not been reflected in the damage curves.

b. Thermal Radiation. A military weapon delivery aircraft properly prepared for its delivery mission with reflective paint and all vulnerable materials shielded from direct thermal radiation will not be damaged by thermal inputs at distances where damage from blast inputs is severe. Other aircraft not so prepared may sustain serious damage at very low thermal levels as a result of ignition of items such as fabric covered control surfaces, rubber and fabric seals, cushions and headrest covers. The radiant exposure levels at which damage to these materials may be expected can be estimated from the data of table 12–2. Aircraft painted with dark paint are especially vulnerable to thermal radiation damage because the dark painted surfaces absorb three to four times the thermal energy that is absorbed by polished aluminum surfaces or surfaces protected with reflective paint. Temporary emergency shielding as provided by trees, buildings, embankments, or similar barriers may be useful for thermal protection of unprepared aircraft, but any of these may increase the blast damage by adding to the flying debris or by multiple reflection of incident overpressures.

9.3 Aircraft in Flight

a. Air Blast. The response of an in-flight aircraft to blast loading is very complex. Factors which influence the response are—

(1) Velocity and altitude of the aircraft.
(2) Orientation of the aircraft with respect to the burst.
(3) Intensity and duration of the overpressure and particle velocity accompanying the blast wave.
(4) Geometry of the aircraft components.
(5) Natural frequency of the aircraft structural components.
(6) Weight and weight distribution at the time of shock arrival.

For weapon delivery aircraft, analytical methods have been developed for predicting response under a variety of flight conditions and for kiloton and megaton yields. These methods require a detailed analysis for each aircraft type. Such analyses have been verified for several aircraft types by observing response at weapon effects tests.

For prediction of weapon effects required to destroy an enemy aircraft in flight, the response problem becomes even more complex. The knowledge of structural behavior and load carrying capacity of aircraft structures in regions above design limit, through ultimate strength to failure, is very limited. Estimates of lethal envelopes for various types of aircraft have been made on the basis of approximate analysis and limited experimental data. Three of these typical envelopes are presented in figure 9–4 to illustrate the general shape and size of regions about a nuclear antiaircraft burst within which an enemy aircraft may be expected to be destroyed by the weapon blast.

b. Thermal Radiation. The radiant exposure of an aircraft in flight varies widely with atmospheric conditions, orientation of the aircraft with respect to the burst, the ground reflecting surfaces, and clouds. Scatter and reflection add to the direct radiation and under some circumstances the thermal energy incident on an aircraft in space may be two to three times that computed at a given slant range from figure 3–6. Conversely, when a heavy cloud layer is between the burst and the aircraft the radiant exposure may be only a fraction of the predicted value for a given range. In other situations, reflected radiation from clouds may contribute significant thermal energy to areas of the aircraft shaded from direct radiation. During weapon effects tests of an aircraft flying in a cloud above the burst, the radiant exposure at the top of the aircraft and its cockpit area was observed to be as much as one-fourth of the direct radiation on the lower surfaces. This experiment demonstrated the need for protection of weapon delivery aircraft from radiant exposure from any direction. For subsonic weapon delivery aircraft which are adequately protected from thermal radiation, the blast loading is usually the limiting effect. However, supersonic aircraft can outrun the shock wave from a delivered weapon, so that thermal inputs determine the minimum safe separation distance of the aircraft and detonation.

Lethal thermal effects are not well defined. It has been estimated that 100 to 135 cal/cm² applied normal to a typical aircraft skin surface would destroy the protective coating and heat the skin to melting temperatures; however, this would not necessarily destroy the aircraft or prevent it from completing its mission. In general, the lethal blast effects extend well beyond the 100 to 135 cal/cm² thermal level from a detonation at operating altitudes for air-breathing-engine aircraft. The thermal envelope representing an expected thermal input of 135 cal/cm² normal to the lifting surfaces is also illustrated on each of the diagrams of figure 9–4 for comparison purposes only.

DAMAGE TO NON-COMBAT AIRCRAFT

Figure 9–1 presents height of burst vs. ground range curves for light, moderate and severe damage to randomly oriented parked transport airplanes, light liaison airplanes, and helicopters. These curves are drawn for 1 KT and are based on the following definitions of damage and corresponding peak overpressure criteria:

Light Damage--That damage which does not prevent flight of the aircraft, though performance may be restricted thereby. Transport airplanes, 1 psi; light liaison airplanes, ½ psi; helicopters, ½ psi.

Moderate Damage—That damage which requires field maintenance to restore the aircraft to operational status. Transport airplanes, 2 psi; light liaison airplanes, 1 psi; helicopters, 1½ psi.

Severe Damage—That damage which requires depot level maintenance to restore the aircraft to operational status. Transport airplanes, 3 psi; light liaison airplanes, 2 psi; helicopters, 3 psi.

Scaling. Height of burst and ground range for a given degree of damage scale as the cube root of the yield:

$$\frac{h_1}{h_2}=\frac{d_1}{d_2}=\frac{W_1^{1/3}}{W_2^{1/3}},$$

where h_1 and d_1 are height of burst and ground distance for yield W_1, and h_2 and d_2 are the corresponding height of burst and distance for yield W_2.

Example.

Given: A 100 KT weapon is to be burst at optimum height to obtain moderate damage to parked transport airplanes.

Find: The ground range at which moderate damage may be expected and the optimum height of burst.

Solution: From figure 9–1, the optimum height of burst for 1 KT is 1,300 feet. The optimum height of burst for 100 KT is $(100)^{1/3}\times 1300=6{,}000$ feet. *Answer*.

Also from figure 9–1, the ground range for moderate damage from a 1 KT burst at a height of burst of 1,300 feet is 1,380 yards. The corresponding ground range for 100 KT is $(100)^{1/3}\times 1{,}380=6{,}400$ yards. *Answer*.

Reliability. These curves are based on full scale test data for military bomber and fighter aircraft and detailed analysis of weapons effects on basic structural components. It is considered that they represent the best available estimates, for the aircraft types specified, of distances at which 50 percent of the aircraft parked at that range may be expected to be damaged to the degree specified.

Related Material.

See paragraph 9.2.

See also figures 9–2 and 9–3.

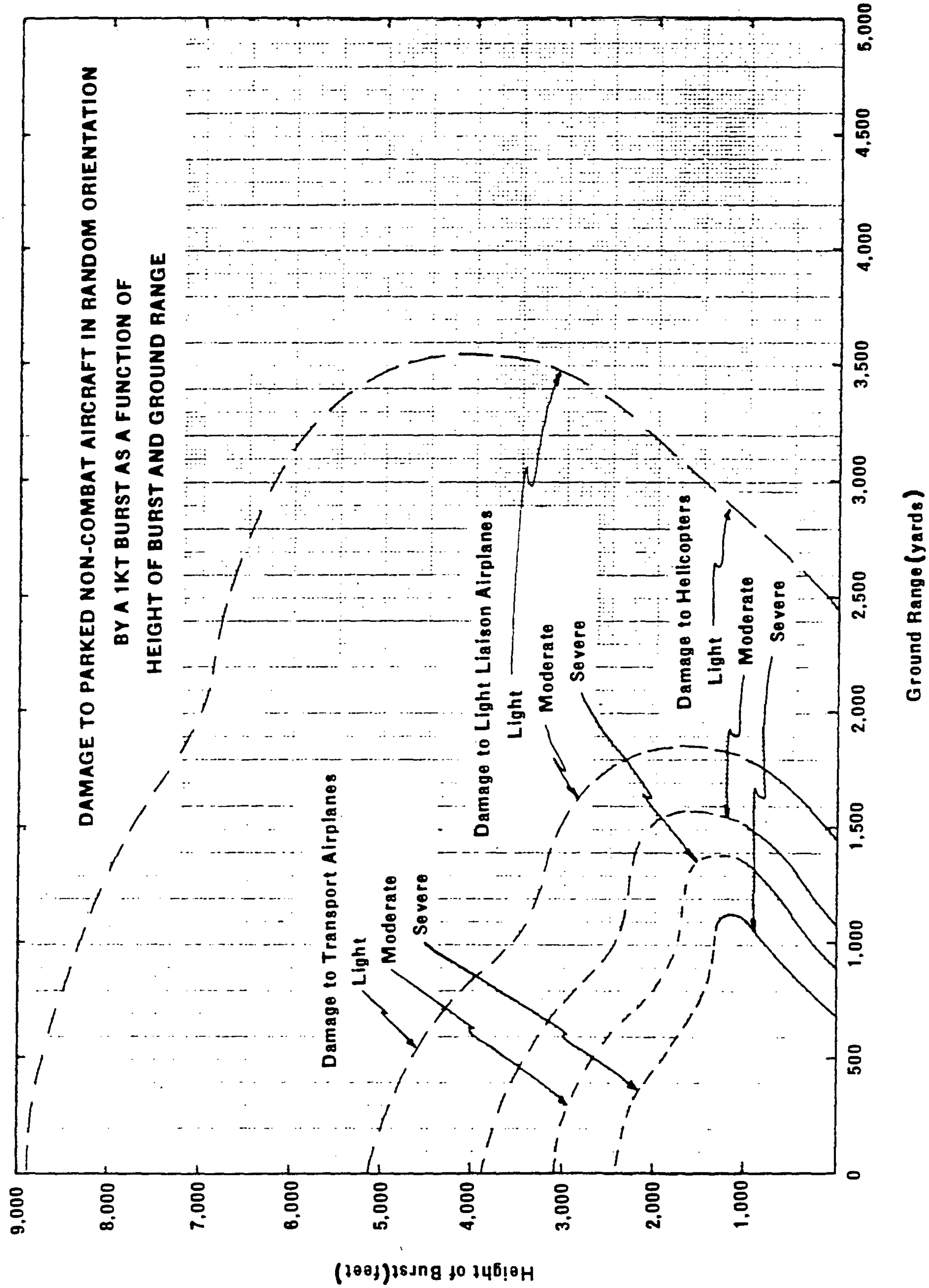
DAMAGE TO PARKED NON-COMBAT AIRCRAFT IN RANDOM ORIENTATION
BY A 1KT BURST AS A FUNCTION OF
HEIGHT OF BURST AND GROUND RANGE
Damage to Transport Airplanes
Light
Moderate
Severe
Damage to Light Liaison Airplanes
Light
Moderate
Severe
Damage to Helicopters
Light
Moderate
Severe
Height of Burst (feet)
9,000
8,000
7,000
6,000
5,000
4,000
3,000
2,000
1,000
Ground Range (yards)
0
500
1,000
1,500
2,000
2,500
3,000
3,500
4,000
4,500
5,000

DAMAGE TO PARKED COMBAT AIRCRAFT, RANDOM ORIENTATION

Figure 9–2 presents height of burst vs. ground range curves for light, moderate and severe damage to bomber and fighter aircraft for random orientation. These curves are drawn for 1 KT and are based on the following definitions of damage and corresponding peak overpressure criteria.

Light Damage—That damage which does not prevent flight of the aircraft, though performance may be restricted thereby. Jet bombers, 1½ psi; propeller fighters, 2 psi; jet fighters, 2 psi.

Moderate Damage—That damage which requires field maintenance to restore the aircraft to operational status. Jet bombers, 2½ psi; propeller fighters, 4 psi; jet fighters, 5 psi.

Severe Damage—That damage which requires depot level maintenance to restore the aircraft to operational status. Jet bombers, 4 psi; propeller fighters, 5 psi; jet fighters, 8 psi.

Scaling. Height of burst and ground range for a given degree of damage scale as the cube root of the yield:

$$\frac{h_1}{h_2}=\frac{d_1}{d_2}=\frac{W_1^{1/3}}{W_2^{1/3}},$$

where h_1 and d_1 are height of burst and ground distance for yield W_1, and h_2 and d_2 are the corresponding height of burst and distance for yield W_2.

Example.

Given: A 50 KT burst at ground level.

Find: At what range from ground zero must a jet fighter be parked in order to be no more than lightly damaged.

Solution: From figure 9–2, the distance from ground zero for light damage to jet fighters for a 1 KT burst is 900 yards. The corresponding distance for a 50 KT burst is $900\times(50)^{1/3}=3{,}300$ yards. *Answer.*

Reliability. These curves are based on full scale test data for military bomber and fighter aircraft and detailed analysis of weapons effects on basic structural components. It is considered that they represent the best available estimates, for the aircraft types specified, of distances at which 50 percent of the aircraft parked at that range may be expected to be damaged to the degree specified.

Related Material.

See paragraph 9.2.

See also figures 9–1 and 9–3.

FIGURE 9-2

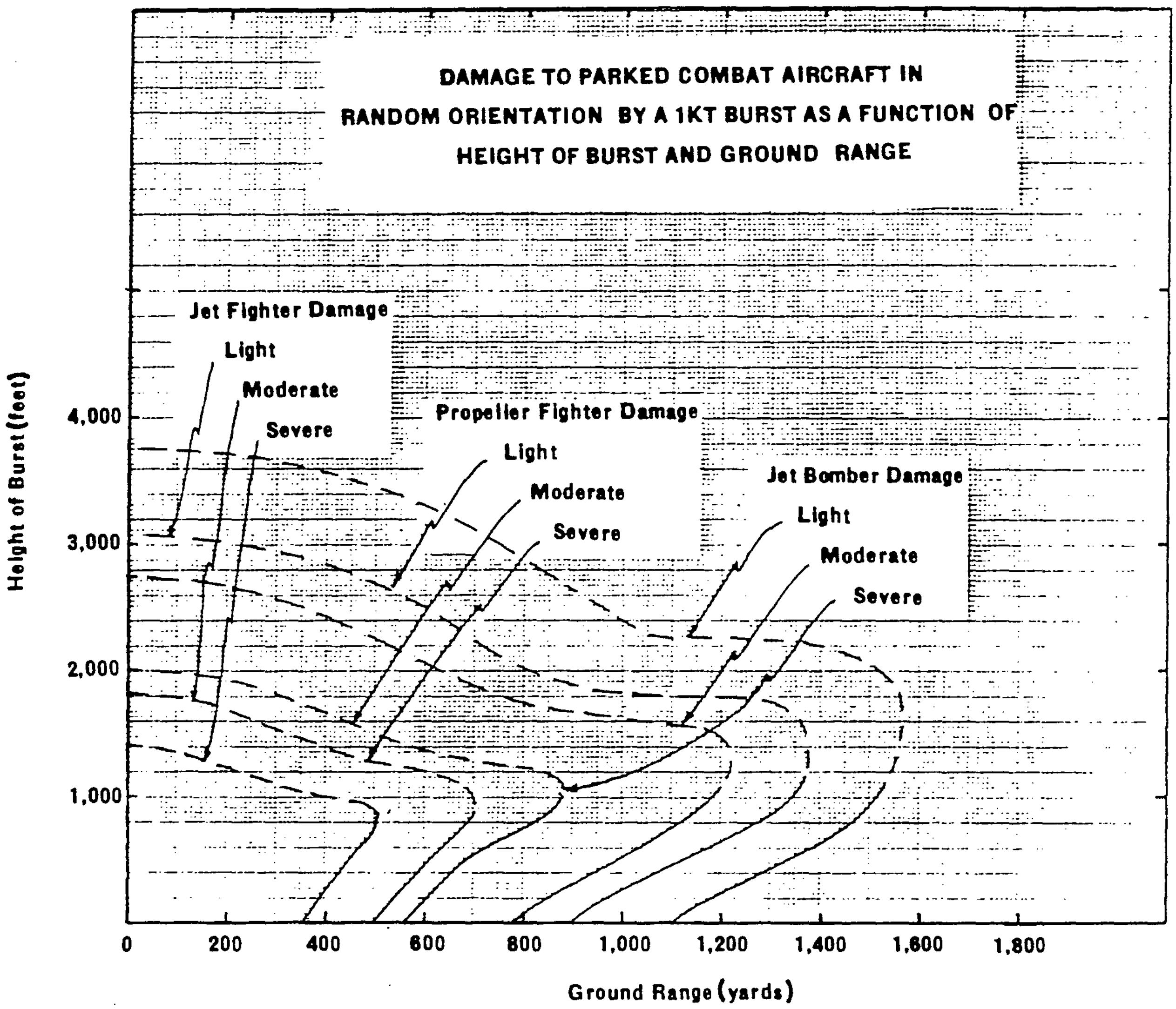
DAMAGE TO PARKED COMBAT AIRCRAFT IN RANDOM ORIENTATION BY A 1KT BURST AS A FUNCTION OF HEIGHT OF BURST AND GROUND RANGE
Jet Fighter Damage
Light
Moderate
Severe
Propeller Fighter Damage
Light
Moderate
Severe
Jet Bomber Damage
Light
Moderate
Severe
Height of Burst (feet)
4,000
3,000
2,000
1,000
0
200
400
600
800
1,000
1,200
1,400
1,600
1,800
Ground Range (yards)

DAMAGE TO PARKED COMBAT AIRCRAFT, NOSE-ON ORIENTATION

Figure 9-3 presents height of burst vs. ground range curves for light, moderate and severe damage to bomber and fighter aircraft for nose-on orientation. These curves are drawn for 1 KT and are based on the following definitions of damage and corresponding peak overpressure criteria.

Light Damage—That damage which does not prevent flight of the aircraft, though performance may be restricted thereby. Jet bombers, 2 psi; propeller fighters, 2 psi; jet fighters, 3 psi.

Moderate Damage—That damage which requires field maintenance to restore the aircraft to operational status. Jet bombers, 3 psi; propeller fighters, 5 psi; jet fighters, 7 psi.

Severe Damage—That damage which requires depot level maintenance to restore the aircraft to operational status. Jet bombers, 5 psi; propeller fighters, 7 psi; jet fighters, 9 psi.

Scaling. Height of burst and ground range for a given degree of damage scale as the cube root of the yield—

$$\frac{h_1}{h_2}=\frac{d_1}{d_2}=\frac{W_1^{1/3}}{W_2^{1/3}},$$

where h_1 and d_1 are height of burst and ground distance for yield W_1, and h_2 and d_2 are the corresponding height of burst and distance for yield W_2.

Example.

Given: A 30 KT weapon is burst 4,000 feet above the terrain and a horizontal distance of 2,500 yards from a jet bomber parked nose-on to the burst.

Find: The corresponding 1 KT height of burst and the degree of damage to be expected.

Solution: The corresponding 1 KT height of burst is $\frac{4,000}{(30)^{1/3}}=1,290$ feet.

The corresponding distance from ground zero is $\frac{2,500}{(30)^{1/3}}=800$ yards.

From figure 9-3, moderate to severe damage would be expected at 2,500 yards from ground zero for a 30 KT weapon burst 4,000 feet above the terrain. *Answer*.

Reliability. These curves are based on full scale test data for military bomber and fighter aircraft and detailed analysis of weapons effects on basic structural components. It is considered that they represent the best available estimates, for the aircraft types specified, of distances at which 50 percent of the aircraft parked at that range may be expected to be damaged to the degree specified.

Related Material.

See paragraph 9.2.

See also figures 9-1 and 9-2.

ESTIMATES OF GUSTS AND THERMAL ENVELOPES FOR TYPICAL COMBAT AIRCRAFT

Figure 9-4 presents an estimate, for each of three typical combat aircraft types, of the lethal envelope in the vertical plane containing the flight path. For each diagram, the silhouette represents the position of the aircraft at burst time; a 1 KT burst anywhere within the envelope is expected to destroy the aircraft. The corresponding lethal volume is approximately that within the surface of revolution generated by revolving the envelope shown about the flight path axis. Also indicated on the diagrams are the ranges at which the radiant exposure of the aircraft would be 135 cal/cm^2, an exposure level at which most aircraft would experience some melting of skin panels by thermal radiation from a 1 KT burst.

Scaling and Reliability. Estimates of lethal envelopes for other yields may be made by scaling the ranges to the blast envelopes by the cube root of the yield and the ranges for the 135 cal/cm^2 envelopes by the square root of the yield. The diagrams are presented to illustrate general shapes and sizes of lethal envelopes for aircraft and it is not intended that the numerical data be applied directly to any specific aircraft models.

Related Material.

See paragraph 9.3.

ESTIMATES OF GUSTS & THERMAL ENVELOPES FOR TYPICAL COMBAT AIRCRAFT

1 KT ANTI-AIRCRAFT BURST

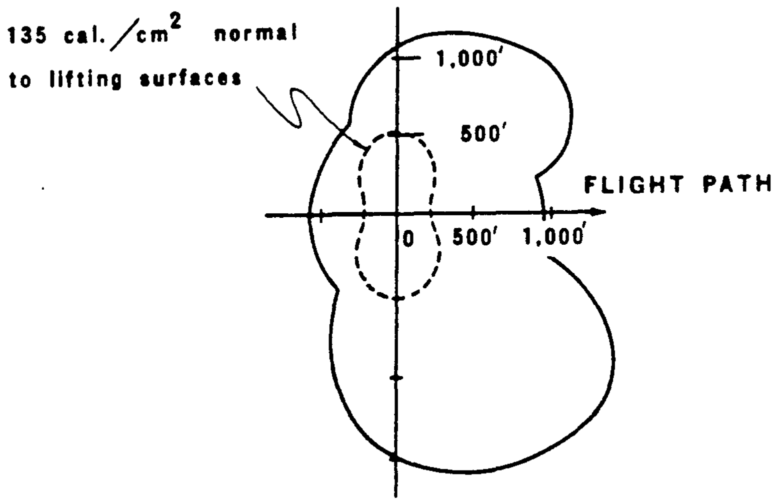

SUBSONIC BOMBER
ALTITUDE 40,000'
SPEED, MACH .9

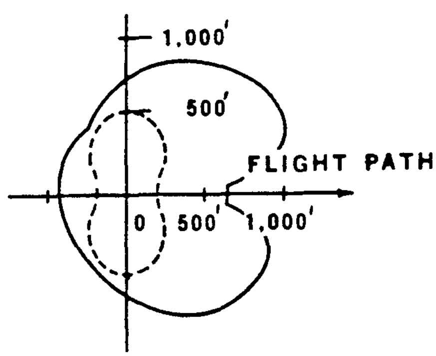

FIGHTER
ALTITUDE 40,000'
SPEED, MACH .95

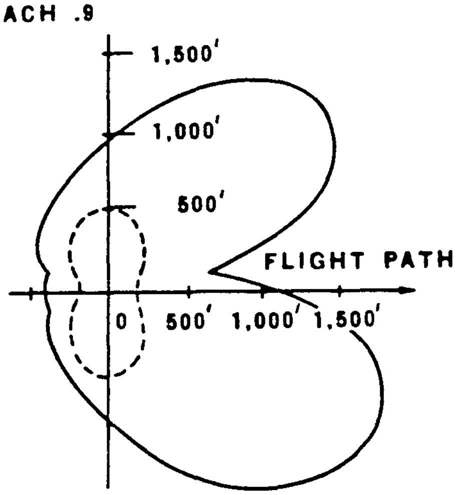

SUPERSONIC BOMBER
ALTITUDE 70,000'
SPEED, MACH 2.5

BLANK

10
Field
Equip.

SECTION X
DAMAGE TO MILITARY FIELD EQUIPMENT

10.1 General

a. Damage Mechanisms. Military field equipment targets are for the most part small, rugged, and free to move, and as such are primarily sensitive to the drag forces associated with the blast wave from a nuclear detonation. Under some circumstances, however, such as when items are shielded from drag forces or lie in the early regular reflection region, crushing by peak blast wave overpressures may be important. The drag forces tend to displace and tumble targets of this type, and in the process damage them. Thermal damage to field equipment in general is not of importance; however, for certain items such as POL dumps, fire effects are important and are treated below.

b. Damage Levels.

(1) Many factors affect the level of damage sustained by military field equipment targets. Among these are orientation of the item of equipment with respect to ground zero; orientation of the blast wave with respect to the surface, i. e., whether the item is in the regular or in the Mach reflection region; shielding effects; the nature of the particulate matter in the blast wave; the presence or lack of flammable materials; and the magnitude of the blast forces. To simplify the presentation of damage criteria for blast effects in the following paragraphs, a height of burst vs. ground range method of presentation for various levels of damage is used. The levels of damage are defined as follows:

(*a*) *Severe.* That damage which is sufficient to prevent the accomplishment of any useful military function, and the repair of which is essentially impossible without removal to a major repair facility.

(*b*) *Moderate.* That damage which is sufficient to prevent any military use until some repairs are effected.

(*c*) *Light.* That damage which does not seriously interfere with immediate military operations but necessitates some repair to restore the item to complete military usefulness.

(2) Specific examples of the type of damage associated with a given level of damage are included for each major item of equipment. Distances shown for moderate damage are those for which the probability of the damage occurring is 50 percent and, where the data permit, 10 percent. Distances shown for severe damage are those for which the probability of damage occurring is 50 percent, and where sufficient data are available, 90 percent and 10 percent. For light damage the distances are those for which the probability of damage is 10 percent. It is intended that the light damage curve and the moderate curve for 10 percent probability be used to indicate approximate limits of light damage and thus may be of value in determining how close equipment may be placed to friendly bursts without endangering the combat usefulness of that equipment. It is assumed for all damage curves, unless stated otherwise, that the items of equipment are oriented in a random fashion with respect to ground zero and lie unshielded on fairly level terrain. A discussion of shielding effects is given below.

c. Terrain Effects. Most of the damage curves presented are the result of a great many exposures of military equipment to full-scale tests, and it is believed that the reliability of the data for a great variety of terrains is excellent. However,

Table 10–1. Damage to Ordnance Items

Item	Damage curves most closely related	Examples of damage
Mortars and recoiless rifles	Figure 10–2	S—Dismemberment. M—Twisted standards and mountings. L—Sight breakage.
Small arms and machine guns	Figure 10–2	S—Dismemberment. M—Broken stocks, twisted and broken mountings. L—Cracked stocks.
Rocket launchers, 3.5 in.	Figure 10–1	S—Torn to pieces. M—Twisted tube. L—Sight damage.
LVT's and DUKW's (on land)	Figure 10–1	S—Great distortion and possible rupture of hull. M—Hull distortion, track damage. L—Glass breakage.

for bursts which are expected to produce a precursor over a terrain which yields no dust, the distances at which a given level of damage occurs may be somewhat less than indicated. Until further evidence is available, however, it is recommended that the criteria shown be used for all types of surface.

d. Subsurface Bursts. It is to be noted that all damage curves of this section extend upward from a zero height of burst. To determine the distance to which a given item of equipment suffers a given level of damage from a subsurface burst, the curves of section X may be used with appropriate reduction from figure 7–18.

e. Scaling. The scaling given with the damage curves of this section have been checked for items of military equipment over a wide range of yields. It is believed that the procedures are valid over a range of yields from 1 KT to 10 MT. Figure II–1 (app. II) gives the values of various numbers raised to the exponents used in this section.

10.2 Ordnance Equipment

a. Blast Damage. Curves are presented in figures 10–1 and 10–2 for damage to tanks, artillery, and vehicles. Tanks and artillery are about equally vulnerable. Table 10–1 indicates which set of curves best fits the experimental data for other items of military ordnance. Examples are also given of damage levels for the various items. Note that figures 10–1 and 10–2 apply to light and heavy vehicles, light, medium, and heavy artillery, and light, medium, and heavy tanks. The artillery curves include antiaircraft artillery except for the electronic fire control equipment, which is discussed in paragraph 10.4.

b. Thermal Damage. Thermal damage to ordnance equipment is generally confined to superficial surface effects. Paint and tires may be scorched. Canvas covers may be ignited from thermal radiation at energies ranging from 15 to 50 cal/cm² from a 1 KT detonation, depending on composition, weight, and impregnation.

10.3 Supply Dumps

a. Blast Damage. Height of burst curves are presented in figure 10–3 for blast damage to POL stored in 5 or 55 gallon drums, ammunition and rations in their standard packaging, and other items normally packaged in small containers. The damage indicated refers to the packaging, and is caused by crushing, by rate of acceleration, by violent impact, or by missiles. The proper use of revetments can considerably reduce the damage radii since the mode of damage then will be limited essentially to overpressure. For POL, rupture of the packaging results in loss of the contents. However, this may not be the case for other items. Individual rounds of ammunition may be serviceable even though thrown for great distances. This may also be true for rations. Note that only severe and light damage are indicated. Moderate damage is not considered because the transition from severe damage to light damage is so abrupt for this type of target. These definitions are as follows:

(1) *Severe.* Rupture of cases and scattering with possible destruction of contents.

(2) *Light.* Scattering of cases, possible cracking of cases, or slight leakage of contents.

b. Thermal Damage. Materials in supply dumps packaged in wooden or metal containers are not significantly affected by thermal radiation. However, serious fires may result in supply dumps from the ignition of kindling fuels such as newspaper, dried weeds and grass, and other litter comprised of thin organic materials. These primary ignitions may lead to fires in less combustible materials in the dumps which otherwise would not ignite. POL dumps are highly susceptible to fire under most conditions, owing to the establishment of ignitions in kindling fuels and the subsequent growth of these ignitions into fires in either accidentally spilled fuels or in fuels spilled from containers ruptured by the blast. Radiant exposures required for ignition of various kindling fuels are given in table 12–2. In the absence of kindling fuels, it is unlikely that POL itself will be ignited, whether in open or closed containers or spilled on the ground.

10.4 Communications Equipment

a. Blast Damage. Radios, telephones, switchboards, and electronic fire control equipment are very susceptible to damage resulting from displacement. Figure 10–4 indicates the range at which damage is expected for this type of equipment. The curves are constructed assuming that the items of interest are unshielded from the effects of the blast wave and that the equipment is not intimately associated with other larger items. If the equipment is intimately associated with other equipment or with a structure, the criteria for damage to the other equipment or the structure should be used to determine the damage to the communication equipment. For example, a radio mounted in a truck is severely damaged if the truck is severely or moderately damaged, and a large switchboard installed in a building is severely damaged if the building collapses. Note that only severe damage is indicated in figure 10–4. Light damage for portable field radios consists of antenna damage for which figure 10–4 provides a damage curve.

For estimating damage to telephone poles connected with wire, the curves of paragraph 11.2 (Forests) may be used. For pole arrays extending radially from ground zero, use figure 11–2, severe damage. For transverse pole line arrays, use figure 11–3, severe damage. Wire on poles is likely to be destroyed by the blast wave out to the limit of pole breakage. However, blast damage to wire on poles cannot be depended upon at greater distances.

b. Thermal Damage. The heat sensitive components of communications and electronic fire control equipment are generally shielded by the casings from thermal radiation. Blast effects usually override thermal effects in cases where thermal effects alone might otherwise be significant. Thus, thermal effects are not usually taken as criteria for damage to this type of equipment.

10.5 Land Mines

a. General. Many factors must be considered in the prediction of the effects of nuclear detonations on minefields. Among these are mine type, soil characteristics, mine spacing, depth of burial of the mines, and the characteristics of the blast wave. Data for all of these factors are not available for all mine types. However, information is available on a number of mine types from which generalized criteria can be developed. Because mines are insensitive to thermal and nuclear radiation, these effects are not treated in the discussion which follows.

b. Effects of Burial Depth and Soil Type. Depth of burial and soil type have some effect on mine detonation. In general, if the soil is not frozen and the depth of burial is not greater than about two feet, the criteria as given below are applicable for soils normally encountered. At present, no information is available on the transmission of pressures through frozen soils, but it is believed that if the soil is frozen, no detonation for buried mines can be depended upon except in the region of cratering.

c. Sympathetic Actuation. Mines are usually spaced so that the pressures from the detonation of one mine do not sympathetically detonate adjoining mines. If the spacing of mines is close enough, it is possible for a mine that is actuated by the overpressure of a nuclear blast wave to cause an adjacent mine not actuated by the nuclear blast to be sympathetically actuated by the addition of the exploded mine's overpressure to that of the nuclear detonation. Gaps in mine fields, if sufficiently large, halt this process so that extensive clearance by sympathetic actuation cannot be depended upon. The criteria as given below do not include any sympathetic actuation effects.

PAGE 10-4 WITHHELD IN ITS ENTIRETY (ARMY (b)(1)) *d. Effects of Blast Wave Characteristics.* In general, land mines are sensitive to the rise time of the blast wave; i. e., if the rise time is long, greater pressures are needed to actuate a given mine than if the rise times are short. Long rise times are characteristic of the precursor zone. Therefore, in the criteria given below, two sets of data must be specified for each mine type, depending upon whether or not the mine is expected to be in a precursor zone. For all bursts, for pressures less than about 8 psi, the rise times are fast. Therefore, for mines which require pressures less than about 8 psi for actuation, the criteria are the same for bursts which produce a precursor as for those which do not. This is also true for mines with fuzes which are insensitive to rise times.

e. Mine Type. Although mines can be detonated by explosions acting on either the main explosive or the more sensitive primer or booster, the overpressures required are so high that blast action on pressure plates is always the controlling effect. Detonation criteria presented in table 10–2 are based on interpolation of test results on fused mines of the pressure plate type. The table does not apply to unfused mines or to other mine types such as those with prong type fuses or double pressure activated pressure plates.

f. Criteria. In table 10–2 are listed mines of various nations. For each mine, criteria are given for 90 percent and 10 percent detonations for precursor and nonprecursor type blast waves and for depths of burial from 0 to 12 inches and from 12 to 24 inches. The distances to which the various pressures extend on the ground can be determined from figure 2–10. Criteria for 50 percent probability of mine detonation are not given, since mine problems are concerned with either substantially complete clearance (90 percent probability), or with substantially little effect on the field (10 percent probability).

10.6 Railroad Equipment

a. Blast Damage.

(1) *General.* Some items of railroad equipment (locomotives, flat cars, and gondolas) are primarily drag sensitive targets for all yields. Others, such as box cars, are primarily overpressure sensitive targets for low yield weapons and drag sensitive for higher yield weapons. For the first type of equipment, the dynamic pressure impulse, when of great enough magnitude, can cause severe tumbling or impact at ranges where overpressure would cause only minor damage. For the second type of equipment and for all yields, overpressure damage occurs early in the loading period. In the low yield range it appears to be the primary damage mechanism. The reason for this is that severe damage can result from overpressure alone at ranges where the dynamic pressure impulse is sufficient only to cause overturning and not tumbling. Further, damage resulting from overturning without tumbling does not significantly increase the overpressure damage incurred earlier. Damage to box cars from high yield weapons, on the other hand, cannot be so simply related to a single damage mechanism. For high yields, the dynamic pressure impulse can cause tumbling at overpressures where, for lower yields, no overturning occurs or where only overturning and no tumbling occurs. Here, other mechanisms of damage must be considered. A box car which was only lightly damaged from overpressure can now become moderately damaged as a result of tumbling and impact. A box car that was moderately damaged and subsequently overturned can now become severely damaged as a result of tumbling and impact.

(2) *Isolated box cars, flat cars, gondolas and full tank cars.* Damage criteria for isolated box cars, flat cars, gondolas, and full tank cars for various orientations are contained in figure 10–5. No attempt has been made to draw separate curves for each type of rolling stock in view of the limited knowledge of the modes of damage for various yields. However, box cars are more susceptible to damage than the other types of rolling stock. This fact should therefore be considered in estimating damage criteria. Furthermore, testing to date has shown that for low yield weapons where overpressure is the primary damage mecha-

nism, severe, moderate, and light damage will occur at approximately 8 psi side-on and 12 psi end-on, 6 psi side-on and 10 psi end-on, and 3 psi side-on and 5 psi end-on, respectively. In addition, a box car having only its underframe and trucks salvable is considered over 80 percent damaged. Therefore, even though it could conceivably be used as a flat car, as a box car it would not be usable without extensive rebuilding.

(3) *Isolated empty tank cars.* Insufficient data exist to permit gradation of damage to tank cars; however, it is known that 13 psi overpressure is sufficient to collapse an empty tank car.

(4) *Isolated locomotives.* Damage criteria for isolated locomotives in various orientations are contained in figure 10–6.

(5) *Roadbeds.* Air bursts are relatively ineffective against roadbeds. However, surface or subsurface bursts are likely to demolish roadbeds out to a distance of 1.5 times the crater radius.

(6) *Marshalling yard structures.* For damage to structures normally associated with a marshalling yard, see paragraph 7.2.

b. Shielding.

(1) There is a decrease in damage to a piece of rolling stock that is shielded from the blast wave by neighboring pieces of rolling stock. For side-on orientation, maximum shielding occurs in the case of a car in the middle of a group of cars on adjacent tracks. Even a car directly exposed to the detonation receives the benefit of a shielding effect, and therefore less damage, if four or more cars are behind it. The effect of shielding essentially vanishes when there are three or more car spaces between cars. In an end-on orientation, the shielding factors are independent of the number of empty tracks located between trains so oriented.

(2) A blast wave having an overpressure of 15 psi will cause overturning of all railroad cars regardless of cargo or shielding, whereas a blast wave having an overpressure of 3 psi will not overturn any but a single unshielded car. An overpressure of 3 psi is also the minimum required to produce damage to box cars when the incident shock is normal to the car sides.

c. Thermal Damage. Compared to the blast damage to railroad equipment described herein, the associated thermal damage is negligible.

10.7 Engineer Heavy Equipment

a. Blast Damage. The vulnerability of engineer heavy equipment to blast damage is directly proportional to its complexity. Truck mounted equipment is doubly vulnerable since damage to either the vehicle or the machinery limits the effectiveness of the whole. Earth moving equipment, which is single purpose and quite sturdy for its heavy work, is least vulnerable. Cabs and housings, which protect the operators and the machinery from ordinary hazards, may become a liability. The broad smooth panel surfaces reflect the shock wave, and in so doing receive approximately double the incident overpressure. If panels tear off or collapse, they become missiles which can damage shafts, pulleys, and power plants. This may also be true of items such as cranes with attachments which add to the area exposed to the high winds and drag forces of the blast wave without increasing the strength of the equipment. Considerable reduction in damage to engineer heavy equipment may be obtained by placing it in bulldozed slots. These permit the protected items to avoid the drag forces, which for exposed equipment are the principal cause of severe or moderate damage. Height of burst curves for both exposed and protected engineer heavy equipment are presented in figures 10–7 and 10–8.

b. Thermal Damage. Thermal damage to engineer heavy equipment is essentially the same as that to ordnance equipment. See paragraph 10.2*b*.

10.8 Miscellaneous Equipment

a. General. Damage criteria for many types of military equipment are omitted; however, they may frequently be associated with like damage to other items of equipment which are specifically mentioned in the preceding paragraphs. For example, from a blast damage standpoint, the pumping equipment normally associated with a POL dump is in general a drag sensitive target.

Therefore, the damage curves for military vehicles and supply dumps can be examined for a determination of damage to pumping equipment. For equipment fabricated from materials that char at low radiant exposures and are destroyed or ignited at higher exposures, a determination of thermal damage can frequently be obtained by utilization of table 12–2, *Critical Radiant Exposure Values for Various Materials*.

b. Wire Entanglements. The variability in vulnerability of wire entanglements is great because of the many factors involved, such as the nature of the soil, the quality of the workmanship and the depth of the picketing. For average soil conditions and U. S. military standards of construction, it has been determined that criteria of figure 10–4 can be used for estimating the distance to which it can be expected that wire entanglements are torn from their picketing or other supports. For double apron barbed wire fences, use the telephone and switchboard curve of figure 10–4, and for concertina entanglements use the radio and electronic fire control instrument curve of figure 10–4.

c. Tentage. Because of the large variability in anchorage of tents, no definite blast damage criteria can be given; however, tents are likely to collapse at overpressures between 0.5 and 3 psi. Thermal damage criteria for tent materials are shown in table 12–2.

10.9 Drag Shielding for Military Equipment

a. Gross Terrain Shielding. As was discussed in section II, the nature of the terrain may have considerable effect in modifying the characteristics of the blast wave. In general these modifications result in an increase in damage for military field equipment located on the side of a hill facing toward the blast, and a decrease in damage for equipment located on the side facing away from the blast, compared to the damage at the same range on level terrain. Quantitatively, it cannot be stated how much greater the damage is on the front face or how much less it is for the rear face. However, the modifications may be so great that offensively, if important targets are located on the rear slope of a hill with respect to a proposed burst point, serious consideration should be given to reselecting the intended ground zero. Defensively, every advantage should be taken of natural terrain features which provide drag shielding for equipment.

b. Effects of "Digging In". The damage curves for military equipment in figures 10–1 through 10–4 are drawn for equipment in the open on fairly level terrain, fully exposed to the drag forces of the blast wave. By digging in military equipment, the equipment is somewhat shielded from these drag forces. The amount of shielding depends upon the type of emplacement used for the item of interest. For example, a shallow open pit provides little drag shielding, whereas a deep pit provides much more effective shielding. In the former case, the damage curves as presented could be used for predicting damage. In the latter case, the damage curves for protected engineer heavy equipment, figure 10–8, can be used. In order to make estimates of the effects of drag shielding for other items of military equipment which are well dug in, the ranges for severe and moderate damage are each reduced to 50 percent of the ranges shown for the unprotected case. Light damage ranges are not reduced. "Well dug in" implies that the item is completely below the surface, but without overhead cover.

PAGES 10-8 THROUGH 10-23 ARE WITHHELD IN THEIR ENTIRETY (ARMY (b)(1))

BLANK

11
Forests

SECTION XI
FOREST STANDS

11.1 General

Although forests or tree stands may afford troops deployed therein significant protection against certain effects of nuclear weapon detonations (e. g. thermal radiation), the forests themselves are quite vulnerable to some of these effects. Falling limbs and trees create a missile hazard and the resultant debris on the forest floor may impede the movement of troops and most vehicles. In dry, windy weather, forest fires may be initiated by a nuclear weapon detonation, with smoke and flame extending the range of hazardous effects from the bomb itself many times. Forest vulnerability depends on recent local weather history and upon the type of tree stand involved. Forest kindling fuels and types of stands are discussed in detail in the paragraphs which follow.

11.2 Air Blast

a. General. For convenience in discussion of blast effects, forest stands are divided into the following types:

(1) *Type I stand: Improved natural or planted conifer forests of European type.* These forests characteristically grow in regular blocks, usually with definite borders. Tree spacing is uniform with only small patches of ground visible through the canopy from above. Trees are of uniform height (100 to 130 feet) and nearly the same in diameter (14 to 24 inches). Stands of this type are vigorous in appearance and fast growing. Viewed from above the crown canopy appears smooth. Within the stand there usually will be found low stumps resulting from thinning, clear lower stems as a result of pruning, and little or no underbrush, combining to give the interior of the stand a clean park-like appearance, and affording good visibility and easy passage into the forest.

(2) *Type II stand: Naturally occurring, unimproved conifer forests that have developed under unfavorable growing conditions.* Unfavorable growing conditions result from: shallow and/or rocky soil, deficient annual rainfall, short growing season with unfavorable temperatures (i. e., higher latitudes and/or higher elevations), and unfavorable topography such as poorly drained flats or steep slopes. Random tree spacing is characteristic, with trees varying in height (10 to 75 feet) and in diameter (1 to 17 inches). The crown canopy generally has an uneven appearance. Large stands often contain bare areas with irregular borders. The stand itself appears low in vigor. The forest floor within the stand is generally cluttered with dead, fallen trees which, when combined with the persistent dead limbs on the dense growing live stems and the heavy underbrush in the numerous stand openings, impede entrance into the stand and decrease visibility.

(3) *Type III stand: All broadleaf forests and naturally occurring, unimproved conifer forests that have developed under favorable growing conditions.* Favorable growing conditions are associated with: deep, generally rock-free soil, adequate annual rainfall, long growing season with favorable temperatures (i. e., middle latitudes and lower elevations), and favorable topography such as well-drained flats and moderate slopes, or along stream courses. Random tree spacing is characteristic with trees varying in height (30 to 120 feet) and in diameter (2 to 25 inches). The crown canopy generally has an uneven appearance. Large stands often contain bare areas with irregular borders. The stand itself appears high in vigor. The forest floor within the stand may be

cluttered with dead, fallen trees which impede entrance into the stand. Underbrush is light or absent, and visibility is fairly good.

b. Air Blast Damage. Height of burst-damage-distance curves for severe and light damage to forests are presented in figures 11–1 to 11–6. Distances to which a given level of damage from a subsurface burst occurs may be derived from figure 7–18 in conjunction with these figures. Examples of scaling accompany figure 11–1. Tree stand types referred to are those given above. Severe and light damage are defined in terms of length of stems down per acre; approximately 1,500 feet per acre for light damage and 9,000 feet per acre for severe damage. These criteria in terms of percentage of trees broken are shown in table 11–1. The approximate number of trees per acre that may be expected for the three stand types is also shown.

Table 11–1. Percentage of Trees Broken for Light and Severe Damage to Forest Stands

Stand type	Total No. of trees per acre	Trees per acre 6 in. or larger in diameter	Light damage, % trees 6 in. or larger in diameter, broken	Severe damage, % trees 6 in. or larger in diameter, broken
I	75	75	15	95
II	475	260	[a] 10	[a] 65
III	215	200	[b] 10	[b] 60

[a] Majority of damage as uprooted trees.
[b] In broadleaf forests majority of damage as branch breakage and uprooting

11.3 Thermal Radiation

a. General. Under certain conditions, the employment of an air burst weapon over a forest or wildland area may cause fires. During the fire season, even when the burning potential (a measure of probable fire aggressiveness) is low, fires may spread. If fires are started in regions of sufficient fuel density when the burning potential is dangerously high, complete evacuation of personnel and equipment may be necessary. Organized control of the spread of the fire is virtually impossible until changes in weather or fuel availability reduce the burning potential.

b. Ignitions. Wildland fuels are generally a mixture of thin and heavy fuel components. Thin fuels are typified by surface litter and grassland; heavy fuels by fallen branches. The thinnest fuel present determines the exposure required for ignition of the mixture. Heavy fuels do not ignite and continue to burn by themselves; however, thin fuels may serve as the source of a pilot flame which substantially lowers heavy fuel ignition exposure requirements, or thin fuels may spread fire after the end of the thermal pulse. During the fire season, ignitions may be expected in kindling fuels wherever the radiant exposures exceed 2 to 3 cal/cm^2 for a 1 KT weapon. As the yield increases the minimum radiant exposures for ignition increase as $W^{1/8}$, i. e., 8 to 10 cal/cm^2 would be required from a 30 MT weapon to ignite the thinnest wildland fuels. These exposures apply to surfaces normal to the direction of radiation; however, wildland fuels rarely present a flat smooth surface. Individual fuel particles are of many shapes and are oriented more or less at random. Consequently, even at low burst altitudes, minimum ignition exposures can be assumed to remain the same, although a reduced number of ignitions is to be expected owing to the increased shielding effect of trees and shrubs. Green leaves and needles on tree crowns smoke and char but do not ordinarily sustain ignition. This smoke production materially reduces the radiant exposure of the ground surface. Ignitions occur in open areas if the dimensions are large enough so that the area is not completely in the shadow of adjacent timber or brush stands. It is estimated that very few ignitions occur within a timber stand in which the tree canopy shades more than 20 percent of the ground surface. Smoldering ignitions are likely to occur in snags and dead limbs on the forest floor. While such ignitions are not an immediate hazard, they may cause fires to break out up to two or three days later, especially if a large amount of blast breakage occurs, opening the stand to the prevailing winds.

c. Fire Seasons. The fire season of an area is primarily a function of the annual rainfall-temperature pattern and its associated vegetation development, and varies widely between geographic locations. Table 11–2 summarizes these conditions for the more important wildland fuels found throughout the world. Once it is determined that fuel conditions meet those prevailing in the fire season, local weather conditions will determine burning potential.

Table 11-2. Condition of Wildland Fuels During Fire Season

Fuel type		Amount and density of fuel required to constitute a fire hazard	Condition during fire season
Grass or heath	Grassland; dry bracken ferns and other seasonal plants; dry regrowth in previously burned areas.	Uniform grass cover one-half ton or more per acre.	Vegetation nearly cured or dead.
Evergreen brush	Perennial evergreen shrubs and brush; chaparral; young evergreen growth.	75 percent or more area covered.	15–25 percent by weight of leaves and associated twigs dead.
Deciduous broadleaf forest.	Forest predominantly of trees such as oak, birch, maple, etc., leaves of which die and fall every year.	Ground covered with more or less continuous layer of dead leaves.	Leaves off trees; ground vegetation dead or nonexistent.
Coniferous forest	Forest of evergreen pines, firs, spruces, etc.; generally the family of needle bearing trees.	Ground covered with more or less continuous layer of dead needles and twigs.	Needles and twigs dry enough to break easily when bent. Grass and other ground vegetation, if present, curing or dead.

d. Kindling Fuels. The majority of thin wildland fuels which serve as kindling material are typed as shown in table 11–3 into four classes corresponding to different minimum exposures required for ignition. Ignition exposures required increase as fuel moisture content increases. Since ignition generally occurs on those surfaces most exposed to the atmosphere, required ignition exposures are a function of relative humidity as shown in figure 11–7. Fires may be blown out by the blast wave, depending on the time interval between ignition and arrival of the shock. Blowout is not expected in overpressure regions below 5 psi for fully exposed fuels. When fires are not blown out, they generally increase in intensity due to action of the blast wind.

Table 11-3. Classes of Thin Wildland Kindling Fuels (Arranged in Order of Decreasing Flammability)

Class	Description
I	Broadleaf and coniferous litter—mixture of fine grass, broken leaves and duff, and thin translucent broadleaf leaves.
II	Hardwood and softwood punk in various stages of decay.
III	Cured or dead grass.
IV	Conifer needles and thick, nearly opaque broadleaf leaves.

e. Burning Potential. The principal factors, aside from the fuels present, that influence the burning potential of a forest or wildland area are—the nature of the terrain, the wind speed close to the ground, the relative humidity and the precipitation history. An approximate guide for evaluating the effects of weather on burning potential is given in table 11–4. Fuels seldom burn vigorously, regardless of wind conditions, when the fuel moisture is greater than 16 percent. This corresponds to an equilibrium moisture content for 80 percent relative humidity. About a quarter inch of rain renders fuels temporarily nonflammable and may extinguish going fires in thin fuels. The time required to restore the burning potential to the value prior to the rain may vary from hours to days depending on local weather conditions. Surface fuels in the interior of timber stands are exposed to reduced wind velocities and generally have high fuel moisture due to shading by the canopy.

f. Fire Spread. Under identical weather conditions, concentrations of heavy fuel are more hazardous than thin fuels, even though they tend to reduce local wind speeds and do not respond as rapidly to changes in relative humidity. Trees and heavy limbs on the forest floor may be ignited by an otherwise nonhazardous surface fire. When heavy fuels are present near the borders of standing timber, fire may travel into the tree crowns and continue to crown (spread

Table 11-4. Burning Potential for Light Wildland Fuels During Fire Season (Terrain With Slopes Less Than 20 Percent)

Wind speed at 20 feet above ground in the open	Relative humidity (percent)			
	Below 15	15-40	40-65	65-80
Below 5 knots	Dangerous*	Dangerous	Low*	Low.
5-10 knots	Critical*	Dangerous	Dangerous	Low.
10-15 knots	Critical	Critical	Dangerous	Low.
Above 15 knots	Critical	Critical	Critical	Dangerous.

*Definitions:

Low—irregular fire perimeter, spread greatly affected by local changes in fuel structure and topography, depth of fire small. Fire generally stops at roads and ridge tops. Control action can be on an individual basis.

Dangerous—continuous intense fire front which moves rapidly, frequently spots ahead. Aggressive organized action required to protect personnel and equipment.

Critical—conflagration-type fire, in heavy fuels readily crowns and spots as much as a mile ahead. Requires personnel and equipment to be evacuated from in front and from near the flanks of such fires. Control action effective only when changes in fuel type or burning conditions permit.

Note 1. For heavy fuels, use the classification for the next higher wind speed.
2. For terrain with slopes greater than 20 percent, use the classification for the next higher wind speed.
3. For canopy shading 20 percent of the ground, reduce wind one class and increase relative humidity one class.
4. For full shading, reduce wind two classes and increase relative humidity two classes.

from top to top) even though ground fuel concentrations are low. Pine species are most likely to crown, fir and spruce less likely, and hardwoods least likely. Where large areas of heavy dry fuels are ignited simultaneously, a large whirling fire may develop. Such fires exhibit erratic spread behavior. Whirls may break off the main fire and travel against the prevailing wind. Whenever a strong upward convection column is built up in the case of a heavy fuel fire, the fire may spread very rapidly by "spotting", i. e., by throwing firebrands. Fires started by spotting may travel toward the main fire due to strong indrafts.

BLANK

DAMAGE TO FOREST STANDS BY TYPE

In figures 11–1 through 11–6 are shown severe and light damage curves for three types of forest stands. Severe damage is defined as approximately 9,000 feet of stems down per acre, and light damage is defined as approximately 1,500 feet of stems down per acre. These criteria in terms of percentages of trees broken in typical stands are shown in table 11–1.

For yields greater than 10 MT, the following scaling procedure applies for height of burst and ground range:

$$\frac{d_1}{d_2}=\frac{W_1^{1/3}}{W_2^{1/3}}=\frac{h_1}{h_2},$$

where d_1=distance for height of burst h_1, and for reference yield W_1, *which is 10 MT* ($10^{1/3}=2.15$); and d_2=distance for height of burst h_2, and for yield W_2 (where W_2 is *in megatons and greater than 10 MT*). This scaling procedure applies only to scaling 10 MT values to higher yields.

Example.

Given: A 20 MT burst at a height of 1,000 feet above a type 1 forest stand.

Find: To what distance light damage extends.

Solution: From the scaling given above,

$$\frac{h_1}{1{,}000}=\frac{2.15}{(20)^{1/3}}, \text{ so that}$$

$$h_1=\frac{2{,}150}{(20)^{1/3}}=790 \text{ feet},$$

the height of burst scaled to 10 MT. From figure 11–4, light damage to a type 1 stand exposed to a 10 MT burst at 790 feet extends to a ground range of 16,000 yards. Therefore, for a 20 MT burst at 1,000 feet, light damage extends to a ground range given by—

$$\frac{16{,}000}{d_2}=\frac{2.15}{20^{1/3}}, \text{ or},$$

$$d_2=\frac{16{,}000\times 2.72}{2.15}=$$

20,200 yards. *Answer.*

Reliability. Based upon observed results of limited full-scale tests and extensive laboratory experiments.

Related material.

See paragraph 11.2.

See also paragraph 11.3 and figure 11–7 for fire effects in forest stands.

SEVERE DAMAGE TO TYPE I FOREST STANDS
AS A FUNCTION OF HEIGHT OF BURST AND GROUND RANGE

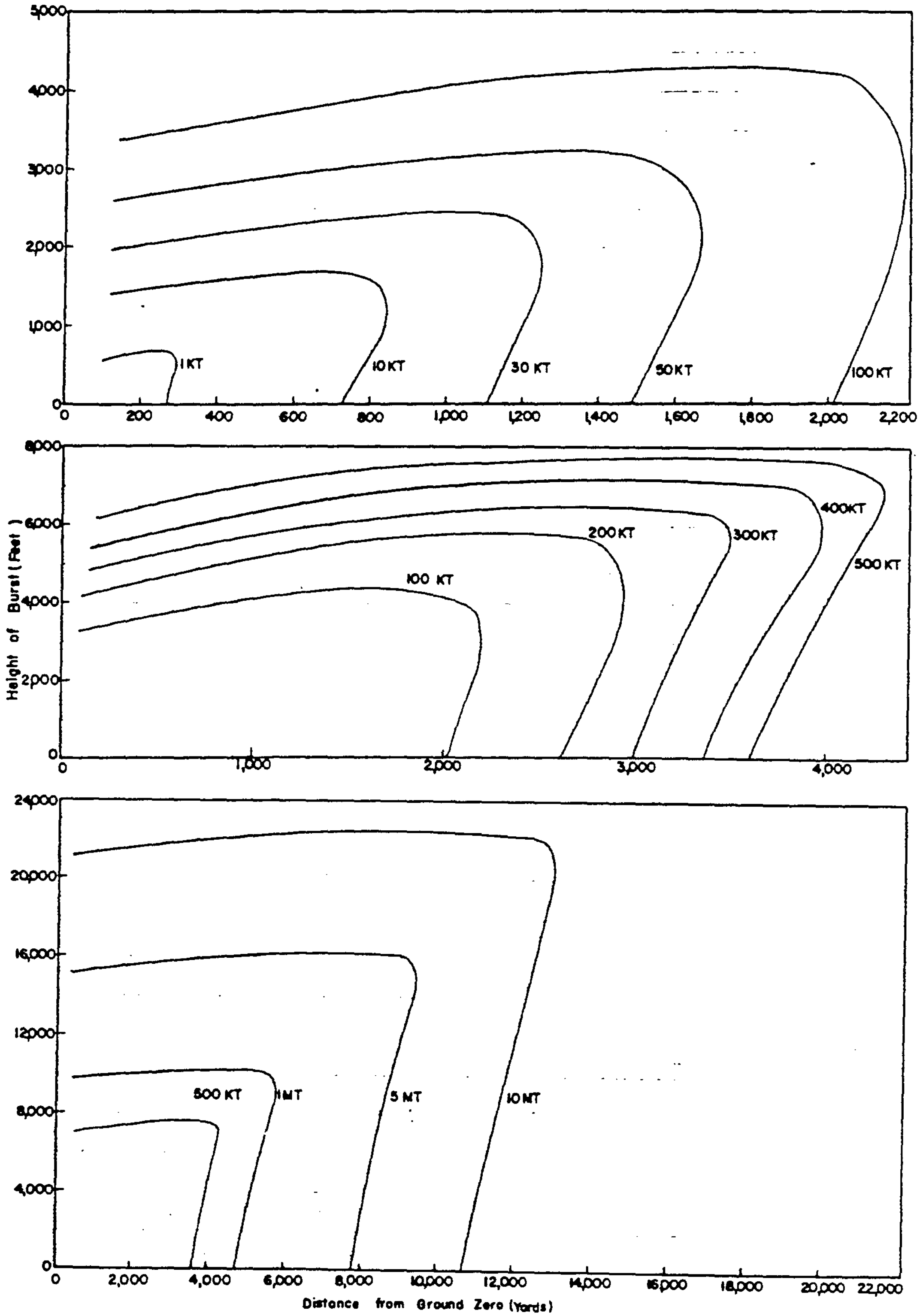

SEVERE DAMAGE TO TYPE II FOREST STANDS
AS A FUNCTION OF HEIGHT OF BURST AND GROUND RANGE

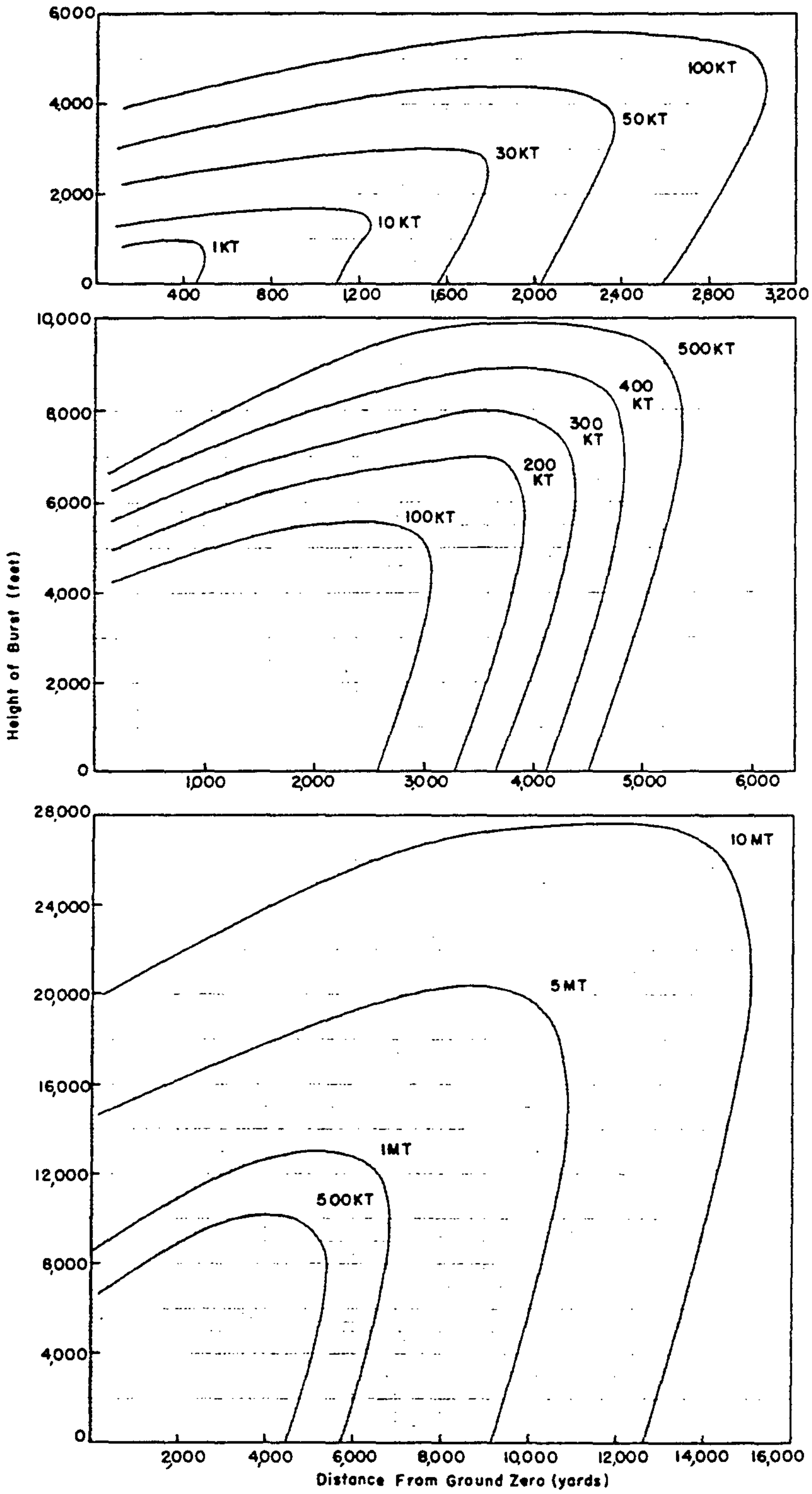

FIGURE 11-3

SEVERE DAMAGE TO TYPE III FOREST STANDS AS A FUNCTION OF HEIGHT OF BURST AND GROUND RANGE

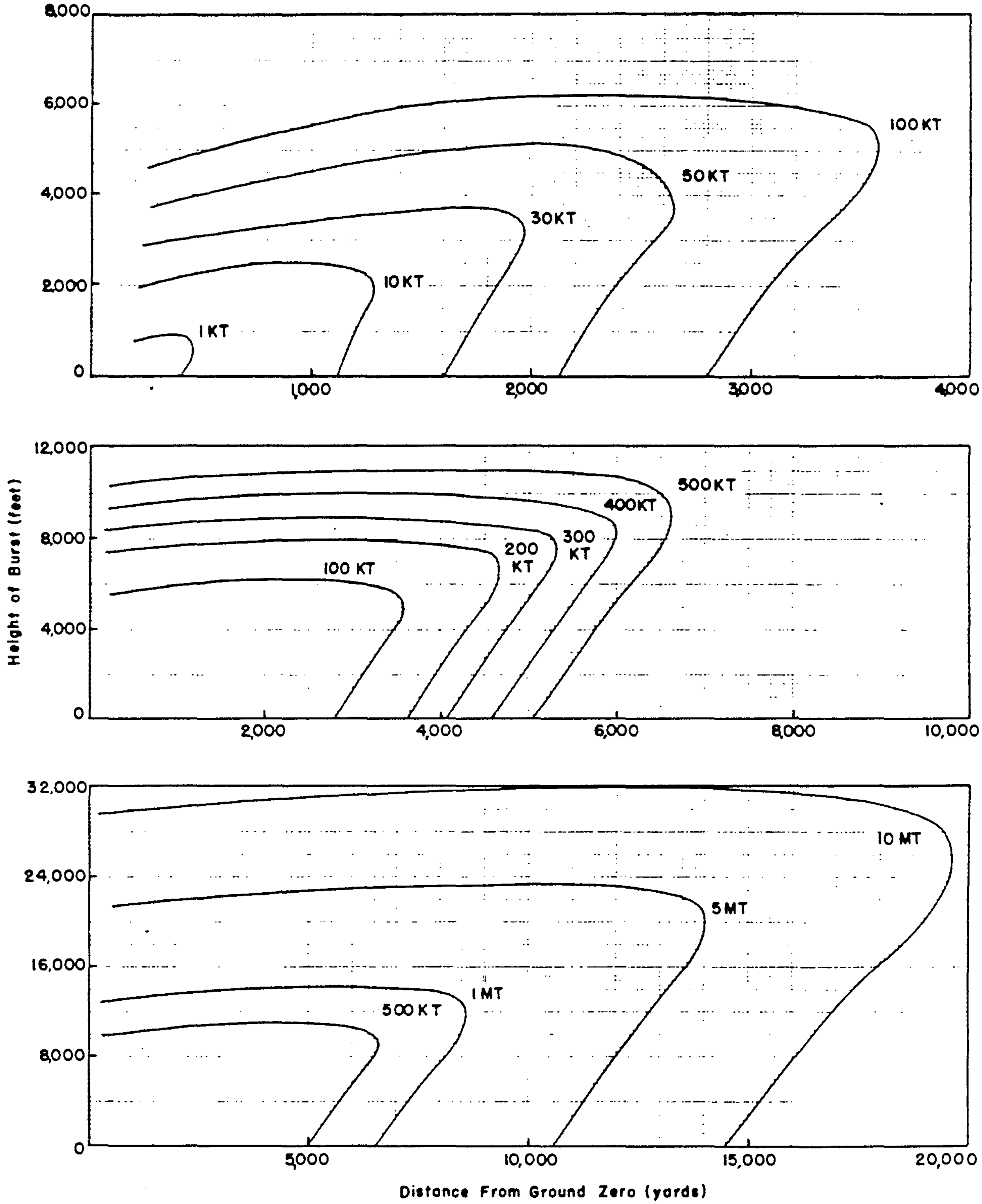

LIGHT DAMAGE TO TYPE I FOREST STANDS AS A FUNCTION OF HEIGHT OF BURST AND GROUND RANGE

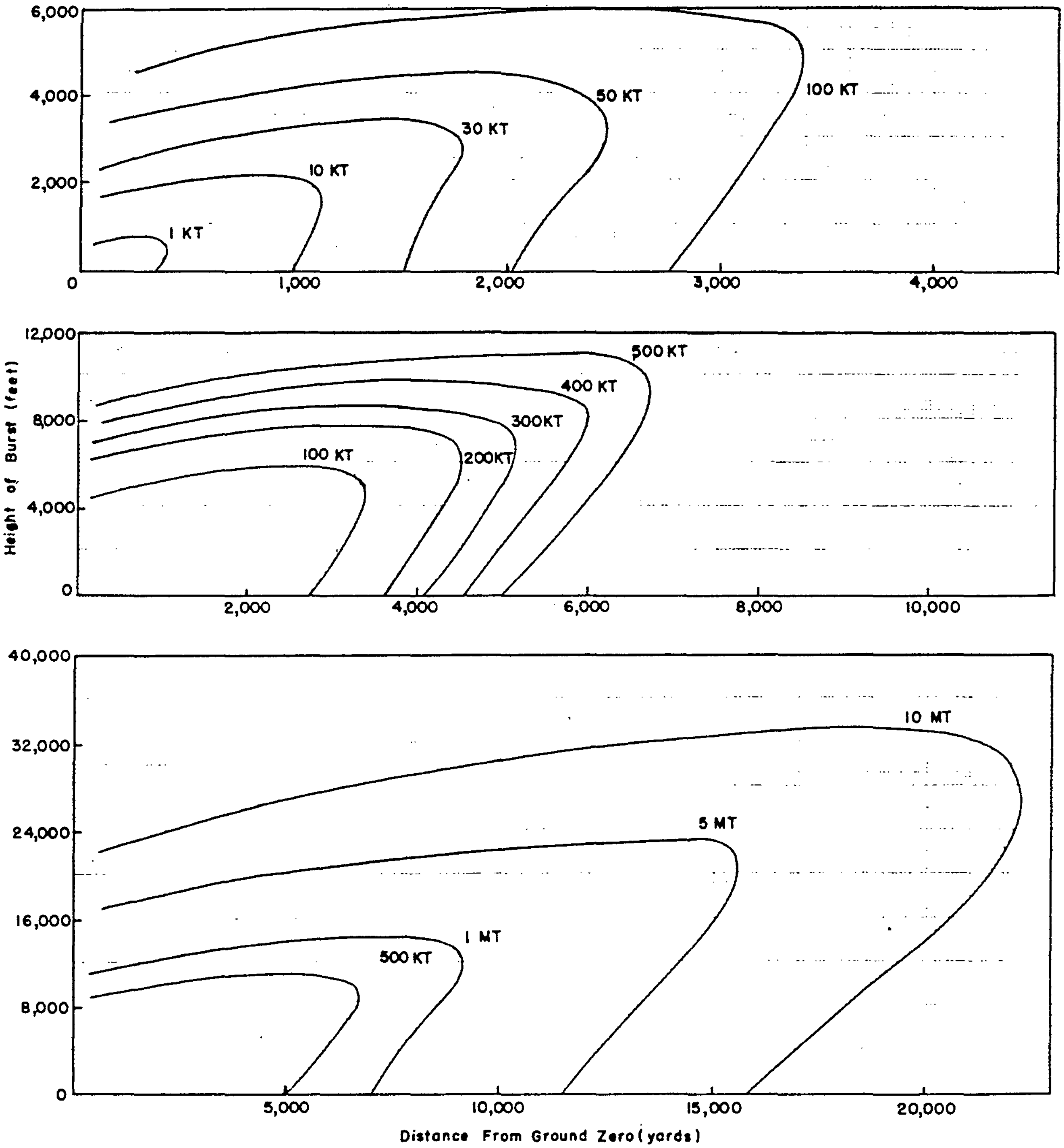

LIGHT DAMAGE TO TYPE II FOREST STANDS
AS A FUNCTION OF HEIGHT OF BURST AND GROUND RANGE

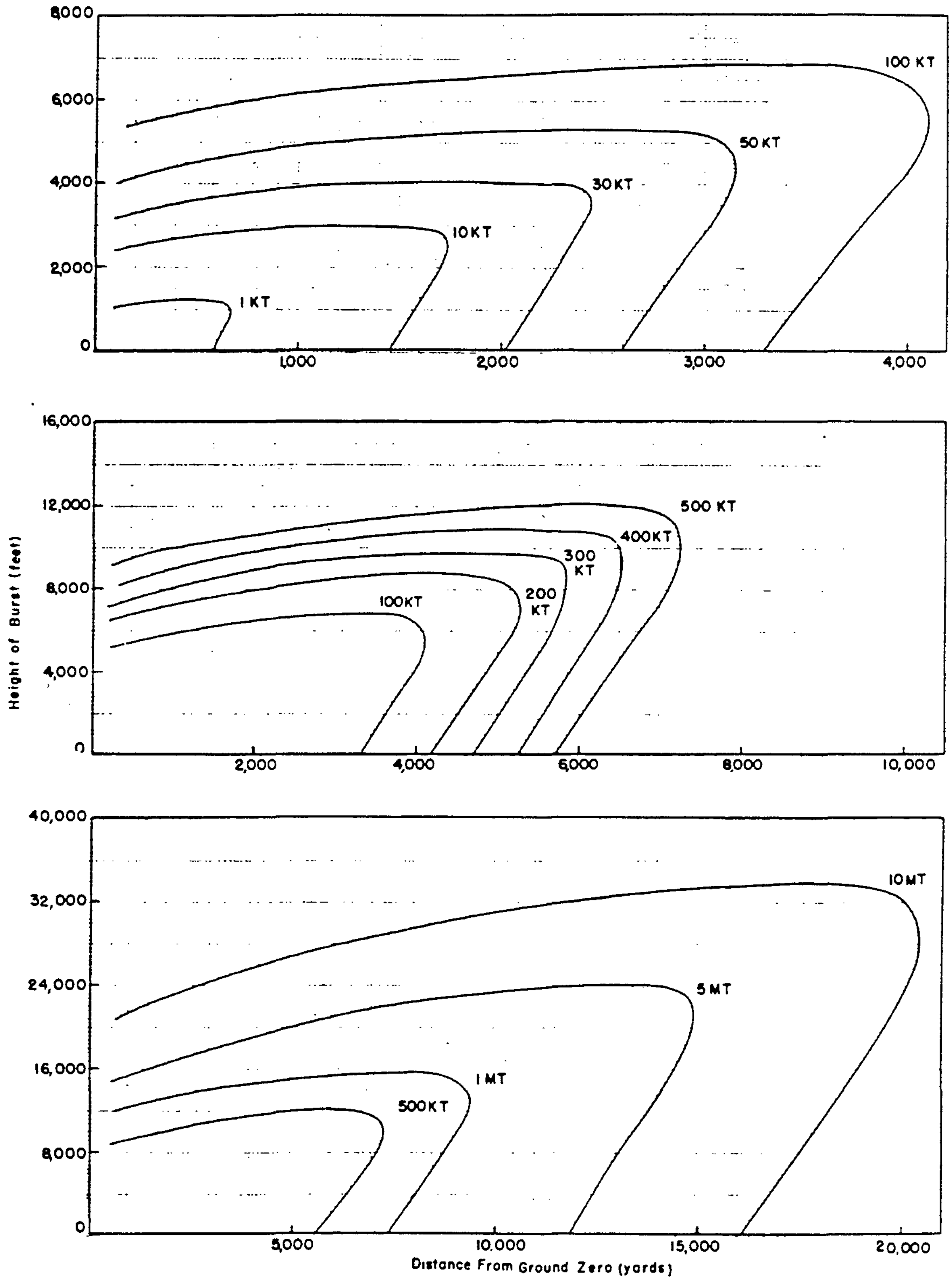

LIGHT DAMAGE TO TYPE III FOREST STANDS
AS A FUNCTION OF HEIGHT OF BURST AND GROUND RANGE

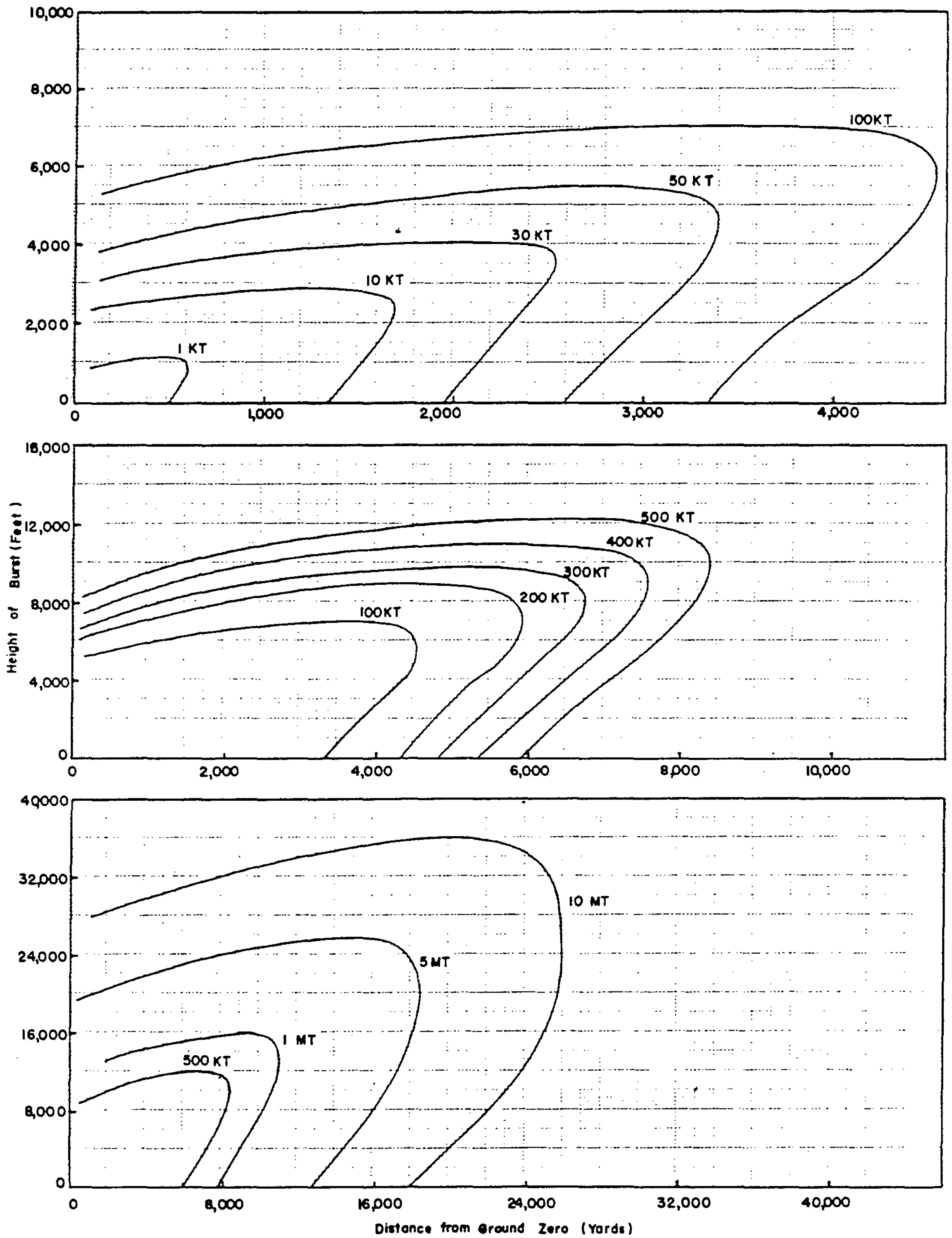

BLANK

WILDLAND KINDLING FUEL IGNITION REQUIREMENTS

The curves of figure 11–7 are presented for various classes of kindling fuels described in table 11–3.

Scaling. To find minimum radiant exposures for another yield W, multiply the exposures read from figure 11–7 by $W^{1/8}$.

Reliability. Based upon observed results of limited full-scale tests and extensive laboratory experiments. The results are not considered reliable in the megaton range.

Related material.

See paragraphs 11.3*b* and 11.3*d*, and table 11–3.

See also figures 11–1 through 11–6 for air blast damage to forest stands.

MINIMUM RADIANT EXPOSURE FOR IGNITION OF WILDLAND KINDLING FUELS BY CLASS SCALED TO 1KT

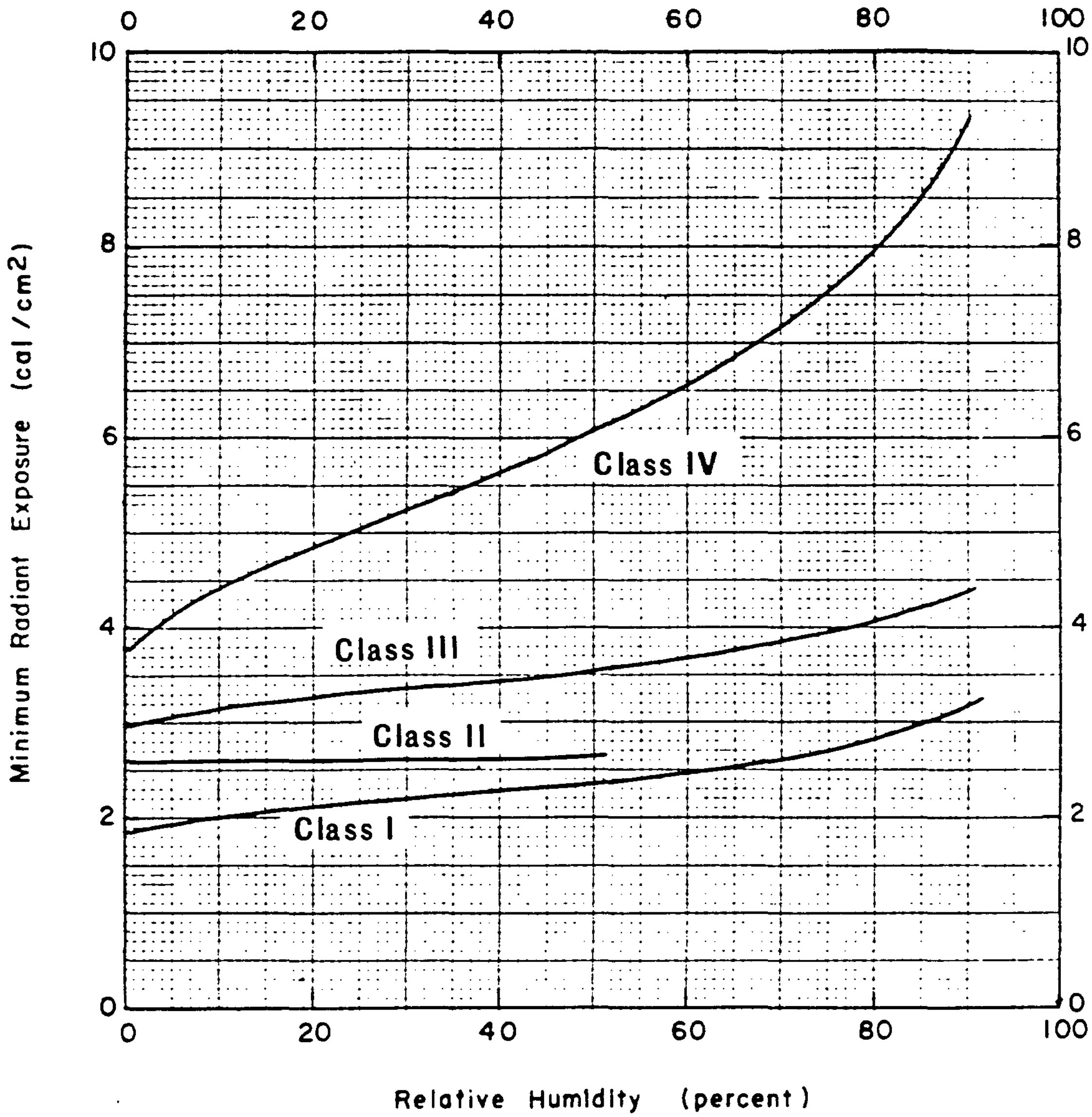

BLANK

12
Misc.

SECTION XII
MISCELLANEOUS RADIATION DAMAGE CRITERIA

12.1 Fire in Urban Areas

a. General. The employment of an air burst weapon over urban areas may produce, in addition to blast damage, mass fires which under proper conditions materially increase the degree and extent of damage. The behavior of such fires, whether they are of primary or secondary origin, follows the pattern of fires in forest and wildland areas. The burning potential for urban areas varies with weather conditions in much the same manner as for wildlands; however, the fire season as such is not as pronounced as in wildlands. During those seasons when weather conditions may reduce exterior potentials to zero, dwellings are usually heated, so that interior fuels are dried out. Fire incidence and subsequent fire buildup depend also upon the amount and distribution of flammable material used in interior furnishing and building construction, the incidence of interior kindling fuels, and the relative cleanliness of the living habits of the population.

b. Ignition Points. A survey of metropolitan areas in the United States indicates that the incidence of exterior ignition points can be correlated with urban land use. Table 12–1 presents a relative tabulation based on exterior kindling fuels. Newspapers and other paper products account for 70 percent of the total, while dry grass and leaves account for another 10 percent in residential areas. Most other exterior kindling fuels are present in small percentages or require radiant exposures in excess of 10 cal/cm² for ignition. Weathered and badly checked fences and building exteriors which contain appreciable dry rot constitute an ignition hazard. The tabulation presented in table 12–1 is not representative of European cities and other areas where fuel is at a premium or where extensive use is made of stone, brick, masonry, and heavy timber construction. Multi-story buildings and narrow streets reduce both interior and exterior primary ignitions, since such ignitions are proportional to the amount of sky seen from the location of the probable ignition point.

Table 12–1. Relative Incidence of Ignitions in Metropolitan Areas of the United States by Land Use (Based on Exterior Kindling Fuels)

Land use	Relative incidence
Downtown retail	1. 0
Large manufacturing*	1. 4
Good residential	1. 6
Small manufacturing	3. 8
Poor residential	5. 2
Neighborhood retail	5. 5
Waterfront areas	8. 0
Slum residential	11. 7
Wholesale	15. 1

*May be likened to a typical fixed military installation in the Z. I.

c. Humidity Effects. Since paper is the major exterior kindling fuel and is also an important interior fuel, the extent of ignitions may be estimated from the minimum radiant exposure requirements for this material (fig. 12–1). Thin exterior kindling fuels respond to hourly changes in relative humidity; however, fire buildup and subsequent fire behavior are best estimated from the average daytime relative humidity. Maximum fire effects occur during daily periods of lowest relative humidity, usually mid-afternoon. Guides for estimating urban burning potentials are given in figures 12–2 and 12–3. Where central heating of dwellings is a common practice, interiors are much drier than would be indicated by exterior relative humidities and temperatures. Based on United States experience, interior heating becomes an important factor when the maximum daily temperature drops below 70° F. Where fuel is scarce or expensive, this temperature may drop to 60° F., or even lower.

d. Fire Spread. The rate of fire buildup in urban areas is expected to be slower than for wildlands. The time to maximum fire intensity is less for the relatively high ignition incidence areas of table 12–1 than for those of lower ignition incidence. Aside from weather conditions, the principal factors which influence fire spread are the continuity, size and combustibility of buildings, fuel value of building contents, and topography. When strong convective action develops and spotting is frequent, the flammability of roof material is an important factor in spread. Spread of the fire front generally occurs by radiation from adjacent buildings; hence, fire stops only when the building spacing becomes great enough to reduce this radiation level below a critical value. This critical spacing is greater for multi-story buildings and varies with building combustibility, but on the average is about 50 to 100 feet.

12.2 Nuclear Radiation Damage

a. Neutron Irradiation.

(1) *Free air neutron flux.* The curves in figure 12–4 show the number of fast neutrons per square centimeter expected per kiloton of yield at various horizontal distances from typical airburst fission weapons detonated at altitudes up to 100,000 feet MSL. It is believed that these curves will give results correct within a factor of five.

(2) *Permanent damage.* Except for photographic film, which is clouded by neutron interaction with particles in the emulsion, and for electronic equipment which utilizes transistors, no permanent damage to equipment results from neutron irradiation. There is evidence that exposure to a neutron flux in excess of 10^{11} neutrons per square centimeter permanently alters the characteristics of transistors. However, any electronic equipment exposed to this flux of neutrons from a nuclear weapon detonation is likely to be severely damaged or destroyed by other effects. Discoloration of glass by neutrons does not occur for fluxes less than about 10^{18} neutrons per square centimeter, and thus can be disregarded as a significant effect.

(3) *Induced activity.* If the neutron flux is sufficiently high, a certain amount of neutron induced gamma activity results for most articles made of steel, due to the manganese which is usually present in commercial steels. The induced activity presents no personnel hazard except for articles exposed within or almost within the fireball, and even then the activity decays so rapidly as to be negligible less than a day after exposure. Significant neutron induced beta activity results in articles made of brass or other copper alloys, if exposed in or near the fireball. The personnel hazard is negligible unless the articles are handled very soon after the detonation. Radioactive decay reduces the activity to negligible levels within a few days.

b. Gamma Radiation. In general, massive quantities of gamma radiation are required to produce any damage to materials, so that damage by some other weapon phenomenon is nearly always more significant. Gamma radiation in excess of 10,000 roentgens can cause deterioration of rubber and other polymers as evidenced by a decrease in breaking strength. Exposure of glass to very high quantities of gamma radiation can produce discoloration. The intensity of radiation required is so great that this may be disregarded as a significant effect. Gamma rays, unlike neutrons, induce negligible radioactivity in materials; therefore, no residual radiation hazard is caused by initial gamma radiation.

c. Electromagnetic Radiation. A large electrical signal is produced by a nuclear weapon detonation. The signal consists of a rather sharp transient signal with a strong frequency component in the neighborhood of 15 kilocycles. Field strengths greater than 1 volt per meter have been detected from megaton yield weapons at a distance of about 2,000 miles. Electronic equipment which responds to rapid, short duration transients can be expected to be actuated by pickup of this electrical noise.

12.3 Thermal Damage to Various Materials

In table 12–2 the critical radiant exposures for specified damage to various materials are shown for three weapon yields. The values presented for fabrics apply for an ambient relative humidity of 65 percent and an ambient temperature of 20° C. For extremely dry conditions the values shown for fabrics should be reduced by 20 percent. For extremely high relative humidities, near 100 percent (at 20° C), the values for fabrics should be increased by 25 percent. If the fabrics are watersoaked, the critical radiant exposures should be increased by 300 percent.

Table 12-2. Critical Radiant Exposure Values for Various Materials

Uniforms	Color	Weight (oz/yd^2)	Damage	Critical radiant exposure Q_c (cal/sq cm) 1 KT	100 KT	10 MT
Army						
Cotton twill (fatigue)	Green	8	Scorched	3	5	9
			Destroyed	8	14	25
Wool serge (winter service)	OD	9	Scorched	3	6	10
			Destroyed	21	37	66
Wool flannel	OD	11	Scorched	3	5	8
			Destroyed	20	40	70
Wool tropical worsted	Khaki	11	Scorched	6	9	13
			Destroyed	13	20	30
Cotton twill shirt and trousers (summer)	Khaki	6	Scorched	4	6	11
			Destroyed	18	31	56
Navy						
Cotton twill (working)	Khaki	8	Scorched	3	5	8
			Destroyed	15	26	46
Cotton denim (dungaree)	Blue	9	Nap Scorched	6	10	17
			Destroyed	7	13	23
Cotton chambray shirting (working)	Blue	3	Scorched	3	6	11
			Destroyed	7	13	22
Cotton twill (white uniform)	White	8	Scorched	4	8	14
			Destroyed	34	60	109
Wool, Melton, (dress blues)	Blue	16	Scorched	1	16	13
			Destroyed	9	18	28
Wool, Kersey (overcoat)	Blue	30	Scorched	1	2	3
			Destroyed	37	65	110
Wool, serge (officer's uniform)	Blue	14	Scorched	5	9	16
			Destroyed	11	21	37
Wool, tropical worsted (officer's uniform)	Khaki	11	Scorched	5	9	16
			Destroyed	11	20	37
Vinyl resin, combined (rain)	Black	13	Scorched	1	1	2
			Destroyed	5	6	8
Marine Corps						
Cotton poplin shirting	OD	6	Scorched	3	6	10
			Destroyed	10	18	32
Wool elastique (winter)	Green	16	Scorched	2	4	7
			Destroyed	25	45	80
		21	Scorched	5	8	15
			Destroyed	30	54	95
Wool, Kersey (winter)	Green	16	Scorched	2	2	6
			Destroyed	27	48	85
Wool serge	Green	12	Scorched	2	3	6
			Destroyed	16	28	50
Air Force						
Cotton twill shirt (tropical)	Khaki	5	Scorched	6	10	19
			Destroyed	9	15	27
Wool gabardine shirt	Gray	8	Scorched	10	17	28
			Destroyed	14	22	37
Wool gabardine shirt	Blue	8	Scorched	1	2	4
			Destroyed	8	14	25
Nylon—flying jacket	OD	5	Scorched	2	3	6
			Destroyed	7	13	23

Table 12–2. Critical Radiant Exposure Values for Various Materials—Continued

Material	Damage	Critical radiant exposure Q_c (cal/sq cm) 1 KT	100 KT	10 MT
Tent material:				
Canvas, white, 12 oz/yd², untreated	Destroyed	12	21	37
Canvas, OD, 12 oz/yd², flame-proofed	Destroyed	5	9	17
Packaging materials:				
Fibreboard, V2S, BT 350 psi, laminated	Flames during exposure	9	16	29
Fibreboard, V3S, BT 275 psi, laminated	Flames during exposure	7	13	23
Fibreboard, V3C, BT 350 psi, corrugated	Flames during exposure	6	11	19
Fibreboard, W5C, BT 200 psi, corrugated	Flames during exposure	5	10	18
Plywood, douglas fir (¼ in.)	Flames during exposure	9	16	20
Airship material, aluminized, N–113A100, 16 oz/yd²	Aluminum surface discolored	20	35	61
	Aluminum surface destroyed	24	43	75
	Fabric destroyed	27	47	82
Airship material, aluminized, N–113A70, 19.4 oz/yd²	Aluminum surface discolored	10	18	31
	Aluminum surface destroyed	15	27	44
	Fabric destroyed	20	35	61
Airship material, aluminized, N–128A170, 8 oz/yd²	Delaminates	2	4	7
	Fabric destroyed	5	10	17
Doped fabrics (used on some aircraft control surfaces):				
Cellulose nitrate covered with 0.0015″ thick aluminum foil.	Sporadic flaming	60	80	140
Cellulose nitrate, aluminized	Persistent flaming	5	6	10
Plastics:				
Laminated methyl methacrylate	Surface melts	73	120	230
USAF window plastic (½ in.)	Bubbling	240	430	750
Vinylite (opaque), ⅛ in. thick	Dense smoking	3	4	6
	Flaming	20	20	25
Sand:				
Coral	Explosion*	15	27	47
Siliceous	Explosion*	11	19	35
Sandbags: Cotton canvas, dry, filled	Failure	10	18	32
Wood, white pine	0.1 mm depth char	10	18	32
White pine, given protective coating	0.1 mm depth char	40	71	126
Construction materials:				
Roll roofing, mineral surface	Surface melts	8	14	25
	Flaming during exposure	22	40	71
Roll roofing, smooth surface	Surface melts	4	7	12
	Flaming during exposure	9	16	29

*"Popcorning."

It should be emphasized that the values in table 12–2 for uniforms refer to damage to the material itself and are not applicable for predicting skin burns under uniforms.

The above discussion does not include the damage to materials when they come in contact with or are enveloped by the fireball. The heat input under these conditions is many orders of magnitude higher than the cases just discussed. Several of the variables considered as influential factors in determining the amount of surface material lost by an object exposed within a fireball include: type of material, surface curvature, orientation, thermal attenuation by the metallic vapors given off by the object, and spallation.

Figures 12–5A and 12–5B give the material loss from spheres of various materials due to ablation or scaling off of the surface material from contact with or envelopment by the fireball. Data for three types of 10-inch diameter spheres are shown; namely, solid steel, solid aluminum, and solid aluminum with small cylindrical wells filled with ceramic inserts. The one curve in figure 12–5A represents all three types.

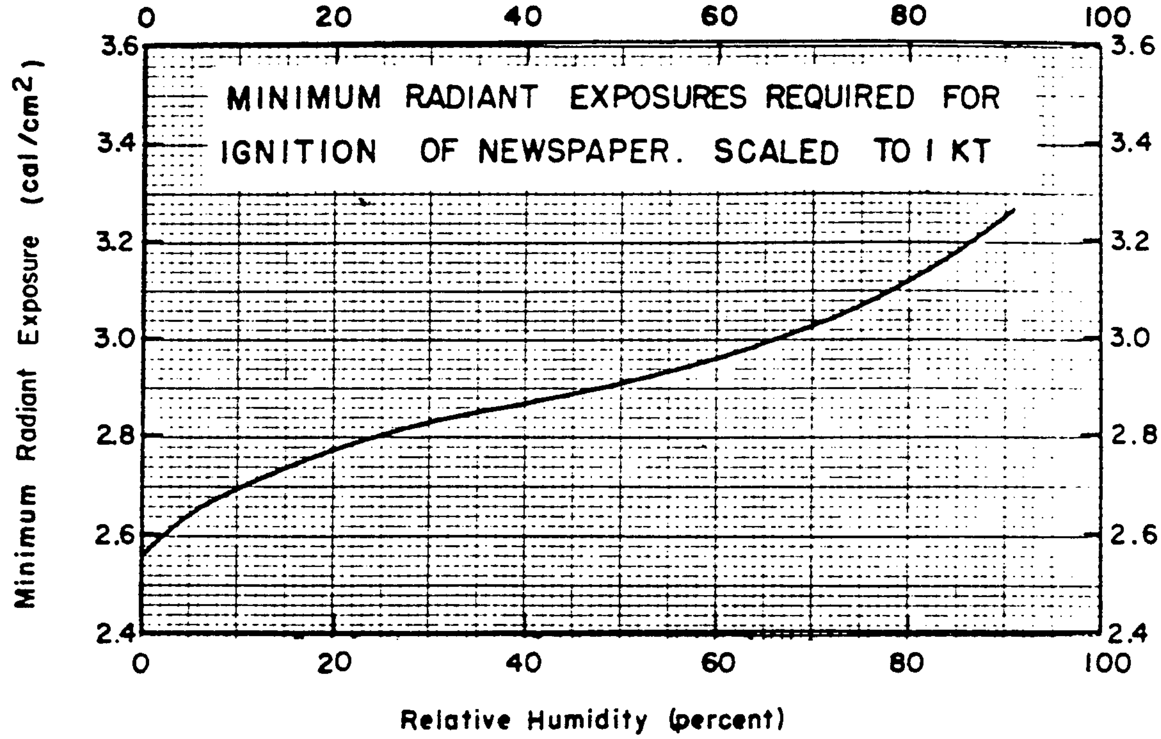

NEWSPAPER IGNITION REQUIREMENTS

Scaling. To find minimum radiant exposures for another yield W at the same relative humidity, multiply the exposures read from figure 12-1 by $W^{1/8}$.

Reliability. Based upon limited empirical data.

Related material.

See paragraphs 12.1*b* and *c*.

See also figure 11-1 for radiant exposures required for wildland kindling fuel ignition.

BURNING POTENTIAL FOR URBAN AREAS
(CENTRAL HEATING NOT IN USE)

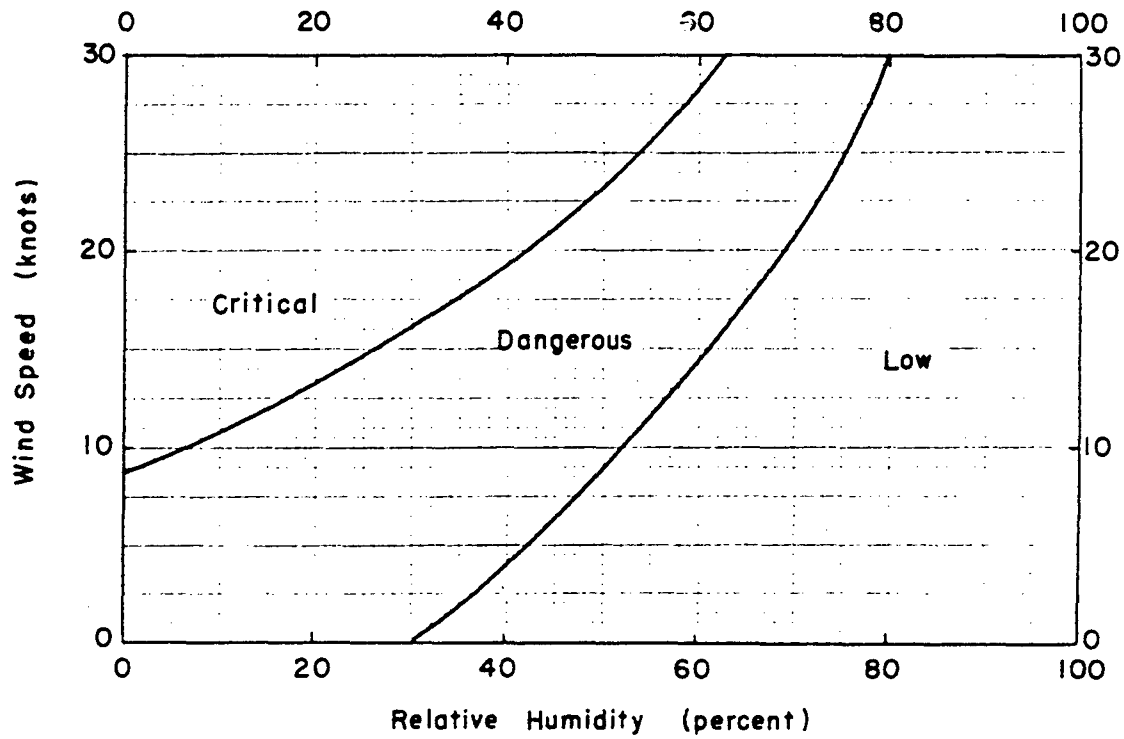

BURNING POTENTIAL FOR URBAN AREAS (CENTRAL HEATING NOT IN USE)

Figure 12-2 represents approximate values of wind speed and average daytime relative humidity conditions corresponding to low, dangerous and critical burning potentials according to the following definitions:

Low. Slow burning fires; fire can be controlled at will. Control action can be on unit structure basis.

Dangerous. Fires burn rapidly; individual building fires combine to form an area fire. Organized action needed to confine fire to area originally ignited.

Critical. Rapid buildup into conflagration-type fires,. high probability of fire storm, spotting frequent and severe. Requires evacuation of fire fighting equipment and personnel; control action effective only at critical breaks in building continuity or density.

Related material.

See paragraphs 12.1*c* and *d*.

See also figure 12-3.

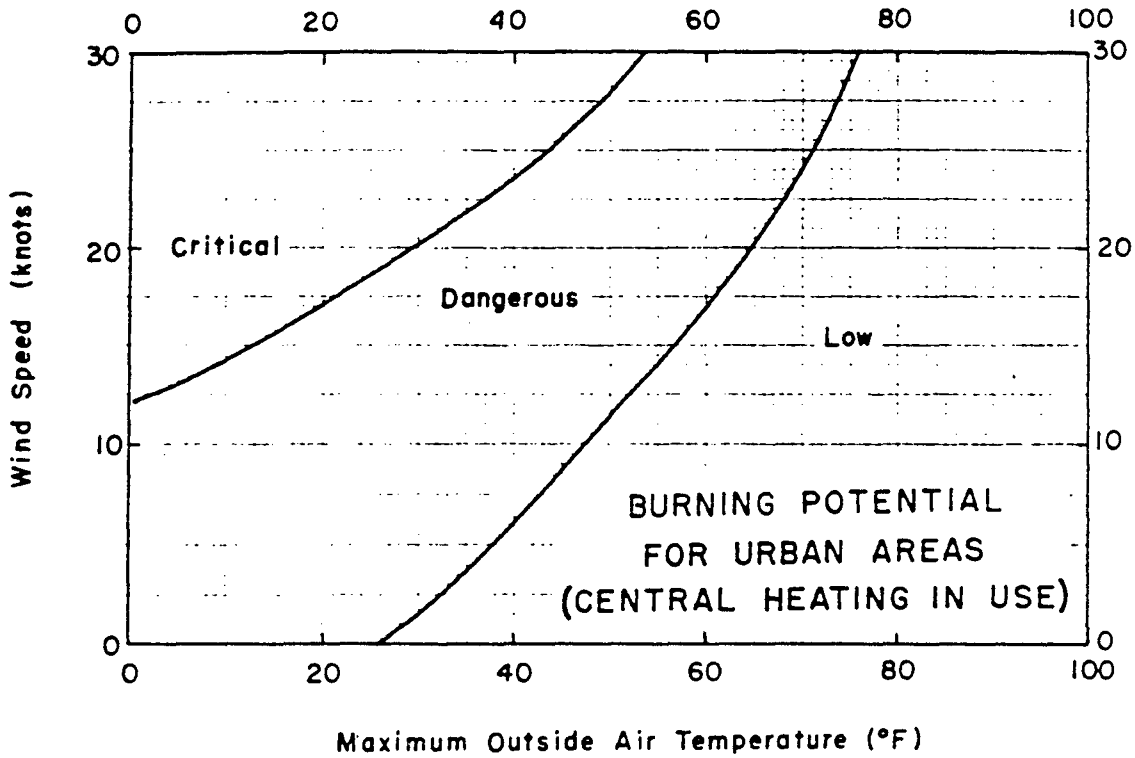

BURNING POTENTIAL FOR URBAN AREAS (CENTRAL HEATING IN USE)

Figure 12–3 shows approximate values of wind speed and maximum outside air temperature conditions corresponding to low, dangerous and critical burning potentials. These burning potentials are defined in the same way as those in figure 12–2.

Note. Temperature must have been below value read on abscissa for at least four consecutive days, with no rain in the previous 24 hours. Snow may be disregarded.

Related material.

See paragraphs 12.1*c* and *d*.
See also figure 12–2.

NEUTRON FLUX FOR A TYPICAL FISSION WEAPON

The curves in figure 12-4 show the number of neutrons per square centimeter per kiloton at various horizontal ranges for different heights of burst of typical fission weapons. The curves are for standard atmospheric conditions. Data are presented in AFSWP-1100, published with a higher security classification, from which neutron flux for specific weapons may be computed.

Scaling. At a given horizontal range and altitude, the neutron flux is proportional to the yield of the weapon.

Example.

Given: A 100 KT air burst at 20,000 feet.

Find: The number of neutrons per square centimeter at a horizontal range of 3,400 yards.

Solution: Reading directly from figure 12-4, the neutron flux from a 1 KT weapon is 10^8 neutrons per cm^2. Since this is a 100 KT burst, 100×10^8 neutrons per $cm^2 =$ 10^{10} neutrons per square centimeter. *Answer.*

Reliability. Neutron flux is dependent upon weapon design. For most fission weapons the curves of figure 12-4 are considered reliable within a factor of 5.

NEUTRON FLUX FROM TYPICAL FISSION WEAPONS
FOR A 1KT BURST IN A STANDARD ATMOSPHERE
AS A FUNCTION OF BURST ALTITUDE AND HORIZONTAL RANGE

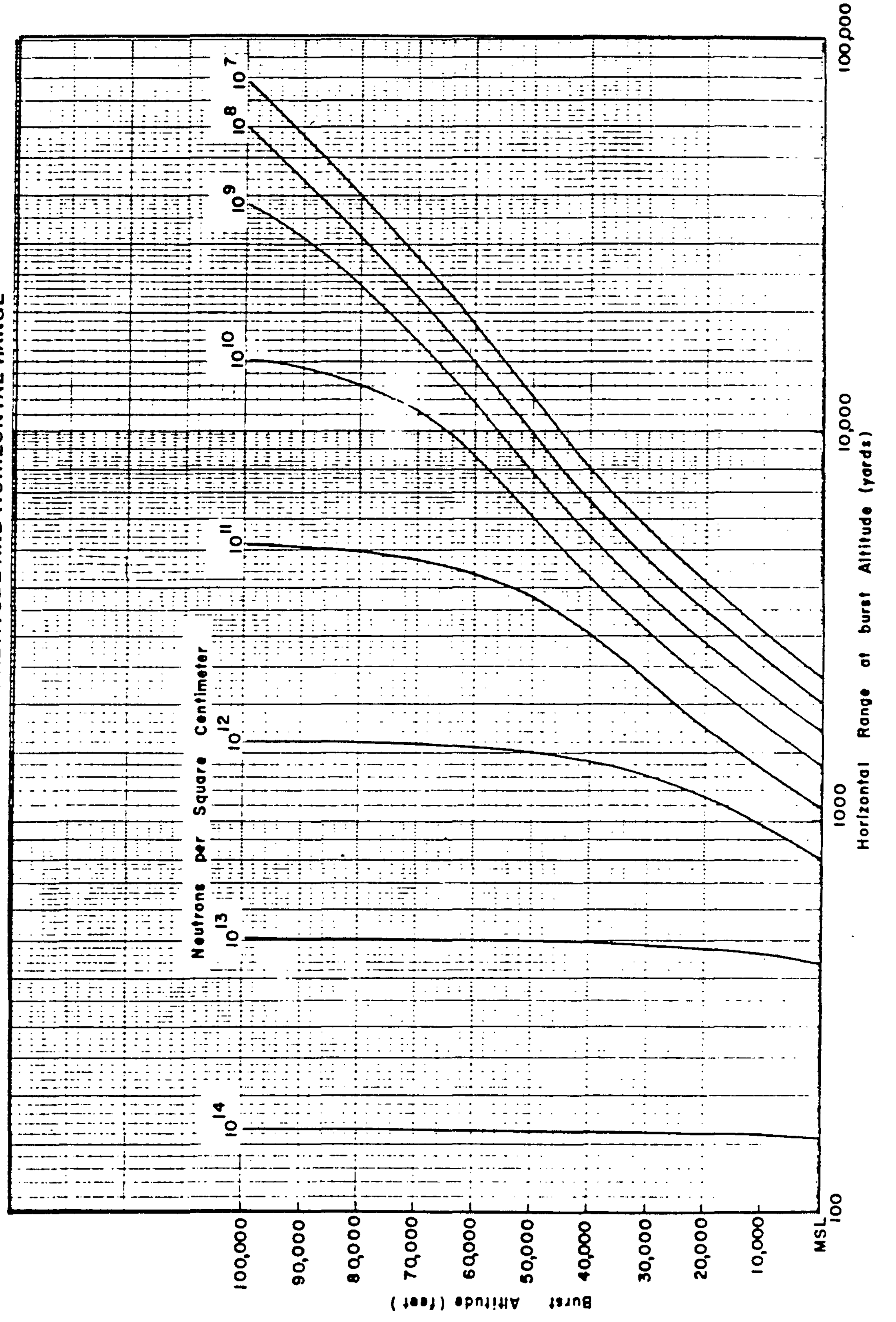

[redacted]

A

WEIGHT LOSS WITH DISTANCE FROM A 23 KT BURST
FOR ALUMINUM, STEEL, CERAMIC INSERT SPHERES

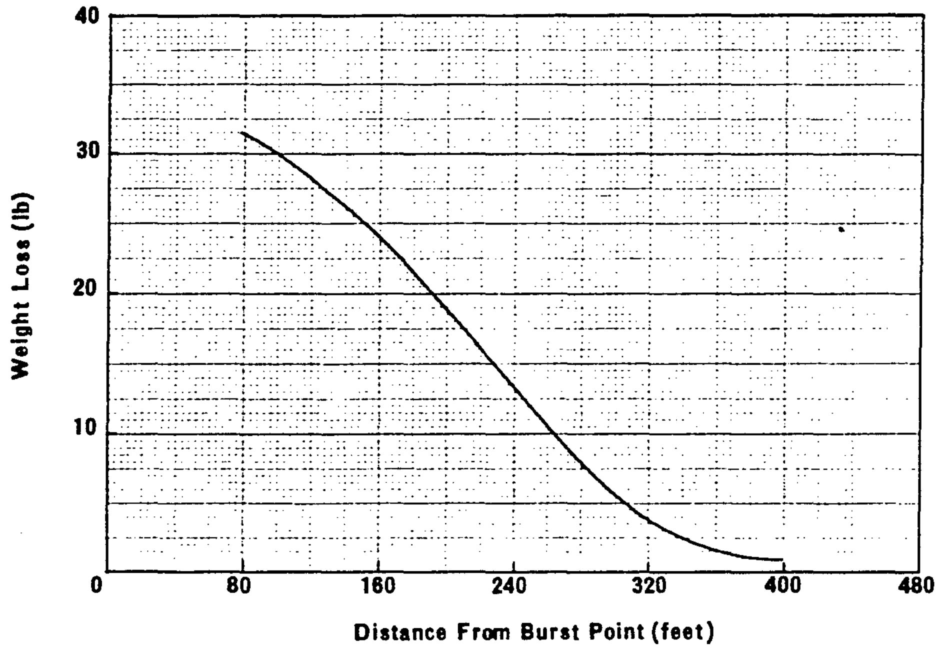

B

REDUCTION OF SPHERE RADIUS WITH DISTANCE FROM A 23 KT BURST
FOR ALUMINUM, STEEL, CERAMIC INSERT SPHERES

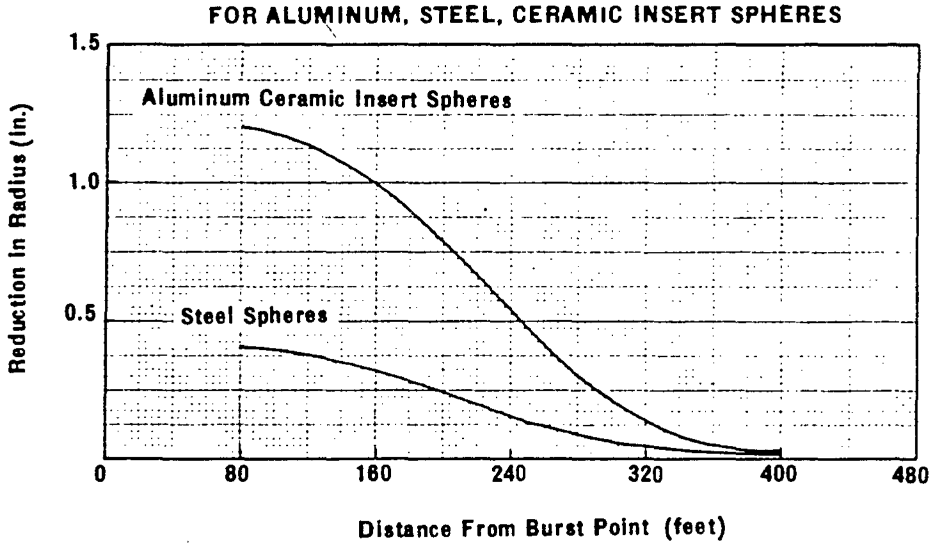

[redacted]

I
Suppl.
Blast Data

APPENDIX I
SUPPLEMENTARY BLAST DATA

I.1 Shock Wave Propagation in Free Air

a. Rankine-Hugoniot Relationships. All of the peak values of the various blast wave characteristics are uniquely related at the shock front for ideal blast waves in free air by the Rankine-Hugoniot equations which are given below:

Shock Velocity—

$$U=C\left(1+\frac{6}{7}\frac{\Delta p}{p}\right)^{1/2},$$

Particle Velocity—

$$u=\frac{5}{7}C\frac{\Delta p}{p}\left(1+\frac{6}{7}\frac{\Delta p}{p}\right)^{-1/2},$$

Peak Density—

$$\rho'=\rho\left[\frac{1+\frac{6}{7}\frac{\Delta p}{p}}{1+\frac{1}{7}\frac{\Delta p}{p}}\right],$$

where ρ=ambient density (slugs/ft^3) ahead of the shock front (0.00238 slugs/ft^3 at sea level),

p=ambient pressure (psi) ahead of the shock front (14.7 psi at sea level),

C=ambient sound velocity (ft/sec) ahead of the shock front (1,116 ft/second at sea level),

ρ'=peak density at the shock front (slugs/ft^3).

Δp=peak overpressure at the shock front (psi),

U=shock velocity (ft/sec), and

u=peak particle velocity (ft/sec) (wind velocity at the shock front).

Values of shock velocity as a function of distance in free air are given in figure I–1. It should be noted that the time of arrival curve, figure 2–2, may be derived from the shock velocity curve of figure I–1 by a successive integration procedure. Values of particle velocity as a function of distance are given in figure I–2.

The relationship between peak dynamic pressure and peak overpressure at the shock front is:

$$q=\frac{5}{2}\frac{(\Delta p)^2}{(7p+\Delta p)},$$

where q, the peak dynamic pressure (psi), is defined as

$$q=\frac{1}{2}\left(\frac{\rho' u^2}{144}\right).$$

The relationship between peak particle velocity and shock velocity is:

$$u=\frac{\frac{5}{7}(U)\frac{\Delta p}{p}}{1+\frac{6}{7}\frac{\Delta p}{p}},$$

where U, u, Δp and p are as previously defined.

The relationship between sound velocity, pressure and density in air is:

$$C=14.2\left(\frac{p}{\rho}\right)^{1/2}=49\ T^{1/2},$$

where C=sound velocity in feet/second.

p=pressure in pounds/sq inch.

ρ=density in slugs/cu ft, and

T=degrees Rankine (degrees F+459).

The relationship between the instantaneous value of the peak overpressure reflected from a surface and the peak overpressure incident upon that surface at a 90° angle is:

$$\Delta p_r=2\Delta p\left(\frac{7p+4\Delta p}{7p+\Delta p}\right),$$

where Δp_r=reflected peak overpressure, and Δp=incident overpressure.

A number of these relationships are shown in figure I–3 as a function of peak overpressure for a sea level atmosphere. Values for many of the variables are given in appendix II.

b. Overpressure Positive Phase Impulse and Wave Form in Free Air. The overpressure positive phase impulse (I_p) is the area under the positive portion of the pressure-time curve, or:

$$I_p=\int_{t=0}^{t=t^+}\Delta p(t)\,dt,$$

where $\Delta p(t)$ is the overpressure as a function of time between $t=0$, the time of arrival of the blast wave at a given range, and $t=t^+$, the end of the positive phase. Values of overpressure positive phase impulse as a function of distance in free air are given in figure I–4. The positive phase pressure-time curve showing the exponential decay of overpressure at a given distance will vary, depending on the peak overpressure and time of duration for a given yield at that distance. A comparison of decay rates for various values of peak overpressure is shown in figure I–5 in terms of normalized coordinates; i. e., the values are expressed as fractions of the peak or maximum values. The use of normalized coordinates permits a comparison on a common basis of the variation of phenomena which differ in absolute magnitude. Where pressures are less than 25 psi, the variation of overpressure with time behind the shock front may be represented by the following semi-empirical equation:

$$\Delta p(t)=\Delta p(1-t/t^+)\ e^{-t/t^+}$$

where $\Delta p(t)$ is the overpressure at any time t, Δp is the peak overpressure, and t^+ is the positive phase duration of the blast wave. The wave form which this exponential equation describes is shown in figure I–6 in terms of normalized coordinates to permit comparison with the dynamic pressure wave form.

c. Dynamic Pressure Impulse and Wave Form. The dynamic pressure impulse is the area under the dynamic pressure-time curve. It may be determined from the following expression:

$$I_q=\int_{t=0}^{t=t_q^+} q(t)dt.$$

This expression is the integral of the curve representing the variation of dynamic pressure behind the shock front as a function of time between $t=0$, the time of arrival of the blast wave, and $t=t_q^+$, the end of the dynamic pressure positive phase. Assuming t_q^+ to be the same as t^+, the overpressure positive phase duration, will not introduce serious error. Values of dynamic pressure impulse as a function of distance in free air are given in figure I–7. The rate of decay varies in an exponential fashion, depending upon the peak dynamic pressure and time of duration. A comparison of decay rates for various values of peak dynamic pressure is shown in figure I–8 in terms of normalized coordinates. Where dynamic pressures are less than 12 psi, the variation of dynamic pressure with time behind the shock front may be represented by the following approximate equation:

$$q(t)=q\ (1-t/t^+)^2\ e^{-2t/t^+},$$

where $q(t)$ is the value of dynamic pressure at any time t, q is the peak dynamic pressure at the shock front, and t^+ is the overpressure positive phase duration. This equation is derived from the expression given in *b* above, with the shock relations given in *a* above, and then simplifying the resulting expression. The positive phase duration of overpressure is used in the above equation instead of positive phase duration of dynamic pressure, since the difference is small and does not affect the total dynamic pressure impulse in a significant manner. The wave form described by the above equation is also shown in figure I–6.

I.2 Blast Wave Perturbations

a. Overpressure Positive Phase Impulse and Wave Forms. The variation of overpressure positive phase impulse with range and height of burst is shown in figures I–9A and I–9B for 1 KT in a sea level homogeneous atmosphere. Figure I–9A applies to good surface conditions where thermal and mechanical effects are minimized and near ideal wave forms may be expected. Figure I–9B applies to average surface conditions where non-ideal wave forms may be expected. It has been found convenient to divide the variations of wave forms into five major classifications, which are illustrated in figure I–10:

Type I. A relatively ideal wave form with a sharp rise to a peak value followed by a rapid exponential decay. Usually the peak pressure is rather high and the duration is rather short in comparison with later wave forms.

Type II. A wave form with two distinct peak values which becomes increasingly non-ideal with increasing range. Usually shock-type rises are evident at the closer ranges. However, as the distance from ground zero increases, the separation of the two peaks and the rise time for the main shock increase, while the first peak

FIGURE I-10

WAVE FORM CLASSIFICATION FOR PEAK OVERPRESSURE

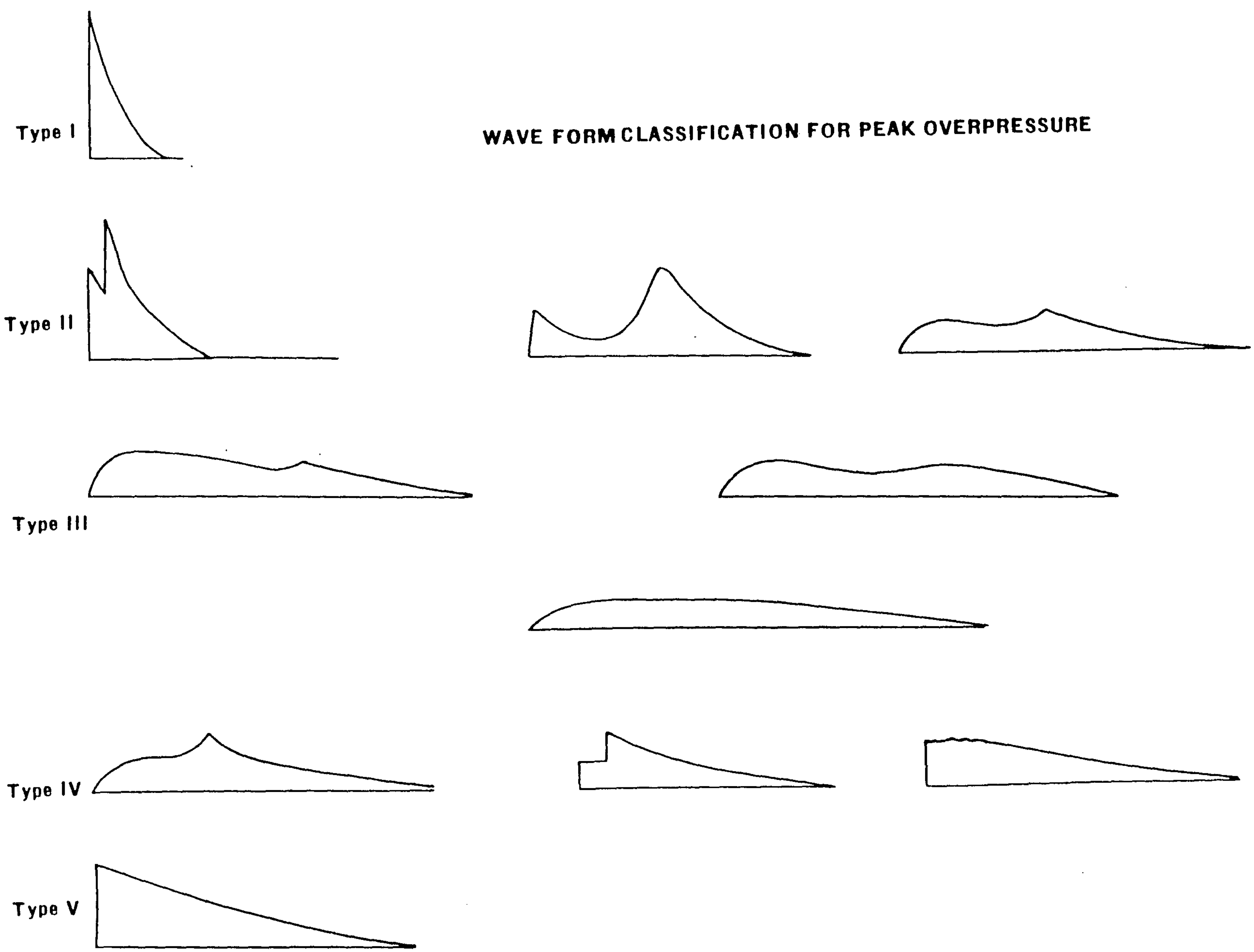

attenuates more rapidly than the second. At midrange, the wave form is characterized by a shock-type rise to a first low peak followed either by a plateau or a slow decay, with a longer rise to a higher second peak preceding a more rapid decay. As the ground range continues to increase, the first peak becomes round and the second peak attenuates more rapidly than the first. This wave form is typical of the early stages of development in the precursor cycle. (A detailed discussion of the precursor is given in par. 2.1*d*(4).)

Type III. A wave form whose peaks and valleys become poorly defined with increasing range. At the closer ranges the wave form shows a first large rounded maximum followed by a slow decay, then a later and smaller second peak. As the distance from ground zero increases, the first peak attenuates more rapidly than the second, so that the two peaks become comparable in magnitude, while the rise times become longer. The second peak disappears at the farther ranges, resulting in a low, rounded, flat-topped wave form with a long initial rise and a rather slow decay marked by considerable turbulence. This wave form is typical of strong precursor action.

Type IV. A wave form which progressively loses its non-classical characteristics with increasing range. At the closer ranges, the wave form shows a compression-type rise to a rounded plateau followed by a slow rise to a second higher peak. As the distance from ground zero increases, the rise times decrease, so that the front of the wave form develops a step-like appearance, and the time separation between the two peaks becomes less. At the farther ranges, the second peak overtakes the first peak to form an almost classical form with a sharp rise to a more or less level plateau, followed by an essentially regular decay. This wave form is typical of the "clean-up" portion of the precursor cycle.

Type V. A classical or ideal wave form with a sharp rise to a peak value followed by an exponential decay. The duration is rather long in comparison with the type I wave form and the rate of decay is slower.

The overpressure wave form types to be expected at a given ground range as a function of height of burst are shown in figure I–11. Since types II, III, and IV are characteristic of precursor action, the figure also delineates the precursor zone.

b. Dynamic Pressure Wave Forms. A tentative classification of the various dynamic pressure wave forms has been made. It is not possible to make a direct correlation of these with the five general types of overpressure wave forms due to the lack of experimental data for dynamic pressure, particularly in the close-in region. The classifications illustrated in figure I–12 are as follows:

Type A. A relatively ideal wave form, with a sharp rise to a peak value followed by a very rapid decay. The duration is usually rather short in comparison with later wave forms.

Type B. A double-peaked wave form with a shock-type initial rise in most cases. The second peak is larger at the closer ranges but becomes comparable in magnitude with the first as the distance from ground zero increases.

Type C. A transitional double-peaked wave form with longer initial rise time. Actual record traces have a very turbulent appearance. The second peak is smaller than the first and becomes somewhat indefinite with increasing range.

Type D. An essentially single-peaked form characterized by a low amplitude plateau with a slow, smooth rise at the closer ranges. Actual traces have a very turbulent appearance. As the distance from ground zero increases, the turbulence becomes less and the plateau develops a shock rise with a flat top or a slow steady increase to a second shock rise followed by a smooth decay. The initial disturbance at the front of the wave form eventually dies out at the farther ranges, leaving a smooth, clean record with a slight rounding after an initial shock-type rise.

Type E. A classical or ideal wave form with a sharp rise to a peak value followed by an exponential decay. The duration is rather long in comparison with type A wave forms and the rate of decay is slower.

It is not possible to draw a wave form-height of burst chart for dynamic pressures at this time due to the lack of experimental data.

I.3 Altitude Conversion of Air Blast Properties

a. General. The air blast parameter curves in this manual are presented for a 1 KT burst in a homogeneous sea level atmosphere. It is sometimes necessary to determine the magnitude of

FIGURE I-12

CONFIDENTIAL

WAVE FORM CLASSIFICATION FOR DYNAMIC PRESSURE

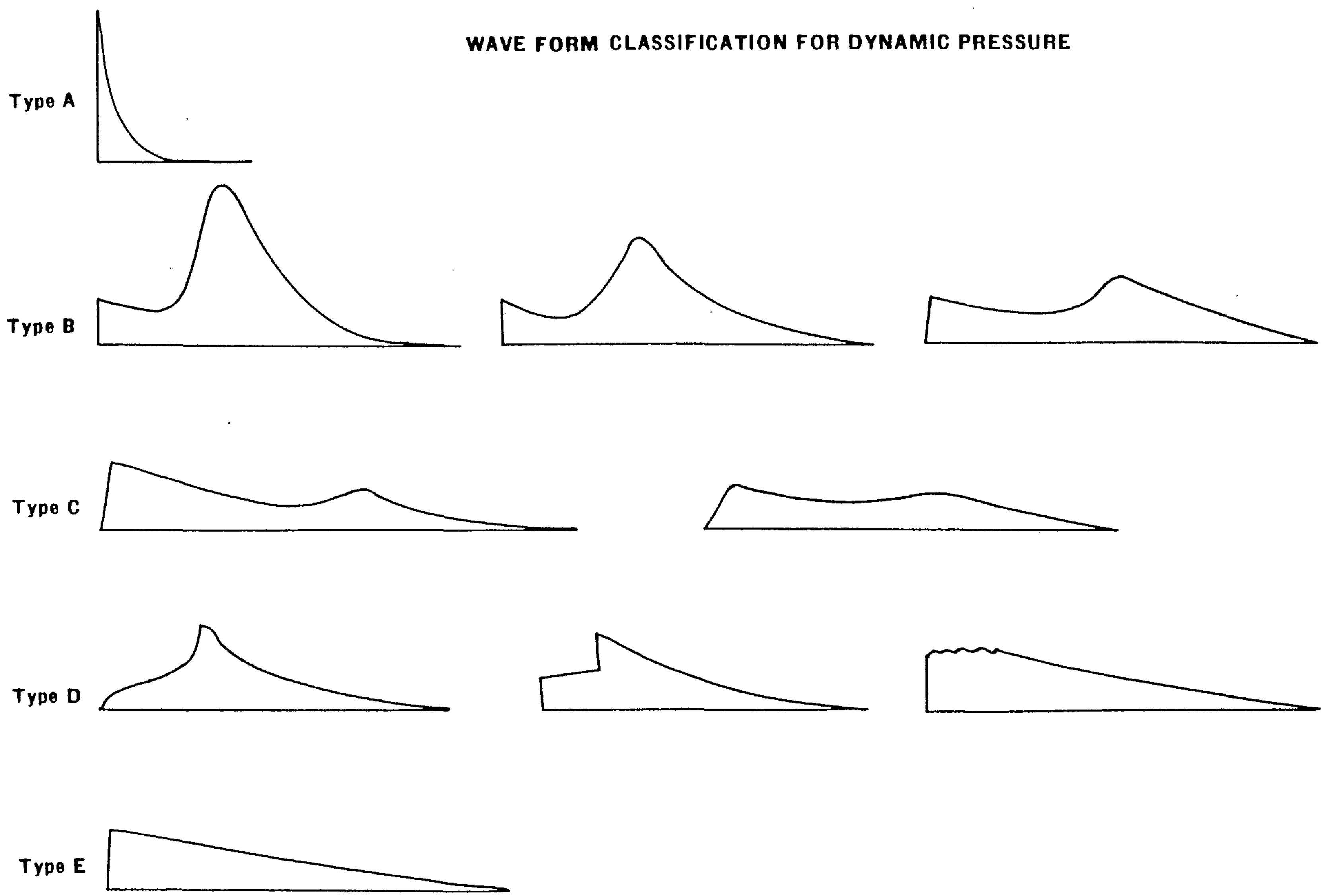

CONFIDENTIAL

the air blast parameters at an altitude other than sea level. When this is the case, the air blast parameters must be converted to reflect the fact that the ambient conditions existing at a particular altitude differ from those existing at sea level. Table II–1 shows how the ambient temperature, sound velocity, density and pressure vary with altitude under standard conditions. The values of these ambient parameters determine the rate of propagation of the blast wave resulting from the detonation of a particular yield and the magnitude of the air blast parameters at a given distance from the point of detonation.

As mentioned in section II, when targets are at mean sea level altitudes of 5,000 feet or less, the differences resulting from conversion of air blast parameters to target altitude are small and are usually of no practical importance. For targets at altitudes in excess of 5,000 feet, conversion of the air blast parameters should be made.

b. Conversion Procedure. An approximate method for relating the air blast parameter values occurring at a point in space at a given altitude, as the result of a nuclear burst at the same or a different altitude, to the blast parameter values of a 1 KT burst occurring in a homogeneous sea level atmosphere, and one which shows good agreement with full scale tests, is a method based on the work of R. G. Sachs. This method assumes that the blast wave propagates in a homogeneous atmosphere of ambient conditions corresponding to those existing at the altitude of the point in space under consideration, regardless of the burst altitude, and that the total energy available for blast is independent of altitude. Therefore, in terms of a similarity transformation, the dependence of pressure and density of the air in the blast wave on distance and time for one set of homogeneous ambient conditions may be obtained from the dependence of pressure and density in the blast wave on distance and time for another set of homogeneous ambient conditions by relating the dimensional scales by which pressure, density, distance, and time in each atmosphere are measured.

The following modified Sachs relations combine both the necessary yield scaling and altitude conversion to compute distance, shock arrival time, peak overpressure, peak dynamic pressure, positive phase duration, peak particle velocity, and peak density at a point in space at a given altitude and specific distance from a burst of yield, W, from the properties of a 1 KT burst in a standard sea level atmosphere:

$$d_z = d_o\, W^{1/3}\, S_d$$

$$t_z = t_o\, W^{1/3}\, S_t$$

$$\Delta p_z = \Delta p_o\, S_p$$

$$q_z = q_o\, S_p$$

$$t_z^+ = t_o^+\, W^{1/3}\, S_t$$

$$u_z = u_o \left(\frac{C_1}{C_o}\right)$$

$$\rho_z' = \rho_o' \left(\frac{\rho_1}{\rho_o}\right)$$

where:

$S_d = \left(\dfrac{p_o}{p_z}\right)^{1/3}$, a factor used to convert distance as measured in a sea level atmosphere to distance measured from the burst to a point at altitude.

$S_t = \dfrac{C_o}{C_z}\left(\dfrac{p_o}{p_z}\right)^{1/3}$, a factor used to convert time of shock arrival and positive phase duration, as measured in a sea level atmosphere, to time of shock arrival and positive phase duration as measured at a point at altitude, at a distance from the burst computed with the factor S_d.

$S_p = \left(\dfrac{p_z}{p_o}\right)$, a factor used to convert peak overpressure and peak dynamic pressure, as measured in a sea level atmosphere, to peak overpressure and peak dynamic pressure at a point at altitude and at a distance from the burst computed with the factor S_d.

p_o, C_o, and ρ_o = ambient pressure, speed of sound, and ambient density of the standard sea level atmosphere. (See appendix II.)

p_z, C_z, and ρ_z = ambient pressure, speed of sound, and ambient density of the atmosphere at the altitude or elevation of the point where blast parameters are to be determined (app. II).

d_o = distance in a sea level atmosphere from a 1 KT burst to a point where the blast parameters are as follows:

time of shock arrival	$=t_o$
peak overpressure	$=\Delta p_o$
peak dynamic pressure	$=q_o$
positive phase duration	$=t_o^+$
peak particle velocity	$=u_o$
peak density	$=\rho_o'$

d_s=distance from a burst of yield W to a point at altitude where the blast parameters are as follows:

time of shock arrival	$=t_s$
peak overpressure	$=\Delta p_s$
peak dynamic pressure	$=q_s$
positive phase duration	$=t_s^+$
peak particle velocity	$=u_s$
peak density	$=p'_s$

Figure I–13 presents values of the above altitude conversion factors S_p, S_d, S_t.

For *surface target* situations at elevations above 5,000 feet, obtain Δp_o, t_o, t_o^+ and q_o from figures 2–2 through 2–5 or figures 2–8 through 2–13. Compute other 1 KT sea level values for use in the above relations from the relationships given in paragraph I.1*a* or obtain from figure I–3.

For *airborne target* situations obtain t_o and t_o^+ from figures 2–2 and 2–4. Obtain Δp_o from figure I–14. Using this value of Δp_o, compute other 1 KT sea level values from the relationships given in paragraph I.1*a* or obtain from figure I–14. Figure I–14 presents higher values of free air peak overpressure for ranges beyond 1,000 feet in a sea level atmosphere than does figure 2–3. The data of figure I–14, when converted to altitude by the above procedure, have correlated well with airborne measurements at weapon effects tests.

I.4 Blast Wave Reflection

As previously discussed in Section 2.1*c*, the reflection of the incident blast wave at the earth's surface produces higher peak overpressures than are obtained at the same range in free air. The characteristics of the blast wave after reflection are dependent upon the yield, height of burst, and the reflecting surface conditions. Under ideal conditions, the peak overpressure in the reflected wave may be determined from figure I–15 on page I–31 by knowing the peak overpressure in the incident wave and the angle at which the blast wave strikes the reflecting surface. This angle between the shock front and the surface is known as the angle of incidence. In the regular region of reflection, the incident and reflected shocks have not merged to form a Mach stem. The limit of regular reflection in the ideal situation is a function of incident pressure and angle of incidence. This limiting condition is shown as a dashed line on figure I–15 on page I–31.

I.5 Surface Burst

For nuclear weapons burst at the surface, reflection of the blast wave takes place immediately and a reinforced shock front is formed which propagates outward in a hemispherical manner. Propagation of the blast wave in free air above the surface after breakaway can be adequately described for military purposes by modified Sachs scaling up to altitudes of 50,000 feet assuming an equivalence of twice the yield in free air. Effects on airborne targets can thus be predicted by this procedure, using a 2W assumption with the curves presented in figure I–14 on page I–30.

In describing the propagation of the blast wave along the surface, an approximate equivalence of 1.6 times the yield in free air, or 1.6W, has been found to hold for the overpressure vs. distance relation over ranges of military interest. No such equivalence factor has been found for other blast wave parameters such as duration or impulse. Consequently, reference should be made to the height of burst curves, figures 2–8 through 2–11 inclusive, to obtain the best values of blast wave parameters at various ranges; however, for convenience an empirical curve of overpressure vs. distance has been prepared based on a large amount of data gathered from a number of nuclear surface bursts which is presented in figure I–16 on page I–32. Due to the limited nature of the precursor on surface bursts, this curve can be used for a variety of surface conditions. It is considered that use of the curve is more appropriate than scaling the free air pressure distance curve by modified Sachs scaling with the 1.6W assumption. There is, however, some uncertainty in the low pressure region (0.1 to 1.0 psi) due to the effect of meteorological conditions such as wind shears and temperature inversions which can cause focusing or degradation of the blast wave. This curve can also be used for predicting overpressures at long range for airbursts with low scaled heights of burst.

FREE AIR SHOCK AND PEAK PARTICLE VELOCITY VS. RANGE

Figures I-1 and I-2 show values of shock velocity and peak particle velocity, respectively. These values hold only at the shock front and are related to other blast parameters by the Rankine-Hugoniot equations discussed in the text.

Scaling. For scaling to other yields, use:

$$\frac{d_1}{d_2}=\frac{W_1^{1/3}}{W_2^{1/3}}$$

where yield W_1 will produce the same peak particle velocity and shock velocity at slant range d_1 as yield W_2 will produce at slant range d_2.

Example.

Given: A 20 KT free air burst in a homogeneous sea level atmosphere.

Find: Shock velocity and peak particle velocity at 3,000 feet.

Solution: Applying the scaling above to scale to 1 KT,

$$d_1=\frac{W_1^{1/3}\times d_2}{W_2^{1/3}}=\frac{1\times 3{,}000}{20^{1/3}}=1{,}100 \text{ feet.}$$

From figure I-1, the shock velocity produced by 1 KT at 1,100 feet (and therefore by 20 KT at 3,000 feet) will be 1,300 feet/sec. *Answer.*

From figure I-2, the peak particle velocity produced by 1 KT at 1,100 feet (and therefore by 20 KT at 3,000 feet) will be 280 feet/sec. *Answer.*

Reliability. Free air shock velocity values are based on full-scale tests, while the peak particle velocity values are calculated using equations described in the text.

Related Material.

See paragraph I.1*a*.

See also figure 2-2, which may be derived from figure I-1 by successive integration; also figures I-3 and I-14.

FIGURE I-1

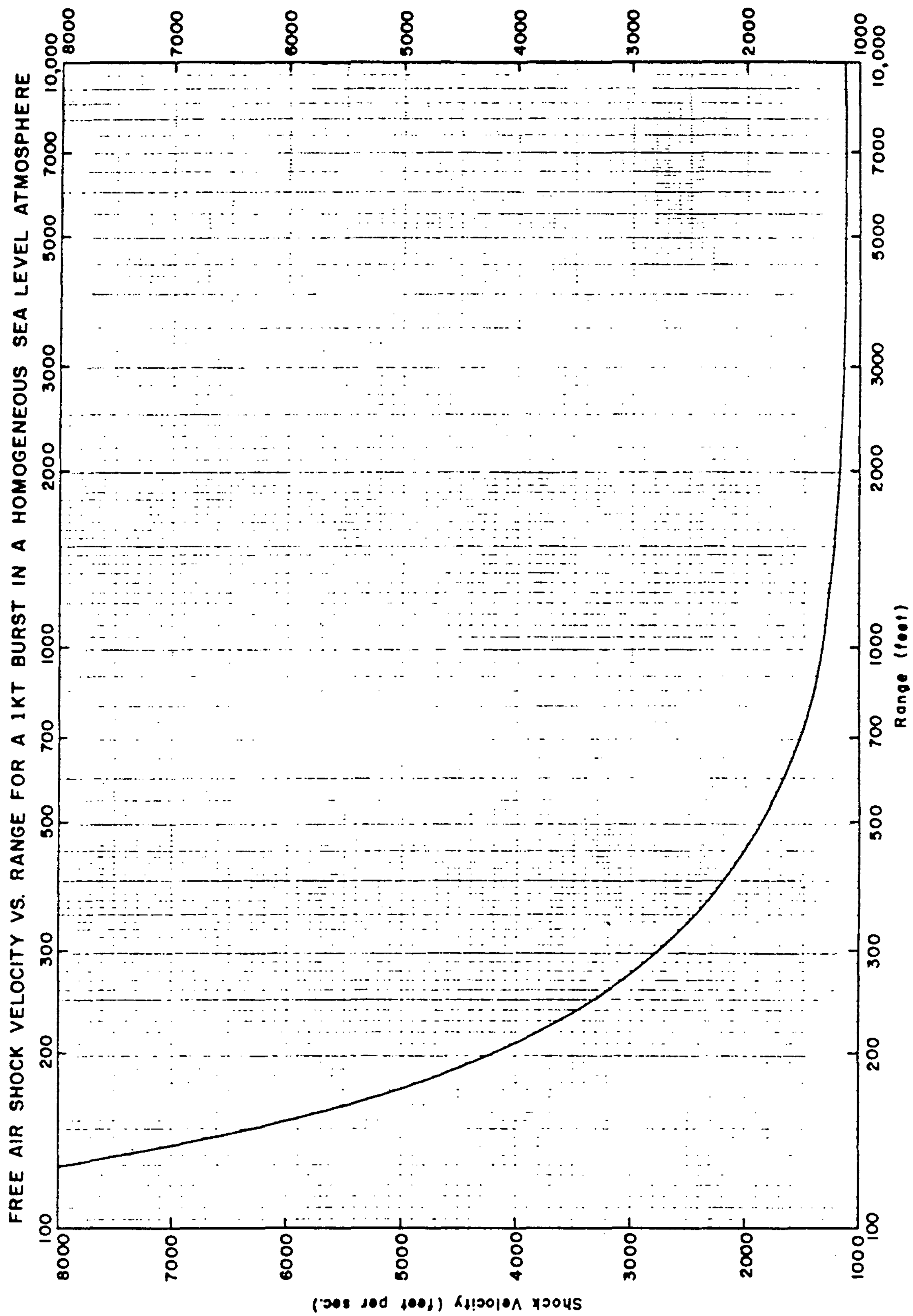
FREE AIR SHOCK VELOCITY VS. RANGE FOR A 1KT BURST IN A HOMOGENEOUS SEA LEVEL ATMOSPHERE
Range (feet)
Shock Velocity (feet per sec.)
100
200
300
500
700
1000
2000
3000
5000
7000
10,000
1000
2000
3000
4000
5000
6000
7000
8000

FREE AIR PEAK PARTICLE VELOCITY VS SLANT RANGE FOR A I KT BURST IN HOMOGENEOUS SEA LEVEL ATMOSPHERE

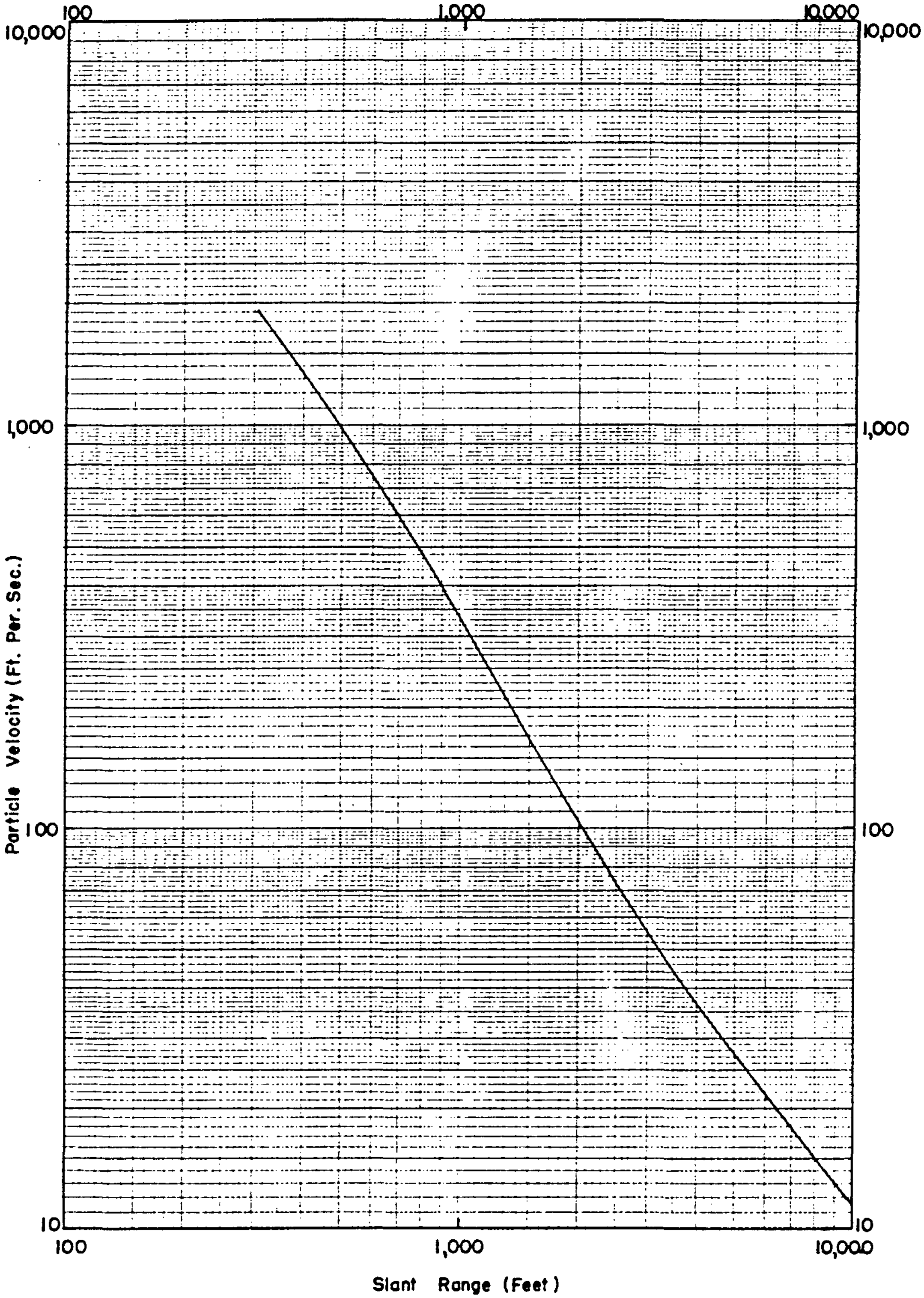

SHOCK FRONT PARAMETERS AS A FUNCTION OF PEAK OVERPRESSURE

FOR SEA LEVEL ATMOSPHERE

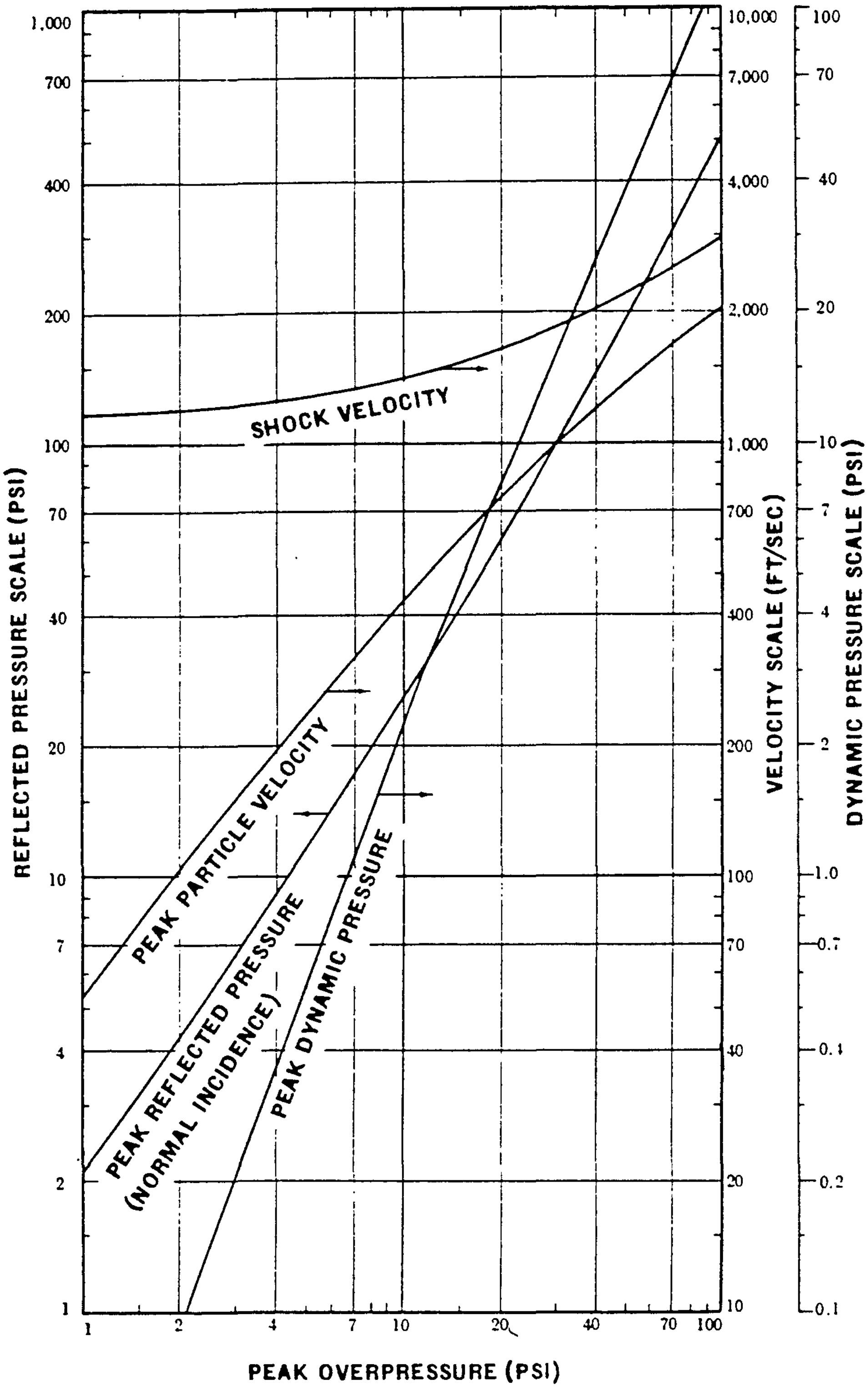

FREE AIR OVERPRESSURE POSITIVE PHASE IMPULSE VS. SLANT RANGE

Figure I-4 gives values of free air overpressure impulse as a function of distance for a 1 KT burst. The overpressure positive phase impulse of the blast wave is derived from the overpressure-time curve as illustrated in figure 2-1. It is the integral of the curve representing the variation of overpressure as a function of time between the time of arrival of the blast wave at a given range and the end of the positive phase at that range.

Scaling. For scaling to other yields, use:

$$\frac{I_1}{I_2}=\frac{d_1}{d_2}=\frac{W_1^{1/3}}{W_2^{1/3}},$$

where yield W_1 will produce, at slant range d_1, an overpressure impulse I_1, and yield W_2 will produce an overpressure impulse I_2 at slant range d_2.

Example.

Given: A 20 KT free air burst in a homogeneous sea level atmosphere.

Find: The overpressure impulse at 3,000 feet slant range.

Solution: Applying the scaling above to scale to 1 KT,

$$d_1=\frac{W_1^{1/3}\times d_2}{W_2^{1/3}}=\frac{1\times 3{,}000}{20^{1/3}}=1{,}100 \text{ ft.}$$

From figure I-4, the overpressure impulse at 1,100 feet from a 1 KT burst would be 0.54 psi-second. Therefore, for a 20 KT burst at 3,000 feet the impulse will be

$$I_2=\frac{I_1\times W_2^{1/3}}{W_1^{1/3}}=0.54\times 2.71=$$

1.46 psi-seconds. *Answer.*

Reliability. Based largely on theoretical considerations with some full scale test data in the low pressure region.

Related Material.

See paragraph I.1*b*.

See also figures 2-1 and I-5 through I-9.

FREE AIR OVERPRESSURE POSITIVE PHASE IMPULSE VS SLANT RANGE FOR I KT BURST IN A HOMOGENEOUS SEA LEVEL ATMOSPHERE

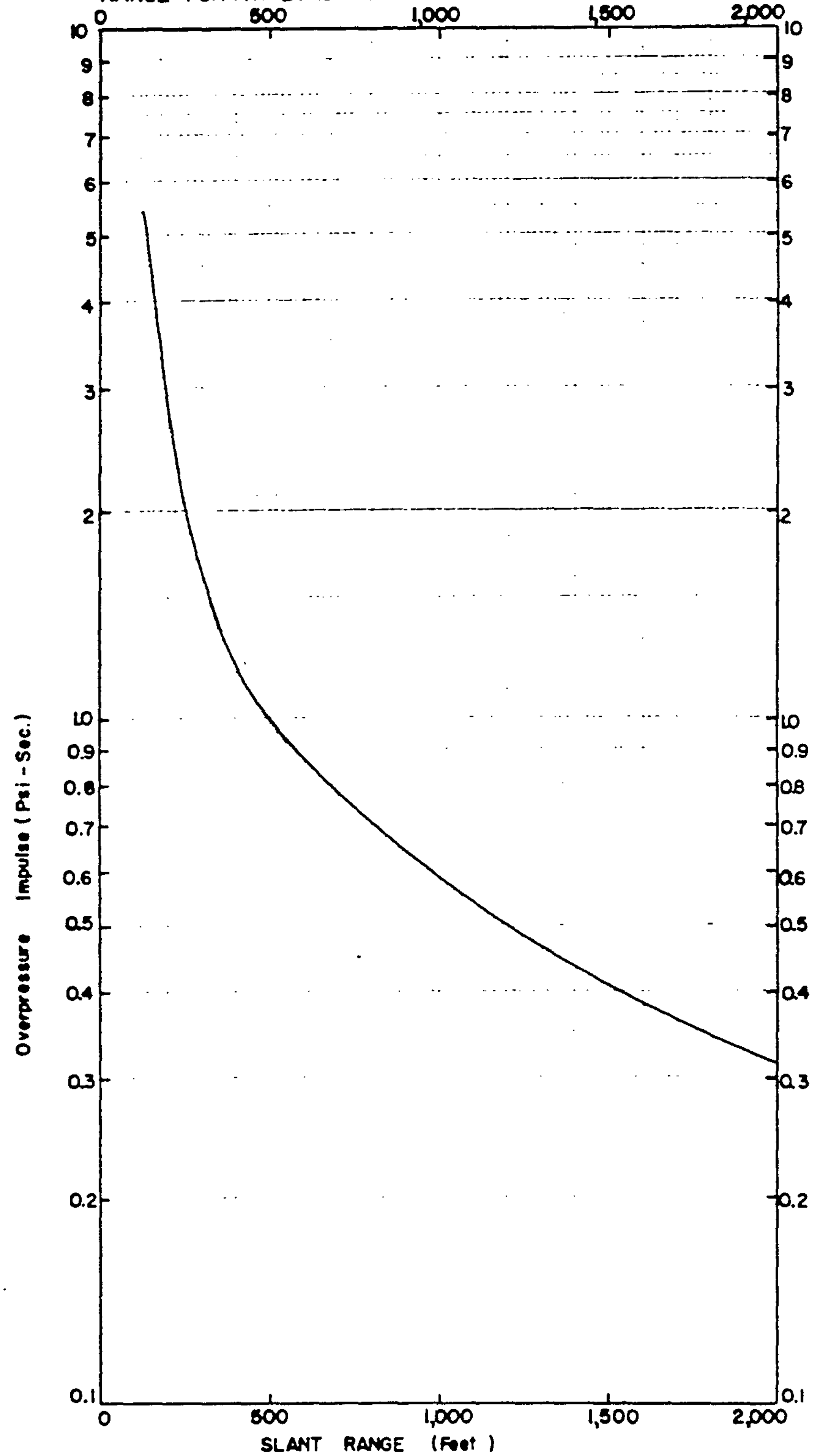

FREE AIR OVERPRESSURE DECAY

At a given point in space, the rate of decay of overpressure after shock front passage depends upon the peak overpressure of the shock front. Figure I-5 shows the variation in overpressure with time for various free air peak overpressures in terms of normalized coordinates; i. e., the overpressure at a given time is expressed as a fraction of the peak overpressure $\left(\frac{\Delta p(t)}{\Delta p}\right)$, and the time is expressed as a fraction of the positive phase duration $\left(\frac{t}{t^+}\right)$, where: $\Delta p(t)$ is the overpressure at the point of interest at a time t after shock front passage.

Δp is the free air peak overpressure at the point of interest, obtained from figure 2-3.

t is the time after shock front passage.

t^+ is the duration of the positive phase at the point of interest, obtained from figure 2-4.

Related Material.

See paragraph I.1*b*.

See also figures 2-1, I-6, and I-8.

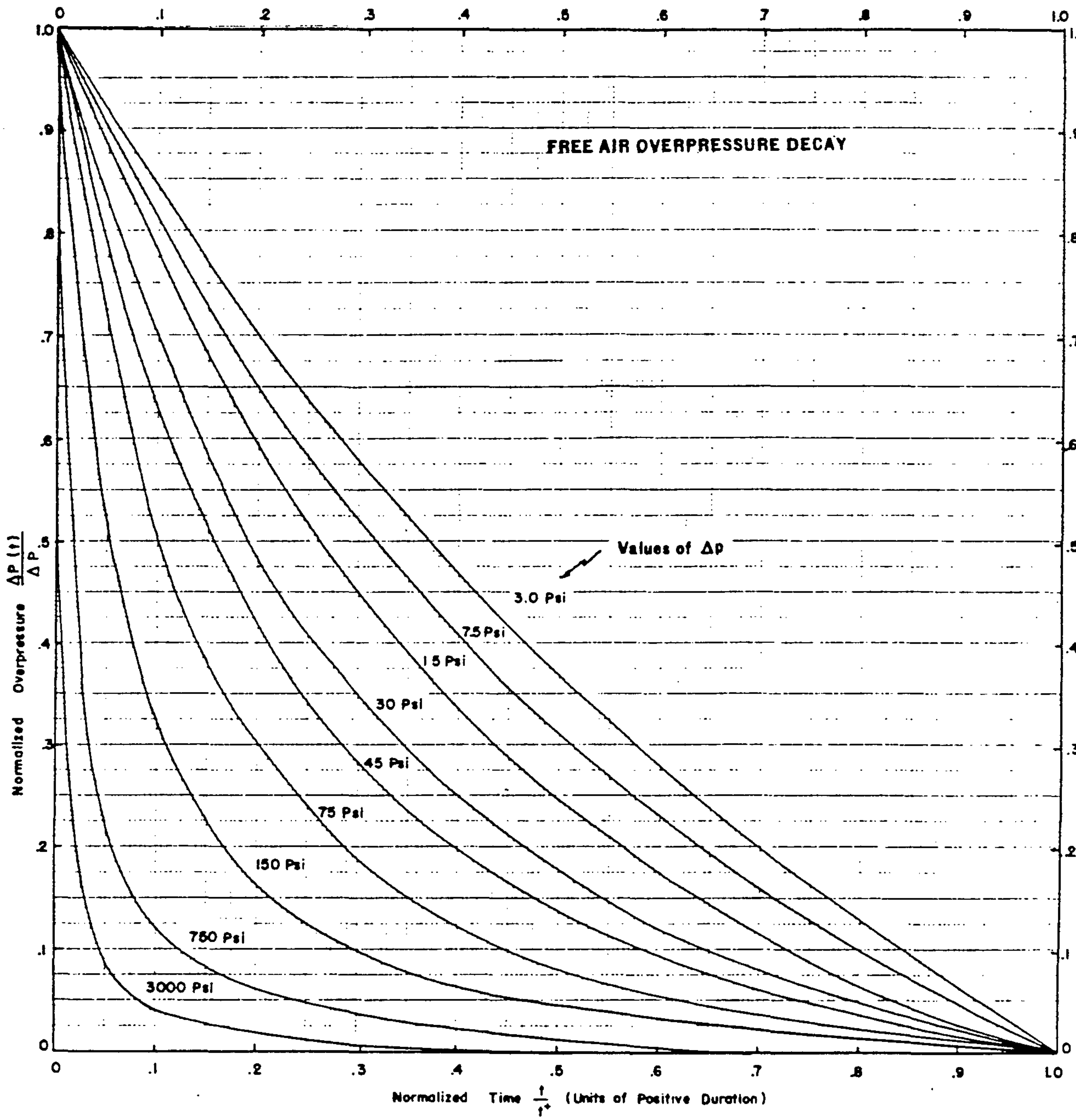
FREE AIR OVERPRESSURE DECAY
Values of Δp
3.0 Psi
7.5 Psi
15 Psi
30 Psi
45 Psi
75 Psi
150 Psi
750 Psi
3000 Psi
Normalized Overpressure ΔP (t) / ΔP
Normalized Time t / t+ (Units of Positive Duration)
0
.1
.2
.3
.4
.5
.6
.7
.8
.9
1.0

COMPARISON OF SIMPLIFIED WAVE FORMS FOR OVERPRESSURE AND DYNAMIC PRESSURE

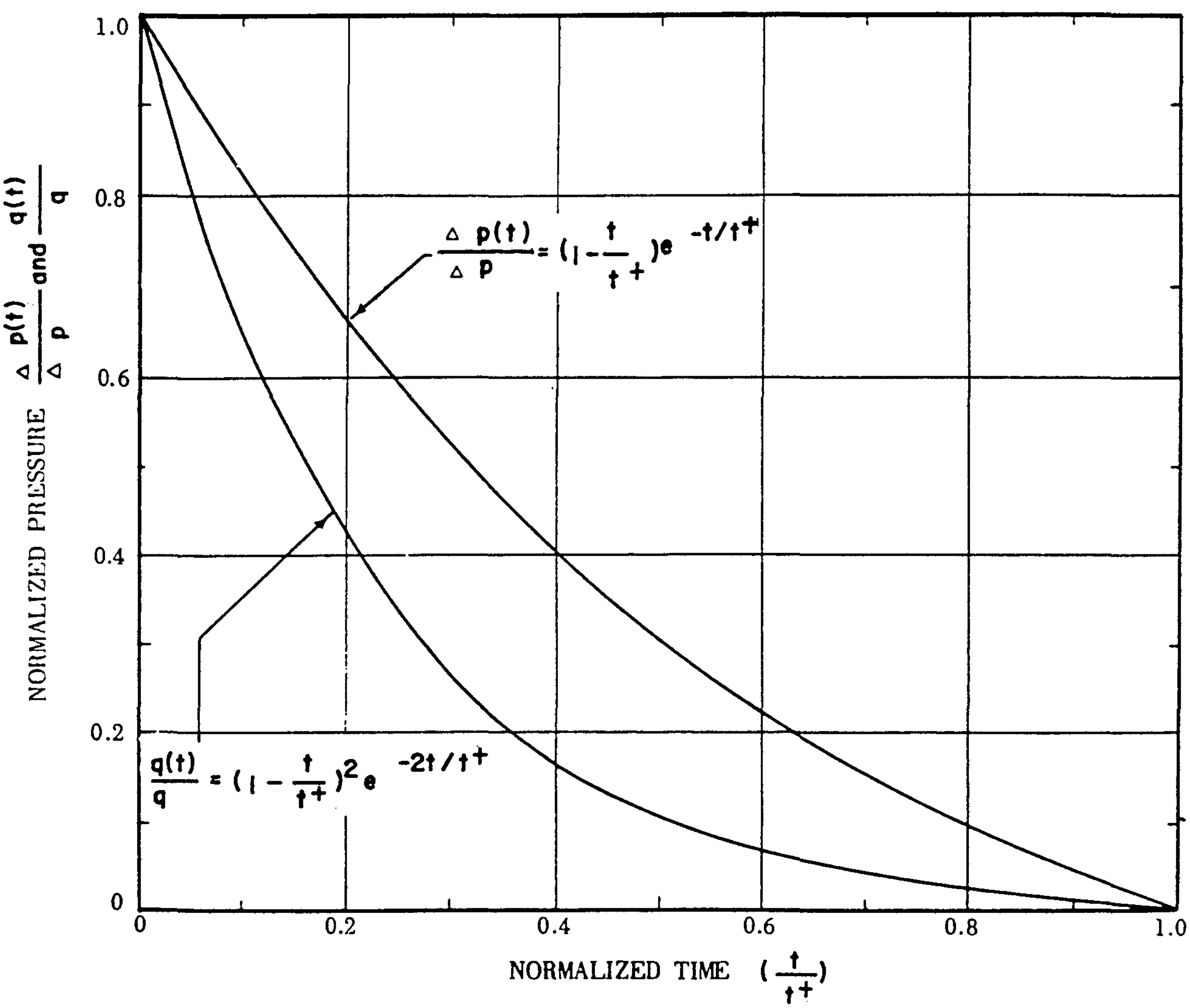

BLANK

FREE AIR DYNAMIC-PRESSURE IMPULSE VS. SLANT RANGE

Figure I–7 gives values of free air dynamic pressure impulse as a function of distance for a 1 KT burst. The dynamic pressure positive phase impulse of the blast wave is derived from the dynamic pressure-time curve as illustrated in figure 2–1. It is the integral of the curve representing the variation of dynamic pressure as a function of time between the time of arrival of the blast wave at a given range and the end of the dynamic pressure phase.

Scaling. For scaling to other yields, use:

$$\frac{I_1}{I_2}=\frac{d_1}{d_2}=\frac{W_1^{1/3}}{W_2^{1/3}},$$

where yield W_1 will produce at a slant range d_1 a dynamic pressure impulse I_1, and yield W_2 at slant range d_2 will produce a dynamic pressure impulse I_2.

Example.

Given: A 20 KT free air burst in a homogeneous sea level atmosphere.

Find: The dynamic pressure impulse at 3,000 feet slant range.

Solution: Applying the scaling above to scale to 1 KT,

$$d_1=\frac{W_1^{1/3}\times d_2}{W_2^{1/3}}=\frac{1\times 3{,}000}{20^{1/3}}=1{,}100 \text{ ft.}$$

From figure I–7, the dynamic pressure impulse at 1,100 feet from a 1 KT burst would be 0.056 psi-sec.

Thus, the overpressure impulse at 3,000 feet from a 20 KT burst will be

$$I_2=\frac{I_1\times W_2^{1/3}}{W_1^{1/3}}=0.056\times 2.71=$$

0.152 psi-sec. *Answer.*

Reliability. Based entirely on theoretical considerations.

Related Material.

See paragraph I.1*c*.

See also figures 2–1, I–4 through I–6, I–8 and I–9.

FIGURE I-7

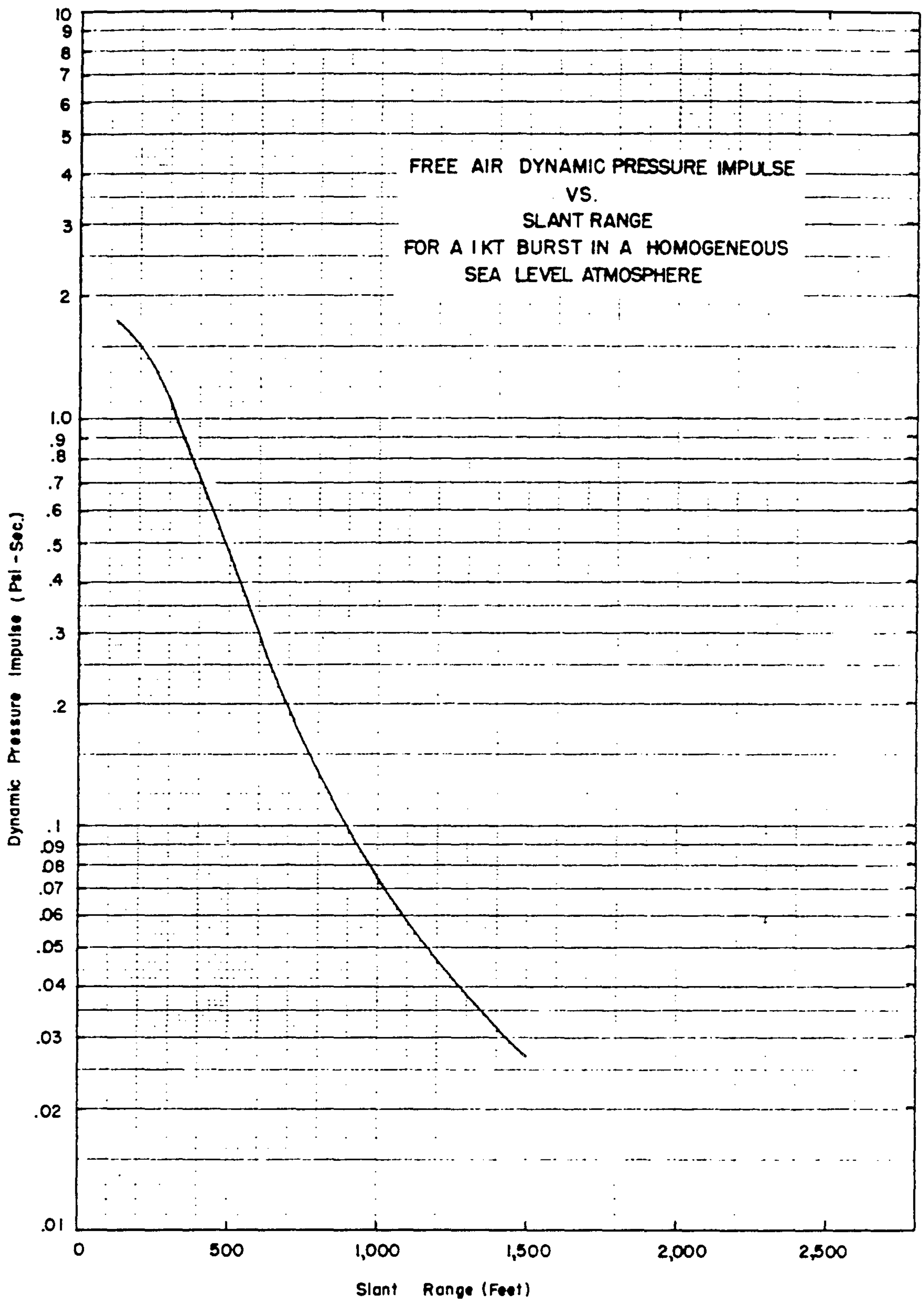
FREE AIR DYNAMIC PRESSURE IMPULSE
VS.
SLANT RANGE
FOR A 1 KT BURST IN A HOMOGENEOUS
SEA LEVEL ATMOSPHERE
Dynamic Pressure Impulse (Psi-Sec.)
10
9
8
7
6
5
4
3
2
1.0
.9
.8
.7
.6
.5
.4
.3
.2
.1
.09
.08
.07
.06
.05
.04
.03
.02
.01
0
500
1,000
1,500
2,000
2,500
Slant Range (Feet)

FREE AIR DYNAMIC PRESSURE DECAY

At a given point in space, the rate of decay of dynamic pressure after shock front passage depends upon the peak dynamic pressure. Figure I-8 shows the variation in dynamic pressure with time for various free air peak dynamic pressures in terms of normalized coordinates; i. e., the dynamic presssure at a given time is expressed as a fraction of the peak dynamic pressure $\left(\frac{q(t)}{q}\right)$, and the time is expressed as a fraction of the positive phase duration $\left(\frac{t}{t^+}\right)$, where:

$q(t)$ is the dynamic pressure at the point of interest at a time t after shock front passage.

q is the free air peak dynamic pressure at the point of interest, obtained from figure 2-5.

t is the time after shock front passage.

t^+ is the duration of the positive phase at the point of interest, obtained from figure 2-4. The overpressure positive phase duration, t^+, is used rather than the dynamic phase duration for reasons discussed in paragraphs 2.1*b*(4)(*b*) and I.1*c*.

Related Material.

See paragraphs 2.1*b*(4)(*b*) and I.1*c*.

See also figures 2-1, I-5 and I-6.

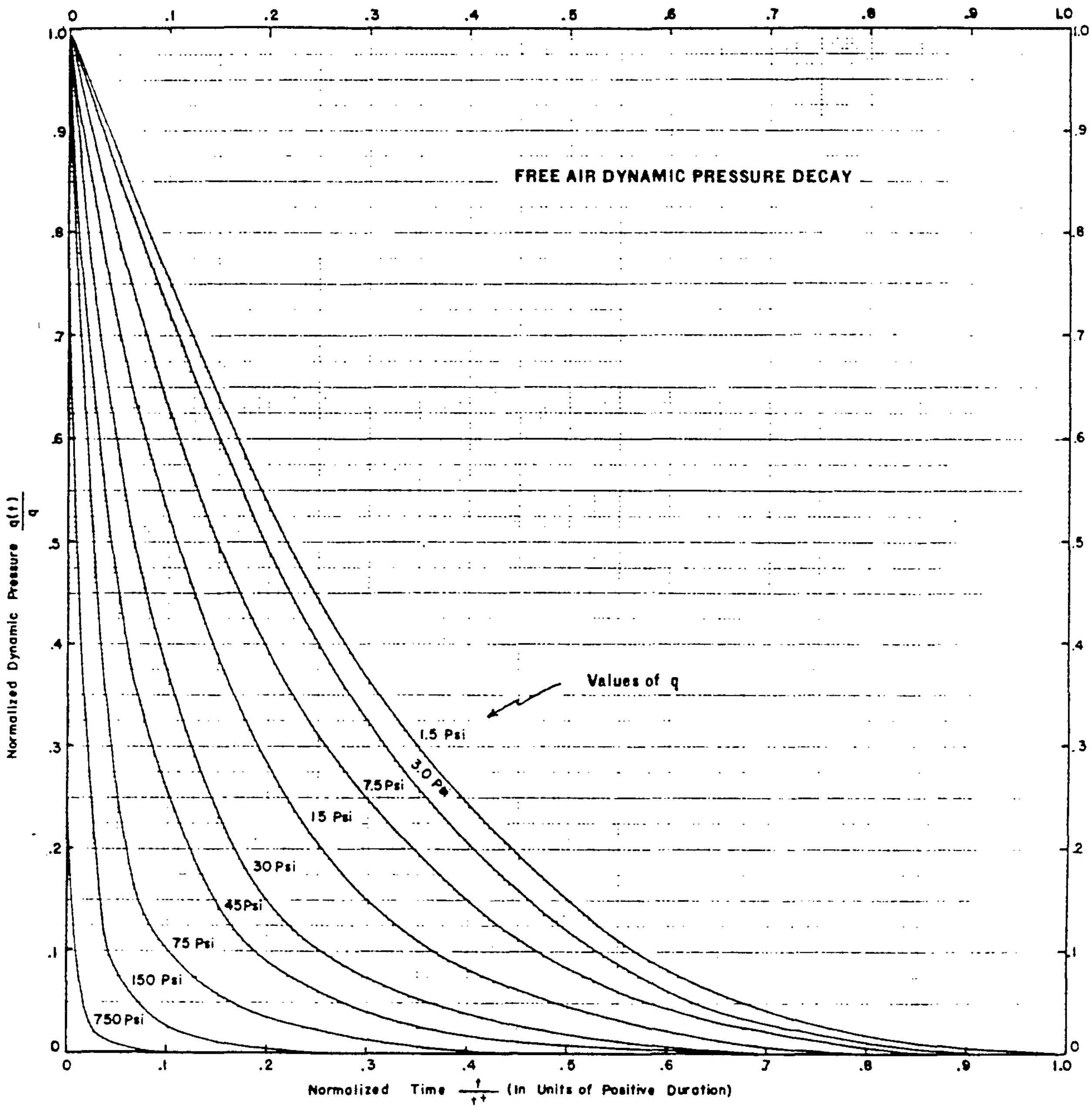
FREE AIR DYNAMIC PRESSURE DECAY
Values of q
1.5 Psi
3.0 Psi
7.5 Psi
15 Psi
30 Psi
45 Psi
75 Psi
150 Psi
750 Psi
Normalized Dynamic Pressure q(t)/q
Normalized Time t/t⁺ (In Units of Positive Duration)
0
.1
.2
.3
.4
.5
.6
.7
.8
.9
1.0

BLANK

OVERPRESSURE POSITIVE PHASE IMPULSE AT THE SURFACE

Figures I–9A and I–9B give overpressure positive phase impulse as a function of height of burst and ground range for a 1 KT burst in a sea level homogeneous atmosphere and represent the area under the positive phase of the overpressure-time curve at or near the reflecting surface. Figure I–9A applies to good surface conditions where thermal and mechanical effects are minimized, i. e., near-ideal wave forms. Figure I–9B applies to average surface conditions where the non-ideal wave forms discussed in paragraph I.2*a* may be expected. The curves in figures I–9A are derived from figures 2–9 and 2–11. The curves in figure I–9B are derived from figures 2–10 and 2–11.

Scaling. To scale to other yields, height of burst, ground range, and impulse scale as the cube root of the yield, or:

$$\frac{I_1}{I_2}=\frac{h_1}{h_2}=\frac{d_1}{d_2}=\frac{W_1^{1/3}}{W_2^{1/3}}$$

where I_1, h_1, and d_1 are impulse, height of burst and ground distance for yield W_1, and I_2, h_2 and d_2 are the corresponding impulse, height of burst and ground range for yield W_2.

Example.

Given: A 30 KT burst at a height of 1,000 feet over an average surface.

Find: The overpressure positive phase impulse on the surface at a ground range of 2,000 yards.

Solution: Using the above scaling to scale to the corresponding ground distance and height of burst for 1 KT,

$$h_1=\frac{W_1^{1/3}\times h_2}{W_2^{1/3}}=\frac{1\times 1{,}000}{(30)^{1/3}}=322\text{ ft.}$$

$$d_1=\frac{W_1^{1/3}\times d_2}{W_2^{1/3}}=\frac{1\times 2{,}000}{(30)^{1/3}}=644\text{ yd.}$$

From figure I–9B for a height of burst of 322 feet and at a ground range of 644 yards the impulse is about 530 psi-msec. Therefore, for 30 KT at a height of burst of 1,000 feet, the overpressure impulse at a ground range of 2,000 yards will be:

$$I_2=\frac{I_1\times W_2^{1/3}}{W_1^{1/3}}=530\times 3.11=1{,}650$$

psi-milliseconds or 1.65 psi-seconds. *Answer.*

Reliability. Based on full scale test data.

Related Material.

See paragraph I.2*a*.

See also figures 2–9 through 2–11, I–4 and I–7.

OVERPRESSURE POSITIVE PHASE IMPULSE AT THE SURFACE AS A FUNCTION OF HEIGHT OF BURST AND HORIZONTAL RANGE
1 KT AT SEA LEVEL FOR GOOD SURFACE CONDITIONS

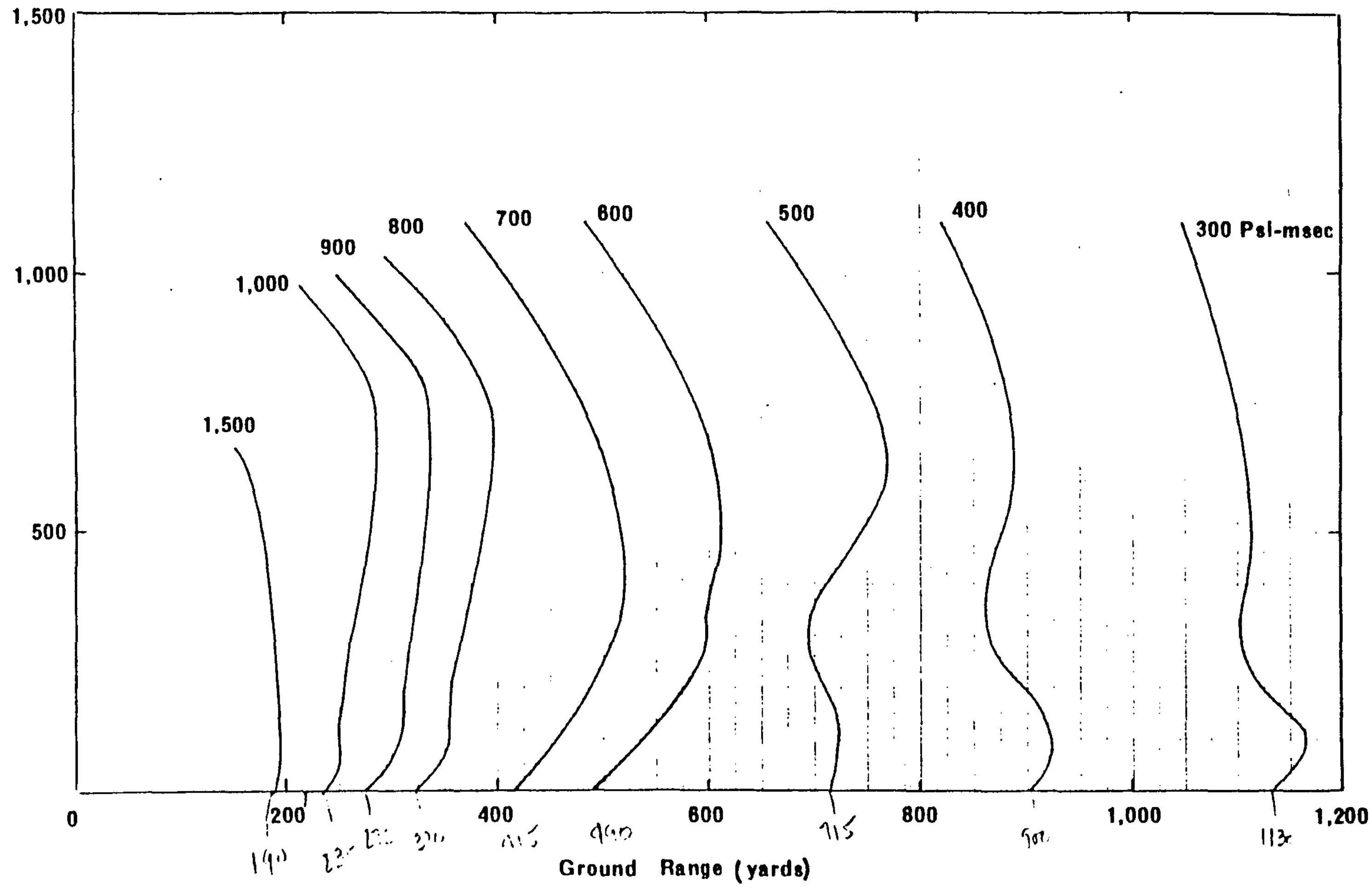

OVERPRESSURE POSITIVE PHASE IMPULSE AT THE SURFACE AS A FUNCTION OF HEIGHT OF BURST AND HORIZONTAL RANGE

1 KT AT SEA LEVEL FOR AVERAGE SURFACE CONDITIONS

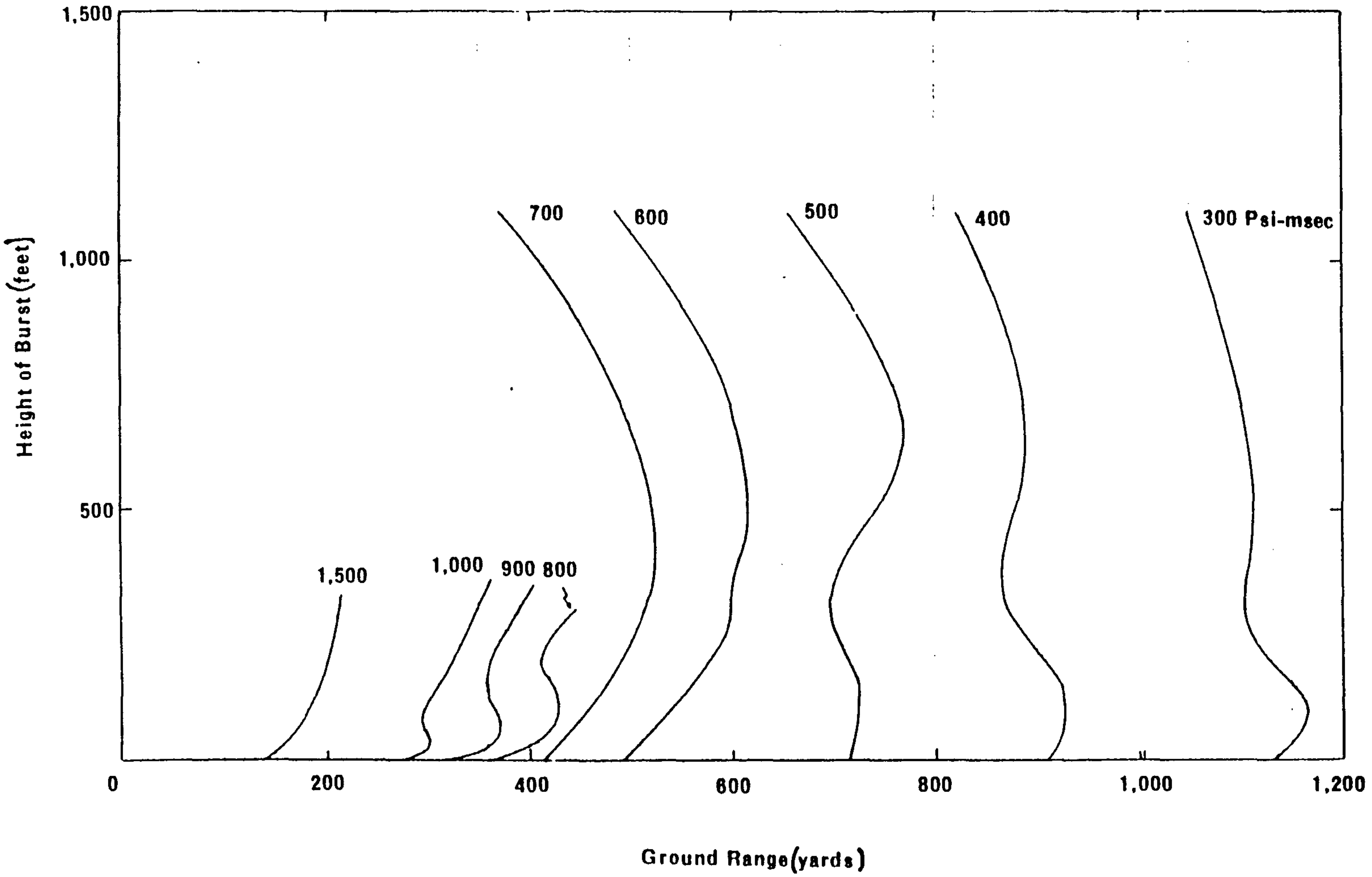

OVERPRESSURE WAVE FORM VARIATIONS AT THE SURFACE

Figure I-11 shows the overpressure wave form types to be expected for a 1 KT burst in a sea level homogeneous atmosphere as a function of height of burst and ground range for average surface conditions. In addition, the precursor zone is depicted.

Scaling. Height of burst and ground distance to which the precursor zone or a wave form type extend scale as the cube root of the yield:

$$\frac{h_1}{h_2}=\frac{d_1}{d_2}=\frac{W_1^{1/3}}{W_2^{1/3}},$$

where h_1 and d_1 are height of burst and ground distance from ground zero for yield W_1, and h_2 and d_2 are the corresponding height of burst and ground distance from ground zero for yield W_2.

Example.

Given: A 100 KT burst at 600 feet over an average surface.

Find: (1) The ground range to which a precursor may be expected to extend; and (2), the wave form to be expected at the surface 660 yards from ground zero.

Solution: (1) Using the above scaling to obtain a corresponding height of burst for 1 KT,

$$h_1=\frac{W_1^{1/3}\times h_2}{W_2^{1/3}}=\frac{1\times 600}{(100)^{1/3}}=129 \text{ ft.}$$

Entering figure I-11 at a height of burst of 129 feet, the precursor zone extends 368 yards for a 1 KT burst. To obtain the corresponding distance for 100 KT,

$$d_2=\frac{W_2^{1/3}\times d_1}{W_1^{1/3}}=\frac{(100)^{1/3}\times 368}{1}=$$

1,710 yards. *Answer.*

(2) The distance at the surface for 1 KT corresponding to 660 yards for 100 KT is:

$$d_1=\frac{W_1^{1/3}\times d_2}{W_2^{1/3}}=\frac{1\times 660}{(100)^{1/3}}=142 \text{ yd.}$$

Entering figure I-11 at a height of burst of 129 feet and a ground distance of 142 yards, the intercept lies within the region of the precursor zone at which the overpressure wave form to be expected at the surface is type II. *Answer.*

Reliability. Boundary lines of precursor and wave form zones are derived primarily from full scale testing over desert surfaces.

Related Material.

See paragraphs 2.1*c* and *d*(4), and I.2*a*.
See also figures 2-16 and 2-17.

VARIATION OF OVERPRESSURE WAVE FORM WITH HEIGHT OF BURST AND GROUND RANGE FOR 1KT IN A SEA LEVEL HOMOGENEOUS ATMOSPHERE FOR AVERAGE SURFACE CONDITIONS

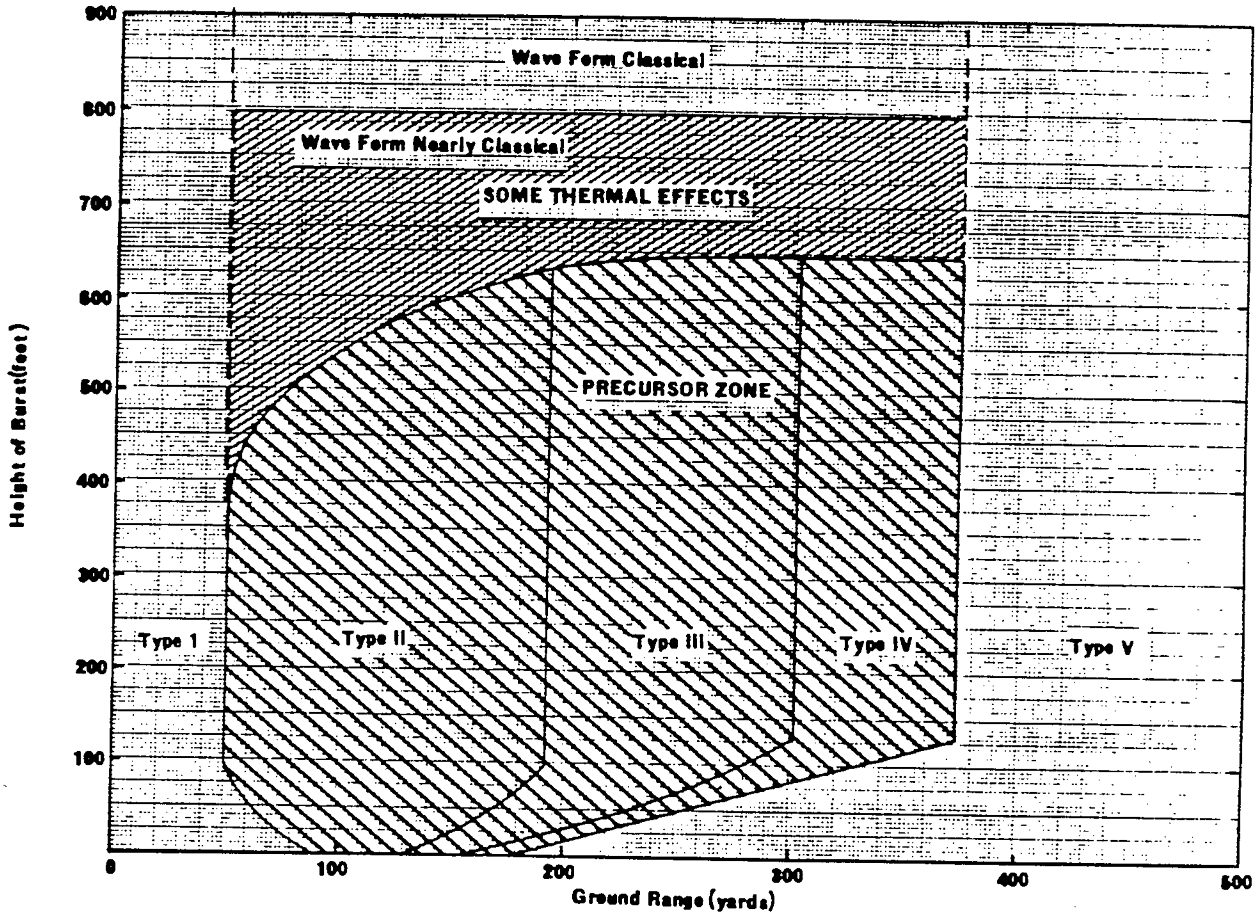

ALTITUDE CONVERSION

Figure I-13 presents altitude conversion factors for distance, pressure and time for use in the modified Sachs procedure for converting 1 KT blast effects data from a sea level standard atmosphere to the atmosphere at target altitude discussed in paragraph I.3.

Figure I-14 presents sea level free air peak overpressure values for use in the altitude conversion procedure in the airborne target situation discussed in paragraph I.3*b*.

The following examples illustrate the altitude conversion procedure for a surface target situation and an airborne target situation.

Example 1. (Surface Target Situation)

Given: A 1 MT detonation at 20,000 feet altitude above a ground surface at an elevation of 7,000 feet.

Find: (1) The time of shock arrival and free air peak overpressure incident at the surface directly below the burst.

(2) The reflected pressure at the surface.

Solution: (1) From figure I-13 the distance, time and pressure conversion factors for a target at an elevation of 7,000 feet are $S_d=1.09$, $S_t=1.11$, and $S_p=0.77$. The 13,000 foot range from burst to ground surface scaled to 1 KT and converted to sea level is:

$$d_o=\frac{d_z}{(W)^{1/3}\,S_d}=\frac{13,000}{(1,000)^{1/3}\,1.09}=1,190 \text{ feet.}$$

From figures 2-2 and 2-3, the 1 KT sea level time of free air shock arrival and free air peak overpressure at a distance of 1,190 feet are 0.6 second and 5.2 psi. Therefore, at a surface at 7,000 feet altitude and 13,000 feet directly below a 1 MT burst, the time of shock arrival and free air peak overpressure incident at the surface are:

$$t_z=t_o\,W^{1/3}\,S_t=0.6\,(1,000)^{1/3}\times1.11=6.6 \text{ seconds.}$$

$$\Delta p_z=\Delta p_o S_p=5.2\times0.77=4.0 \text{ psi.}$$

Answers.

(2) From paragraph I.1a a free air peak overpressure of 4.0 psi at normal incidence to a surface produces a reflected pressure of about 9 psi. *Answer.*

Example 2. (Airborne Target Situation)

Given: At shock arrival time, an aircraft is flying at 25,000 feet altitude and at a horizontal range of 15,000 feet from a point directly above a 1 MT burst which is 5,000 feet above a sea level surface.

Find: The peak overpressure and peak particle velocity at the aircraft position.

Solution: The slant range

$$d_z=\sqrt{(15,000)^2+(25,000-5,000)^2}=25,000 \text{ feet.}$$

From figure I-13 for the 25,000 feet target altitude, the distance conversion factor $S_d=1.39$ and the pressure conversion factor $S_p=0.37$.

The range from target to burst scaled to 1 KT and converted to sea level is:

$$d_o=\frac{d_z}{S_d(W)^{1/3}}=\frac{25,000}{1.39\times(1,000)^{1/3}}=1,800 \text{ feet.}$$

From figure I-14, the sea level peak overpressure Δp_o and the peak particle velocity u_o at a distance of 1,800 feet are 2.80 psi and 150 feet per second, respectively.

Therefore, at 25,000 feet altitude and a slant distance of 25,000 feet from a 1 MT burst, the peak overpressure Δp_z is:

$\Delta p_z=\Delta p_o\,S_p=2.80\times0.37=1.04$ psi, and the peak particle velocity u_z is:

$$u_z=u_o\left(\frac{C_z}{C_o}\right)=150\times\frac{1,016}{1,116}=137 \text{ feet per second.}$$

Answers.

Reliability. The altitude conversion factors of figure I-13 introduce no significant additional error and do not change the reliability of the basic data to which they are applied. The sea level data from figure I-14 is considered reliable within ±20 percent when converted to altitudes up to 50,000 feet and scaled for yields up to 20 MT.

Related Material.

See paragraphs 2.1*d*(2)(*c*) and I.3.

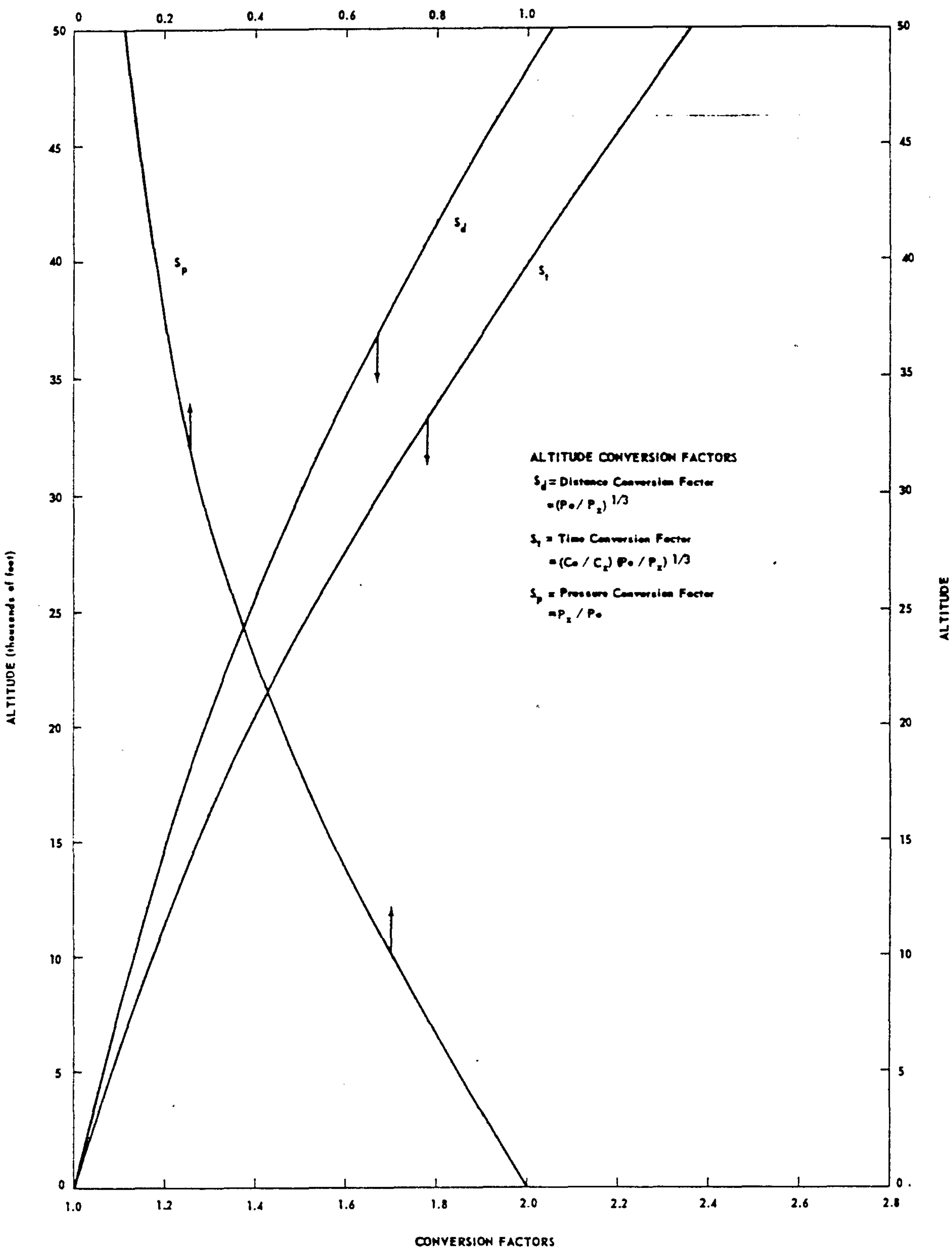
0
0.2
0.4
0.6
0.8
1.0
50
45
40
35
30
25
20
15
10
5
0
1.0
1.2
1.4
1.6
1.8
2.0
2.2
2.4
2.6
2.8
ALTITUDE (thousands of feet)
ALTITUDE
CONVERSION FACTORS
S_p
S_d
S_t
ALTITUDE CONVERSION FACTORS
S_d = Distance Conversion Factor
$=(Po/P_z)^{1/3}$
S_t = Time Conversion Factor
$=(Co/C_z)(Po/P_z)^{1/3}$
S_p = Pressure Conversion Factor
$=P_z/Po$

SEA LEVEL BLAST PARAMETERS FROM A 1KT BURST

FOR ALTITUDE CONVERSION FOR AIRBORNE TARGETS

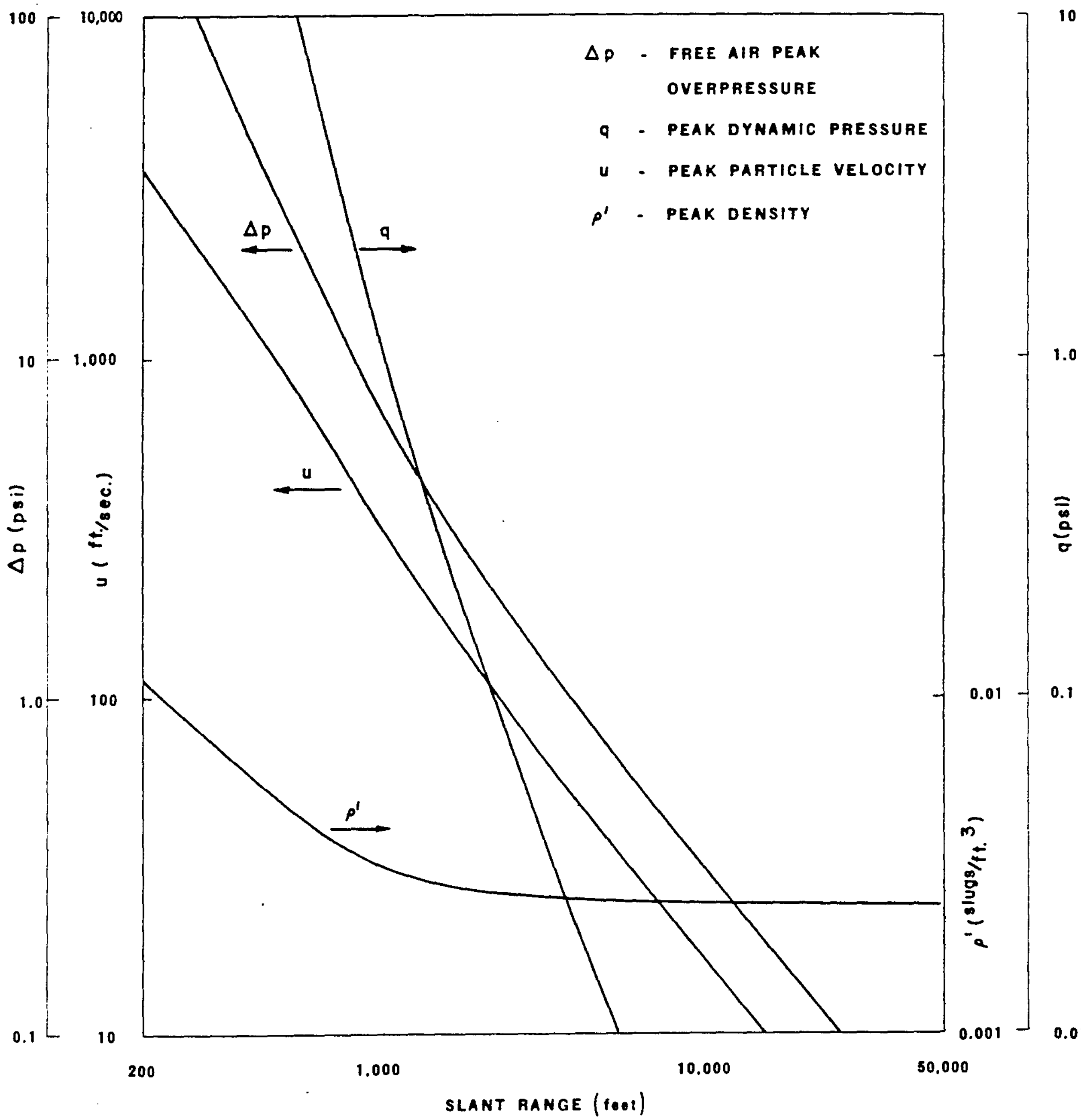

REFLECTION CHART FOR PEAK OVERPRESSURE UNDER IDEAL CONDITIONS

INCIDENT PRESSURE Pi

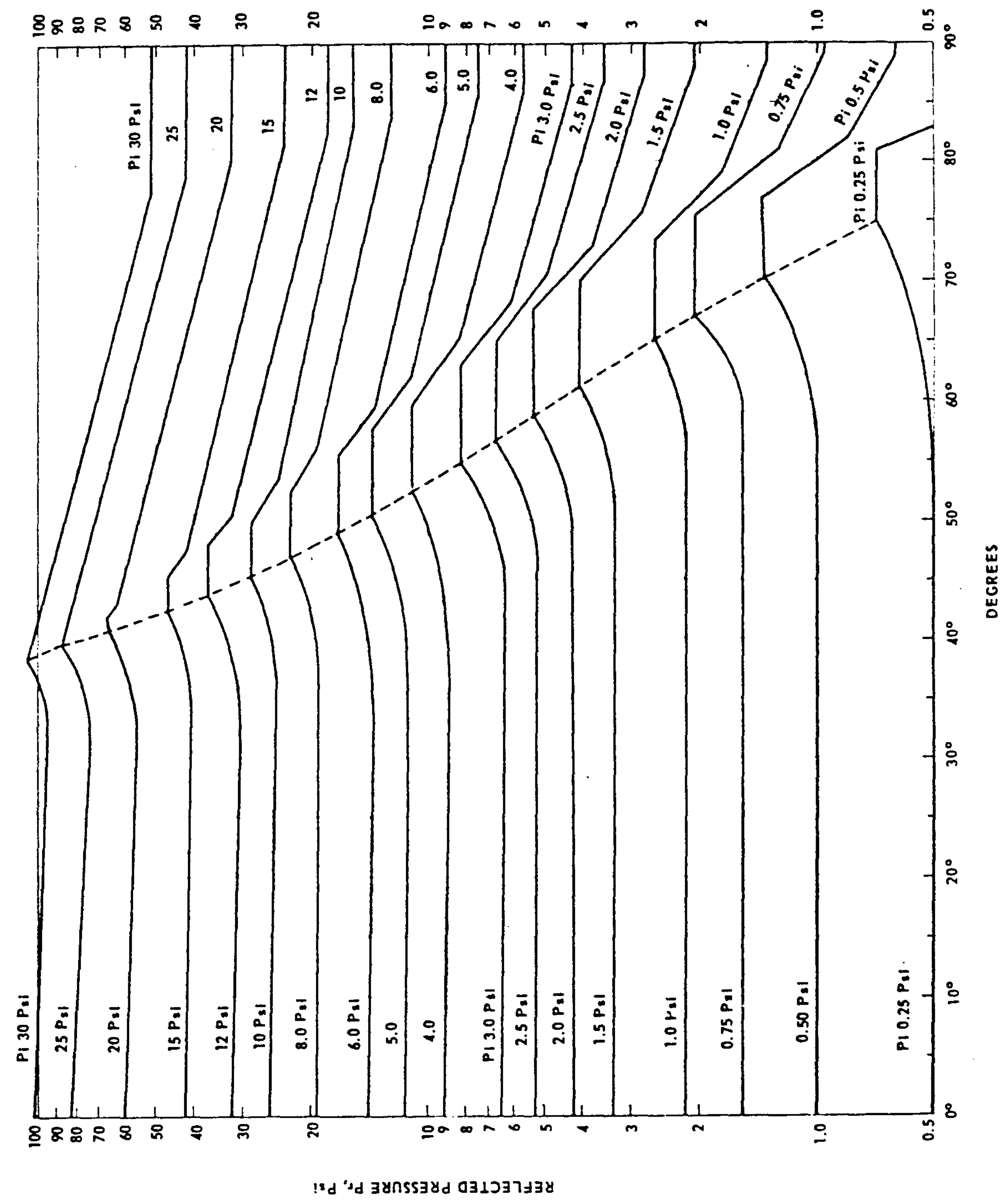

PEAK OVERPRESSURE VS. DISTANCE

HOMOGENEOUS ATMOSPHERE OF STANDARD SEA LEVEL CONDITIONS

1 KT SURFACE BURST

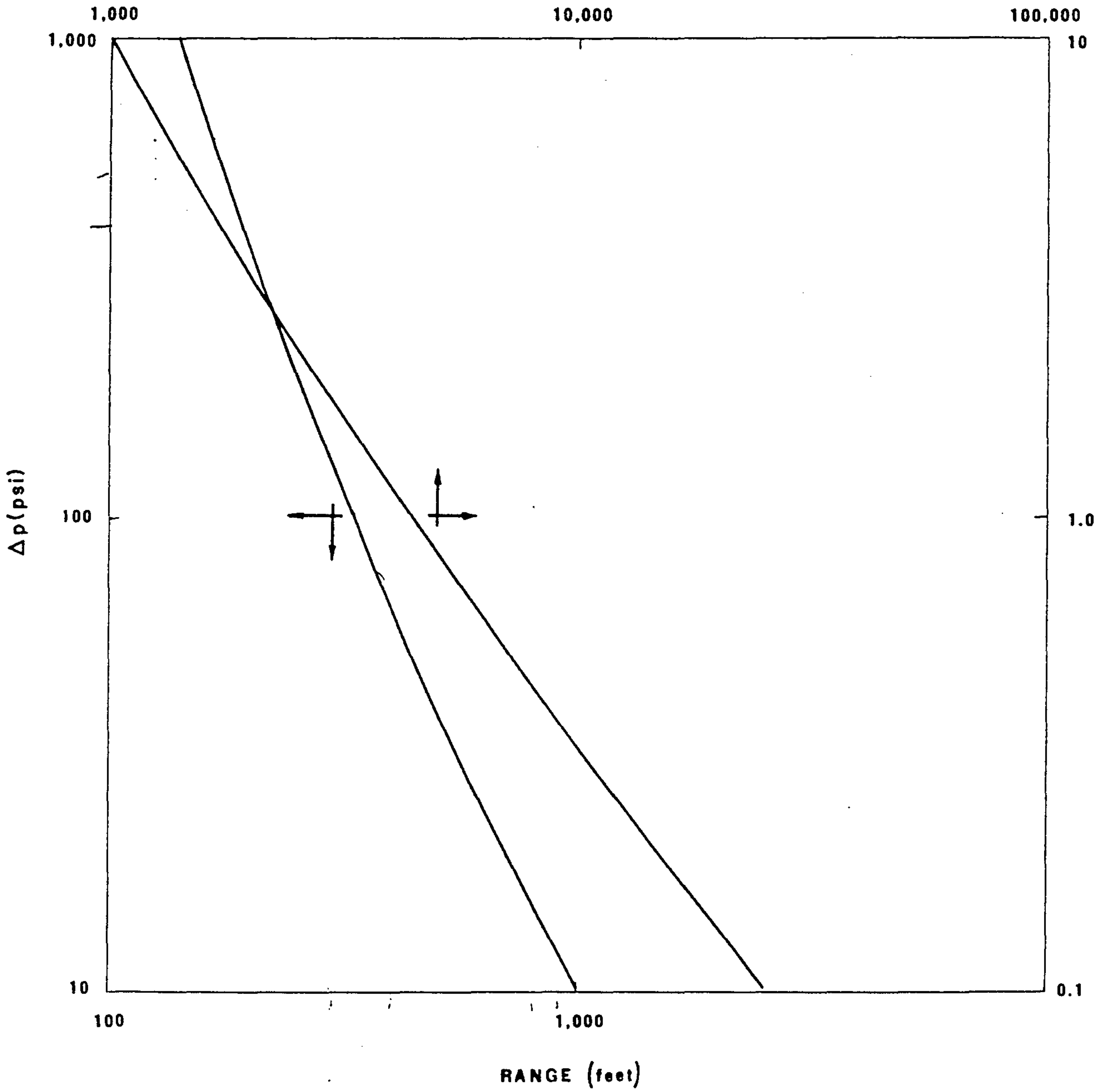

II
Useful
Relationships

447555 O - 58 - 31

APPENDIX II
USEFUL RELATIONSHIPS

II.1 General

Equivalents:

1 KT is equivalent to 10^{12} calories of energy.

1 MT=1,000 KT=10^{15} calories of energy.

(Ultimately all the energy from a nuclear weapon appears as heat.)

1 KT represents about 1.5×10^{23} fissions.

Energy equivalents:

1 calorie =4.184 joules
=3.086 foot-pounds
=2.61×10^{13} Mev
=3.966×10^{-3} Btu.

Mass-energy conversion: 1 gram mass=5.61×10^{26} Mev.

The temperature associated with one electron-volt is 11,605.9 degrees Kelvin.

1 millibar=1,000 dynes/cm^2=0.0145 psi.

Relative air density:

Given air pressures at detonation and target altitude.

$$R=25.8\,\frac{p_1-p_2}{h_1-h_2},$$

where p_1-p_2 is pressure difference in millibars
h_1-h_2 is the altitude difference in feet

Given detonation and target at same altitude,

$$R=0.27\,\frac{p}{T}=\frac{\rho}{0.00129},$$

where p=pressure in millibars
T=absolute temperature in degrees Kelvin
ρ=air density in gm/cm.^{3}

Given detonation and target altitude only, standard atmosphere assumed, use figure II–3.

Constants:

Velocity of light: 3×10^8 meters per second.

Avogadro's number: 6.023×10^{23} molecules per mole.

Planck's constant: 6.624×10^{-34} joule-second

Boltzmann constant: 1.38×10^{-16} erg per degree.

Loschmidt number: 2.687×10^{19} molecules per cubic centimeter at 0° C.

Mass of electron: 9.11×10^{-28} gram.

Mass of proton: 1.67×10^{-24} gram.

Mass of alpha particle: 6.64×10^{-24} gram.

Classical electron radius: 2.82×10^{-13} cm.

Standard sea-level atmosphere:

Pressure=14.6960 lbs./square inch
=29.92 in. of mercury (at 0° C.)
=76 cm of mercury (at 0° C.)
=33.9 ft. of water (at 4° C.)
=1,013.25 millibars
=2,117 lbs./square foot

Temperature=59.000 degrees Fahrenheit
=15.000 degrees Centigrade

Density=0.0023779 slug per cubic foot

Speed of sound=1,116.215 ft/sec.

II.2 Thermal

Temperature scale conversions:

°K=°C.+273; °C.=5/9 (°F.−32)
°F.=9/5°C.+32; °R=°F.+459.4

Thermal radiation from a nuclear weapon:

For air bursts under 50,000 feet,

$$E=\frac{W}{3}\,KT=\frac{W}{3}\times10^{12}\text{ calories } (W\text{ in }KT)$$

For surface bursts viewed from the ground,

$$E=\frac{W}{7}\,KT=\frac{W}{7}\times10^{12}\text{ calories } (W\text{ in }KT)$$

A radiant exposure of approximately 1 cal/sq cm will be received at a slant range of 1 mile from a 1 KT air burst on a clear day.

At a given slant range the radiant exposure for ground targets is proportional to weapon yield.

Time to radiant power minimum:

$$t_{min}=\frac{W^{1/2}}{370}=0.0027\,W^{1/2}\text{ seconds } (W\text{ in }KT)$$

Time to second radiant power maximum:

$$t_{max}=\frac{W^{1/2}}{31.2}=0.032\,W^{1/2}\text{ seconds } (W\text{ in }KT)$$

Second radiant power maximum:
For air bursts under 50,000 feet:

$$P_{max}=4\ W^{1/2}\ KT/\text{sec}=4\ W^{1/2}\times 10^{12}\ \text{cal/sec}\ (W \text{ in } KT)$$

Less than 1 percent of the thermal radiation from a nuclear detonation near sea level is emitted before the radiant power minimum.

II.3. Nuclear

1 KT fission yield makes available 300 megacuries of radioactive fission product gamma activity at a time of one hour after a detonation.

1 curie is that quantity of radioactive material which undergoes 3.7×10^{10} disintegrations per second.

The roentgen is a measure of *quantity of ionization*, and is equivalent to:

83.8 ergs per gram of air; or
1.64×10^{12} ion-pairs per gram of air; or
5.24×10^{7} Mev per gram of air.

0.7 Mev is the approximate mean effective energy for the gamma rays from a residual fission product field.

To obtain the radiation intensity in roentgens per hour three feet above a plane residual fission product field, multiply the concentration of the contaminant in curies per square foot by 120, or in megacuries per square mile by 4.

Total dose in roentgens accumulated to infinite time from one hour after a burst is numerically equal to five times the dose rate in roentgens per hour at $H+1$ hour. (Fission product activity.)

The radioactive decay of gross fission products is approximately exponential with time, so that—

$$I=I_1\ t^{-1.2}$$

where I is the dose rate at any time t, and I_1 is the dose rate at unit time.

The velocity of a thermal neutron ($E=1/40$ ev) is 2,200 meters per second.

Shielding thicknesses in inches required to cut incident gamma radiation by a factor of ten are:

Material	*Initial bomb gamma*	*Residual gamma*
Lead	2.1	1.0
Iron	4.5	2.8
Concrete	18	9.5
Soil	26	14
Water	41	21

As a rough rule of thumb, the area of effect for a given degree of contamination resulting from a nuclear surface burst can be considered directly proportional to the fission yield of the weapon.

Greatest cloud diameter at 9 minutes after burst time (for kiloton yields) is approximately given by—

$$d=10{,}000\ W^{1/3}\ \text{feet}$$

The dose rate inside the bomb cloud is independent of yield (in the kiloton range) and is given by the formula,

$$D=1.31\times 10^{5}t^{-2.06}\ \text{roentgens per hour,}$$

where t is the time after detonation in minutes.

*Table II-1. Standard Atmospheric Conditions**

Geometric altitude ft (meters)	Temp. °F. (°C.)	Pressure pounds/in.² (millibars)	Density lb/ft³ (kg/m3)	Sound velocity ft/sec (cm/sec)
0	59.00	14.692	0.076475	1116.44
(0)	(15.0)	(1013.25)	(1.2250)	(34,029.1)
1,000	55.43	14.17	0.074262	1112.59
(304.79)	(13.02)	(977.17)	(1.1895)	(33,911.7)
2,000	51.87	13.66	0.072099	1108.74
(609.57)	(11.04)	(942.13)	(1.1549)	(33,794.4)
3,000	48.30	13.17	0.069984	1104.87
(914.36)	(9.05)	(908.13)	(1.1210)	(33,676.4)
4,000	44.74	12.69	0.067918	1100.98
(1219.14)	(7.08)	(875.13)	(1.0879)	(33,557.9)
5,000	41.17	12.23	0.065899	1097.09
(1523.9)	(5.09)	(843.11)	(1.0556)	(33,439.3)
10,000	23.36	10.11	0.056483	1077.40
(3047.9)	(−4.80)	(696.94)	(0.90474)	(32,839.2)
15,000	5.55	8.29	0.048137	1057.35
(4571.8)	(−14.69)	(572.06)	(0.77106)	(32,228.0)
20,000	−12.26	6.76	0.040773	1036.92
(6095.7)	(−24.59)	(466.00)	(0.65310)	(31,605.3)
25,000	−30.05	5.46	0.034306	1016.10
(7619.6)	(−34.47)	(376.50)	(0.54951)	(30,970.7)
30,000	−47.83	4.37	0.028657	994.84
(9143.6)	(−44.35)	(301.48)	(0.45903)	(30,322.7)
35,000	65.61	3.47	0.023751	973.14
(10,667.5)	(−54.22)	(239.09)	(0.38044)	(29,661.3)
40,000	−69.70	2.73	0.018895	968.07
(12,191.4)	(−56.49)	(188.23)	(0.30266)	(29,506.8)
45,000	−69.70	2.15	0.014873	968.07
(13,715.3)	(−56.49)	(148.16)	(0.23823)	(29,506.8)
50,000	−69.70	1.69	0.011709	968.07
(15,239.3)	(−56.49)	(116.64)	(0.18755)	(29,506.8)
60,000	−69.70	1.05	0.0072588	968.07
(18,287.1)	(−56.49)	(72.31)	(0.11627)	(29,506.8)

*Reference, U.S. Extension To The ICAO Standard Atmosphere—Tables and Data to 300 Standard Geopotential Kilometers.

*Table II-2. Average Atmosphere**

Geometric altitude	Temperature	Pressure	Density	Sound velocity	Mean free path
Meters (feet)	°C. (°F.)	Millibars (psi)	kg/m^3 (lb/ft^3)	m/sec (ft/sec)	m (ft)
0	+15.0	1013.25	1.2250	340.29	6.6317×10^{-8}
(0)	(+59.0)	(14.69)	(7.648×10^{-2})	(1116.49)	(21.7586×10^{-8})
10,000	−49.90	265.00	4.135×10^{-1}	299.53	1.9646×10^{-7}
(32,810)	(−57.82)	(3.84)	(2.581×10^{-2})	(982.76)	(6.4458×10^{-7})
20,000	−56.49	55.293	8.891×10^{-2}	295.07	9.1374×10^{-7}
(65,620)	(−69.70)	(0.802)	(5.55×10^{-3})	(968.12)	(29.9798×10^{-7})
30,000	−41.92	11.855	1.786×10^{-2}	304.83	4.5484×10^{-6}
(98,430)	(−43.46)	(1.72×10^{-1})	(1.11×10^{-3})	(1000.15)	(14.9233×10^{-6})
40,000	−12.25	2.9977	4.003×10^{-3}	323.80	2.0296×10^{-5}
(131,240)	(+9.95)	(4.35×10^{-2})	(2.50×10^{-4})	(1062.39)	(6.6591×10^{-5})
50,000	+9.50	8.786×10^{-1}	1.083×10^{-3}	337.03	7.5023×10^{-5}
(164,050)	(+49.1)	(1.27×10^{-2})	(6.76×10^{-5})	(1105.80)	(24.6150×10^{-5})
60,000	−19.94	2.581×10^{-1}	3.492×10^{-4}	321.71	2.3266×10^{-4}
(196,860)	(−3.90)	(3.74×10^{-3})	(2.18×10^{-5})	(1055.53)	(7.6336×10^{-4})
70,000	−53.82	6.321×10^{-1}	1.004×10^{-4}	296.88	8.0912×10^{-4}
(229,670)	(−64.89)	(9.17×10^{-3})	(6.27×10^{-6})	(974.06)	(26.5472×10^{-4})
80,000	−76.29	1.224×10^{-2}	2.165×10^{-5}	281.26	3.752×10^{-3}
(262,480)	(−105.34)	(1.77×10^{-4})	(1.35×10^{-6})	(922.81)	(12.3103×10^{-3})
90,000	−76.29	2.258×10^{-3}	3.995×10^{-6}	281.26	2.033×10^{-2}
(295,290)	(−105.34)	(3.27×10^{-5})	(2.49×10^{-7})	(922.81)	(6.6703×10^{-2})
100,000	−66.15	4.629×10^{-4}	7.123×10^{-7}	—	1.043×10^{-1}
(328,100)	(−87.09)	(6.71×10^{-6})	(4.45×10^{-8})	—	(3.4221×10^{-1})
110,000	−45.06	1.187×10^{-4}	1.589×10^{-7}	—	4.481×10^{-1}
(360,910)	(−49.11)	(1.72×10^{-6})	(9.92×10^{-9})	—	(14.7022×10^{-1})
120,000	−40.46	3.610×10^{-5}	1.216×10^{-7}	—	1.629
(393,720)	(−40.83)	(5.23×10^{-7})	(7.59×10^{-9})	—	(5.3447)
130,000	+11.74	1.256×10^{-5}	1.299×10^{-8}	—	5.291
(426,530)	(+53.13)	(1.82×10^{-7})	(8.11×10^{-10})	—	(17.3598)
140,000	+89.53	5.336×10^{-6}	4.296×10^{-9}	—	1.585×10^{-1}
(459,340)	(+193.17)	(7.74×10^{-8})	(2.68×10^{-10})	—	(5.2004×10^{-1})
150,000	+166.82	2.698×10^{-6}	1.779×10^{-9}	—	3.803×10^{-1}
(492,150)	(+332.31)	(3.91×10^{-8})	(1.11×10^{-10})	—	(12.4776×10^{-1})
160,000	+243.61	1.531×10^{-6}	8.554×10^{-10}	—	7.872×10^{-1}
(524,960)	(+470.55)	(2.22×10^{-8})	(5.34×10^{-11})	—	(25.8280×10^{-1})
225,000	+494.59	1.308×10^{-7}	4.308×10^{-11}	—	1.368×10^{-3}
(738,225)	(+922.35)	(1.90×10^{-9})	(2.69×10^{-12})	—	(4.4884×10^{-3})
500,000	+1120.73	8.541×10^{-10}	1.197×10^{-13}	—	3.807×10^{-5}
(1,640,500)	(+2049.51)	(1.24×10^{-11})	(7.47×10^{-15})	—	(12.4908×10^{-5})

*Handbook of Geophysics, for Air Force Designers—1957.

FRACTIONAL POWERS AND DIMENSION SCALING NOMOGRAM

Figure II-1A presents several fractional powers of numbers between 1 and 100,000. The fractional powers presented are those which are necessary in the application of various scaling procedures presented elsewhere in the text.

Figure II-1B is a nomogram from which actual dimensions may be obtained from various scaled dimensions for yields from 0.1 KT to 100 MT. The scaling power for which the scaled dimensions are applicable is indicated at the top of the scale in each case. A straight line connecting a yield with any scaled dimension will cross the actual dimension scale at the proper value according to the scaling which is being used. The dimensions may be in any units for which scaling is given, but the scaled dimension and the actual dimension will always be in the same units.

Examples.

1. *Given:* A 500 KT weapon is to be burst at the minimum height of burst at which fallout is not expected.

Find: The actual height of burst at which the weapon is to be detonated.

Solution: From paragraph 4.3*d* the minimum burst height for a 500 KT weapon at which fallout is not expected is 180 $W^{0.4}$ feet.

a. From figure II-1A:

$(500)^{0.4}=12$

$180\times 12=2{,}160$ feet. *Answer.*

b. From figure II-1B:

A straight line connecting 500 on the yield scale with 180 on the 2/5 power scaled dimension scale crosses the actual dimension scale at 2,160. The desired height of burst is thus *2,160 feet. Answer.*

(*Note.* Conversion from one scaling procedure to another is particularly easy with the nomogram. The line mentioned above crosses the cube root scaled dimension scale at 270. Thus 180 $W^{0.4}$ feet corresponds to 270 $W^{1/3}$ feet for 500 KT.)

2. *Given:* A ground range of 2,580 yards from an 80 KT surface burst.

Find: The proper scaled range for determining overpressure from the 1 KT graphs.

Solution: The applicable scaling is:

$$\frac{d_1}{d_2}=\frac{W_1^{1/3}}{W_2^{1/3}}.$$

a. From figure II-1A:

$$(80)^{1/3}=4.3$$

$$d_1=\frac{W_1^{1/3}\times d_2}{W_2^{1/3}}=\frac{1\times 2{,}580}{4.3}=600 \text{ yards.}$$

b. From figure II-1B:

A straight line from 80 on the yield scale through 2,580 on the actual dimension scale intersects the cube root scaled dimension scale at 600. The scaled distance is thus 600 yards. *Answer.*

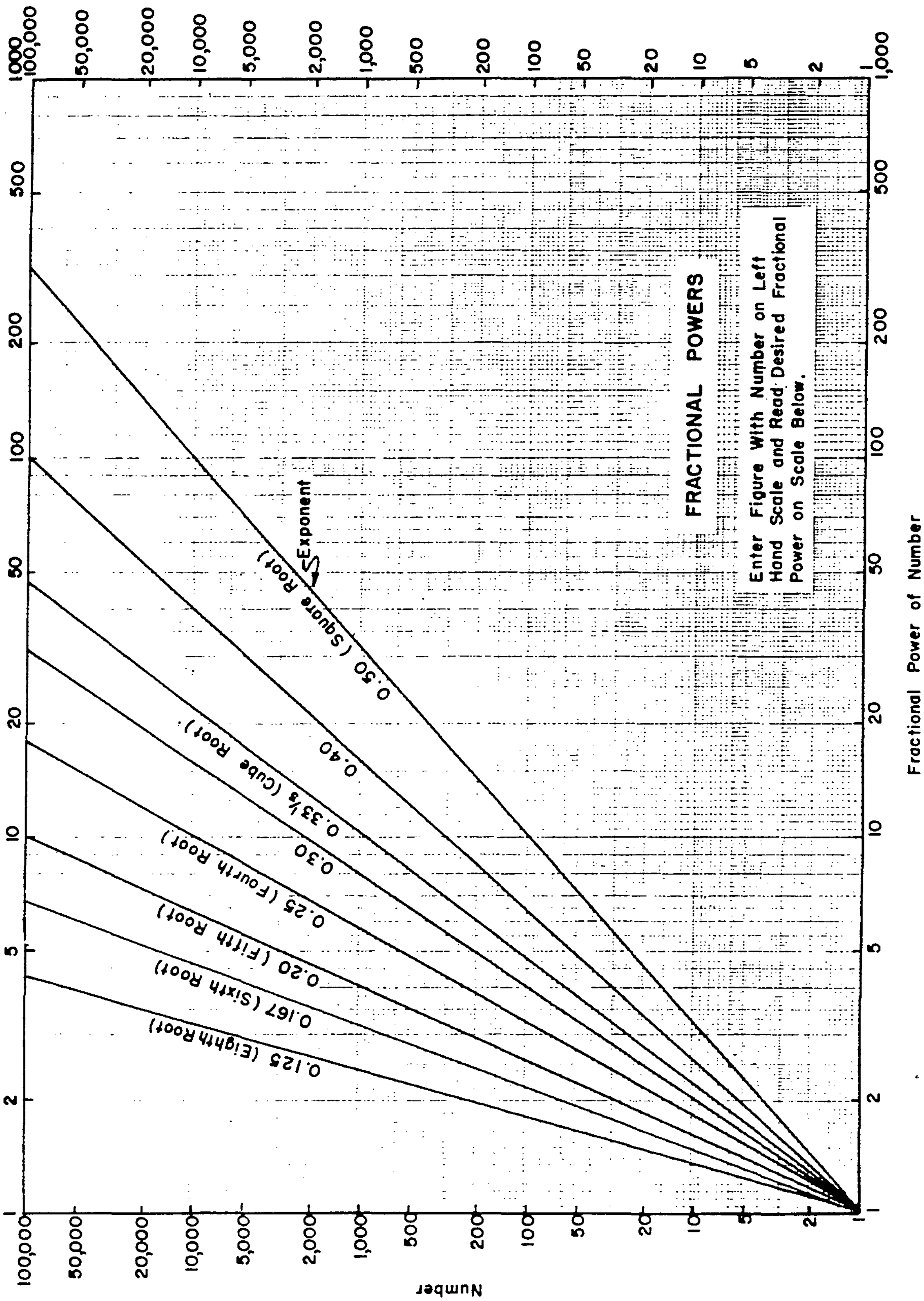
FRACTIONAL POWERS
Enter Figure With Number on Left Hand Scale and Read Desired Fractional Power on Scale Below.
Exponent
0.50 (Square Root)
0.40
0.33⅓ (Cube Root)
0.30
0.25 (Fourth Root)
0.20 (Fifth Root)
0.167 (Sixth Root)
0.125 (Eighth Root)
Number
Fractional Power of Number
100,000
50,000
20,000
10,000
5,000
2,000
1,000
500
200
100
50
20
10
5
2
1

DIMENSION SCALING NOMOGRAM

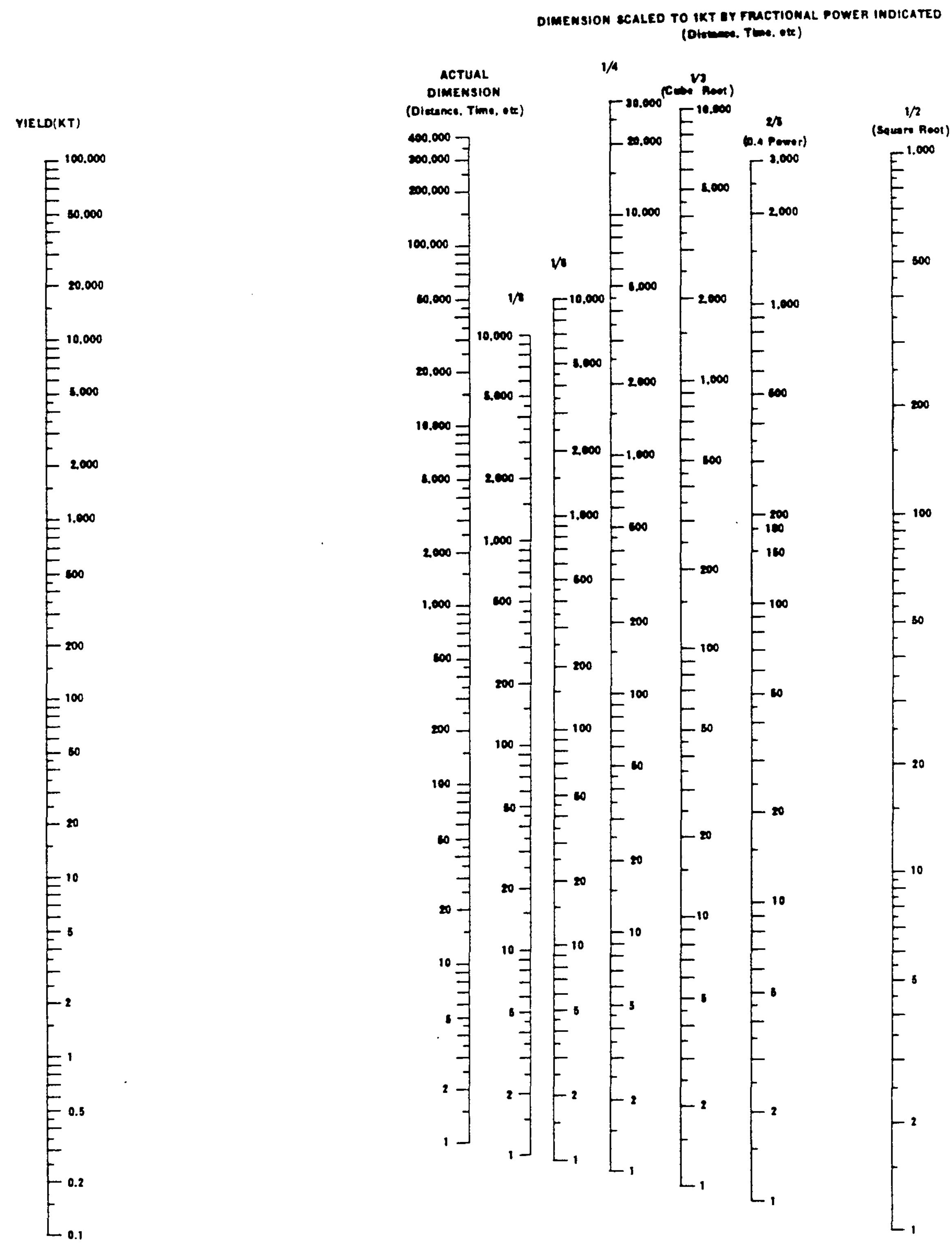

NOMOGRAM RELATING HEIGHT OF BURST HORIZONTAL DISTANCE AND SLANT RANGE

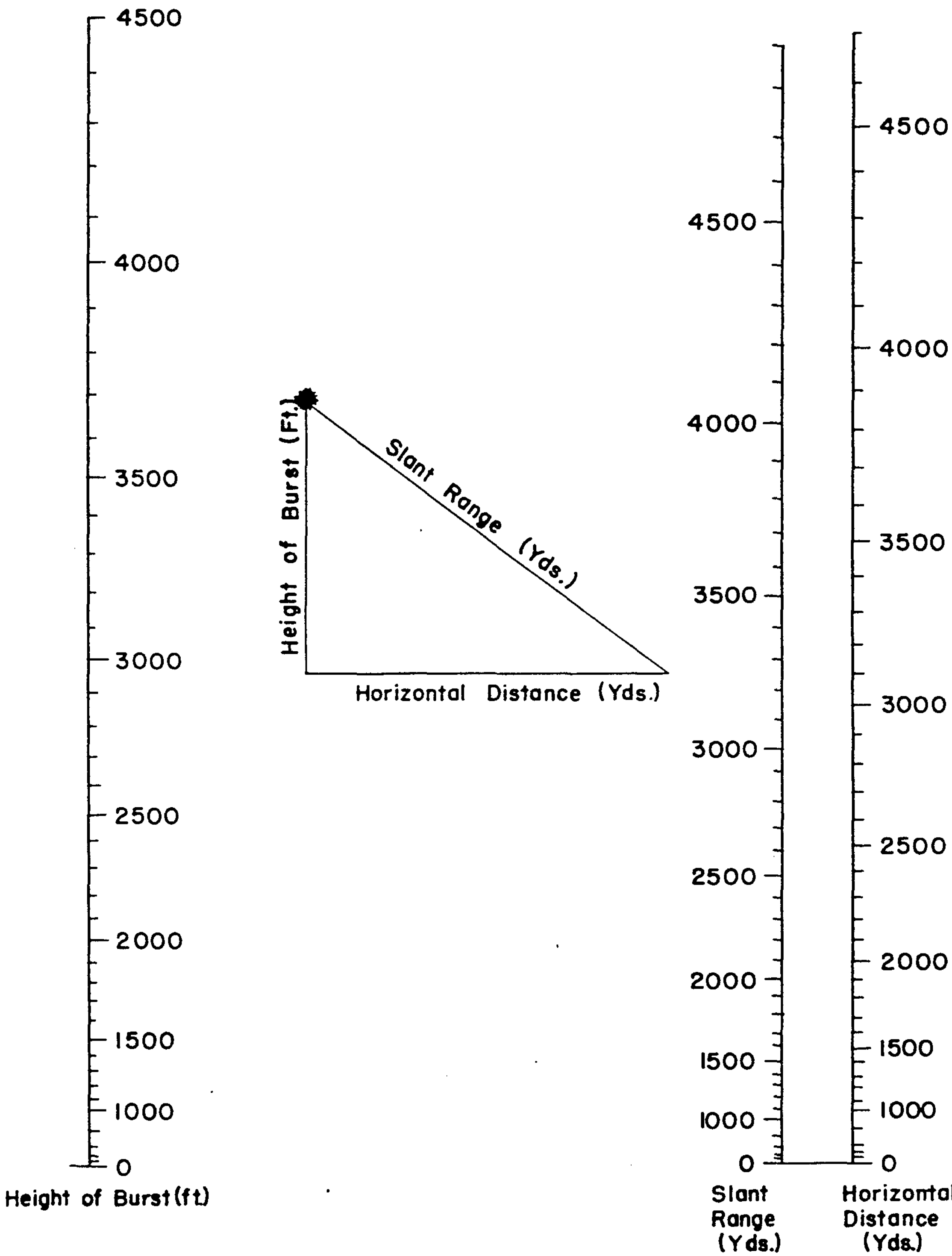

RELATIVE AIR DENSITY
(STANDARD ATMOSPHERE)

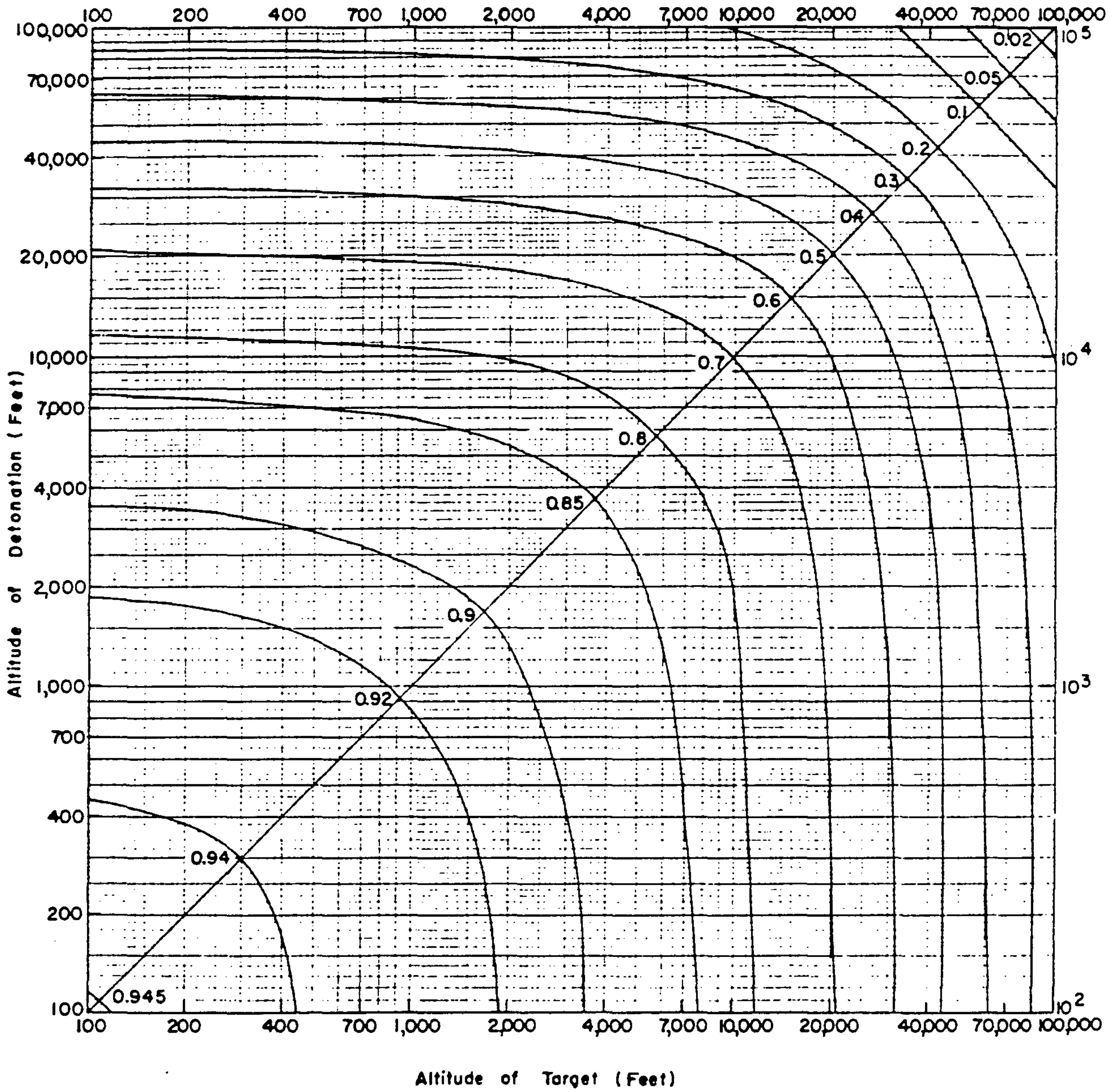

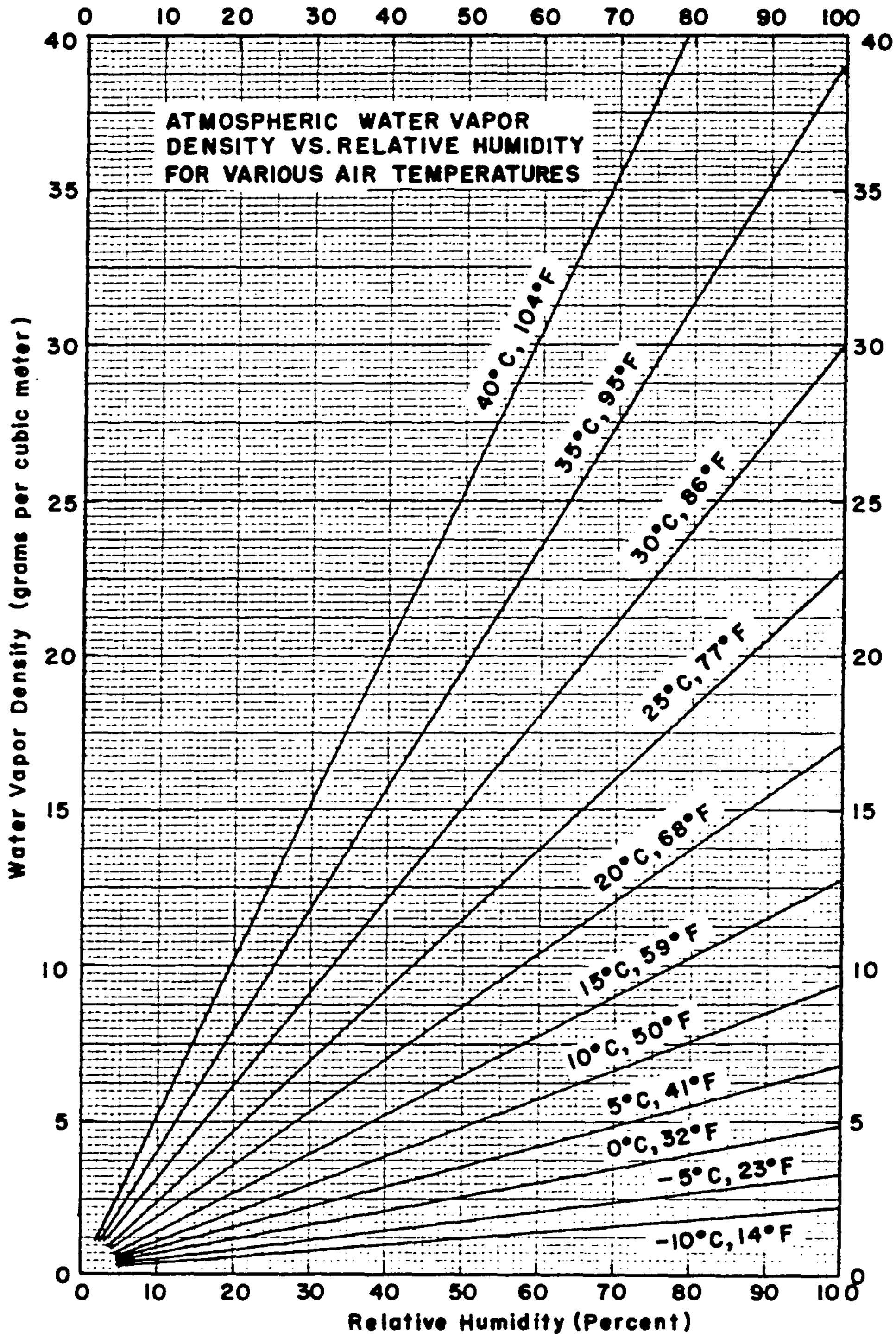
ATMOSPHERIC WATER VAPOR
DENSITY VS. RELATIVE HUMIDITY
FOR VARIOUS AIR TEMPERATURES
Water Vapor Density (grams per cubic meter)
Relative Humidity (Percent)
40°C, 104°F
35°C, 95°F
30°C, 86°F
25°C, 77°F
20°C, 68°F
15°C, 59°F
10°C, 50°F
5°C, 41°F
0°C, 32°F
-5°C, 23°F
-10°C, 14°F
0
10
20
30
40
50
60
70
80
90
100
5
15
25
35

III
Glossary

APPENDIX III
GLOSSARY

Absorption coefficient—A number characterizing a given material with respect to its ability to absorb radiation. The linear absorption coefficient refers to the ability of a given material to absorb radiation per unit thickness; it is expressed in reciprocal units of thickness. The mass absorption coefficient refers to the ability of a given material to absorb radiation per unit mass; it is expressed in units of area per unit mass, and it is equal to the linear absorption coefficient divided by the density of the absorbing material.

Acceleration—Time rate of change of velocity. The acceleration due to gravity (g) is 32.2 ft/sec^2.

Activity—The rate of decay of radioactive material expressed as the number of nuclear disintegrations per second.

Air burst—See *Burst types*.

Albedo—The fraction of the incident radiation reflected in any manner by a material.

Alpha particle—A particle ejected spontaneously from the nuclei of some radioactive elements. It is identified with the helium nucleus, which has an atomic weight of four and an electric charge of plus two.

Amplitude—The maximum displacement of an oscillating particle from its position of equilibrium.

Angle of incidence—The angle between the perpendicular to a surface and the direction of propagation of a wave.

Apparent crater—See *Crater*. The visible crater remaining after a nuclear detonation.

Atmospheric transmissivity ($\overline{T}$)—The fraction of the radiant exposure received at a given distance after passage through the atmosphere relative to that which would have been received at the same distance if no atmosphere were present.

Atomic cloud—An all-inclusive term, identified as the hot gases, the smoke and the vapors formed in the ball of fire produced by the burst of a nuclear weapon, which from large yield weapons may penetrate the tropopause and spread out because of temperature inversions and winds existing aloft. The cloud contains radioactive fission products. See *Fireball*.

Atomic weapon—See *Nuclear weapon*.

Attenuation—Reduction in intensity of radiation or blast by passage through any medium.

Ball of fire—See *Fireball*.

Base surge—A cloud which rolls out from the bottom of the column produced by a subsurface burst of a nuclear weapon. For underwater bursts the surge is, in effect, a cloud of liquid droplets which has the property of flowing almost as if it were a homogeneous fluid. For subsurface land bursts the surge is made up of small solid particles, but still behaves like a fluid.

Beta particle—A small particle ejected spontaneously from a nucleus of either natural or artificially radioactive elements. It carries a charge of one electronic unit and has an atomic weight of 1/1840. The charge may be either positive (positrons) or negative (electrons). The charge is thus one-half that of the alpha particle and the mass is 1/7360 that of an alpha particle. The electron is much lighter than the hydrogen atom (atomic weight = 1), which is the lightest atom.

Blast wave—See *Shock wave*. The shock wave transmitted through the air as the result of an explosion, through usage, is referred to as a blast wave or air blast.

Blast yield—That portion of the total energy of a nuclear detonation which manifests itself as a blast or shock wave.

Bomb debris—See *Weapon debris*.

Breakaway—The onset of a condition in which the shock front moves away from the periphery of the expanding ball of fire.

Breaking wave—A wave of such steep slope that it is unable to maintain its shape and hence loses height by tumbling or falling over.

Burst geometry—The location of a nuclear detonation with respect to the ground surface, water surface, or bottom.

Burst types:

Air burst—The explosion of a nuclear weapon at such a height that the weapon phenomenon of interest is not significantly modified by the earth's surface. For example, these heights are such that for—

Blast—the reflected wave passing through the fireball does not overtake the incident wave above the fireball ($\sim 160\ W^{1/3} \pm 15$ percent).

Thermal radiation—the apparent thermal yield viewed from the ground is not affected by heat transfer to the earth's surface nor by distortion of the fireball by the reflected shock wave ($\sim 180\ W^{0.4} \pm 20$ percent for 10 KT to 100 KT and ± 30 percent for other yields).

Fall-out—militarily significant local fall-out of radioactive material will not occur. For $W<100$ KT, $H_B=100\ W^{1/3}$; see Section 4.3 for reliability discussion; for $W>100$ KT, in the absence of data, H_B may be conservatively taken to equal $180\ W^{0.4}$. For certain other phenomena of interest, e. g., neutron induced activity, initial gamma or neutron flux, the height of burst at which an air burst occurs is difficult or impossible to distinguish.

Surface burst—the explosion of a nuclear weapon at the earth's surface (either ground or water surface).

Subsurface burst (underground or underwater)—the explosion of a nuclear weapon in which the center of the detonation lies at any point beneath the earth's surface (either ground or water surface).

Calorie—The amount of heat required to raise the temperature of 1 gram of water from 15° C. to 16° C. at 760 mm Hg pressure.

Camouflet—See *Crater*.

Casualty—As used in this manual, an individual who, as a result of injury, requires medical attention.

Cavitation—The separation of the water particles and the forming of cavities, as a result of water's inability to withstand the tensional wave reflected from the water surface.

Cloud chamber effect—See *Condensation cloud.*

Column—The visible column of particulate matter which may extend to the tropopause (the boundary between the troposphere and the stratosphere) subsequent to the explosion of a nuclear weapon. Also, the hollow cylinder of material thrown up from a subsurface nuclear detonation.

Combat ineffective—An individual whose injuries are of such nature that he is no longer capable of carrying out his assigned task.

Condensation cloud—A mist or fog which temporarily surrounds the ball of fire following a nuclear detonation in a comparatively humid atmosphere. As it is similar to the cloud observed by physicists in the Wilson cloud chamber, it is also called the "Wilson cloud." Rapid cooling of the previously heated air surrounding the ball of fire during the negative pressure phase of the shock wave causes the moisture in the air to condense temporarily, forming a cloud. The cloud is dispelled within a second or so upon return of the air pressure to normal.

Contamination (radioactive)—The deposit of radioactive material on the surface of structures, areas, personnel, or objects. See *Decontamination.*

Contour method—The representation of the degree of contamination resulting from a nuclear burst by the use of contour lines to connect points of equal radiation dose or dose rate. See *Isodose lines.*

Coupling—The energy transfer of a shock wave traveling in one medium which produces a shock wave in a second medium at their common interface.

Crater—The pit, depression, or cavity formed in the surface of the earth by an explosion. May range from saucer shaped to conical, depending largely on the depth of burst. In the case of a deep underground burst no rupture of the surface may occur. The resulting cavity is termed a camouflet. See also *True crater* and *Apparent crater.*

Crater depth—The maximum depth of the crater measured from the deepest point of the pit to the original ground level.

Crater radius—The average radius of the crater measured at the level corresponding to the original surface of the ground.

Critical radiant exposure (Q_c)—The radiant exposure required for a particular effect on a material. The unit of critical radiant exposure is the cal/sq cm.

Curie—By definition, the quantity of any radioactive nuclide in which the number of disintegrations per second is 3.7×10^{10}.

Decontamination—The process of removal of contaminating radioactive material from an object, a structure, or an area. The problem of decontamination consists essentially of reduction of the level of radioactivity, and thus reduction of the hazard it imposes, to a reasonably safe limit. See *Contamination*.

Diffraction—The bending of waves around the edges of objects.

Diffraction loading—The forces exerted upon an object or structure by the blast wave overpressures as the shock front strikes and engulfs it.

Direct shock wave—A shock wave traveling through the medium in which the explosion occurred, without having encountered an interface, is referred to as the direct shock wave.

Dose (*dosage*)—The total amount of nuclear or ionizing radiation absorbed by an individual exposed to the radiating source, such as would be received from a nuclear explosion and resulting radioactive products. X-rays and gamma ray doses are measured in roentgens; alpha, beta, and neutron doses are measured in *rem* or *rep*. See *Dose-rate*.

Dose-rate—The amount of nuclear radiation received per unit of time. See *Dose*.

Dosimeter—An instrument for measuring the amount of radiation received. Dosimeters include film badges, pocket chambers, and pocket dosimeters; also glass, crystal, and liquid dosimeters.

Drag loading—The forces exerted upon an object or structure by the dynamic pressures from the blast wave of an explosion, influenced by certain characteristics (primarily the shape) of the object or structure.

Ductility—The ability of a material or object to undergo large permanent deformations without rupture.

Dynamic pressure (q)—$q = \frac{1}{2}\rho u^2$, where ρ is the density of the medium and u is the particle velocity behind the shock front. The drag force on an object is directly proportional to the dynamic pressure.

Dynamic pressure impulse—See *Impulse*.

Electromagnetic radiation—Radiation made up of oscillating electric and magnetic fields and propagated with the speed of light. Includes gamma radiation, X-rays, ultraviolet, visible and infrared radiation, and radar and radio waves.

Electromagnetic spectrum—The frequencies (or wave lengths) present in a given electromagnetic radiation. A particular spectrum could include a single frequency or a wide range of frequencies.

Energy partition—The distribution of the total energy released by a nuclear detonation among nuclear radiation, thermal radiation, and blast. The exact distribution is a function of time and of the weapon yield and the medium in which the weapon is detonated.

Factor—A multiplier, frequently used to indicate range of coverage. For example, "correct within a factor of two" means correct within a possible range of values between twice and one-half the stated value.

Fall-out—The process of the gradual settling out of small particles and the rapid fall of larger particles thrown up by the explosion. The local or militarily significant fall-out area may extend from the crater or immediate vicinity of the detonation out to distances of many miles, depending upon meteorological and surface conditions. Detectable amounts of fall-out may occur over distances of hundreds or thousands of miles for several months after an explosion.

Film badge—A photographic film packet in the form of a badge, carried by personnel, for obtaining a measure of gamma ray dosage. See *Dosimeter*.

Fireball—The visible luminous sphere of hot gases formed by a nuclear weapon.

Fire storm—A wind blowing toward a large burning area from all sides, reaching as much as 40 miles per hour and persisting for perhaps several hours caused by the updraft of heated air over the burning area. This phenomenon may occur after a nuclear explosion over or in a city or other combustible area. The conditions required to initiate a fire storm are poorly understood at this time. The winds of a fire storm tend to limit the spread of the fire causing the storm.

Fission—The process of splitting an atom, usually into two major portions. This is the type of fission that occurs in materials used in nuclear weapons. The fission of U^{235} or Pu^{239} and certain other radionuclides releases large amounts of energy in extremely short intervals of time.

Fission products—The substances produced as a result of the fission of the nuclear material of nuclear weapons. The fission of uranium 235, for example, yields more than 60 direct products, sometimes called fission fragments, which are formed by the actual splitting of the uranium nuclei. These direct products, being radioactive, immediately begin to decay, forming additional daughter products.

Free air—A region of homogeneous air sufficiently remote from reflecting surfaces or other objects that the characteristics of the direct shock are not modified in any way by reflected shocks or other disturbances arising from scattering objects.

Free air overpressure (sometimes called *free air pressure*)—The unreflected pressure in excess of atmospheric or ambient pressure created in the air by the incident shock of any explosion.

Fusion—The process whereby the nuclei of light elements combine to form the nucleus of a heavier element; not to be confused with nuclear fission, which is the process whereby the nucleus of a heavy element splits into two nuclei of lighter elements.

Gamma rays—Electromagnetic radiations, similar to X-rays, originating from the atomic nucleus.

Ground zero (*GZ*)—The point on the surface of land or water vertically below or above the center of a burst of a nuclear weapon; also called surface zero.

Height of burst—The height above the earth's surface at which a weapon is detonated. *Altitude*, by contrast, is the height above mean sea level.

Hogging—The causing of tensile stresses above and compressive stresses below the longitudinal neutral axis of a ship by a wave crest passing amidships.

Hot spots—Regions in a contaminated area in which the level of radioactive contamination is considerably higher than in neighboring regions. See *Contamination*.

Impulse (*I*)—The product of the average force and the time during which it acts at a given point, or the integral of the curve representing variation of force with time, with integration over the time of interest. In considering the effectiveness of a shock wave in producing damage, it is generally more convenient to employ the concepts of *overpressure impulse* and *dynamic pressure impulse*. The *overpressure impulse* (I_p) of the positive phase of a blast wave is the integral of the curve representing the variation of overpressure with time, the integration being performed from $t=0$, the time of arrival of the shock front at a given location, to $t=t^+$, the end of the positive phase. The *dynamic pressure impulse* (I_q) is a similar integral of the dynamic pressure-time curve.

Induced radioactivity—Radioactivity resulting from certain nuclear reactions in which exposure to radiation results in the production of unstable nuclei. Many materials near a nuclear explosion enter into this type of reaction, notably as a result of neutron bombardment.

Induced shock wave—The shock wave induced in a medium when a shock wave traveling in another medium crosses the interface between the two media.

Infrared—That portion of the electromagnetic spectrum occurring between the wave lengths 0.7 and 12 microns.

Initial radiation—The nuclear radiation accompanying a nuclear explosion and emitted from the resultant ball of fire and atomic cloud. It includes the neutrons and gamma rays given off at the instant of the explosion, and the alpha, beta, and gamma rays emitted in the rising ball of fire and column. In contrast to residual radiation, its effect on persons and objects on the earth's surface is terminated about ninety seconds after the explosion, because of the removal of the final source (fission products in the atomic cloud) from within radiation range of the earth at the end of that period of time. See *Residual radiation*.

Intensity—Energy incident per unit surface. See also *Radiant exposure* and *Radiant power*.

Inversion (*atmospheric temperature inversion*)—A region in the atmosphere in which the temperature rises with increasing altitude instead of dropping, as it does in the more general case.

Ionization—The production of charged particles (ions) by dislodging electrons from atoms or molecules.

Irradiance (H)—The incident radiant energy per unit time per unit area. The unit of irradiance is the cal/sq cm/sec.

Isobaric—Constant pressure condition.

Isodose lines—A term applied to imaginary contours in a radioactive field on which the total accumulated radiation dosage is the same.

Kelvin scale—The absolute temperature scale for which the zero is $-273°$ C. Conversion from centigrade to Kelvin is made by adding 273° C. to the centigrade reading.

KT (kiloton)—Refers to the energy release of a thousand tons of TNT, where 1 ton equals 2,000 pounds and where the energy content of TNT is defined as 1,100 calories per gram.

Lethal gust envelope—The boundary of the area in any given plane within which the gust loading effects from a detonation inflict sufficient structural damage to destroy a given aircraft.

Lip height—The height above the original surface to which earth is piled around the crater formed by an explosion.

Loading—The forces imposed upon an object.

Luminous—See *Visible*.

Mach stem—The shock formed by the fusion of the incident and reflected shocks from an explosion. The term is usually used with reference to an air-propagated wave reflected from the surface of the earth, generally nearly vertical to the reflecting surface. See *Shock front*.

Median lethal dose—The amount of radiation received over the whole body which would be fatal to about 50 percent of human beings, animals, or organisms. It is usually accepted that a dose of 400 to 450 roentgens received over the whole body in the course of a few minutes represents the median lethal dose for human beings. The term is sometimes abbreviated as MLD or LD–50.

Micron (μ)—A unit of length equal to 10^{-6} meter, 10^{-3} millimeter, or 10^4 Angstrom units.

Millibar—One thousand dynes per square centimeter, a unit of measure of atmospheric pressure.

MT (*megaton*)—Refers to the energy release of a million tons of TNT (10^{15} calories).

Negative phase—That portion of the blast wave in which pressures are below ambient atmospheric pressure.

Neutron—An electrically neutral particle which is one of the fundamental particles making up all atoms. It has nearly the same weight as the hydrogen nucleus (atomic weight 1). The neutron under appropriate conditions is capable of causing fission of U^{235} or Pu^{239} and certain other radionuclides. In the fission process other neutrons are produced, which can cause fission in additional U^{235} or Pu^{239} atoms. This multiplication process, triggered by neutrons, gives rise to the chain reaction which makes nuclear explosions possible.

Nominal weapon—A weapon with a 20 KT yield.

"*Non-linear zone*"—A wedge-shaped zone in water which increases in depth as the range from the burst point increases and within which anomalous reflections affect the underwater pressure history.

Nuclear radiation—Any or all of the radiations emitted as a result of the radioactive decay of a nucleus. The radiations include gamma radiation (of electromagnetic character) and particle radiation (alpha particles, positive and negative beta particles, and neutrons).

Nuclear weapon—A general name given to any weapon in which the explosion results from the energy released by reactions involving atomic nuclei, either fission or fusion or both. Also called *Atomic weapon*.

Nuclide—A general term referring to all nuclear species, both stable and unstable, of the chemical elements as distinguished from the two or more nuclear species of a single chemical element which are called isotopes.

Overpressure—The transient pressure, usually expressed in pounds per square inch, exceeding existing atmospheric pressure manifested in the blast wave from the explosion. During some period of the passage of the wave past a point, the overpressure is negative.

Overpressure impulse—See *Impulse*.

Period of vibration (*period*)—The time for one complete cycle of oscillation or vibration.

Plastic deformation—That deformation from which a deformed object does not recover upon removal of the deforming forces.

Popcorning—The ejection of dust particles from certain types of surface upon absorption of the thermal radiation emitted by a nuclear detonation.

Positive phase—That portion of the blast wave in which pressures are above ambient atmospheric pressure.

Precursor—A pressure wave which precedes the main blast wave of a nuclear explosion.

Radiant energy—See *Thermal radiation*.

Radiant exposure (Q)—The incident radiant energy per unit area, expressed in cal/sq cm. Also referred to as *Intensity*.

Radiant power (P)—Time rate of radiant energy emission. Also sometimes referred to as *Intensity*. The units of radiant power are KT/sec. or cal/sec.

Radioactive—Refers to the state of a material in which the atoms decay spontaneously by the emission of nuclear radiation.

Rarefaction wave—When a shock wave in a medium strikes the interface between this medium and a less dense medium, part of the energy of the shock wave induces a shock wave in the less dense medium. The remainder of the energy forms a rarefaction or tensile wave which travels back through the denser medium.

Reflected pressure—The pressure along a surface at the instant a blast wave strikes the surface.

Reflected shock wave—When a shock wave traveling in a medium strikes the interface between this medium and a denser medium, part of the energy of the shock wave induces a shock wave in the denser medium and the remainder of the energy results in the formation of a reflected shock wave which travels back through the less dense medium.

Relative air density—The ratio of the air density under a given condition to the air density at 0° C. and 1,013 millibars.

Rem (*roentgen equivalent mammal*)—One rem is the quantity of ionizing radiation of any type which, when absorbed by man or other mammal, produces a physiological effect equivalent to that produced by the absorption of 1 roentgen of X-ray or gamma radiation.

Rep (*roentgen equivalent physical*)—The quantity of ionizing radiation which upon absorption in the body tissue produces 93 ergs of energy per gram of tissue.

Residual radiation—Nuclear radiation emitted by the radioactive material after a nuclear burst. Following a burst, the radioactive residue is in the form of fission products, unfissioned nuclear material, and material such as earth and water constituents, exposed equipment, etc., in which radioactivity may have been induced by neutron bombardment. It is sometimes referred to as lingering radiation. See *Initial radiation*.

Response—The action of an object under the applied loading.

Rise time—The time interval from blast wave arrival to the time of peak overpressure in the blast wave.

Roentgen—A unit of X- or gamma-ray dose. The exposure dose of X- or gamma-radiation such that the associated corpuscular emission per 0.001293 gram of air produces, in air, ions carrying one electrostatic unit of quantity of electricity of either sign.

Scaling wind—An idealized representation of the winds aloft in the atmosphere used to draw the fall-out contours for contaminating bursts.

Scattering—Change in direction of propagation of radiation caused by collision with particles.

Scavenging—That process by which fission products are removed from the radioactive cloud by becoming attached to earth, rain, or other particles.

Shielding—1. Material of suitable thickness and physical characteristics used to protect personnel from radiation during the manufacture, handling and transportation of fissionable and radioactive materials.

2. Obstructions which tend to protect personnel or materials from the effects of a nuclear explosion.

Shock front—The boundary at which the medium being traversed by a shock or blast wave undergoes abrupt changes in velocity, pressure, and temperature.

Shock strength—The ratio of the peak blast wave overpressure plus ambient pressure to the ambient pressure.

Shock wave—The steep frontal compression or pressure discontinuity rapidly advancing through a medium as the consequence of a sudden application of pressure to the medium. Its form depends on the magnitude of the pressure and the displacement of the medium as the wave progresses. In soil the shock wave is commonly referred to as the ground shock; in water, the water shock; and in air, the air blast.

Slant range—The direct distance between an explosion and a point.

Slug—That mass to which a force of one pound imparts an acceleration of one foot per second per second.

Spectral distribution—Refers to the distribution of energy by wave length over the electromagnetic spectrum.

Subsurface burst—See *Burst types*.

Surface burst—See *Burst types*.

Tensile wave—See *Rarefaction wave*.

Thermal energy—See *Thermal radiation*.

Thermal pulse—The radiant power vs. time pulse from a nuclear weapon.

Thermal radiation—Electromagnetic radiation from a nuclear weapon which is emitted in the wavelength range from 0.2 micron in the ultraviolet, through the visible, to 12 microns in the infrared. Also called *Thermal energy* and *Radiant energy*.

Thermal yield—That part of the total yield of a nuclear weapon which appears as thermal radiation. See *Thermal radiation*.

Thermonuclear—An adjective referring to the process involving the fusion of light nuclei such as those of deuterium and tritium.

TNT effects equivalence—The expressing of the effect of a particular phenomenon of a nuclear detonation in terms of the amount of TNT which would produce the same effect.

TNT energy equivalence—Total energy of a nuclear detonation expressed in terms of the amount of TNT required to produce an equivalent energy.

Tolerance dose—The amount of radiation which may be received by an individual within a specified period with negligible effect.

Transition zone (region)—A zone extending above the earth's surface in which the weapon phenomenon of interest from a burst in the zone will be modified by the presence of the earth's surface. See ***Burst types: Air burst*** for extent of this zone for various phenomena.

Transmissivity—See ***Atmospheric transmissivity***.

Triple point—The intersection of the incident, reflected, and fused shock fronts produced by an explosion in the air. Because of the variation of the angle of incidence as the blast wave expands, and because the reflected wave, in a heated, denser medium, travels faster than the incident wave, the height of the triple point increases with the distance from the explosion. See *Mach stem*.

Tropopause—The boundary between the troposphere and the stratosphere.

True crater—See *Crater*. The crater excluding fall-back material.

Ultraviolet—That portion of the electromagnetic spectrum occurring between the wavelengths 0.2 and 0.4 micron.

Underground burst—See *Burst types*.

Underwater burst—See *Burst types*.

Visible—That portion of the electromagnetic spectrum occurring between 0.4 and 0.7 micron. The term luminous also is applied to radiation in this region.

Visibility—The horizontal distance at which a large, dark object can just be seen in daylight near the horizon.

Wave length—The distance between two similar and successive points on an alternating wave, as between maxima.

Wave train—A series of alternating crests and troughs of a wave system resulting from a surface disturbance.

Weapon debris—The residue of a nuclear weapon after it has exploded; that is, the materials used for the casing and other components of the weapon, plus unexpended plutonium or uranium, together with fission products.

Wilson cloud—See *Condensation cloud*.

Wind shear—A relatively abrupt change with altitude of wind direction or magnitude.

Yield (*W*)—The energy released in a nuclear explosion, usually measured by the estimated equivalent amount of TNT required to produce the same energy release. See *TNT energy equivalence*.

BLANK

IV
Bibliog.

APPENDIX IV
BIBLIOGRAPHY

This biblography contains many of the sources of data and information contained in this volume other than weapon test reports. It should not be considered inclusive, however, of all sources actually used. Many of the references listed herein contain extensive bibliographies on a particular subject. Further assistance in locating specific test data may be obtained from *Cumulative Subject Guide to Weapons Test Information*, TID 9004 (8th Rev.) (S) or the current *Abstracts of Weapon-Test Reports*, both published by Technical Information Service, Oak Ridge, Tennessee. Identification of Corporate Author Codes appears on the last page of this appendix.

GENERAL

1. *The Effects of the Atomic Bomb on Hiroshima, Japan*, Volumes I, II, III (Physical Damage Div. of U. S. Strategic Bombing Survey), May 1947 (U).
2. *The Effects of the Atomic Bomb on Nagasaki, Japan*, Volumes I, II, III (Physical Damage Div. of U. S. Strategic Bombing Survey), June 1947 (U).
3. *The Effects of Nuclear Weapons*, U. S. Govt. Printing Off., 1957 (U).

BLAST AND SHOCK PHENOMENA

1. *Airblast Peak Pressure Along the Water Surface from Shallow Underwater Explosions*, NAVORD 2571, C. R. Niffenegger (NOL), 1 Aug 52 (C).
2. *Behavior of Missiles from Underground Explosions at Dugway Covering Research from April to October 1951*, SRI-317-TR-5, R. B. Vaile, Jr. (SRI), Nov 51 (S).
3. *The Behavior of Soils Under Dynamic Loadings. III. Final Report on Laboratory Studies*, R. V. Whitman, et al. (MIT), Aug 54 (U).
4. *The Behavior of Soils Under Dynamic Loadings. IV. Review and Preliminary Correlation of Laboratory and Field Studies*, R. V. Whitman (MIT), Jun 55 (C).
5. *Blast Wave*, LA 1020–1022 (LASL), Aug 47 (S).
6. *A Comparison of Altitude Corrections for Blast Overpressures*, Haskell (AFCRC), Sep 54 (S).
7. *Comparison of the Modified Sachs Scaling with Experiments* (SC), TM 274-54-51, C. D. Broyles, 14 Dec 54 (SRD).
8. *Conference: Weather Effects on Nuclear Detonations*, AFSG 31 (AFCRC), Feb 53 (SRD).
9. *Convective Heating of Air Above an Inorganic Surface Heated by Radiation from a Nuclear Weapon*, AFSWP-862, F. M. Sauer and W. Lai (For. Serv.), Nov 55 (C).
10. *Correlation of Experimental Peak Overpressures in the Fused Shock Region*, (ARA) 236, David C. Knodel, Jan 57 (S-FRD).
11. *Crater and Slope Tests with Explosives, Part I. Testing Program and Procedure*, Memo 282-P (Panama Canal, Dept. of Op. and Main.), Jun 48 (U).
12. *Cratering from Atomic Weapons*, AFSWP-514 TAR, W. J. Christensen (AFSWP), 29 Jun 56 (SRD).
13. *Curves of Atomic Weapons Effects for Various Burst Altitudes (Sea level to 100,000 ft.)*, SC-3282 (TR), Cook and Broyles (SC), 9 Mar 54 (SRD).
14. *The Effect of Earth Cover in Protecting Structures Against Blast*, AFSWP-357, R. B. Vaile, Jr. (SRI), 30 Sep 54 (CRD).
15. *Effects of the Explosion of 45 Tons of TNT Under Water at a Depth Scaled to Test BAKER*, G. A. Young (NOL), 1 Dec 54 (S).

16. *Effects of Explosions in Shallow Water, Final Report,* (WES), Apr 55 (C).
17. *The Effect of Rain or Fog on Air Blast,* NAVORD–2944, G. K. Hartmann (NOL), 1 Aug 53 (S).
18. *Effects of Topography on Shock Waves in Air,* Condit, et al (AFSWC), TR 57–9, Aug 56 (C).
19. *Effects of Underground Explosions, Volumes I through III* (CFD/NRC), Jun 44 (U).
20. *The Effects Produced by the Explosion of Charges in Shallow Water with Particular Reference to the Atomic Bomb,* NCRE/R 43 (G. B. Naval Const. Res. Est.), Sep 48 (U).
21. *Height of Burst for Atomic Weapons,* LA–1665, F. B. Porzel (LASL), May 1954, (SRD).
22. *Height of Burst for Atomic Bombs,* LA–1406, Francis B. Porzel (LASL), Mar 52 (SRD).
23. *Height of Burst for Nuclear Weapons,* RM 1107, H. L. Brode (RAND), 1 June 54 (SRD).
24. *The Influence of Atmospheric Pressure and Temperature Variations on Shock-Wave Propagation,* AFSWP–264, NAVORD–2707, Part I—Development of Theory and Calculation of Illustrative Examples, F. Theilheimer and L. Rudlin (NOL), 7 Oct 53 (S).
25. *The Influence of Atmospheric Pressure and Temperature Variations on Shock-Wave Propagation,* Part II, AFSWP–265, L. Rudlin (NOL), 1 Aug 54 (SRD).
26. *The Interaction of Shock Waves with a Thermal Layer,* Robert Varwig and Jay Zemel (NOL), 18 Jun 55 (OUO).
27. *Underwater Explosions, A Summary of Results,* E. H. Kennard (DTMB), (C).
28. *Mach Shock Formation from a Nuclear Detonation,* AFSWP–510 TAR, R. J. Hesse and J. R. Kelso (AFSWP), 10 Mar 55 (SRD).
29. *Numerical Solution of Spherical Blast Wave,* Brode, RM 1363–AEC (RAND), 29 Sept 54 (U).
30. *On the Acoustical Theory of Transmission of a Spherical Blast Wave from Water to Air,* A. B. Arons (Woods Hole), 1956 (C).
31. *On the Oblique Reflection of Underwater Shock Waves from a Free Surface,* Parts I–IV, J. H. Rosenbaum (NOL), 1953–54 (C).
32. *Operation TEAPOT—Underground Shot Base Surge Analysis,* AFSWP–876, M. L. Milligan and G. A. Young (NOL), 31 Jan 56 (SRD).
33. *The Pelican Report: Preliminary Studies of an Underwater Atomic Explosion at Deep Submergence* (AFSWP), 10 Apr 52 (SRD).
34. *Phenomenology of a High Altitude Atomic Explosion,* SC–3363, Shelton (SC), 28 Apr 54 (SRD).
35. *The Precursor—Its Formation, Prediction and Effects,* SC–2850 (TR), Frank H. Shelton (SC), 27 Jul 53 (SRD).
36. *Prediction of Dynamic Pressure,* TM 121–54–51, R. J. Buehler (SC), 12 Jul 54 (SRD).
37. *Predictions on the Effect of Refraction on Peak Pressure and Duration of Explosion Pressure Waves,* R. R. Brockhurst (Woods Hole Oceanographic Institute), 1955 (S).
38. *Prediction of Incident Pressure-Time Curves for Nuclear Explosions,* SC–5112 (82), Luke J. Vortman (SC), Jan 54 (SRD).
39. *A Preliminary Estimate of the Effect of Fog and Rain on the Peak Shock Pressure from an Atomic Bomb,* AFCRD AFSG–16, H. P. Gauvin and J. H. Healy (AFCRC), Sep 52 (SRD).
40. *The Preshock Sound Velocity Field over Inorganic and Organic Surfaces,* AFSWP–420, F. M. Sauer (For. Serv.), Dec 54 (C).
41. *Rain, Fog and Cloud Effects on Blast Damage from Atomic Weapons,* SC–3008 (TR), Thomas B. Cook (SC), 22 Oct 53 (SRD).
42. *Refraction and Diffraction of Explosion Pressure Pulses by Gradients in the Propagation Velocity,* R. R. Brockhurst (Woods Hole), 1957 (C).
43. *Response of Non-Linearly Supported Boundaries to Shock Waves, Case of the Spherical Cavity,* M. L. Baron (Col. U.), Mar 56 (C).
44. *A Scale Model Study of the Effects of Symmetric Ridges on Blast Overpressures,* SC–3335 (TR), J. Todd (SC), 3 May 54 (C).

45. *The Scaling of Base Surge Phenomena of Shallow Underwater Explosions*, AFSWP–484, M. L. Milligan and G. A. Young (NOL), 1 May 54 (C).
46. *Shock Wave Diffraction*, N7onr-32104, Sachs and Sauer (SRI), (SRD).
47. *Small Explosion Tests*, Project MOLE, Volumes I and II, D. C. Sachs and L. M. Swift (SRI), Dec 55 (SRD).
48. *Spherical Wave Propagation in Water*, Part I, S. C. Lowell (NYU), Oct 55 (U).
49. *Study of Blast Effects in the Regular Reflection Region*, Task VI, Phase Report No. III of Ad Hoc Analytical Services, ARF–M044-Phase II (ARF), 4 May 54 (S).
50. *Study of Underwater Blast*, F. B. Porzel (ARF), 1956 (CRD).
51. *Theoretical Blast Wave Curves for Cast TNT*, OSRD–5481, J. G. Kirkwood and S. R. Brinkley, Jr. (OSRD), Aug 45 (U).
52. *Underground Explosion Test Program*, Final Report, Volume I—"Soil," Volume II—"Rock" (ERA), 30 Apr 52 (C).
53. *Underwater Explosions*, R. H. Cole (Princeton U. P.), 1948 (U).
54. *Water Waves Produced by Explosions*, H. C. Kranzer and J. B. Keller (NYU), Sep 55 (U).
55. *Wave Propagation in Solids*, Edmund Pinney (Calif. U.), Jan 55 (U).

THERMAL RADIATION PHENOMENA

1. *Airborne Thermal Radiation Measurements at Operation CASTLE*, USNRDL–TR–87, R. P. Day, A. Guthrie, and W. B. Plum (NRDL), 17 May 56 (SRD).
2. *Airborne Thermal Radiation Measurements at Operation IVY*, USNRDL–412, T. R. Broida and A. Broida (NRDL), 14 Aug 53 (SRD).
3. *Atmospheric Attenuation of Thermal Radiation from a Nuclear Detonation*, AFSWP–509, L. B. Streets and Harvey Marron (AFSWP), Dec 1, 54 (C).
4. *Attenuation of Thermal Radiation by a Dispersion of Oil Particles*, AFSWP–749, C. M. Sliepcevich, et al. (ERI), May 54 (C).
5. *Basic Characteristics of Thermal Radiation from an Atomic Detonation*, AFSWP–503 TAR, L. B. Streets (AFSWP), Nov 53 (SRD).
6. *High Altitude Effects on Blast-Thermal Partition of Energy from Nuclear Explosions, and Associated Scaling Laws*, SC–2969 (TR), F. H. Shelton (SC), 15 Sep 53 (SRD).
7. *Horizontal Attenuation of Ultraviolet and Visible Light by the Lower Atmosphere*, NRL 4031, Lawrence Dunkelman (NRL), 10 Sep 52 (U).
8. *Infrared Transmission of Blackbody Radiation through the Atmosphere* (AFCRC–TN–55–857), D. Burch and J. N. Howard (Ohio St. U.), May 55 (U).
9. *Reflected Radiation from an Infinite Lambert Plane*, NRL Memo–122, William B. Fussell (NRL), Jan 53 (U).
10. *Reflection of ABD Thermal Radiation by a Diffusing Ground Surface*, Part 28, NML 5046–3 (NY Naval Shipyard, ML), 5 Nov 53 (C).
11. *Reflections of Radiant Energy from Perfectly Diffusing Surfaces to Horizontal, Flat Targets*, AFSWP–513 TAR, H. Marron and L. B. Streets (AFSWP), 1 Dec 55 (U).
12. *Reflection of Radiation from an Infinite Plane*, Part I, DR–1434, Ralph Zirkand (DN BuAer), Jun 53 (U).
13. *Scaling of Thermal Radiation from Nuclear Detonations*, AFSWP–795, A. Broida (NRDL), 10 Mar 54 (SRD).
14. *Spectral and Radiometric Comparisons of Wasp and HA*, NRL Rpt 4555 RD 538 (NRL), May 1955 (SRD).
15. *A Study of the Effects of Environment on Thermal Radiation*, AFSWP–601, L. B. Streets (AFSWP), Jun 53 (C).

16. *Thermal Data Handbook*, AFSWP–700 (TOI), 1 Nov 54 (SRD).
17. *Total Transmission of the Atmosphere in the Near-Infrared*, NRL 3858, Harold Yates (NRL), 10 Sep 51 (U).

NUCLEAR RADIATION PHENOMENA

1. *Contamination Patterns at Operation JANGLE*, USNRDL–399, R. K. Laurino and I. G. Poppoff (NRDL), 30 Apr 53 (SRD).
2. *The Effects of Soil, Yield, and Scaled Depth on Contamination from Atomic Bombs*, R. D. Cadle (SRI), 29 Jun 53 (SRD).
3. *An Estimate of the Relative Hazard of Beta and Gamma Radiation from Fission Products*, AD–95 (H), R. I. Condit, J. P. Dyson, and W. A. S. Lamb (NRDL), Apr 49 (C).
4. *Delayed Gamma-Rays from Uranium Photofission*, AFSWP–991, J. M. Wyckoff and H. W. Koch (NBS), 30 Sep 55 (U).
5. *Evaluation of Radioactive Fall-Out*, AFSWP–978, R. D. Maxwell (AFSWP), 15 Sep 55 (SRD).
6. *Fall-Out Symposium*, AFSWP–895 (AFSWP), Jan 55 (SRD).
7. *The Fast Neutron Hazard*, Titus C. Evans, Nucleonics 4:3, Mar 49 (U).
8. *Gamma Radiation in Air Due to Cloud or Ground Contamination*, AFSWP–465, M. J. Berger and J. A. Doggett (NBS), 1 Jun 53 (U).
9. *Gamma-Ray Spectral Measurements of Fall-Out Samples from Operation CASTLE*, AFSWP–822, C. S. Cook (NRDL), 26 Jan 55 (SRD).
10. *Hazard Due to Beta Radiation from Fission Products Deposited on the Ground After an Atomic Explosion*, CREL–529, F. S. Goulding and G. Cowper, Atomic Energy Commission of Canada, Ltd., Jan 53 (U).
11. *Interim Report on the NDA–NBS Calculation of Gamma Ray Penetration*, NDA Memo 15c–20, H. Goldstein, et al. (NDAI), 8 Sep 53 (U).
12. *Investigation of Gamma Radiation Hazards Incident to an Underwater Atomic Explosion*, W. E. Strope (BuShips, DN), 1948 (C).
13. *The Nature of Individual Radioactive Particles. I. Surface and Underground ABD Particles from Operation JANGLE*, USNRDL–374, C. E. Adams, I. G. Poppoff, and N. R. Wallace (NRDL), 28 Nov 52 (S).
14. *Radioactive Fall-Out Hazards from Surface Bursts of Very High Yield Nuclear Weapons*, AFSWP–507, D. C. Borg, L. D. Gates, T. A. Gibson, Jr., and R. W. Paine, Jr. (AFSWP), May 54 (SRD).
15. *The Relative Importance of Nuclear Radiation from Atomic Weapons Detonated at High Altitudes*, AFSWP–500, P. W. Ifland (AFSWP), 1953 (SRD).
16. *The Residual Radiological Hazard from the Air Detonation of an Atomic Weapon in the Rain*, AFSWP–501, L. D. Gates, et al. (AFSWP), May 53 (SRD).
17. *Scaling of Contamination Patterns, Surface and Underground Detonations*, NRDL–TR–1, C. F. Ksanda, et al. (USNRDL), Sep 53 (SRD).
18. *Spectral Distribution of Gamma Rays Propagated in Air*, AFSWP–502A, L. D. Gates and C. Eisenhauer (AFSWP), Jan 54 (U).
19. *Spectrum and Attenuation of Initial Gamma Radiation from Nuclear Weapons*, AFSWP–502B TAR, D. C. Borg and C. Eisenhauer (AFSWP), Jan 55 (SRD).
20. *Studies on the Propagation of Gamma Rays in Air, June 30–October 15, 1953. Final Progress Report*, AFSWP–449, W. Bernstein, et al. (BNL), 1953 (U).
21. *Survey of Data on Residual Gamma Spectra*, AFSWP–427, S. Miller, et al. (NBS), 30 Jul 54 (C).
22. *Transport and Early Deposition of Radioactive Debris from Atomic Explosions*, S. M. Greenfield, W. W. Kellogg, F. J. Krieger, R. R. Rapp (RAND), Jul 54 (SRD).
23. *Nuclear Radiation Handbook*, AFSWP–1100 (NDA), Mar 25, 1957 (SRD).
24. *Prediction of Neutron-Induced Activity in Soils*, AFSWP–518, J. F. Canu and P. J. Dolan (AFSWP), 11 Jun 57 (SRD).

PERSONNEL CASUALTIES

1. *The Acute Radiation Syndrome, A Study of Ten Cases*, LA–1095–1097, Hempleman (LASL), Mar 50 (OUO).
2. *Biological Effectiveness of Nuclear Radiation from Fission Weapons*, LA–1987, Payne S. Harris (LASL), Aug 55 (SRD).
3. *The Biological Effects of Blast*, TID–5251, C. S. White (AEC), 15 Sep 54 (SRD).
4. *The Burn Problem in Atomic Warfare*, E. I. Evans, Journal of the American Medical Association, CXLIII, 1143, 1950 (U).
5. *The Effects of Blast Phenomena on Man: A Critical Review* (CHABA–3), Armed Forces-National Research Council Committee on Hearing and Bio-Acoustics, Jun 55 (U).
6. *The Combined Effects of Thermal Burns and Whole-Body X-Irradiation on Survival Time and Mortality*, AFSWP–470, and 473, 474, 475, E. L. Alpen, et al. (NRDL), May, Oct, 53 (U).
7. *The Dose Received by Partially Shielded Gamma Ray Detectors*, AFSWP–466, M. J. Berger (NBS), 8 Oct 54 (U).
8. *The Effect of Atomic Explosions in Causing Temporary Blindness*, ORO–T–115, J. Green (ORO/JHU), 28 Sep 50 (U).
9. *Effect of Nuclear Weapon Yield on Effectiveness of Thermal Energy for Burn Production*, AFSWP–734, E. L. Alpen (NRDL), 30 Aug 54 (SRD).
10. *Effects of Spectral Distribution of Radiant Energy of Cutaneous Burn Production in Man and Rat*, AFSWP–737, E. L. Alpen, et al. (NRDL), 25 Apr 55 (U).
11. *The Effects of Total-Body Fast Neutron Irradiation in Dogs*, AFSWP–760, V. P. Bond, et al. (NRDL), 10 Jan 55 (U).
12. *Experimental Work on Physiological Effects of Blast*, RC–108, S. Zuckerman (G. B., Ministry of Home Sec.), June 40 (S).
13. *Exposure of Monkeys to High Doses of Fission Neutrons from Godiva*, LA–1838, W. H. Langham, et al. (LASL), Oct 54 (SRD).
14. *Extension to Man of Experimental Whole Body Radiation Studies*, Vol. 112, F. C. McLean, J. H. Rust, A. M. Budy, Military Surgeon, Mar 53 (U).
15. *Heat-Reflecting Textiles as Protective Barriers Against Intense Thermal Radiation*, AFSWP–849, R. C. Maggio and T. B. Gilhooly (NML), 25 Mar 55 (U).
16. *Maximum Permissible Amounts of Radioisotopes in the Human Body*, Handbook 52 (NBS), 20 Mar 53.
17. *Mechanical and Thermal Injury from the Atomic Bomb*, E. H. Pearse and J. T. Payne (NEJM, CCXLI, 647), 1949 (U).
18. *Ocular Lesions Following the Atomic Bombing of Hiroshima and Nagasaki*, MDDC 936, J. J. Flick (AEC Oak Ridge, Tenn.), 13 May 47 (U).
19. *Pathologic Effects of Atomic Radiation*, NAS–NRC 452, 1956 (U).
20. *Permissible Doses from External Sources of Ionizing Radiation*, Handbook 59 (NBS), 24 Sep 54.
21. *Reflectance and Absorptance of Human Skin*, AFSWP–840, W. Derksen (NML), 31 Mar 55 (U).
22. *The Relative Biological Efficiency of Different Ionizing Radiations*, AFSWP–436, John W. Boag (NBS), 30 Dec 53 (U).
23. *The Relative Biological Effectiveness of Fast Neutrons in Mice*, AFSWP–759, R. E. Carter, et al. (NRDL), 17 Nov 54 (U).
24. *Report of the International Committee on Radiological Units and Measurements*, Handbook 62 (NBS), 10 Apr 57.
25. *Report on the Medical Studies of the Effects of the Atomic Bomb*, M. Tsuzuki (Gen. Rpt., Atomic Bomb Casualty Commission, Washington National Research Council, App. 9), 1947 (U).
26. *Research Report on the Accuracy With Which Flash Burns May Be Predicted From the Temperature History of a Skin Stimulant*, AFSWP–953, W. L. Derksen (NML), 19 Jun 56 (U).

27. *Research Report on the Influence of Air Supply and Air Flow on Burns Behind Irradiated Fabrics*, AFSWP-1000, W. L. Derksen and J. J. Bates (NML) (U).
28. *Studies of the Effects of Massive, Rapid Doses of Gamma Rays on Mammals*, LA-1643, W. H. Langham, et al. (LASL), 1953 (U).
29. *A Study of Radiant Energy Burns: The Effect of Exposure Time and Intensity*, UR-217, J. B. Perkins, H. E. Pearse, and H. D. Kingsley (Univ. of Rochester A. E. Proj. Rpt.), 1952 (U).
30. *Thermal and Combined Thermal and Ionizing Radiation, Effects on Biological Systems*, AFSWP-471, 475 and 735, E. L. Alpen (NRDL), 1953-1954.

DAMAGE TO STRUCTURES

1. *Air Blast Loading on a Scaled Three-Dimensional Structure*, AFSWP-813, C. N. Kingery and J. H. Keefer (BRL), Jul 55 (U).
2. *Air Blast Loading Test on Structures*, Operation DRAGON, Int. Rpt. SRI-P-678 Int. 3, S. R. Hornig and D. C. Sachs (SRI), Jul 54 (C).
3. *Air Blast Loading on Three-Dimensional Scale Models of Dome Shape*, AFSWP-773, E. Rines, et al. (BRL), Apr 55 (U).
4. *Analysis of Gravity Dams Subjected to Underwater Explosions*, Int. Rpt., C. H. Norris (MIT), 1 Jul 53 (S).
5. *Behavior of Reinforced Concrete Structural Elements Under Long Duration Impulsive Loads*, Part I. Summ. Rpt., MIT-25A, Robert J. Hansen (MIT), Sep 49 (U).
6. *Behavior of Truss Bridges Under Blast From an Atomic Bomb, Phase I and II*, MIT 29 and MIT 29A, J. S. Archer, W. B. Delano and S. Namyet (MIT), 1950-51, Phase I (C); Phase II (OUO).
7. *Blast Loading End Effects I*, AFSWP-461, C. C. Hudson (SC), 24 Aug 54 (C).
8. *Blast Pressure Requirements for Structural Damage*, AFSWP-805, N. M. Newmark (Ill. Univ.), Aug 54 (S).
9. *Deformation Model Studies of Buildings Subjected to Blast Loading*, AFSWP-166 (Stan. U. VRL TR-20), H. A. Williams and A. K. Ruby (Stan. U.), 1 Dec 54 (U).
10. *Deformation Model Analysis of Building 2, Army Test Structure, Operation GREENHOUSE*, AFSWP-167 (Stan. U. VRL TR-21), Harry A. Williams (Stan. U.), 15 Dec 54 (C).
11. *Design of Structures to Resist the Effects of Atomic Weapons*, EM-1110-34 (MIT) (U).
12. *Diffraction of a Mach Stem Shock over a Square Block*, AFSWP-704, E. B. Turner, et al. (ERI), Jan 56 (U).
13. *Dynamic Analysis of a One Story Rigid Frame*, AFSWP-605, R. C. DeHart (AFSWP), 29 Sep 55 (U).
14. *The Effect of Blast Loading Duration on Structural Damage*, AFSWP-508 TAR, S. B. Smith, et al. (AFSWP), May 54 (S).
15. *The Effect of Earth Cover in Protecting Structures Against Blast*, AFSWP-357A, R. B. Vaile, Jr. (SRI), 30 Sep 54 (CRD).
16. *The Effects of Surface Roughness*, AFSWP-990, G. Naguma and A. H. Wiedermann (ARF), Dec 55 (C).
17. *An Engineering Approach to Blast Resistant Design*, N. M. Newmark (Proceedings American Society of Civil Engineers), Separate No. 306, Oct 53 (U).
18. *Field Fortifications Test, Exercise Desert Rock VI*, Technical Rpt. 1468-TR (ERDL), 2 Nov 56 (SRD).
19. *Investigation of Shear Walls*, Parts I and II (U), III through V (C), Williams and Benjamin (Stan. U.), 1952-53.
20. *Load Deformation Characteristics of Simulated Beam Column Connections in Reinforced Concrete*, AFSWP-174 (Ill. U. SRS-76), R. M. McCollister, et al. (U. of Ill.), Jun 54 (U).
21. *Loading Analysis of Five Story Reinforced Concrete Frame Structures* (in the Regular Reflection Region, Two-Dimensional), (ARF), 16 Jul 56 (C).
22. *Methods for Estimating Blast Loading on Simple Structures*, AFSWP-226, Vortman, L. J., Merritt, M. L. (SC), Sep 53 (SRD).

23. *On the Effect of Slow Rise Times on the Blast Loading of Structures*, AFSWP-4[illegible], M. L. Merritt (SC), 25 Sep 53 (CRD).
24. *Response of a Single Story Heavy Steel Frame Industrial Building to Atomic Blast*, AFSWP-782, A. Finerman and J. H. King (MIT), Dec 55 (S).
25. *Self-Shielding from Blast Waves by Structural Members*, AFSWP-225, C. C. Hudson (SC), May 53 (U).
26. *Shielding of Three-Dimensional Blocks*, AFSWP-989 (ARF), Nov 55 (C).
27. *A Simple Method for Evaluating Blast Effects on Buildings*, ARF-EMR-1 (ARF), Jul 52 (U).
28. *Study of Atomic Blast Damage to Buildings at Hiroshima and Nagasaki*, AFSWP-808, J. S. Archer (MIT), Jul 54 (C).
29. *The Theoretical Elastic Response of Shear Walls Subjected to Dynamic Loads*, AFSWP-818, A. Finerman (MIT), Aug 56 (U).

DAMAGE TO NAVAL EQUIPMENT

1. *Model Studies on Effects of Underwater Atomic Explosions on Ships*, Parts I-V, W. W. Murray (UERD), 1957 (C).
2. *On the Prediction of the Hull Splitting Standoff of Submarines from Atomic Depth Charges*, A. H. Keil and H. M. Schauer (UERD), 1956 (C).
3. *Proceedings of Seventh Symposium on Underwater Explosion Research*, Parts I (C) and II (DTMB), 1956 (SRD).
4. *Submarine Lethality Curves for Underwater Atomic Explosions*, D. S. Cohen (UERD), 1956 (C).
5. *Underwater Explosion Research, Vol. III*, (ONR Compendium) (U).

DAMAGE TO AIRCRAFT

1. *The Effects of Atomic Explosions on Aircraft*, 7 Volumes, WADC TR 52-244 (MIT), 1953 (SRD).
2. *General Design Considerations for Aircraft Operating in the Vicinity of a Nuclear Burst*, WADC TR-53-238, David J. Fink (WADC), Jul 53 (SRD).
3. *Résumé of the Effects of Very High Yield Atomic Explosions on Aircraft Structures—Explosion Characteristics, Structural and Aeroelastic Blast Effects, and Thermal Radiation Effects*, WADC Tech. Rpt. 54-386, E. A. Witmer, et al. (WADC), 10 Aug 56 (SRD).
4. *Three-Dimensional Lethal Envelopes for the B-52 at 35,000-foot and 45,000-foot Altitudes Subjected to 2.0 KT and 0.5 KT Atomic Bursts* (C), ARA-185, D. J. Fink, P. B. Athens, (ARA), 18 Aug 54 (SRD).
5. *The Vulnerability of the MIG-17 (FRESCO) to Free-Air Nuclear Detonations*, ARA-220, D. J. Fink, et al. (ARA), 10 Jun 55 (SRD).
6. *The Vulnerability of Parked Army Aircraft to Nuclear Detonations*, WADC Tech. Rpt. 56-354, D. H. Whitford (WADC), Jun 56 (SRD).

DAMAGE TO MILITARY FIELD EQUIPMENT

1. *The Effects of Atomic Weapons on Engineer Heavy Equipment*, ERDL-1443 (ERDL), 25 Apr 56 (U).
2. *Exercise Desert Rock I* (Hq III Corps, Ft McArthur), Oct 51 (SRD).
3. *Report of Test Exercises Desert Rock II and III* (Hq Camp Desert Rock), 15 Dec 51 (SRD).
4. *Exercise Desert Rock IV* (Hq Sixth Army), Apr-Jun 1956 (SRD).
5. *Exercise Desert Rock V* (Hq Camp Desert Rock), Jan-Jun 53 (SRD).
6. *Analysis of Atomic Weapons Effects Upon Army Ground Operations Equipment*, ORO Repts., Phases I through V, Dec 50-Jul 52 (S).
7. *Damage to Field Military Equipment from Nuclear Detonations*, AFSWP-511 TAR, R. J. Hesse (AFSWP), 1 Feb 56 (SRD).
8. *The Influence of Atomic Weapons on Signal Communications in an Infantry Division* (SigC Board Study No. 93A), 14 Jan 53 (S).

9. *Influence of Atomic Weapons on Signal Communications in Corps and Army Areas* (SigC Board Study No. 95), 2 Apr 52 (S).
10. *Studies of Railroad Marshalling Yards*, ARF Project No. M055 (Final Report) (ARF) (C).

FOREST STANDS

1. *Burning Potential—Forest and Wildland Areas*, Phase Rpt. 1/52, Keith Arnold, et al. (For. Serv.), Jan 52 (C).
2. *Comparison of Field and Laboratory Forest Fuel Ignition Energies and Extrapolation to High-Yield Weapons*, AFSWP–870, F. M. Sauer (For. Serv.), Mar 56 (SRD).
3. *A Study of the Influences of a Forest on the Effects of an Atomic Weapon*, AFSWP–602, L. B. Streets (AFSWP), Jun 53 (C).
4. *Thermal Conductivity of Some Common Forest Fuels*, AFSWP–405, G. M. Byram, et al. (For. Serv.), 1 Dec 52 (U).
5. *Thermal Properties of Forest Fuels*, AFSWP–404, G. M. Byram, et al. (For. Serv.), Oct 52 (U).
6. *Blast Effects on Forest Stands by Nuclear Weapons*, AFSWP–971, W. L. Fons, F. M. Sauer, and W. Y. Pong (For. Serv.), 1957 (C).

MISCELLANEOUS RADIATION DAMAGE CRITERIA

1. *Apparatus and Methods for the Exposure of Materials to Thermal Radiation*, AFSWP–246, G. E. Davis (NML), 2 Oct 52 (U).
2. *Critical Thermal Energies of Construction Materials*, AFSWP–839, L. Banet and J. Bracciaventi (NML), 30 Dec 54 (U).
3. *Distribution of Primary Ignition Points Following Atomic Attack on Urban Targets-Transient Exterior Fuels*, AFSWP–412, G. C. Chandler and Keith Arnold (For. Serv.), Mar 53 (U).
4. *Effects of Thermal Radiation on Materials, Final Report On*, A. F. Robertson (NBS), 1 Nov 53 (C).
5. *Frequency of Urban Building Fires as Related to Daily Weather Conditions*, AFSWP–866, A. R. Pirsko (For. Serv.), Mar 56 (U).
6. *Investigation of Optical Transmittance, Reflectance, and Absorptance of Materials*, AFSWP–396, R. F. Byrne and L. N. Mancinelli (NML), 12 Mar 54 (U).
7. *A Method for Estimating Probable Ignitions of Interior Fuels by Atomic Weapon Explosion* (*Survey of Boston and Detroit*), AFSWP–340, H. D. Bruce and L. E. Downs (Forest Products Lab), 1 Feb 56 (SRD).
8. NML Reports on Critical Thermal Energies of Various Specific Materials as follows:

    Metallized rayon fabric, AFSWP–390; Doped fabrics, AFSWP–389, 388, 244, 393; Aluminized fabrics, 384; Protective coatings on wood, 382; Awning material, 381; Aluminized asbestos cloth, 380; Packaging materials, 379; Special fabrics (window shades, rugs, curtains, upholstery), 245; Plastics, 243; Flight clothing, 392; Rubber hose and gasket materials, 395; Canopy materials, 397; Plastic radome materials, 399; Curtain materials (aircraft), 400; Chemical warfare protective materials, 401; Ceramics, 402; Flame proofed cotton fabric, 403.
9. *Primary Ignitions Following Atomic Attack on Urban Targets-Transient Exterior Fuels*, AFSWP–413, F. M. Sauer, et al. (For. Serv.), Jun 53 (U).
10. *Remarks on Estimation of the Number of Fires Due to the Ignition of Transient Exterior Kindling Fuels*, AFSWP–861, F. M. Sauer (For. Serv.), Oct 55 (U).
11. *Relative Protection Against Radiation Burns Provided by Heat-Treated Orlon*, NML 5046–3 Pt–20, Final, W. J. Bates and M. S. Kelly (NML), 13 Aug 52.
12. *Research Report on the Relative Spectral Energy Distribution of the NML Carbon-Arc Source of Intense Thermal Radiation*, AFSWP–1002, W. L. Derksen (NML), 31 Jul 56 (U).
13. *Research Report on Thermal Damage to Cloths as a Function of Time of Exposure, Nuclear Weapon Pulses*, AFSWP–996, J. J. Bates (NML), 1956 (C).

14. *Temperatures Attained in Wood Exposed to High Intensity Thermal Radiation*, FRL/MIT-TR-3. H. C. Hottel and R. Gordon (Fuels Research Lab., MIT), Apr 53 (U).

15. *Thermal Radiation Characteristics of Liquid Fuels*, AFSWP-833, J. J. Bates and T. I. Monahan (NML), 5 Nov 54 (C).

16. *Thermal Radiation Damage to Cloths as a Function of Time of Exposure, Rectangular Pulses*, AFSWP-841, J. J. Bates and T. I. Monahan (NML), 16 Jun 55 (U).

IDENTIFICATION OF CORPORATE AUTHOR CODES

AEC	Atomic Energy Commission
AFCRC	Air Force Cambridge Research Center, Cambridge, Mass.
AFSWP	Armed Forces Special Weapons Project
ARA	Allied Research Associates
ARF	Armour Research Foundation, Illinois Inst. of Tech., Chicago, Ill.
BNL	Brookhaven National Laboratory
BRL	Ballistic Research Laboratories, Aberdeen Proving Ground, Md.
CFD	Committee on Fortification Design
DTMB	David Taylor Model Basin
ERA	Engineering Research Associates
ERDL	Engineer Research and Development Laboratory, Ft. Belvoir, Va.
ERI	Engineering Research Institute
For. Serv.	Forest Service, Dept. of Agriculture
LASL	Los Alamos Scientific Laboratory
MIT	Massachusetts Institute of Technology, Cambridge, Mass.
NAS	National Academy of Science
NBS	National Bureau of Standards
NDA	Nuclear Development Corporation of America
NML	Naval Material Laboratory, N. Y. Naval Shipyard
NOL	Naval Ordnance Laboratory, Silver Spring, Md.
NRC/DMS	National Research Council, Division of Medical Sciences
NRDL	Naval Radiological Defense Laboratory, San Francisco, Calif.
NRL	Naval Research Laboratory
ONR	Office of Naval Research
ORO/JHU	Operations Research Organization, Johns Hopkins Univ.
RAND	RAND Corp., Santa Monica, Calif.
SC	Sandia Corporation, Albuquerque, New Mexico
SRI	Stanford Research Institute, Menlo Park, Calif.
TOI	Technical Operations, Inc.
UERD	Underwater Explosions Research Division, Norfolk Naval Shipyard
WADC	Wright Air Development Center, Wright-Patterson AFB
WES	Waterways Experiment Station, Vicksburg, Miss.

BLANK

Index

INDEX

Note. Numbers and letters in roman type refer to paragraphs; numbers in italics refer to figures.

BLANK

U. S. GOVERNMENT PRINTING OFFICE : 1960 O - 552794

~~CONFIDENTIAL~~

APR 17 1975

21 SEP 1975

~~CONFIDENTIAL~~

WARNING NOTICES

Authority for release of this document to a foreign government must be secured from the Assistant Chief of Staff, Intelligence, Headquarters, Department of the Army.

When this document is released to a foreign government, it is released subject to the following conditions: This information is furnished with the understanding that it will not be released to another nation without specific approval of the United States of America, Department of the Army; that it will not be used for other than military purposes; that individual or corporation rights originating in the information whether patented or not will be respected; and that the information will be afforded substantially the same degree of security as afforded by the United States of America, Department of the Army.

This document contains information affecting the national defense of the United States within the meaning of the Espionage Laws, Title 18 U. S. C., sections 793 and 794. The transmission or the revelation of its contents in any manner to an unauthorized person is prohibited by law.

U.S. DEPARTMENT OF COMMERCE
Technology Administration
National Technical Information Service
Springfield, VA 22161 (703) 605-6000